

Calibration of the Massachusetts and
Cape Cod Bays Hydrodynamic Model:
1998-1999

Massachusetts Water Resources Authority

Environmental Quality Department
Report 2001-12



Citation:

HydroQual and Signell RP. 2001. **Calibration of the Massachusetts and Cape Cod Bays Hydrodynamic Model: 1998-1999**. Boston: Massachusetts Water Resources Authority. Report ENQUAD 2001-12. 170 p.

TABLE OF CONTENTS

<u>Section</u>	<u>Page</u>
1	INTRODUCTION 1-1
1.1	PROJECT OVERVIEW 1-1
1.2	PHYSICAL SETTING 1-1
2	MODEL IMPLEMENTATION 2-1
2.1	NUMERICAL SCHEME 2-1
2.2	MODEL GEOMETRY AND BATHYMETRY 2-3
2.3	VERTICAL MIXING 2-3
2.4	HORIZONTAL MIXING 2-3
2.5	SURFACE AND BOTTOM STRESS 2-5
2.6	SURFACE HEAT FLUX 2-5
2.7	FRESHWATER INPUT 2-7
2.8	OPEN BOUNDARY CONDITIONS 2-11
2.9	TIME STEP 2-17
2.10	SIGMA-COORDINATE CORRECTION 2-17
3	CALIBRATION 3-1
3.1	SALINITY AND TEMPERATURE 3-1
3.1.1	Temporal Comparisons 3-1
3.1.2	Buoy Data 3-15
3.1.3	RMS Error 3-19
3.2	VERTICAL PROFILES 3-22
3.3	CURRENTS 3-26
3.4	SHORT TERM EVENTS 3-36
4	SUMMARY 4-1
4.1	CONCLUSIONS 4-1
4.2	RECOMMENDATIONS 4-2
5	REFERENCES 5-1
APPENDIX A	BOUNDARY CONDITION DATA STATION LOCATIONS
APPENDIX B	BOUNDARY CONDITION INPUTS FOR TEMPERATURE AND SALINITY
APPENDIX C	MONTHLY CURRENT METER MODEL VERSUS DATA COMPARISONS AT THE BOSTON BUOY
APPENDIX D	MONTHLY CURRENT METER MODEL VERSUS DATA COMPARISONS AT THE SCIUATE BUOY

LIST OF FIGURES

<u>Figure</u>	<u>Page</u>
2-1. Hydrodynamic Grid	2-4
2-2. Meteorological Forcings	2-8
2-3. Freshwater Input	2-9
2-4. Freshwater Input (continued)	2-10
2-5. Station Locations from which Temperature and Salinity Data were Available to Specify Boundary Conditions from Jan. through April 1998	2-13
2-6. Open Boundary Conditions off the New Hampshire Coast and East of Cape Ann	2-16
3-1. Study Area	3-2
3-2. 1998 Salinity and Temperature Calibration at MWRA Stations F26, F27 and F29	3-3
3-3. 1998 Salinity and Temperature Calibration at MWRA Stations F31, N01 and N10	3-5
3-4. 1998 Salinity and Temperature Calibration at MWRA Stations N04, N07 and F17	3-6
3-5. 1998 Salinity and Temperature Calibration at MWRA Stations F07, F01 and F02	3-7
3-6. 1998 Sigma-t Calibration at MWRA Stations F26, F27, F29, F07, F01 and F02	3-9
3-7. 1998 Sigma-t Calibration at MWRA Stations F31, F17, N01, N10, N04 and N07	3-10
3-8. 1999 Salinity and Temperature Calibration at MWRA Stations F26, F27 and F29	3-11
3-9. 1999 Salinity and Temperature Calibration at MWRA Stations F31, N01 and N10	3-12
3-10. 1999 Salinity and Temperature Calibration at MWRA Stations N04, N07 and F17	3-13
3-11. 1999 Salinity and Temperature Calibration at MWRA Stations F07, F01 and F02	3-14
3-12. 1999 Sigma-t Calibration at MWRA Stations F26, F27, F29, F07, F01 and F02	3-16
3-13. 1999 Sigma-t Calibration at MWRA Stations F31, F17, N01, N10, N04 and N07	3-17
3-14. 1998 Temperature and Salinity Calibration at the Boston Buoy and Scituate Buoy	3-18
3-15. 1999 Temperature and Salinity Calibration at the Boston Buoy and Scituate Buoy	3-20
3-16. Model Versus Salinity Data Vertical Profile Comparisons for Six Far Field Stations in June 1998	3-23
3-17. Model Versus Salinity Data Vertical Profile Comparisons for Four Near Field and Two Far Field Stations in June 1998	3-24
3-18. Model Versus Temperature Data Vertical Profile Comparisons for Six Far Field Stations in June 1998	3-25
3-19. Model Versus Temperature Data Vertical Profile Comparisons for Four Near Field Stations and Two Far Field Stations in June 1998	3-27
3-20. Model Versus Temperature Data Vertical Profile Comparisons for Six Far Field Stations in August 1999	3-28
3-21. Model Versus Temperature Data Vertical Profile Comparisons for Four Near Field Stations and Two Far Field Stations in August 1999	3-29
3-22. Model Versus Salinity Data Vertical Profile Comparisons for Six Far Field Stations in August 1999	3-30
3-23. Model Versus Salinity Data Vertical Profile Comparisons for Four Near Field Stations and Two Far Field Stations in August 1999	3-31

LIST OF FIGURES - continued

<u>Figure</u>	<u>Page</u>
3-24. Comparison Between Current Meter and Model Results at the Scituate Buoy for November 1998 at 5 and 17 Meters	3-32
3-25. Comparison Between Current Meter and Model Results after Being Filtered by a 33-hour Lowpass Filter at the Scituate Buoy for Nov. 1998 at 5 and 17 Meters	3-33
3-26. Comparison Between Current Meter Data and Model Results at the Scituate Buoy for July 1999 at 5 and 17 Meters	3-34
3-27. Comparison Between Current Meter and Model Results after Being Filtered by a 33-hour Lowpass Filter at the Scituate Buoy for July 1999 at 5 and 17 Meters	3-35
3-28. Comparison Between Current Meter and Model Results after Being Filtered by a 33-hour Lowpass Filter at the Boston Buoy for Nov. 1998 at 5 and 23 Meters	3-37
3-29. Comparison Between Current Meter and Model Results after Being Filtered by a 33-hour Lowpass Filter at the Boston Buoy for July 1999 at 5 and 23 Meters	3-38
3-30. Model Versus Data Comparison During a Wind Mixing Event	3-40
3-31. 34-hour Lowpass Salinity and Currents Along a Transect Through the Boston Buoy as Shown in Figure 3-1 (May 8 - May 14, 1998)	3-41
3-32. 34-hour Lowpass Salinity and Currents Along a Transect Through the Boston Buoy as Shown in Figure 3-1 (May 15 - May 20, 1998)	3-43
3-33. Model Versus Data Comparison During a Cooling Event	3-44
3-34. 34-hour Lowpass Temperature and Currents Along a Transect Through the Boston Buoy as Shown in Figure 3-1 (June/July 1999)	3-45
3-35. Model Versus Data Comparison During a Fall Turnover Event	3-46
3-36. 34-hour Lowpass Temperature and Currents Along a Transect Through the Boston Buoy as Shown in Figure 3-1 (October, 1999)	3-47

LIST OF TABLES

<u>Table</u>	<u>Page</u>
2-1. Availability of Temperature and Salinity Boundary Condition Data	2-14
3-1. RMS Error	3-21

SECTION 1

INTRODUCTION

1.1 PROJECT OVERVIEW

The Massachusetts Water Resources Authority (MWRA), as part of its discharge permit for the Deer Island Wastewater Treatment Plant, is required to use the coupled hydrodynamic/water quality model developed for Massachusetts and Cape Cod Bays to analyze impacts of the treatment plant effluent on the bays following the September 6, 2000 startup of the offshore outfall. MWRA has decided to analyze the years 1998 and 1999 with the model and therefore requires the hydrodynamic/water quality model to be setup and run for this period. The first phase of this project is the setup and calibration of the hydrodynamic model while the second phase will be the setup and running of the water quality model. The hydrodynamic model was originally set up and calibrated for the period of October 1989 through December 1994 by Dr. Richard Signell at the U.S. Geological Survey (USGS) in Woods Hole. Dr. Signell has since transferred the model to HydroQual to conduct the modeling work for the 1998-1999 period.

This report includes the final calibration of the hydrodynamic model for the years 1998 and 1999. The report also includes the model inputs and the calibration process. This final report addresses comments made by the MEG in March, 2001.

1.2 PHYSICAL SETTING

Massachusetts Bay is a semi-enclosed embayment that opens into the Gulf of Maine at its eastern boundary. It is roughly 100 km long, 50 km wide and has an average water depth of 35 m. The bay is bounded on the east by Stellwagen Bank, which rises to within 20 m of sea surface. Boston Harbor empties into western Massachusetts Bay, providing one source of nutrients to the region.

Circulation in Massachusetts Bay is driven by a combination of local and remote processes that vary with season (Geyer et al, 1992). Throughout the year water flows southward in the western Gulf of Maine, and although most of this current continues flowing southward over the eastern flank of Stellwagen Bank (largely bypassing Massachusetts Bay), a small portion flows into the bay and drives a weak counter-clockwise flow that enters at Cape Ann, on the north and exits on the south at Race Point, located to the north of Cape Cod. The magnitude of this flow varies from less than 1 cm/s off Boston to about 3-4 cm/s along the western portions of Massachusetts Bay.

The remotely driven mean circulation pattern is modified by seasonal current regimes. During the winter, the bay is well-mixed vertically, and the wind is principally from the northwest, reinforcing the counterclockwise circulation. In the spring, surface warming and freshwater intrusions from rivers that discharge to the Gulf of Maine cause the bay to become stratified. During this period, surface currents in the bay are dominated by the strong, yet variable, density-driven flow associated with these Gulf of Maine intrusions. By summer, the stratification has intensified due to further surface warming. The dominant wind direction in summer is from the southwest, which drives strong upwelling events along the western and northern shores of the bay. In the fall, rapid cooling on the shallow western side of the bay results in a density field that temporarily reverses the surface mean flow.

Tidal currents in Massachusetts Bay are dominated by the semi-diurnal M_2 constituent (period = 12.42 hours). The currents are largely bidirectional and the magnitude ranges from about 10 cm/s in the interior of Massachusetts Bay to more than 50 cm/s off the tip of Cape Cod and in the entrances to Boston Harbor and Plymouth Harbor (Blumberg et al, 1993, Irish and Signell, 1992). Although the transport due to tides is generally oscillatory and, therefore, does not give rise to net transport of material, they are an important source of bottom-generated turbulent mixing.

SECTION 2

MODEL IMPLEMENTATION

2.1 NUMERICAL SCHEME

The model used in this study is called ECOM-si, a semi-implicit variant of the three-dimensional Estuary, Coastal and Ocean Model (ECOM) described by Blumberg and Mellor (1987). ECOM-si was selected because it includes a free surface, nonlinear advective terms, coupled density and velocity fields, river runoff, heating and cooling of the sea surface, and a 2.5 level turbulence closure scheme to represent vertical mixing (Mellor and Yamada, 1982). In addition, the combination of orthogonal curvilinear coordinates in the horizontal plane and sigma-coordinates in the vertical dimension allows grid refinement in regions of interest without sacrificing the advantages of a Cartesian grid.

The basic equations are expressed in a sigma coordinate system:

$$\sigma = \frac{z - \eta}{H + \eta} \quad 2-1$$

where $H(x,y)$ is the bottom topography, $\eta(x,y)$ is the surface elevation and z is the depth varying from η to $-H$. The basic governing equations are presented here in Cartesian coordinates to facilitate discussion. The equations as expressed in curvilinear coordinates may be found in Blumberg and Mellor (1987).

The continuity equation is:

$$\frac{\partial \eta}{\partial t} + \frac{\partial uD}{\partial x} + \frac{\partial vD}{\partial y} + \frac{\partial w}{\partial \sigma} = 0 \quad 2-2$$

the x momentum equation is:

$$\begin{aligned} \frac{\partial uD}{\partial t} + \frac{\partial u^2D}{\partial x} + \frac{\partial uvD}{\partial y} + \frac{\partial uw}{\partial \sigma} - f vD + gD \frac{\partial \eta}{\partial x} = \\ \frac{\partial}{\partial \sigma} \left\{ \frac{K_M}{D} \frac{\partial u}{\partial \sigma} \right\} - \frac{gD^2}{\rho_o} \frac{\partial}{\partial x} \int_{\sigma}^0 \rho d\sigma + \frac{gD}{\rho_o} \frac{\partial D}{\partial y} \int_{\sigma}^0 \frac{\partial \rho}{\partial \sigma} d\sigma + F_x \end{aligned} \quad 2-3$$

and the y momentum equation is:

$$\begin{aligned} \frac{\partial \mathbf{u}D}{\partial t} + \frac{\partial \mathbf{uv}D}{\partial x} + \frac{\partial v^2 D}{\partial y} + \frac{\partial v w}{\partial \sigma} + f \mathbf{u}D + \mathbf{g}D \frac{\partial \eta}{\partial y} = \\ \frac{\partial}{\partial \sigma} \left\{ \frac{K_M}{D} \frac{\partial v}{\partial \sigma} \right\} - \frac{\mathbf{g}D^2 \partial}{\rho_o \partial y} \int_{\sigma}^0 \rho d\sigma + \frac{\mathbf{g}D \partial D}{\rho_o \partial y} \int_{\sigma}^0 \frac{\partial \rho}{\partial \sigma} d\sigma + \mathbf{F}_y \end{aligned} \quad 2-4$$

where η is the surface elevation, \mathbf{u} and \mathbf{v} are the x and y components of velocity, D is the total water depth $D = H + \eta$, w is the transformed vertical velocity (normal to sigma surfaces), K_M is the vertical eddy viscosity, ρ is the water density, ρ_o is a reference water density, f is $1/2$ the earth's rotation rate (Coriolis parameter), and F_x and F_y are the horizontal viscous terms defined by:

$$F_x = \frac{\partial}{\partial x} \left(2A_M D \frac{\partial u}{\partial x} \right) + \frac{\partial}{\partial y} \left[A_M D \left(\frac{\partial u}{\partial y} + \frac{\partial v}{\partial x} \right) \right] \quad 2-5$$

and

$$F_y = \frac{\partial}{\partial x} \left[A_M D \left(\frac{\partial u}{\partial y} + \frac{\partial v}{\partial x} \right) \right] + \frac{\partial}{\partial y} \left(2A_M D \frac{\partial v}{\partial y} \right) \quad 2-6$$

where A_M is the horizontal eddy viscosity. The parameterizations of K_M and A_M are discussed in Sections 2.3 and 2.4, respectively. The model also solves prognostically for temperature, salt, turbulence kinetic energy and turbulence macroscale.

ECOM-si differs from the Blumberg and Mellor (1987) ECOM model in that it uses a semi-implicit scheme for calculating the free surface, therefore avoiding the gravity wave CFL condition required by explicit schemes (e.g., Casulli, 1990). This has the advantage that larger time steps may be taken (on the order of minutes, rather than tens of seconds). A potential disadvantage of implicit schemes is that they more readily damp free wave motions, but in strongly forced and damped shallow regions such as Massachusetts Bay, the effect is small. This was determined by halving the time step and observing negligible differences in simulation results. Another disadvantage is that because the calculation of surface elevation requires solving a large matrix equation at each time step and efficient solution of this equation requires positive definiteness, boundary conditions for elevation must be formulated in matrix form and must not destroy the positive definiteness of the matrix. We use a combination of clamped and gravity wave radiation conditions on the open boundary, made possible by the implementation of the partially-clamped formulation of Blumberg and Kantha (1985) discussed in Section 2.8.

2.2 MODEL GEOMETRY AND BATHYMETRY

The model is configured on a 68 x 68 horizontal curvilinear orthogonal grid (Figure 2-1) with segment (1,1) in the lower left corner. The grid spacing ranges from approximately 600 m in Boston Harbor to about 6000 m along the open boundary with the Gulf of Maine. The grid extends well offshore of Massachusetts Bay to allow exchange with the Gulf of Maine inside the model domain, and extends far enough north to include the Merrimack River, a large source of fresh water to the region. Twelve sigma levels are used in the vertical dimension. The top three layers are defined at 1%, 4% and 10% of the local water column depth with the bottom nine layers equally distributed (i.e., each representing 10%) over the remaining 90% of the water column.

The bathymetry for the model was obtained by interpolating NOAA sounding data on to the model grid using an inverse distance method. The resulting grid was Shapiro filtered (Shapiro, 1975) to remove 2 grid length variability, and a maximum depth of 140 m was set to eliminate the deep complex topography offshore of Massachusetts Bay. The minimum depth was set to 3 m to avoid having segments flood and dry.

2.3 VERTICAL MIXING

The vertical mixing parameterization was the level 2.5 turbulence closure scheme of Mellor and Yamada (1982) with the extensions by Galperin et al. (1988). An important feature of these extensions include a length-scale limitation that prevents the mixing length from becoming too large during strongly stratified conditions. The minimum “background mixing” value, below which the eddy viscosity never falls, was set to $5 \times 10^{-6} \text{ m}^2/\text{s}$. This value is comparable to the value of vertical mixing observed by Geyer and Ledwell (1994) from a dye experiment near the new outfall site.

2.4 HORIZONTAL MIXING

The horizontal mixing parameterization used the Smagorinsky (1963) formulation in which the magnitude of the horizontal mixing is proportional to horizontal current shear. The Smagorinsky coefficient was set to 0.1, which results in typical horizontal eddy viscosities and diffusivities between 5 -- 20 m^2/s over much of Massachusetts Bay. Ideally, the magnitude of this mixing would simulate processes occurring at scales smaller than the mesh can resolve. In western Massachusetts Bay the grid cell spacing is 1--2 km, and using the rule of thumb that 6--8 grid cells motions are the minimum length that are realistically represented, the model should well resolve mixing processes occurring at scales of 10 km or so. From Okubo (1971), we expect that observed horizontal mixing at a scale of 10 km should be about 10 m^2/s , and at a scale of 1 km should be about 1 m^2/s . Since the model partially resolves shear (and thus produces mixing) at scales between 1 and 10 km, the ideal mixing level should probably be somewhere between 1 and 10 m^2/s .

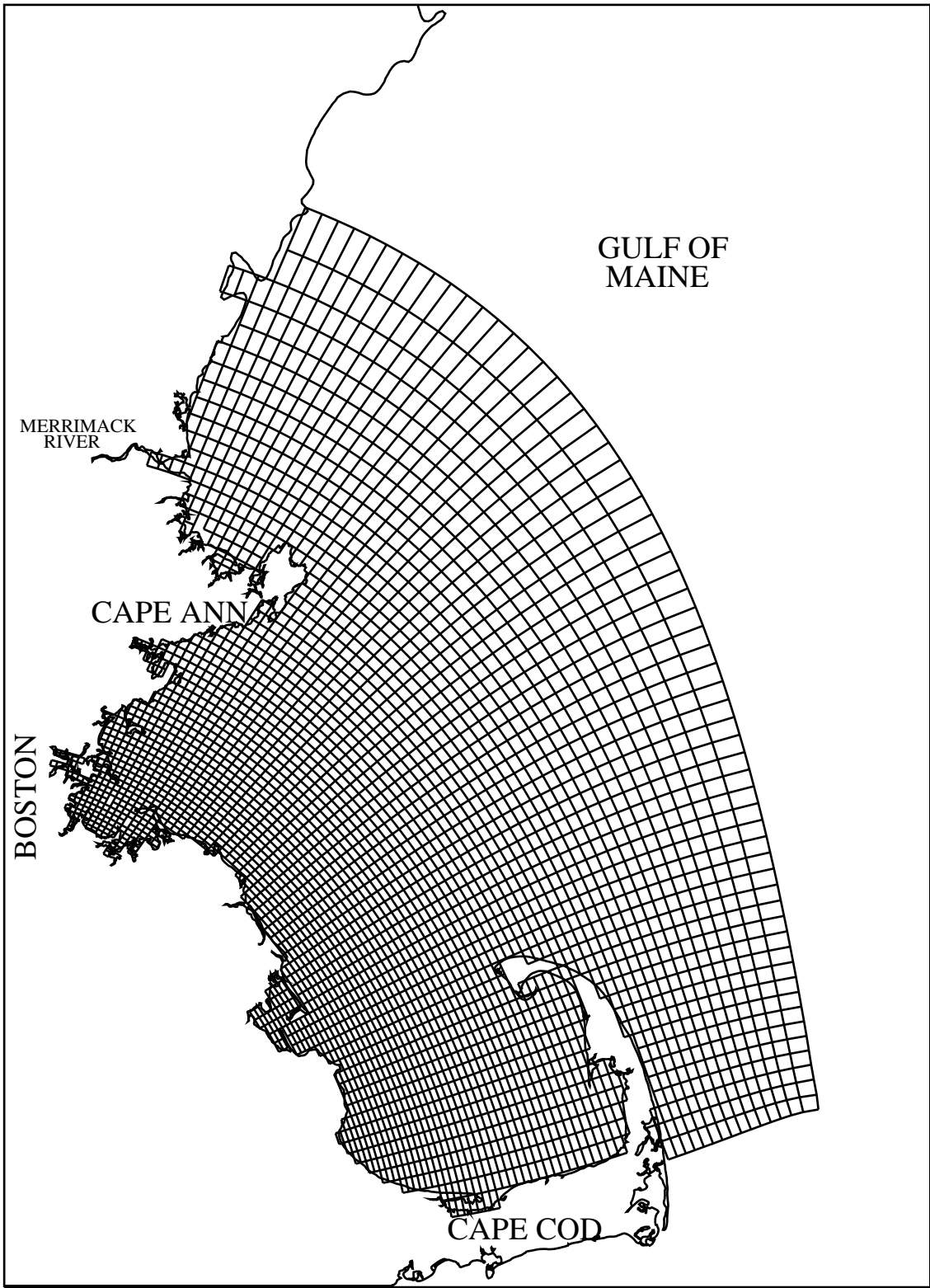


Figure 2-1. Hydrodynamic Grid

In addition to the specified horizontal viscosity, the velocity field was Shapiro filtered every 2 hours to remove 2 grid length energy. This was necessary to prevent 2 grid length energy along the open boundary from growing large enough to violate the advective CFL condition. By applying a 4th order Shapiro filter at 2 hour intervals, the longer wavelength energy is largely unaffected. For example, it can be shown over 20 filter applications (two days of simulation), the amplitude of 6 grid length structure is reduced less than 5% (see appendix of Signell, 1989).

2.5 SURFACE AND BOTTOM STRESS

The surface wind stress was assumed to be uniform over the model domain and was determined from wind measurements at the Boston Buoy using the Large and Pond (1981) formulation. Although the scale of the bay is relatively small compared to most synoptic wind features, there is some wind variability over the bay, caused in part by local effects such as sea breeze. Wind speed and direction was specified at three hour increments for input into the model. A gap in the available Boston Buoy data existed for the period of November 13 to December 1, 1999. Data from Boston's Logan Airport were used to supplement the Boston Buoy data.

The bottom stress is determined from the quadratic drag law applied at the point closest to the bed where there is a velocity estimate. This is in the middle of the lowest grid cell. Because the distance between the lowest velocity point and the bed varies with location, the bottom roughness length z_0 is specified at each location, and then a constant stress layer is assumed so that an effective drag coefficient can be computed at the velocity point. Currently, ECOMsi uses a constant z_0 throughout the model domain. The bottom roughness length is a calibration parameter that is used to accurately reproduce the tides. For this study, z_0 was assigned a value of 0.003 m which is equivalent to a drag coefficient of 2.5×10^{-3} at 10 m above the bottom (which is in turn a typical value used for depth-averaged models of coastal seas). In these runs, the bottom sigma layer thickness is 10% of the water depth, so the lowest velocity point is 5% of the water depth above the bed. Within Massachusetts Bay, the maximum distance between the lowest velocity point and the bed is 4.8 m in Stellwagen Basin, where the model water depth reaches 96 m.

2.6 SURFACE HEAT FLUX

The surface heat flux was calculated using techniques described by Weller et al. (1995). The technique differed somewhat from what Signell et al. (1996) used in the original calibration of the Massachusetts Bay model. In that effort, the total heat flux, including the short wave radiation, was introduced into the top sigma layer at each grid location. Using that method, the top sigma layer, which represents only the top one percent of the water column depth, became too warm during the summer months, as compared to observed data. Although more than half of the insolation that enters the coastal ocean is absorbed within the top half

meter of the water column (Rosati and Miyakoda, 1988), the remaining fraction that penetrates through the water column may have a significant impact of the development of the thermal structure. Martin (1985) found that modeling simulations are very sensitive to the optical characteristics of the coastal oceans which varies significantly both spatially and temporally. Simpson and Dickey (1981) demonstrated that proper parameterization of downward irradiance is crucial to accurate prediction of upper ocean thermal structure. Following Martin (1985) and Simpson and Dickey (1981), the current study has adopted an innovative technique of parameterization for the absorption of downward irradiance by specifying what portion of the total irradiance is allowed to be absorbed in the top layer and what portion is allowed to penetrate through the water column. Spatially-variable extinction coefficients, developed by HydroQual (1995), have been used to account for the spatially-variable optical characteristics of Massachusetts Bay.

As part of an earlier water quality analysis, HydroQual and Normandeau (1995) estimated spatially varying extinction coefficients for Massachusetts and Cape Cod Bays. The extinction coefficients were based on light transmissivity data collected as part of the Harbor and Outfall Monitoring Program. An analysis of the light transmissivity data found that higher light extinction coefficients were found closer to shore, in shallower waters, probably the result of greater sediment resuspension and algal growth. Using these data, a curve was fitted to the light extinction coefficient as a function of water column depth. The shortwave radiation penetrating the water column is then controlled via the Equation 2-7.

$$I(z) = I_0 e^{-k_c z} \quad 2-7$$

where I_0 is the surface insolation, k_c is the extinction coefficient, z is the depth and $I(z)$ is the insolation at depth z .

In the version of the heat flux model used for this analysis, the absorbance of shortwave radiation can be specified in two ways. The modeler can use either of the two methods separately or a combination of the two methods. In the first method, the modeler can specify the fraction of the total shortwave radiation, that reaches the water surface, that will be absorbed by the surface layer of the model. Within the framework of Signell's model, this is the method that was applied with a fraction of 1.0 assigned to the surface layer. The heat would then be distributed to other layers via flow and dispersion. In the second method, shortwave radiation is absorbed based on a spatially variable extinction coefficient.

It was anticipated that a combination of these two methods would be used in this calibration effort. However, the use of extinction coefficients alone produced good results as will be shown by comparisons of the model results to vertical temperature data. Therefore, while Signell used a fraction of 1.0 to assign all the shortwave radiation to be absorbed in the surface layer, a fraction of 0.0 was used in this application

of the model. This does not mean that no shortwave radiation was absorbed in the surface layer in this application of the model. Rather, the fraction absorbed in the first layer was controlled by Equation 2-7, and was dependent on the spatially varying extinction coefficient. The remaining portion of the shortwave radiation was then absorbed by lower layers in the model.

The heat flux model requires information concerning precipitation, evaporation, air temperature, relative humidity, atmospheric pressure, shortwave radiation (insolation), wind speed and direction, and a light extinction coefficient. Due to the lack of evaporation data, precipitation and evaporation were assumed to offset one another and were set to zero in the model inputs. Wind speed and direction, air temperature, and barometric pressure were retrieved from the Boston Buoy. Relative humidity data were obtained from Logan Airport, and insolation data were obtained from the Woods Hole Oceanographic Institution. During periods where data were missing from the Boston Buoy, Logan Airport data were used in their place. The model input was specified at three-hour increments. The input is shown in Figure 2-2. The meteorological forcings to the model were spatially constant over the model domain. Due to the spatially varying extinction coefficients and spatially varying sea surface temperature calculated by the model, the heat flux varies over the model domain.

2.7 FRESHWATER INPUT

Freshwater was introduced directly into the model at grid cell locations representing the mouths of the Merrimack, Charles, Neponset and Mystic rivers, as well as at the existing effluent discharges at Nut and Deer Islands, and the South Essex Sewerage District outfall in Salem Sound. Flows for the Merrimack and Charles rivers were obtained from the US Geological Survey. Flows for the Neponset and Mystic rivers were inferred by multiplying the daily flows from the Charles River by 0.431 and 0.195 respectively, factors determined from the ratio of the annual average flows. This method was used previously by Signell et al.(1996). Flows for Nut and Deer Island were obtained from MWRA and the annual average South Essex plant flow was taken from Menzie-Cura (1991). Figures 2-3 and 2-4 present the input flows. The Merrimack River is by far the largest source of freshwater in the model domain. High flows are observed in the spring as well as in June/July 1998 and September 1999. The other rivers have similar seasonal patterns as the Merrimack River.

The Nut Island discharge was diverted to Deer Island in July 1998 and this change was reflected in the model inputs. An additional constant discharge of $1.0 \text{ m}^3/\text{s}$ (Menzie-Cura, 1991) was included to represent the flow at the South Essex treatment plant. This discharge was not included in previous model calibrations. The South Essex treatment plant flow was added to improve the flushing of nutrients discharged at this location in the water quality model.

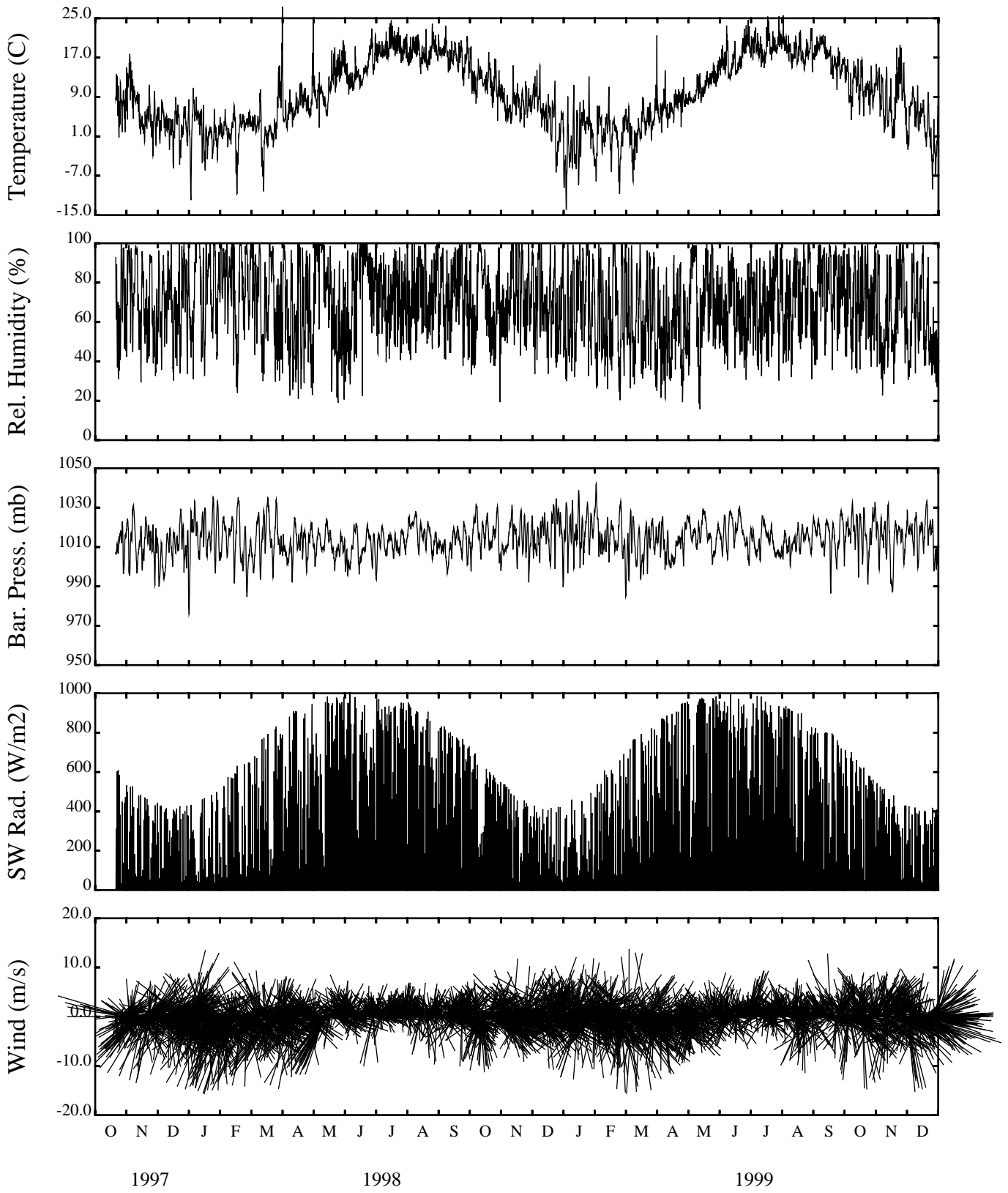


Figure 2-2. Meteorological Forcings

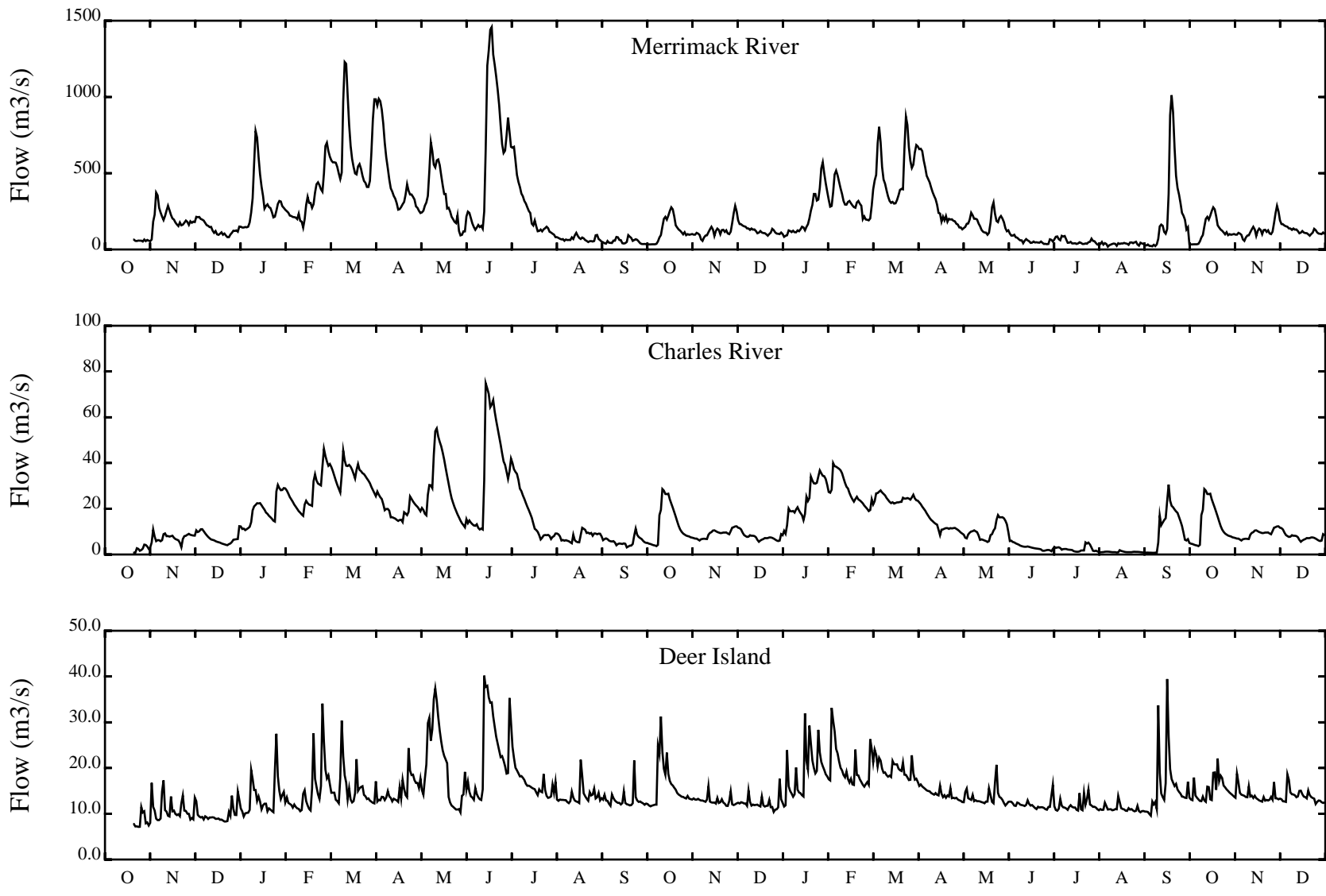


Figure 2-3. Freshwater Input

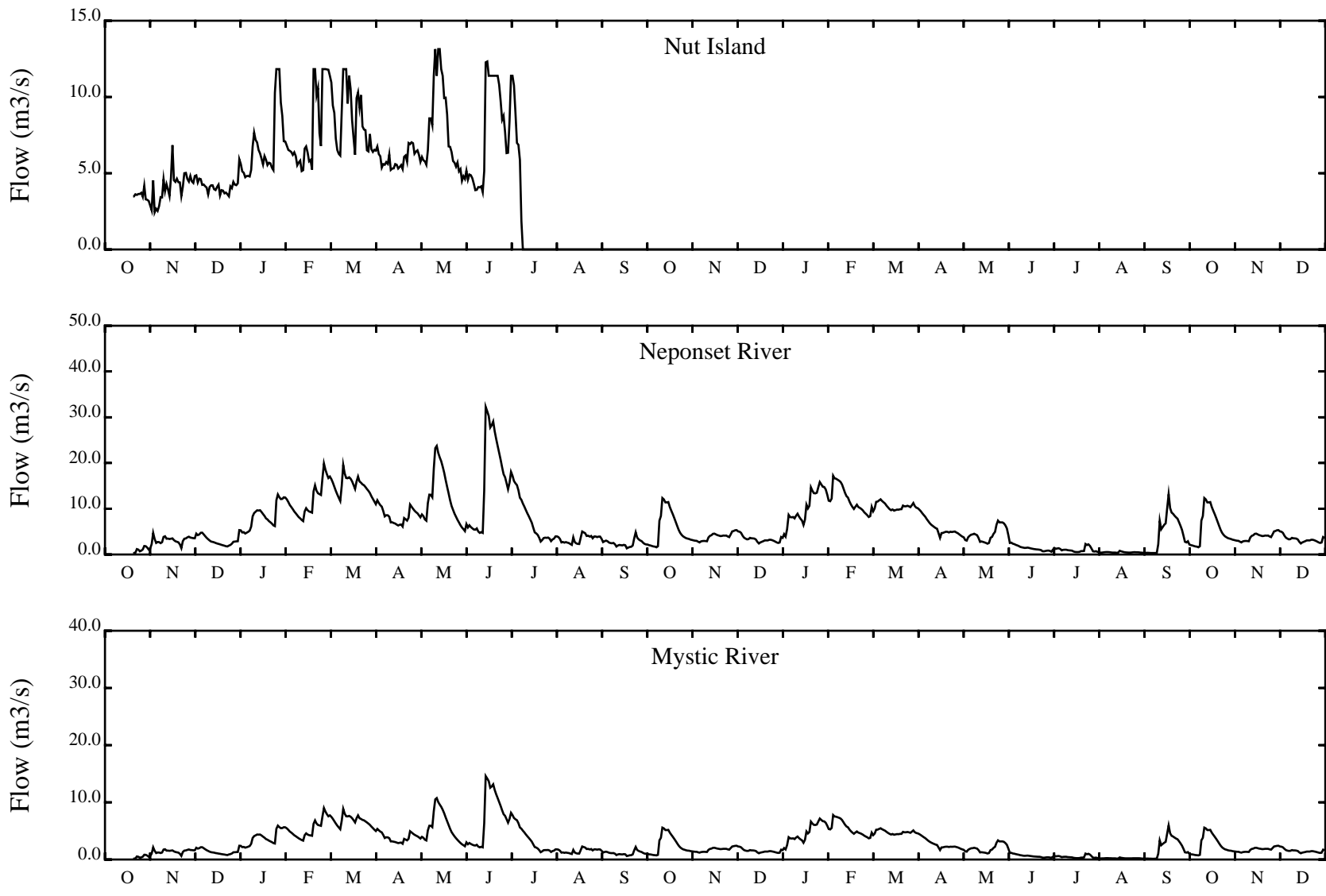


Figure 2-4. Freshwater Input - continued

2.8 OPEN BOUNDARY CONDITIONS

Open boundary conditions are required for elevation, temperature and salinity. Because the elevation field at each time step is solved for using a fully implicit scheme, the boundary condition must be specified as part of the matrix solution for the elevation field. In addition, the matrix solver used in the ECOMsi code requires the matrix to be symmetric and positive definite, which puts further constraints on the type of boundary condition imposed. The partially clamped boundary condition of Blumberg and Kantha (1985) can be shown to satisfy these constraints, and is expressed as:

$$\frac{\partial \eta}{\partial t} + \sqrt{gD} \frac{\partial \eta}{\partial x} = \frac{\eta - \eta_{\text{data}}}{T_{\text{lag}}} \quad 2-8$$

where η_{data} is specified from data, and T_{lag} is the relaxation time. If T_{lag} is very large a pure radiation boundary condition is approached, and if T_{lag} is very small a purely clamped (specified) condition is approached. In the Massachusetts Bay model, the northern and offshore boundary elevations are clamped while the southern boundary (perpendicular to the offshore boundary) radiated gravity waves. The values used for elevation along the northern and offshore boundaries were a combination of M_2 , N_2 and S_2 tidal elevations derived from the tidal model of Lynch and Naimie (1993) and low frequency fluctuations were developed by the method described below. The M_2 tidal elevations obtained from Lynch were used to synthesize S_2 and N_2 constituents by scaling the M_2 amplitudes by the observed S_2/M_2 and N_2/M_2 ratios at the Boston Buoy and shifting the S_2 and N_2 phases by the amount observed at the Boston Buoy. Low frequency fluctuations in elevation were obtained from a density driven flow analysis using assigned temperature and salinity boundary conditions based on a geostrophic balance. A flow normal to the boundary was specified at the 50 m depth. A reference flow was specified to diminish offshore from 10 cm/s at the coast to 5 cm/s at 50 km offshore to 0 cm/s 100 km offshore. The justification for this parameterization is that it gives about the right flow along the 50-100 m isobath, as determined by Vermersch, et al. (1979) and year-round USGS data collected on Stellwagen Bank.

Temperature and salinity are also specified along the open boundaries. If the flow is directed out of the domain, the interior values are simply advected out of the domain. When outflow turns to inflow, the water property values slowly move toward specified values over a defined relaxation time to avoid artificial fronts from developing. In the Massachusetts Bay model, the relaxation time was specified to vary linearly from 3 days at the most northern boundary cell to 30 days at the southern boundary cell.

The majority of the data used to develop boundary conditions were obtained from the National Marine Fisheries Service database for Massachusetts Bay and the Gulf of Maine. These data were supplemented with data from the MWRA Harbor and Outfall Monitoring Program (HOM3) and the AFMIS/LOOPS/AOSN collaborative effort in Massachusetts Bay conducted in August-October 1998. The

latter data are found on the Harvard University web site. Figure 2-5 presents an example of the spatial and temporal distribution of the available temperature and salinity data. The figure displays the period from January 1998 to April 1998. Also included on the figure is the model grid, and a square 10x10 km grid to aid in determining the location of stations on the map. Figures showing data availability for the remaining months of the calibration period can be found in Appendix A. The stations represented by circles are actual data stations, those represented by triangles (for example in October 1998 at the northern boundary) are fabricated data stations. Results of the interpolation are presented in Appendix B. These figures present the temperature and salinity boundary conditions. Boundary condition time one is October 20, 1997, time two is November 1, 1997. Each time after time two is a period of thirty days later. The three panels would more properly represent the boundary if placed end to end with each number representing a segment at a particular standard level. The vertical line in the bottom panel indicates where the model boundary changes from the north-south direction to the east-west direction.

The temperature and salinity values assigned to the boundary were developed by interpolating the available temperature and salinity data over space and time using the OAX (version 5) software package, which was developed at the Bedford Institute of Oceanography. OAX uses optimal linear interpolation (objective analysis) to estimate data values at grid points (eg., the open boundary) based on data at a finite number of nearest neighbors. Documentation for the OAX system can be found on-line at http://dformr.mar.dfo-mpo.gc.ca/science/ocean/coastal_hydrodynamics/oax.html. Output from OAX was generated every 30 days beginning November 1, 1997. If required, OAX can provide output on a more or less frequent basis. Table 2-1 presents the perceived availability of the temperature and salinity data. The results of the OAX interpolation were further smoothed by MATLAB using a weighted average. Results of the temperature and salinity interpolation provided a density field which was used to determine the low frequency changes in the model boundary elevation as described earlier.

In a previous study, Signell et al. (1996) used the Gulf of Maine Model (GOMM) to specify elevation, temperature and salinity boundary conditions for the period of October 1989 to December 1992. Difficulties using the GOMM for the period of 1993-1994 caused Signell to abandon the GOMM approach in favor of the approach used in this modeling study. As preparation began for the 1998-99 modeling study, the OAX interpolation method for specifying boundary conditions was attempted first due to the speed and simplicity of the method. After the first calibration model run was completed and produced favorable results, it was determined that enough data were available to provide boundary conditions, and that the OAX interpolation method would be adopted for this modeling study in lieu of the GOMM.

During model calibration it was determined that the model results could be improved by modifying the boundary conditions. Modification of the boundary could be implemented in several ways. One method is to change how often results are to be generated by OAX interpolation. However, ultimately this procedure

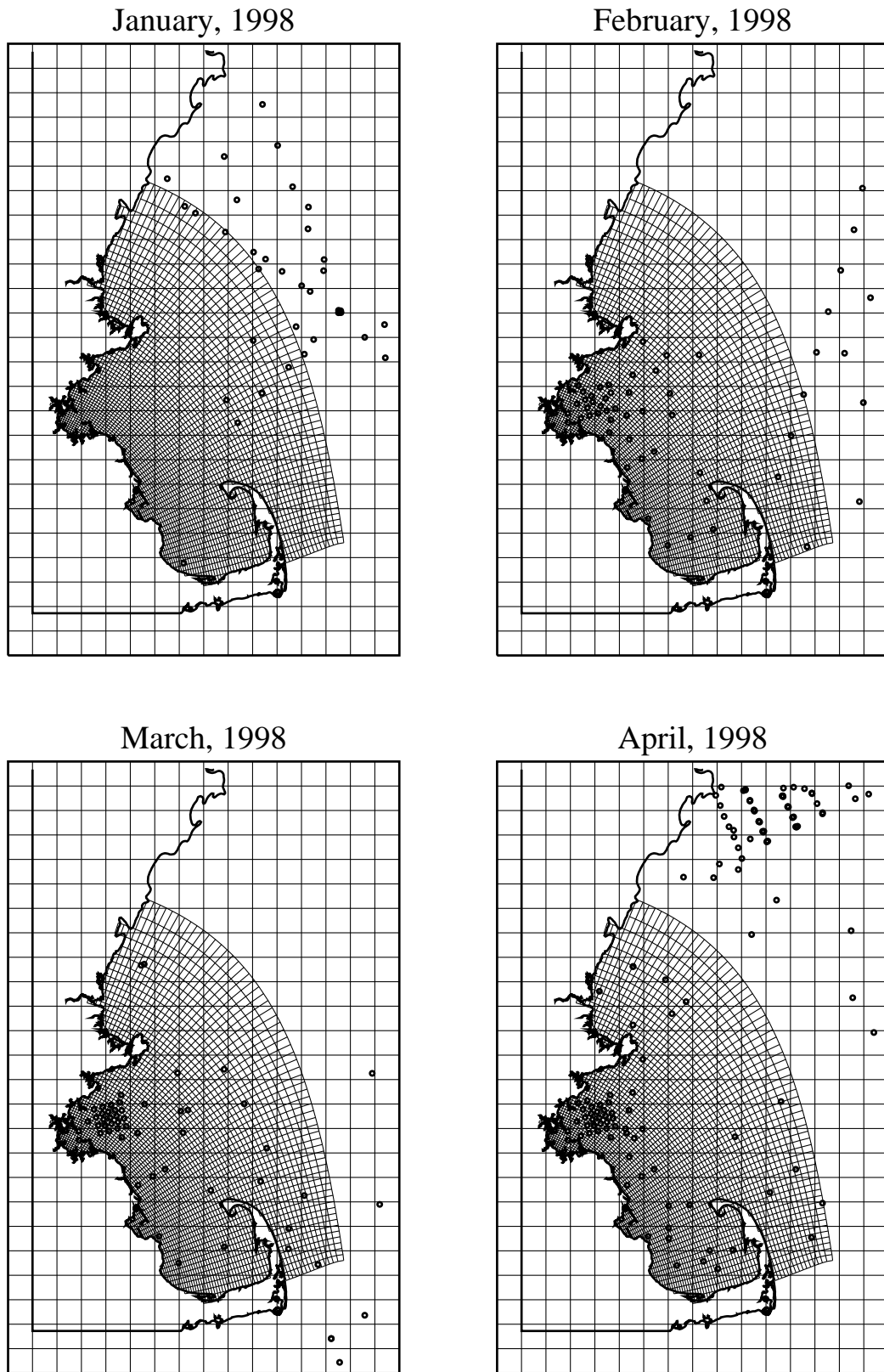


Figure 2-5. Station Locations from which Temperature and Salinity Data were Available to Specify Boundary Conditions from Jan. through April 1998

Table 2-1. Availability of Temperature and Salinity Boundary Condition Data.

<u>Month</u>	<u>Rating</u>
October 1997	+
November	-
December	-
January 1998	+
February	-
March	-
April	+
May	+
June	+
July	+
August	0
September	0
October	0
November	-
December	-
January 1999	-
February	0
March	+
April	+
May	-
June	0
July	-
August	-
September	-
October	-
November	+
December	-

+ = good

0 = fair

- = poor - none

is data-dependent and given the paucity of available data, a period of thirty day output was selected. A second procedure is to change the data sets that OAX uses for interpolation. This recognizes the inherent limitations of spatial and temporal interpolation of salinity and temperature data. For example, it was noted that some unusually high surface temperature data in Cape Cod Bay were influencing the estimation of the boundary data during a data poor period. It is more likely that the Cape Cod Bay temperatures were a product of local climate and physical affects and should not be used to determine boundary temperature in the Gulf of Maine. Therefore, they were deleted from the OAX data interpolation data set for that period. In two instances, data were fabricated during periods when data were sparse. These periods were October-December 1998, and June-July 1999. Although setting boundary conditions using only “real” data would have been preferred, the fabrication of data seemed justified based on the paucity of available data during certain times within the calibration period. If the GOMM were to have been used in lieu of the interpolation method, a similar degree of uncertainty would have existed during these periods due to the lack of observed data with which to compare the GOMM model results. A third method for modifying the boundary conditions depends on setting the reference flow used to determine the geostrophic balance. The 10 cm/s velocity at the 50 m isobath is based on a year-round average of the velocities. Based on Signell (personal communication) this velocity could be as high as 15 cm/s. As is discussed below to improve the calibration during the period of May through July 1998 this reference velocity was increased to 15 cm/s.

Figure 2-6 presents the boundary conditions for temperature and salinity at two boundary grid cells for the period of October 1997 to December 1999. The top two panels present temperature and salinity boundary conditions at depths of 1 and 20 meters at a point 10 km off of the New Hampshire coast. The boundary conditions are well mixed from October 1997 through February 1998. During March, stratification develops and there are two periods, April and June, when fresher water enters through the boundary. The greatest degree of temperature stratification in 1998 occurs during the summer. Water column overturn occurs in November, with the 20 m depth reaching its highest temperature at this point. The water column is fairly well mixed with respect to temperature from November to March, however, the salinity boundary condition is not completely mixed. In the spring and summer of 1999, there is not as much salinity stratification as estimated for 1998. The surface water at the boundary is warmer in 1999 than in 1998.

The bottom two panels of Figure 2-6 present the temperature and salinity boundary conditions at the 1 m, 20 m and 140 m depths at a point 50 km east of Cape Ann. The boundary conditions here follow a similar seasonal pattern as were estimated for the northern boundary segment with some notable differences. The influence of the Maine rivers, located outside the model domain, are not as evident this far offshore. The surface salinity does not decline as much nor does it change as rapidly. The dip in the surface temperature that is observed in August 1998 at the more northerly segment is not apparent here. Also, the 20 m temperature boundary conditions reach their peak earlier, in September, and reach a higher temperature.

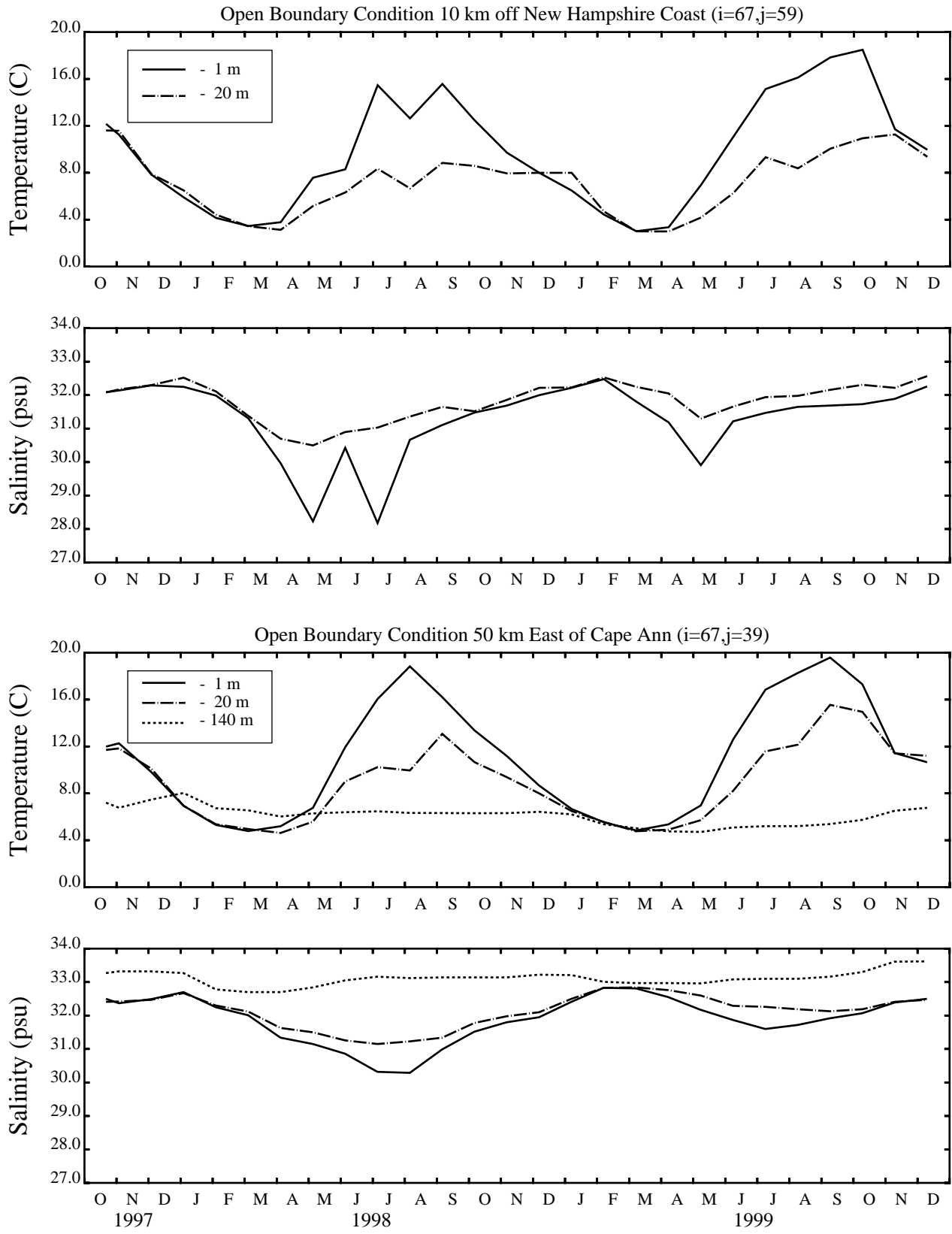


Figure 2-6. Open Boundary Conditions Off the New Hampshire Coast and East of Cape Ann

The boundary conditions at the 140 m depth do not vary much during the calibration with temperatures ranging between 4-8 °C and the salinity hovering around 33 psu.

2.9 TIME STEP

A time step of 207 seconds was chosen for the 1998-1999 period. This time step was chosen based on previous usage of the model, where time steps ranged from 103.5 seconds to 414 seconds. While a larger time step could be used for portions of the year, this would have to have been determined through trial and error and it was determined not to be worth the effort. Although ECOM-si is not restricted by the gravity wave CFL condition, it is limited by the advective CFL condition.

2.10 SIGMA-COORDINATE CORRECTION

In regions of steep topography, sigma-coordinate models are prone to errors in the calculation of pressure gradient and horizontal diffusion terms (Beckman and Haidvogel, 1993). Based on previous modeling this error was reduced in Massachusetts Bay by removing the domain-averaged vertical salinity, temperature and density profiles, via subtraction, before calculating horizontal differences. In essence, if you consider density (for example) at a location to be composed of the mean density plus the deviation from the mean density, removing the mean allows the derivation to be solved for only the deviation from the mean. This technique preserves the relative differences within the domain and allows the numerical solution to be calculated with greater accuracy. The effectiveness of this technique depends on the degree to which the vertical structure varies over the domain. In domains such as Massachusetts Bay, in which the stratification is nearly uniform over the region, this technique greatly improves the model comparison to observed data.

SECTION 3

CALIBRATION

3.1 SALINITY AND TEMPERATURE

3.1.1 Temporal Comparisons

Model inputs were developed for the period of October 20, 1997 to December 31, 1999. The approximate 10 week period, representing the end of 1997 was included to permit model spin-up, i.e., to allow the model to reach dynamic equilibrium from its initial resting state. The figures included in this section present surface and bottom comparisons of model computations versus observed temperature and salinity data for the calibration period. The surface model computation represents the third vertical layer of the 12 layer model. This third sigma-layer corresponds to the top 4-10% of the water column and corresponds best to the depth at which the salinity and temperature were recorded. Figures of sigma-t or density are also included to indicate how well the model reproduces the density differences throughout the water column. Figure 3-1 presents the MWRA station locations for reference to the calibration figures that follow.

The first series of four figures presents the temperature and salinity calibration for the period of October 1997 through December 1998. Figure 3-2 presents three stations close to the boundary of the water quality model. At station F26, the northernmost station, the model tracks the bottom salinity fairly well including the marked decrease in salinity that occurs in late February 1998. At the surface, the model is approximately 1 ppt too high in early February, and again too high in October 1998. However, the model matches the remaining data points fairly well and reproduces the freshening event observed in June. Further south at station F27, the model again matches the bottom water salinity fairly well. Surface layer computations appear too saline in January and February, but match the remaining data quite well. Note, the surface water was not as fresh in June as was observed at station F26, and the model reproduces this feature well. Near Race Point (F29), the model does a good job reproducing the temporal trends observed in the data, but appears to be too fresh in the latter part of the year.

The model reproduces the surface temperature at these three stations fairly well. At F26, the model does not reproduce the high bottom temperature observed in October, but matches the remaining data points very well. From the data there appears to be a large gradient between F26 and F27 bottom waters in October. The model is in fair agreement with the data at F27 with temperatures slightly lower than the data in June, August and October. At F29, the model matches the surface temperature data quite well, but underestimates the bottom temperature in June and September. However, the model generally reproduces the observed seasonal trends in vertical stratification of temperature.

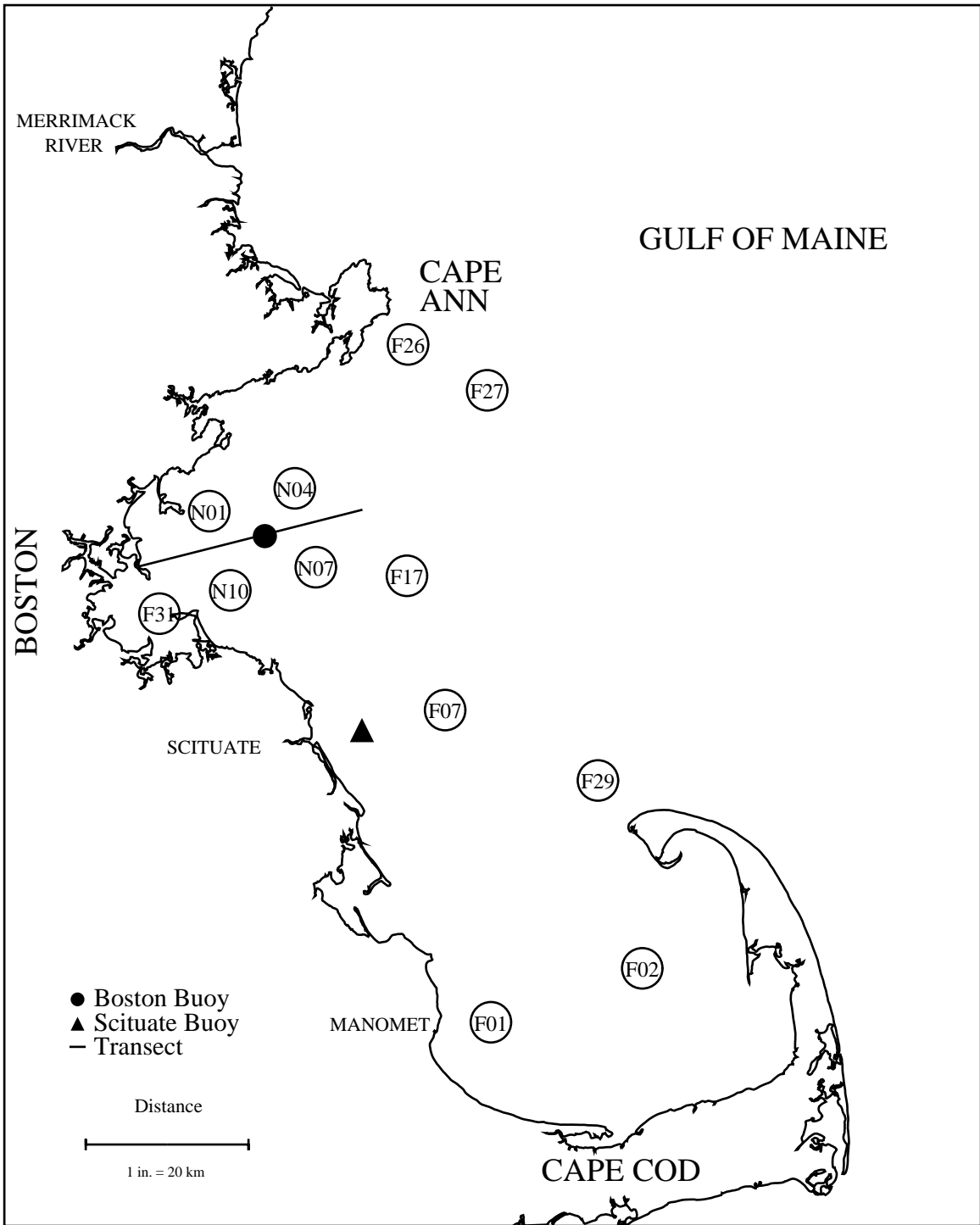


Figure 3-1. Study Area

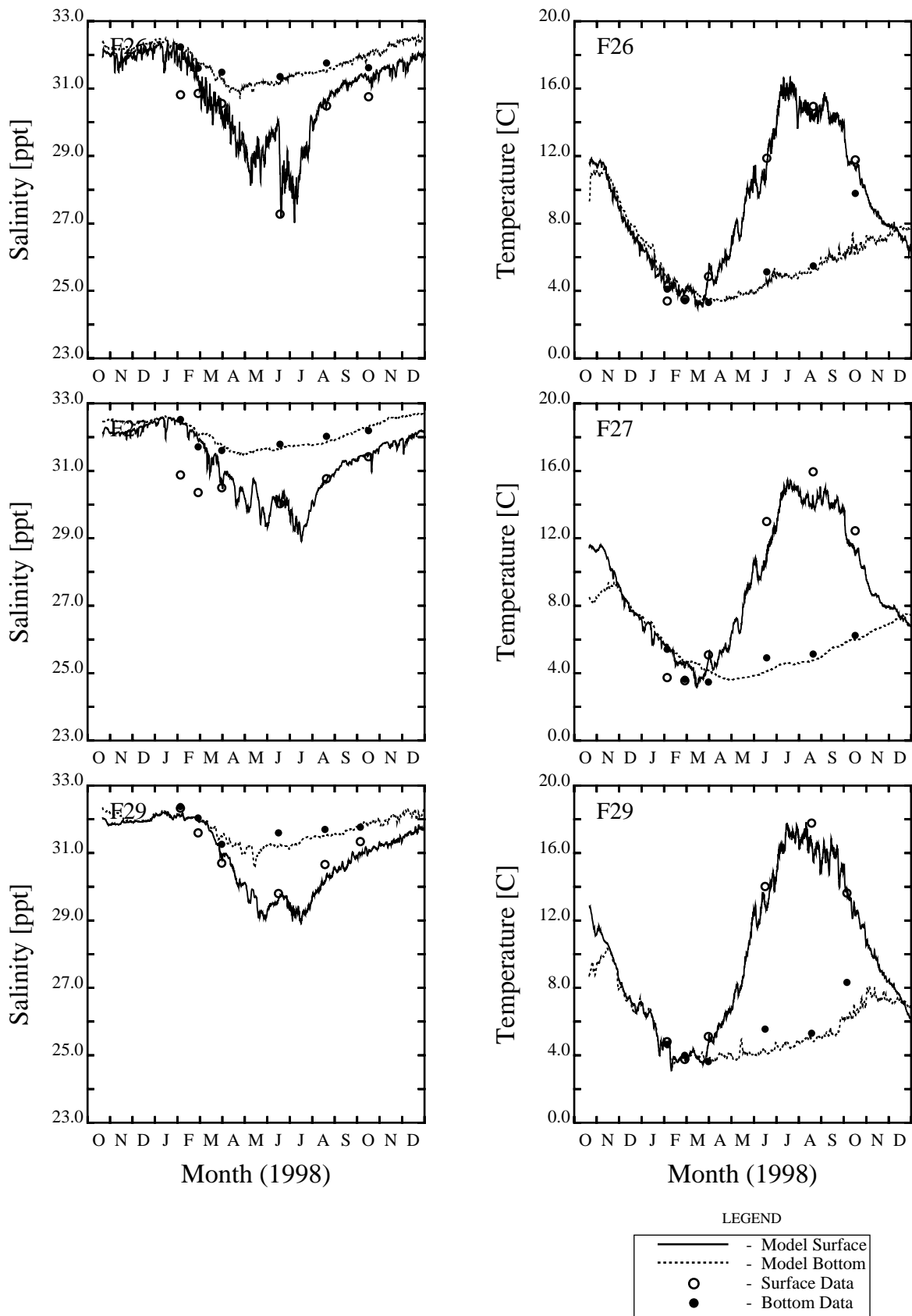


Figure 3-2. 1998 Salinity and Temperature Calibration at MWRA Stations F26, F27 and F29

Figure 3-3 presents model versus data comparisons for three stations located in Boston Harbor and in the northwestern portion of Massachusetts Bay. At station F31, in Boston Harbor, the observed salinity data were not strongly stratified except during June. The model reproduces most of the observed data fairly well, but model computations appear to be too fresh during June, especially in the bottom water. At station N01, in the nearfield area, the model does not reproduce the extreme low surface salinity observed in June although it does compute a 3 ppt decrease in salinity. The model also appears to take longer to recover from the freshwater event than do the observed data. During the remaining portions of the year the model does quite well reproducing both the surface and bottom salinities. The same generalities, with respect to the status of the calibration can be stated for station N10. The model reproduces most of the salinity data fairly well slightly under predicting the data, but misses the extreme low salinity event observed in June. It is interesting to note that the average surface salinities of approximately 25 - 25.5 ppt are lower than observed for the boundary stations, F26 and F27, and are lower than observed in Boston Harbor for the same time period. This may suggest a large unaccounted for source of freshwater or questionable data.

The calibration to temperature comparison at these three stations is encouraging. The model does exceedingly well reproducing the markedly different bottom temperatures at all three locations. The model reproduces the general temporal trends in the surface temperatures but appears to slightly lag in warming during the spring. The model reproduces most of the Boston Harbor data, but appears to miss a mixing event that occurred in August.

Figure 3-4 presents model versus data calibration results at three stations, two located more central to northern Massachusetts Bay and one located towards the middle of Massachusetts Bay. Results for stations N04 and N07 are similar to stations N01 and N10 in terms of where the model matches the data and where it misses. Overall, in the bottom waters the temperature calibrations are very good, while the bottom salinity calibrations are reasonably good at these stations. At station F17, the model results are in general agreement with the temporal trends observed in bottom salinity data but the model appear too fresh in June and August. At the surface, the model is too saline in January and February and too fresh during the summer months. The temperature results for the surface at F17 are high with respect to the data during February, June and August, but fewer data are available for this station, limiting more complete model versus data comparisons.

Stations found in the southern portion of the model domain are presented in Figure 3-5. The model does a fair job reproducing the data at station F07. The model reproduces most of the salinity data, but appears to be slightly too fresh during the summer months. The temperature data is also fairly well reproduced at station F07. Calibration results are presented for the Cape Cod Bay stations, F01 and F02. In general, the model reproduces the observed salinity reasonably well, save for some questionable data in June for F01 and being too fresh, by approximately 0.25 ppt, during the summer. The model reproduces the bottom

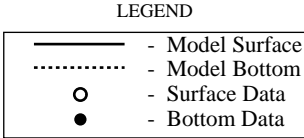
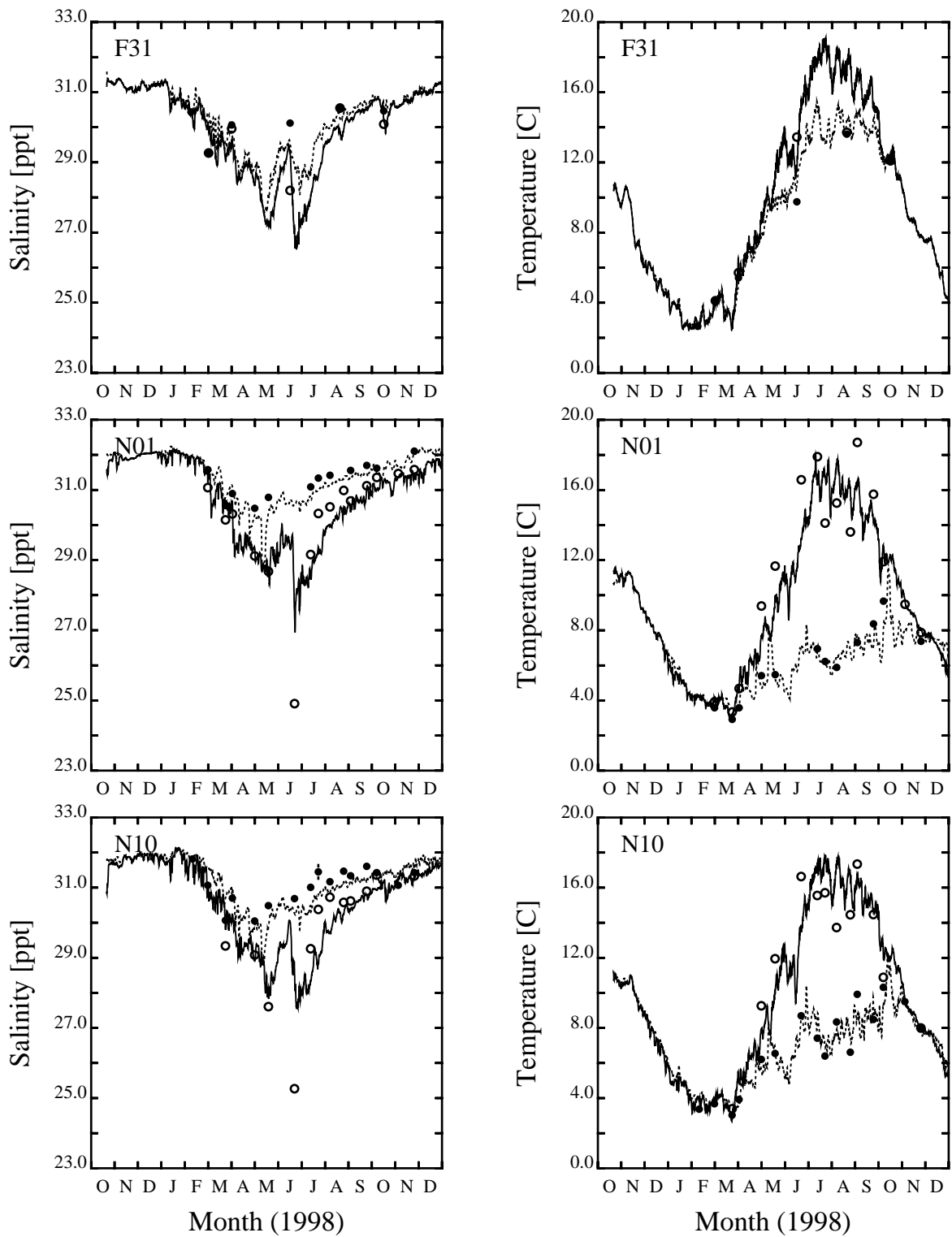


Figure 3-3. 1998 Salinity and Temperature Calibration at MWRA Stations F31, N01 and N10

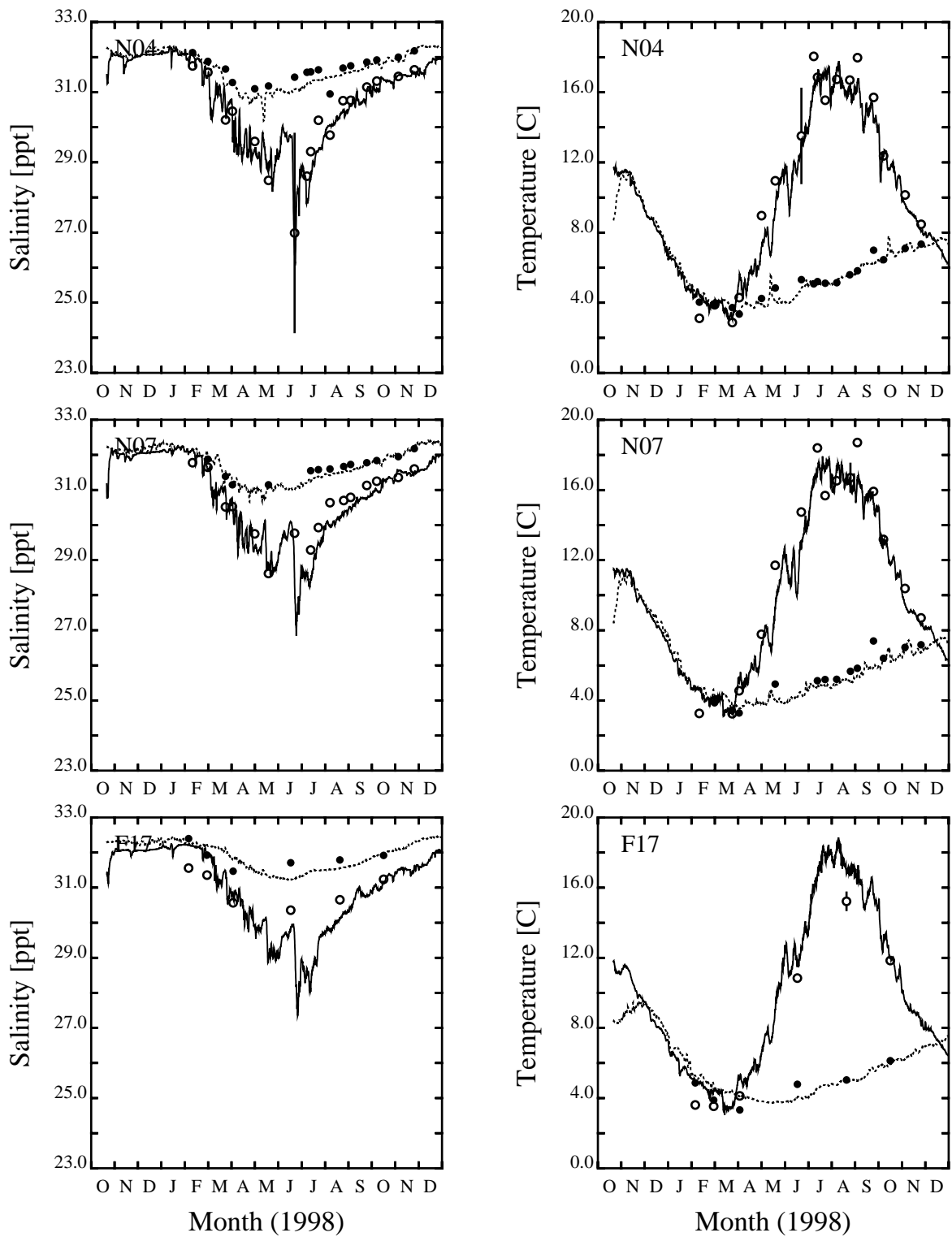


Figure 3-4. 1998 Salinity and Temperature Calibration at MWRA Stations N04, N07 and F17

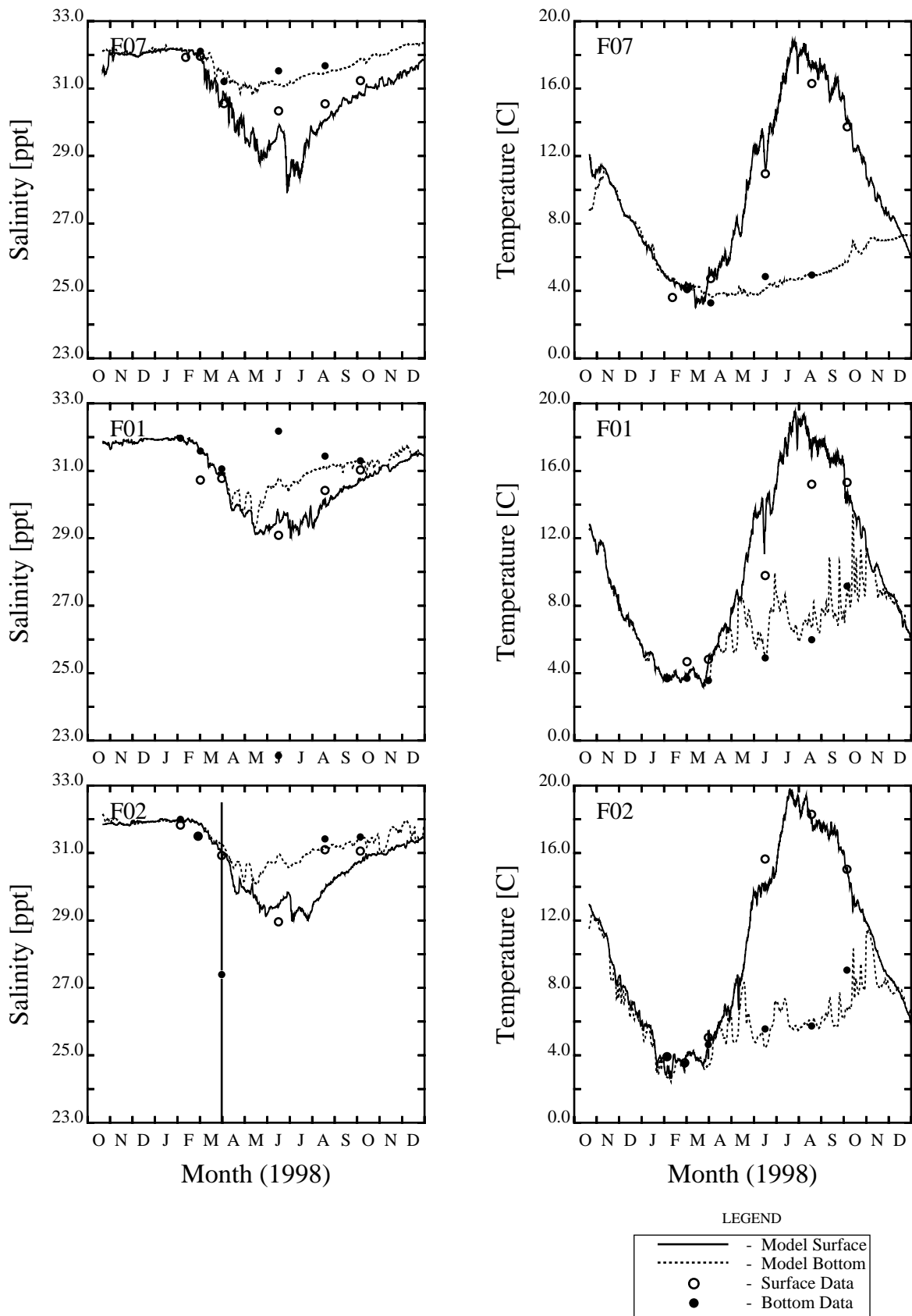


Figure 3-5. 1998 Salinity and Temperature Calibration at MWRA Stations F07, F01 and F02

temperature at the Cape Cod Bay stations. During the summer, the model seems to reproduce the temperatures at station F02 quite well, and partially reproduces a large cooling event observed in June at station F01 (as well as F07). However, the model appears to be about 2°C too warm in August compared to the observed data for F01.

Water density has been calculated from model results and temperature and salinity data. In terms of providing input for the water quality model, it is important that the appropriate degree of water column stratification is computed by the hydrodynamic model. Figure 3-6 presents model versus data comparisons for sigma-t at six far field stations for the period of October 1997 through December 1998. As would be expected, where the model compares favorably with data for salinity and temperature, the model compares favorably with sigma-t. As the overall temporal temperature and salinity calibration is good, the same is true for sigma-t. Except for overestimating the surface density at stations F26, F27 and F29 during the early portion of 1998, the model results compare favorably with the estimated sigma-t at the stations near the Atlantic Ocean boundary of Massachusetts and Cape Cod Bays. At station F07, the model results compare favorably with the available data. In Cape Cod Bay (stations F01 and F02), the model underpredicts the density at the bottom during July and at the surface in August, but matches the remaining data fairly well.

Model versus data comparisons for sigma-t at two additional far field stations and four near field stations are presented in Figure 3-7. Again, where the model results compare favorably with temperature and salinity data, the model results for density compare well with the calculated density data. At station F31, bottom waters were calculated to be too fresh during June. Consequently, the model underestimates the density during this period. The model results match the data fairly well during the remainder of the year. At station F17 the model does a fair job reproducing sigma-t. At stations N01 and N10, the model misses the extreme low densities observed in June, and remains stratified for longer than is observed in the data in July and August. During the remainder of the year the model reproduces the bottom and surface density data quite well. The model matches the density data at stations N04 and N07 very well. Overall the model does a good job at reproducing the temporal variations in density (and differences between surface and bottom) at all stations, as well as the density differences between stations.

Figures 3-8 through 3-11 present model versus data comparisons at the same stations for 1999. In general, the data indicate that 1999 was a warmer and dryer year than 1998. The boundary stations are shown in Figure 3-8. With respect to salinity, the model overestimates salinity in February and April at stations F26 and F27. However, the model generally reproduces the remaining data. The salinity at station F29 is fairly well reproduced except perhaps for the recovery from the spring freshet in the surface layer. For temperature, model computations are slightly cooler (0.1 - 1.0°C) than the observed summer/fall bottom temperatures. For June 1999, there is an interesting spatial pattern observed in the temperature data. Although stations F26 and F27 are reasonably close together there is approximately a two degree Celsius

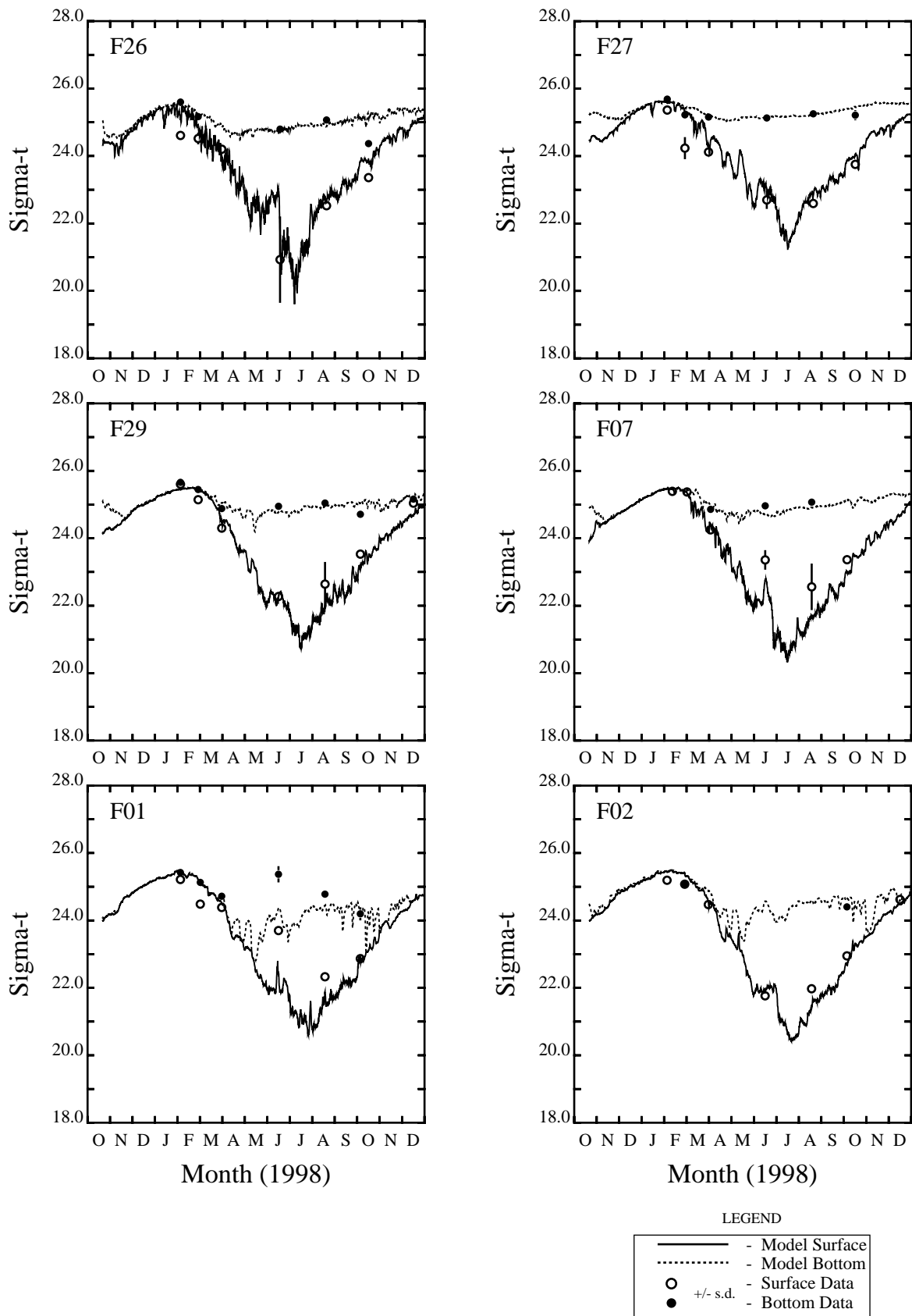


Figure 3-6. 1998 Sigma-t Calibration at MWRA Stations F26, F27, F29, F07, F01 and F02

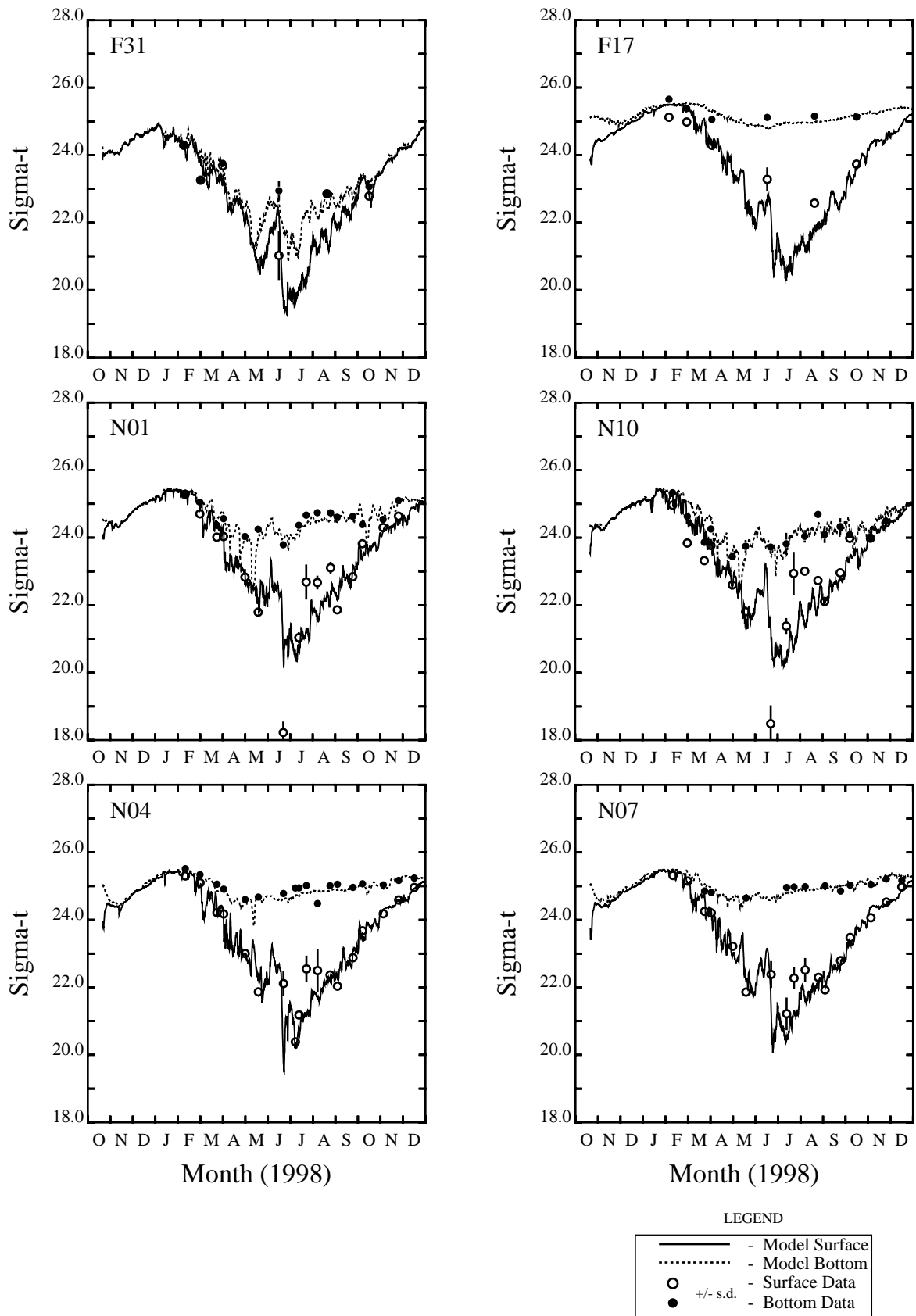


Figure 3-7. 1998 Sigma-t Calibration at MWRA Stations F31, F17, N01, N10, N04 and N07

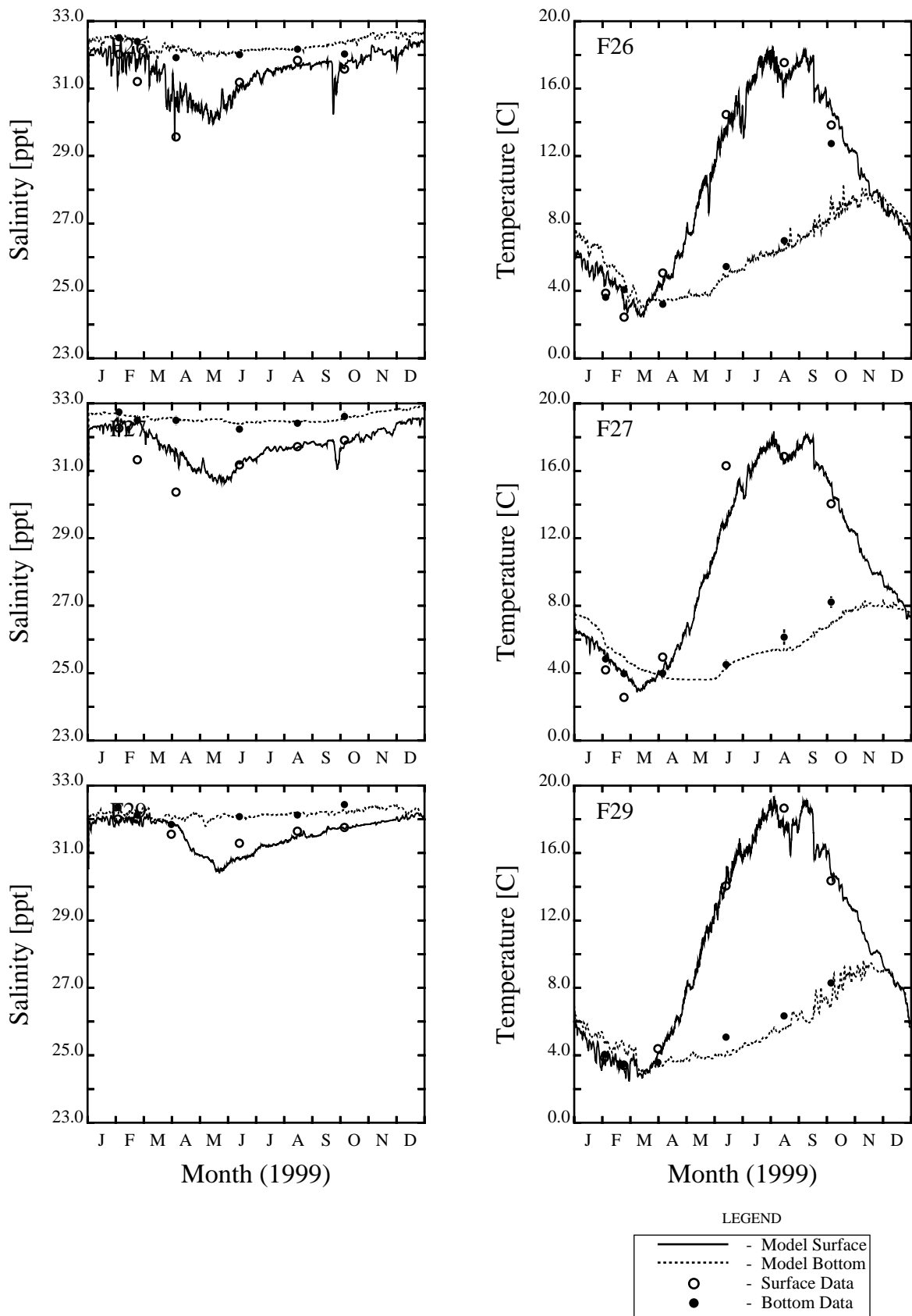


Figure 3-8. 1999 Salinity and Temperature Calibration at MWRA Stations F26, F27 and F29

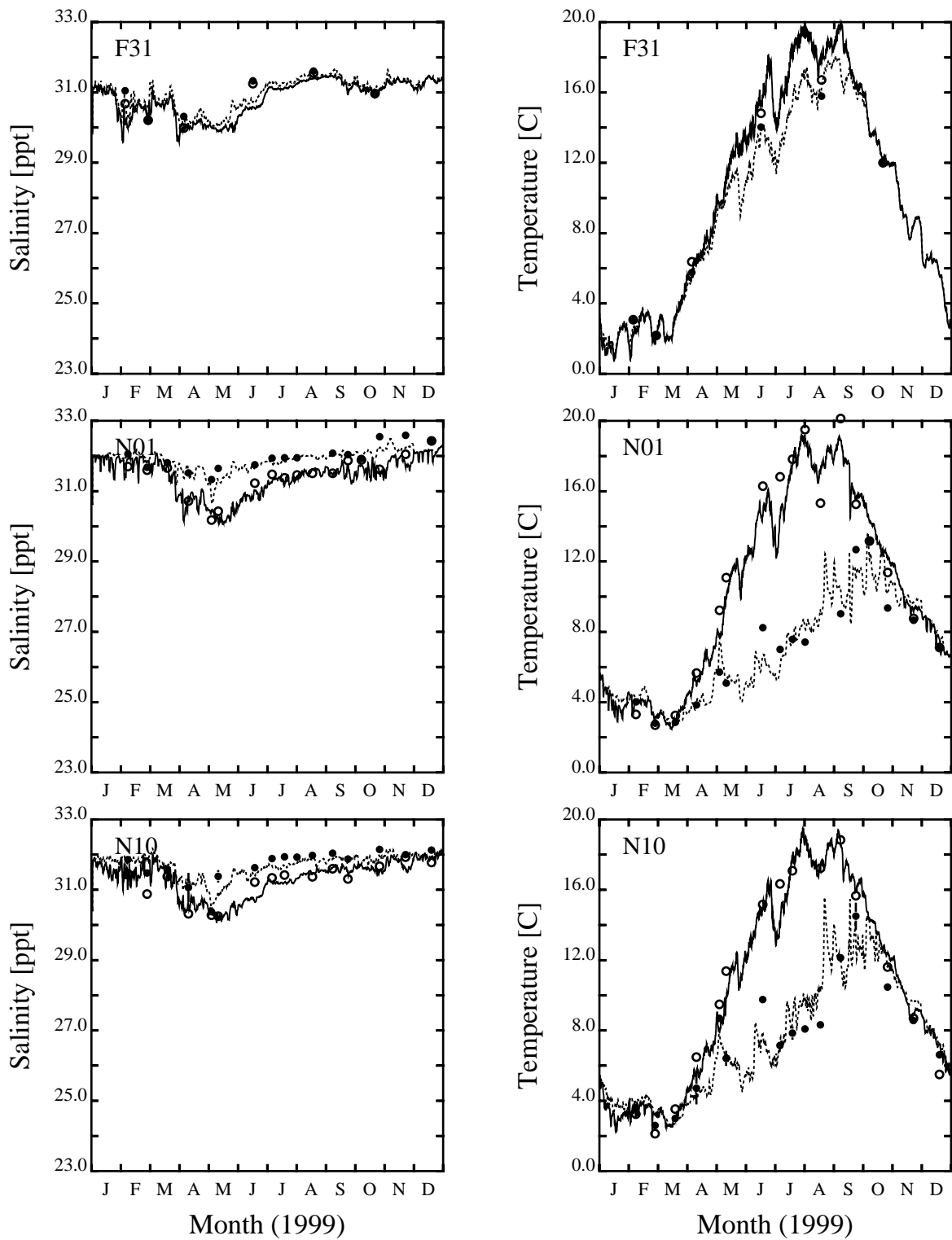


Figure 3-9. 1999 Salinity and Temperature Calibration at MWRA Stations F31, N01 and N10

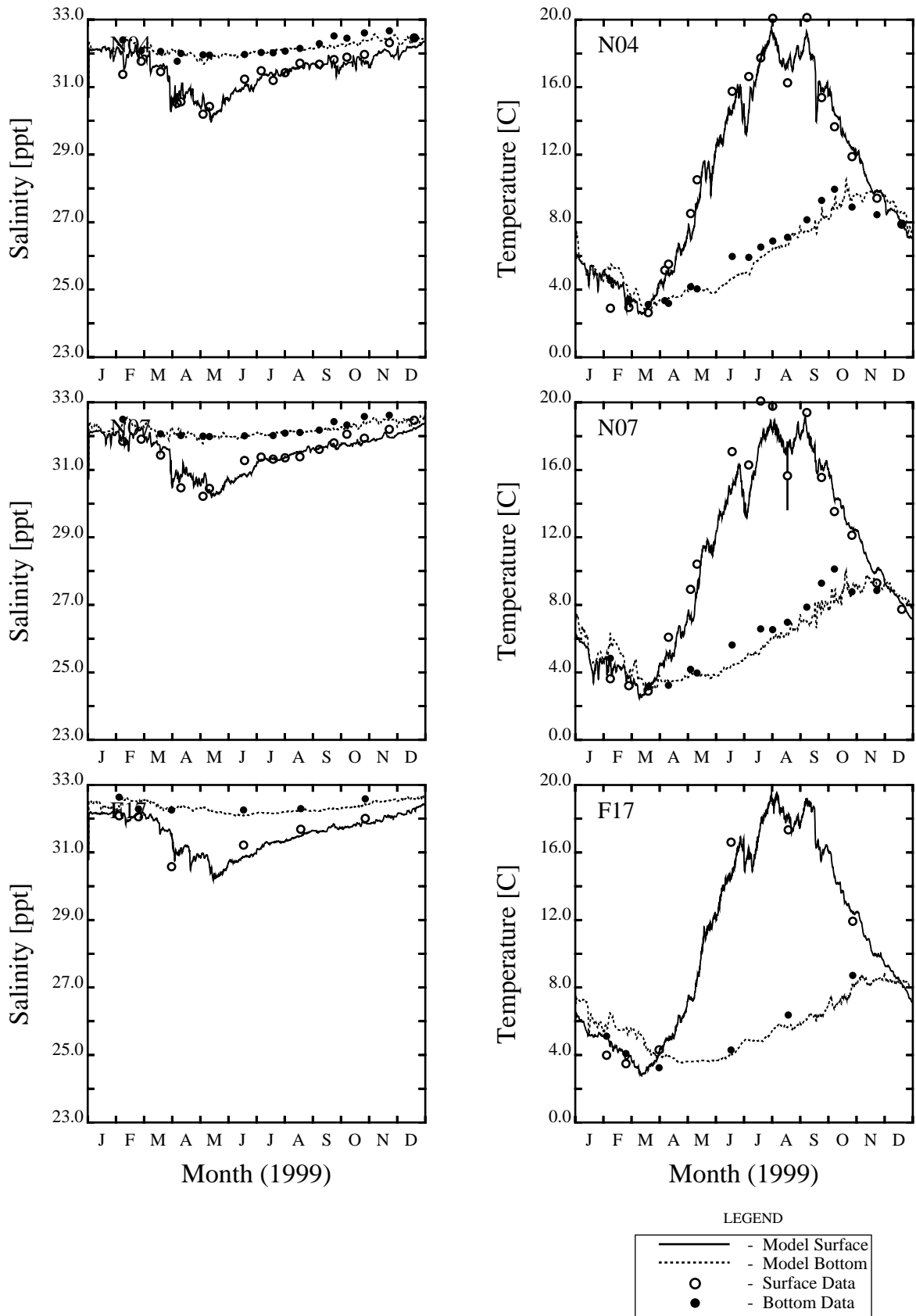


Figure 3-10. 1999 Salinity and Temperature Calibration at MWRA Stations N04, N07 and F17

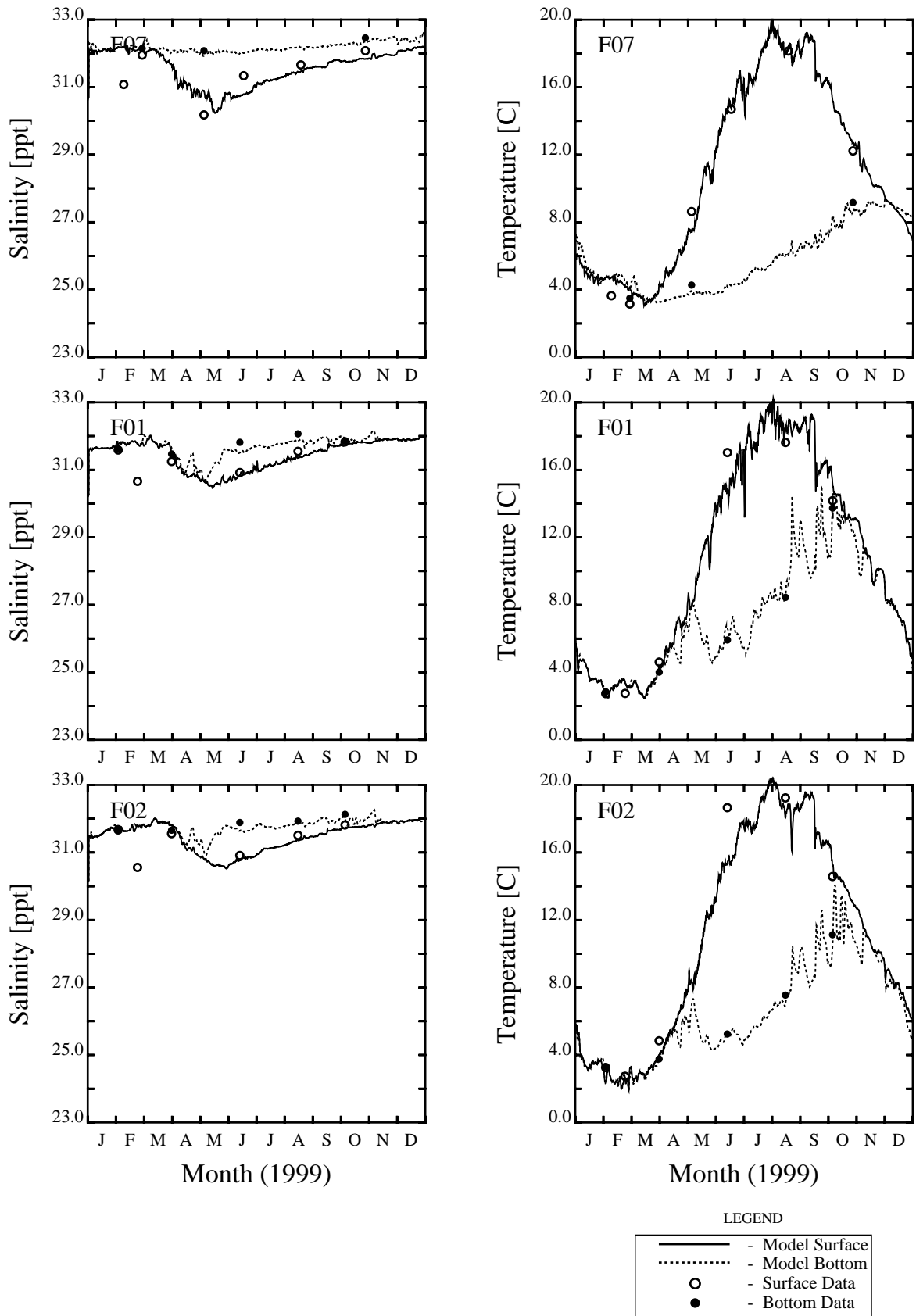


Figure 3-11. 1999 Salinity and Temperature Calibration at MWRA Stations F07, F01 and F02

difference in the surface temperatures. The model, however, computes similar temperatures for these two stations during June, suggesting that the model greatly underpredicts the temperature at F27. In another case, the data indicate that the water column is more vertically mixed during October at station F26. The model does not reproduce this feature. However, at station F27 the data indicate that the water column is stratified with regard to temperature, and the model agrees well with the observed data.

Figure 3-9 presents the 1999 model versus data calibration for temperature and salinity at the northwestern stations (F31, N01, and N10). Less salinity stratification is observed here than was observed in 1998. In general, the model reproduces the salinity data quite well although the model does slightly (~0.1 ppt) underestimate bottom salinity for N10. The model generally reproduces the observed temperature data well including the spatial differences between stations. There is a period in June where the model computes a marked decline in the surface temperature, which is not apparent in the data. This will be discussed further with the analysis of the Boston Buoy data.

The central bay (N04, N07, and F17) stations shown in Figure 3-10 have similar model data comparisons as the previous figure. The salinity data is reproduced quite well at all three stations. The bottom temperature is computed to be approximately 0.5 - 1°C too low beginning in June and continuing into September. Again, the model computes a drop in the surface temperature during June that is not observed in the data.

Figure 3-11 presents the 1999 salinity and temperature calibration for three of the southern MWRA stations. The model reproduces the limited bottom salinity data, slightly underpredicting the June data. The model also calibrates well to the observed temperature data at these stations. The drop in temperature during June that is computed in the northern and central portions of the model domain is not as apparent in Cape Cod Bay.

In 1999, the water column did not experience as great a density stratification as was observed in 1998, as shown in Figures 3-12 and 3-13. The model compares favorably with the density data calculated at the six far field stations presented in Figure 3-12. The model reproduces the timing and magnitude of stratification fairly well overall. In a similar fashion the model reproduces the density and density differences between top and bottom for Boston Harbor, the near-field stations and station F17 (Figure 3-13).

3.1.2 Buoy Data

The Boston Buoy and Scituate Buoy provide data on a more continuous basis than the HOM3 sampling program. Data are collected every 20 minutes at the buoys. Figure 3-14 presents temperature and salinity

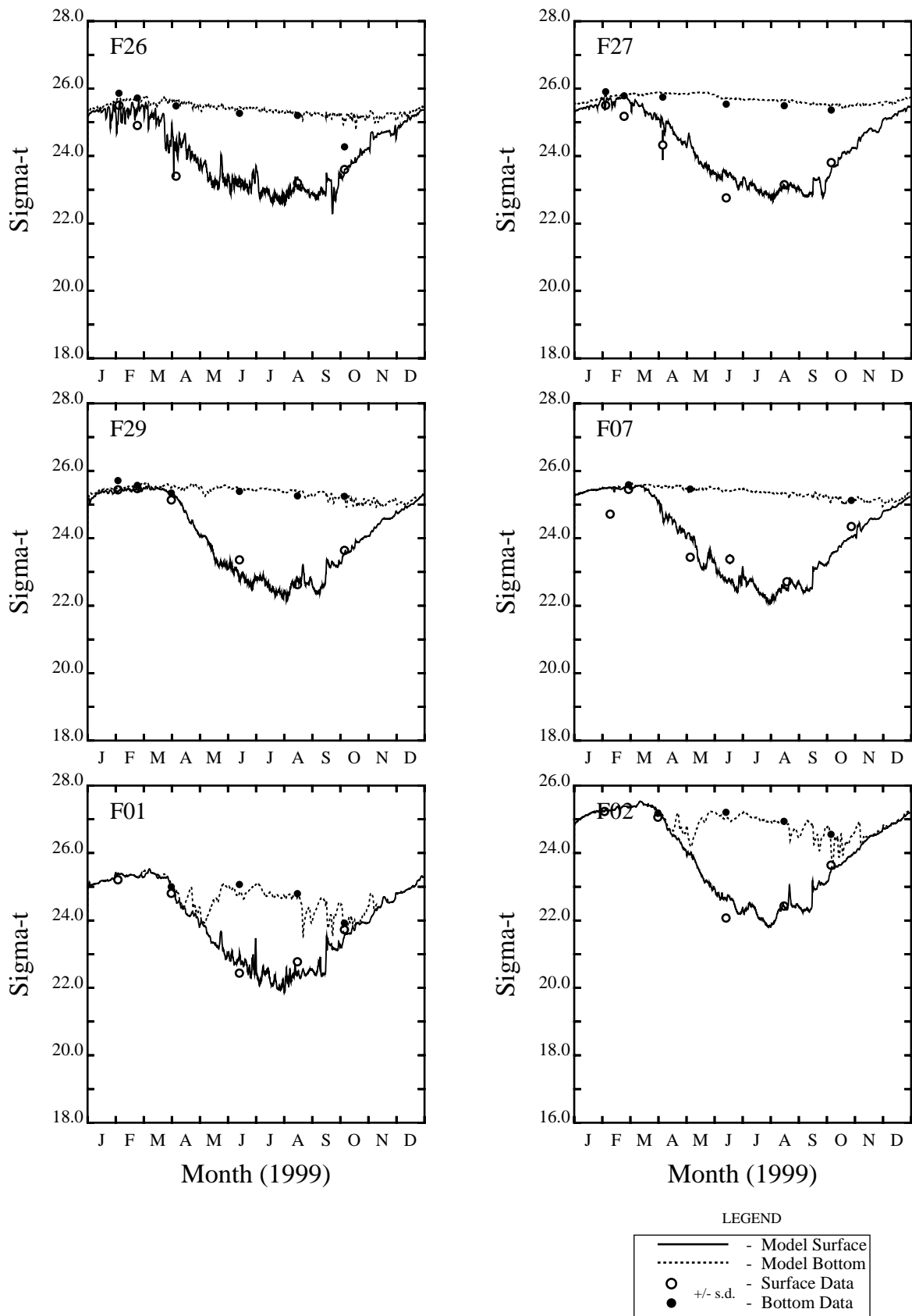


Figure 3-12. 1999 Sigma-t Calibration at MWRA Stations F26, F27, F29, F07, F01 and F02

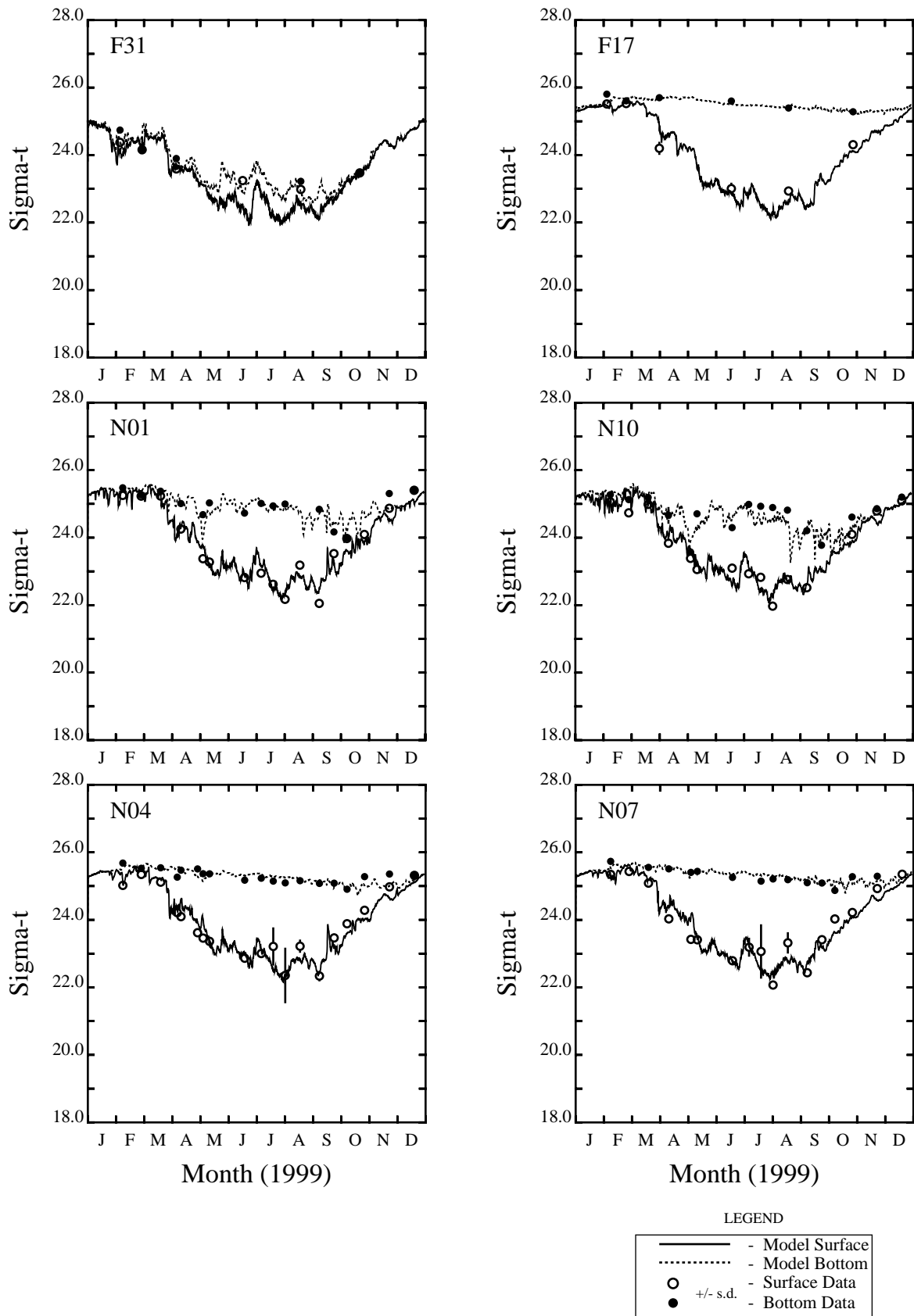


Figure 3-13. 1999 Sigma-t Calibration at MWRA Stations F31, F17, N01, N10, N04 and N07

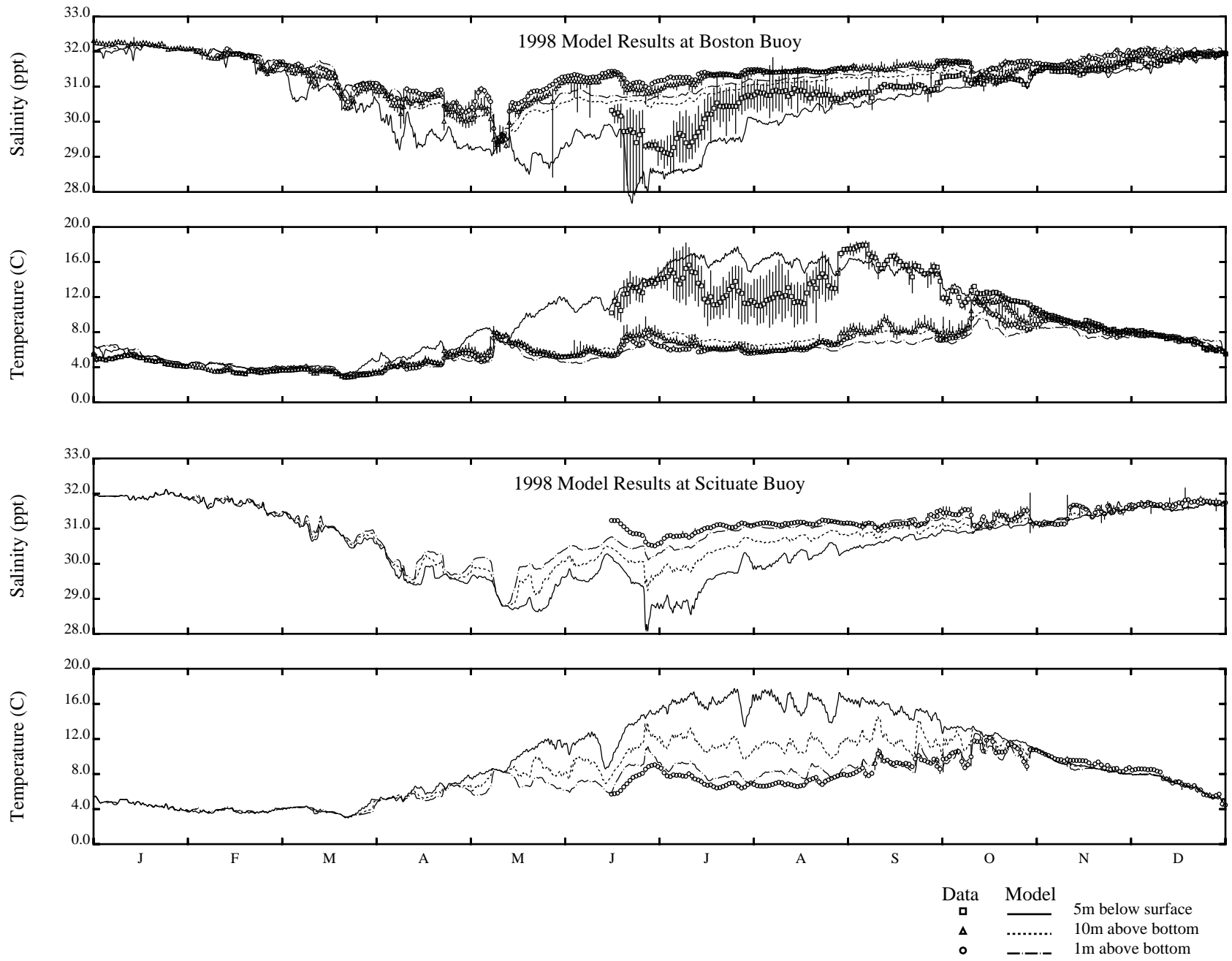


Figure 3-14. 1998 Temperature and Salinity Calibration at the Boston Buoy and Scituate Buoy

data collected at these buoys in 1998 and compares them to model results. Data were collected at three depths at the Boston Buoy, 1.0 meter above the bottom, 10 meters above the bottom and 5 meters below the surface. The water depth at the Boston Buoy is approximately 30 meters. Reliable data at the Scituate Buoy were measured 1.0 meter above the bottom. The depth at the Scituate Buoy is approximately 23 meters.

At the Boston Buoy, the model compares favorably with the bottom salinity data from January through mid-May. Beyond mid-May the model tends to under predict the bottom and mid-depth salinity by several tenths of a ppt. At the 5m depth, the model is on the order of one ppt too fresh during the summer. The bottom and mid-depth model comparison to the data is very favorable throughout the year. The model is able to reproduce some of the small time scale changes in the bottom temperature. The model reproduces the mid-to late-June 5m depth data, but substantially over predicts the temperature during July and August. The model begins to reproduce the appropriate temperature during September.

Measurements at one meter above the bottom were all that were available at the Scituate Buoy. During the summer of 1998, the model under predicts the salinity by up to 0.5 ppt, and over predicts the temperature by 1-2°C. Part of the reason for the inaccuracy of the model may be the depth of the segment that contains the Scituate Buoy. The model segment here is 18.4m deep whereas the buoy itself is located in 23 meters of water.

Figure 3-15 presents the temperature and salinity comparisons for model results versus data at the buoys during 1999. During 1999 more data are available. The water column did not become as stratified with regard to salinity 1999 as compared to 1998 and the model reproduces this feature. The model over predicts the salinity during April and a portion of May at the surface. The model under predicts the surface salinity slightly during June and July. During the remainder of the year the model favorably reproduces the salinity. The model also reproduces the temperature quite well. The mid-depth temperatures are reproduced quite well. Except for a period during July and August where the model over predicts the surface temperature, the model reproduces the surface temperature quite well.

At the Scituate Buoy, the model reproduces the bottom data very well during 1999. The comparison to bottom salinity is quite good throughout the year. Except for a period in July and August where the model over predicts the bottom temperature, the model reproduces the bottom temperatures quite well.

3.1.3 RMS Error

The RMS error was calculated at 13 of the HOM3 stations for the period of 1998-99 and are shown in Table 3-1. The available data file did not include the sampling time so data were compared to daily averaged model

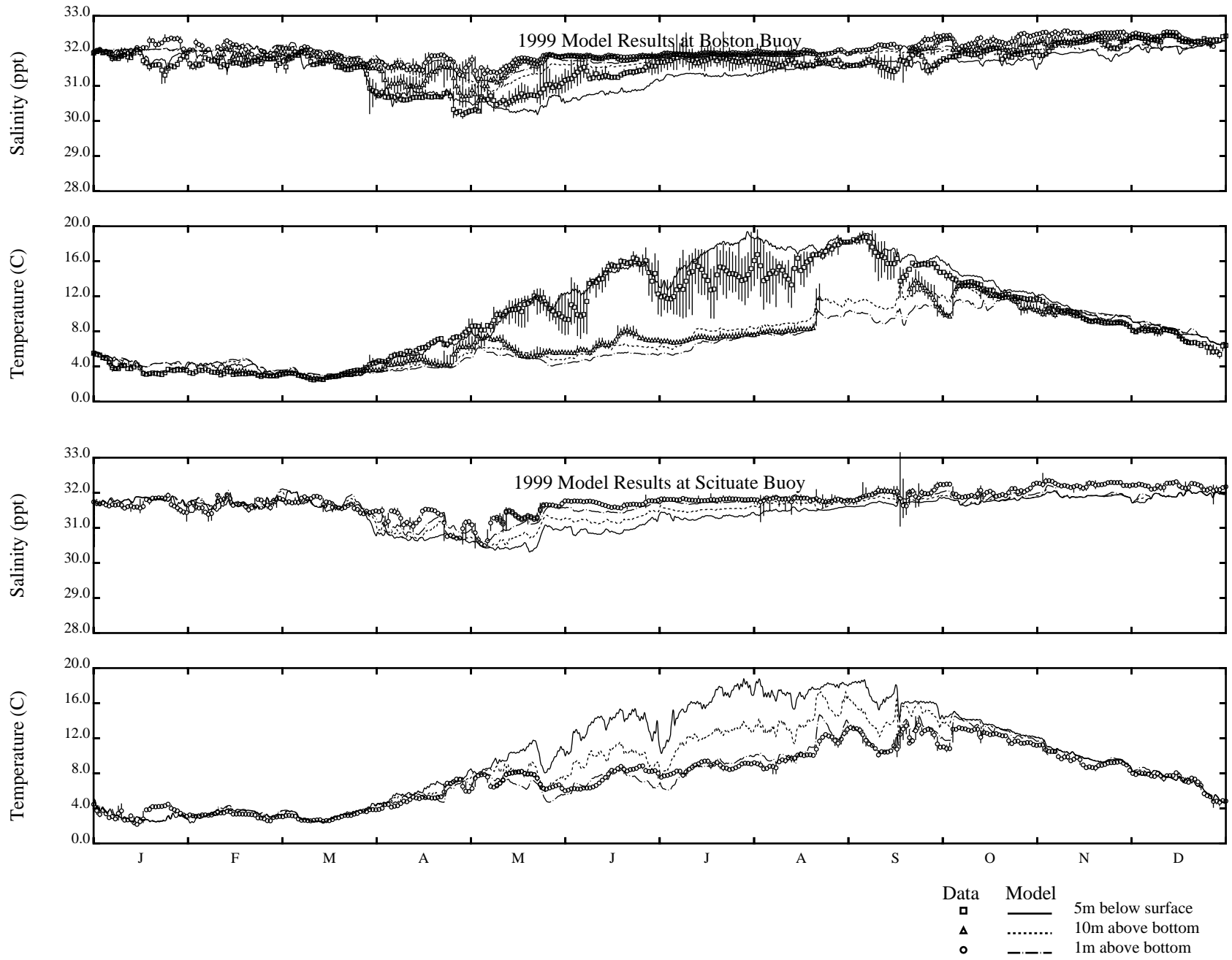


Figure 3-15. 1999 Temperature and Salinity Calibration at the Boston Buoy and Scituate Buoy

Table 3-1. RMS Error

Station	Surface Salinity	Bottom Salinity	Surface Temperature	Bottom Temperature
N01	0.542	0.238	1.434	1.055
N04	0.547	0.223	1.271	0.922
N07	0.421	0.179	1.245	1.019
N10	0.829	0.321	1.543	0.855
F01	0.478	0.386	1.162	0.672
F02	0.345	0.281	1.208	1.184
F07	0.507	0.410	0.655	0.835
F17	0.490	0.237	1.203	0.756
F26	0.629	0.192	0.823	1.328
F27	0.485	0.155	1.344	0.727
F28	0.459	0.381	1.244	1.016
F29	0.700	0.235	0.820	1.078
F31	0.554	0.428	1.312	0.423

	Salinity			Temperature		
	5m	10m above bottom	1m above bottom	5m	10m above bottom	1m above bottom
Boston Buoy	0.408	0.393	0.338	1.606	1.246	0.743
Scituate Buoy	N/A	N/A	0.234	N/A	N/A	0.844

results. Since the far field stations are sampled only six times per year it was decided that annual and seasonal statistics would not be computed. RMS error for the surface and bottom temperature range from 0.65 to 1.54°C and 0.42 to 1.32°C, respectively. For salinity the model has an RMS error ranging from 0.34 to 0.83 ppt at the surface and from 0.16 to 0.43 ppt at the bottom. The comparisons are generally more favorable at the bottom where there is less variability in the data.

The same analysis was done at the Boston and Scituate Buoys. The results are presented in Table 3-1. At the Boston Buoy the model compares more favorably at the bottom than at the five meter level.

3.2 VERTICAL PROFILES

The following set of figures present vertical profiles of salinity and temperature data and model results during two periods where vertical salinity or temperature stratification is observed. The first period presented is from the MWRA survey WF987 which was completed in mid-June 1998. During this period, low surface salinities were observed in the bay. Figure 3-16 presents salinity data versus model comparisons for six far field stations. Station F26 is the northernmost station where fresh water plumes are observed to enter the bay. The model reproduces the salinity here fairly well. A little further south at station F27, a freshwater plume is not as apparent and the model reproduces this feature. The model matches the salinity fairly well at the other far field stations presented.

Figure 3-17 presents salinity data versus model comparisons at four near field stations and two Cape Cod Bay far field stations. The two westernmost near field stations N01 and N10 show a great deal of stratification that the model does not reproduce. The surface salinity is less than the salinity observed in Boston Harbor (F31) and at the boundary (F26). The origin of this fresher water could be from either Boston Harbor or the boundary; the latter because sampling was conducted on separate days six days apart and there is a time lag between what occurs at the boundary and what is observed in the near field area. In the more eastern near field area (N04 and N07), the fresher water is not observed and the model reproduces the data. Down in Cape Cod Bay, at station F01, the model underpredicts the salinity.

Vertical profiles for temperature at the same six far field stations as Figure 3-16 are presented in Figure 3-18. The model versus data comparisons show mixed results. Temperatures are over predicted by the model at stations F31 and F07. As the flow exits the bays at F29 the model underpredicts the temperature. The temperature profiles at stations F17, F26 and F27 are matched fairly well by the model.

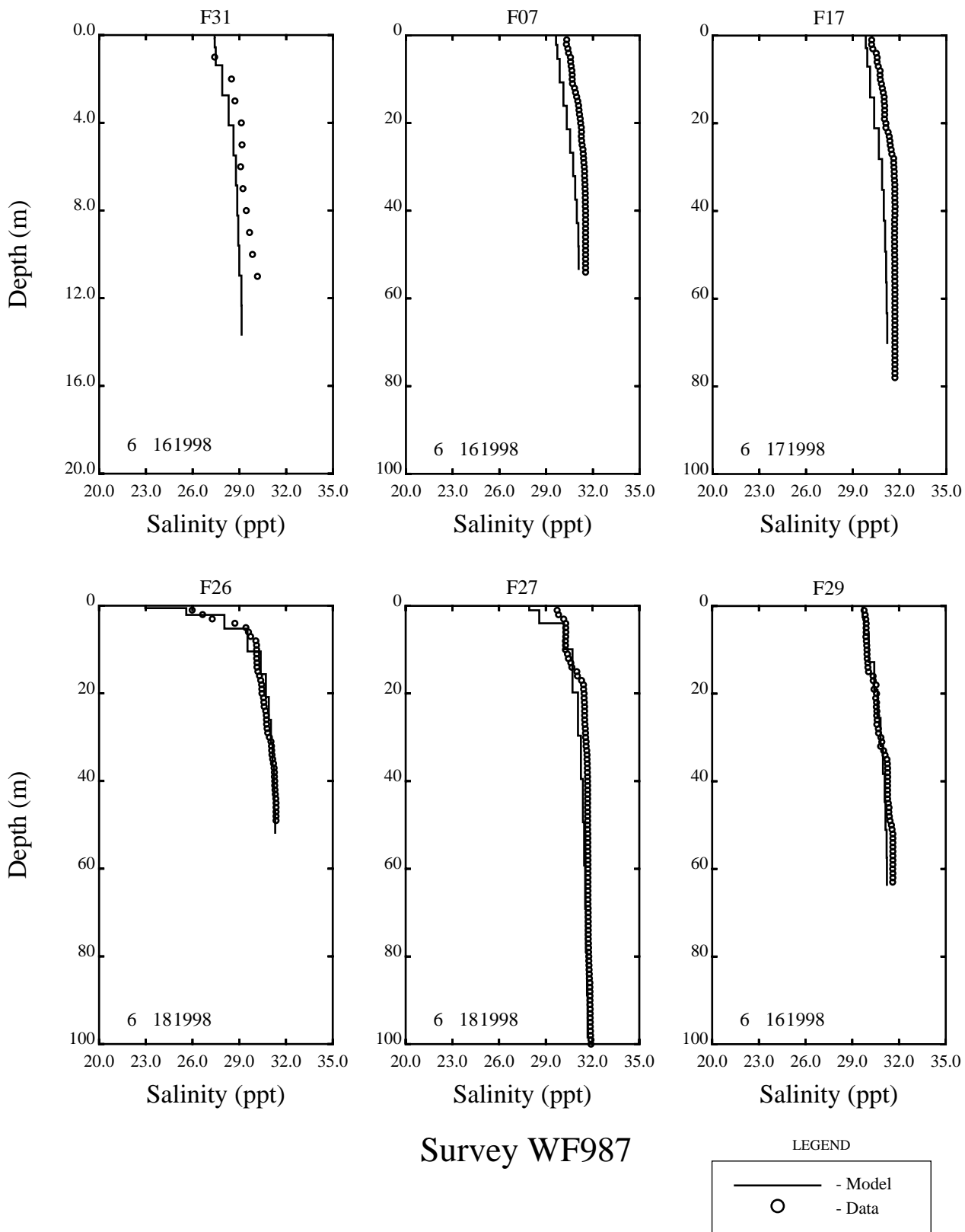


Figure 3-16. Model versus Salinity Data Vertical Profile Comparisons for Six Far Field Stations in June 1998

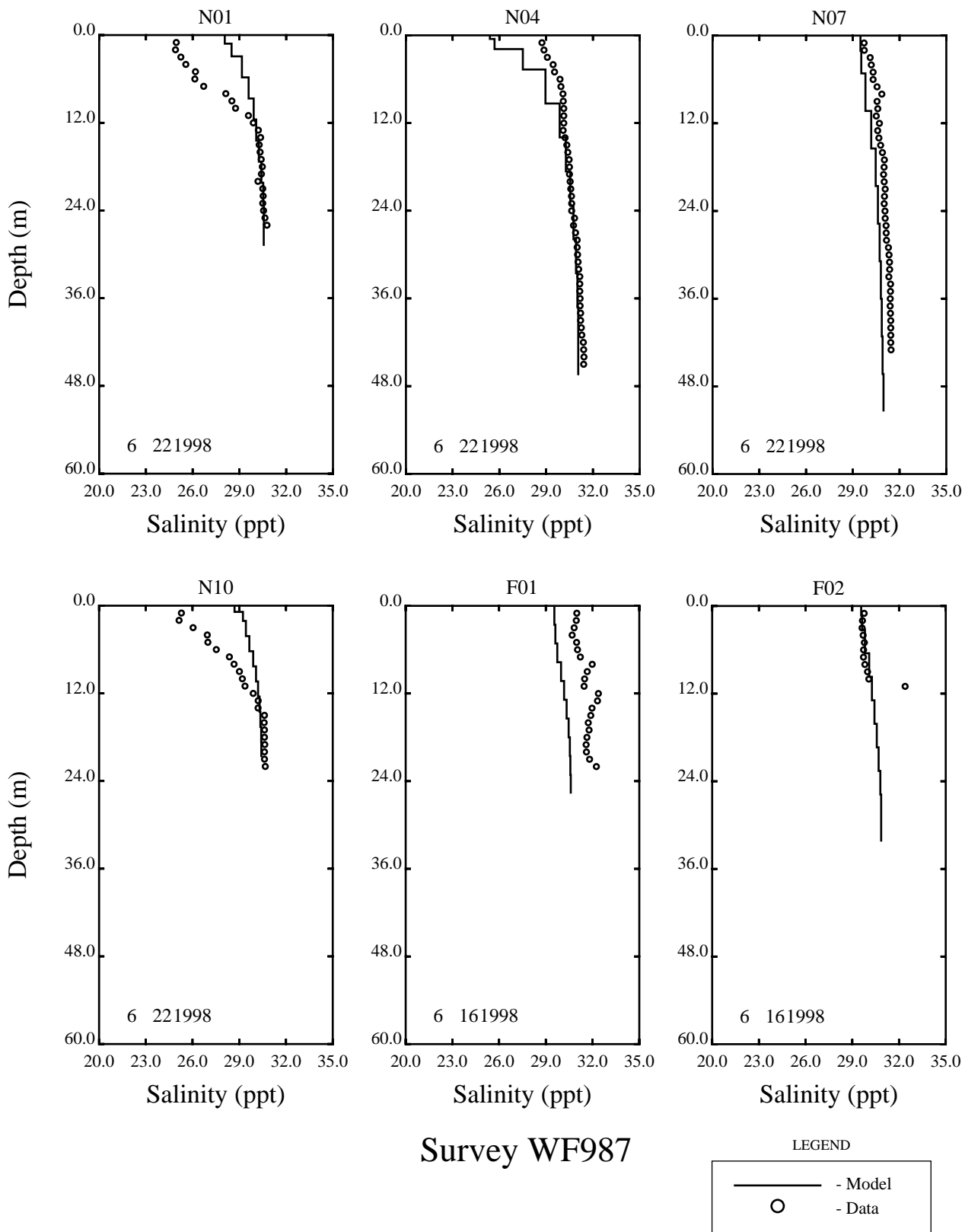


Figure 3-17. Model versus Salinity Data Vertical Profile Comparisons for Four Near Field and Two Far Field Stations in June 1998

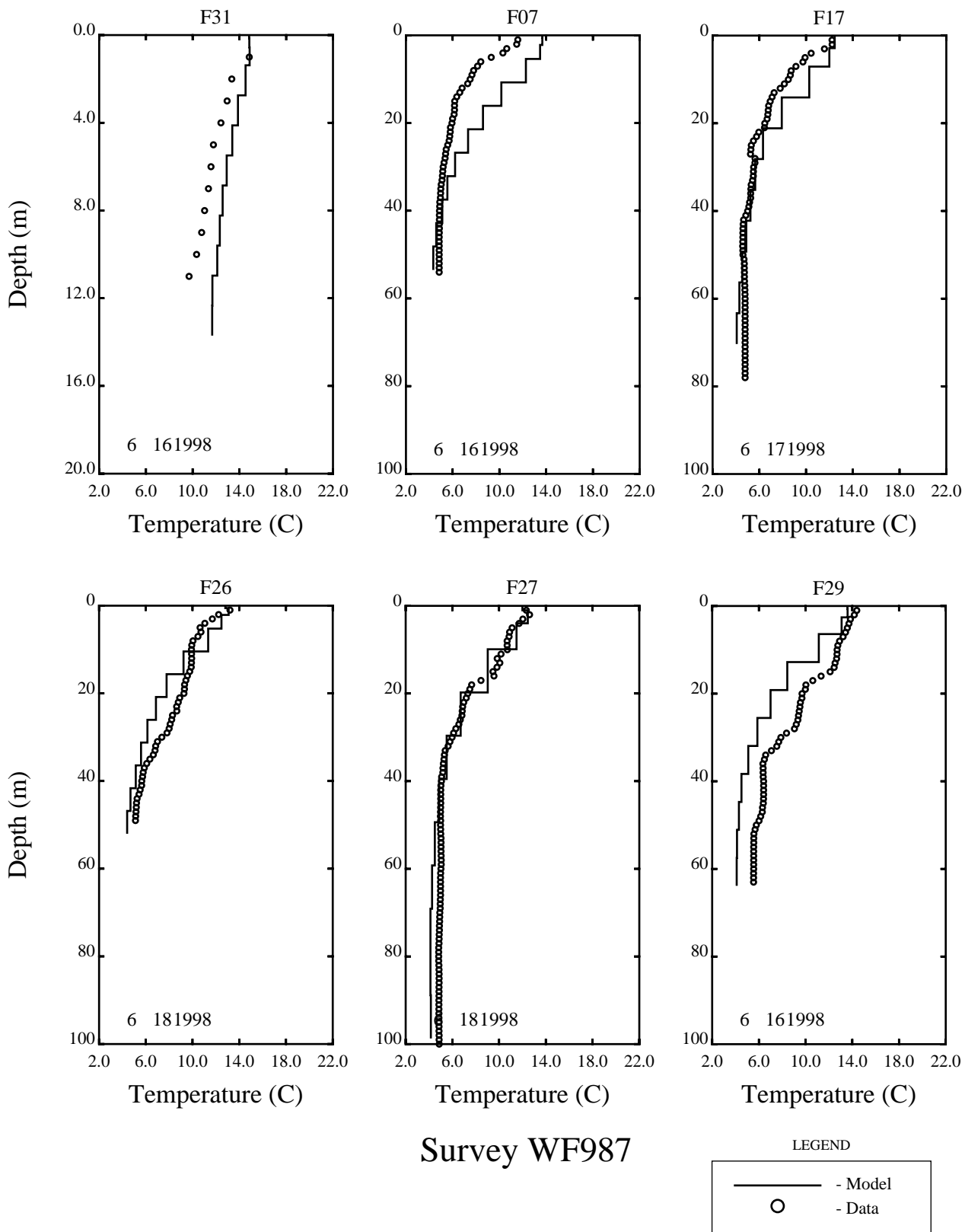


Figure 3-18. Model versus Temperature Data Vertical Profile Comparisons for Six Far Field Stations in June 1998

Similarly, mixed results for the model calibration are observed in Figure 3-19. Surface temperatures are underpredicted by the model at stations N01, N10 and F02, and over predicted at F01. The model produces fair results at stations N04 and N07. The data show a greater spatial variation than the model is able to reproduce.

Figures 3-20 through 3-23 present vertical profiles for temperature and salinity, at the same 12 stations presented above, for the MWRA survey WF99B completed in August 1999. During this period the bays were very temperature stratified, but not very stratified with respect to salinity. As shown in Figures 3-20 and 3-21, the model compares favorably at 10 out of the 12 stations, slightly over predicting temperatures at stations N01 and N10. The model is able to reproduce the different levels of temperature stratification observed in Boston Harbor, Cape Cod Bay, and near the boundary of the water quality model.

Figures 3-22 and 3-23 present the vertical profile model versus data comparison for salinity. During this period the system is not stratified with respect to salinity. The model matches the data very closely at all of the locations presented.

3.3 CURRENTS

Current velocity data were available at two meter depth intervals from both the Scituate Buoy and the Boston Buoy. Figure 3-24 presents the wind input to the model as well as data and model results during a well mixed period (November 1998) at the Scituate Buoy at a depth of 5 meters and a depth of 17 meters. The current vectors represent two hour averages of the model results and data. During this period the wind direction was quite variable. The model appears to reproduce the data quite well at both depths in the water column, reproducing the timing, the magnitude and the direction of the currents. There is strong coherence between the observed data, the model results and the wind data. Figure 3-25 presents the 33-hour low pass filter results for the same period. While the model results are in slight disagreement with the data in the early portion of the month, during the later portion of the month, the model performs quite well.

During the more stratified period of July 1999, the model had difficulty reproducing the data. Figure 3-26 shows that the current data rapidly change magnitude and direction. The model results have the same general characteristics. The model also reproduces the difference in magnitude between the currents at the 5 m depth and the 17 meter depth. The 33-hour low pass filtered results presented in Figure 3-27 show the model has more difficulty reproducing the non-tidal component of the velocity during this stratified period.

Signell et al. (1996) had similar difficulties with his 1989-1991 calibration of Massachusetts Bay. Signell wrote “The quality of the comparison between modeled and observed currents varies substantially with space and time. At Boston Buoy, for example, events are frequently well-represented during the winter, but are only

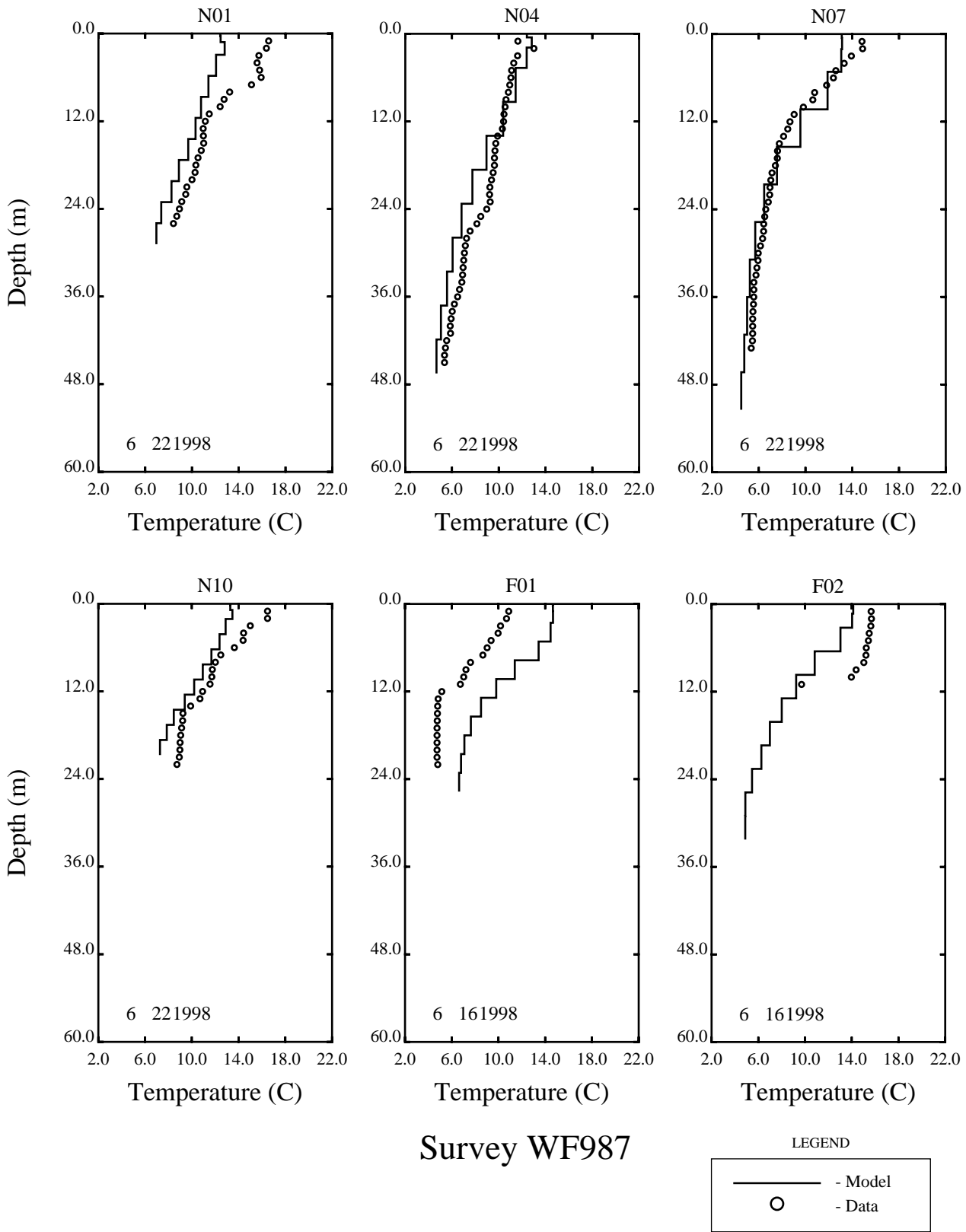


Figure 3-19. Model versus Temperature Data vertical Profile Comparisons for Four Near Field Stations and Two Far Field Stations in June 1998

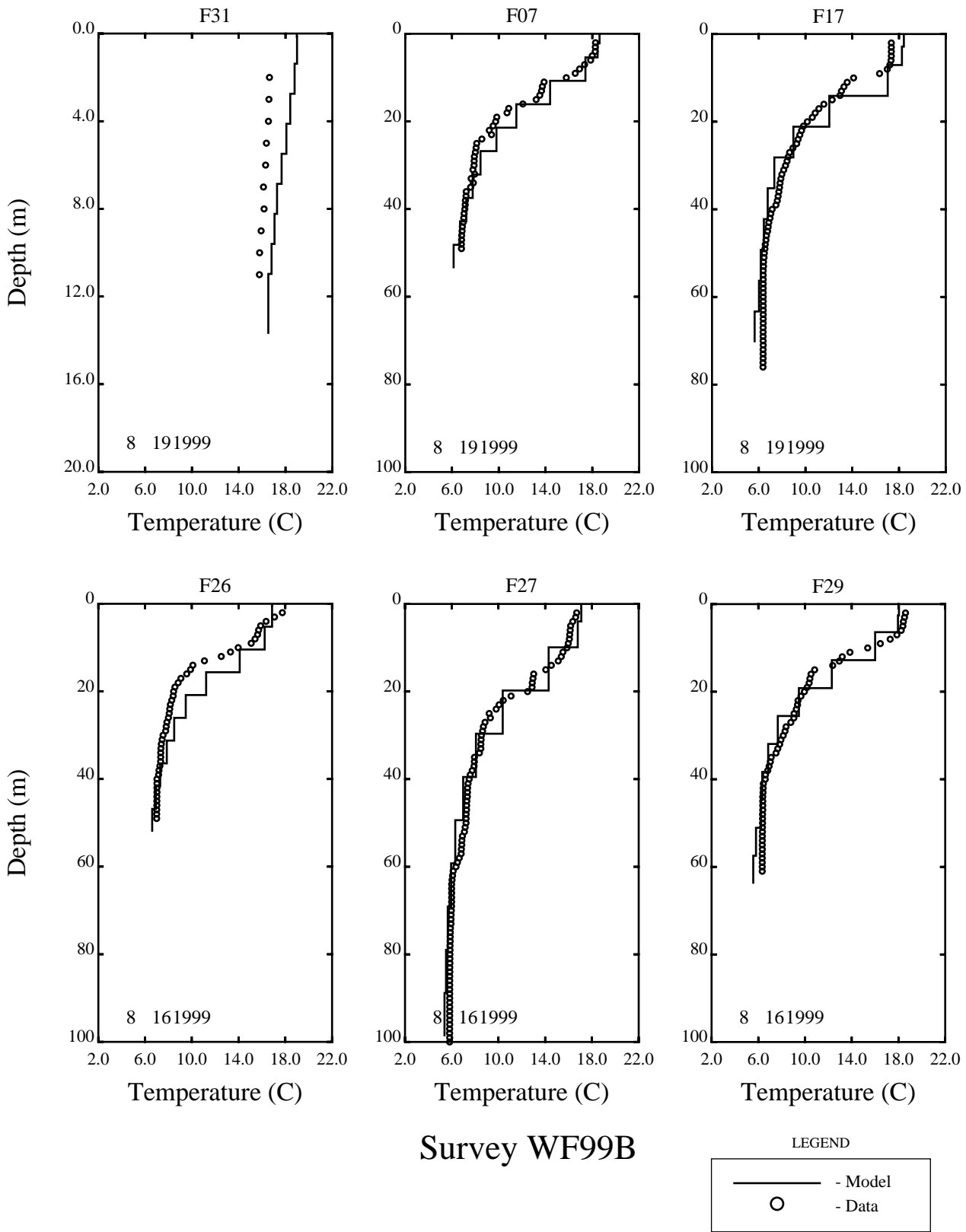


Figure 3-20. Model versus Temperature Data Vertical Profile Comparisons for Six Far Field Stations in August 1999

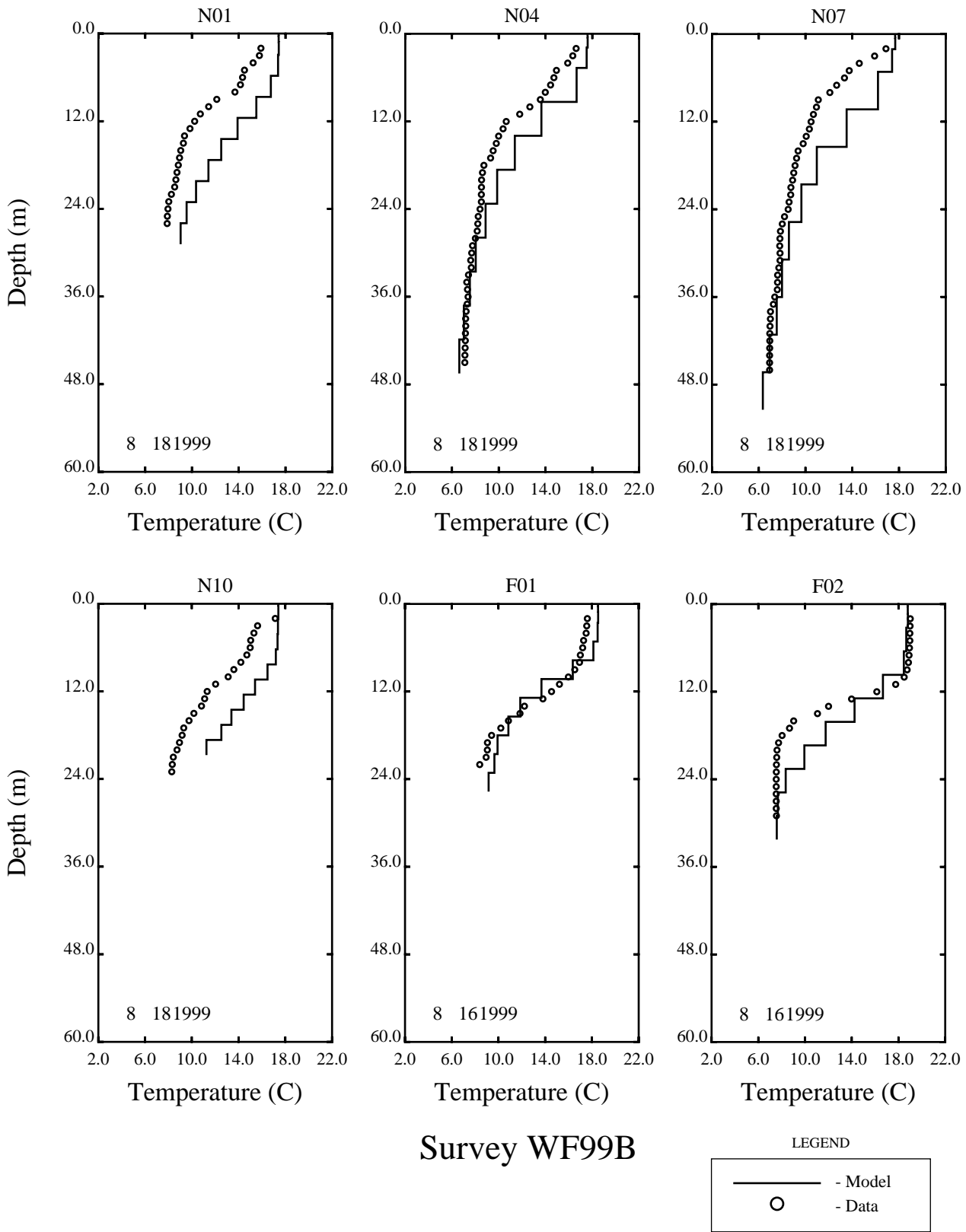


Figure 3-21. Model versus Temperature Data Vertical Profile Comparisons for Field Stations and Two Far Field Stations in August 1999

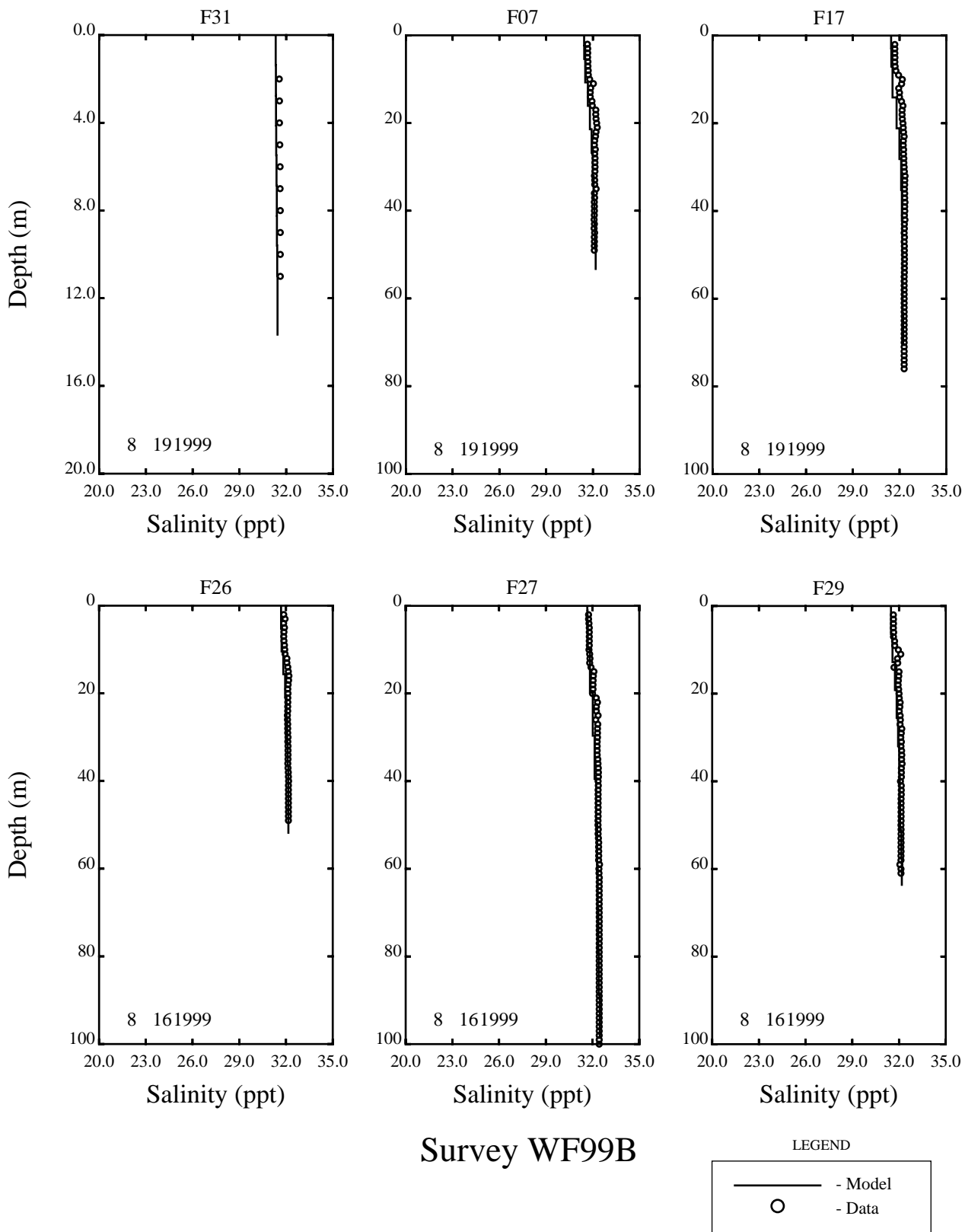


Figure 3-22. Model versus Salinity Data Vertical Profile Comparisons for Far Field Stations in August 1999

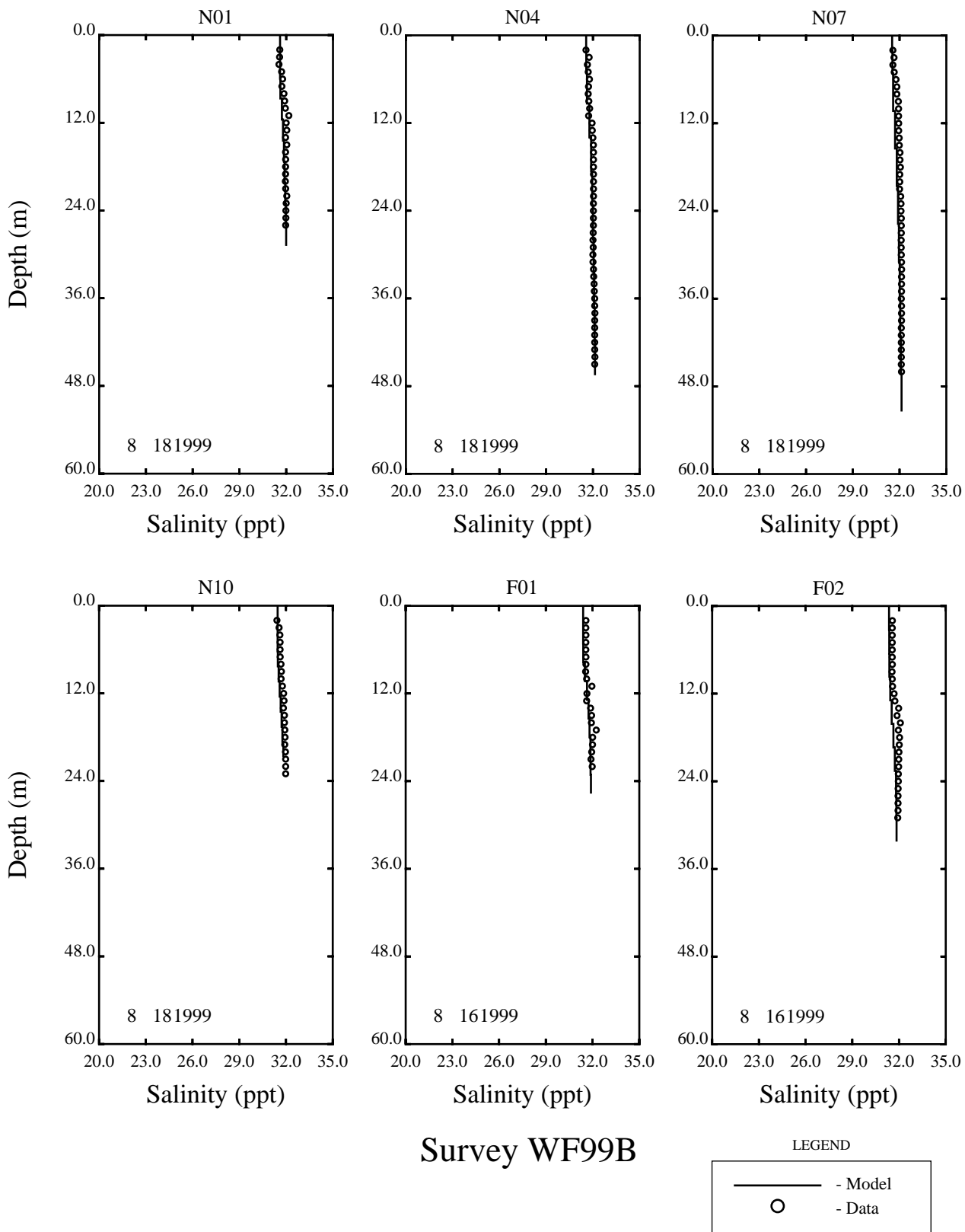


Figure 3-23. Model versus Salinity Data Vertical Profile Comparisons for Four Near Field Stations and Two Far Field Stations in August 1999

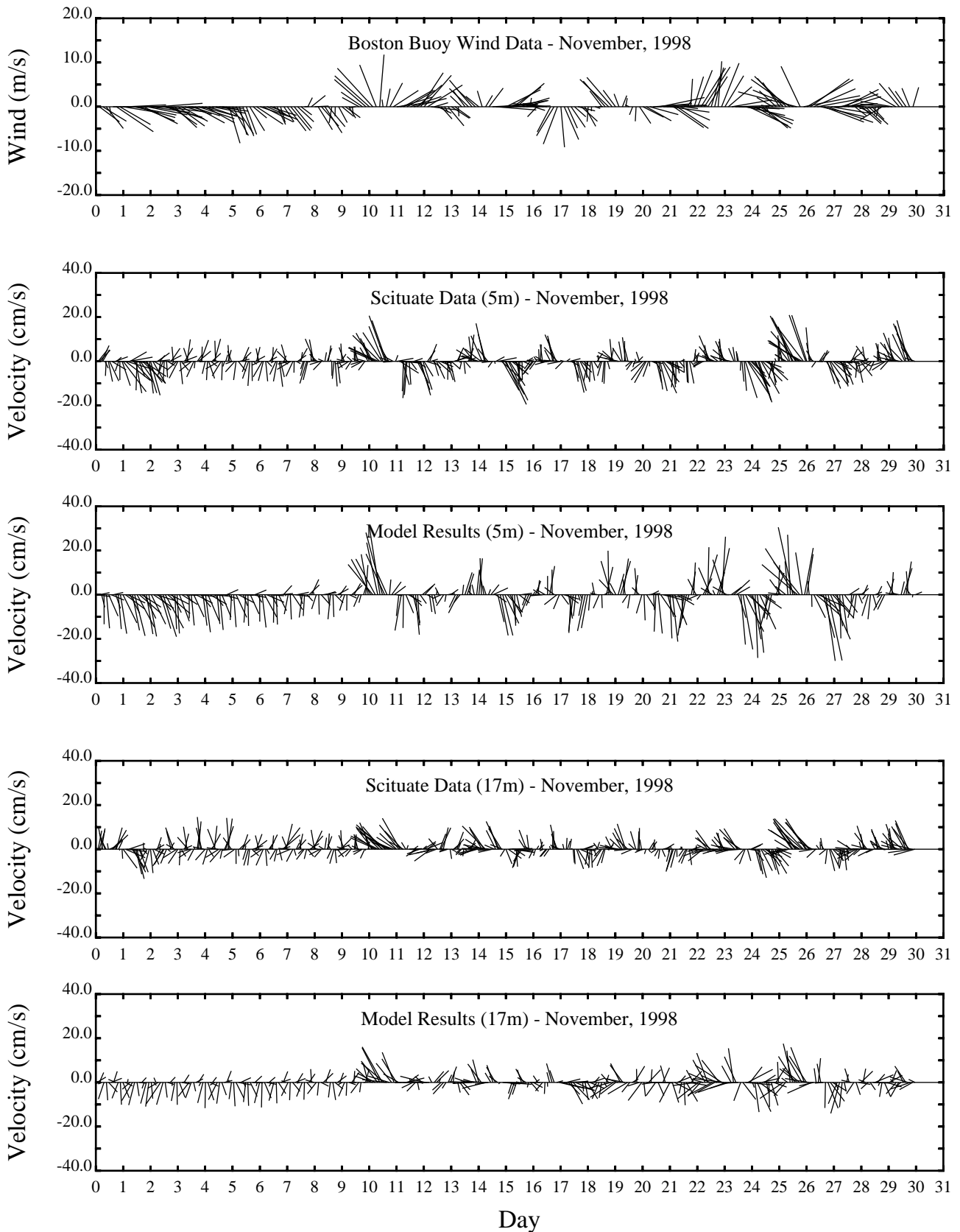


Figure 3-24. Comparison Between Current Meter and Model Results at the Scituate Buoy for November 1998 at 5 and 17 Meters

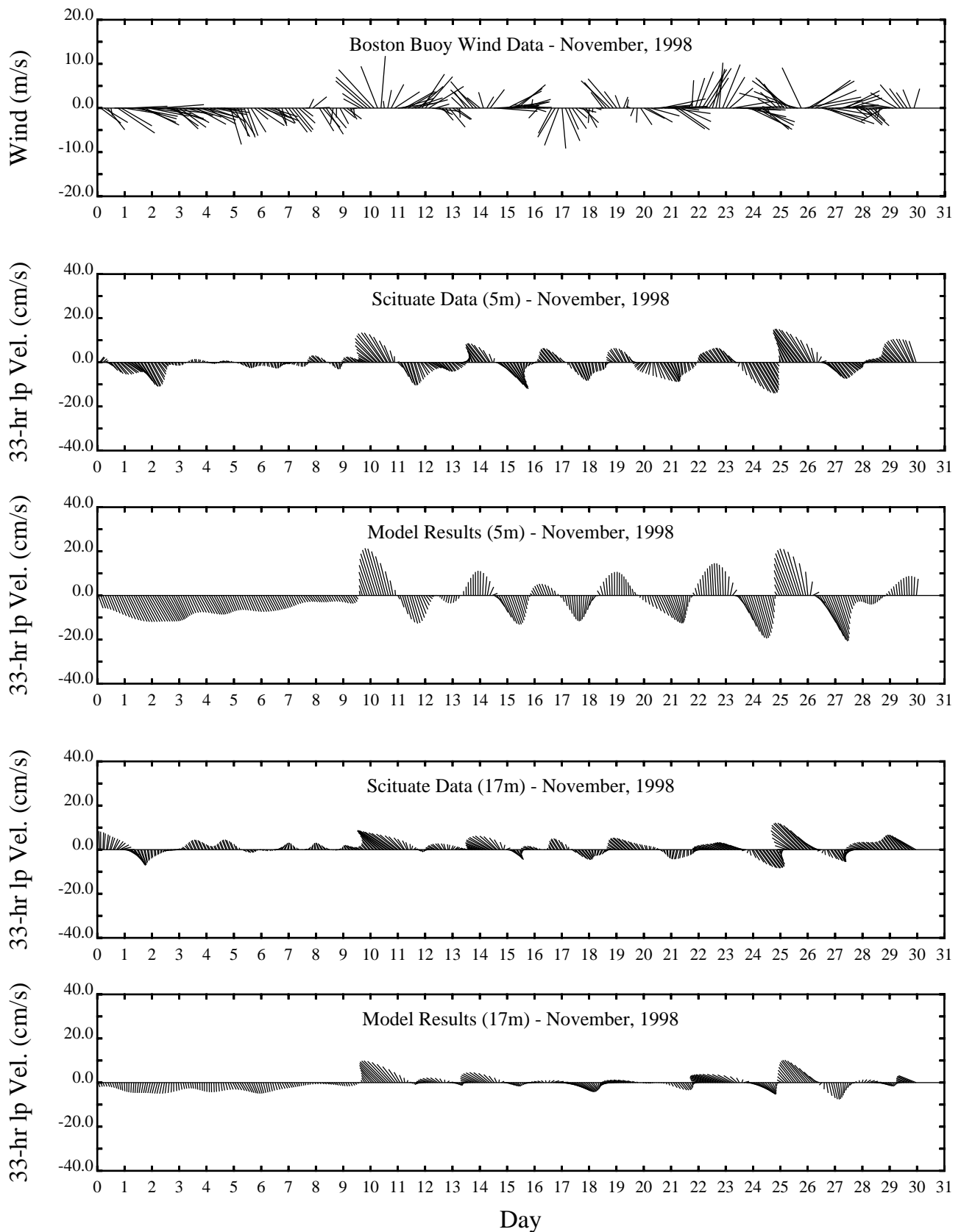


Figure 3-25. Comparison Between Current Meter and Model Results after being Filtered by a 33-hour Lowpass Filter at the Scituate Buoy for Nov. 1998 at 5 and 17 Meters

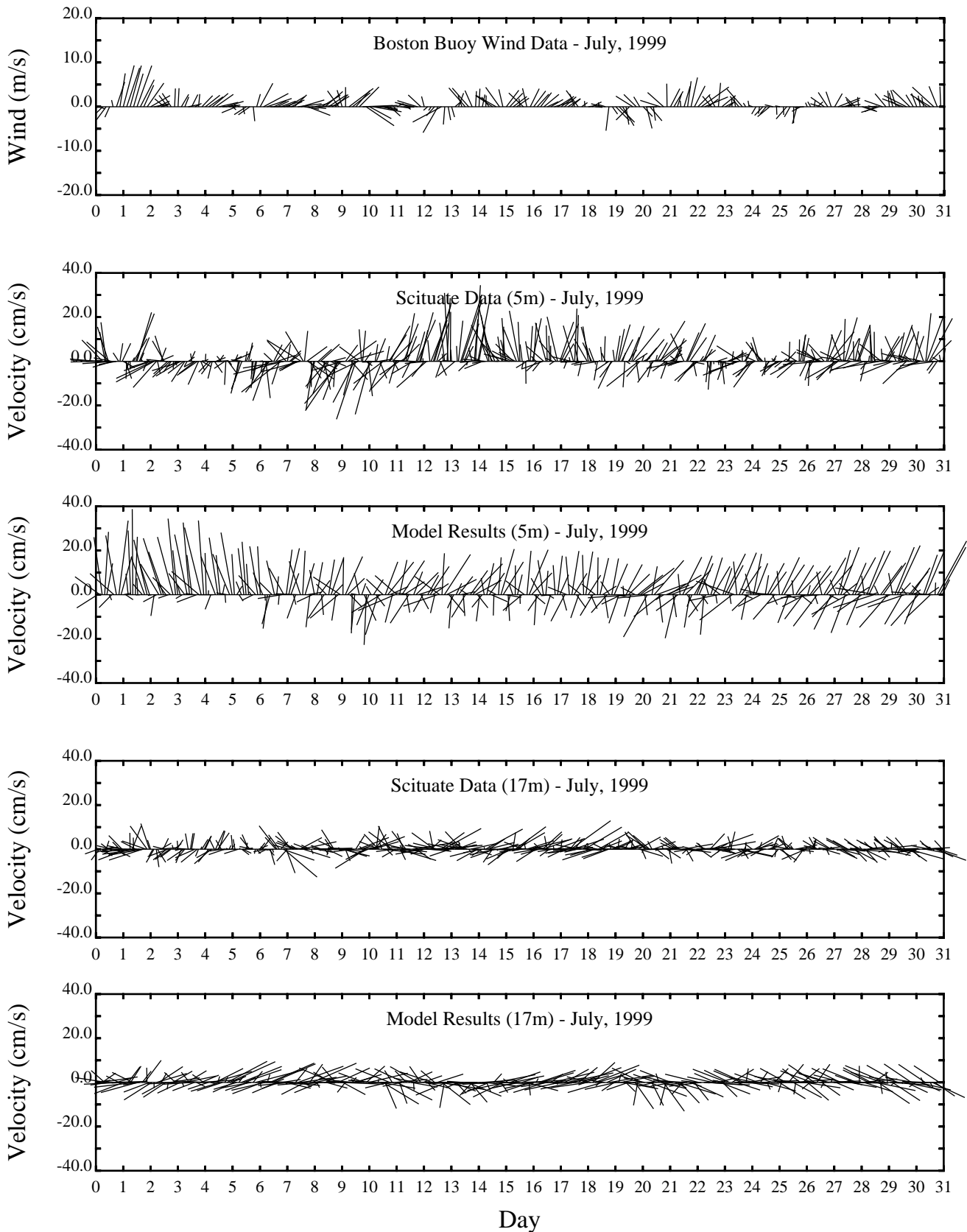


Figure 3-26. Comparison Between Current Meter Data and Model Results at the Scituate Buoy for July 1999 at 5 and 17 Meters

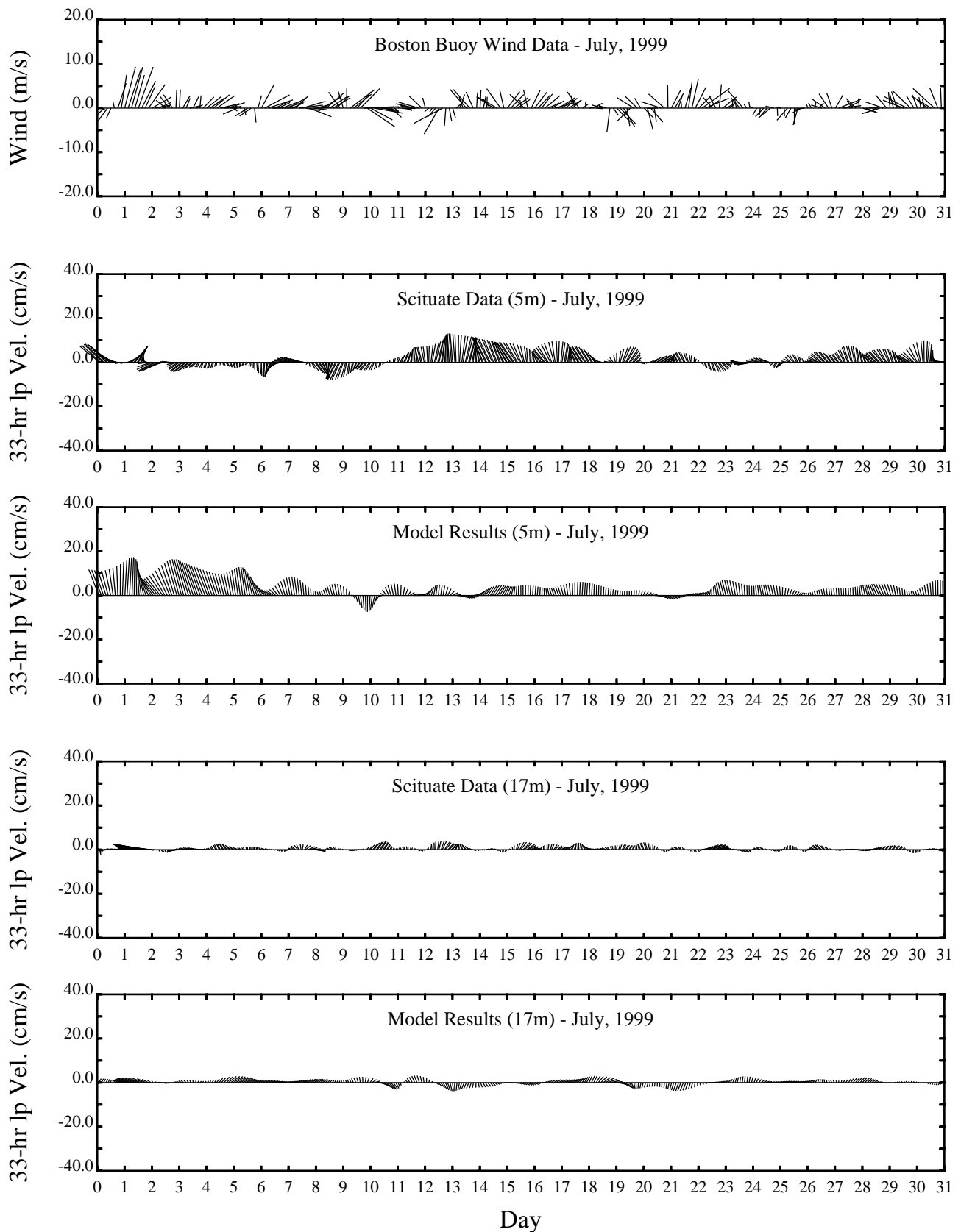


Figure 3-27. Comparison Between Current Meter and Model Results after Being Filtered by a 33-hour Lowpass Filter at the Scituate Buoy for July 1999 at 5 and 17 Meters

occasionally well represented during the summer. As explained in Signell et al. (1994), this is because the flow regime in winter is largely wind-driven with large spatial scales. Thus small deviations in the structure or timing of the circulation between the current meter data collected at the Boston Buoy are highly variable and there is little coherence between the wind and the raw current data. For this reason, only low pass filtered comparisons are presented for the Boston Buoy.

Figure 3-28 presents the data and model results after applying a 33-hour low pass filter to the November 1998 Boston Buoy data and model results. At the 5 meter depth the model is able to reproduce a number of the features observed in the data resulting from wind effects. At the 23 meter depth some of the general features of the data are reproduced by the model, but the model does not compare as favorably as at the Scituate Buoy.

The 33-hour low pass filtered results for July 1999 are shown in Figure 3-29. The model reproduces some of the features observed in the data towards the end of the month at the 5 meter depth, but does a poor job in other portions of the month. At the 23 meter depth, the model reproduces the approximate magnitude of the data, but is often in the wrong direction.

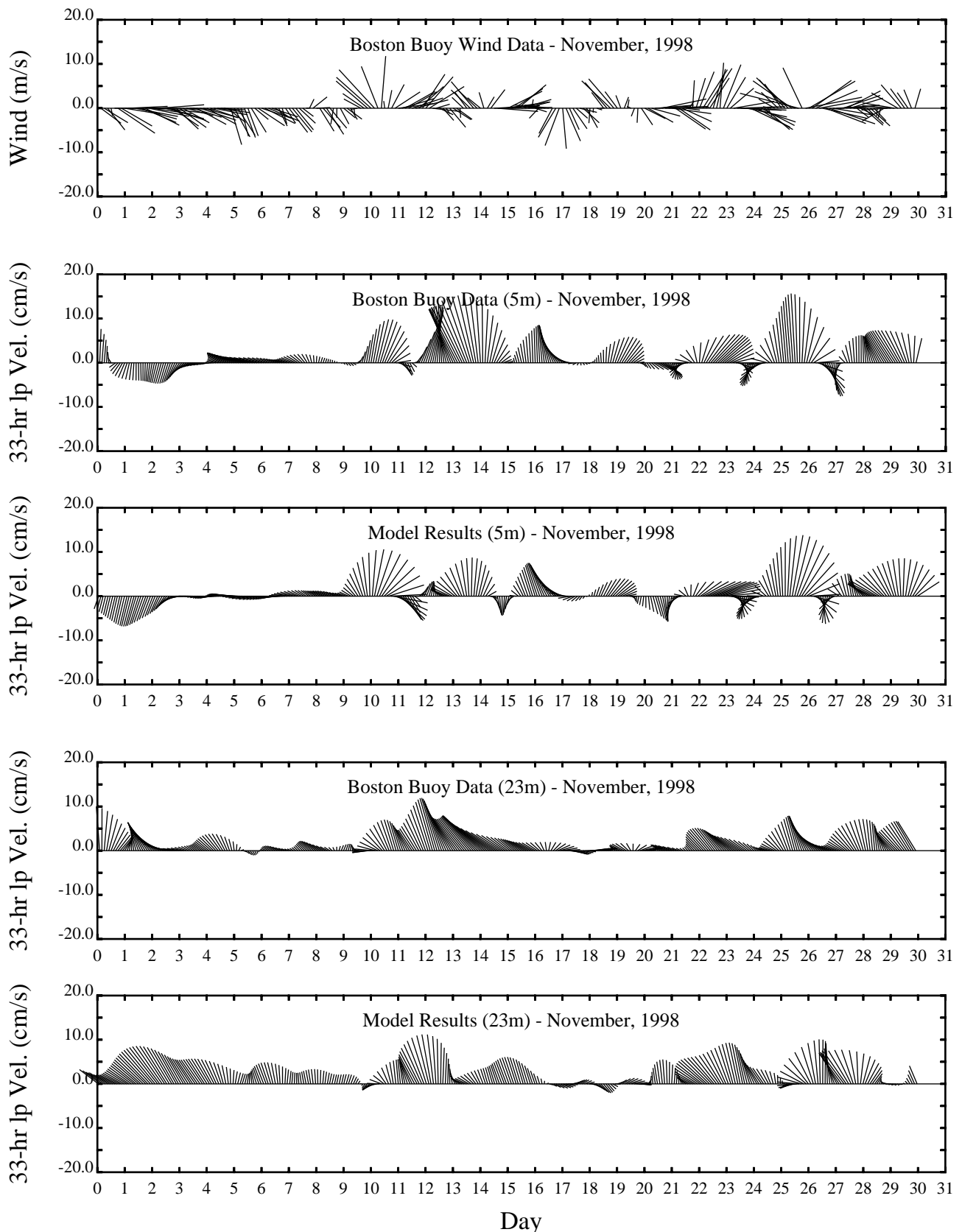
model and reality will not result in large errors at the mooring locations. During the stratified seasons, however, the spatial scales are considerably smaller due to upwelling, intrusions of Gulf of Maine river water, etc. Small deviations in the structure or timing during the stratified seasons will therefore result in larger errors at the mooring locations.”

The remaining current meter calibration figures for each month of the calibration period at both buoys can be found in Appendices C and D.

The previous analyses have shown that the model is able to reproduce the long-term seasonal events that are observed in the Massachusetts and Cape Cod Bays Systems. This section will show the model’s ability to reproduce shorter term mixing and stratification events.

3.4 SHORT TERM EVENTS

Astronomical tides have been considered the major source of mixing energy for destratification processes. Stratification and destratification as a result of neap-spring tidal mixing have been reported by Ruzecki and Evans (1985) in the York River estuary. Geyer and Signell (1992) have argued that the effectiveness of tidal dispersion and mixing depends on the relative scale of the tidal excursion to the spacing between major bathymetric and shoreline features. They concluded that in estuaries where the typical spacing of topographic features is less than the tidal excursion, tidal dispersion may contribute significantly to the



Day
 Figure 3-28. Comparison Between Current Meter and Model Results after Being Filtered by a 33-hour Lowpass Filter at the Boston Buoy for Nov. 1998 at 5 and 23 Meters

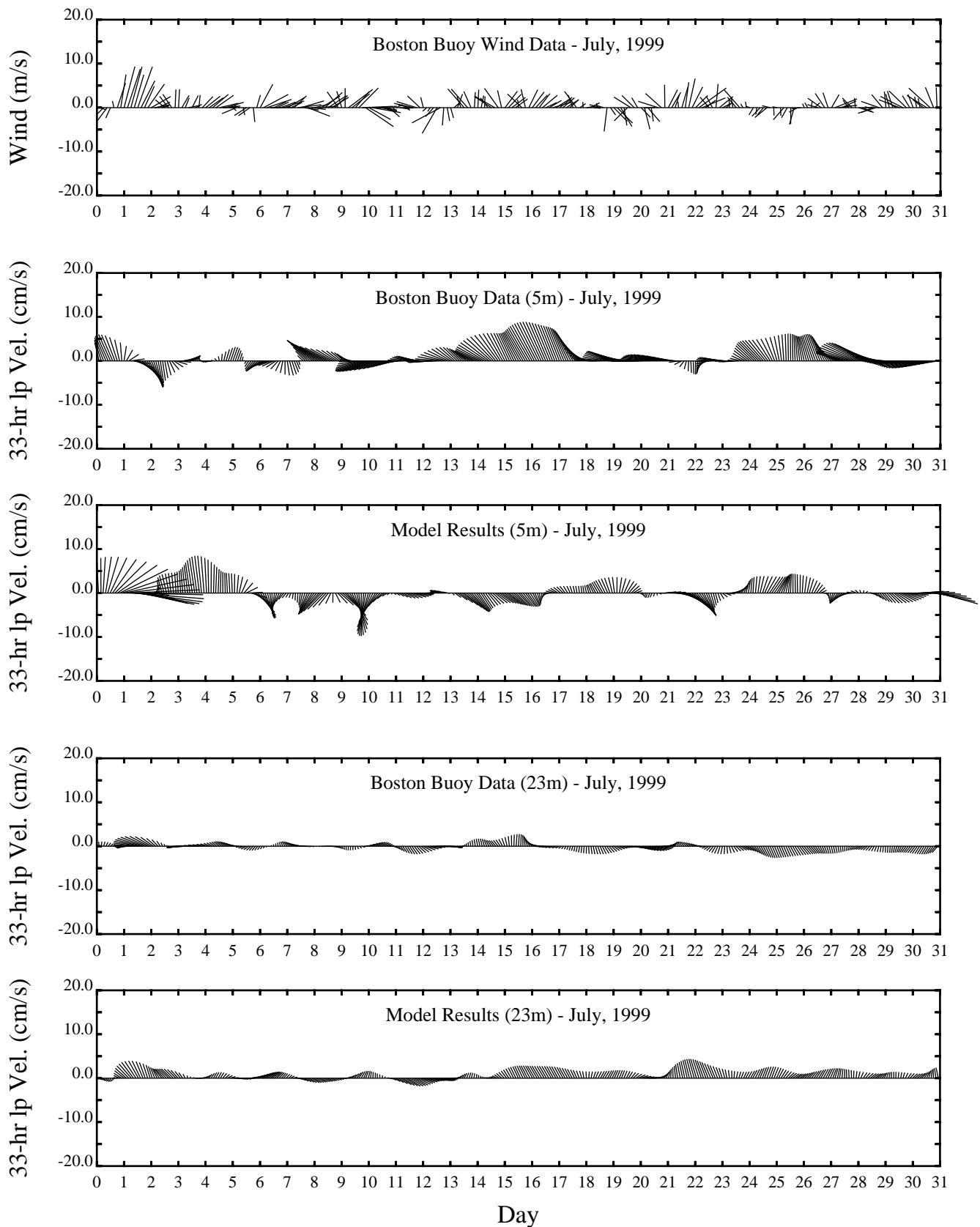


Figure 3-29. Comparison Between Current Meter and Model Results after Being Filtered by a 33-hour Lowpass Filter at the Boston Buoy for July 1999 at 5 and 23 Meters

mixing processes. In Chesapeake Bay, Blumberg and Goodrich (1990) have found that wind-driven internal shear is a more effective mechanism of inducing destratification than turbulence generated at the surface.

In general, wind mixing tends to raise the potential energy of a water column by redistributing the density gradient over depth and, thereby, altering the horizontal pressure gradient which essentially generates the gravitational flow. Several studies have demonstrated that a depth-dependent response to local wind forcing is a very effective mechanism in maintaining stratification as well as destratification. Among these studies, work completed in Chesapeake Bay by Weisberg (1976), Wang (1979), Grano and Pritchard (1982), Goodrich (1985), Goodrich et al. (1987), and Blumberg and Goodrich (1990), and in Mobile Bay, by Noble et al., (1996) and Schroeder et al. (1990) are notable.

Several wind driven events have been identified during the two-year simulation period. Three are examined in this section. The model has been reasonably successful in reproducing these events. A strong mixing event following a stratified condition was observed on May 10, 1998, as illustrated in Figure 3-30. The destratification process observed during this period was almost invariably preceded by strong north-northeast winds that began on May 9, 1998. This mixing mechanism was closely tied with wind-generated internal velocity shear during a downwelling episode associated with the north-northeast winds as illustrated in Figure 3-31. Figure 3-31 illustrates the event in six sequential snap shots, approximately one day apart, along a transect indicated in Figure 3-1 during May 8 through May 14, 1998. The color contours and shades indicate 34 hour lowpass salinity and the arrows indicate the 34 hour lowpass currents across the section. The wind rose diagram indicates the wind speed and its direction. During this period, in the coastal downwelling zone, a near balance exists between north-northeast wind stress, Coriolis force, and internal pressure gradient. Due to the onshore currents in the surface layer and compensating offshore currents at depths, a vertical instability occurred due to the net generation of shear across the pycnocline, causing sufficient mixing to destratify the entire water column on May 11 and part of May 12 as shown in Figures 3-30 and 3-31. As the downwelling process continued to set in for several days, a weaker vertical density structure was established as it tends to bring fresher water downward introducing buoyancy in the lower layer. Consistent higher wind speeds and the weaker stratification allowed the wind forcing to penetrate deeper into the water column and complete the full mixing episode, as can be seen in Figure 3-31, on May 12, 1998 at 2:24 hour. The success of the model in capturing these events is a general indication that the overall circulation in the bay is well reproduced by the hydrodynamic model.

It is evident that the mixing events are not permanent in nature, but rather are highly transient. This process is demonstrated by the quick restratification that occurred when the wind abated or changed its direction, particularly towards the north or northeast. Such an event can be seen in both the model and observed data immediately after the complete mixing event that occurred in May 12, 1998 as shown in Figure 3-31.

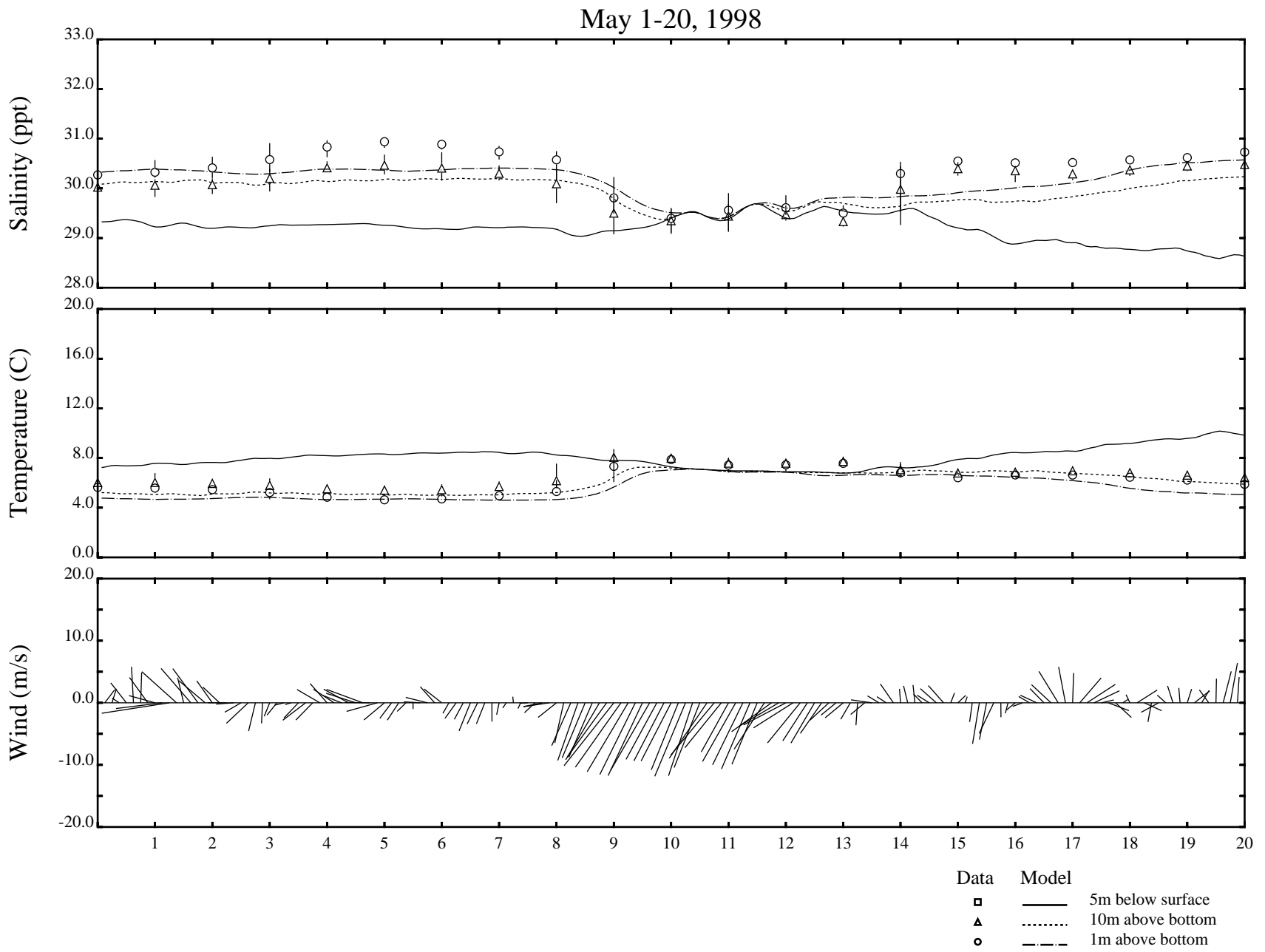


Figure 3-30. Model versus Data Comparison during a Wind Mixing Event

May 1998

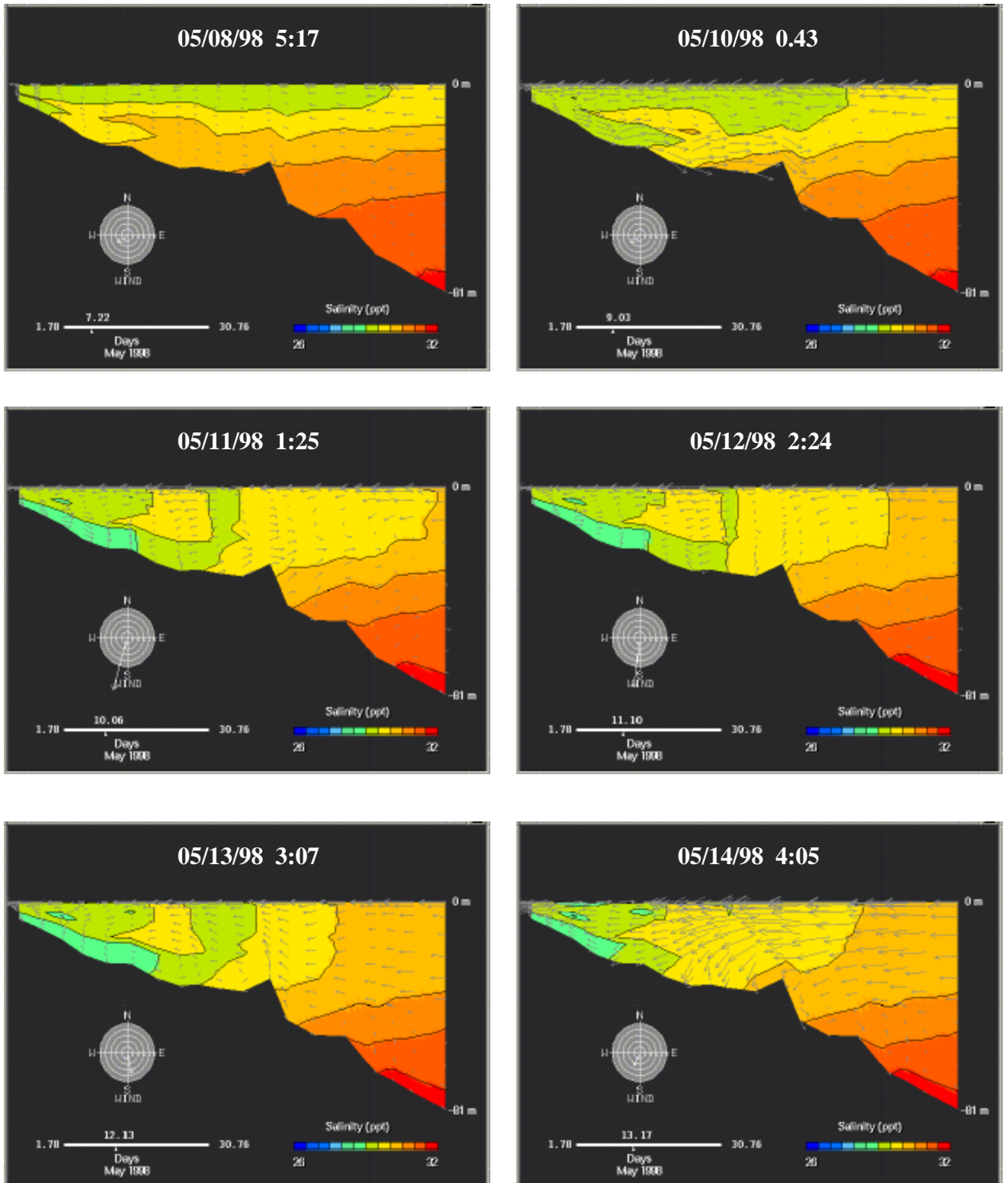


Figure 3-31. 34-hour Lowpass Salinity and Currents along a Transect through the Boston Buoy as shown in Figure 3-1 (May 8 - May 14, 1998)

Beginning mid-day May 12 through May 13, although the wind was consistently blowing towards south and southwest, its strength was substantially diminished. Beginning early May 14 through May 15, the wind completely changed its direction towards the north, which marks the onset of the upwelling episodes (Figure 3-32) and reestablishment of the stratification regime. The re-establishment of stratification and, in certain cases, enhancement of stratification is primarily the result of horizontal advection of more saline offshore water at depths by the compensating onshore flow and Coriolis force associated offshore flow in the surface. As shown in Figure 3-32, the model reproduces these events very well.

A major cooling event occurred in June 29 through July 8, 1999 as shown in Figure 3-33. The model and the observed data both show a drop of about 5°C in temperature during this cooling episode. It is interesting to note that although the surface salinity variation is not as pronounced as the temperature, however, surface to bottom salinity differences became smaller during this event and finally became completely mixed on July 9, 1999. While the surface temperature continued to drop during this period, the bottom temperature remained relatively unchanged. However, the surface temperature quickly recovers between July 6 and 13, suggesting a significant atmospheric source of heat in the surface mixed layer.

A careful investigation of this cooling event suggests that consistent but relatively weak south-southwest winds existed until June 27, however, during June 28 through July 3, the wind became significantly strong with an exception on June 30, when the wind was briefly weaker, and triggered an upwelling episode. The temperature variation during this period is significantly dominated by this upwelling event. The upwelling event is characterized by an upward movement of the thermocline, which eventually broke the surface on July 3, 1999 as can be seen in Figure 3-34. On June 30 and July 1, the wind changed its courses several times within a day, which caused enormous turbulence to erode the thermocline and deepen the surface mixed layer. This event mixed the surface water with the cooler lower layer water which resulted in a drop in surface temperature. This episode is followed by a stronger south-southwest wind for a short period of time until the wind subsided for next several days. During this weaker wind event the system readjusted itself and with the continuous source of atmospheric heat, the surface temperature recovered by July 13.

As previously described, the depth-dependent mechanism introduced by wind stress acting on the water surface is very effective in generating vertical shear, which produces mixing and finally destratifies the entire water column. Such a mixing event during fall turnover was observed during October, 1999, as shown in Figures 3-35 and 3-36. Before the turnover event occurred, the wind was predominantly blowing towards north-northeast between October 1 and 3, 1999 (see Figure 3-35). This caused an upwelling event as indicated by the upward movement of the isotherm which began to break the surface on October 3 near the coast as can be seen in Figure 3-36. During the following two days the wind changed its direction and consistently blew towards the south which triggered a downwelling event. The consecutive upwelling and downwelling events that occurred within a few days generates enormous internal shear, which is very

May 1998

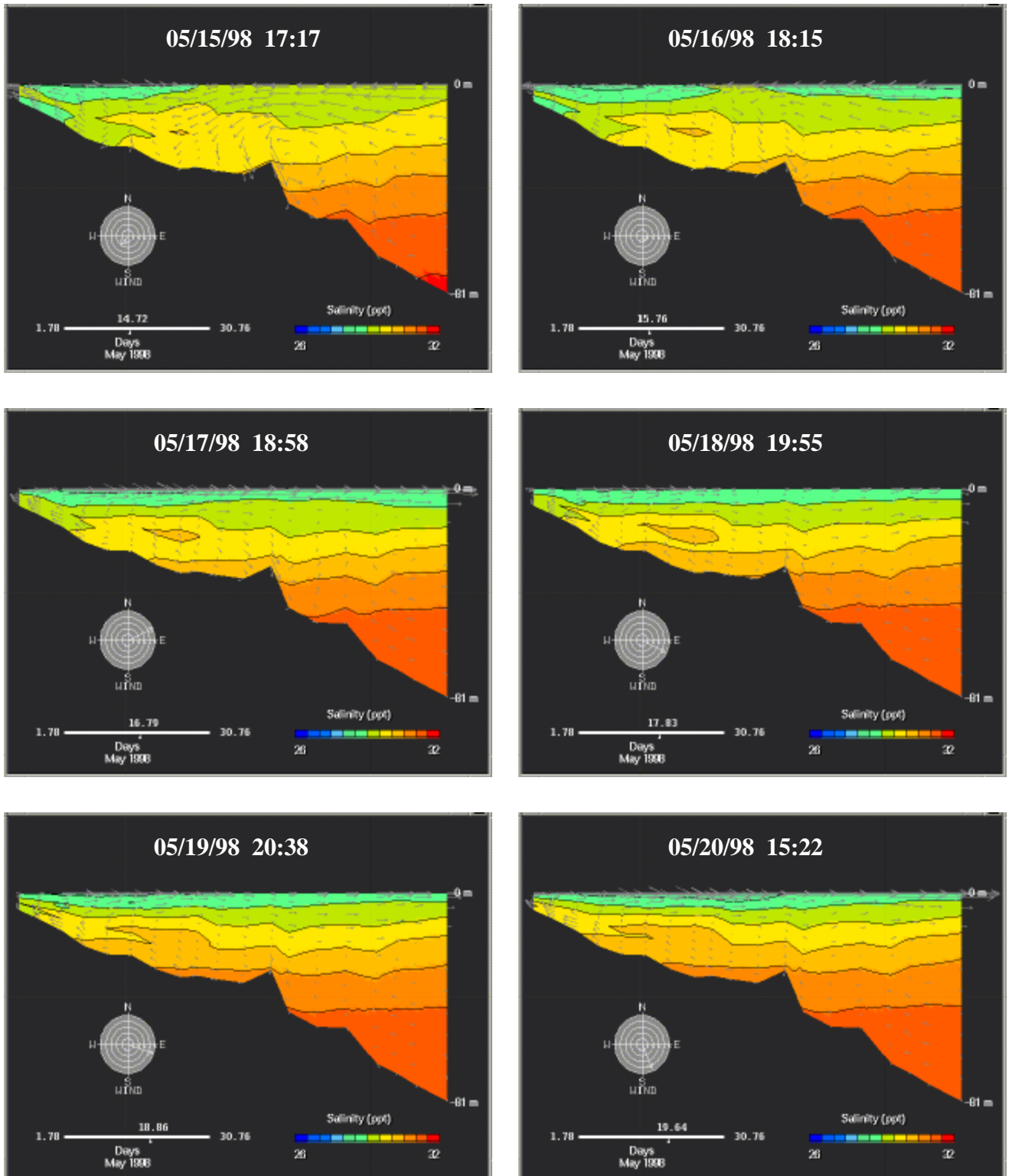


Figure 3-32. 34-hour Lowpass Salinity and Currents along a Transect through the Boston Buoy as shown in Figure 3-1 (May 15 - May 20, 1998)

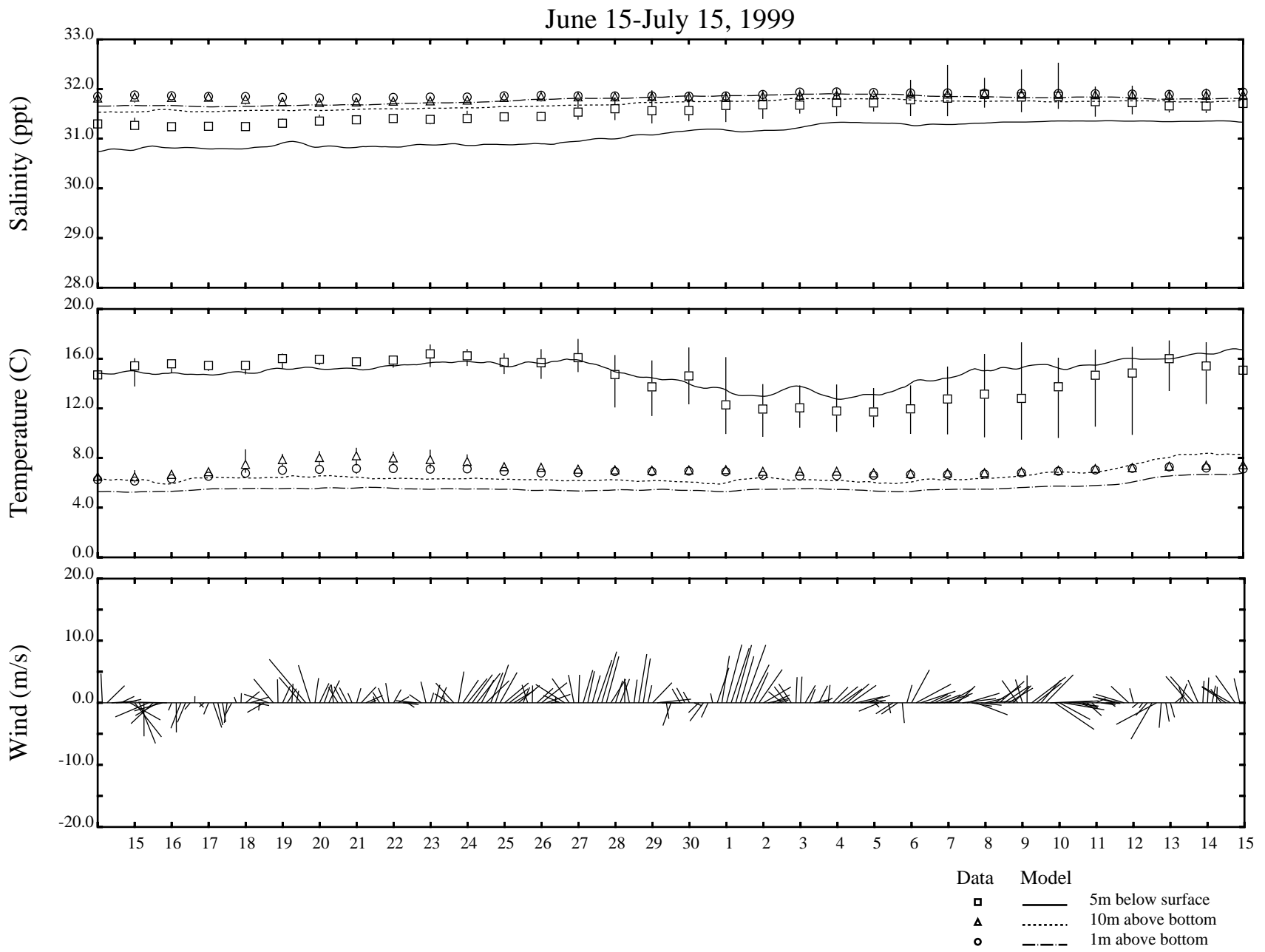


Figure 3-33. Model versus Data Comparison during a Cooling Event

June/July 1999

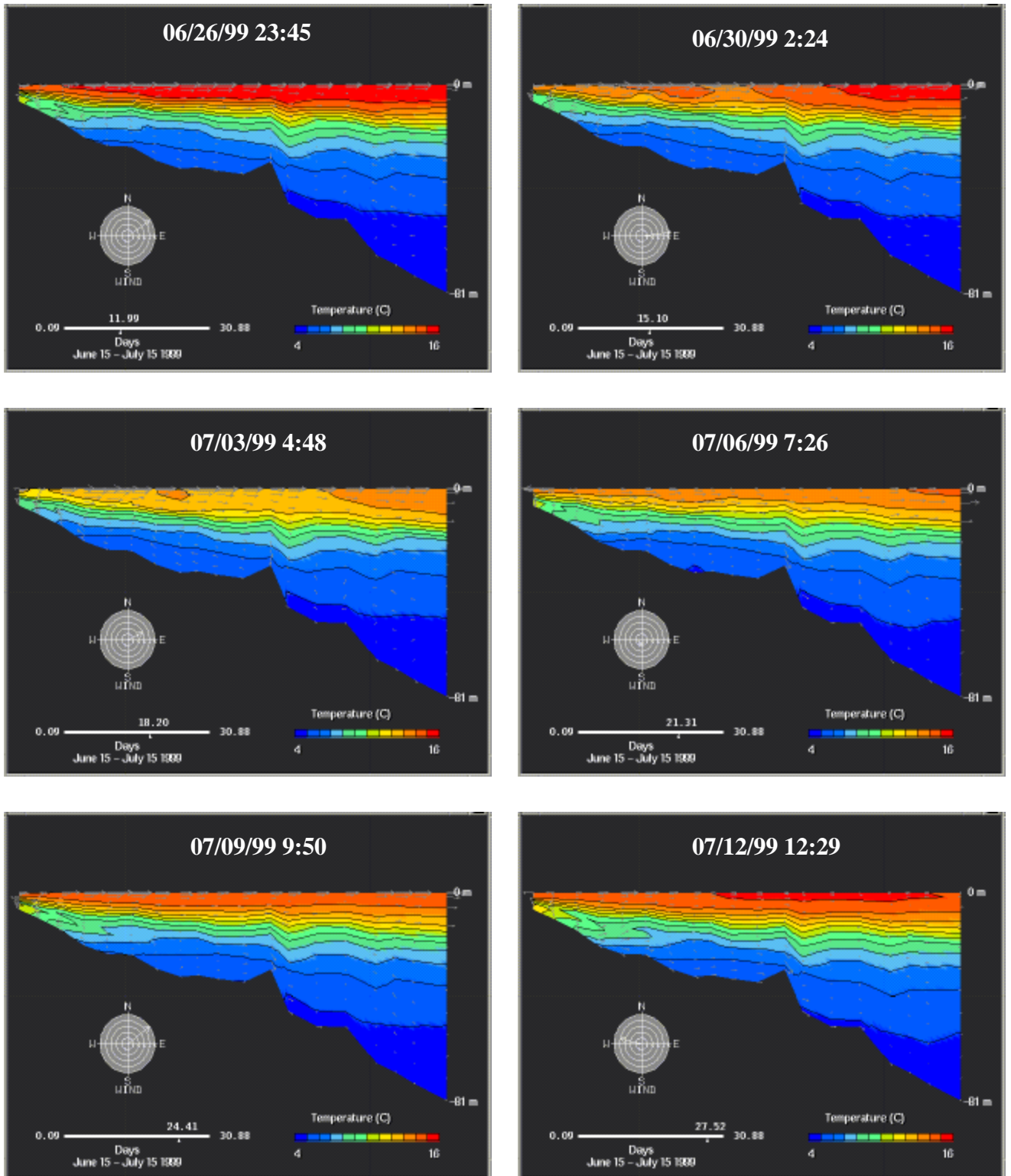


Figure 3-34. 34-hour Lowpass Temperature and Currents along a Transect through Boston Buoy as shown in Figure 3-1 (June/July 1999)

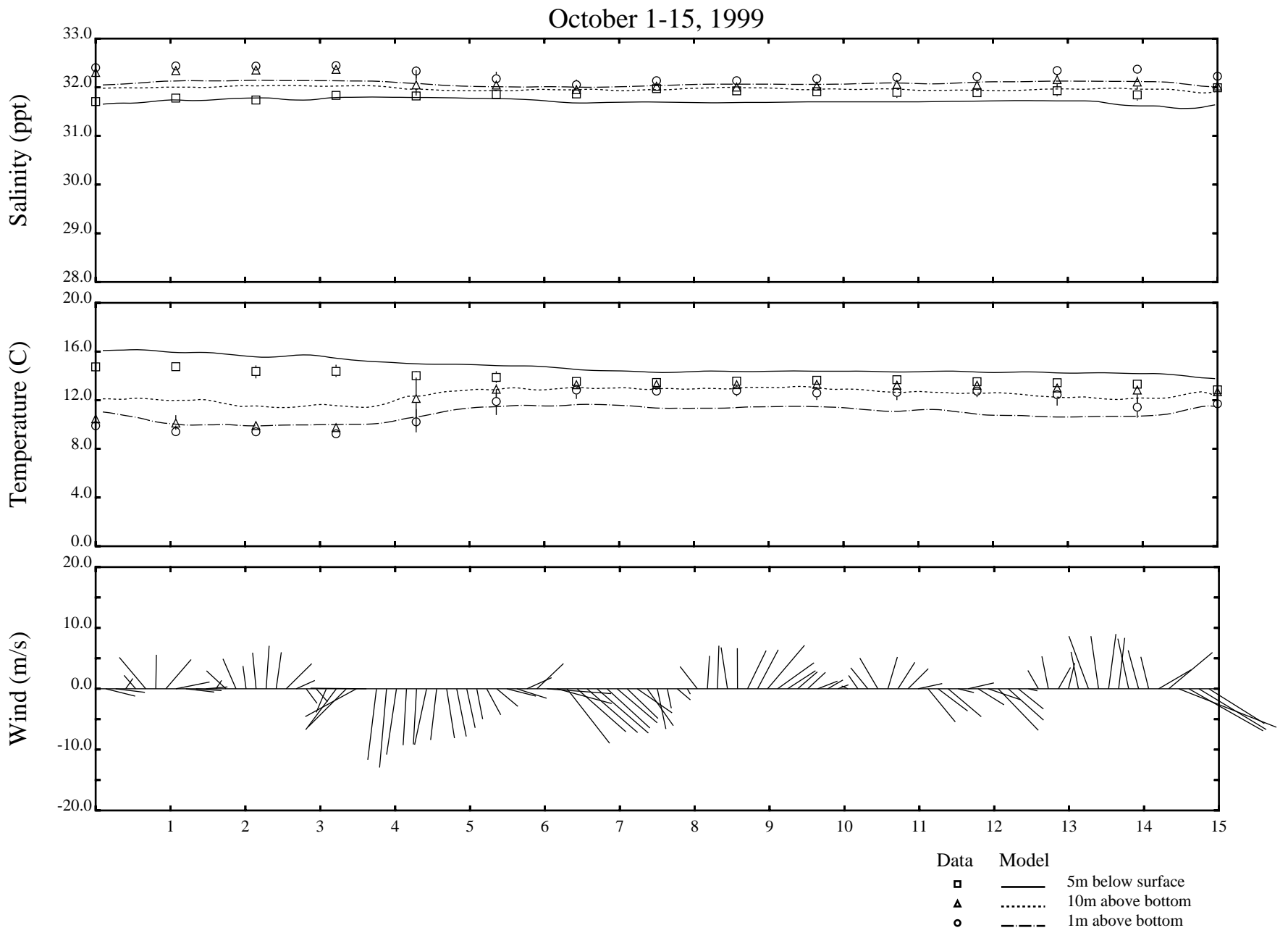


Figure 3-35. Model versus Data Comparison during a Fall Turnover Event

October 1999

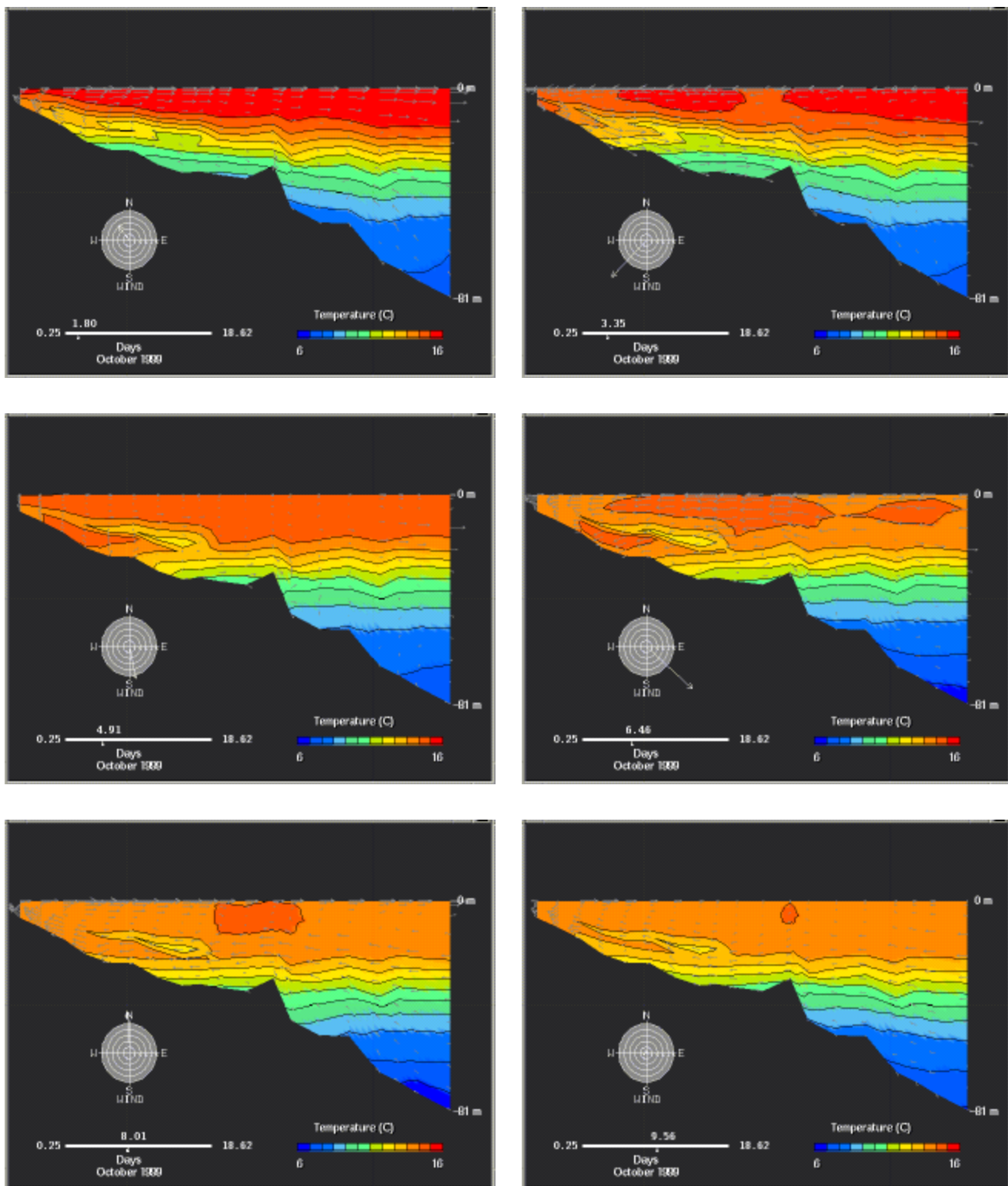


Figure 3-36. 34-hour Lowpass Temperature and Currents along a Transect through the Boston Buoy as shown in Figure 3-1 (October, 1999)

effective in eroding the thermocline and deepening the surface mixed layer. Within three days (between day 1.8 and 4.9) the surface mixed layer depth increased by 100% as shown in Figure 3-36. For the next few days (October 6 through 8) the wind again changed its direction from north-northwest to south (see Figure 3-35). This frequent change in wind direction of considerable strength would produce tremendous turbulent energy which penetrates deep into the water column. A permanent mixed layer depth of over 25 meters developed by October 8 near the Boston Buoy location as shown in Figure 3-36. After the complete mixing event, as observed in the data on October 9, 1999 (Figure 3-35) the model computed bottom temperature seemed to be about 1-1/2 degrees lower than the observed data. However, the model was able to reproduce the temperature 10m above the bottom very accurately, suggesting that the model was able to successfully reproduce the surface mixed layer.

SECTION 4

SUMMARY

4.1 CONCLUSIONS

This report presents the calibration of the Massachusetts and Cape Cod Bays Hydrodynamic model for the years 1998 and 1999. The focus of this effort was to calibrate an existing model to new environmental conditions, not to develop a new model. However, some modifications were made to the model to enhance its performance. In the course of model calibration, observations were made that the model computed very high temperatures in the surface layer during the warmer months of the year. In the original heat flux model, all of the short wave radiation entering the water column was absorbed in the top one percent of the water column which caused excessive heating. This prompted a modification to the heat flux code as described in Section 2.6. This modification allowed more short wave radiation to penetrate deeper into the water column. Thus, temperatures at the surface of the water column were reduced and the temperatures in the water column were more accurately reproduced. This was the only change made to the model during this study.

The calibration procedure was the same as was used by Signell during his 1992-1994 calibration of the hydrodynamic model although it differed somewhat from the procedure Signell (1996) used for the original 1989-1992 calibration. During the 1989-1992 calibration, Signell used the Gulf of Maine Model (GOMM) to specify the boundary conditions. Difficulties encountered with the GOMM when calibrating 1993-1994 prompted Signell to develop a new procedure for generating boundary conditions from data using the interpolation method described in Section 2.8. During that effort Signell also revisited the 1992 calibration and created a new three-year calibration for 1992-1994. Based on the availability of boundary data and the success of the 1992-1994 calibration effort, the interpolation method was chosen for the specification of boundary conditions for the 1998-1999 calibration study.

The calibrated model itself performs well overall. While day to day variability may not be fully reproduced, the model reproduces the seasonal trends observed in the data, as well as some of the short-term events. The model reproduces the temperature data to within 1.54°C based on the RMS error and the salinity data to within 0.83 ppt. The model does a fair job reproducing the current velocity data at the Boston Buoy and a very good job reproducing the data at the Scituate Buoy. Based on the analysis of the hydrodynamic model calibration, the following conclusions can be made:

- 1998 and 1999 are very different years in terms of temperature and salinity and provide a good test of the model's flexibility and applicability to year to year variations
- The available meteorological and river gage data were adequate to specify these inputs to the model

- The available MWRA, NMFS, and AFMIS/LOOPS/AOSN data were adequate to specify temperature, salinity and low frequency elevation changes at the boundary
- Modifications to the way solar insolation is distributed vertically in the water column improved the hydrodynamic model's ability to reproduce the temperature data
- The hydrodynamic model compared favorably to temperature, salinity and current data for both of the years 1998 and 1999 despite the differing conditions between the years in Massachusetts and Cape Cod Bays
- The current hydrodynamic model calibration should be adequate for use as input to the water quality model.

4.2 RECOMMENDATIONS

The Gulf of Maine has a large influence on what occurs within Massachusetts and Cape Cod Bays in terms of circulation, stratification, temperature and salinity. Therefore, specifying boundary conditions is an important part of reproducing conditions within the bays. It is recommended that additional data collection efforts be made at the northern boundary in the Gulf of Maine. These efforts can include sampling stations that are visited regularly, the placement of a buoy to measure currents, temperature and salinity, or a more coordinated effort with the sampling conducted by the NMFS. Further, the use of sea-surface data from satellite imagery could be used to help establish boundary data.

As Massachusetts and Cape Cod Bays experience a great deal of year to year variation, it is recommended that additional years be modeled.

SECTION 5

REFERENCES

- Beckmann, A. and D. B. Haidvogel, 1993. Numerical Simulation of Flow around a Tall Isolated Seamount. Part I: Problem Formulation and Model Accuracy, *J. Phys. Oceanogr.*, 23, 1736-753.
- Blumberg, A., R. Signell and H. Jenter, 1993. Modeling Transport Processes in the Coastal Ocean, *Journal of Environmental Engineering*, 1, 31-52.
- Blumberg, A. F. and D. M. Goodrich, 1990. Modeling of Wind-Induced Destratification in Chesapeake Bay, *Estuaries*, 13(3), 236-249.
- Blumberg, A. F. and L. H. Kantha, 1985. Open Boundary Condition for Circulation Models, *J. Hydraulic Engineering*, 111, 273-255.
- Blumberg, A. F. and G. L. Mellor, 1987. A Description of a Three-dimensional Coastal Model, 1-16, *Coastal and Estuarine Sciences*, Vol. 4. AGU, Washington, DC.
- Blumberg, A. F. and G. L. Mellor, 1987. A Description of a Three-Dimensional Coastal Ocean Circulation Model. In: Three-Dimensional Coastal Ocean Models, Coastal and Estuarine Sciences, Vol. 4, N. Heaps (Ed.), American Geophysical Union, Washington, D.C., 1-6.
- Casulli, V., 1990. Semi-Implicit Finite Difference Methods for the Two-dimensional Shallow Water Equations, *J. Computational Physics*, 86, 56-4.
- Galperin, B., L. H. Kantha, S. Hassid and A. Rosati, 1988. A Quasi-equilibrium Turbulent Energy Model for Geophysical Flows, *J. Atmosph. Sci.*, 45, 55-62.
- Geyer, W., G. Gardner, W. Brown, J. Irish, B. Butman, T. Loder and R. Signell, 1992. Physical Oceanographic Investigation of Massachusetts and Cape Cod Bays, Technical Report MBP-92-03, Massachusetts Bays Program, U.S. EPA Region I/Massachusetts Coastal Zone Management Office, Boston, Massachusetts, 1-497.
- Geyer, W. R. and J. Ledwell, 1994. Final Report: Massachusetts Bay Dye Study. Boston: Massachusetts Water Resources Authority. Report ENQUAD 1994-17, 1-39.

- Geyer, W. R. and R. P. Signell, 1992. A Reassessment of the Role of Tidal Dispersion in Estuaries and Bays. *Estuaries* 15: 97-108.
- Goodrich, D. M., W. C. Boicourt, P. Hamilton and D. W. Prichard, 1987. Wind-Induced Destratification in Chesapeake Bay, *J. Phys. Oceanogr.*, 17: 2232-2240.
- Goodrich, D. M., 1985. On Stratification and Wind-Induced Mixing in the Chesapeake Bay. Ph.D. thesis, Marine Sciences Research Center, State Univ. of New York, Stony Brook, NY.
- Grano, V. and D. W. Pritchard, 1982. A Study of Spatial Variations in the Non-Tidal Currents of the Upper Chesapeake Bay. Chesapeake Bay Institute, the Johns Hopkins Univ. PPRP-62. NTIS No. PB82-229550.
- HydroQual, Inc. and Normandeau, 1995. A Water Quality Model for Massachusetts and Cape Cod Bays: Calibration of the Bays Eutrophication Model, Boston: Massachusetts Water Resources Authority. Report ENQUAD 1995-08. 1-402.
- Irish, J.D. and R. P. Signell, 1992. Tides of Massachusetts and Cape Cod Bays. Woods Hole Oceanographic Institution. Tech. Report WHOI-92-35, 1-62.
- Large, W. G. and S. Pond, 1981. Open Ocean Momentum Flux Measurements in Moderate to Strong Winds, *J. Phys. Oceanogr.*, 11, 324-336.
- Lynch, D. and C. Naimie, 1993. The M2 Tide and its Residual on the Outer Banks of the Gulf of Maine, *J. Phys. Oceanogr.*, 23, 2222-2253.
- Martin, P.J., 1985. Simulation of the Mixed Layer at Ows November and Papa with Several Models, *J. Geophys. Res.*, 90 (C0), 903-916.
- Mellor, G. and T. Yamada, 1982. Development of a Turbulence Closure Model for Geophysical Fluid Problems, *Rev. Geophys. Space Phys.*, 20, 851-875.
- Menzie-Cura & Associates, 1991. Sources and Loadings of Pollutants to Massachusetts Bay. Task 1 of the Massachusetts Bays Program. Prepared for the Massachusetts Bay Program, Massachusetts Coastal Zone Management/U.S. EPA. Technical Report No. MBP-91-01.

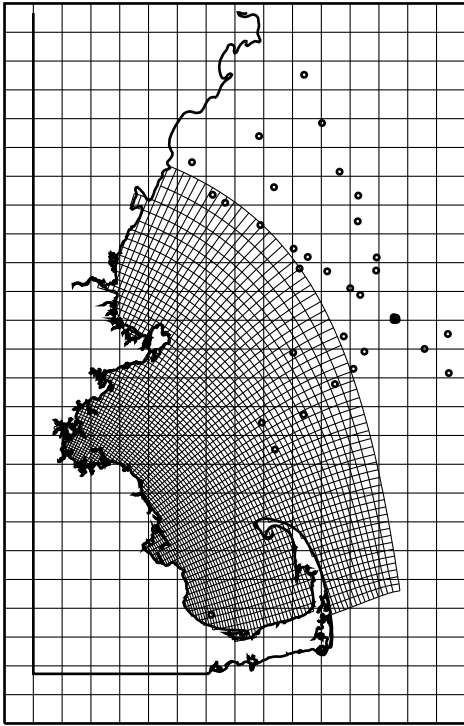
- M.W R.A., 1988. Final Secondary Treatment Facilities Plan, Technical report, MWRA.
- Noble, M. A., W. W. Schroeder, W. J. Wiseman, Jr., H. F. Ryan and G. Gelfenbaum, 1996. Subtidal Circulation Patterns in a Shallow, Highly Stratified Estuary: Mobile Bay, Alabama. *Journal of Geophysical Research* 96: 25689-25703.
- Okubo, A., 1971. Oceanic Diffusion Diagrams. *Deep-Sea Research* 18:789-802.
- Rosati, A. and K. Miyakoda, 1988. A General Circulation Model for Upper Ocean Simulation, *J. Phys. Oceanogr.*, 18, 11.
- Ruzecki, E. and D. Evans, 1985. Temporal and Spatial Sequencing of Destratification in a Coastal Plain Estuary, in M. Bowman, W. Peterson, and C. Yentsch, eds. Tidal Mixing and Plankton Dynamics. New York: Springer-Verlag, Lecture Notes on Coastal and Estuarine Studies. Volume 19.
- Schroeder, W. W., J. R. Pennock and W. J. Wiseman, Jr., 1990. Salinity Stratification in a River-Dominated Estuary. *Estuaries*, 13, 145-154, 1990.
- Shapiro, R., 1975. Linear Filtering, *Mathematics of Computation*, 29, 1094-1097.
- Signell, R. P., 1989. Tidal Dynamics and Dispersion Around Coastal Headlands, Ph. D. Thesis, Woods Hole Oceanogr. Inst./Mass. Inst. of Technol. Joint Program in Oceanography, Cambridge, Mass., 1-159.
- Signell, R. P., H. L. Jenter, and A. F. Blumberg, 1996. Circulation and Effluent Dilution Modeling in Massachusetts Bay: Model Implementation, Verification and Results, U.S. Geological Survey Open File Report 96-015.
- Signell, R. P., 1994. Modeling the Seasonal Circulation in Massachusetts Bay, In *Estuarine and Coastal Modeling*, Proceedings of the 3rd International Conference, edited by M. L. Spaulding, 578-590. American Society of Civil Engineers, ASCE, New York.
- Signell, R. P. and B. Butman, 1992. Modeling Tidal Exchange and Dispersion in Boston Harbor, *Journal of Geophysical Research*, 97, 15,591-16, 606.
- Simpson, J.J. and T. D. Dickey, 1981. The Relationship Between Downward Irradiance and Upper Ocean Structure, *J. Phys. Oceanogr.*, 11, 309-323. Smagorinsky, J., 1963. General Circulation Experiments with the Primitive Equations I. The Basic Experiment, *Monthly Weather Review*, 91, 99-164.

- U.S.E.P.A., 1993. Assessment of Potential Impact of the MWRA Outfall on Endangered Species, Technical report, EPA Region 1, JFK Federal Building, Boston, Massachusetts 02203.
- Vermersch, J., R. Beardsley and W. Brown, 1979. Winter Circulation in the Western Gulf of Maine: Part 2. Current and Pressure Observations, *J. Phys. Oceanogr.*, 9, 786-784.
- Wang, D.P., 1979. Wind Driven Circulation in the Chesapeake Bay, Winter 1975. *J. Phys. Oceanogr.*, 9, 564-572.
- Weisberg, R., 1976. The Nontidal Flow in the Providence River of Narragansett Bay: a Stochastic Approach to Estuarine Circulation. *J. Phys. Oceanogr.*, 8, 225-232.
- Weller, R., D. Rudnick and N. J. Brink, 1995. Meteorological variability and air-sea fluxes at a closely spaced array of surface moorings, *J. Geophys. Res.*, 100, 4867-4883.

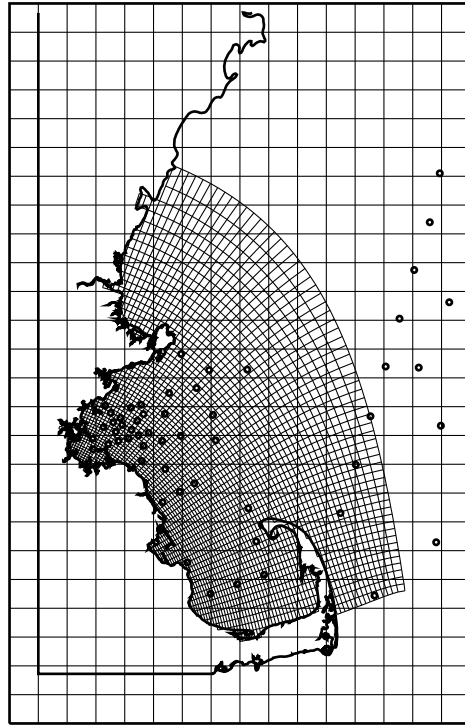
APPENDICES

APPENDIX A
Boundary Condition Data
Station Locations

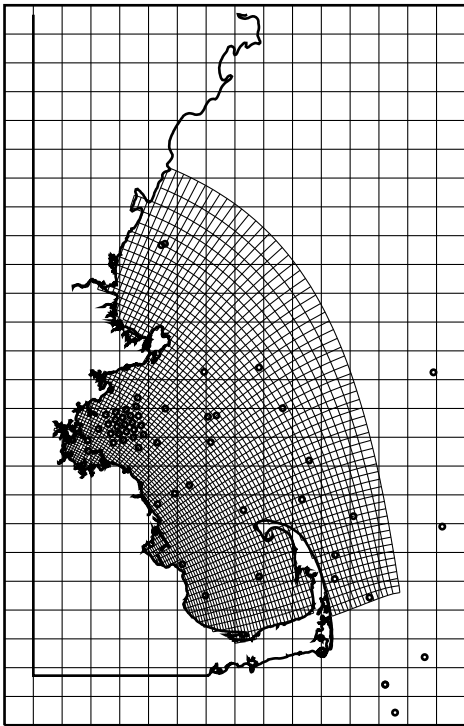
January, 1998



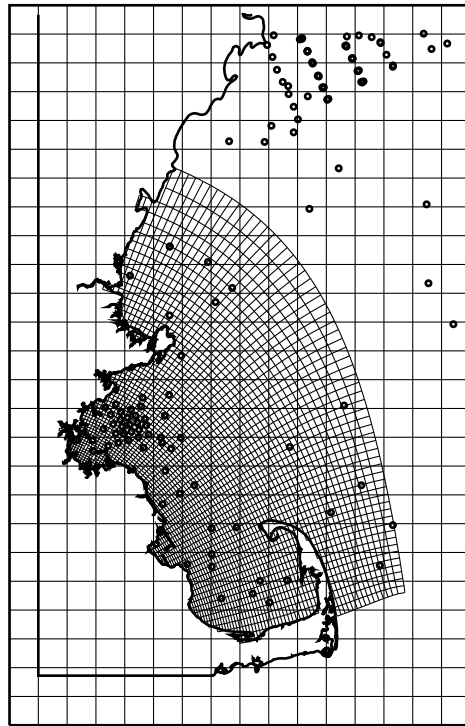
February, 1998



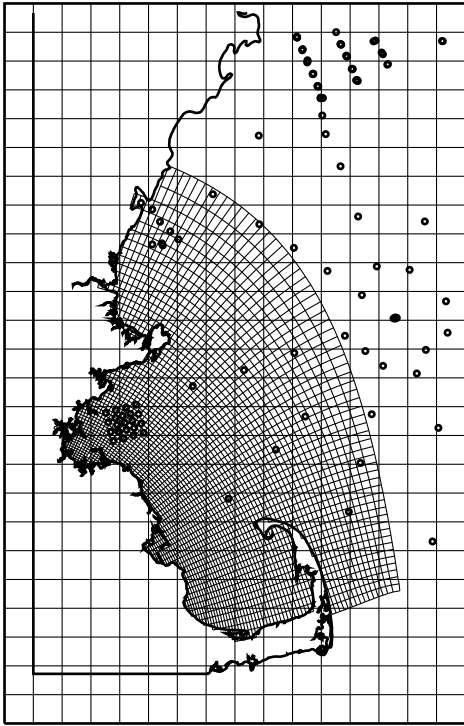
March, 1998



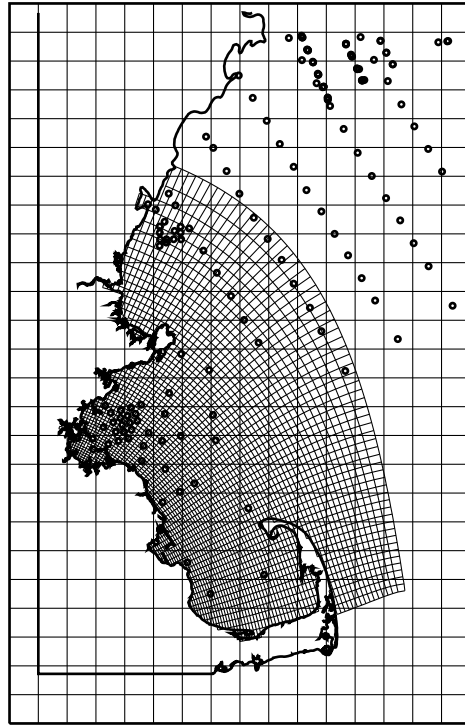
April, 1998



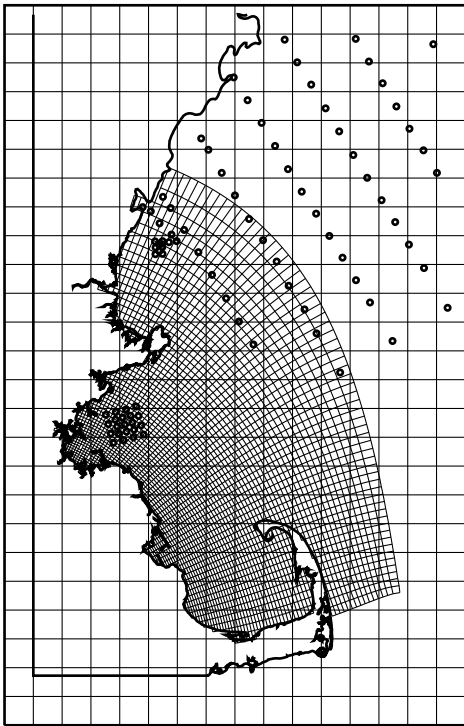
May, 1998



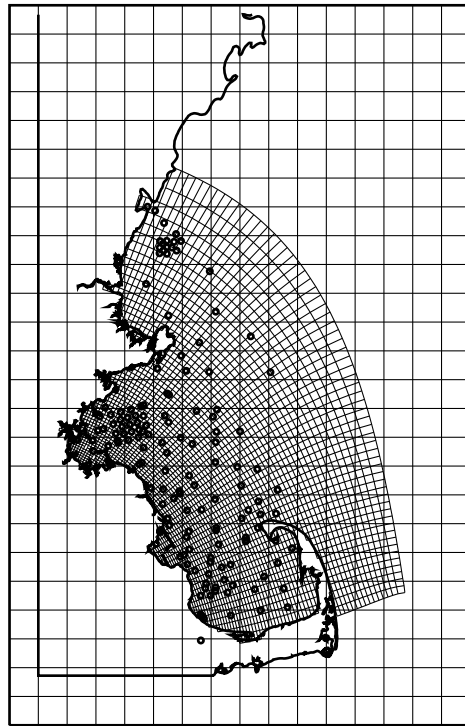
June, 1998



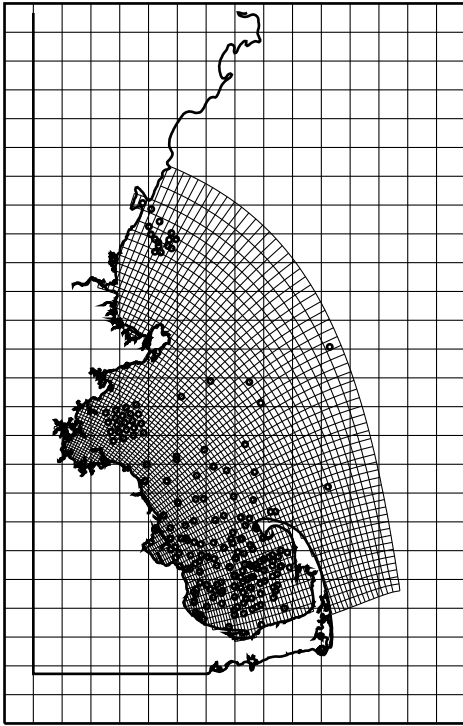
July, 1998



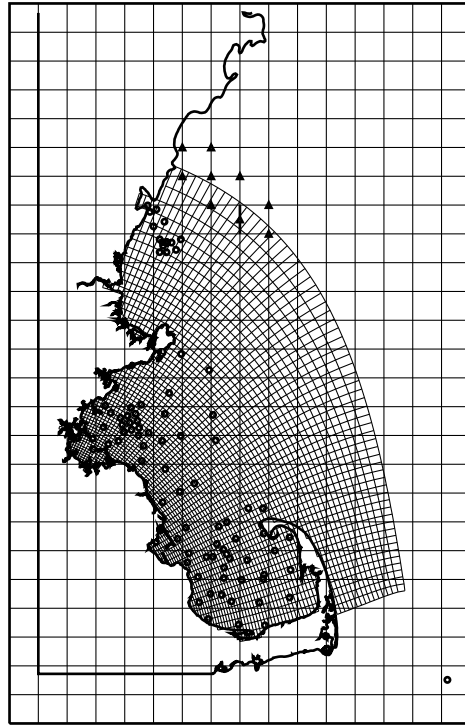
August, 1998



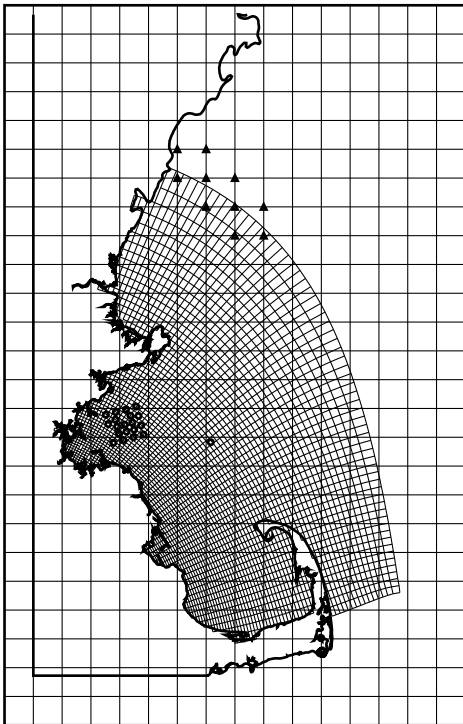
September, 1998



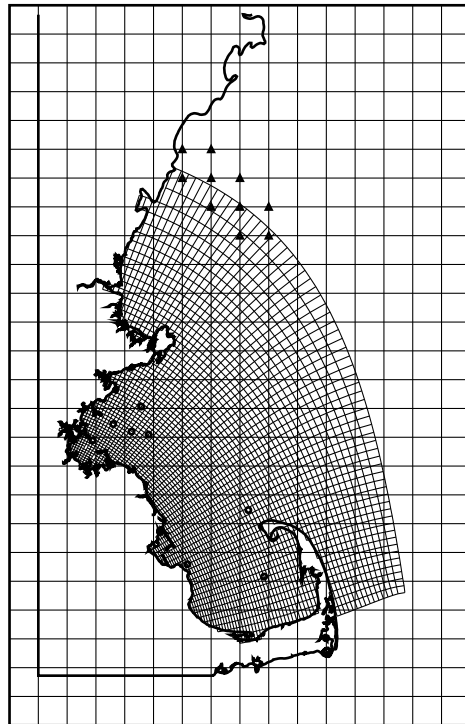
October, 1998



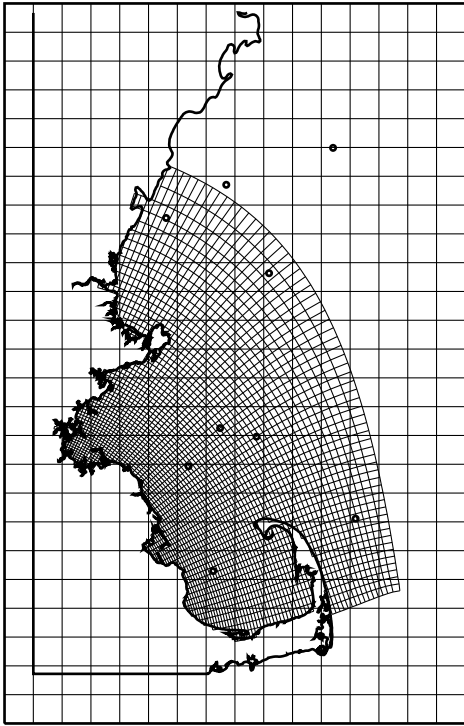
November, 1998



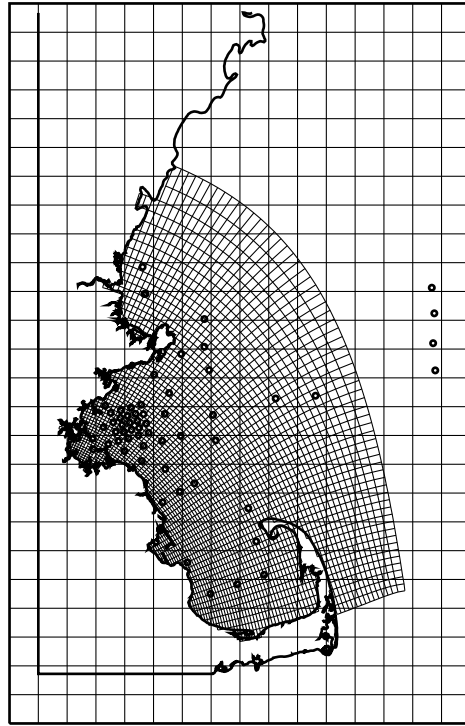
December, 1998



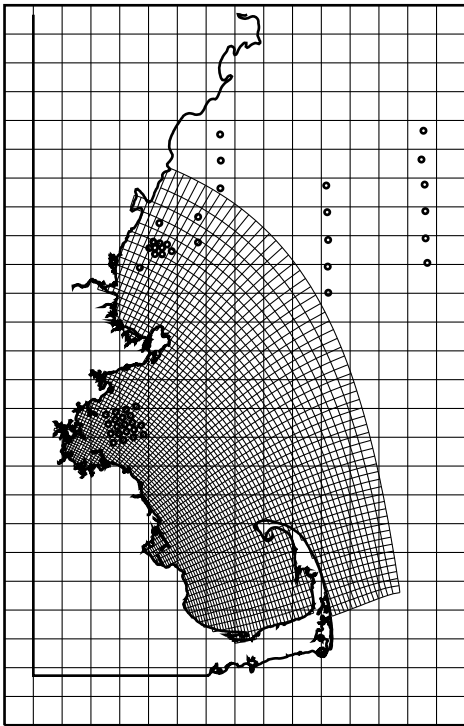
January, 1999



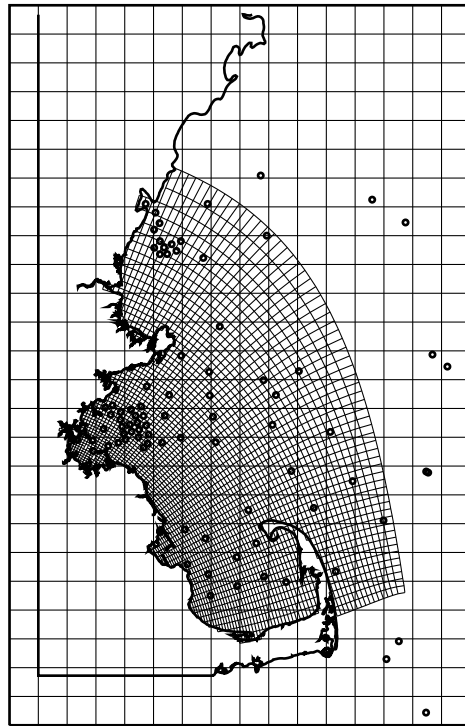
February, 1999



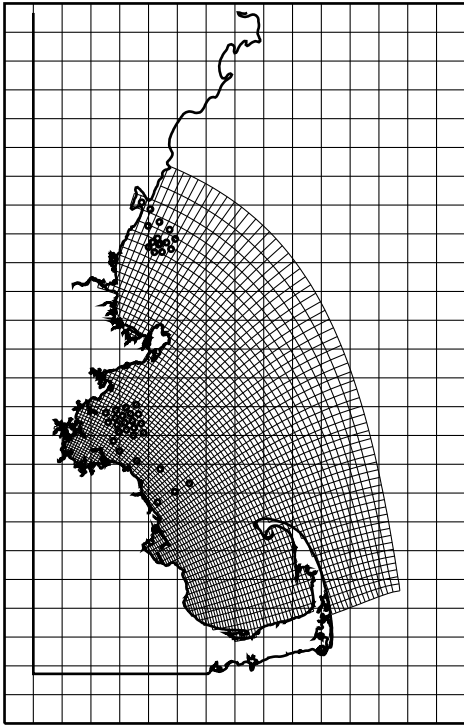
March, 1999



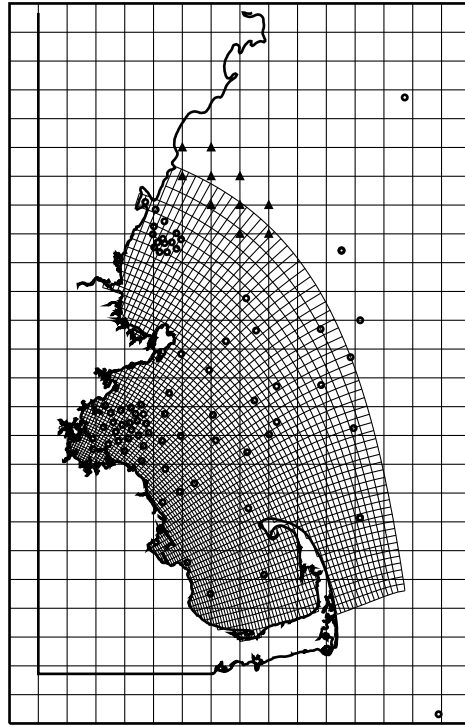
April, 1999



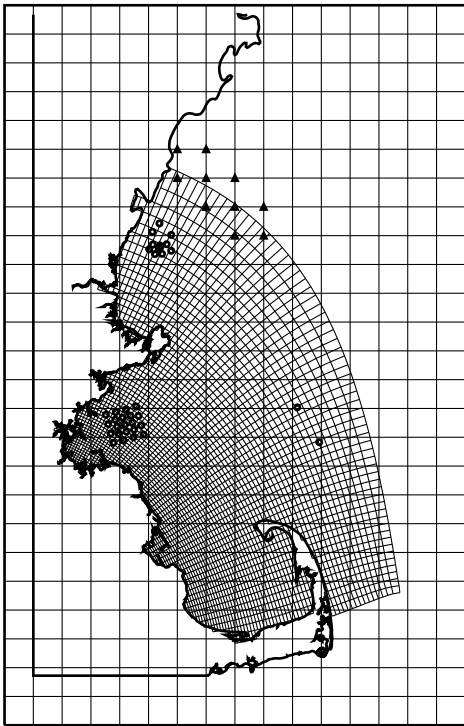
May, 1999



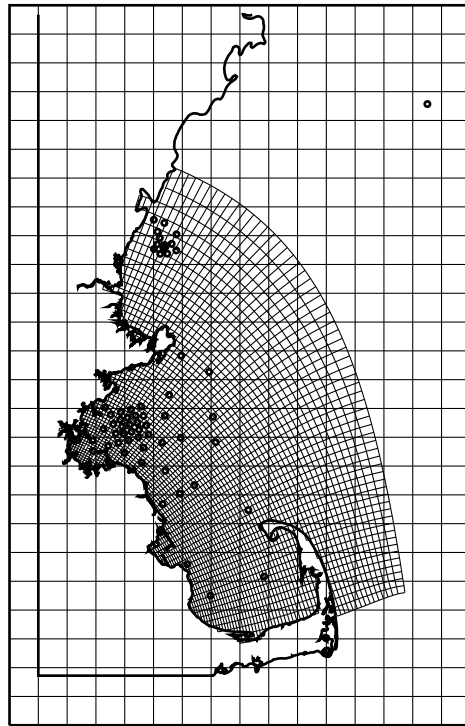
June, 1999



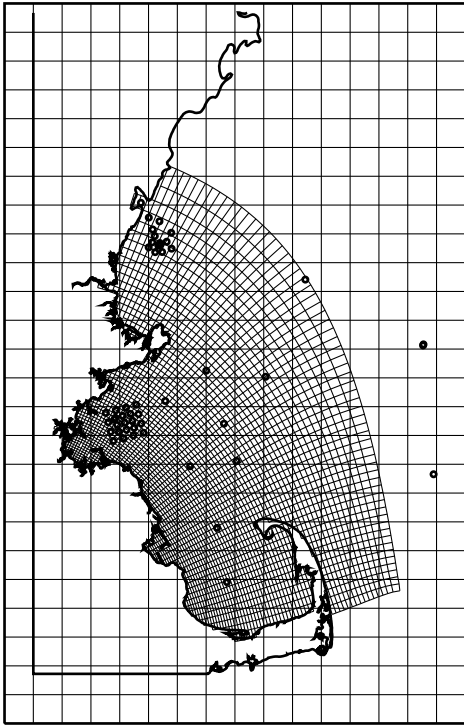
July, 1999



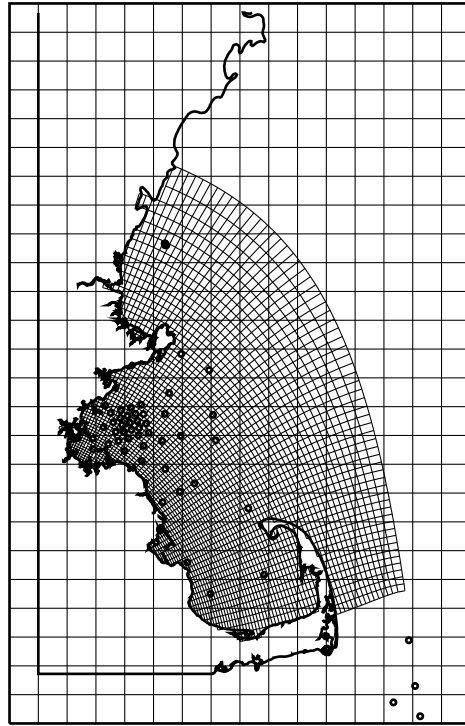
August, 1999



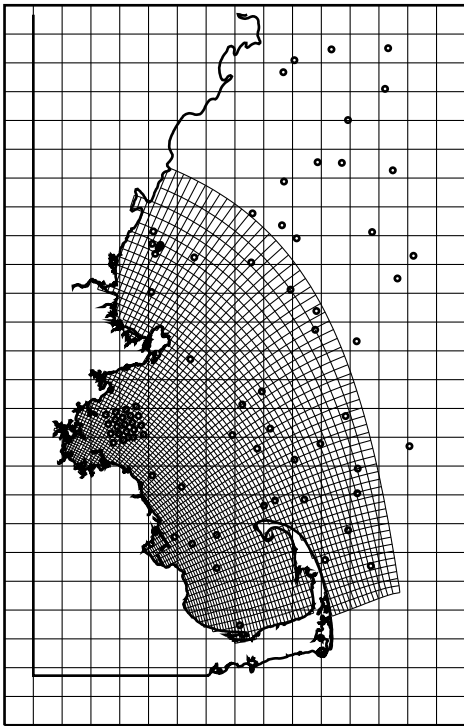
September, 1999



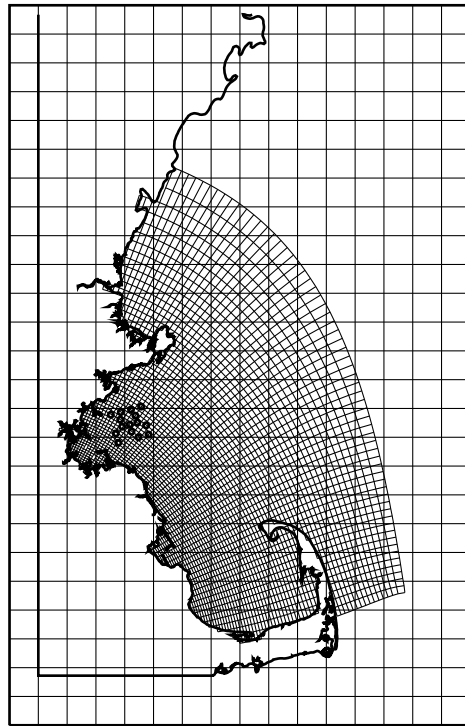
October, 1999



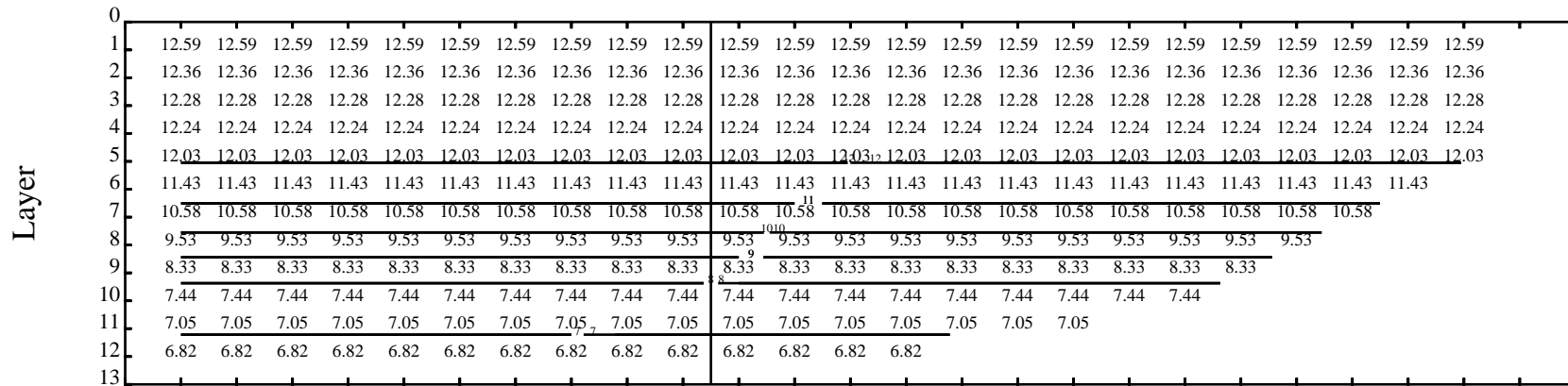
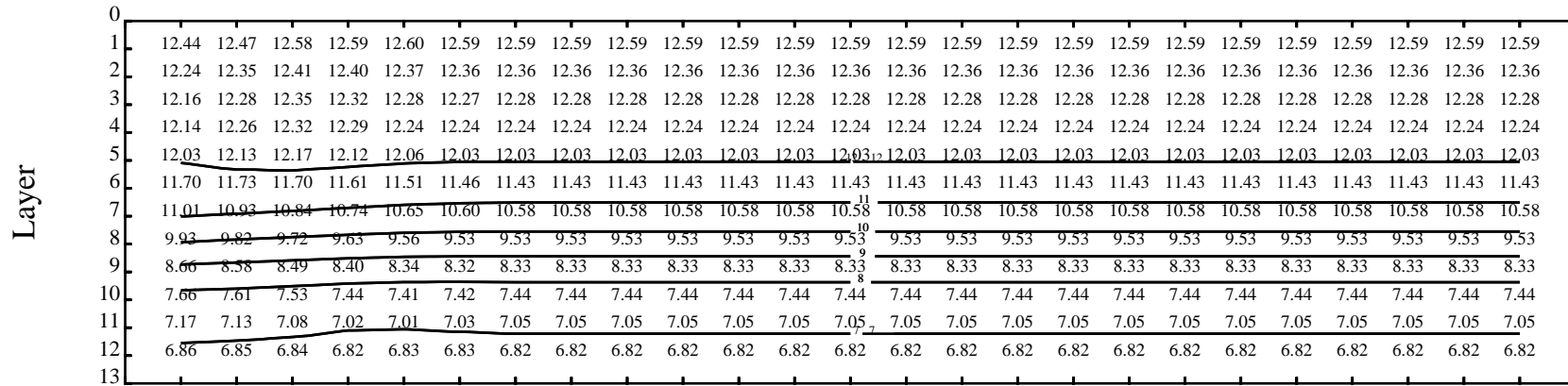
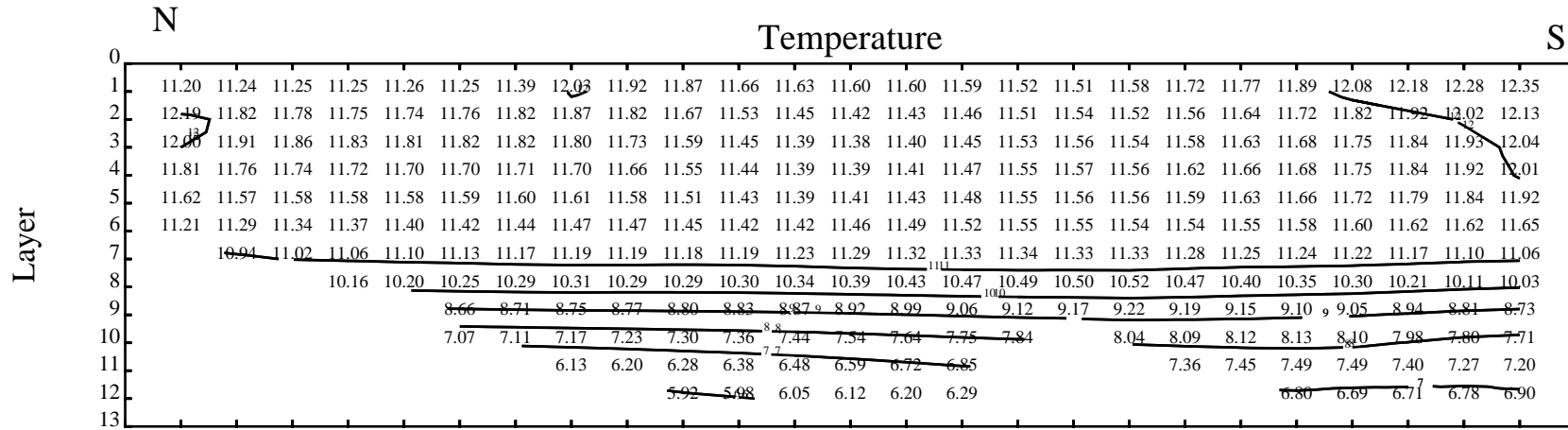
November, 1999

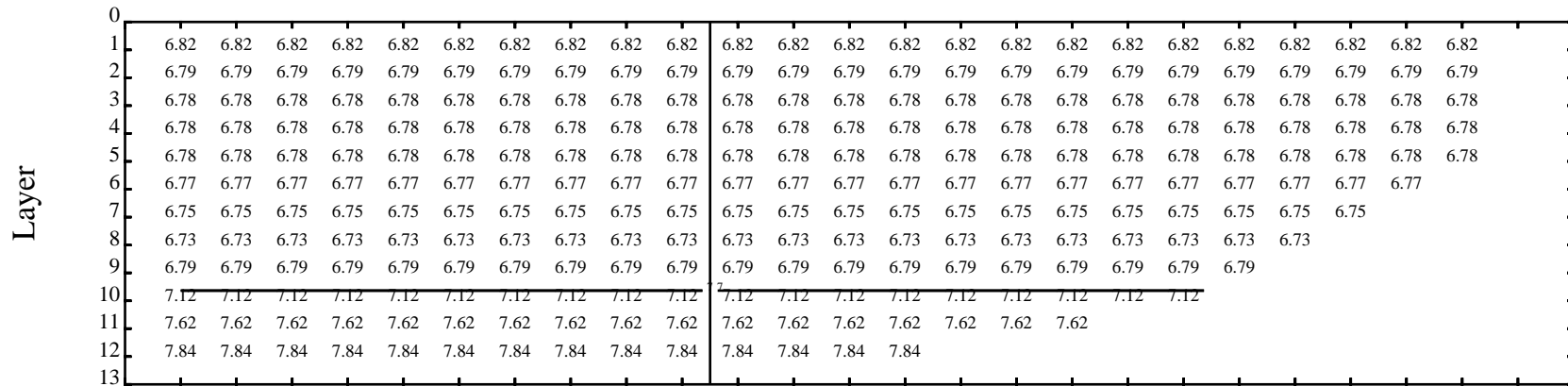
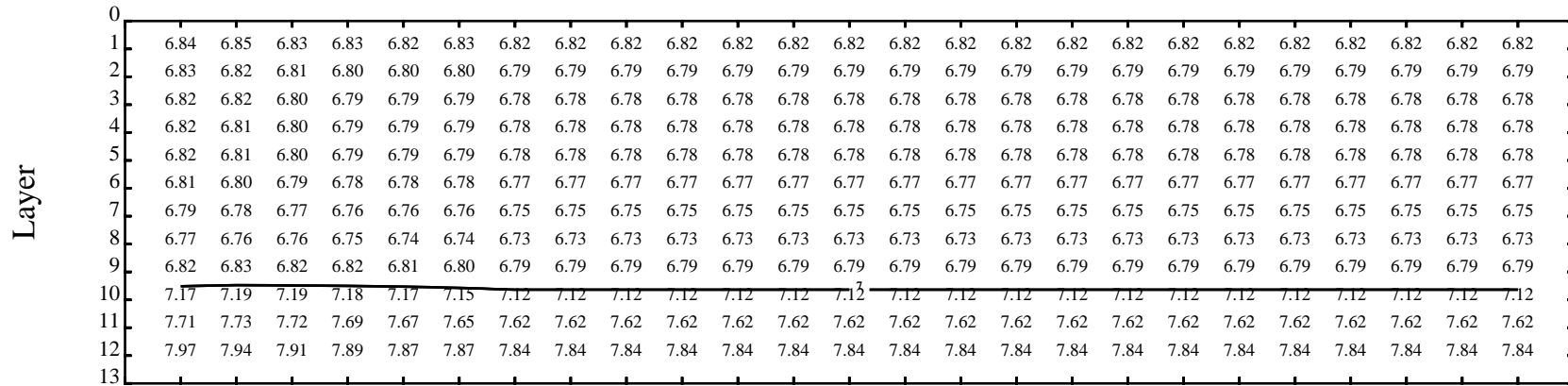
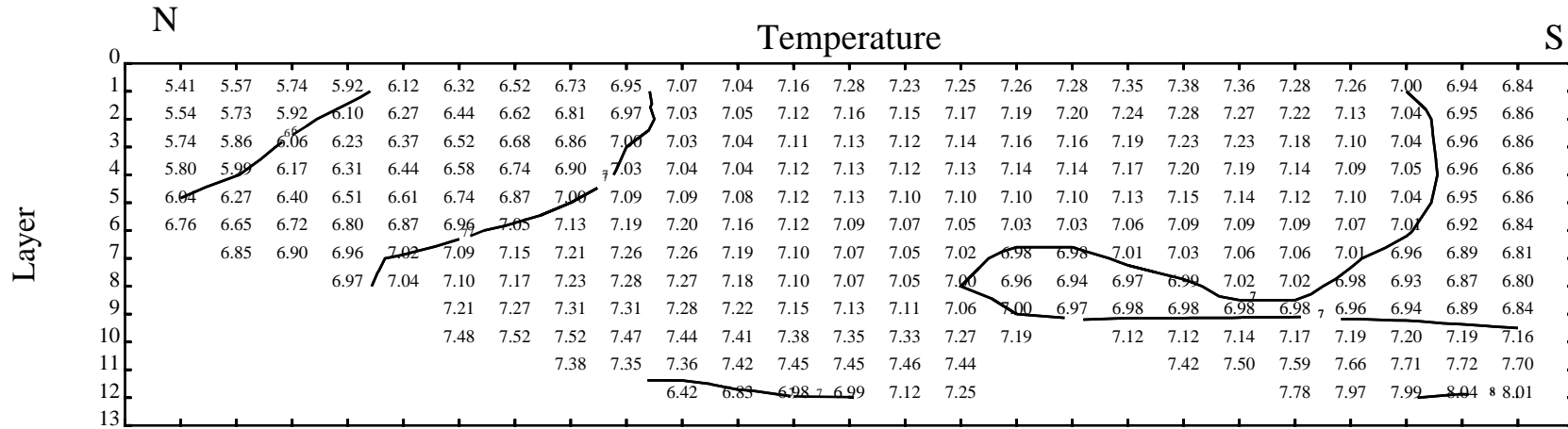


December, 1999

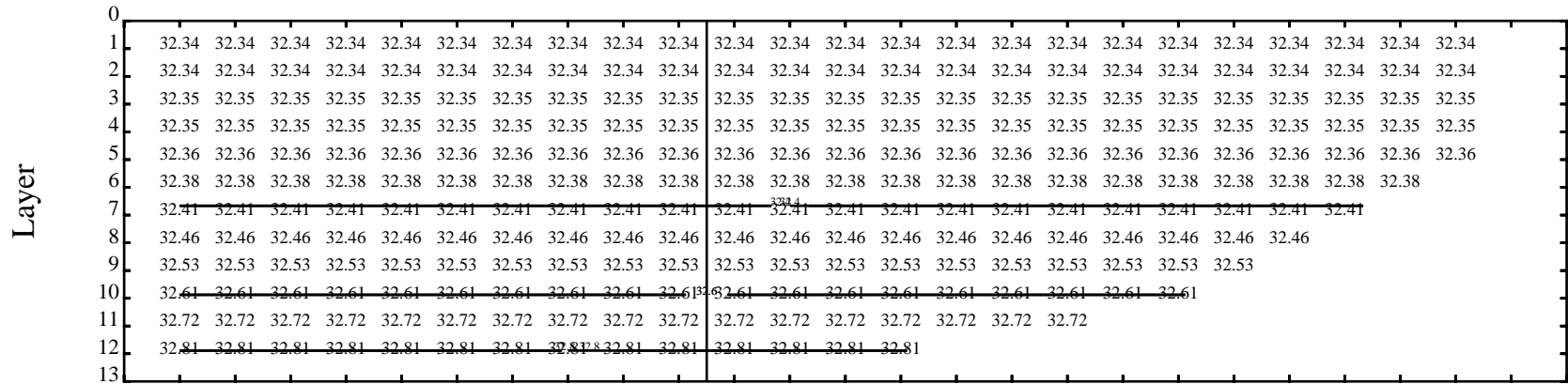
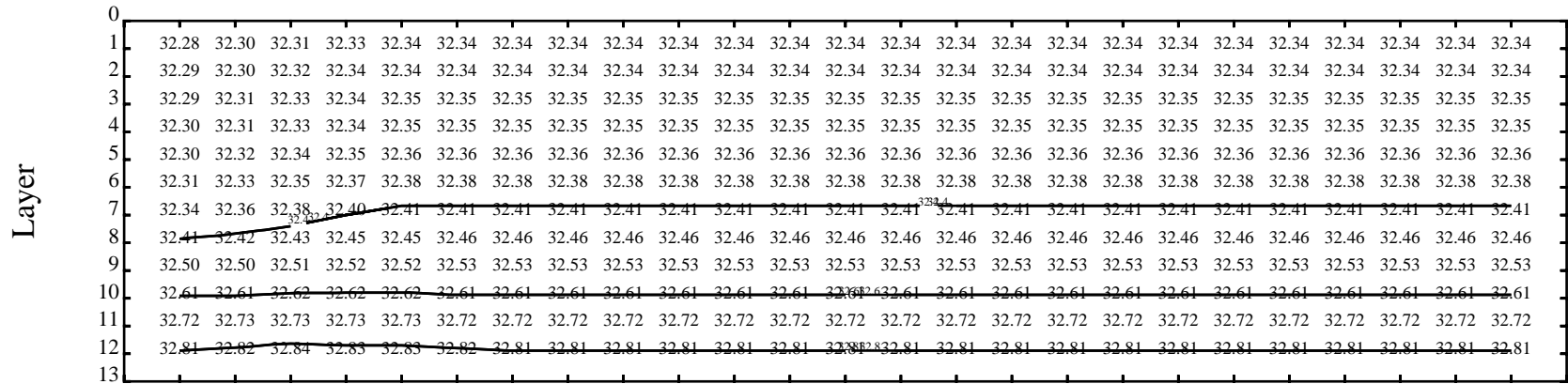
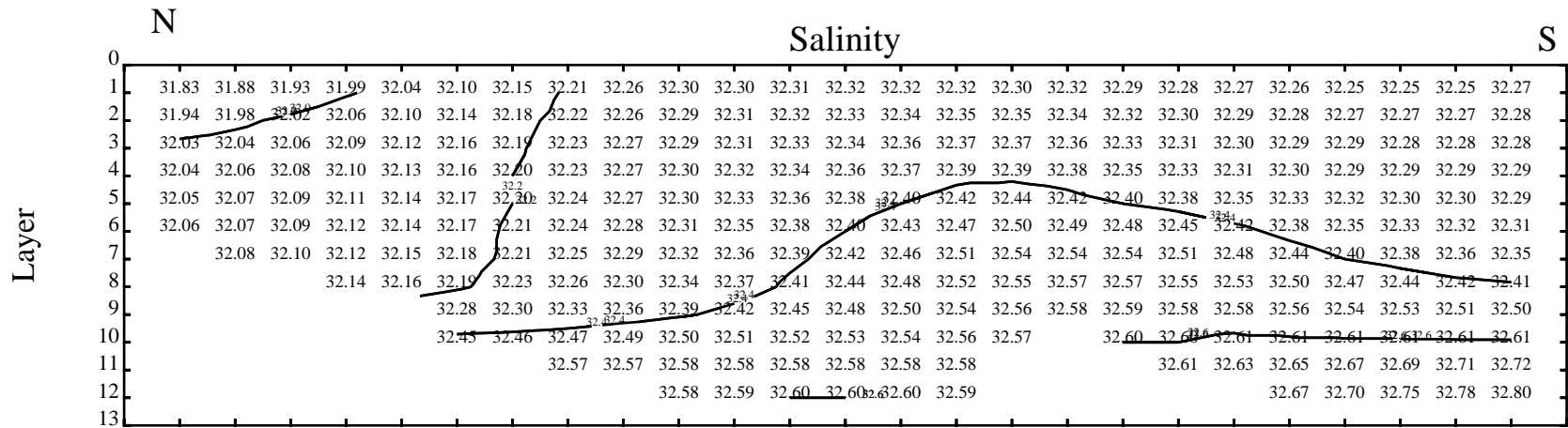


APPENDIX B
Boundary Condition Inputs for
Temperature and Salinity

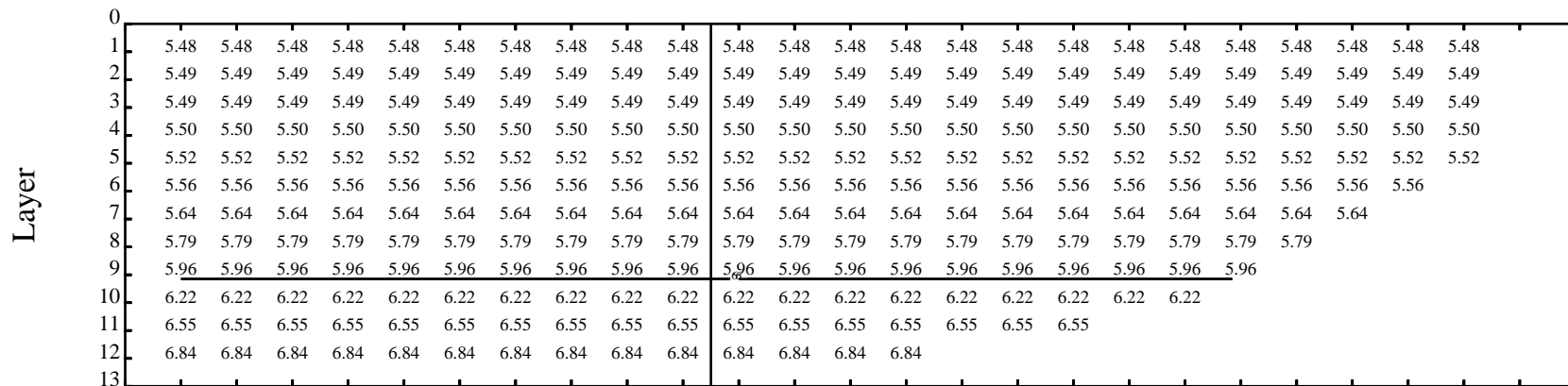
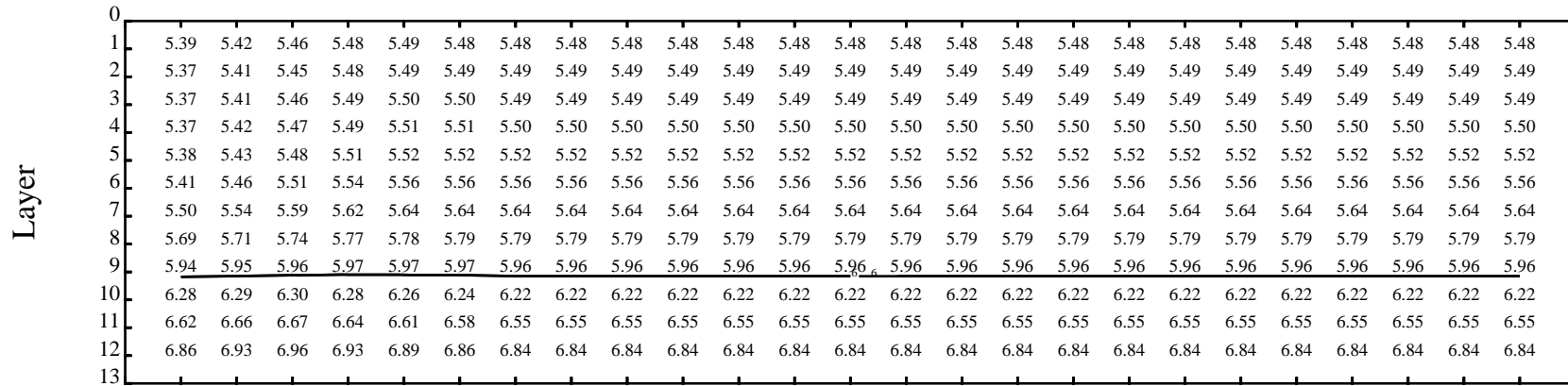
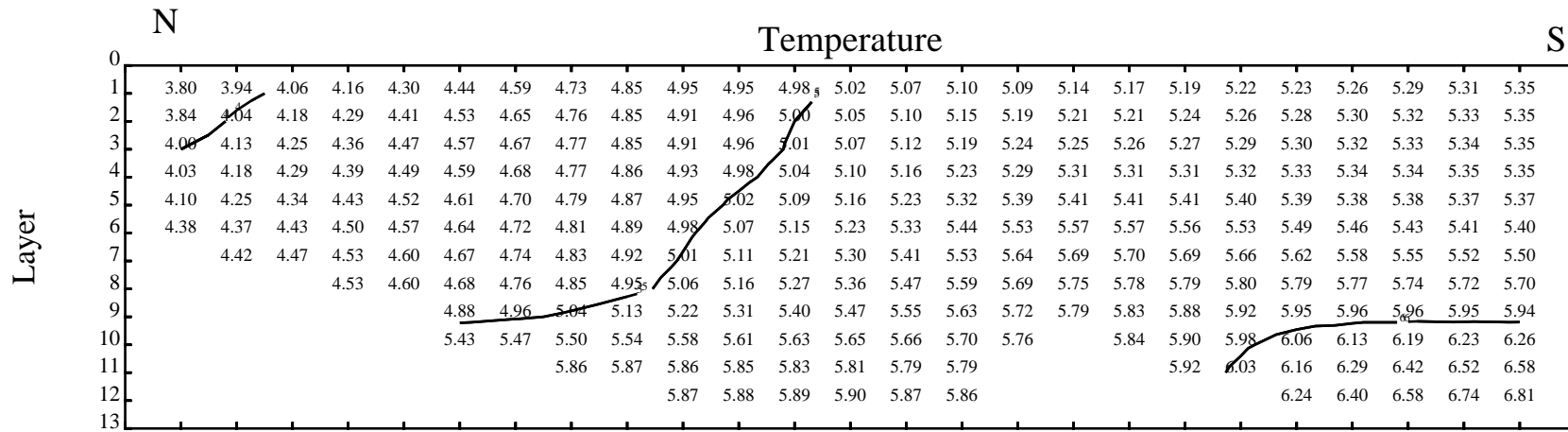


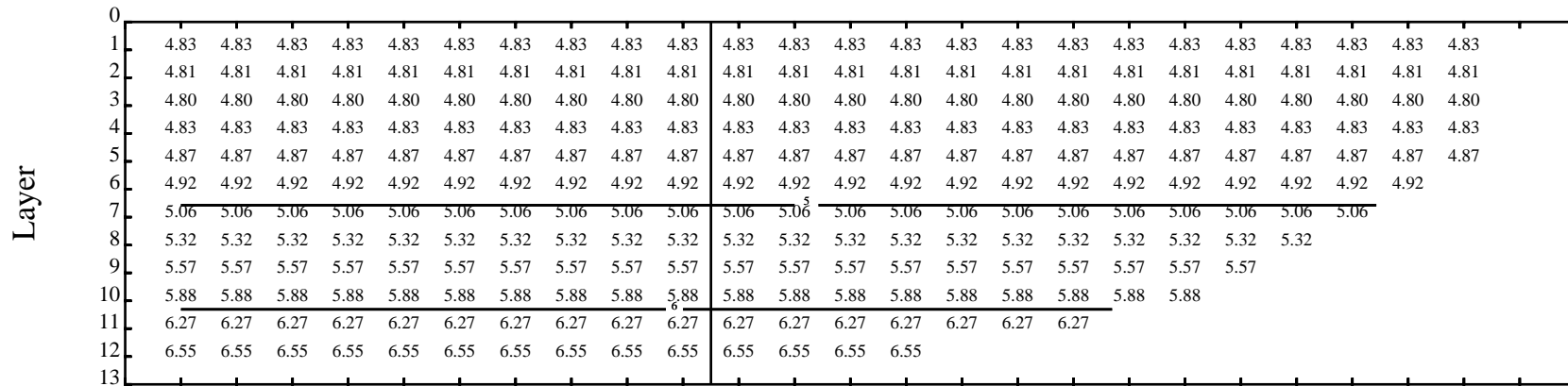
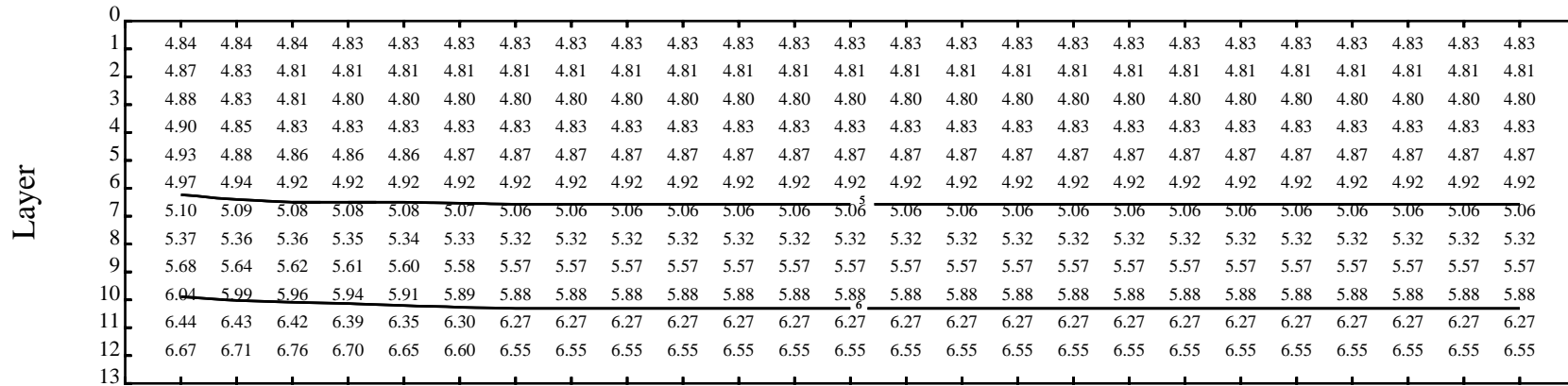
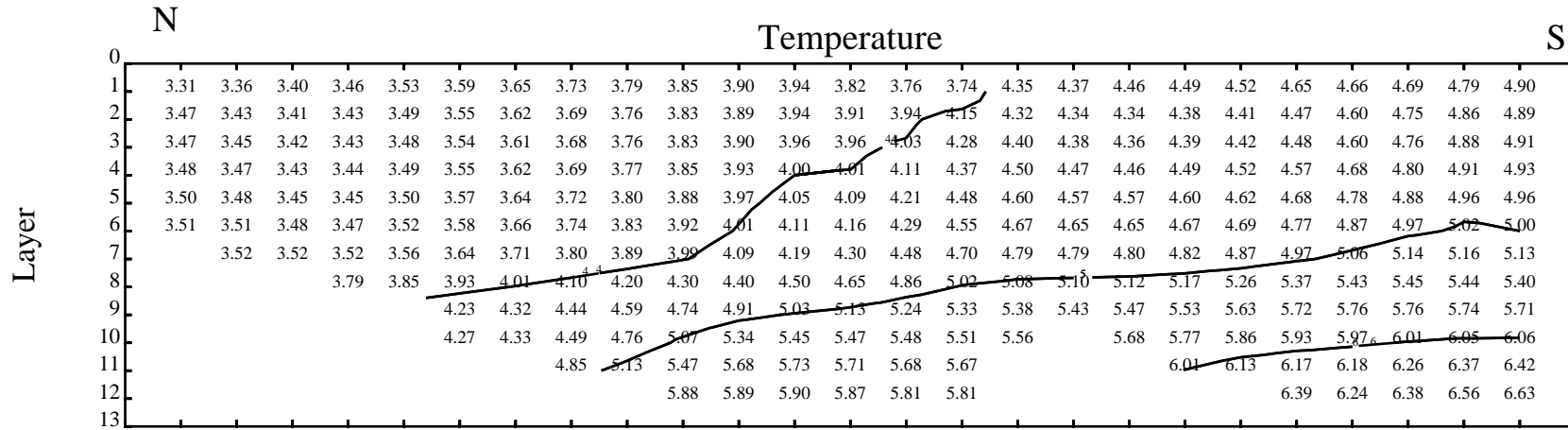


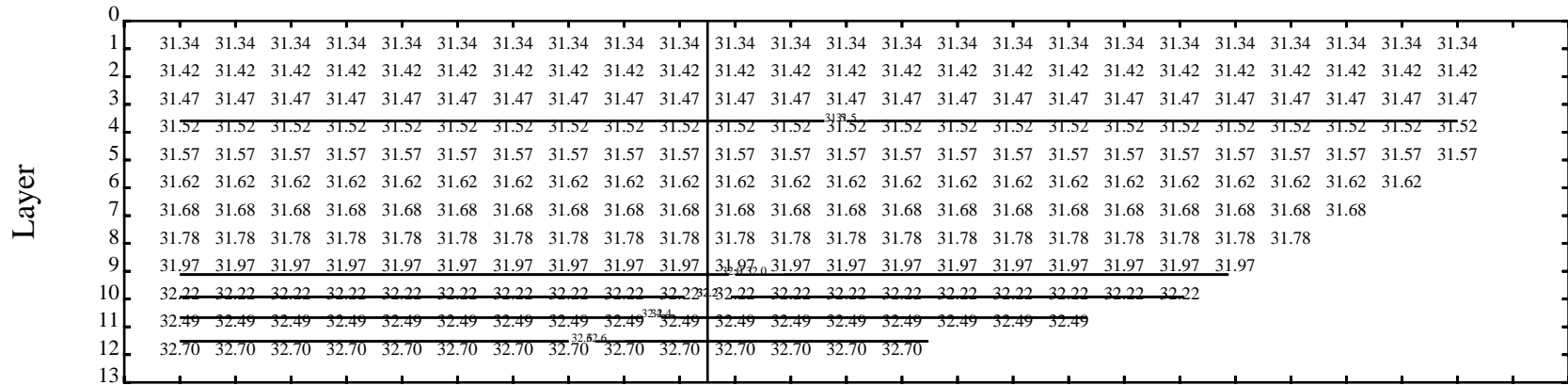
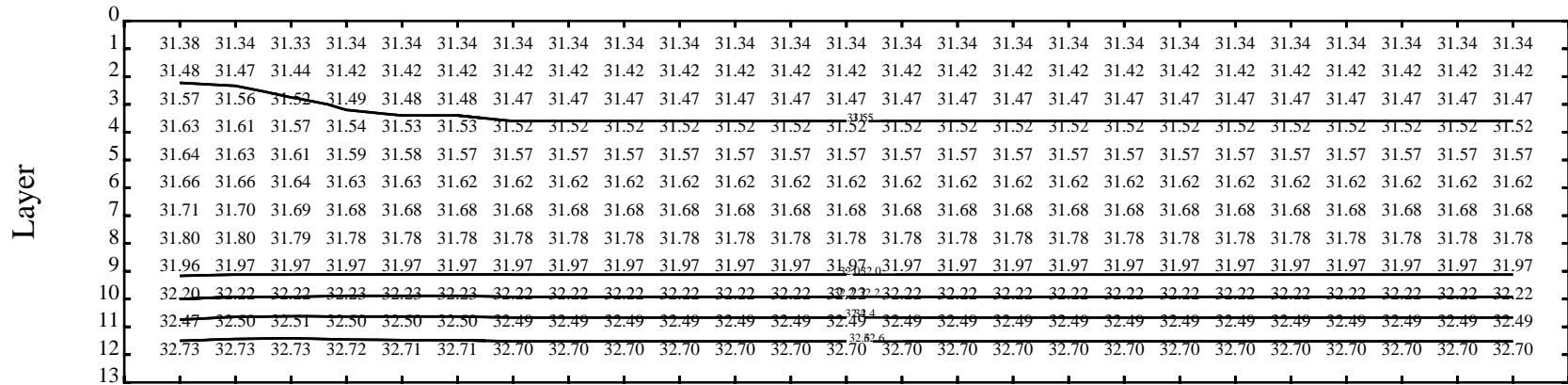
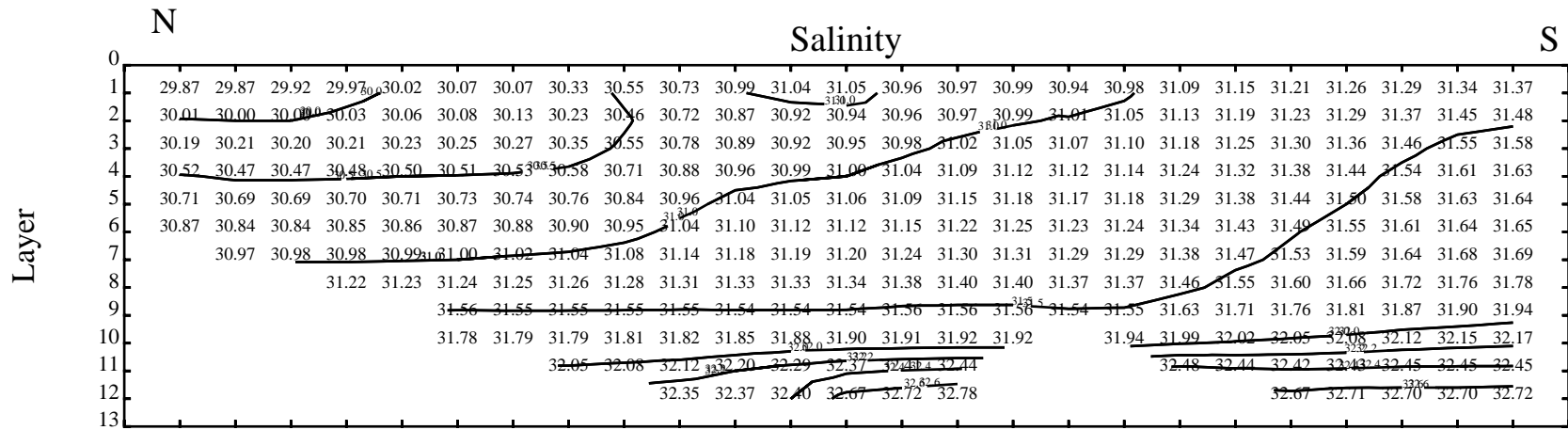
BC Time 4



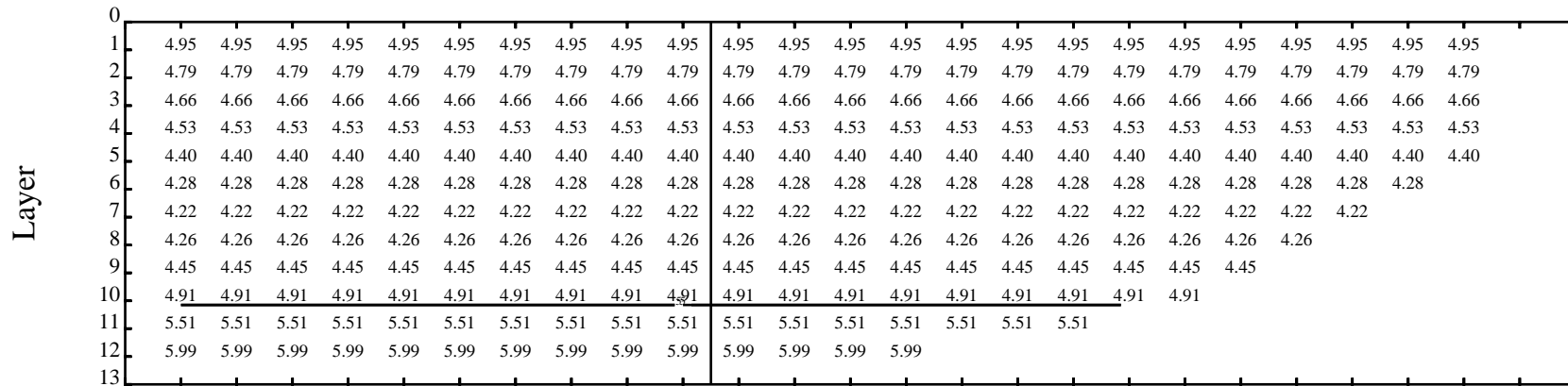
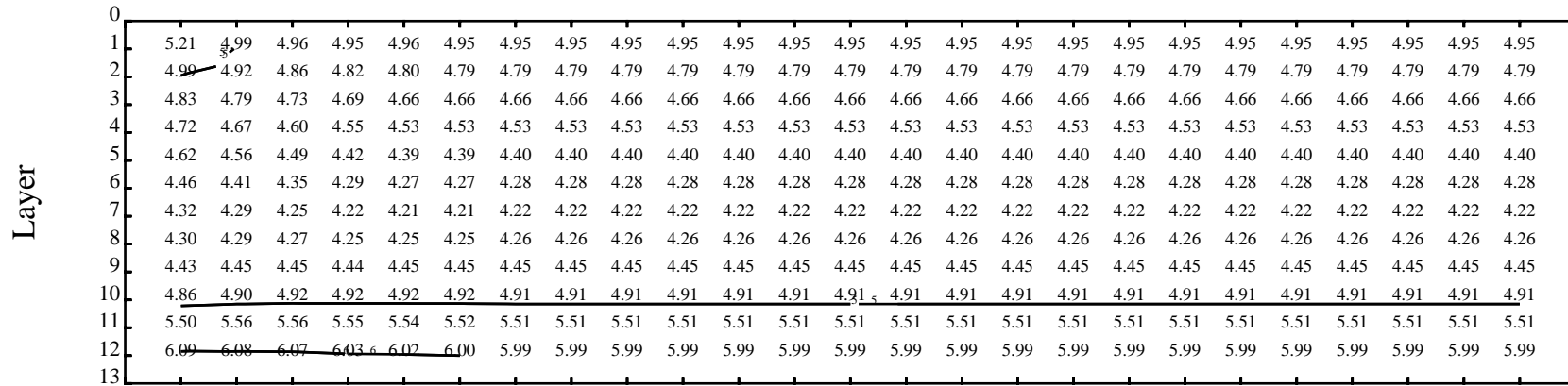
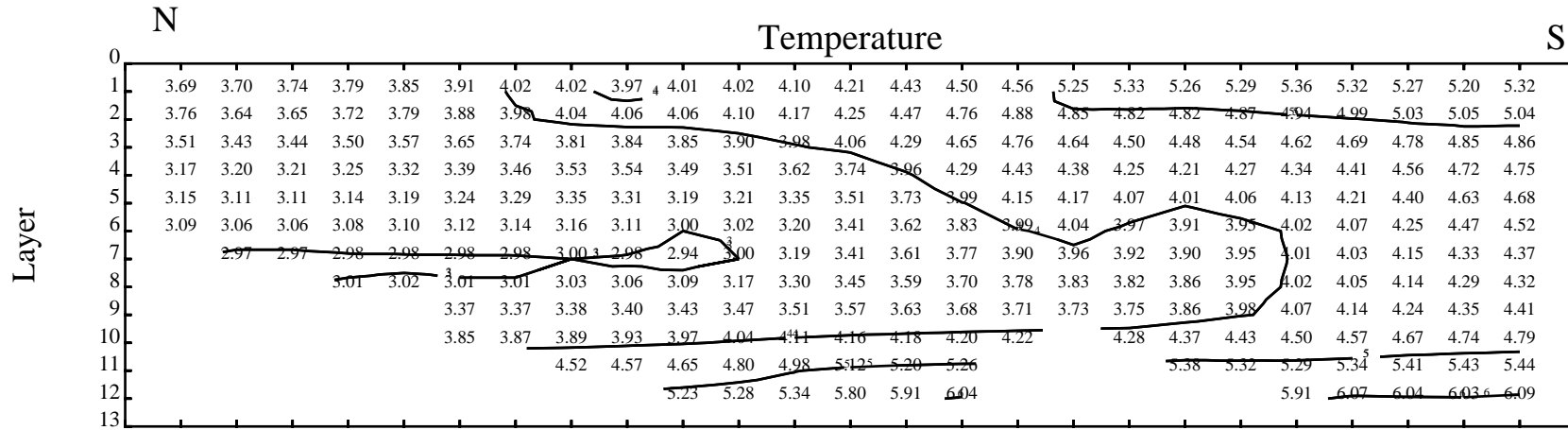
BC Time 5

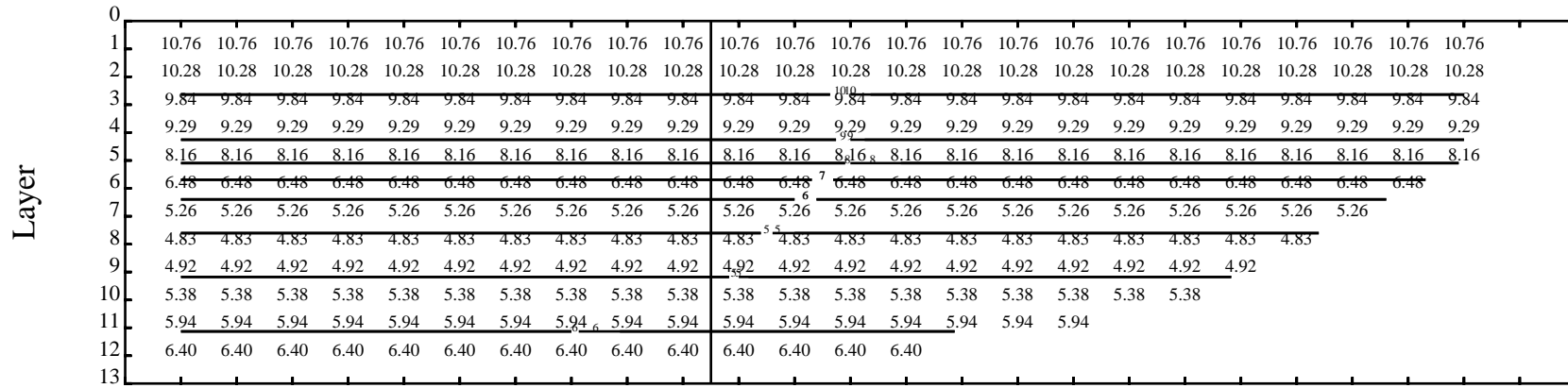
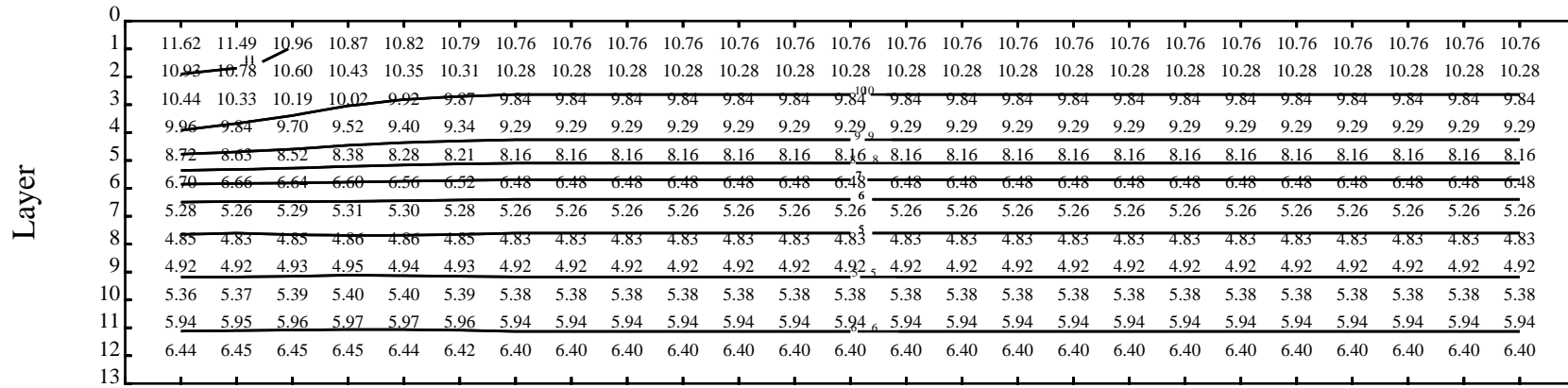
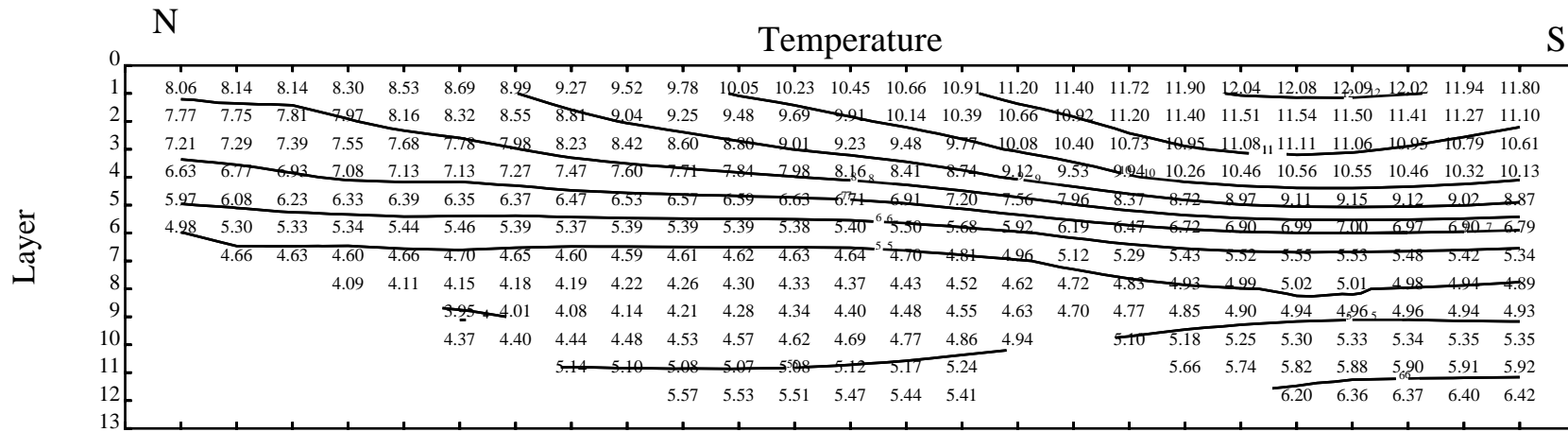






BC Time 7

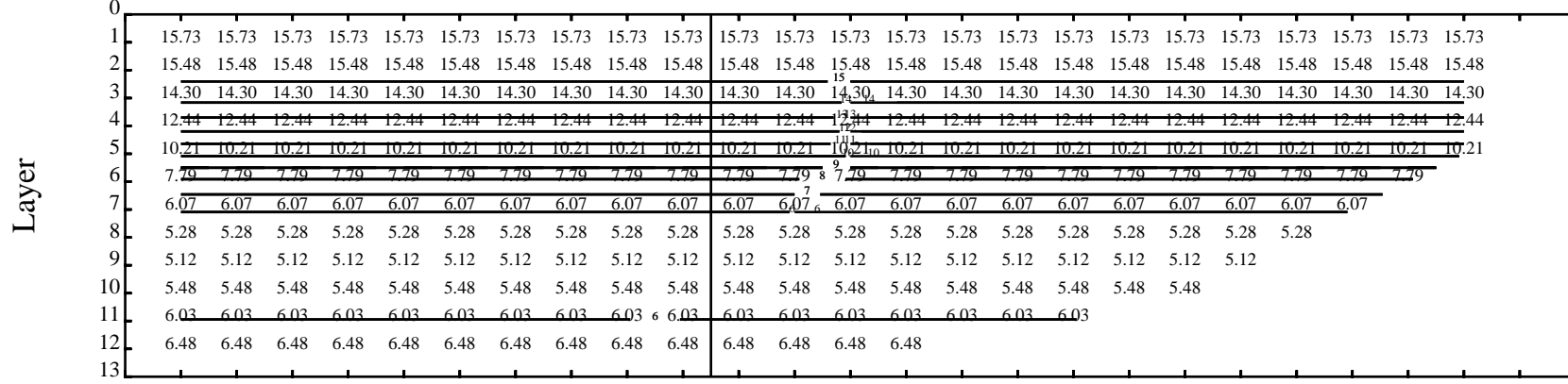
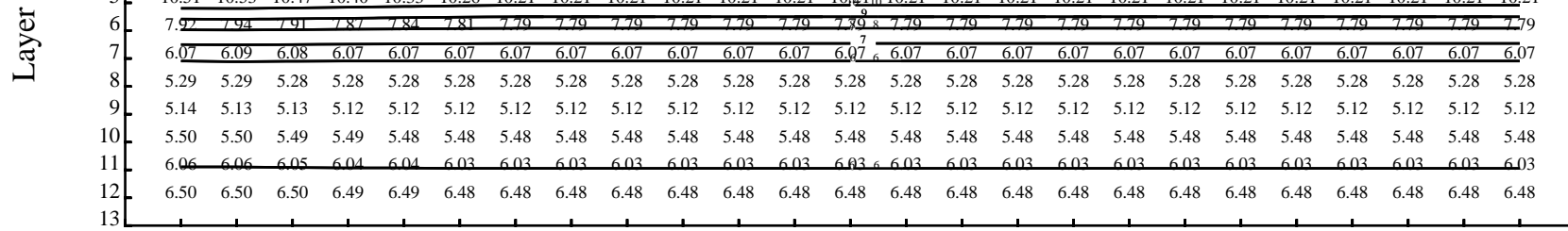
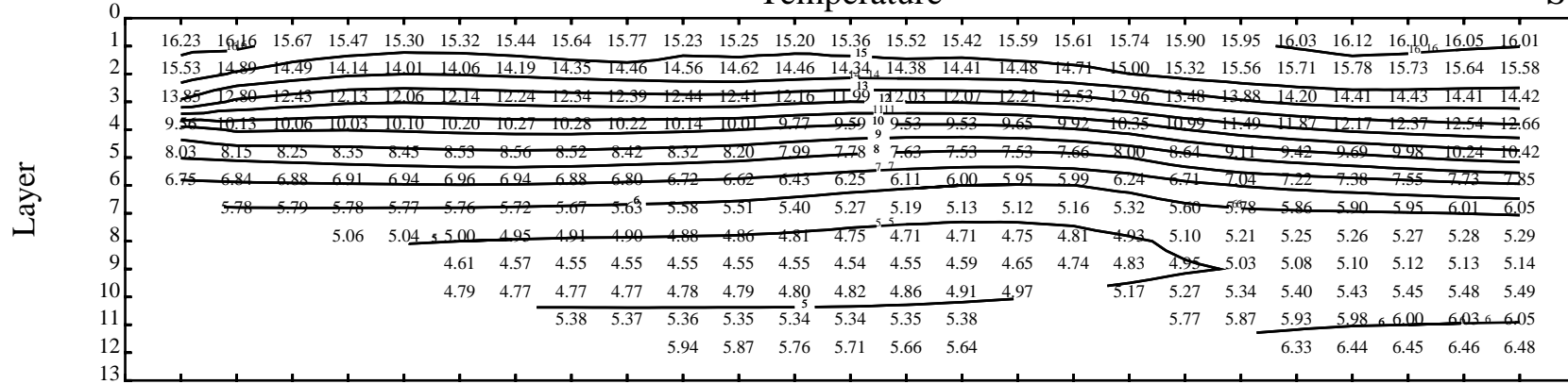


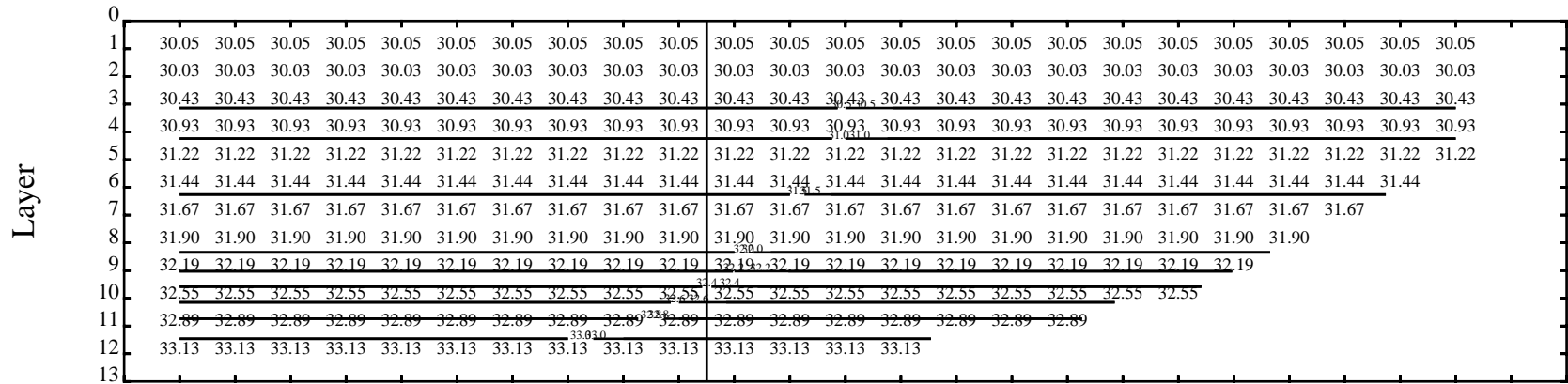
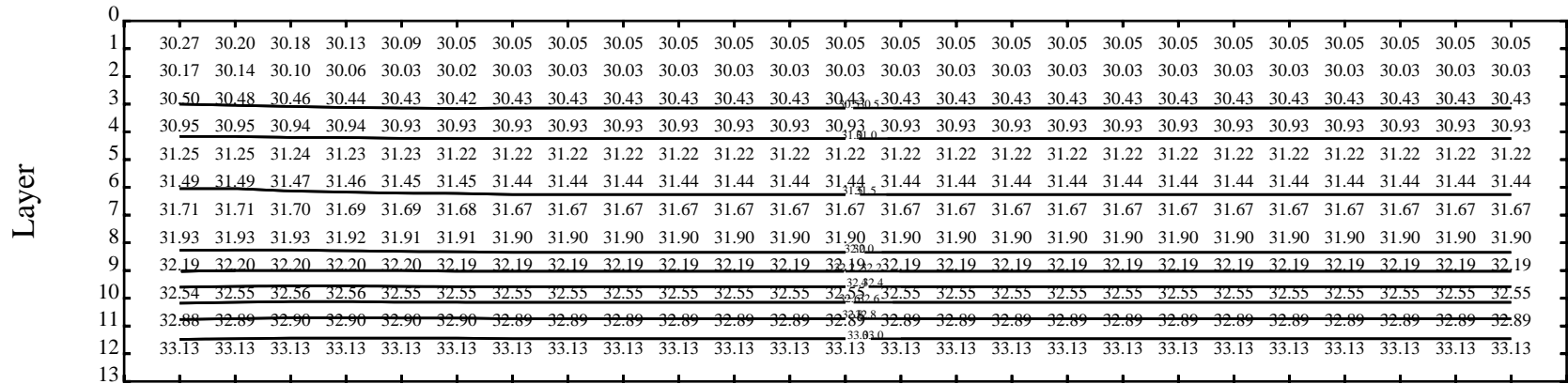
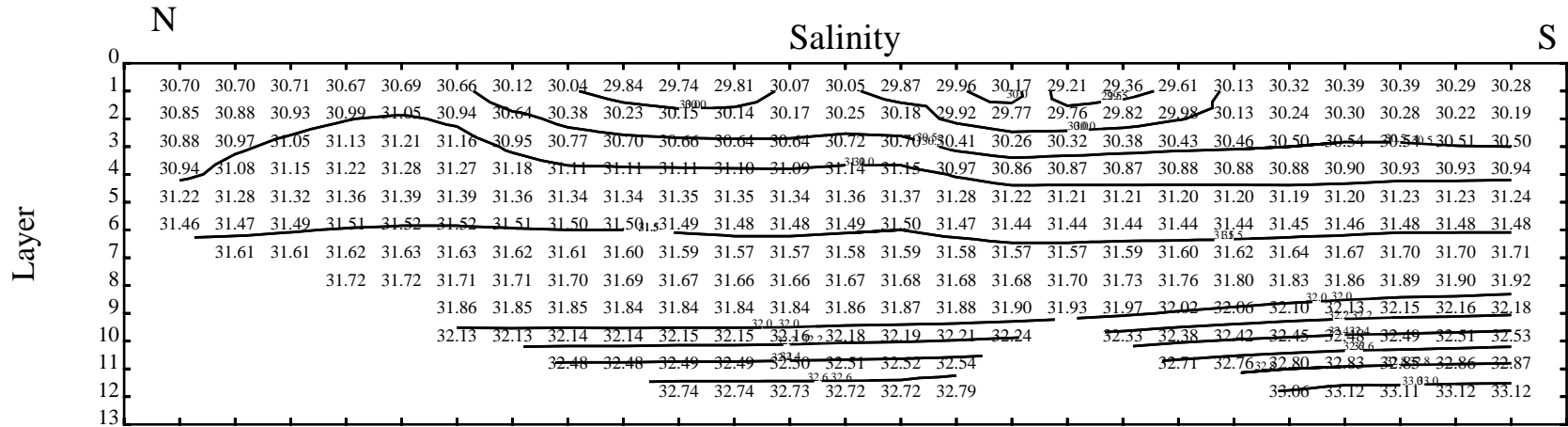


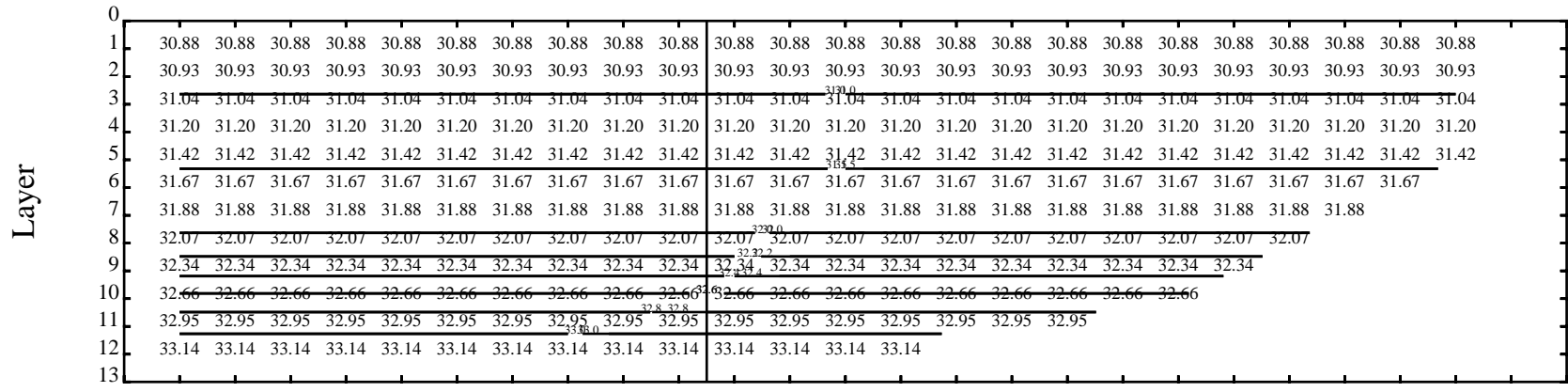
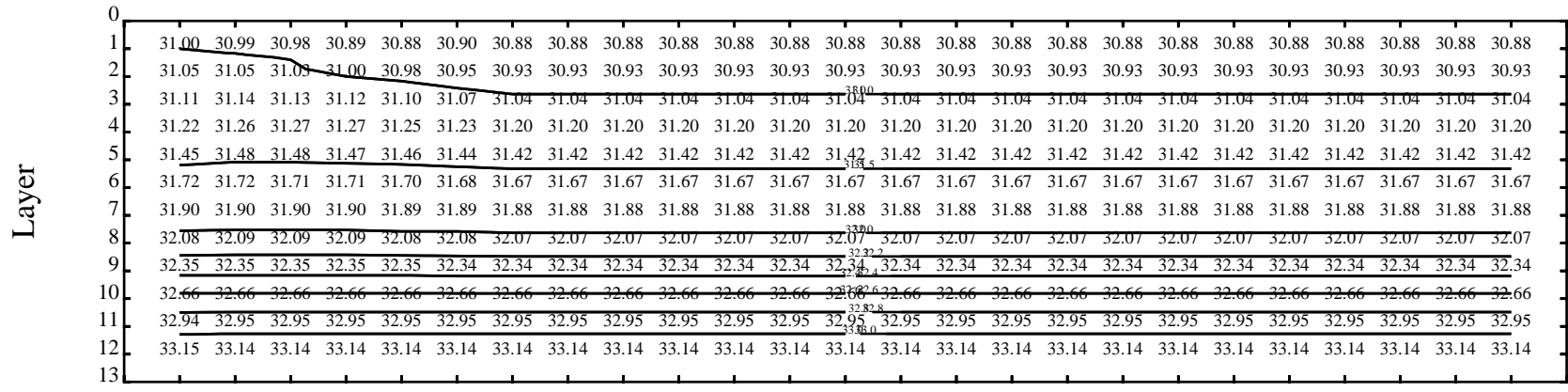
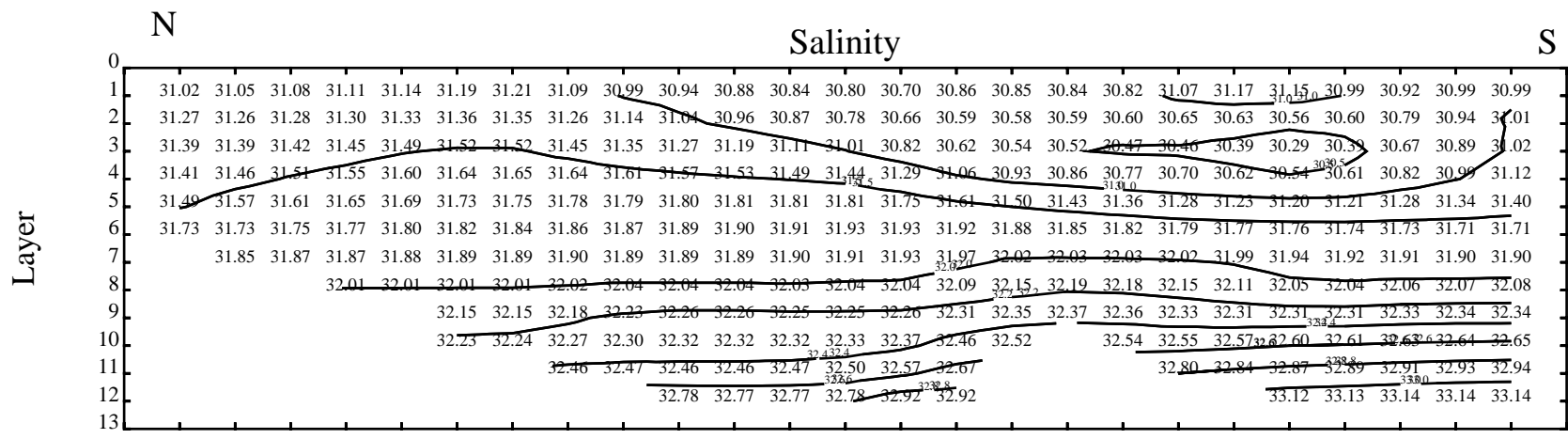
N

Temperature

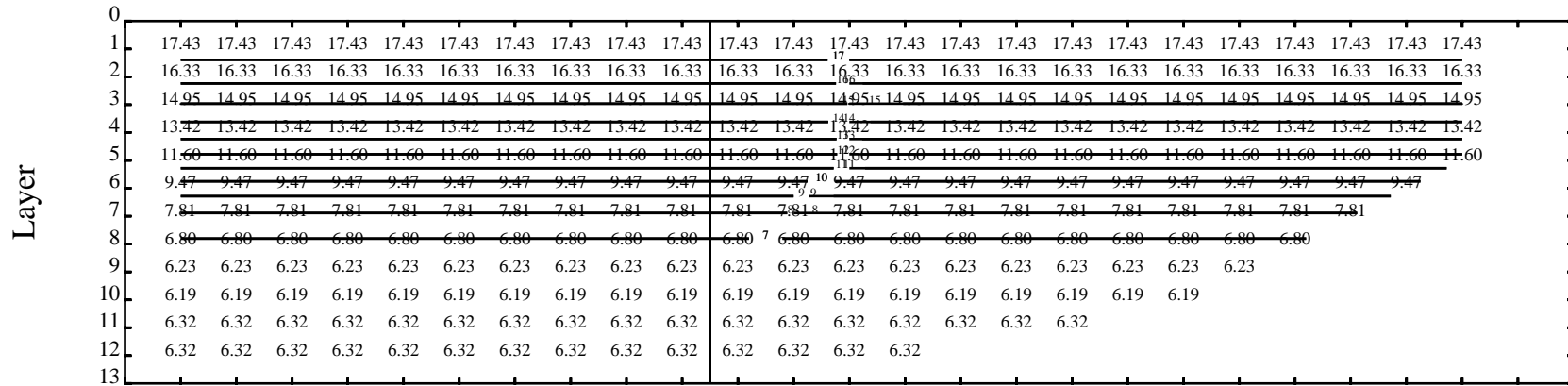
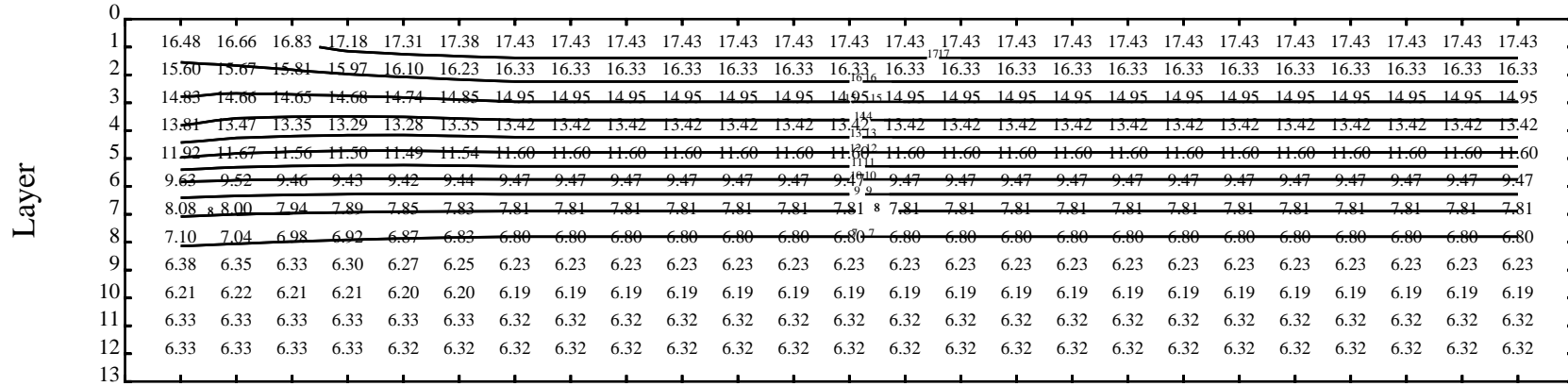
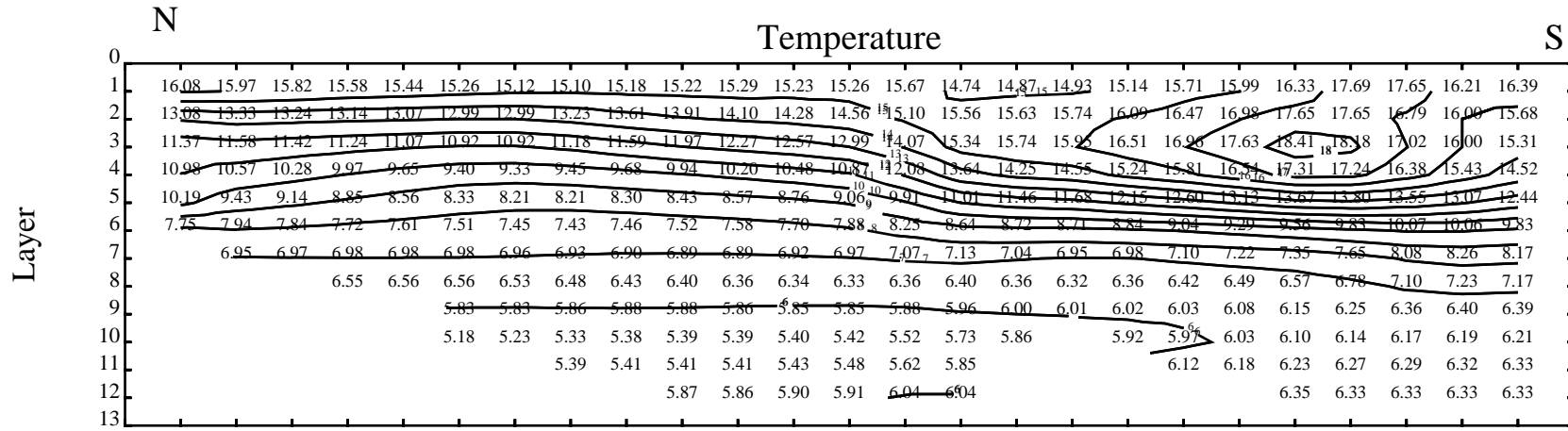
S



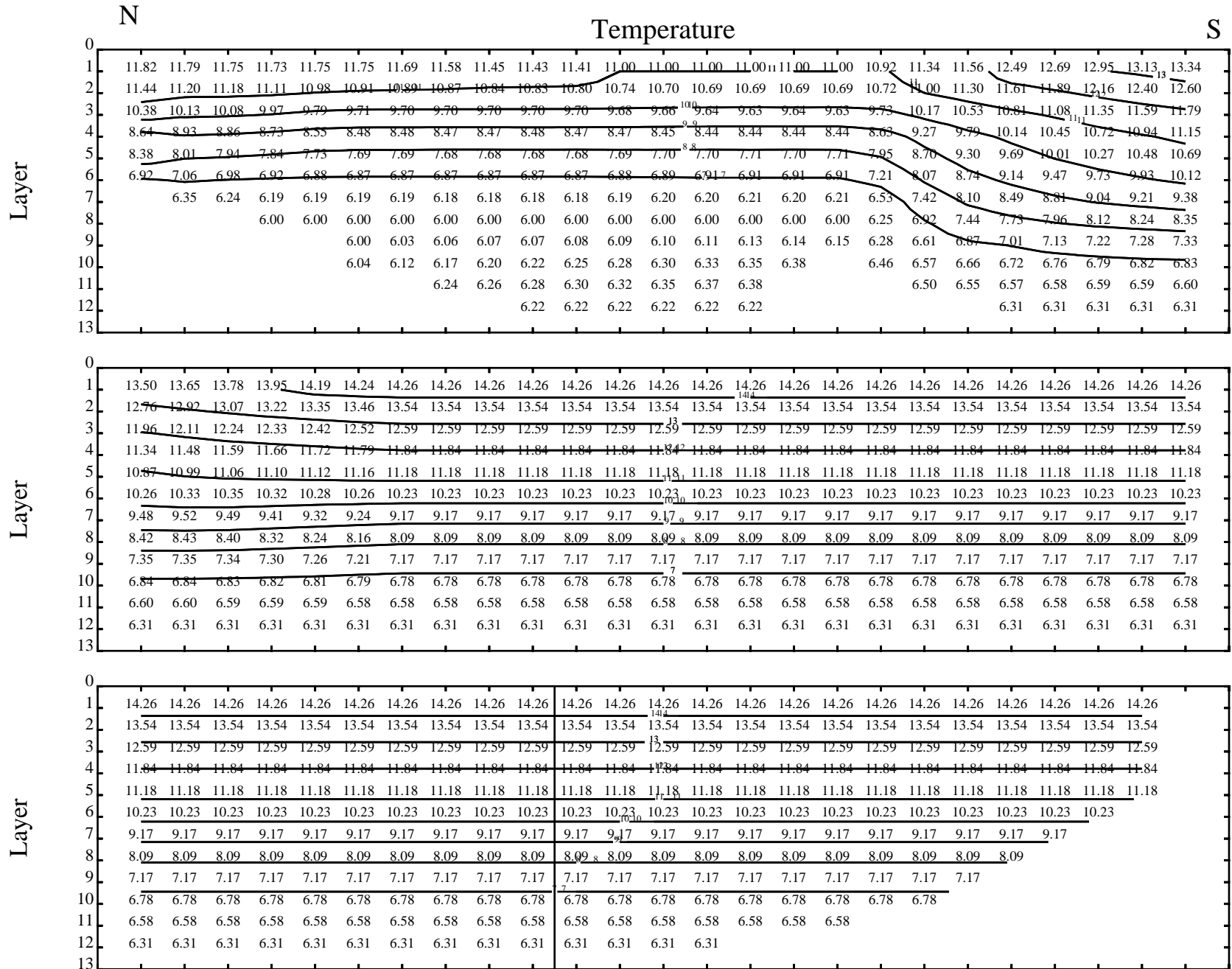




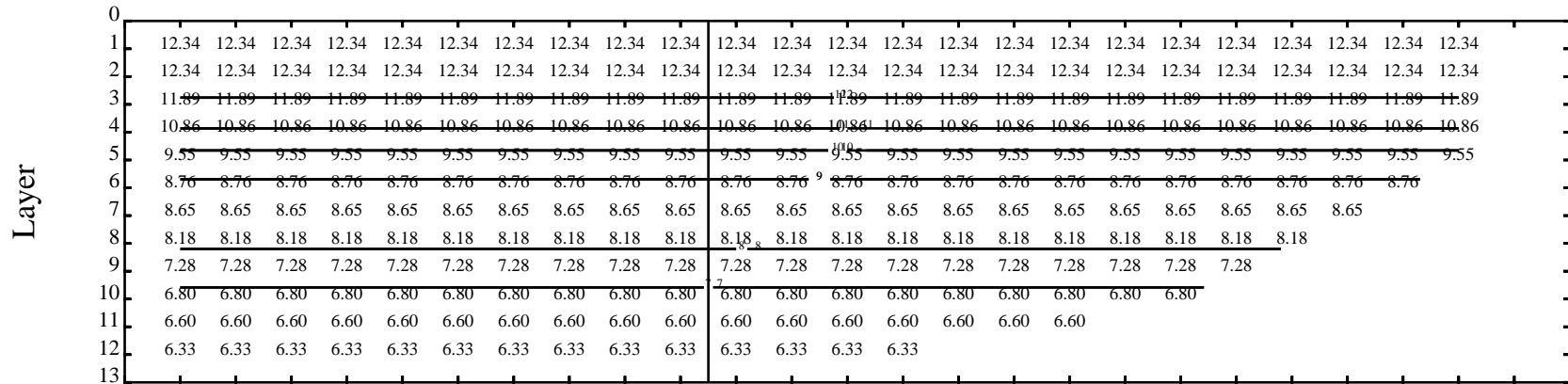
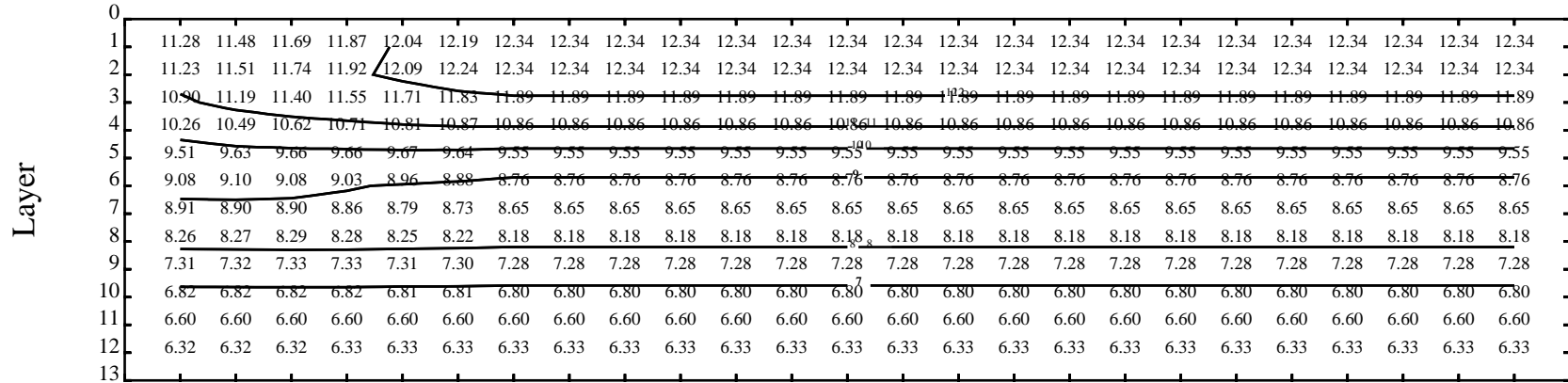
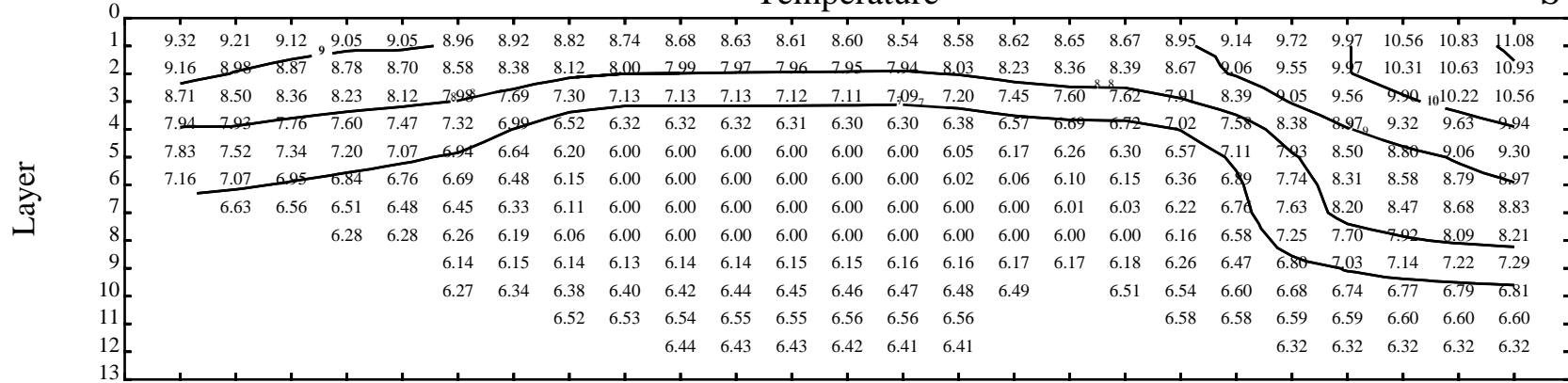
BC Time 12

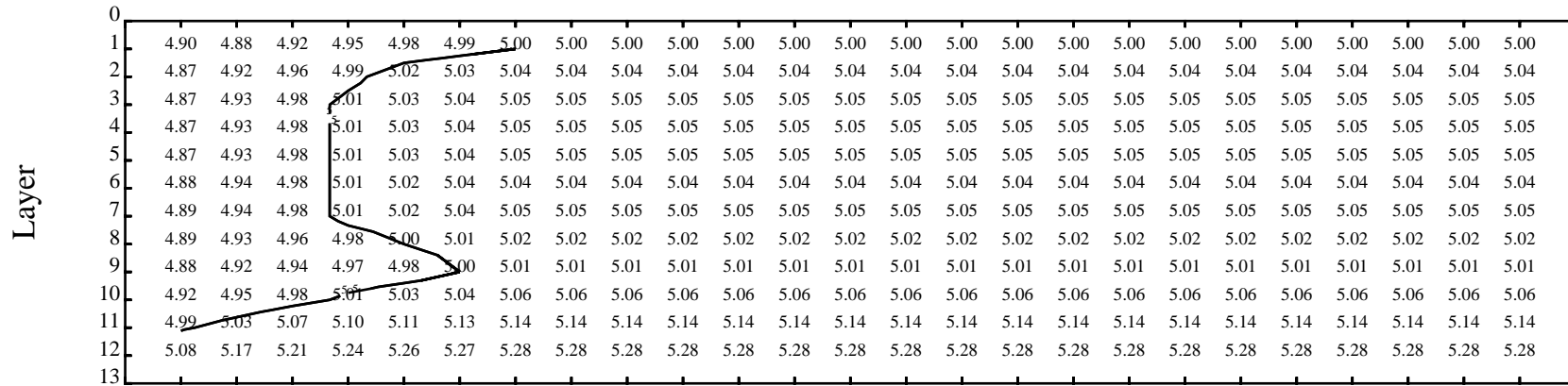
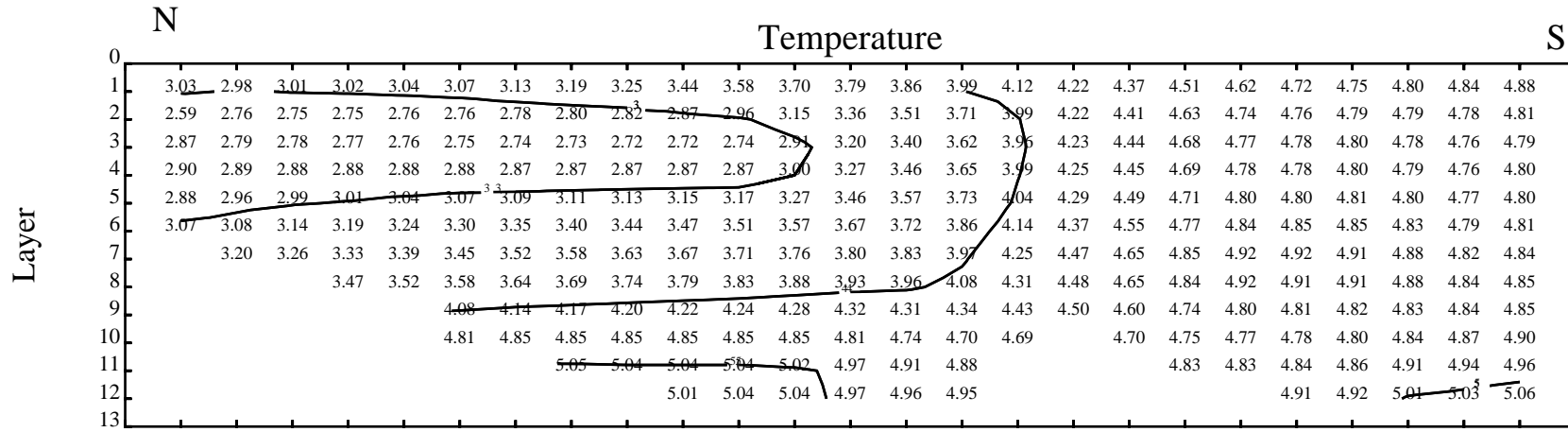


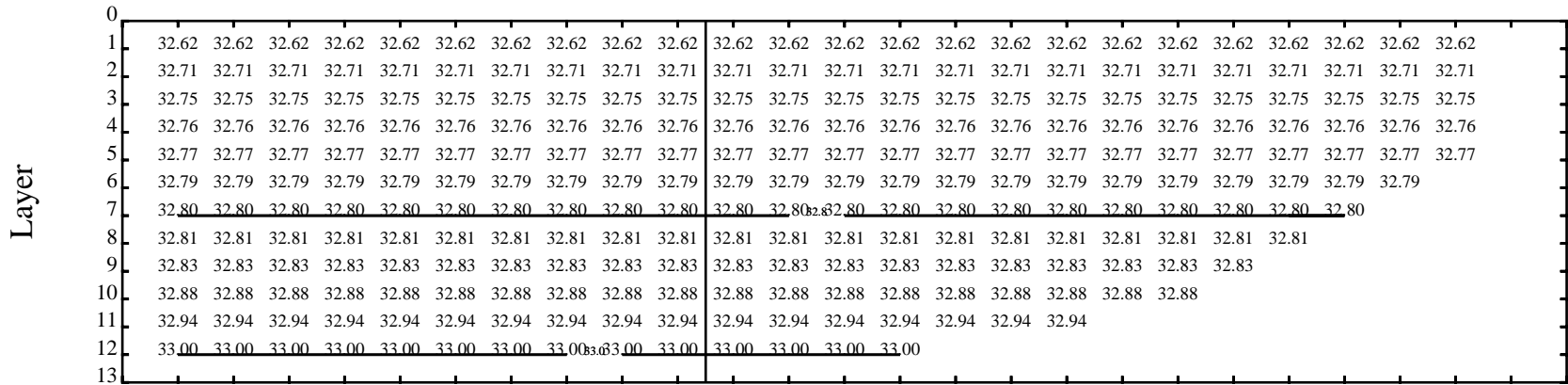
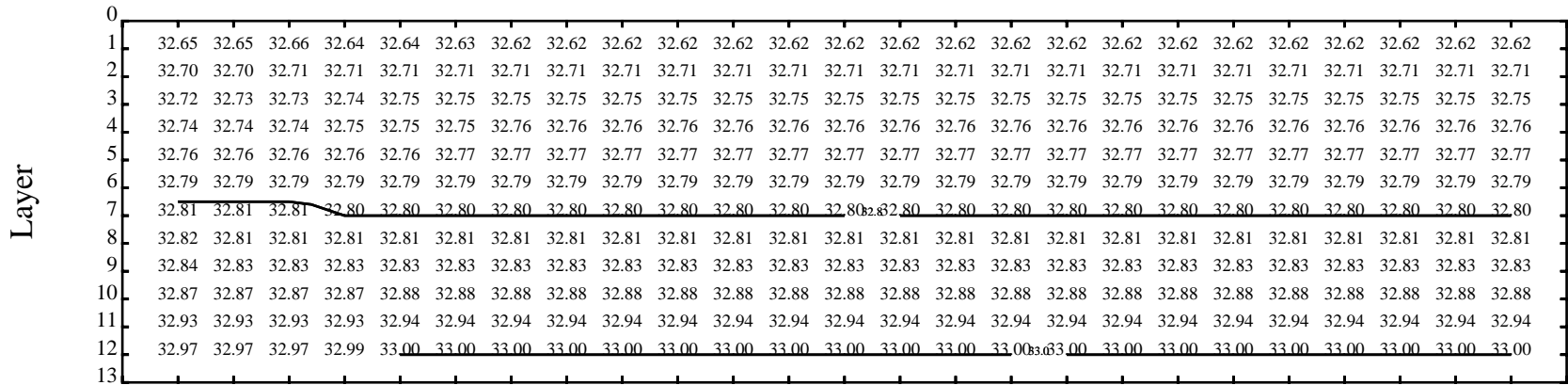
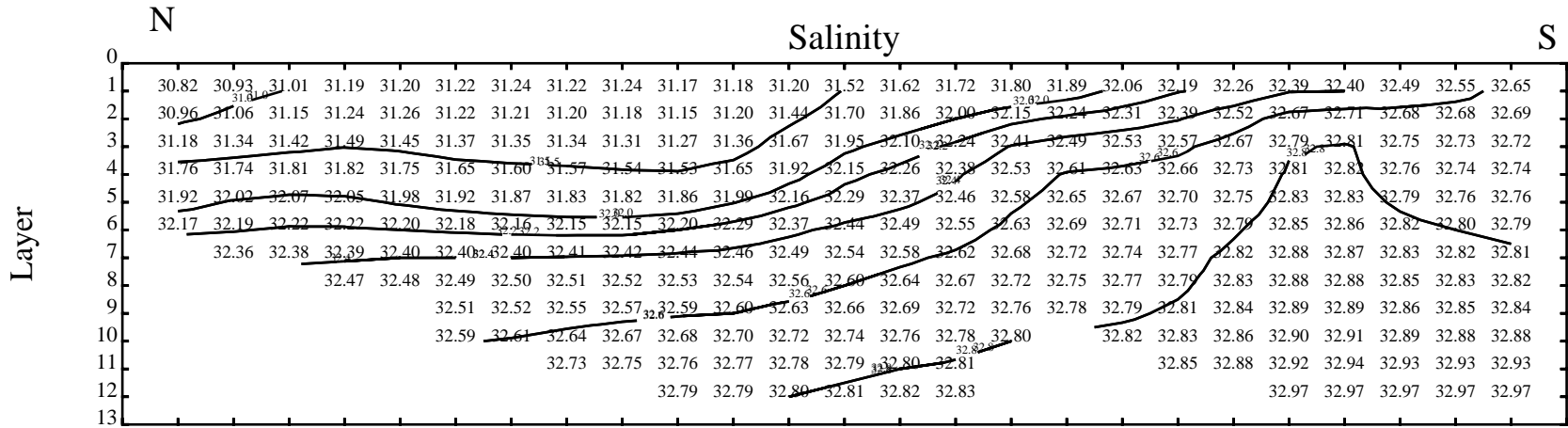
BC Time 12

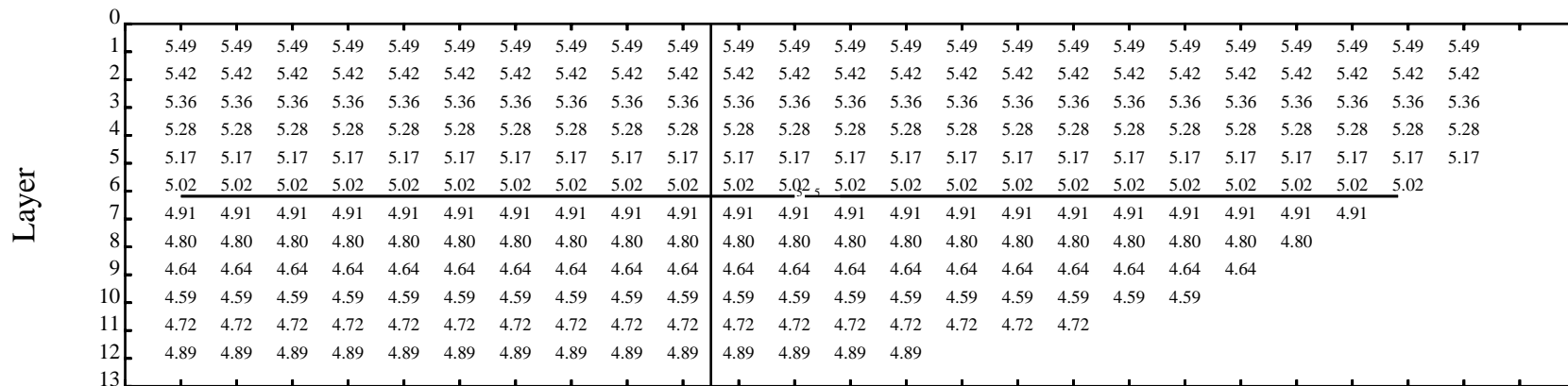
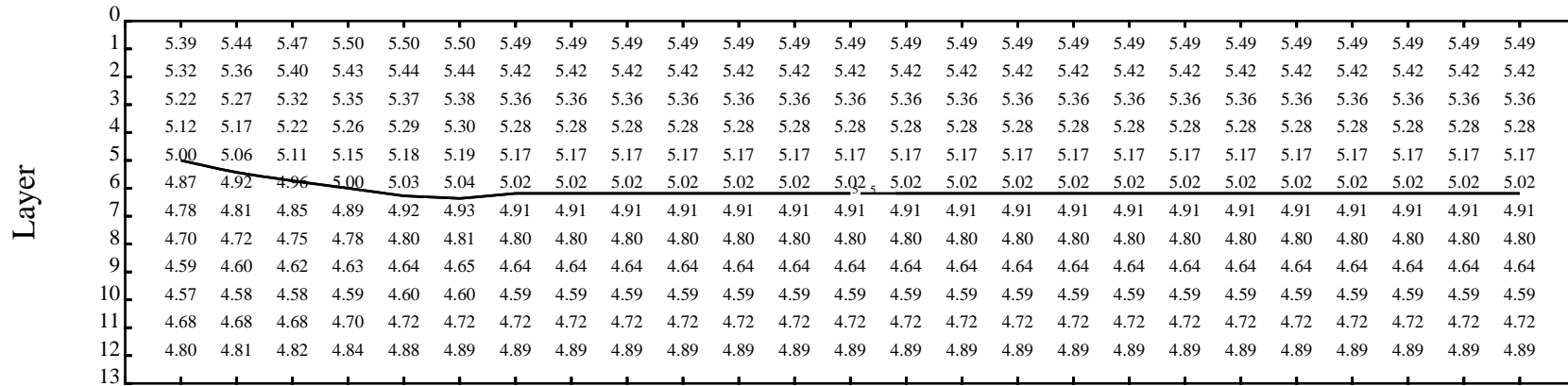
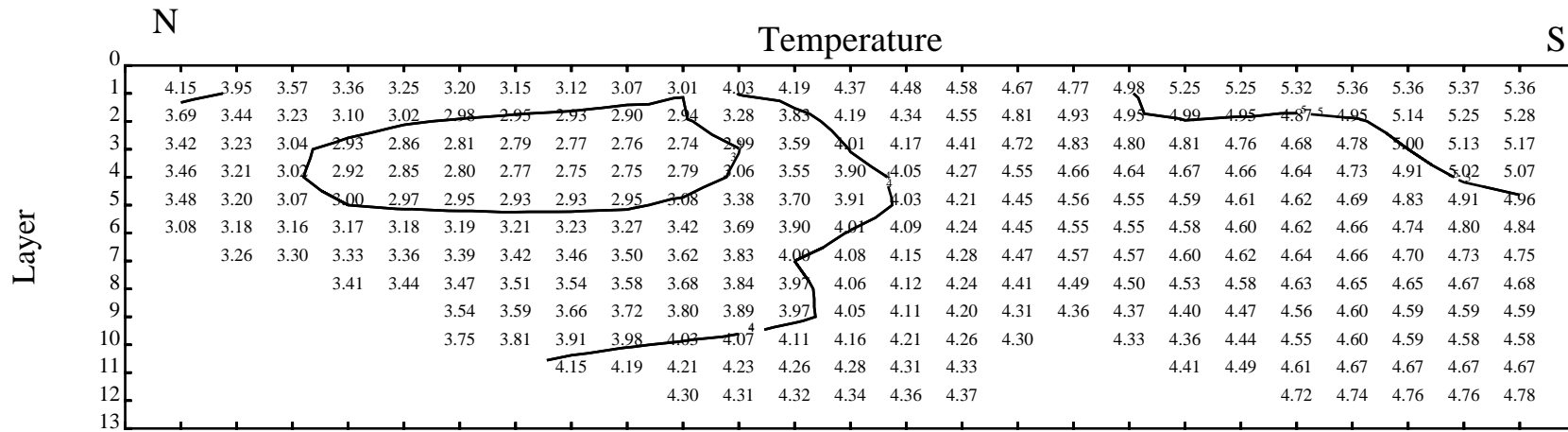


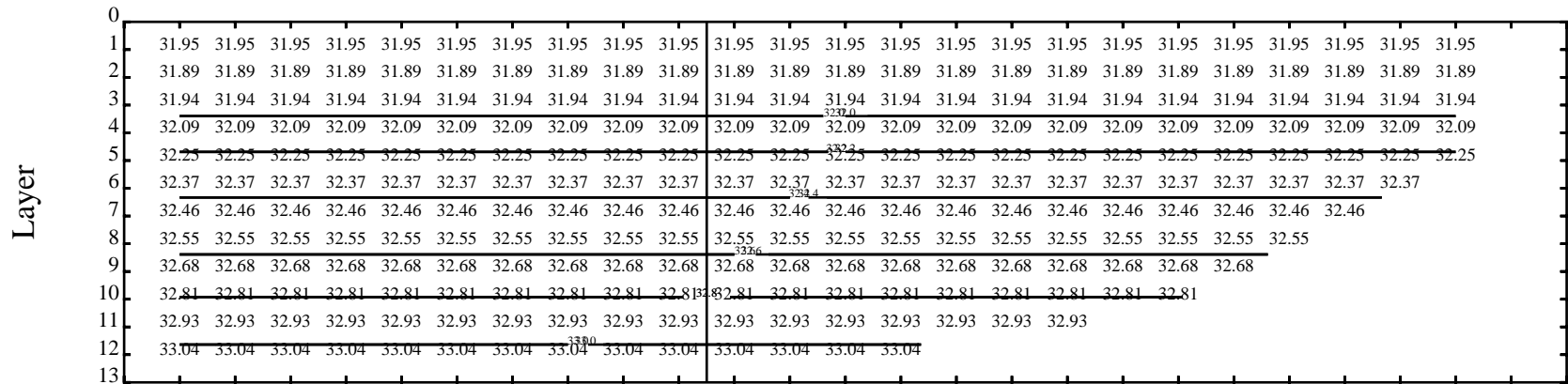
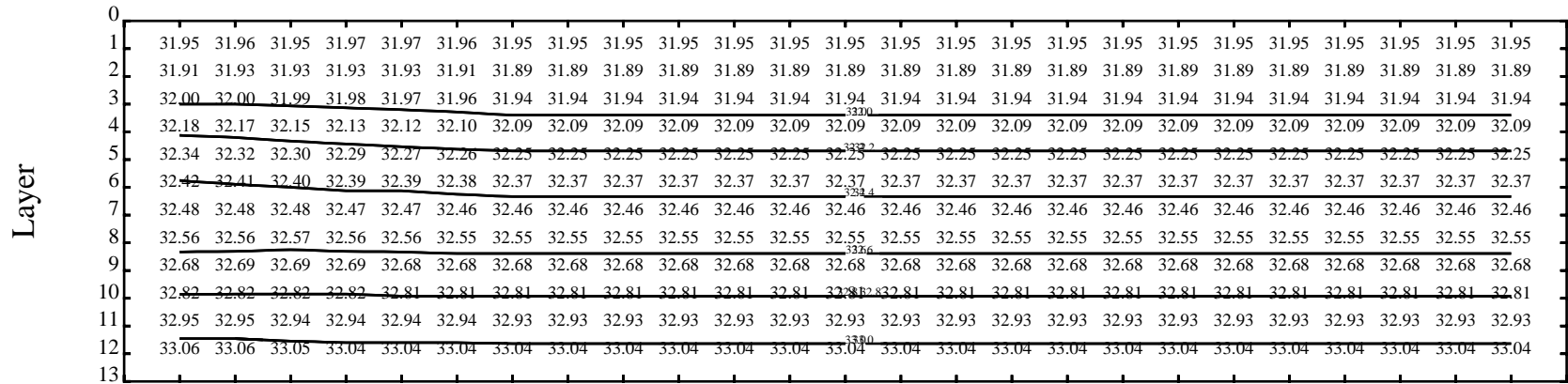
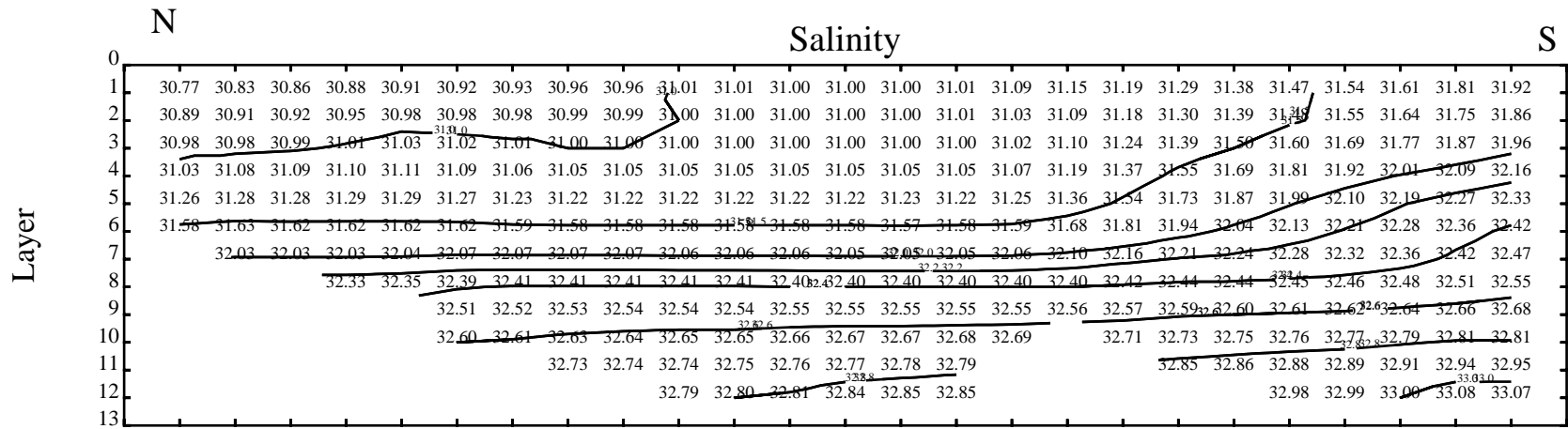
N Temperature S

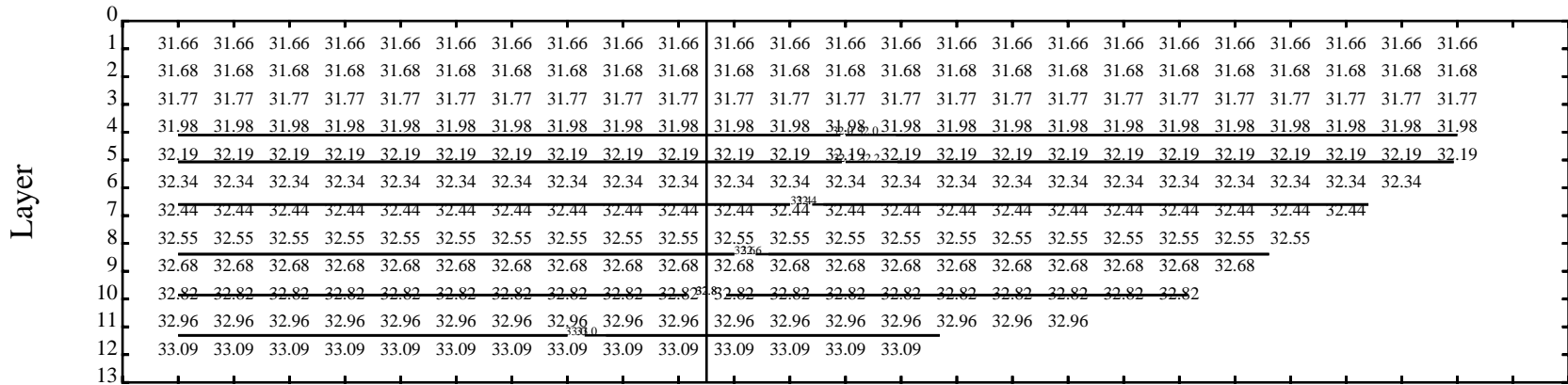
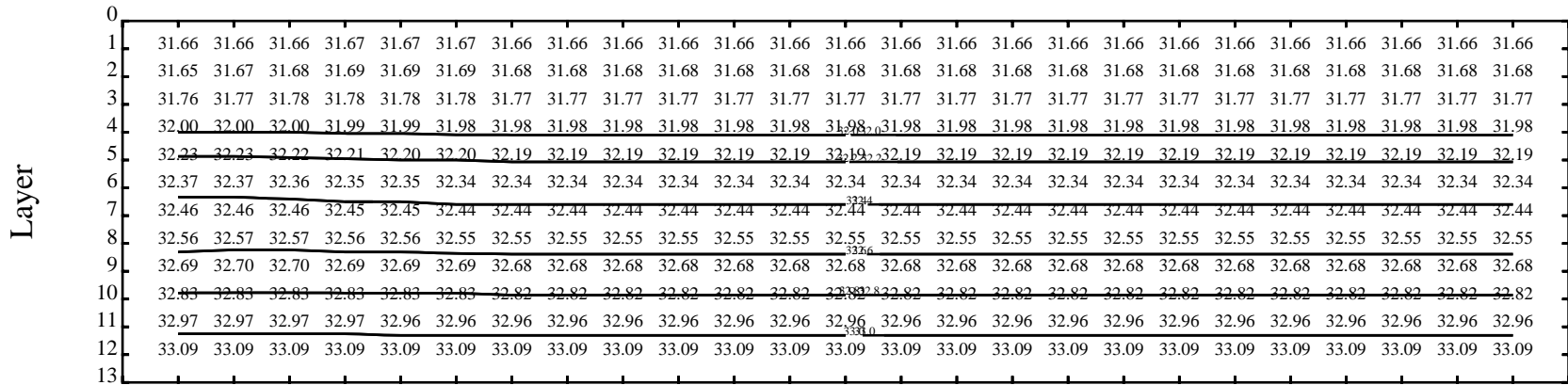
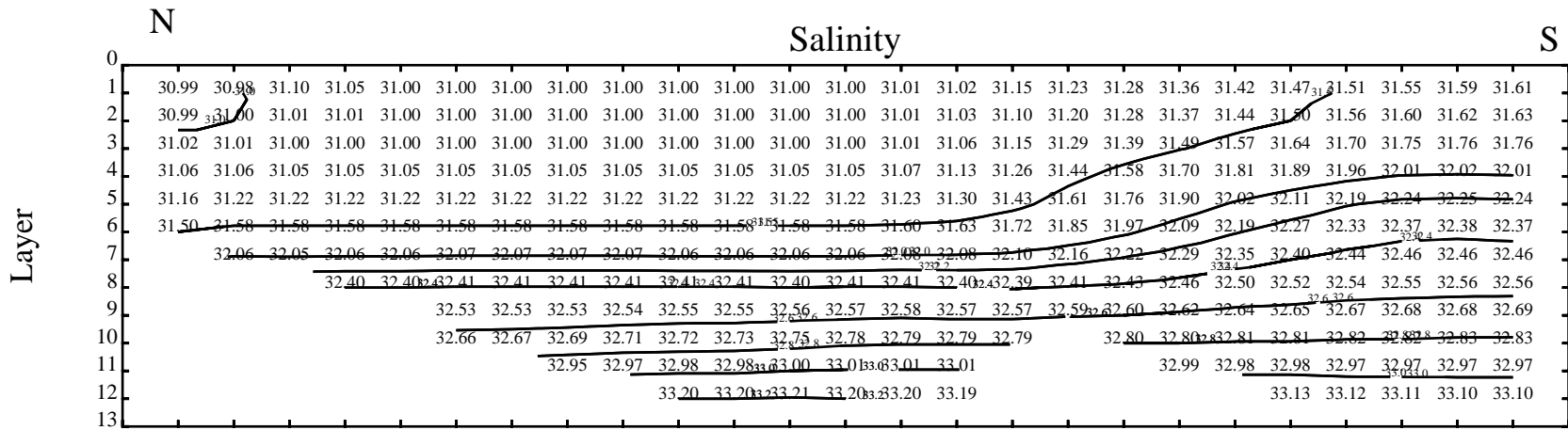








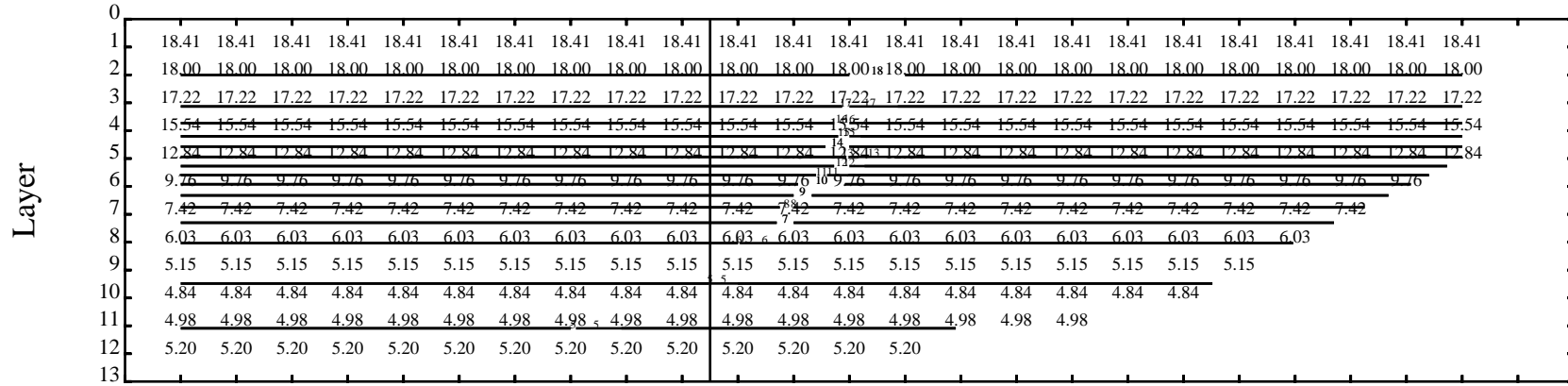
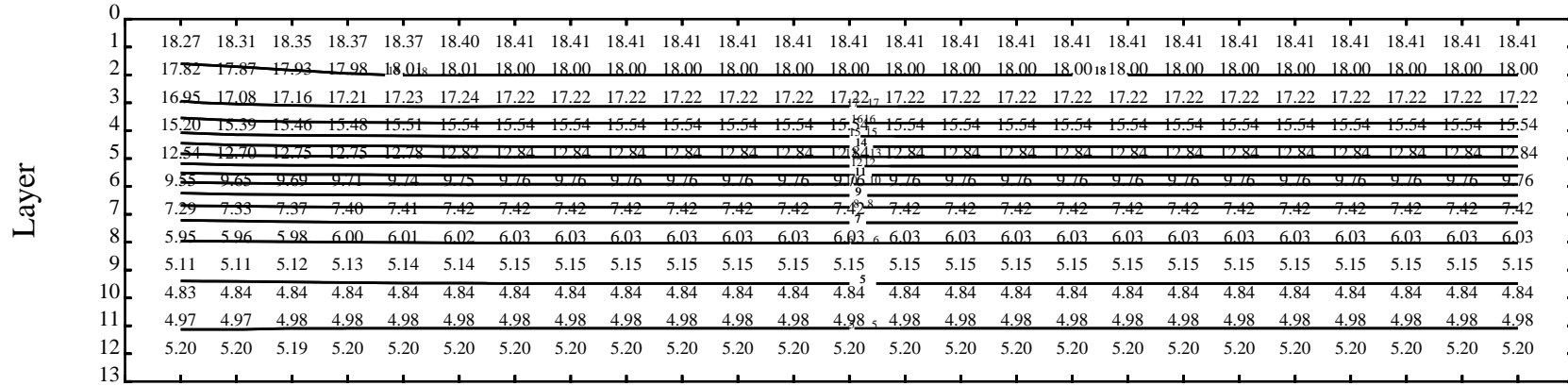
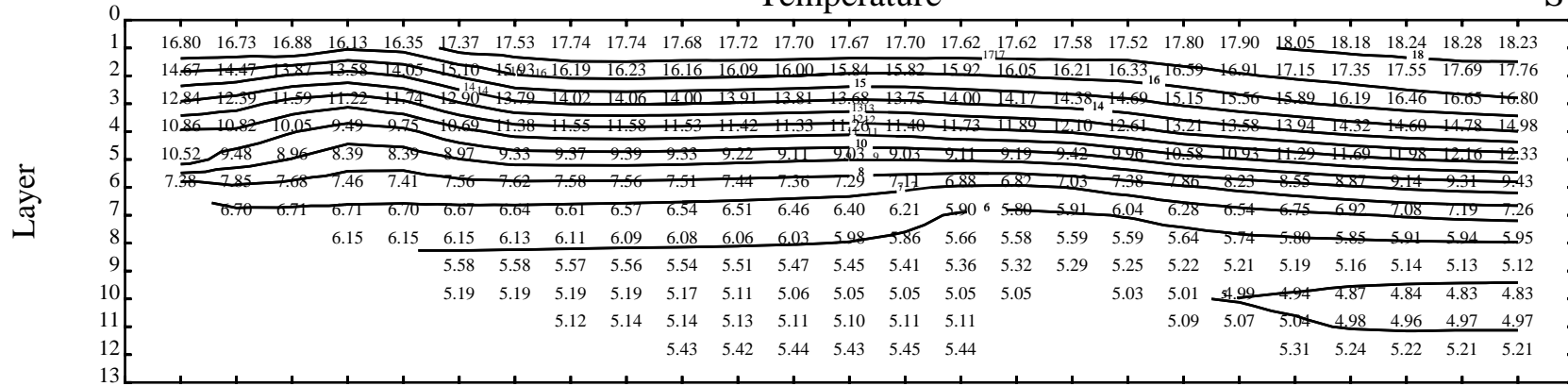




N

Temperature

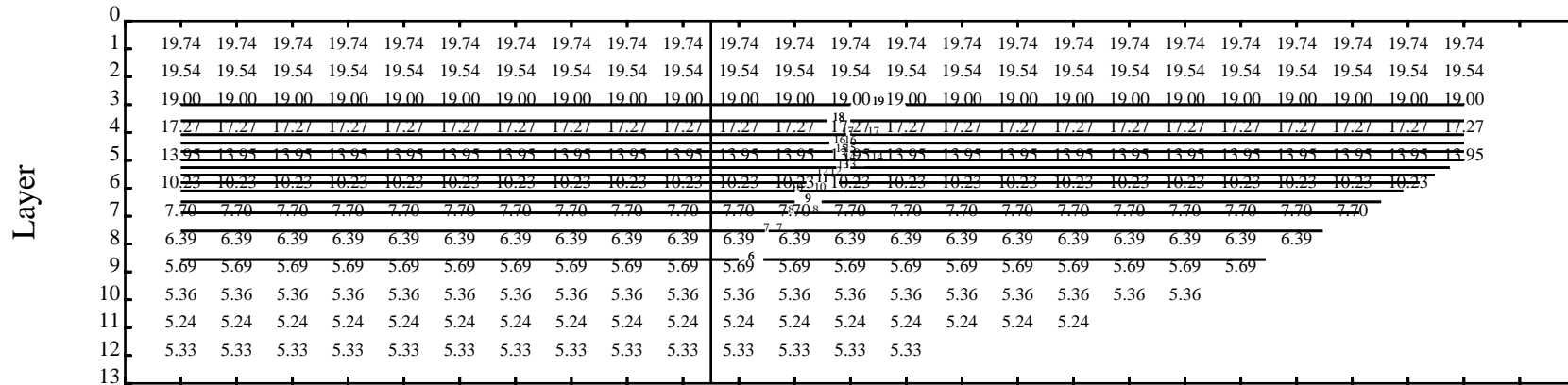
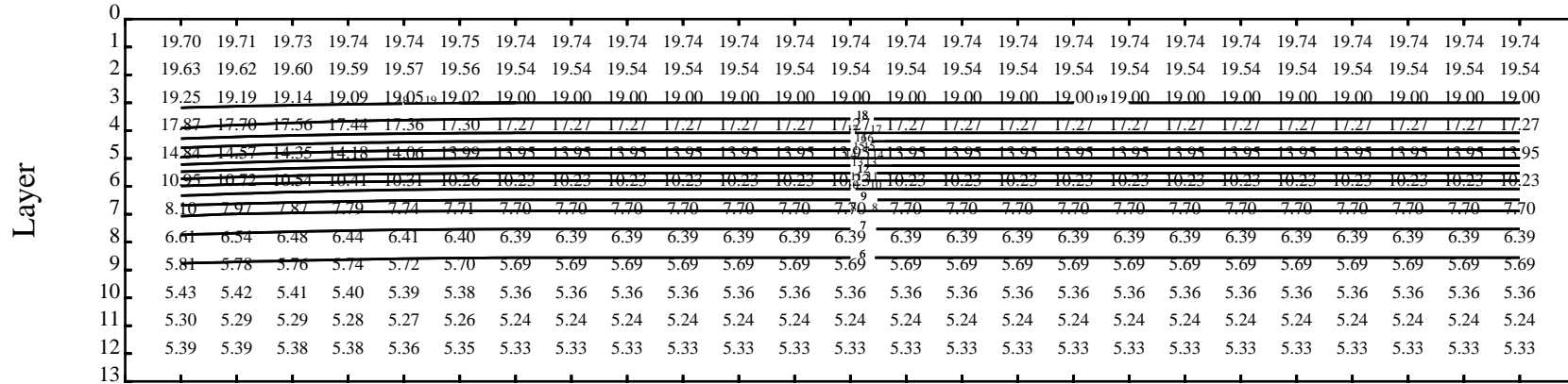
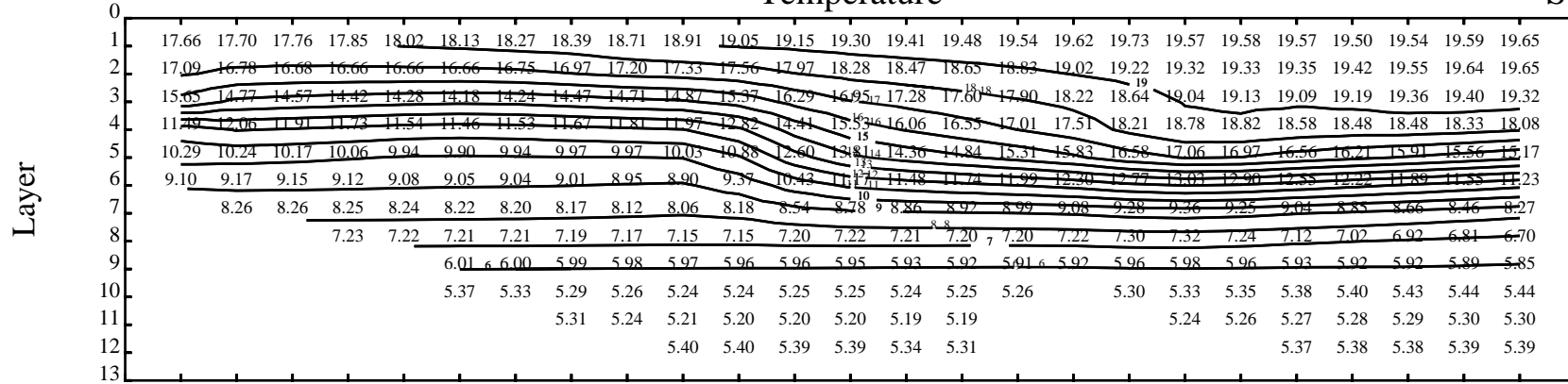
S

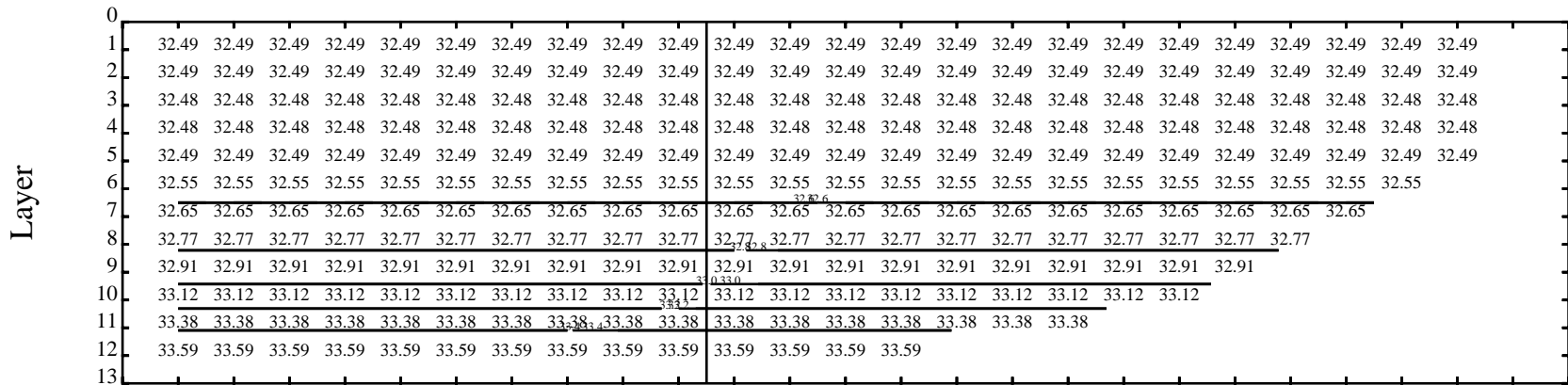
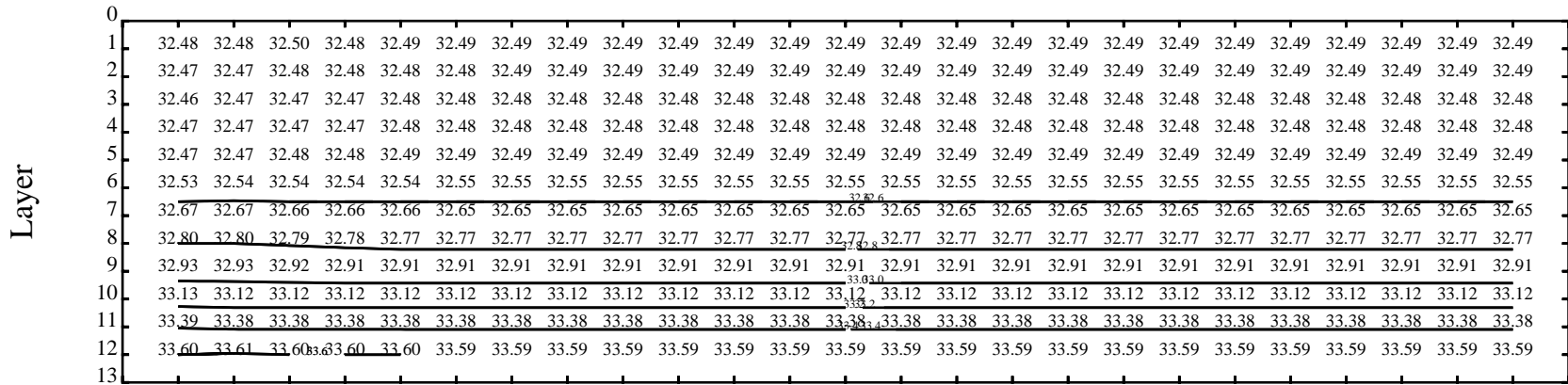
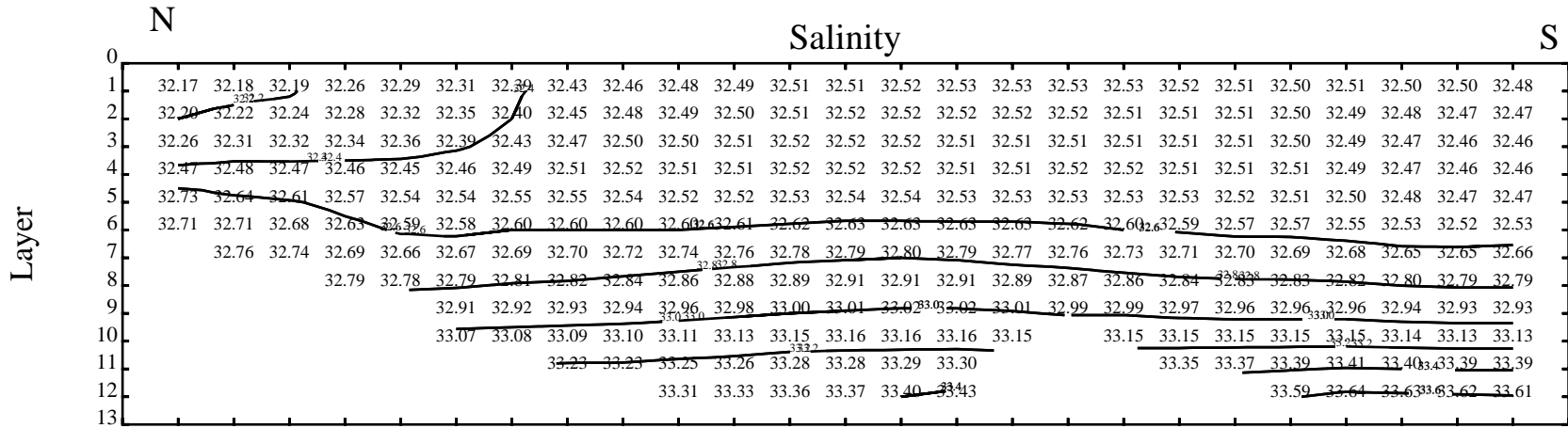


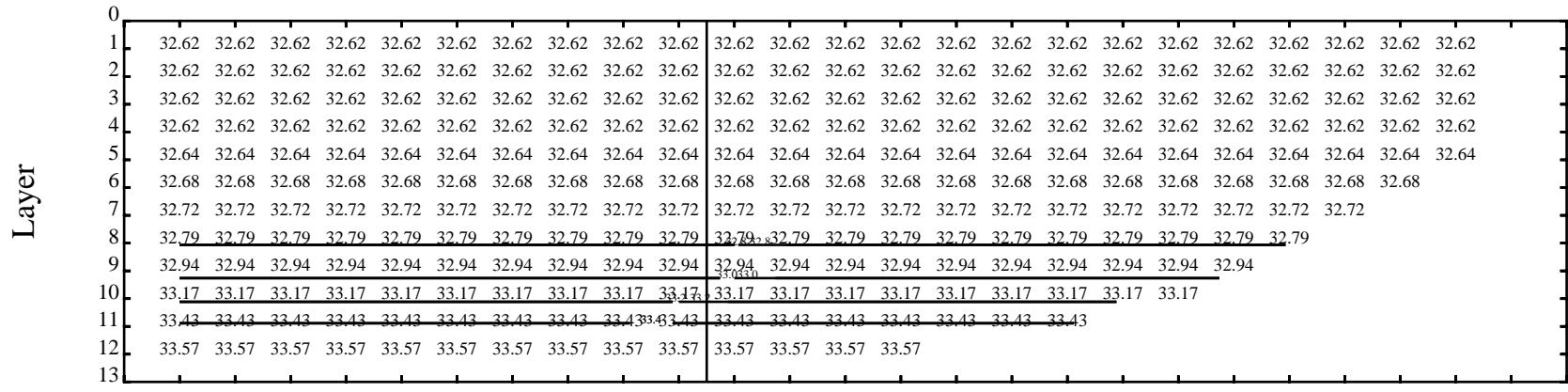
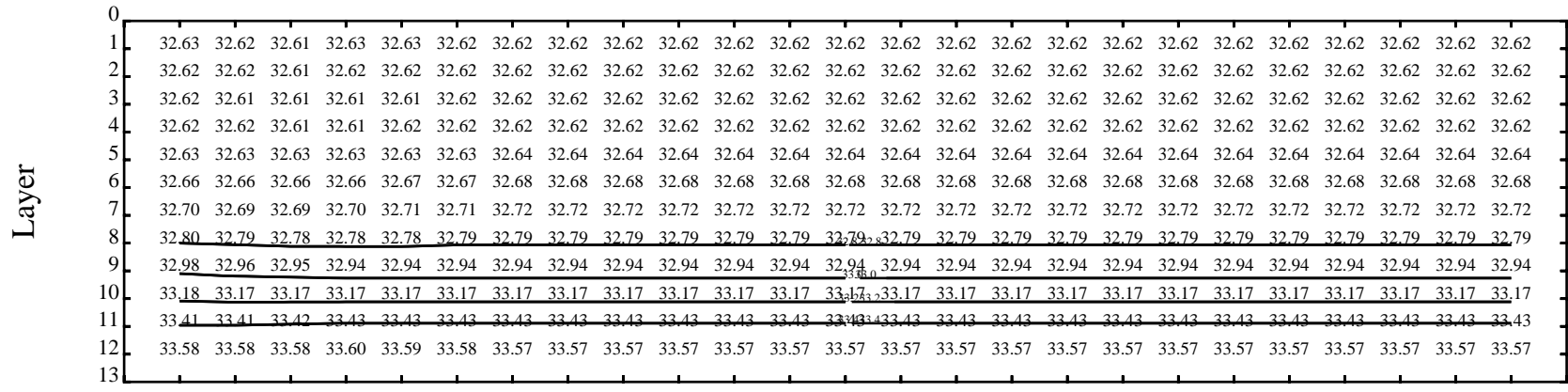
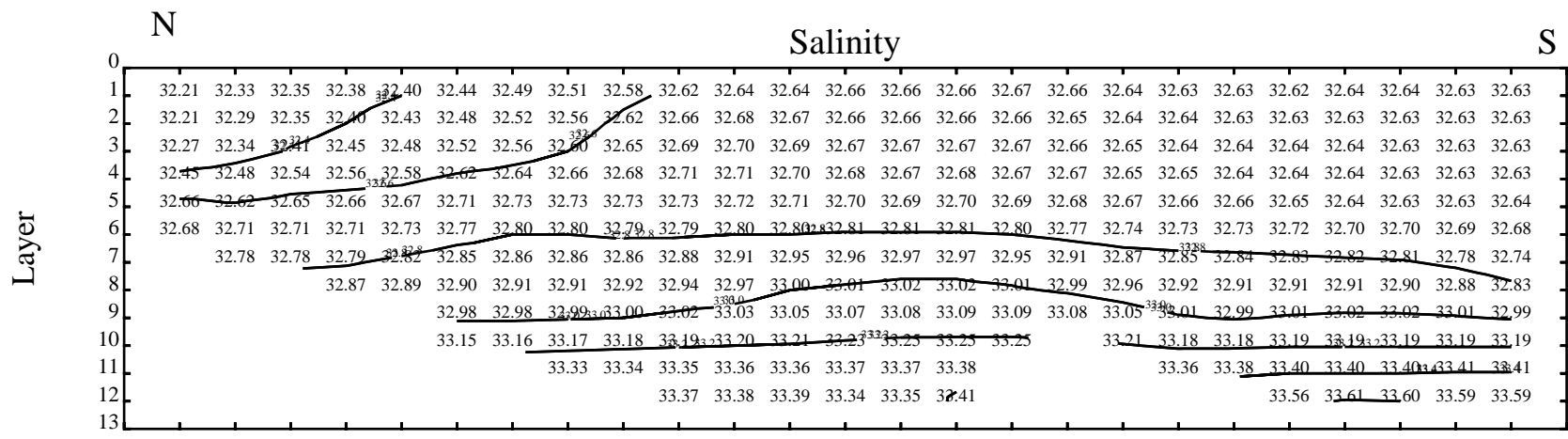
N

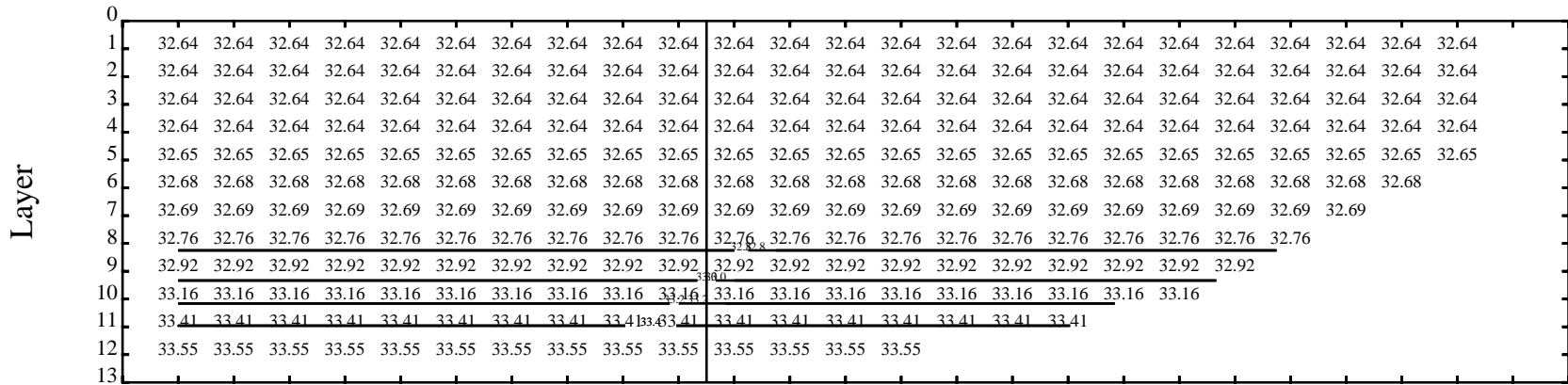
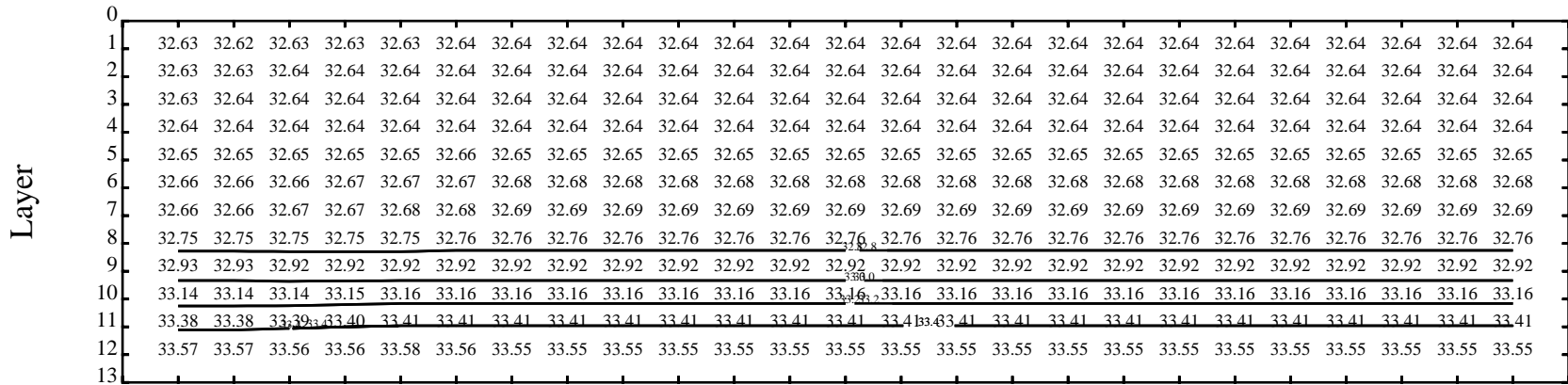
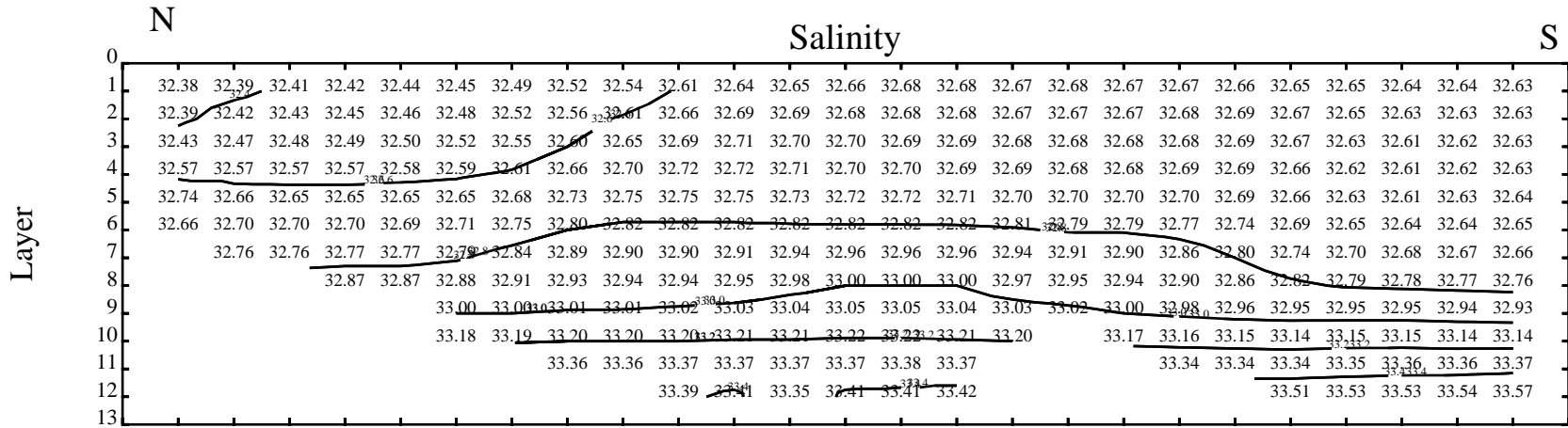
Temperature

S

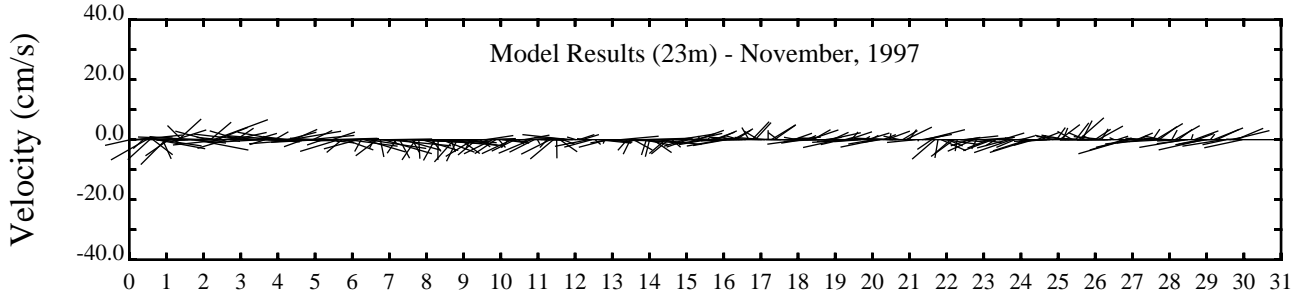
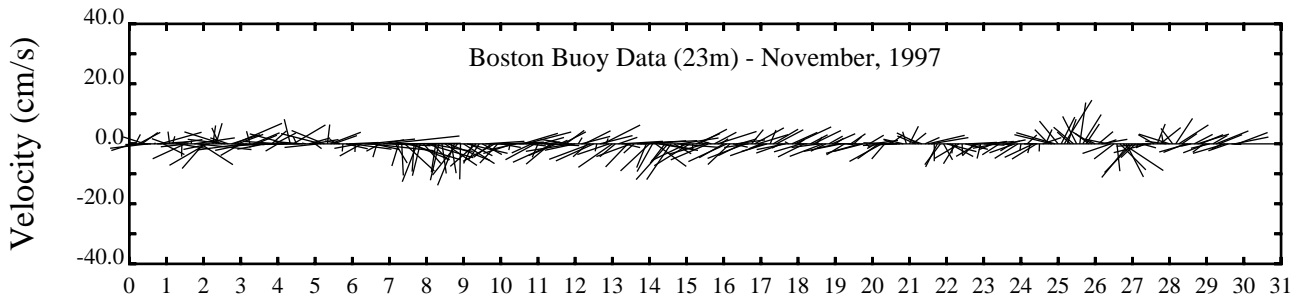
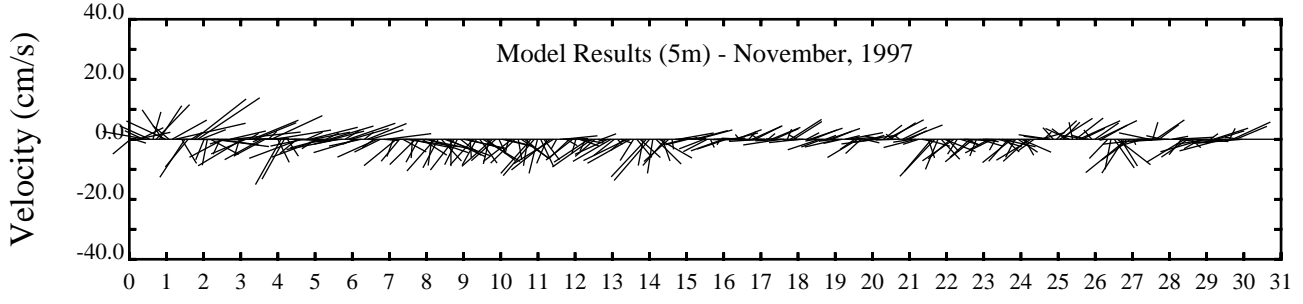
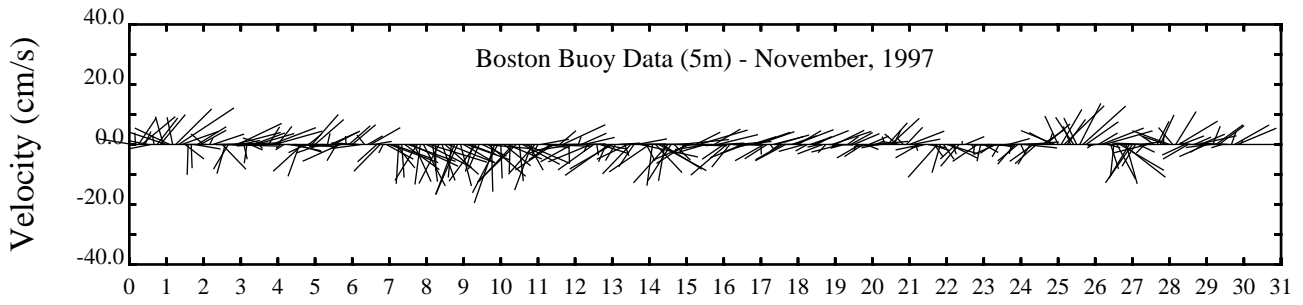
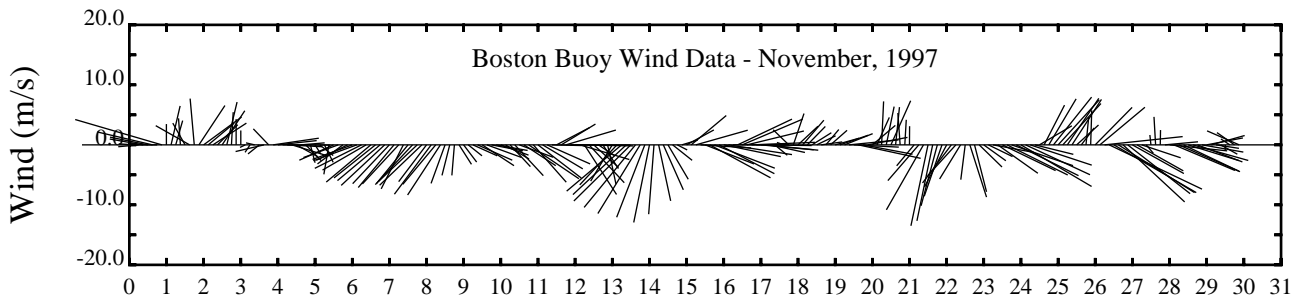




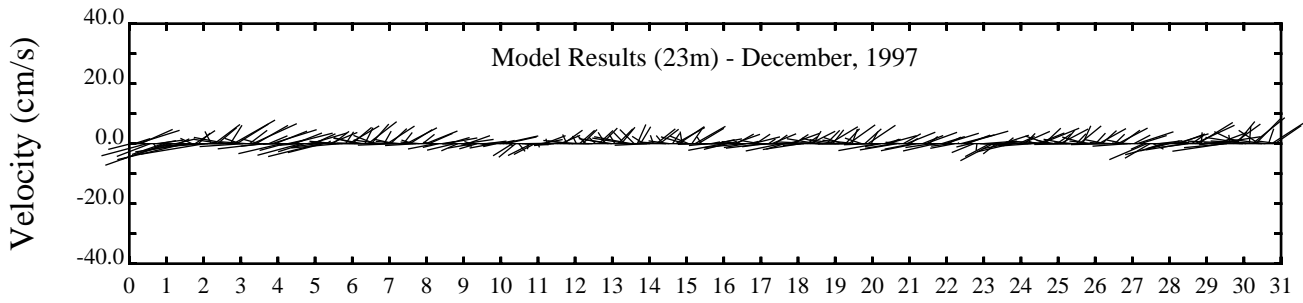
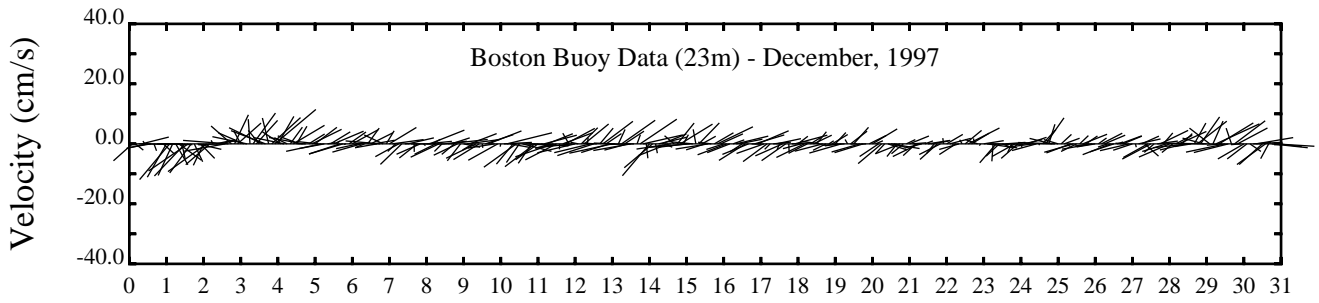
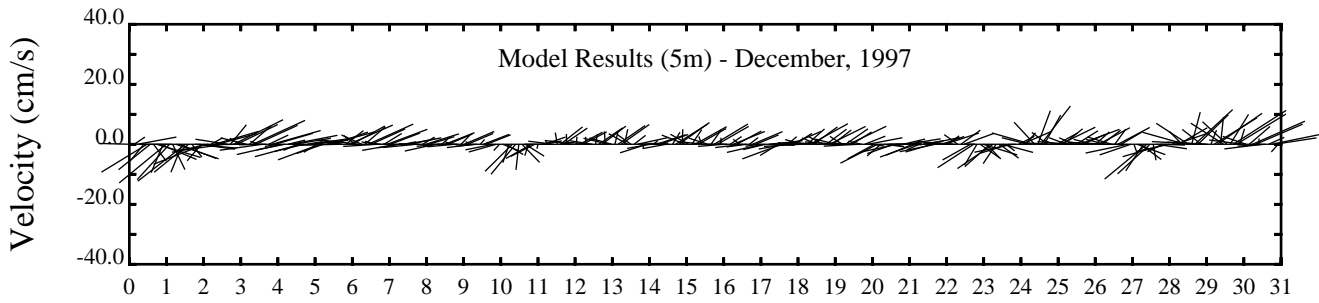
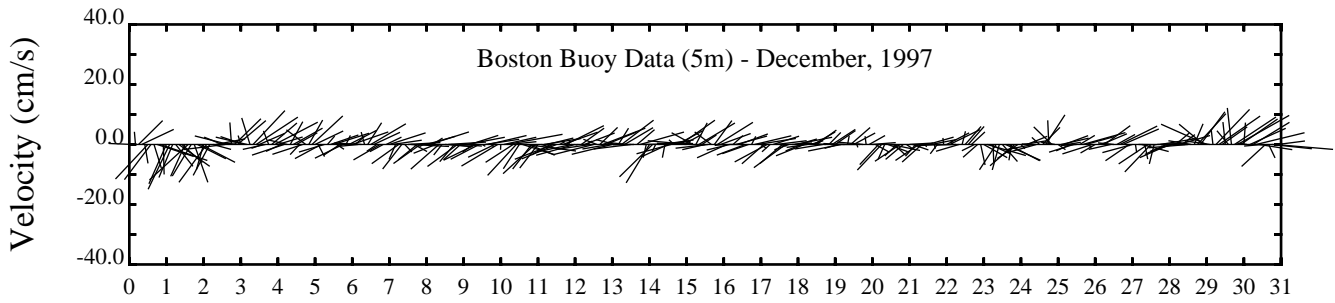
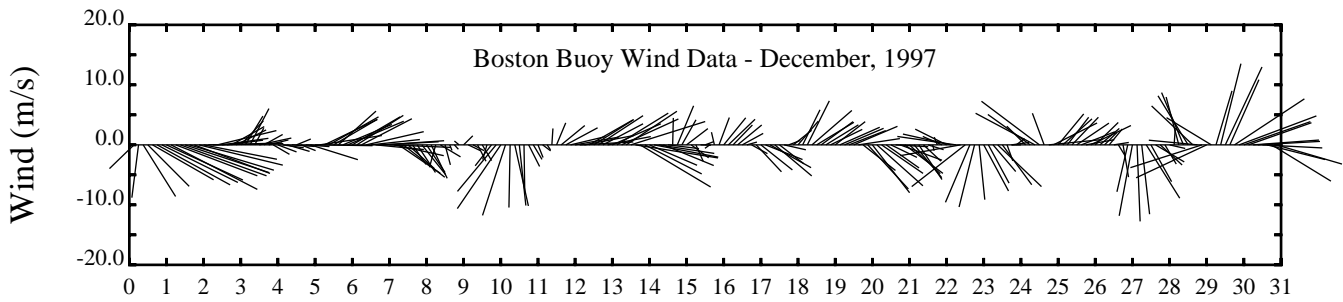




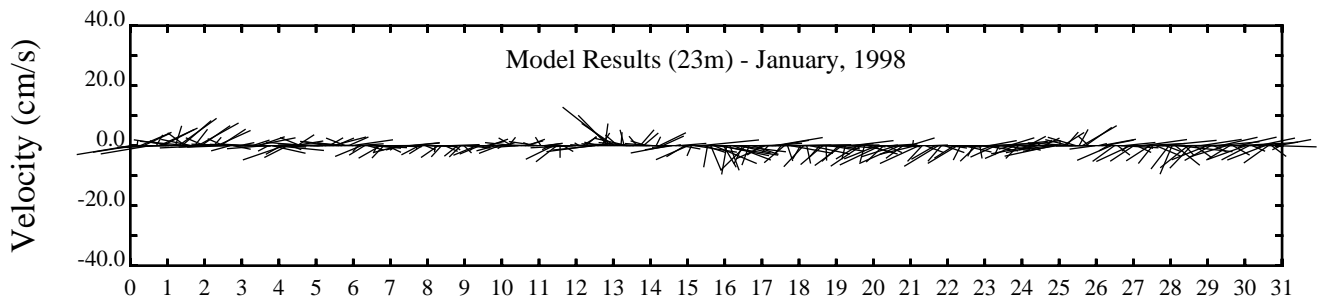
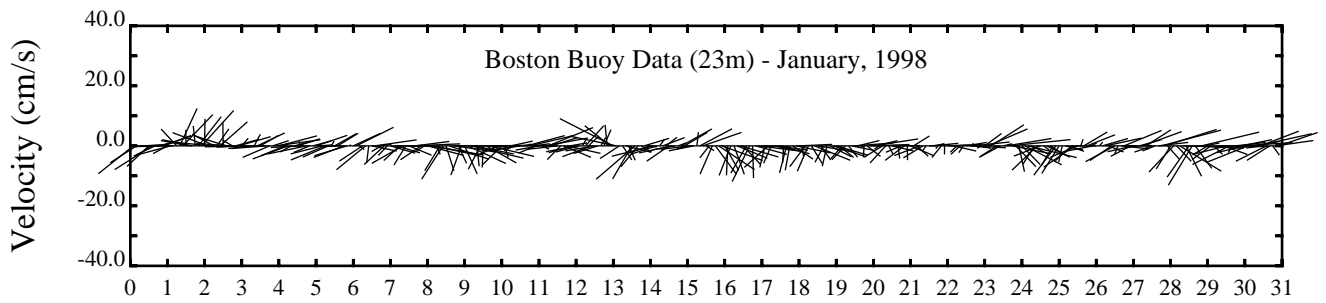
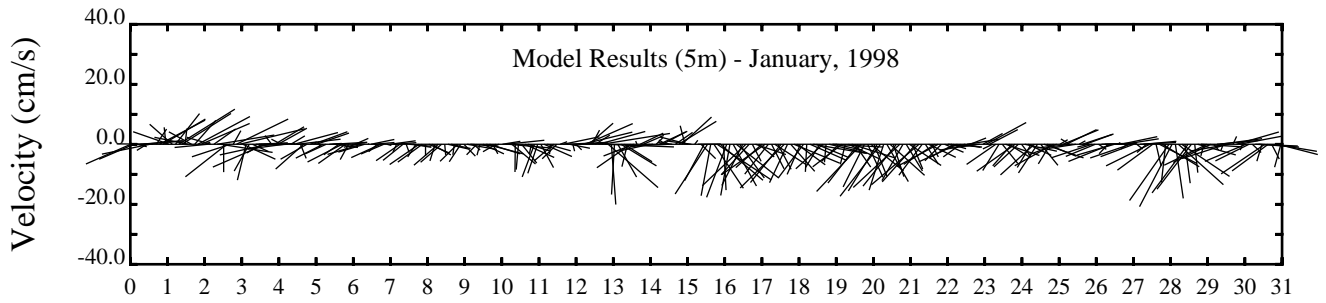
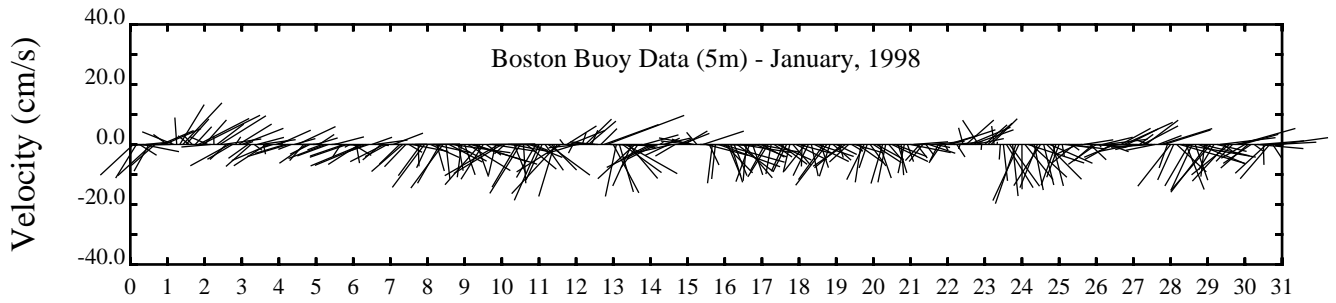
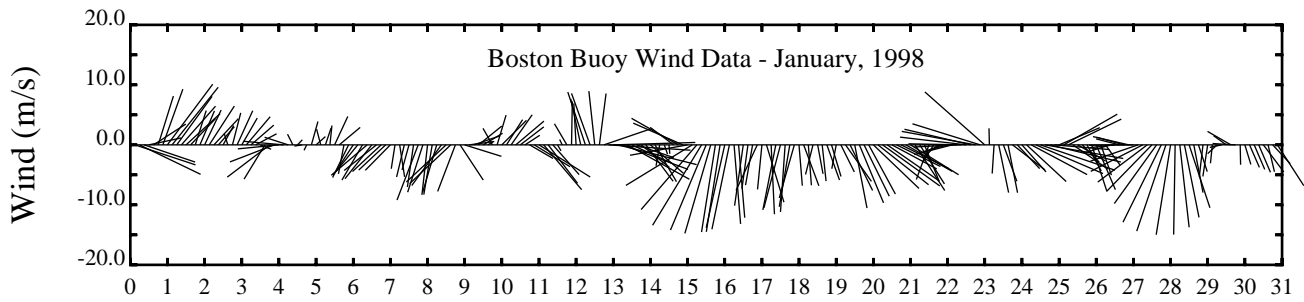
APPENDIX C
Monthly Current Meter Model versus
Data Comparisons at the Boston Buoy



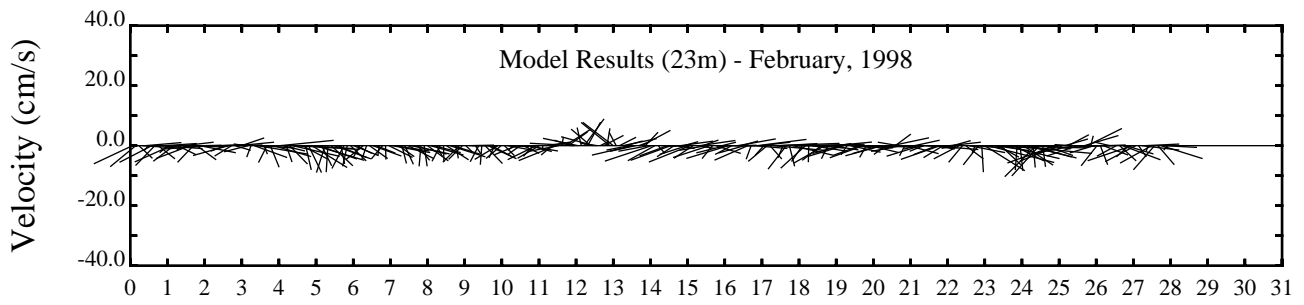
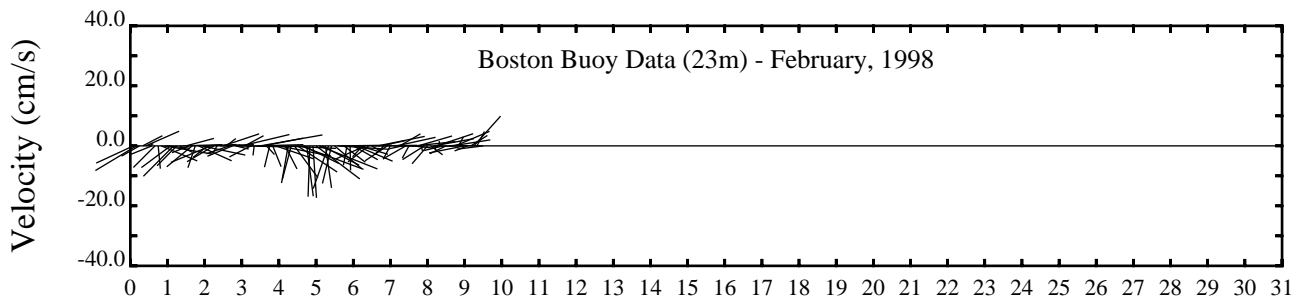
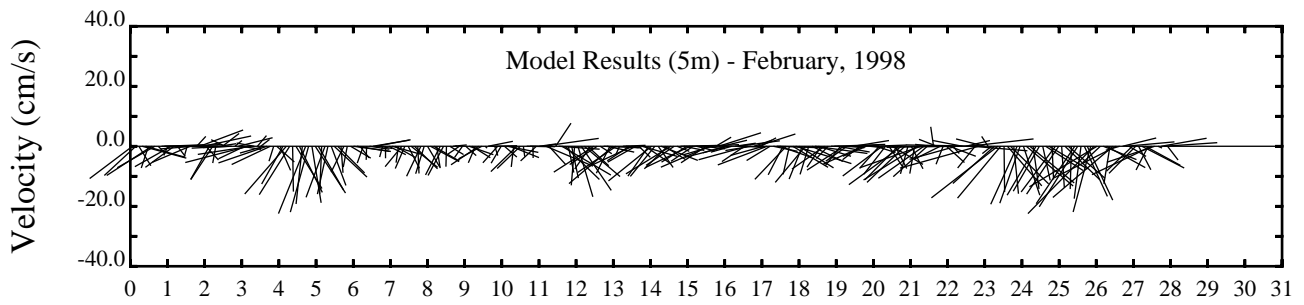
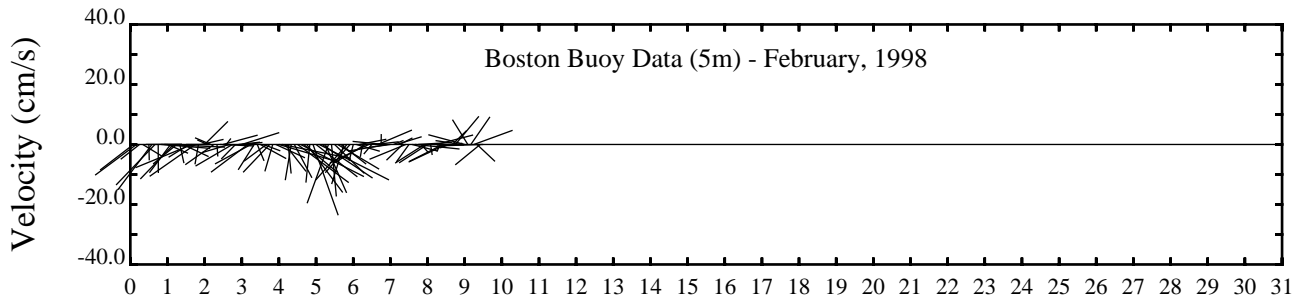
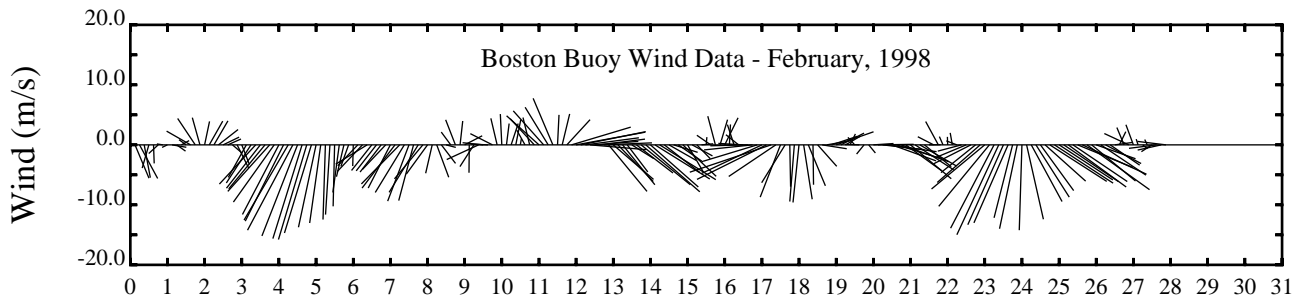
Day

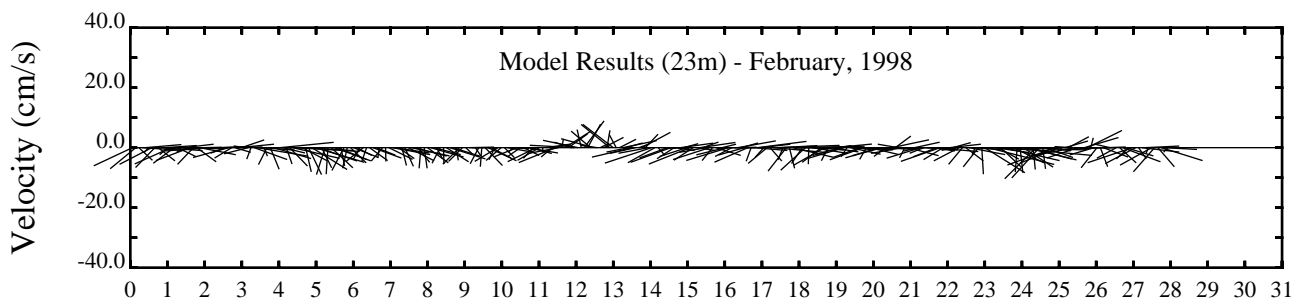
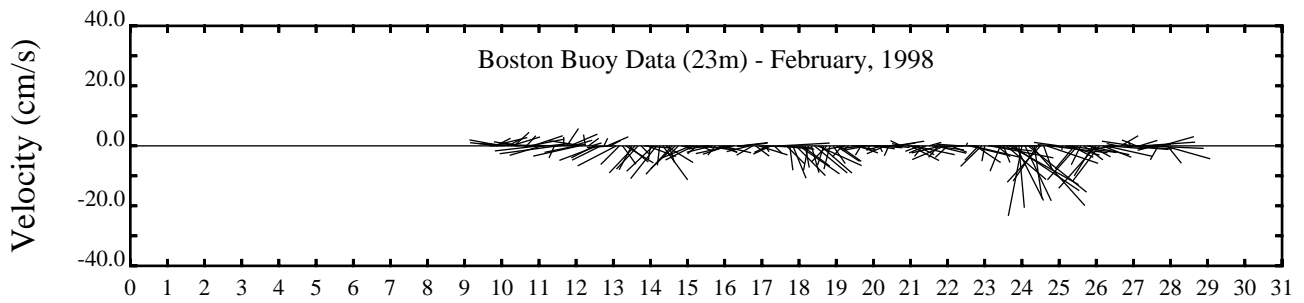
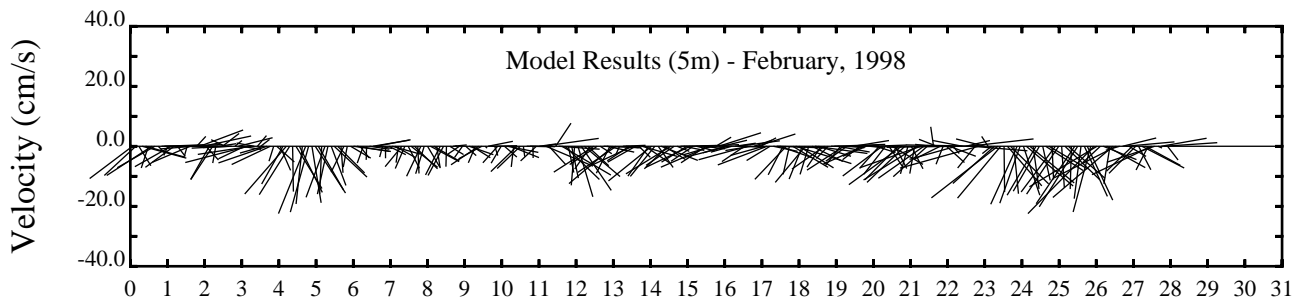
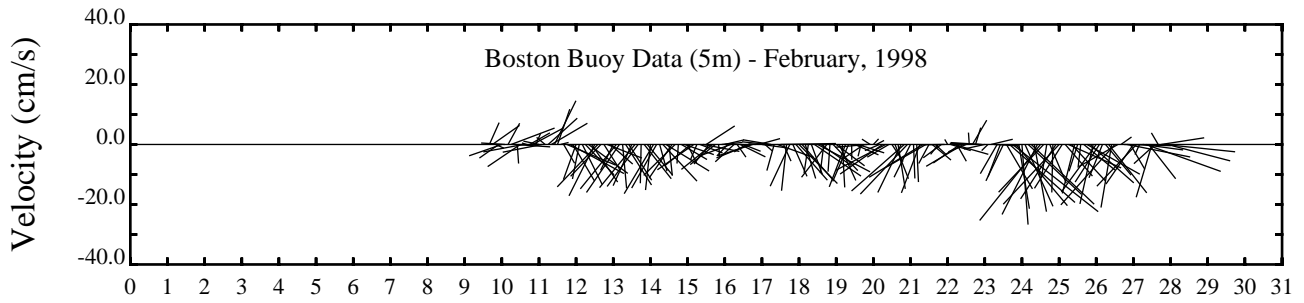
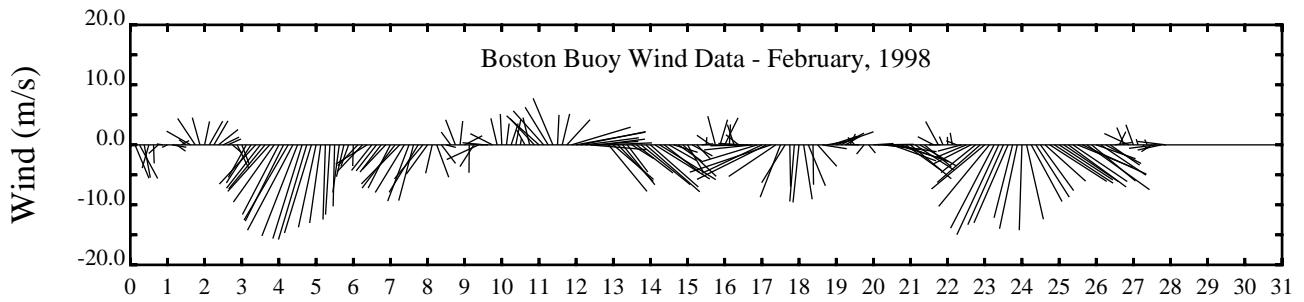


Day

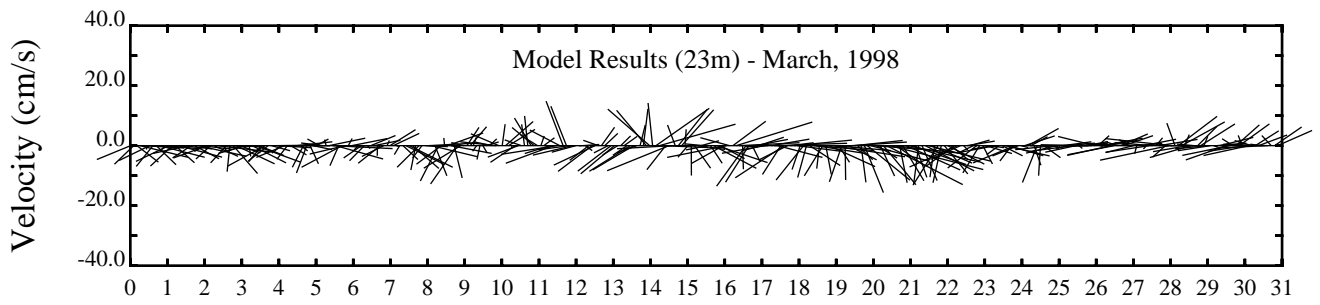
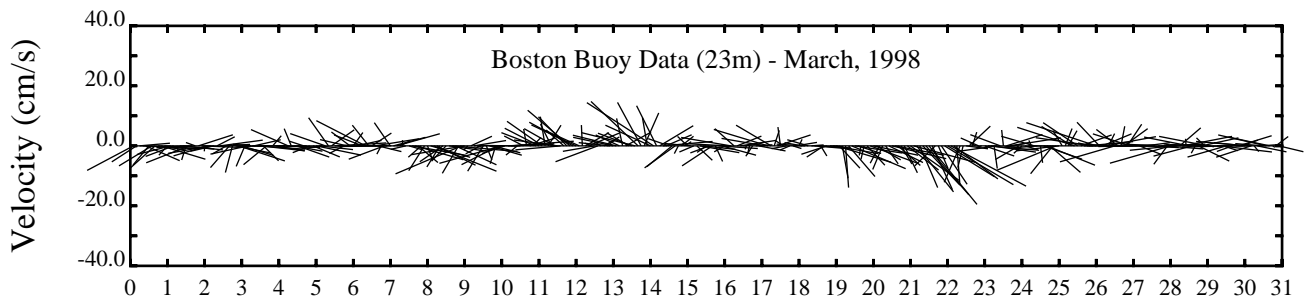
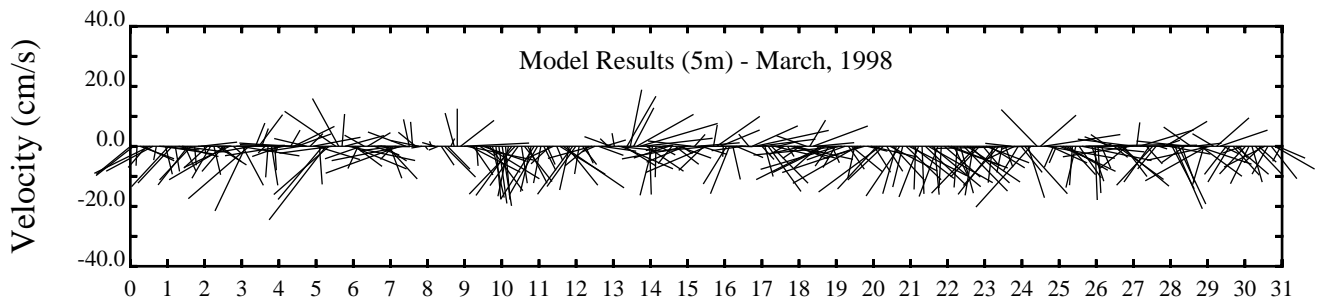
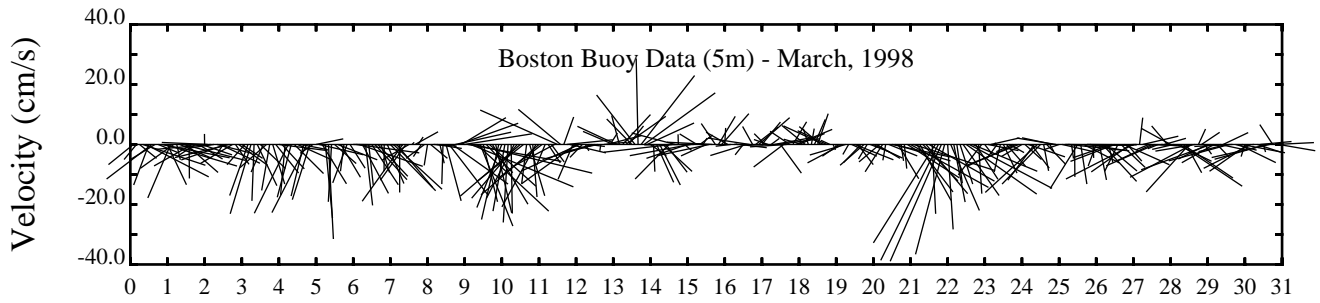
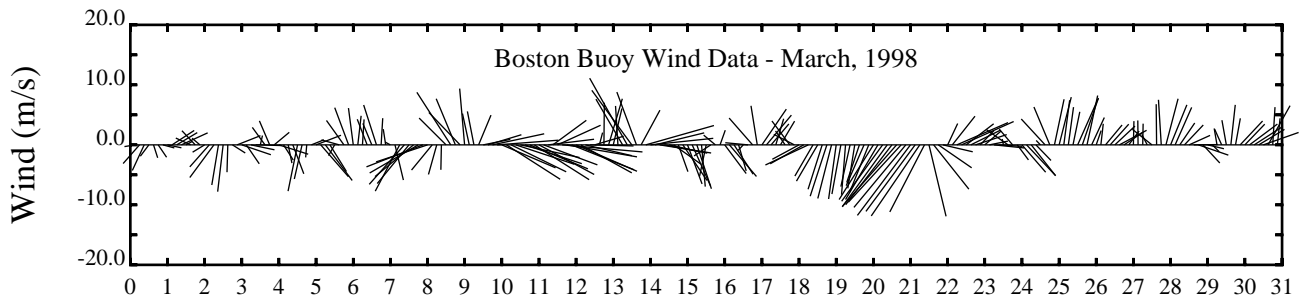


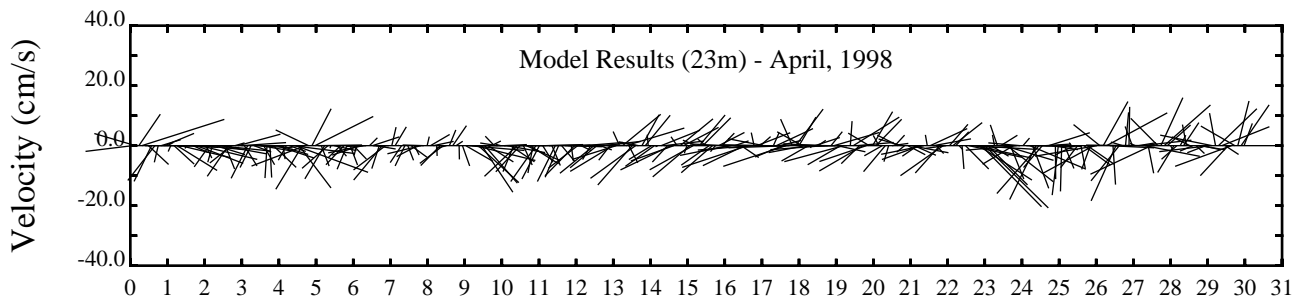
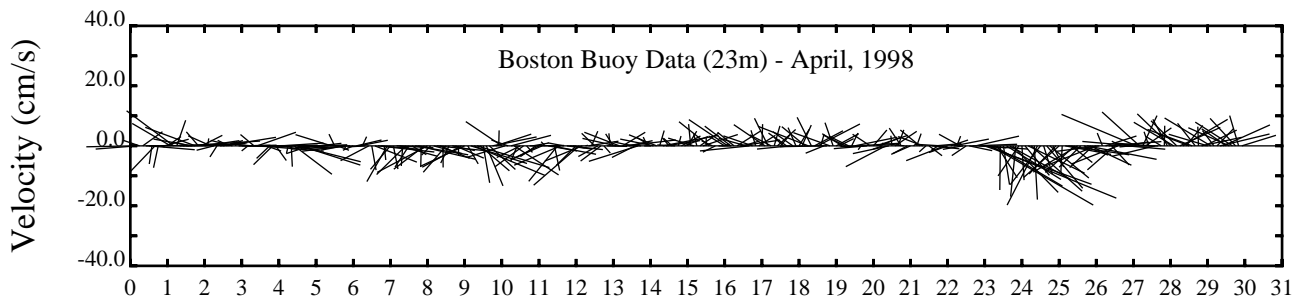
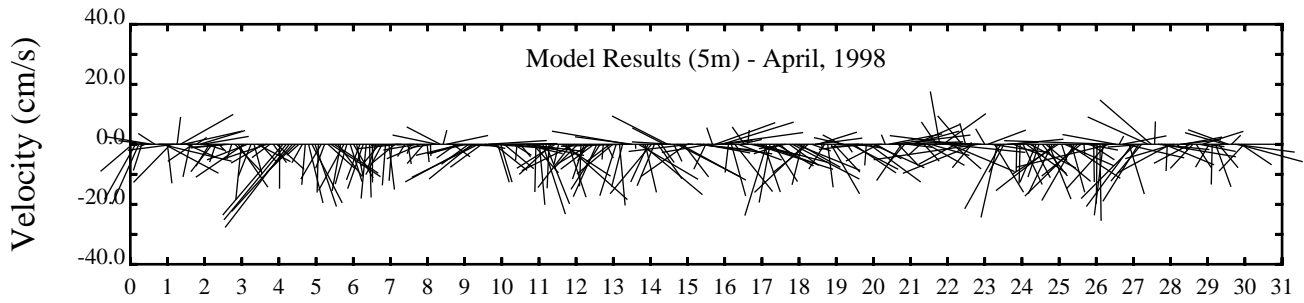
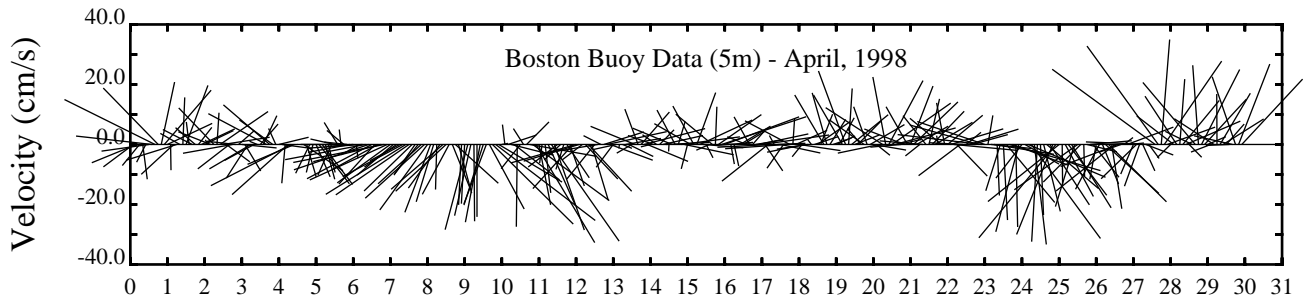
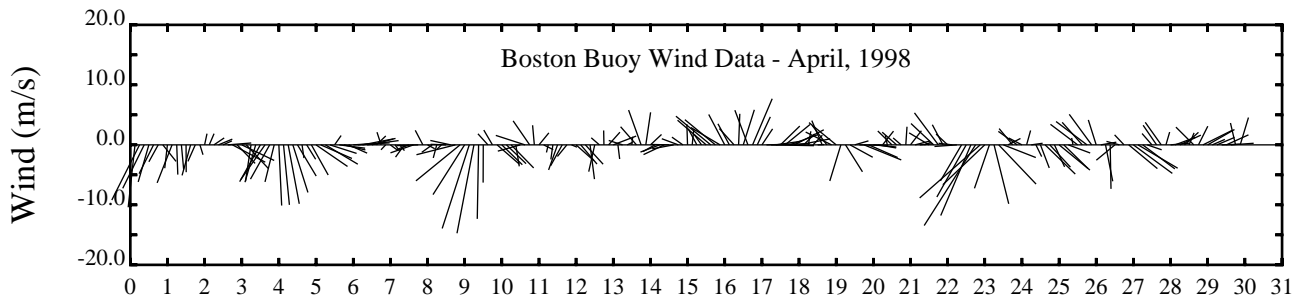
Day

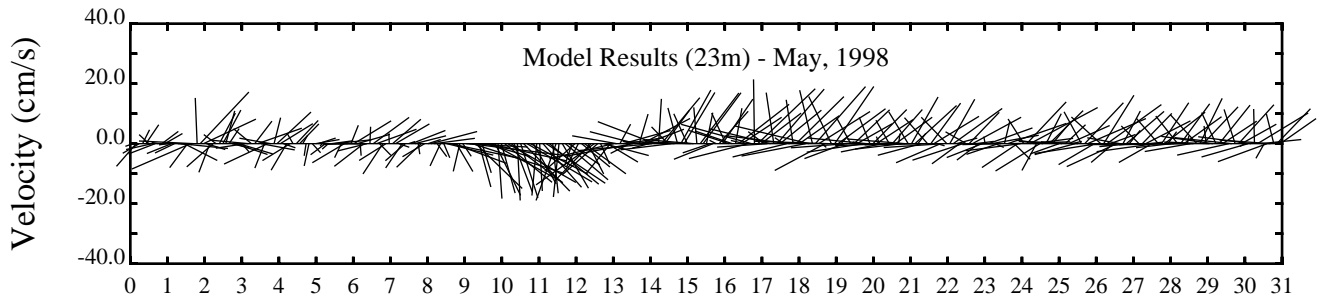
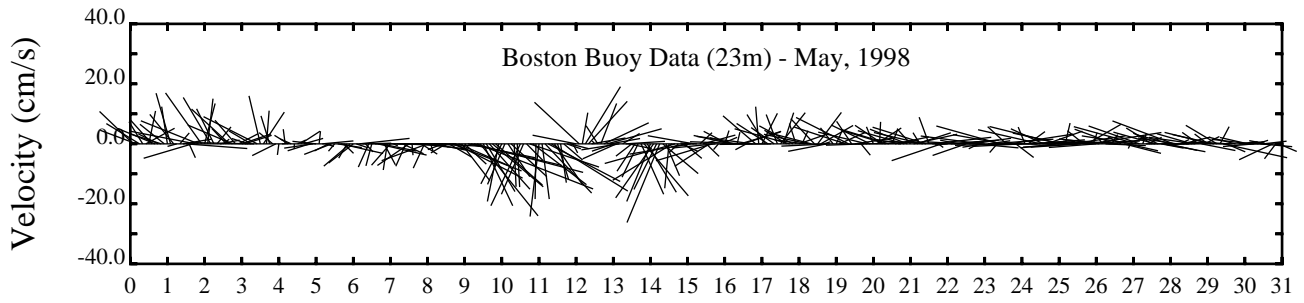
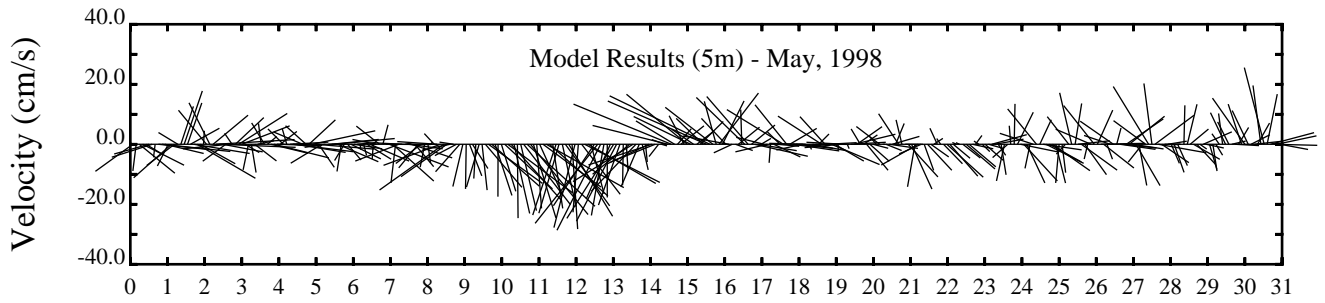
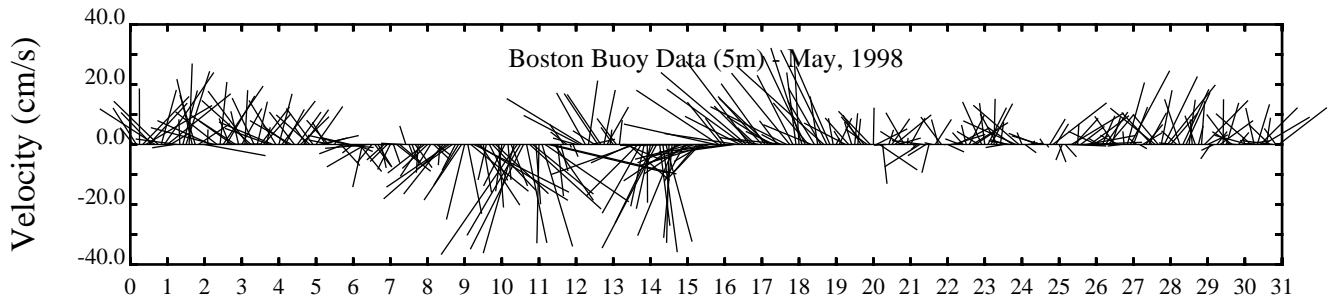
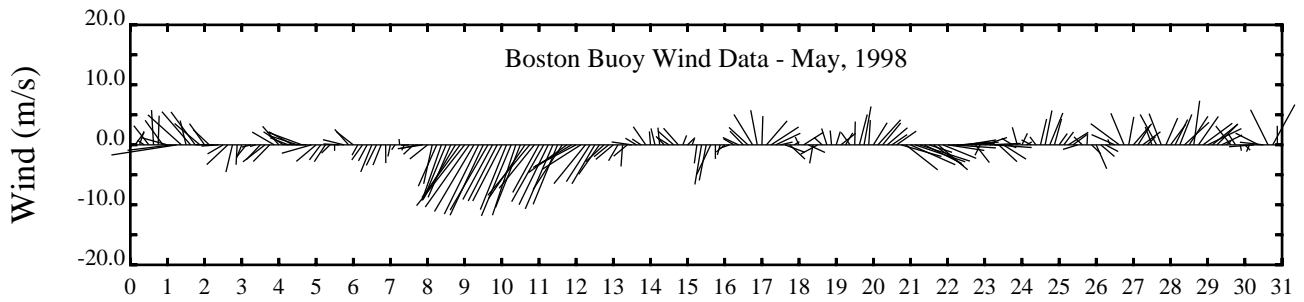


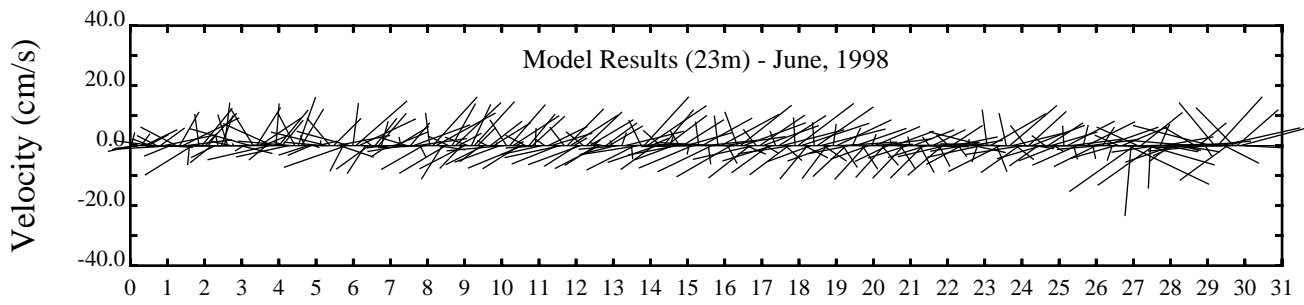
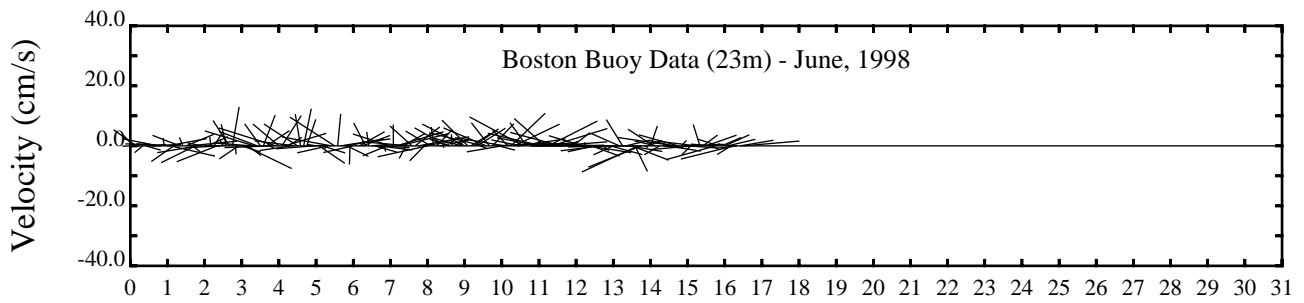
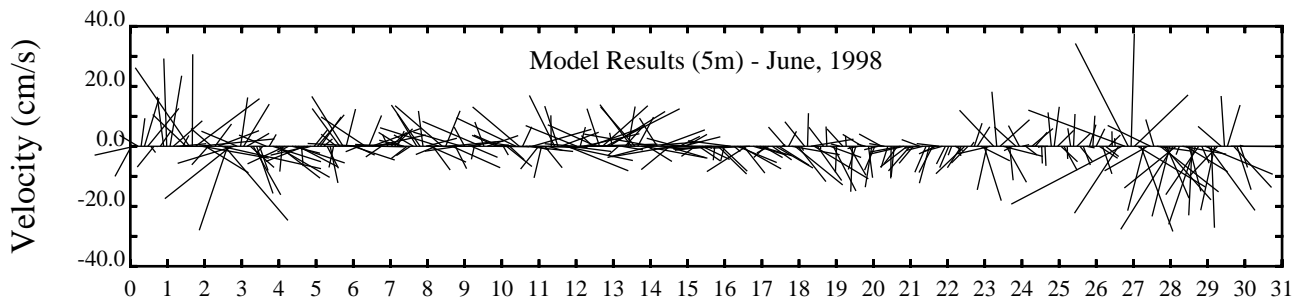
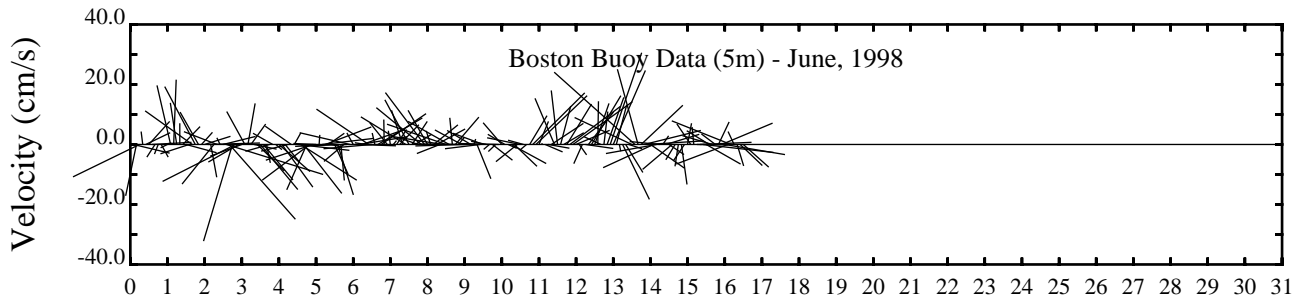
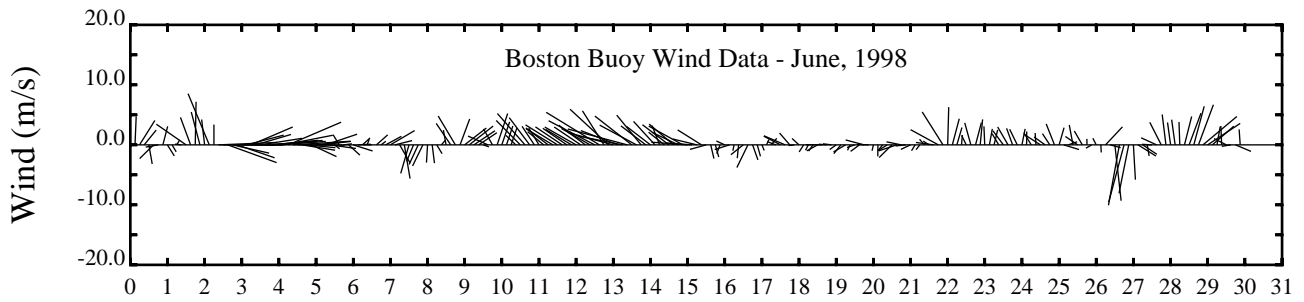


Day

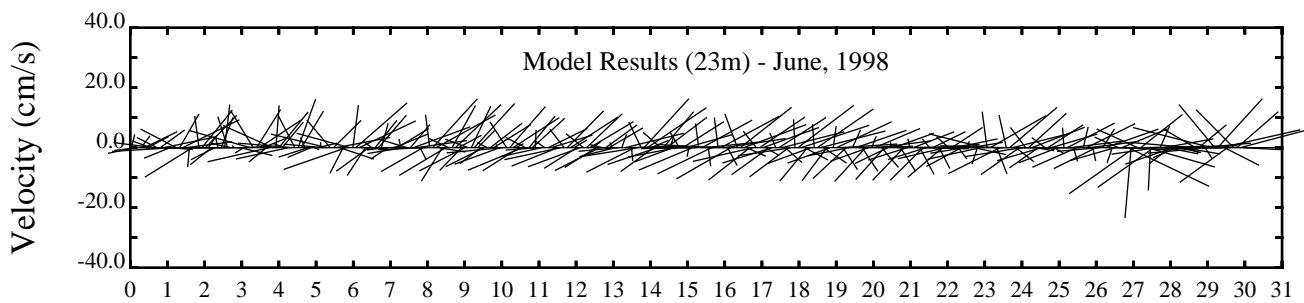
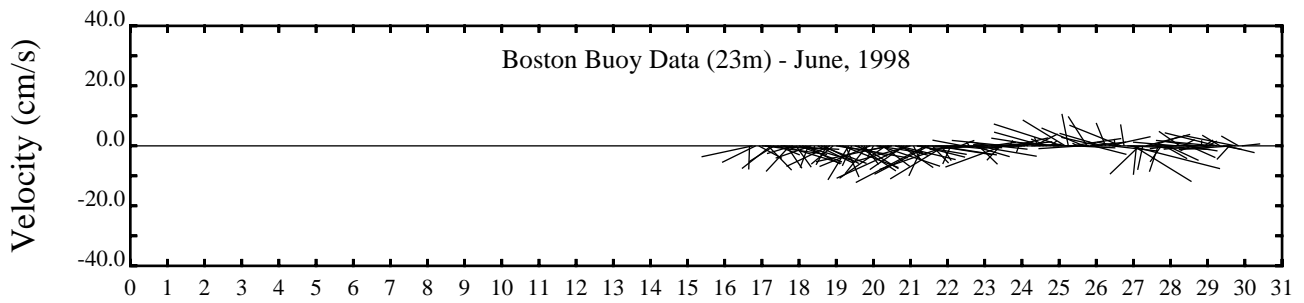
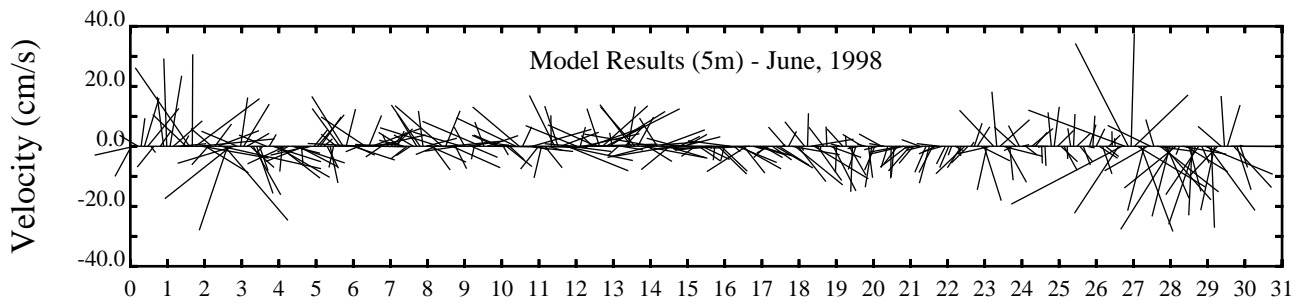
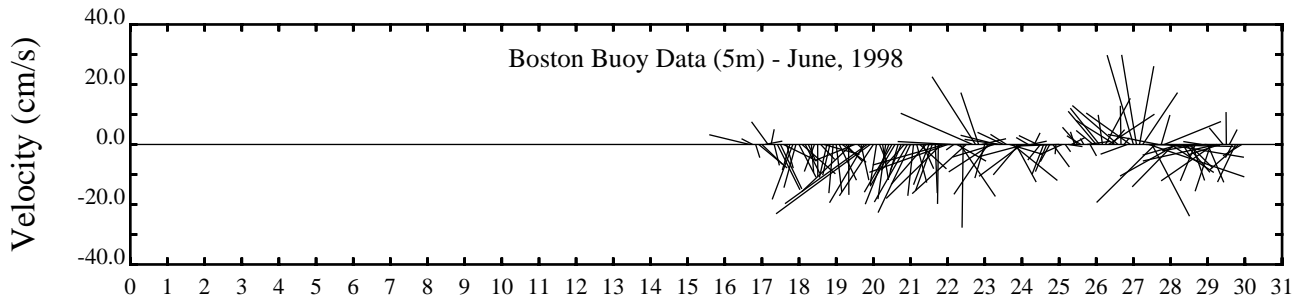
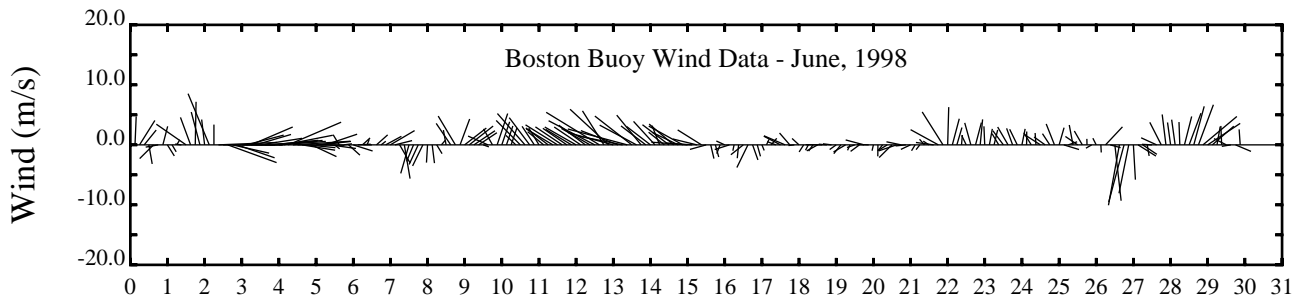




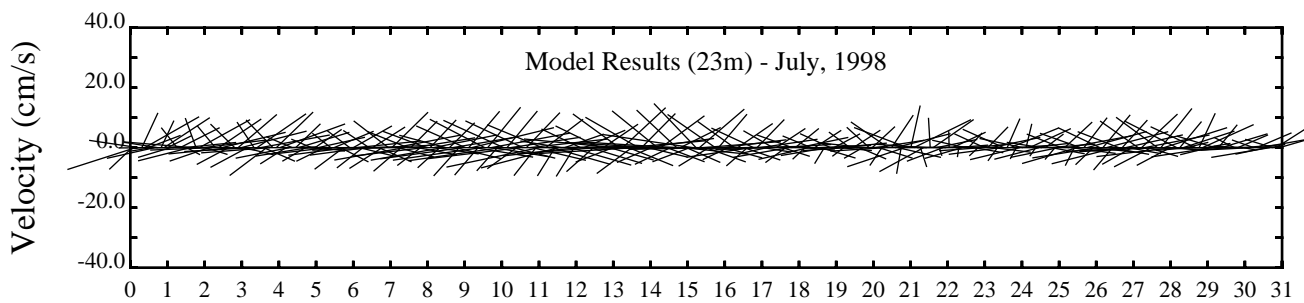
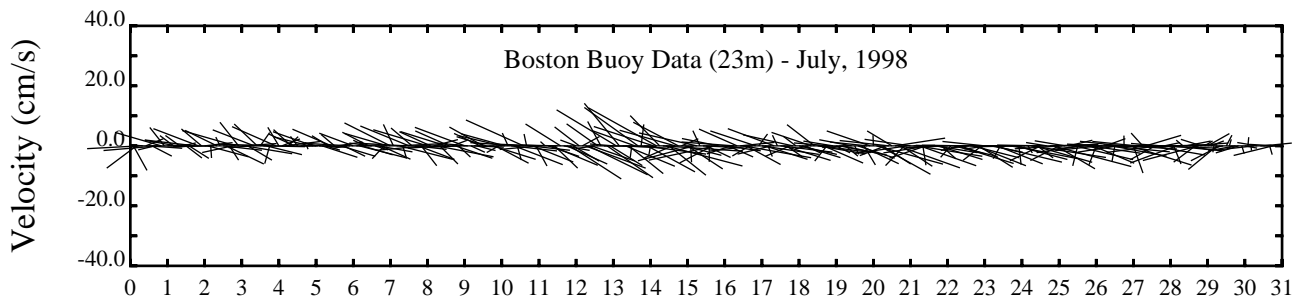
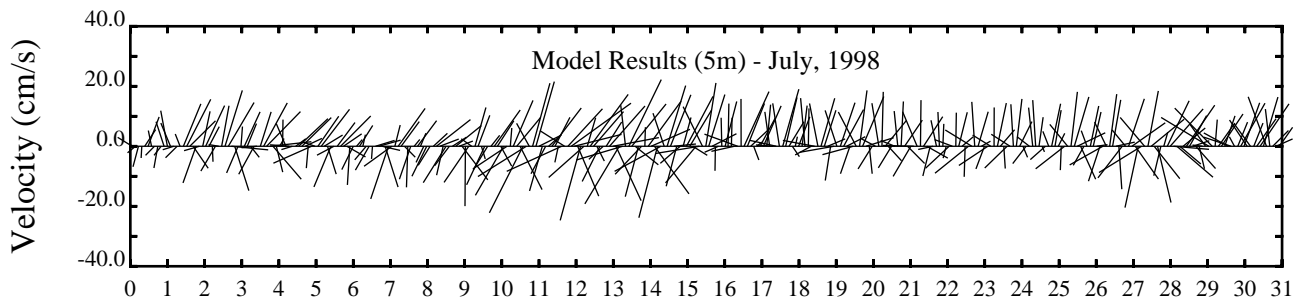
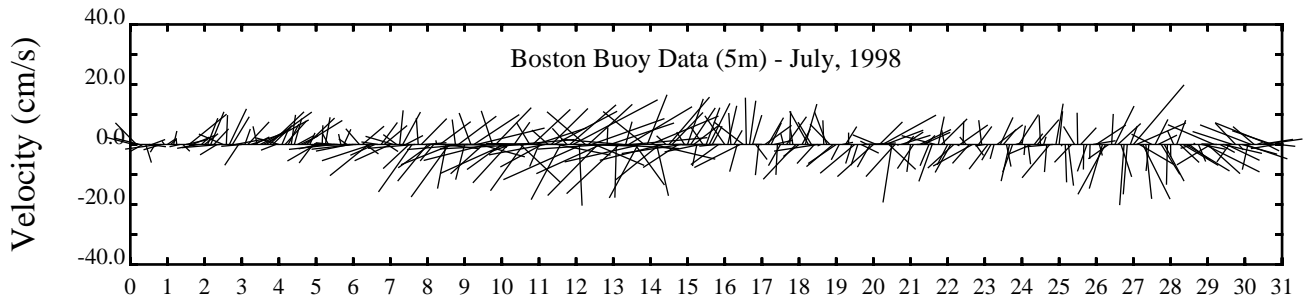
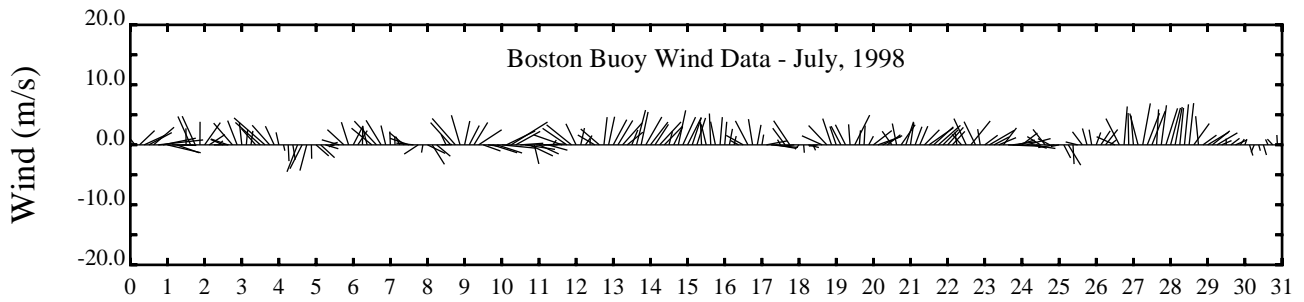




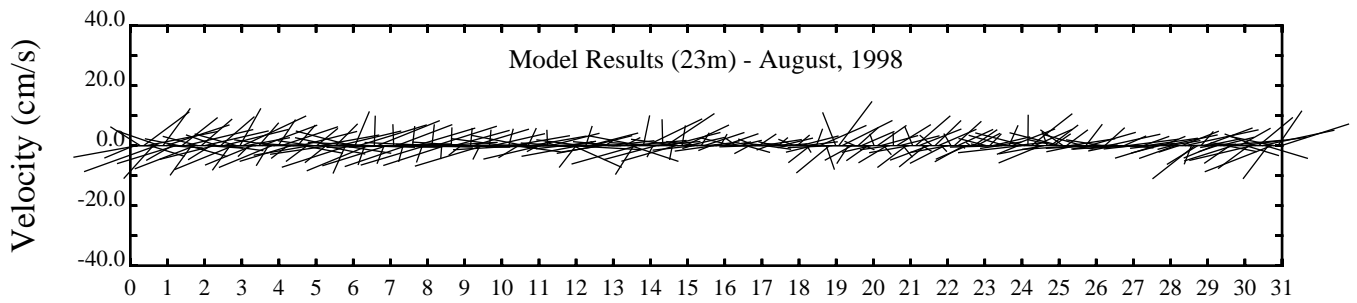
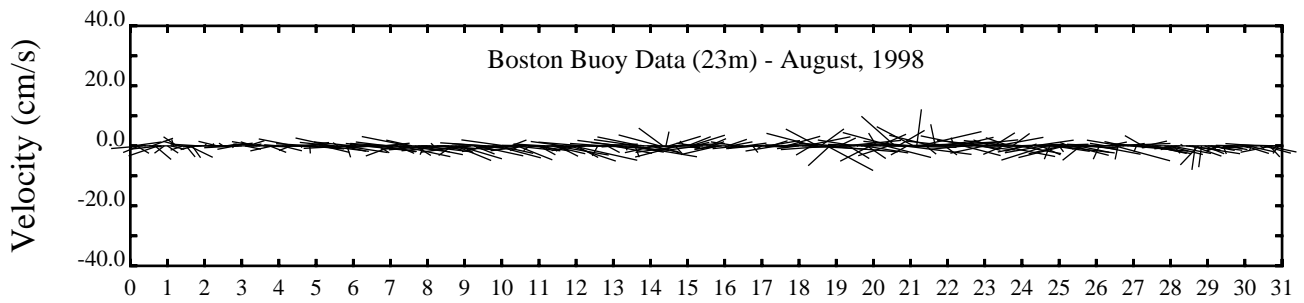
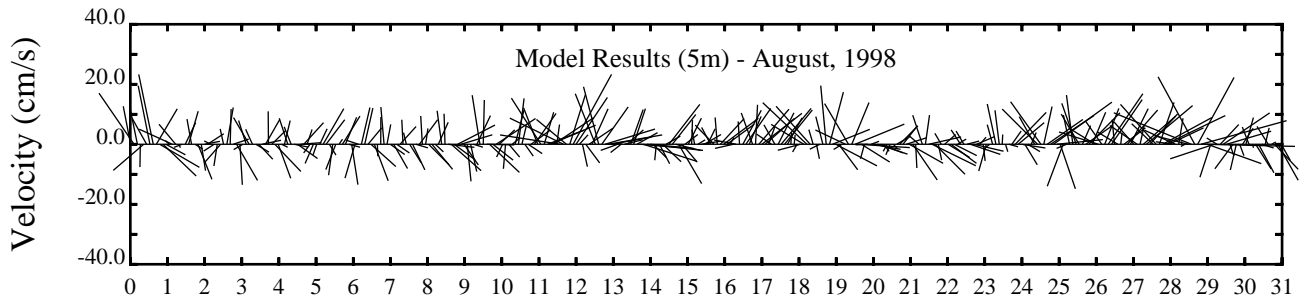
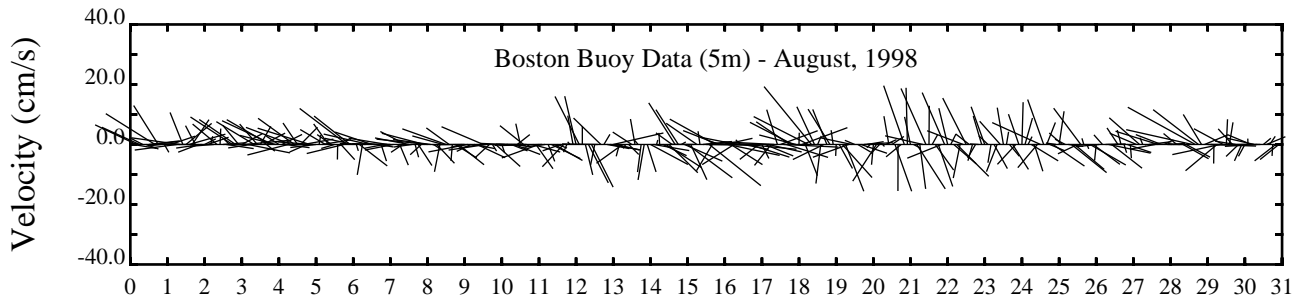
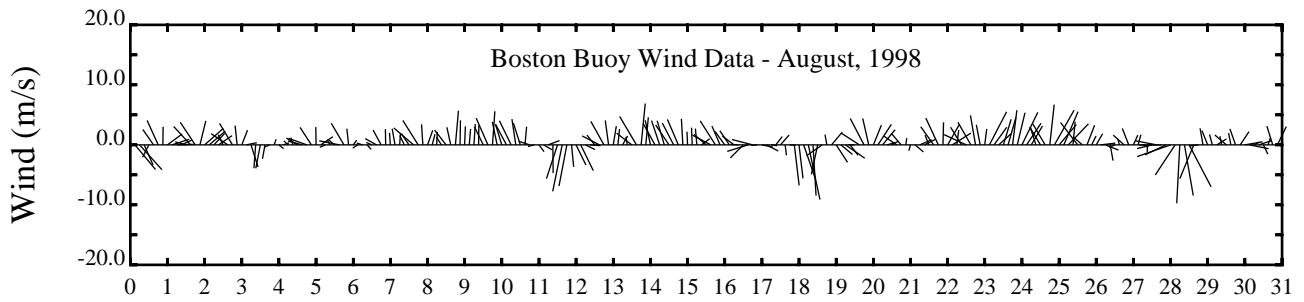
Day



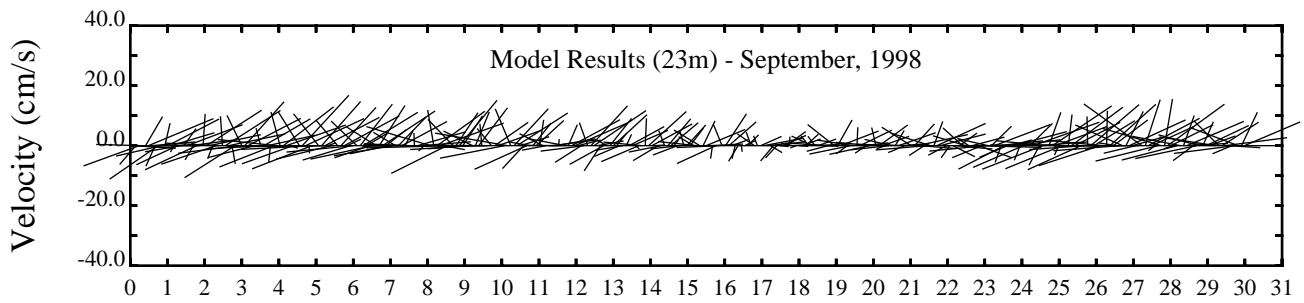
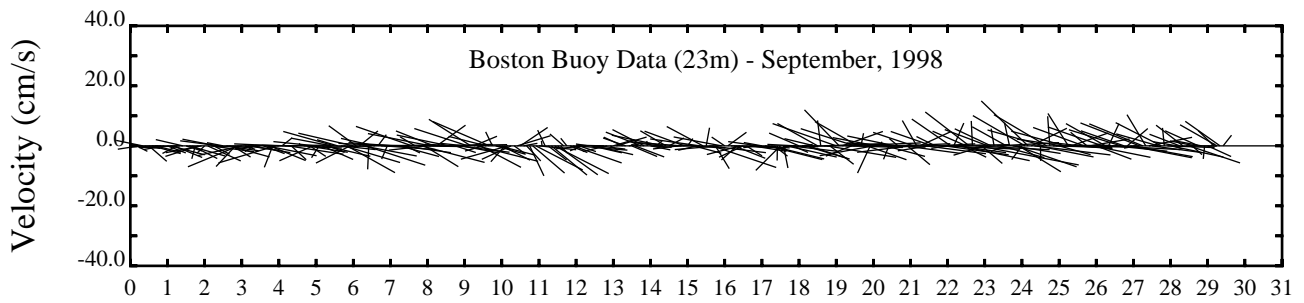
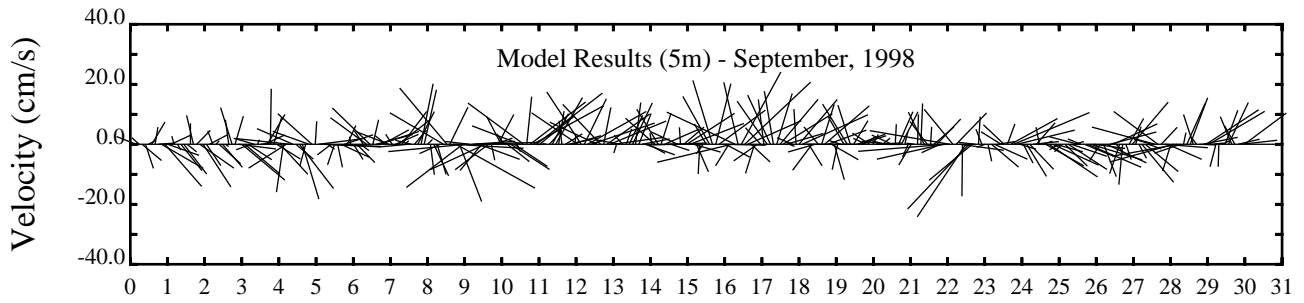
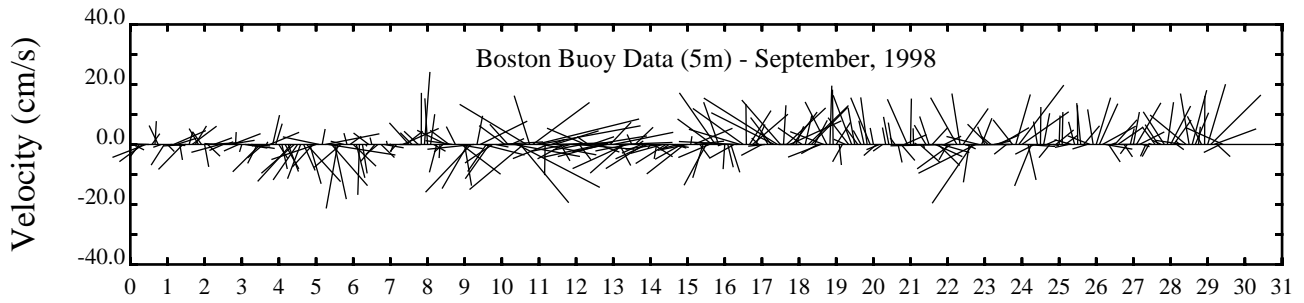
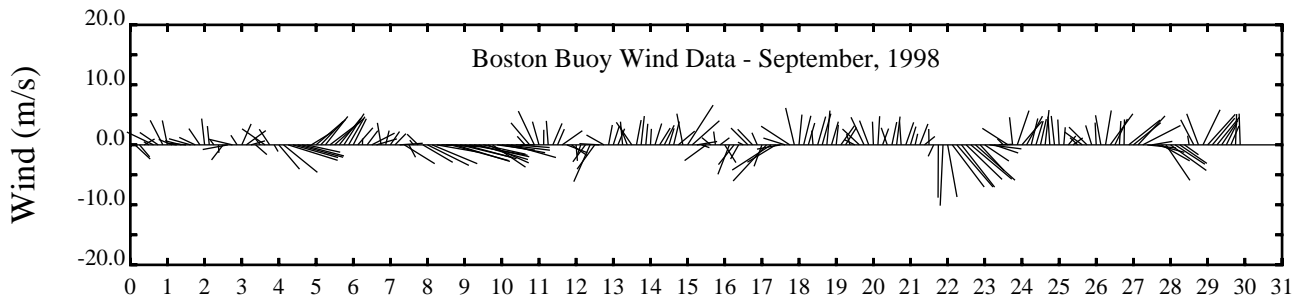
Day



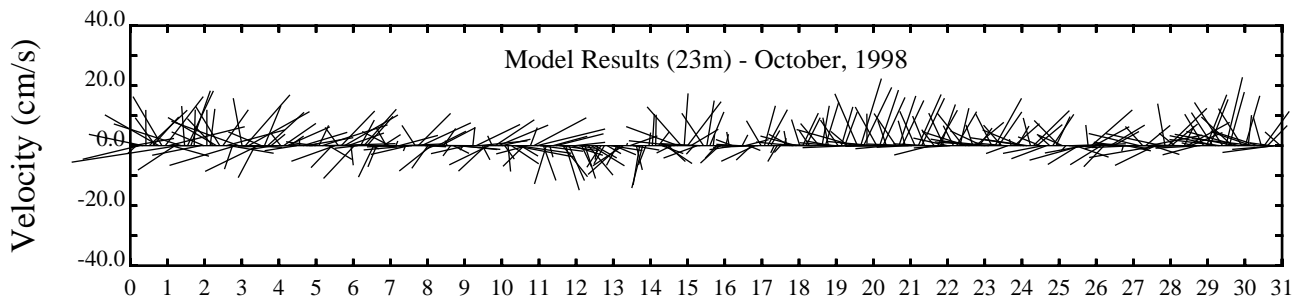
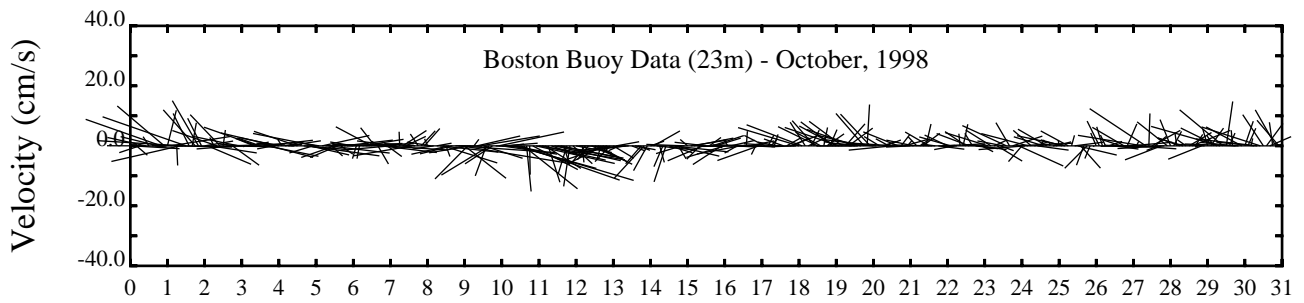
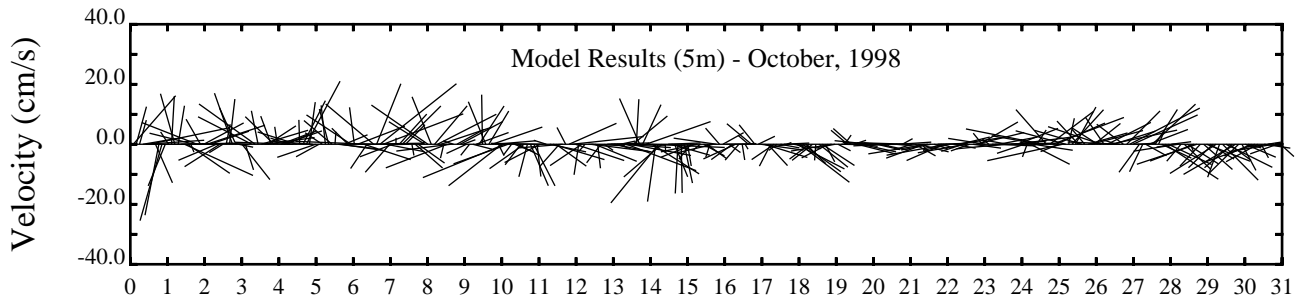
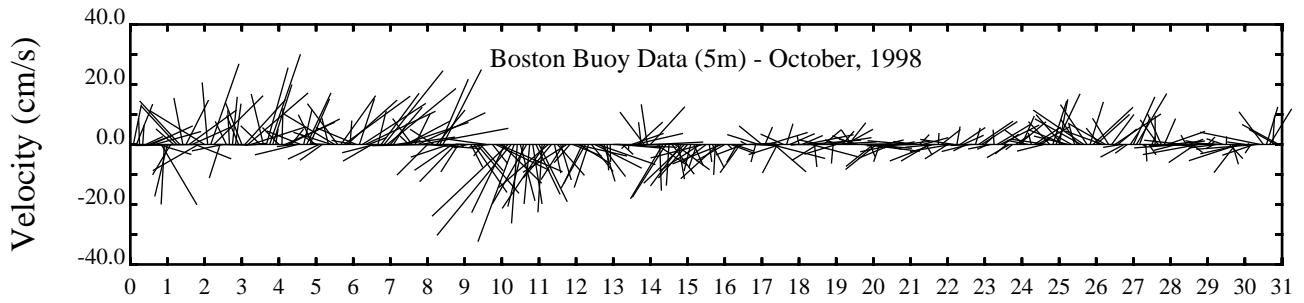
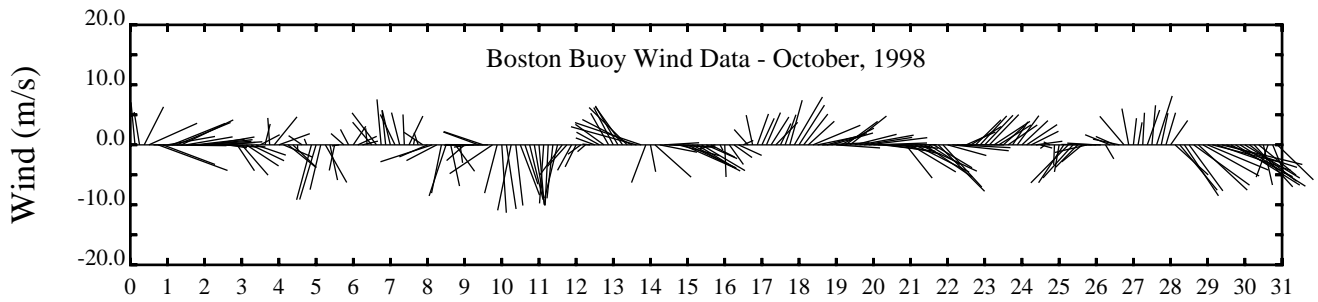
Day



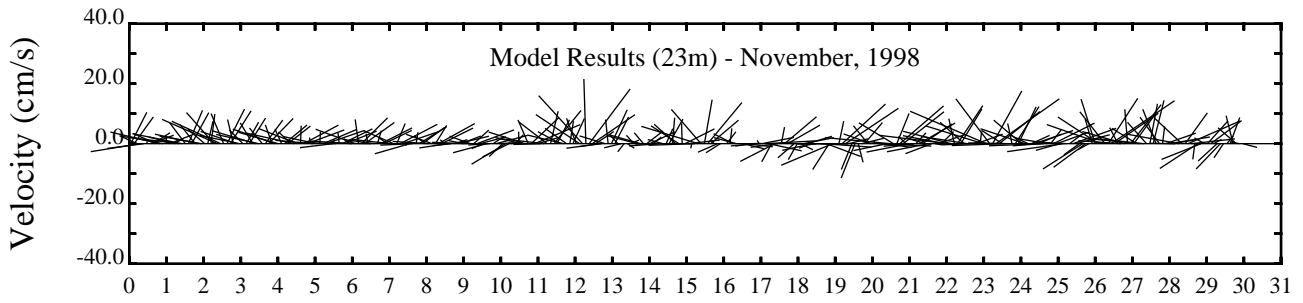
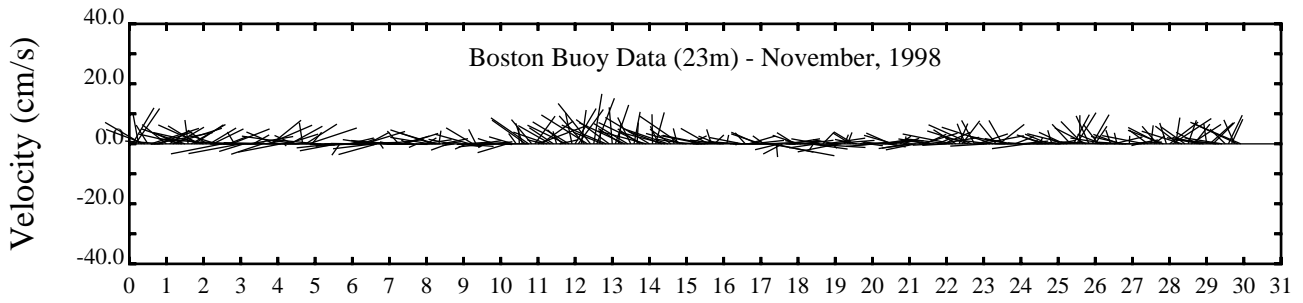
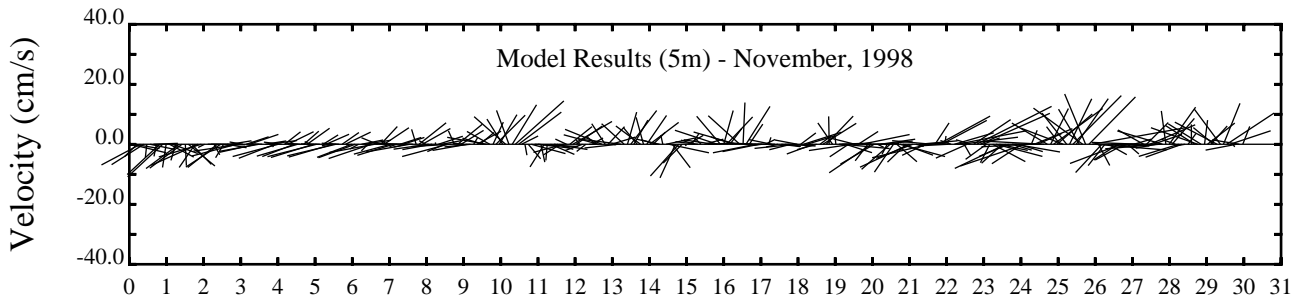
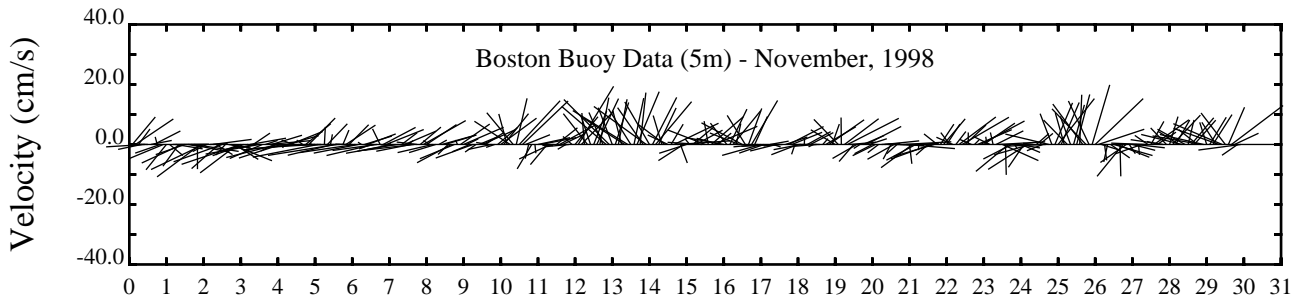
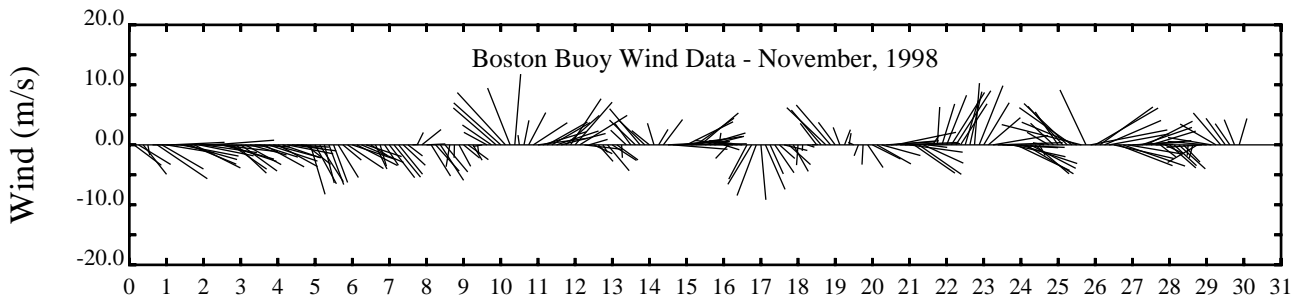
Day

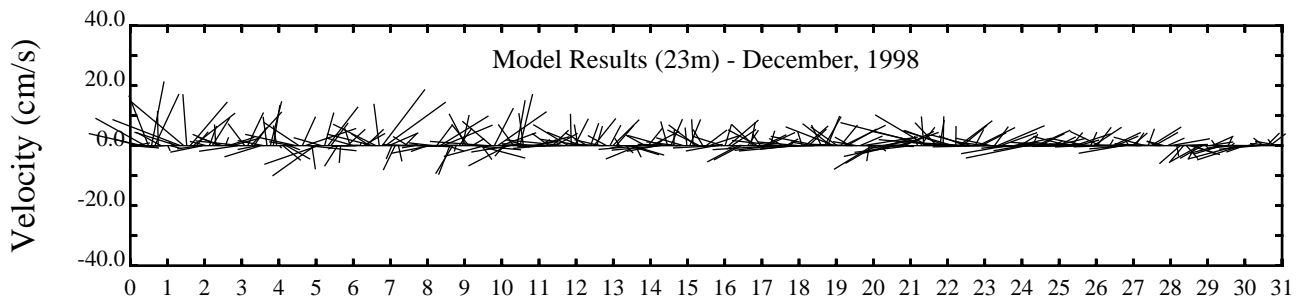
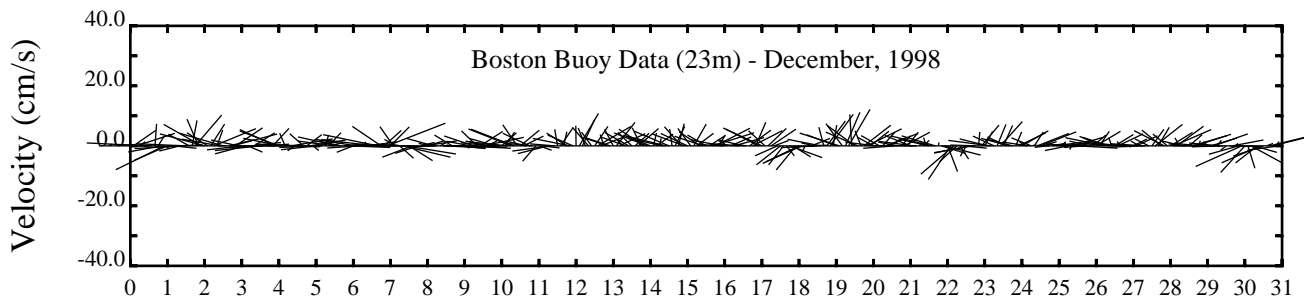
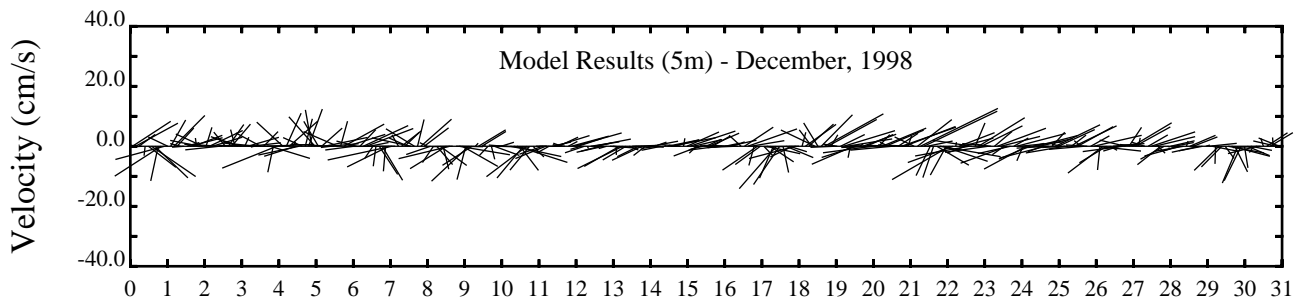
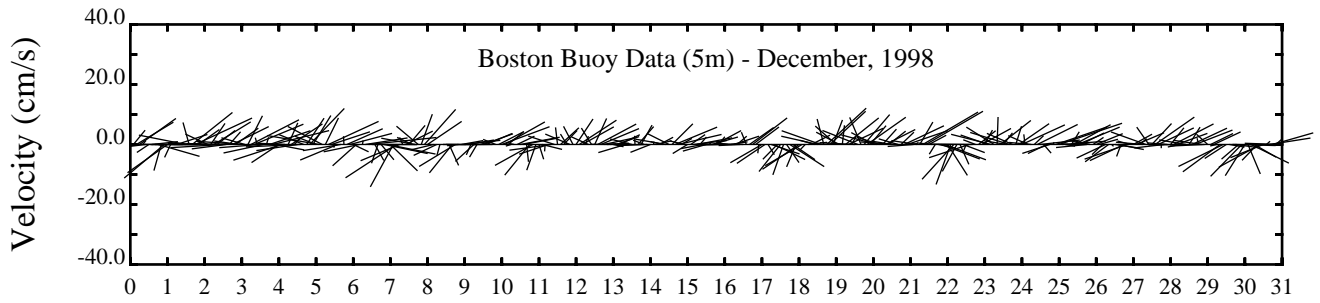
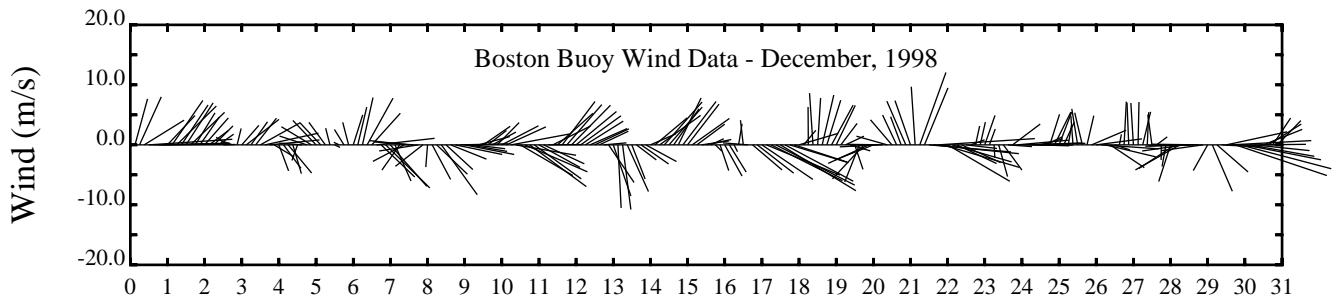


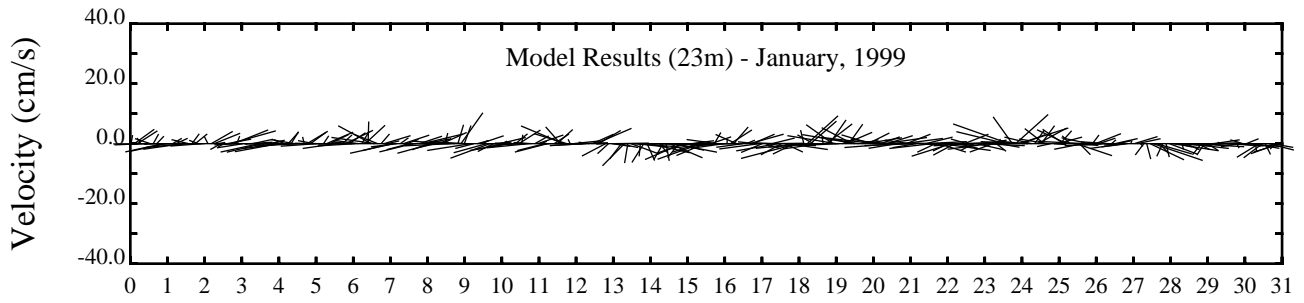
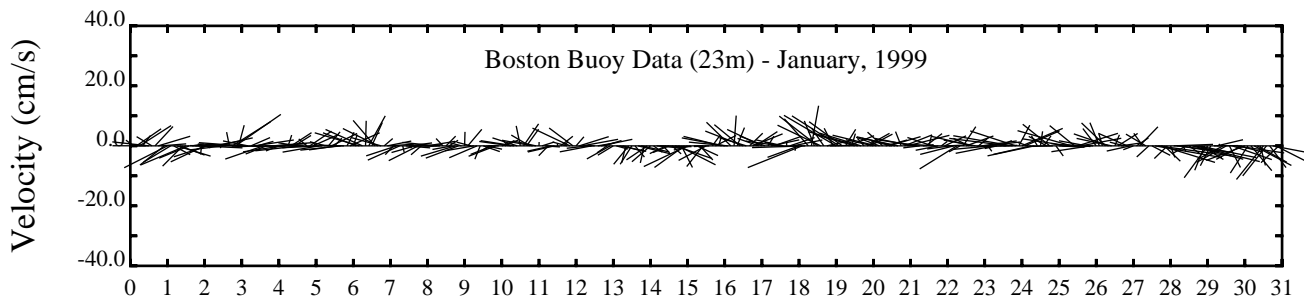
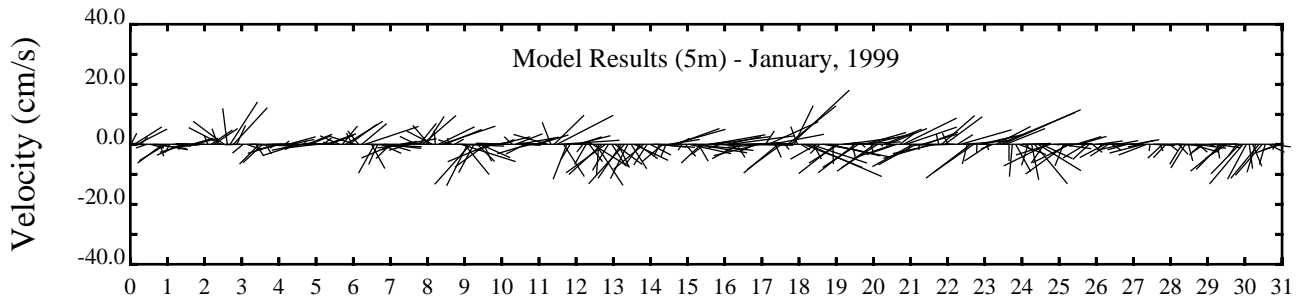
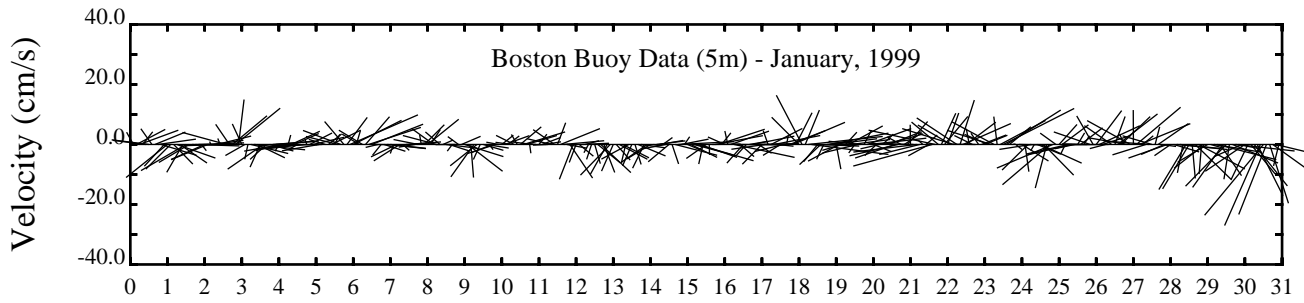
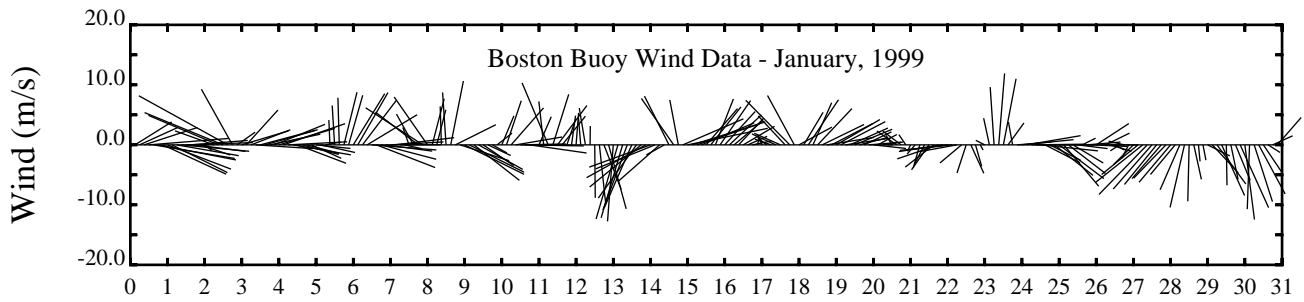
Day

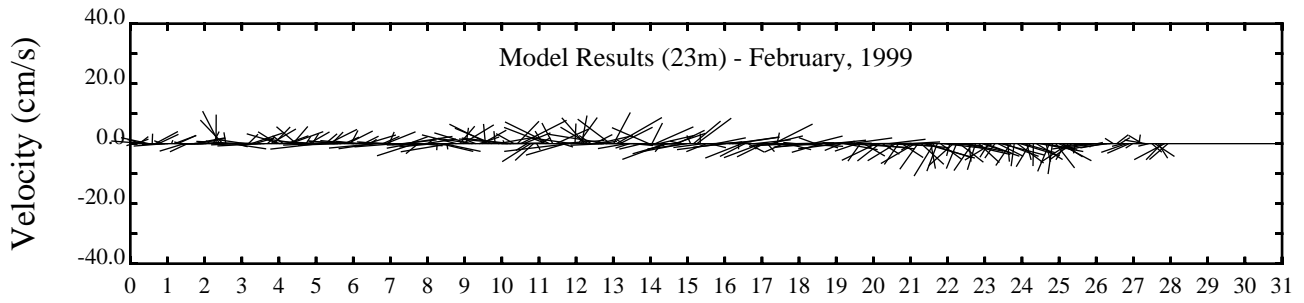
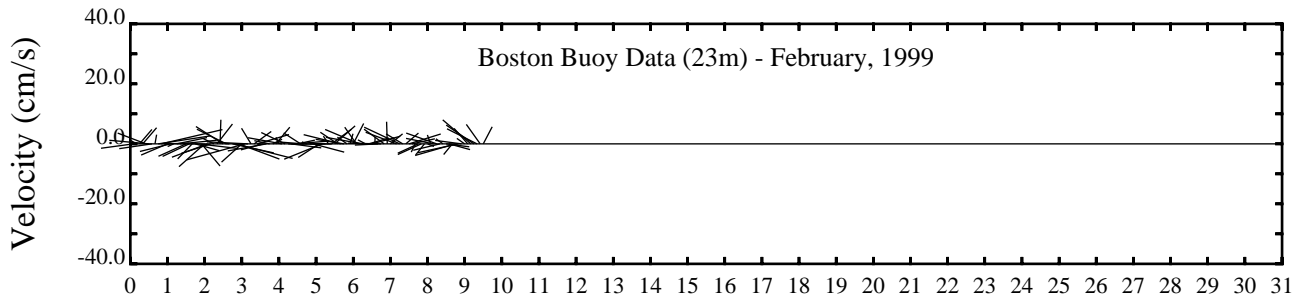
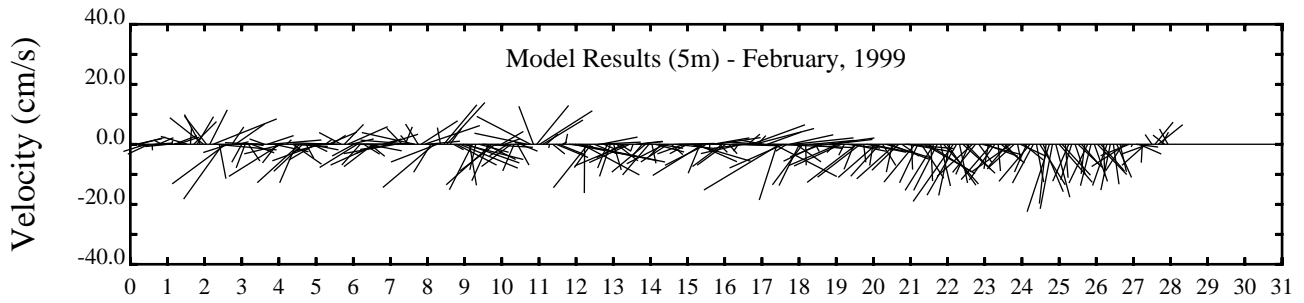
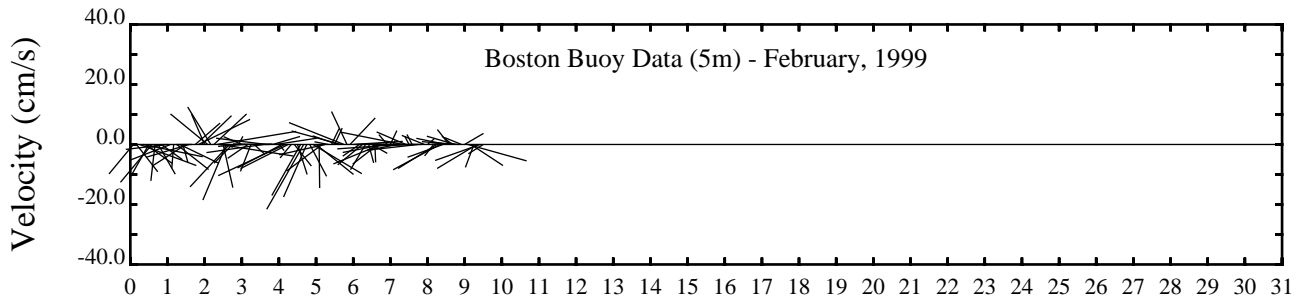
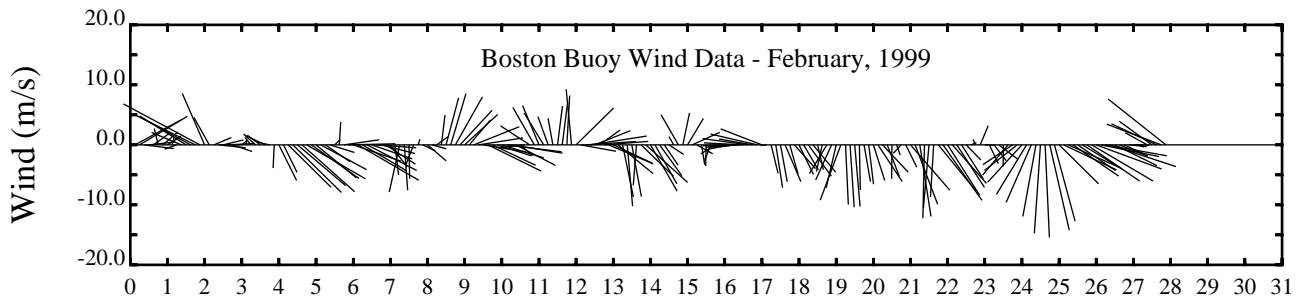


Day

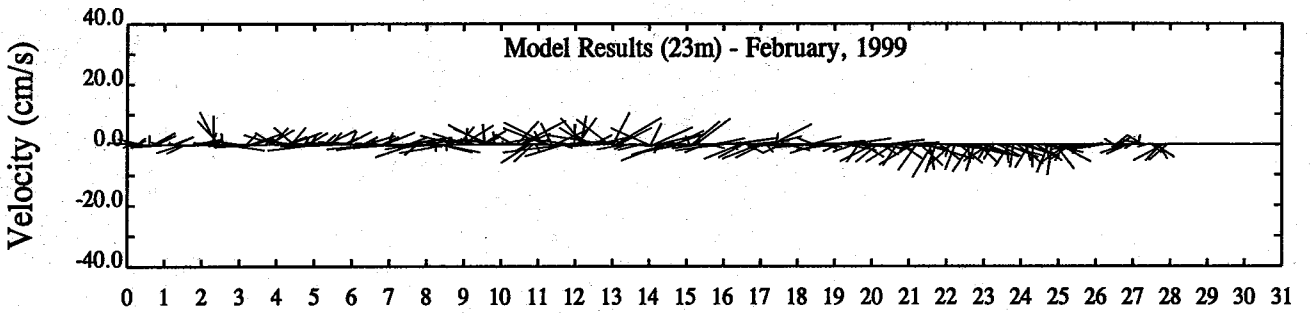
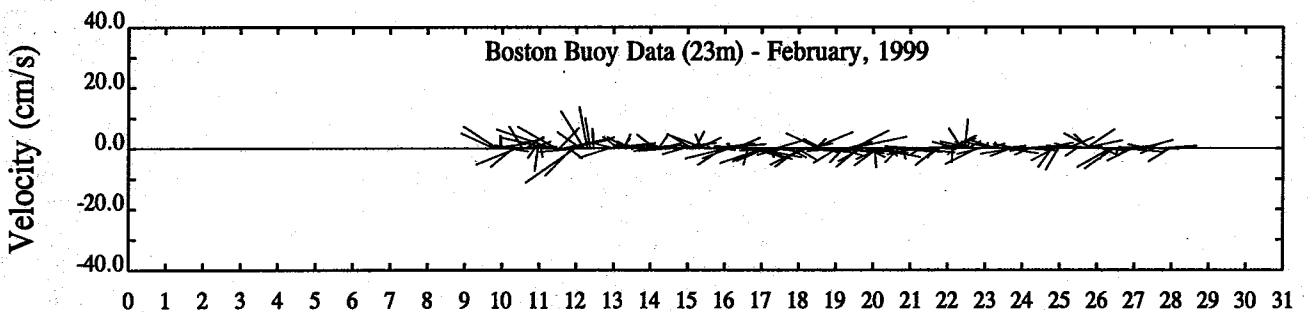
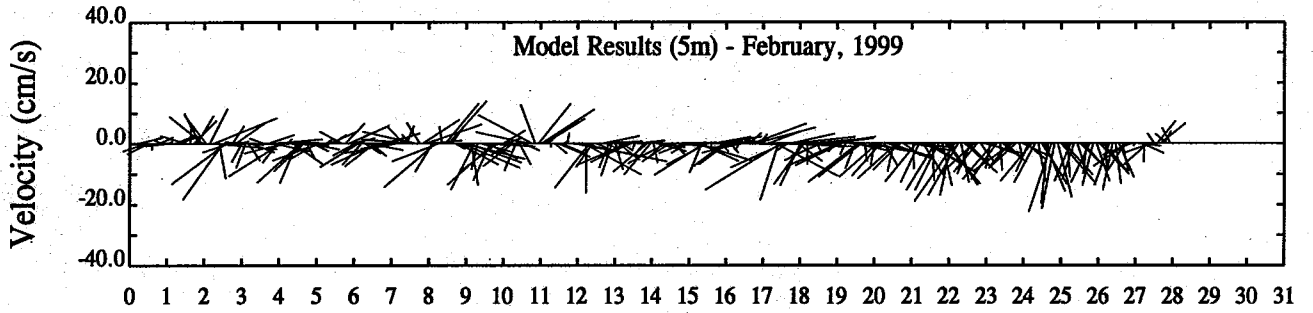
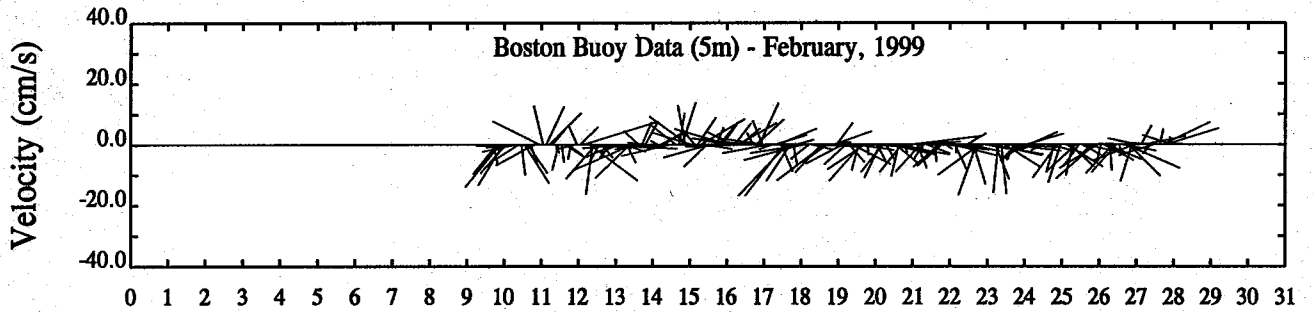
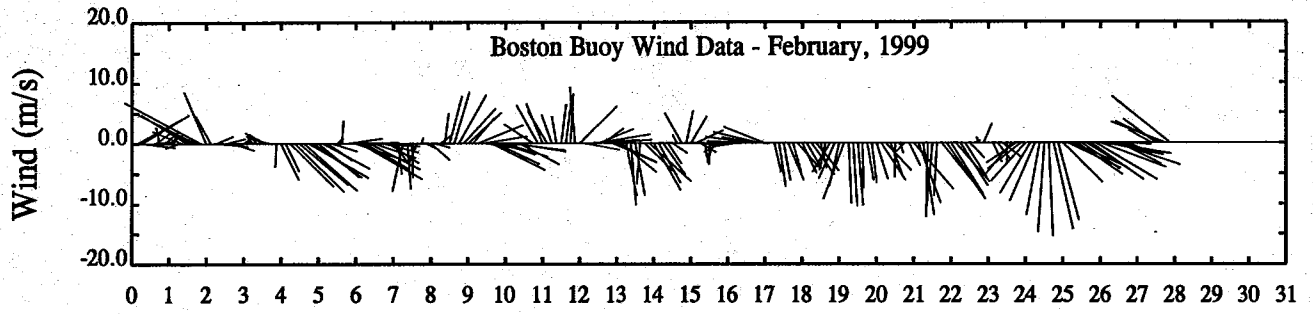


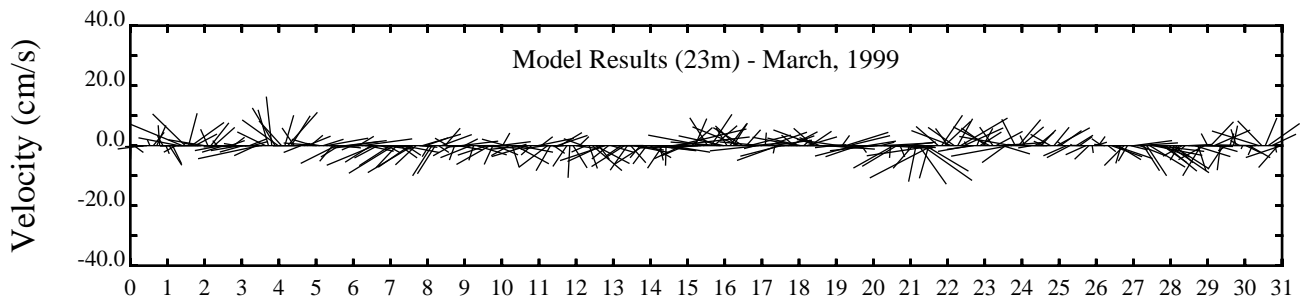
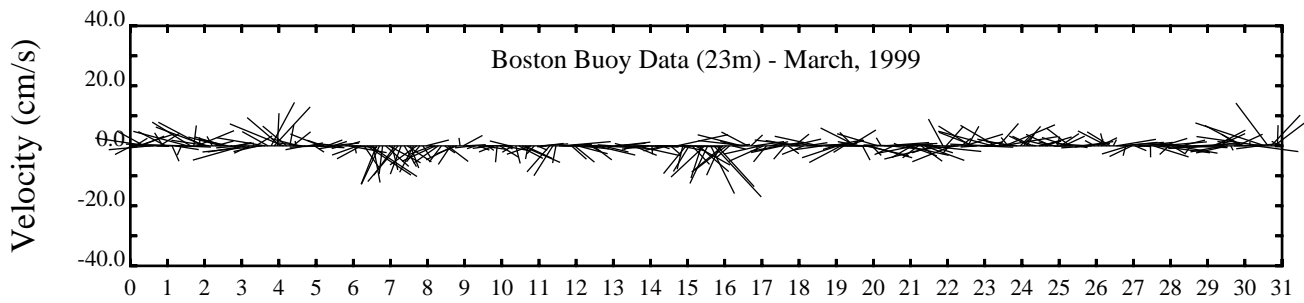
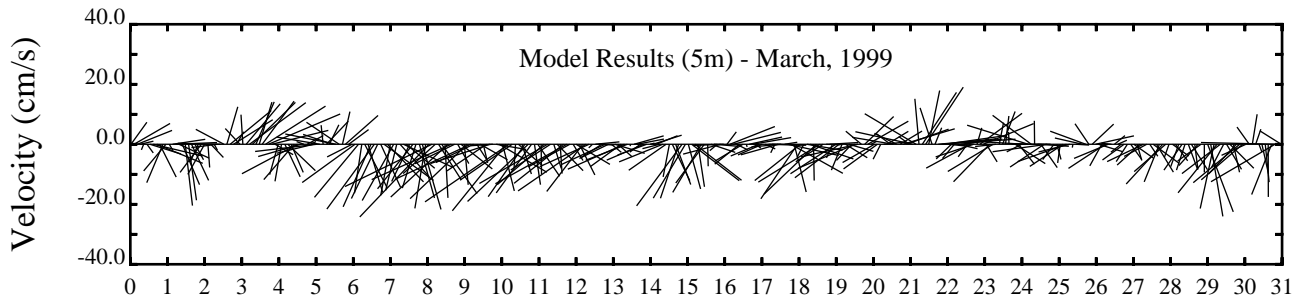
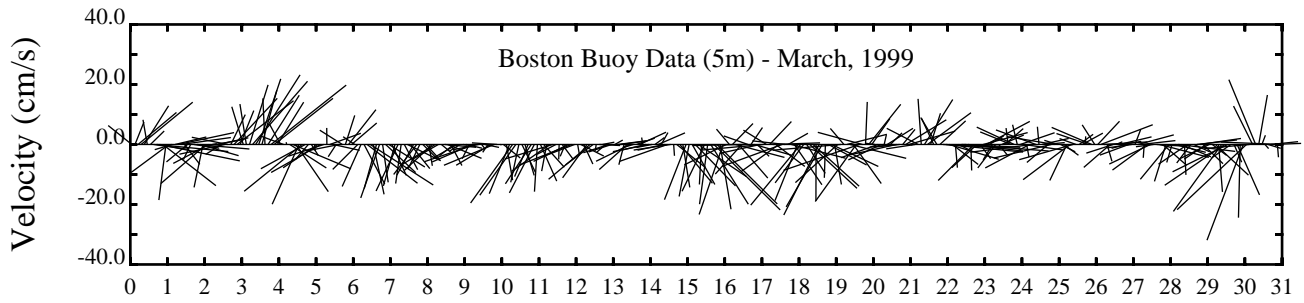
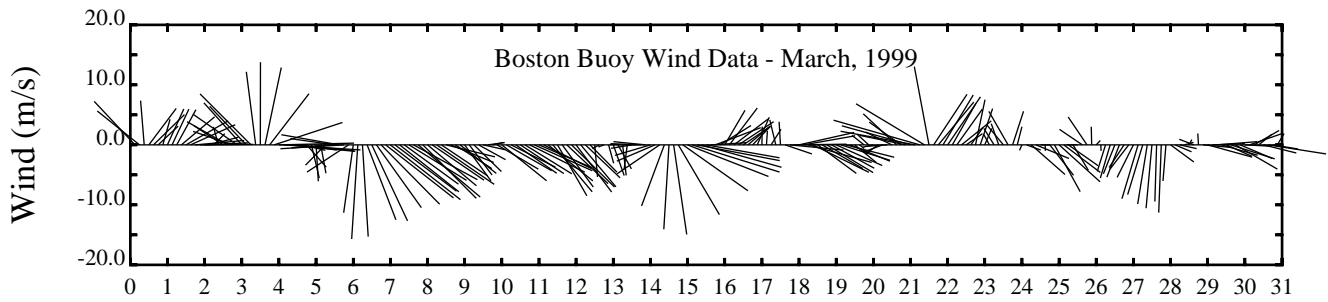


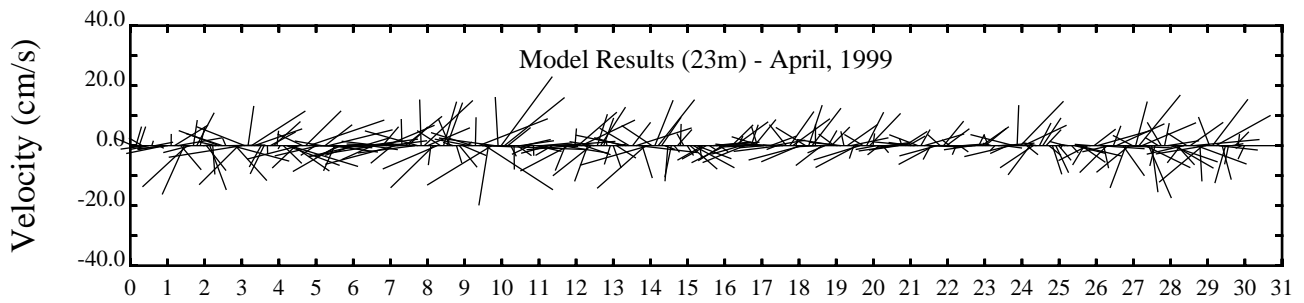
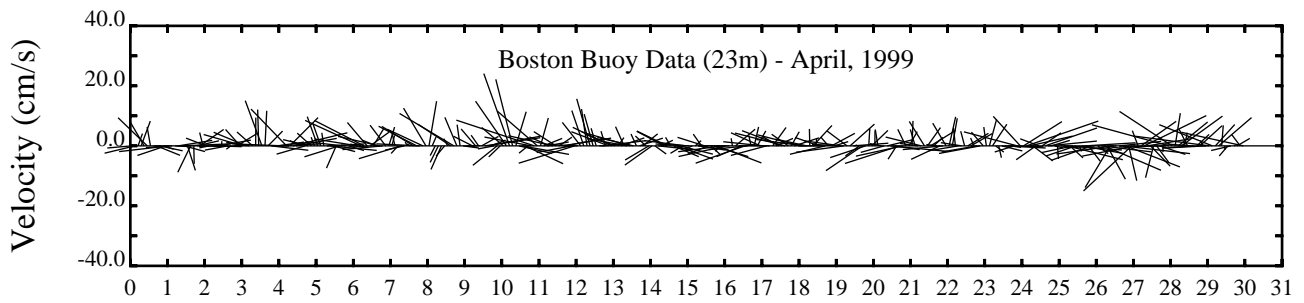
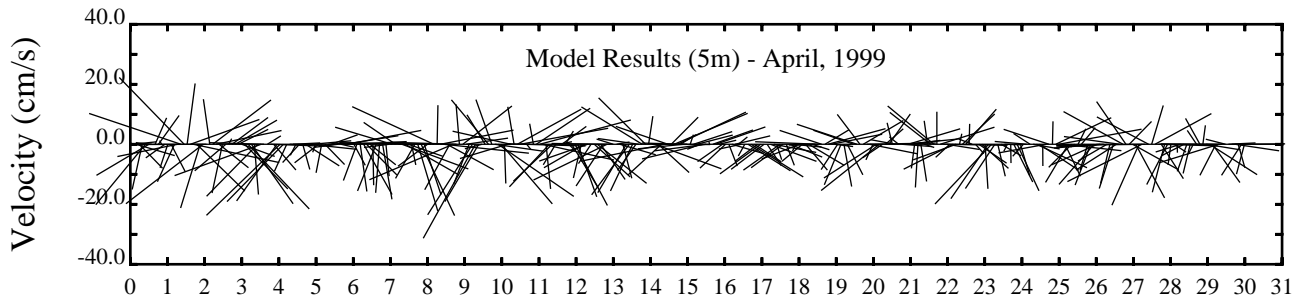
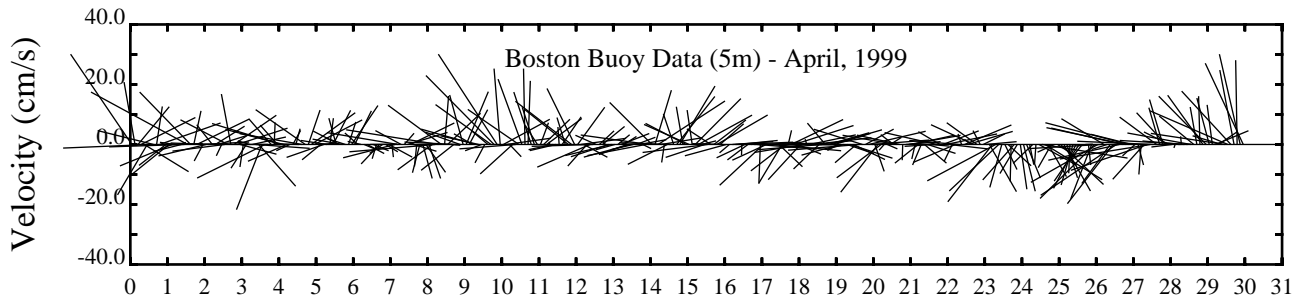
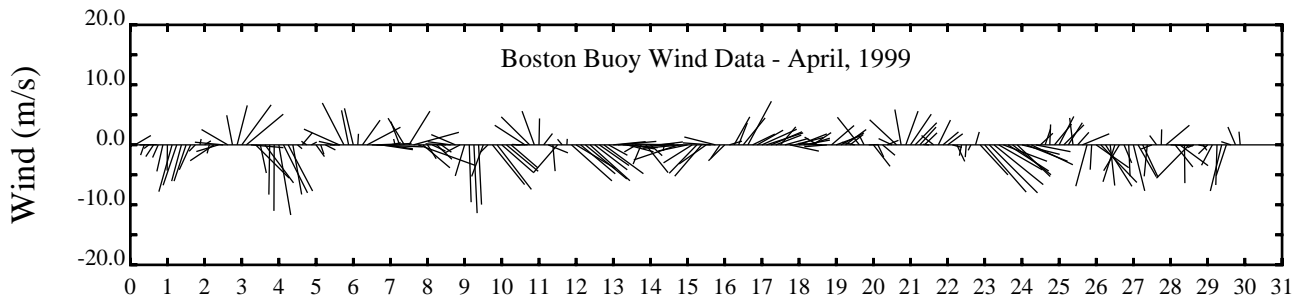




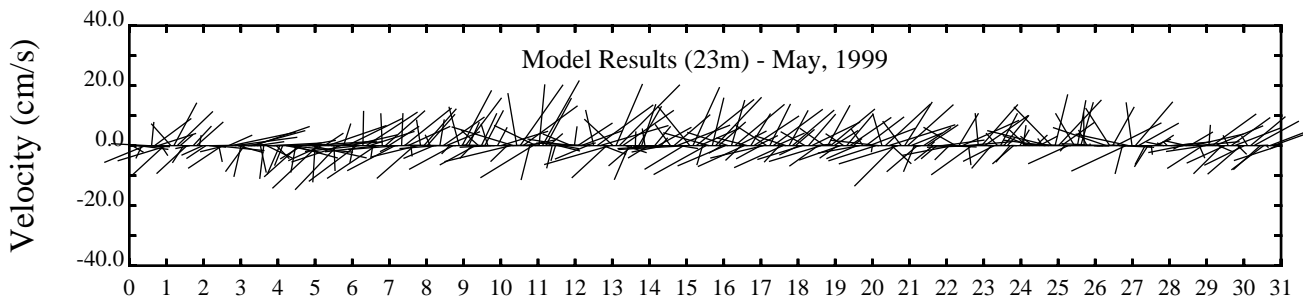
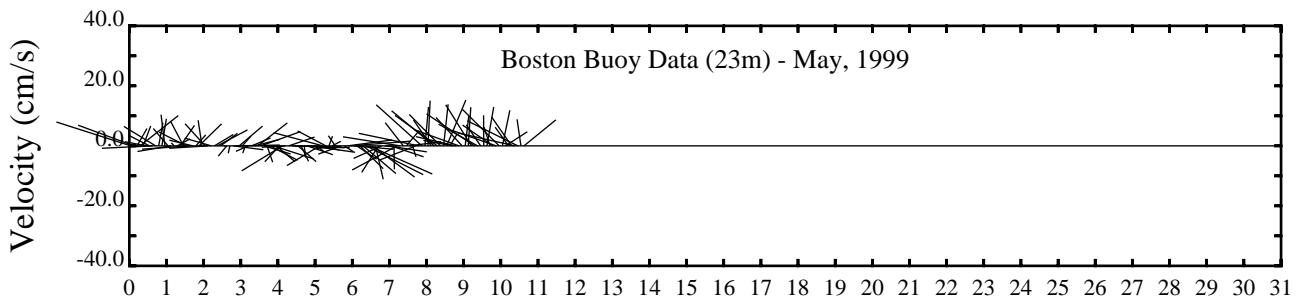
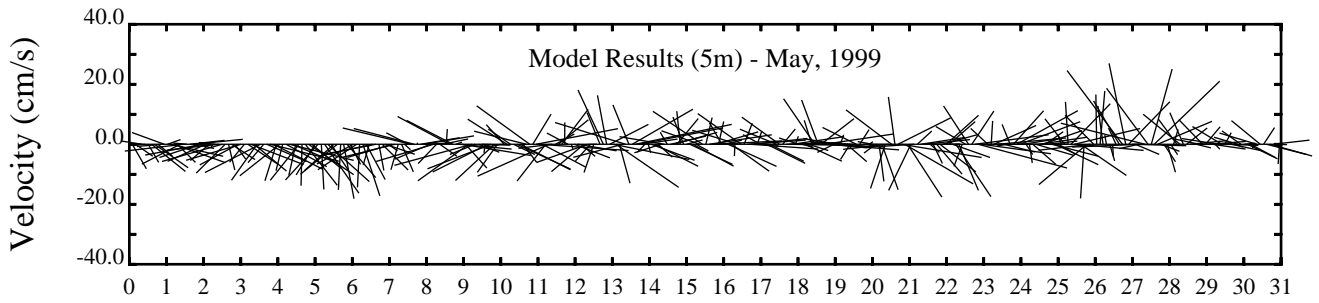
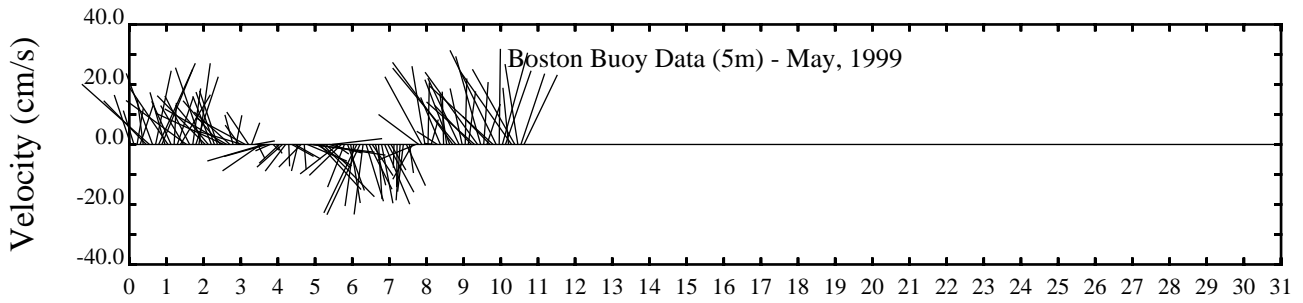
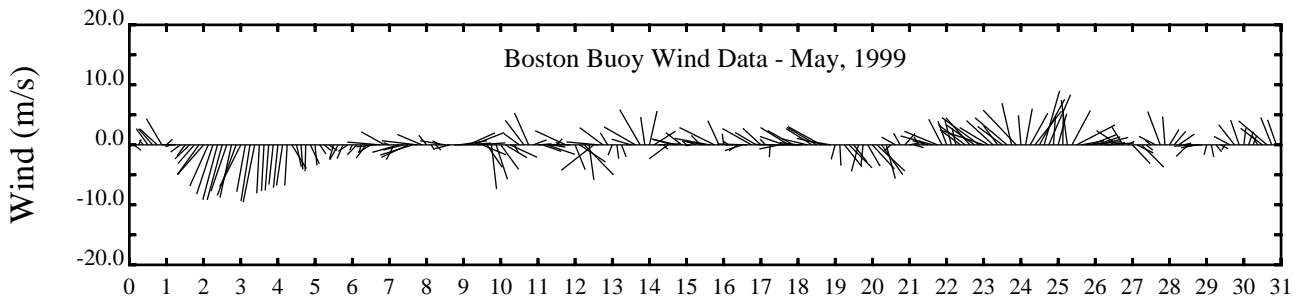
Day



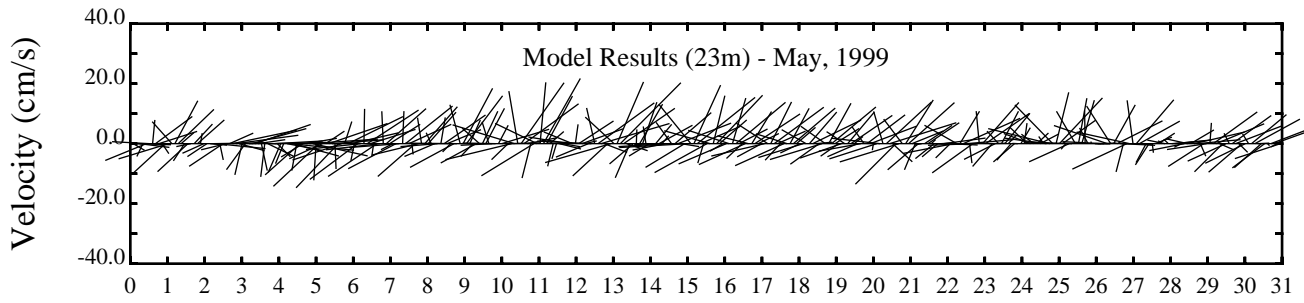
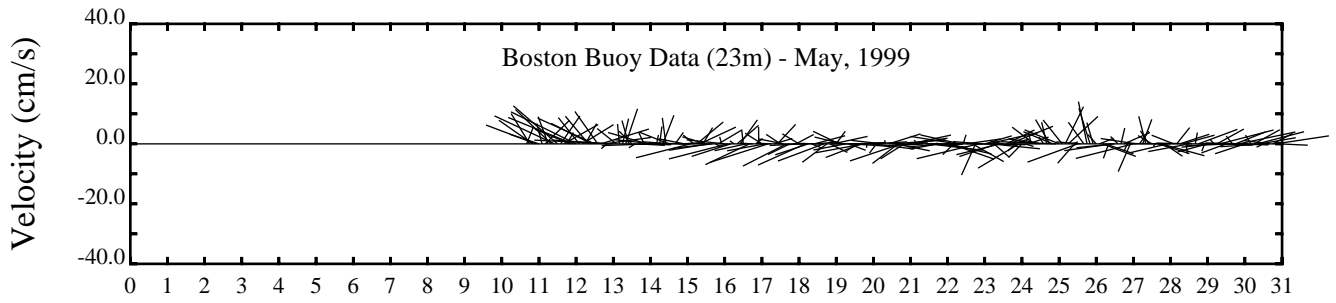
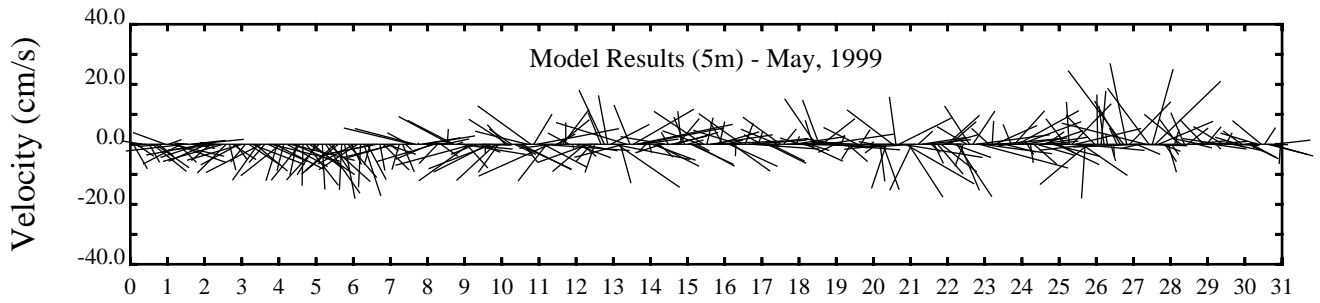
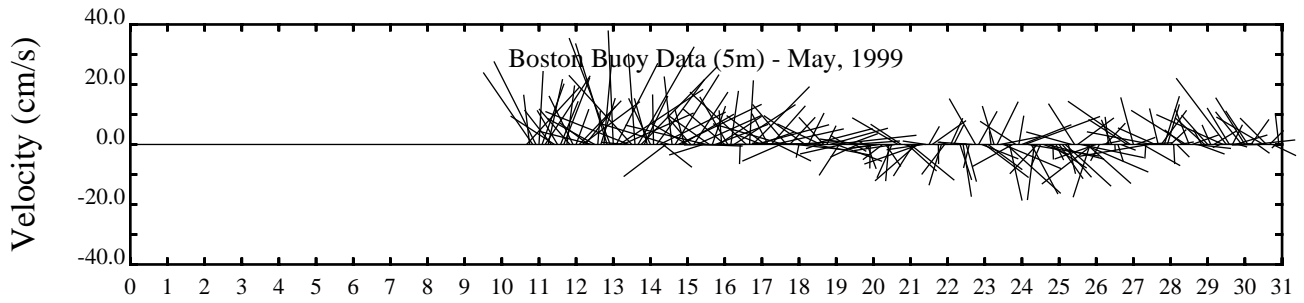
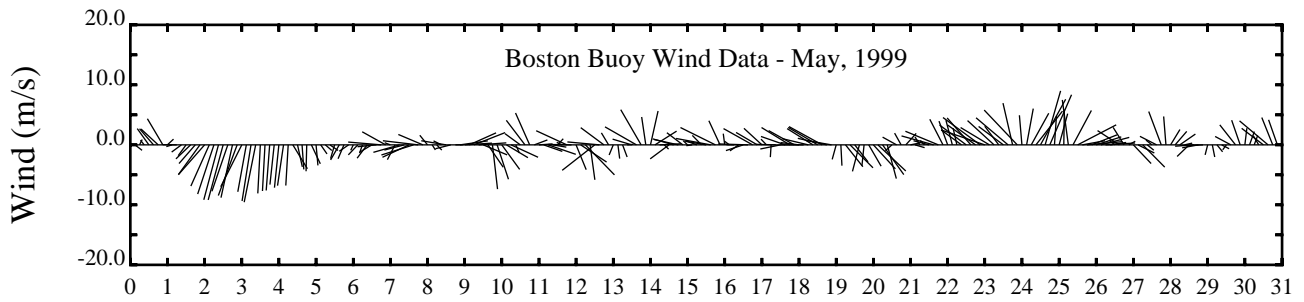




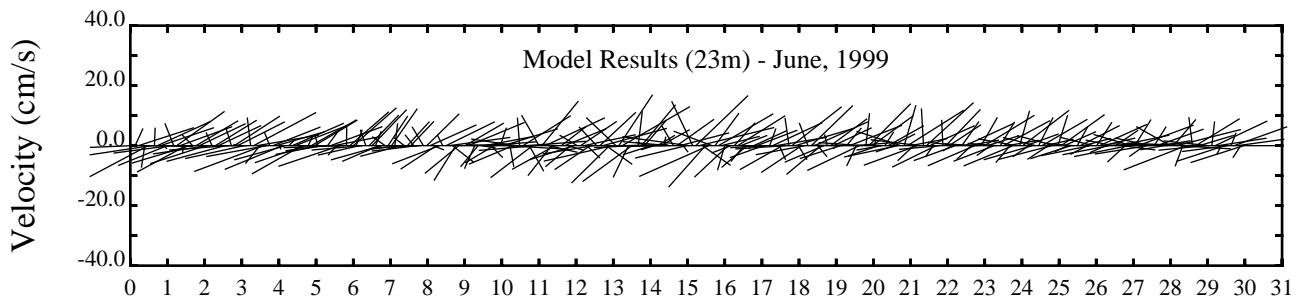
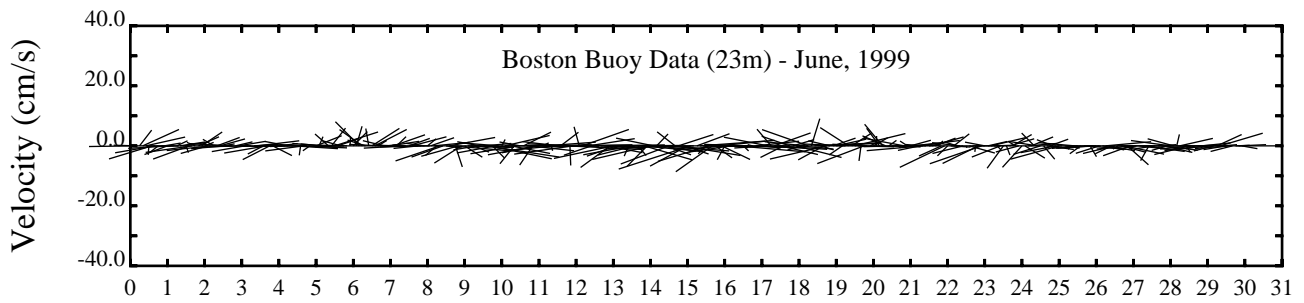
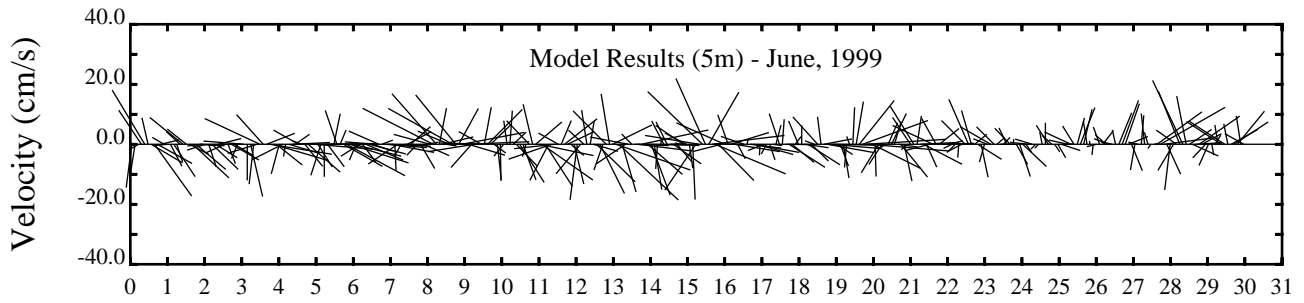
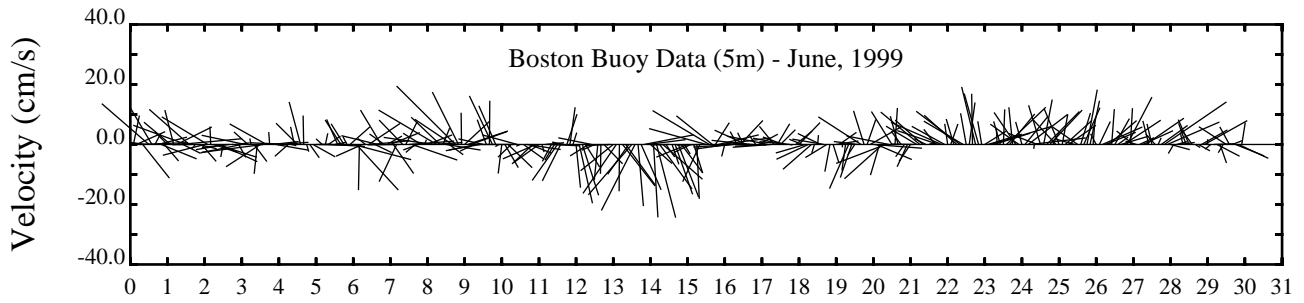
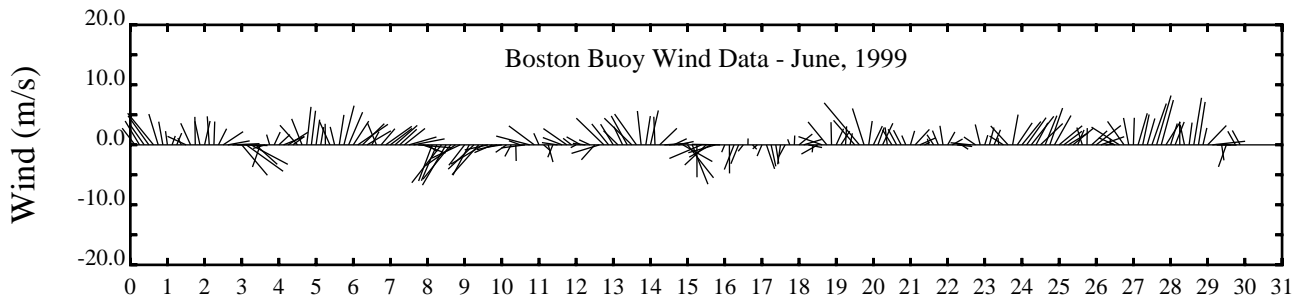
Day

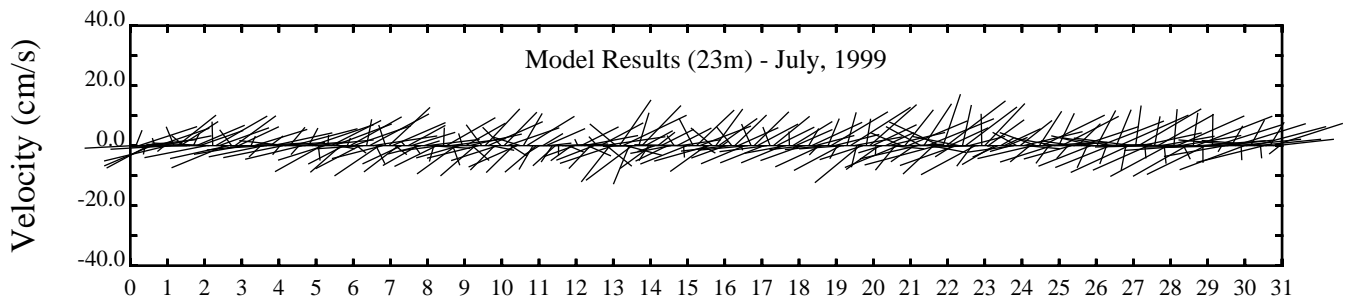
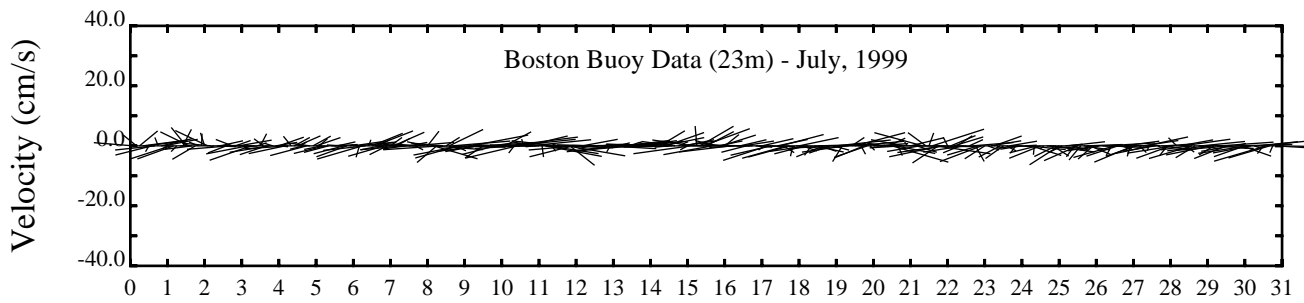
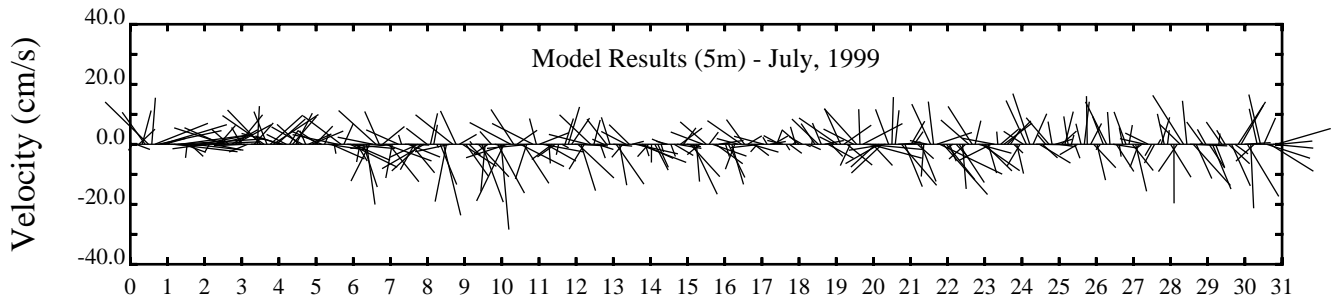
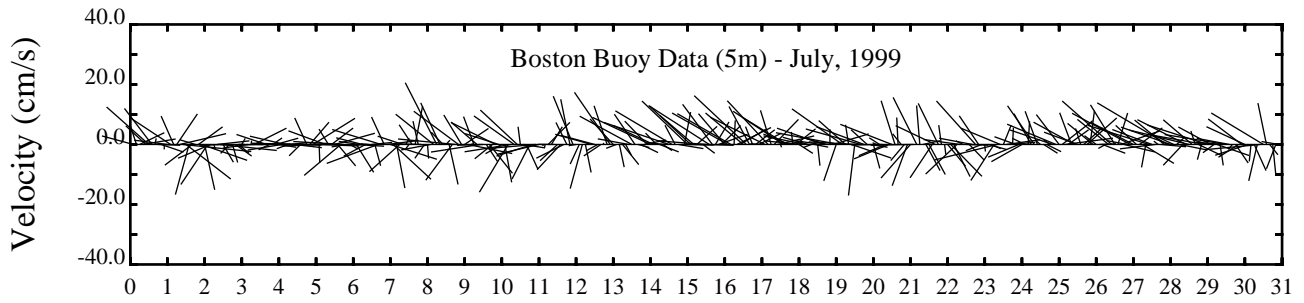
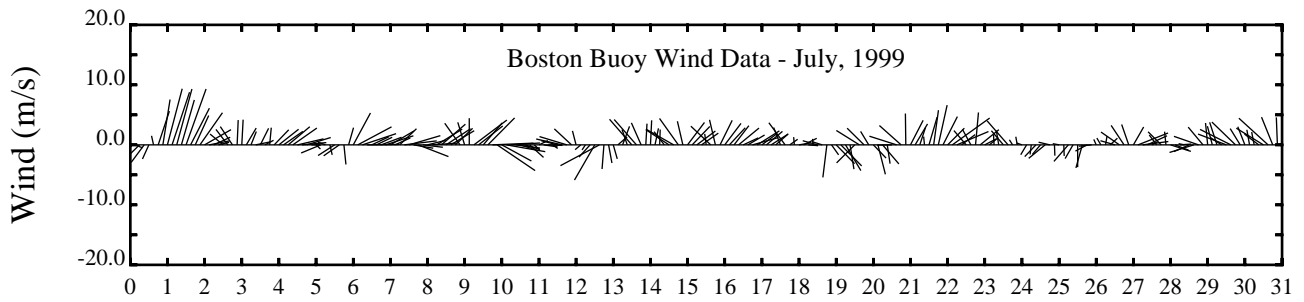


Day

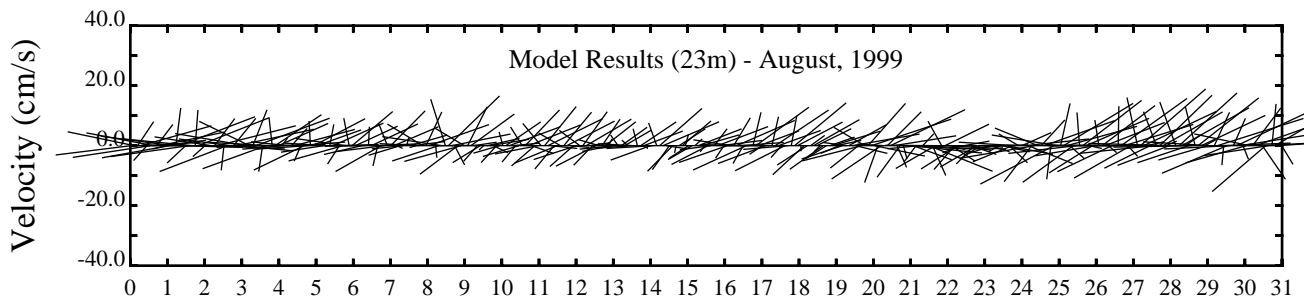
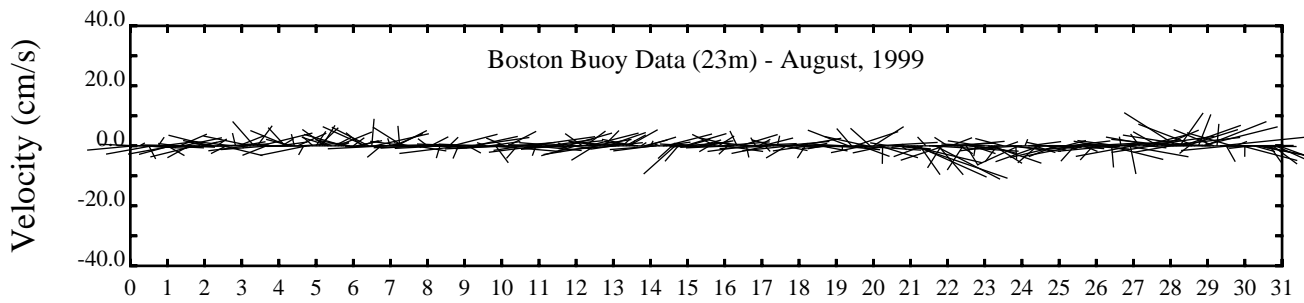
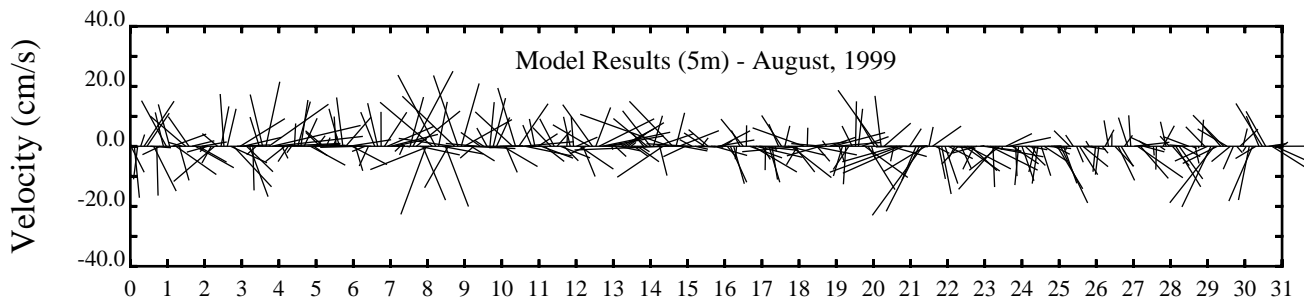
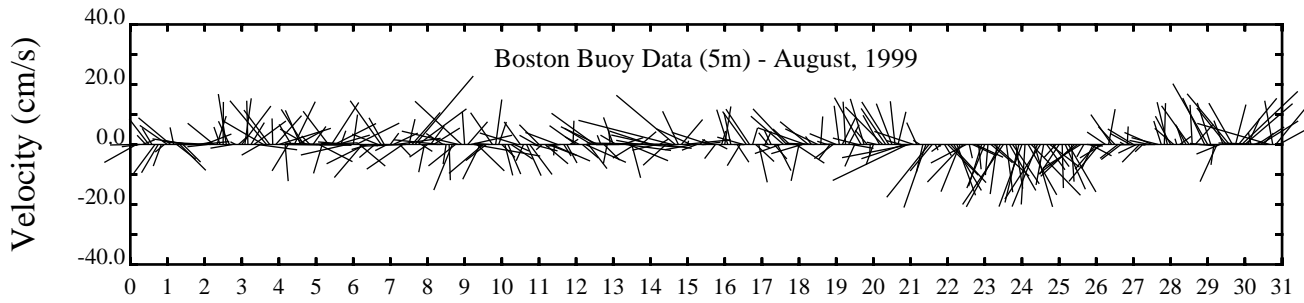
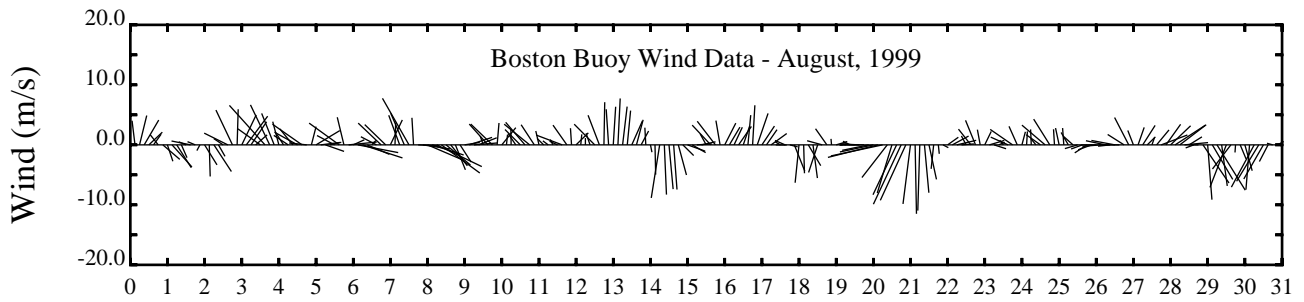


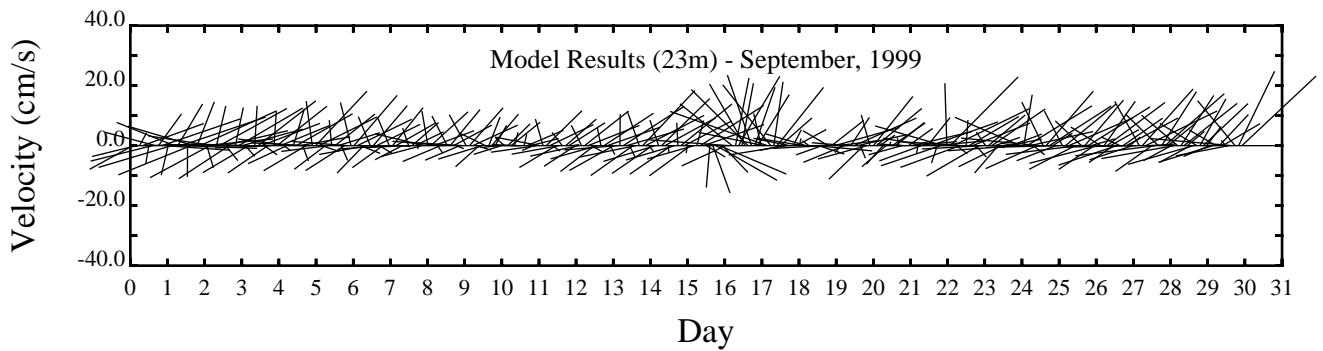
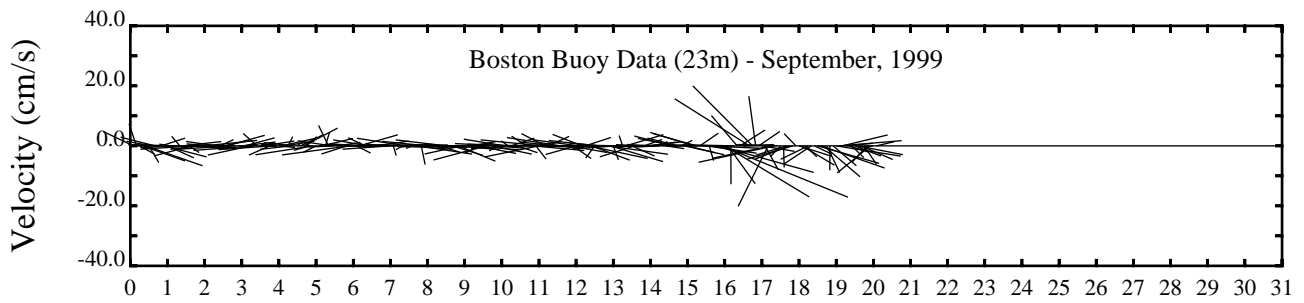
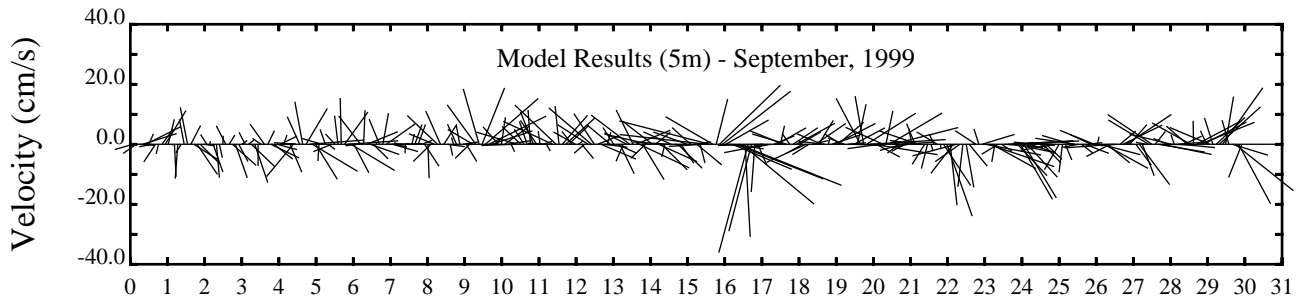
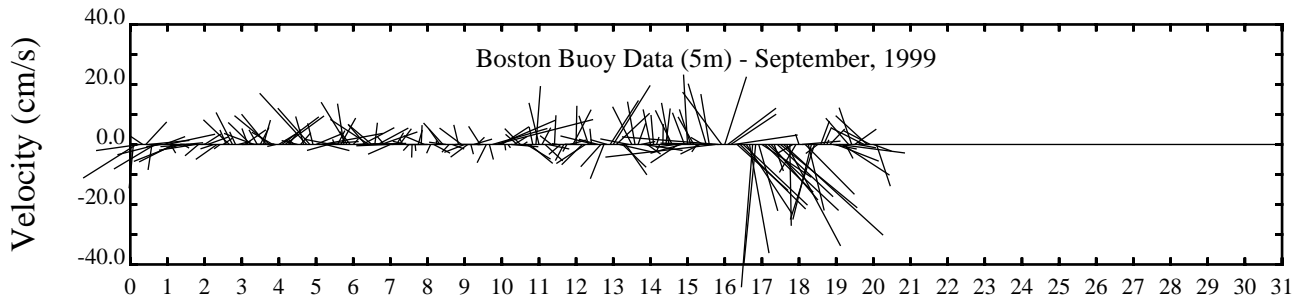
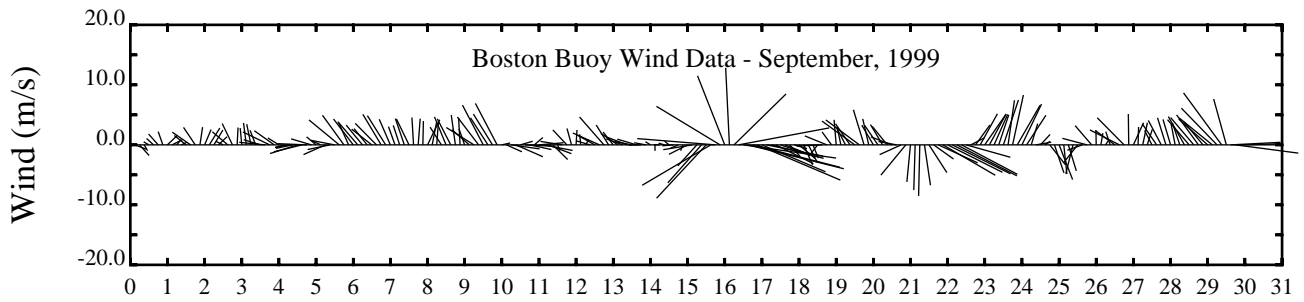
Day

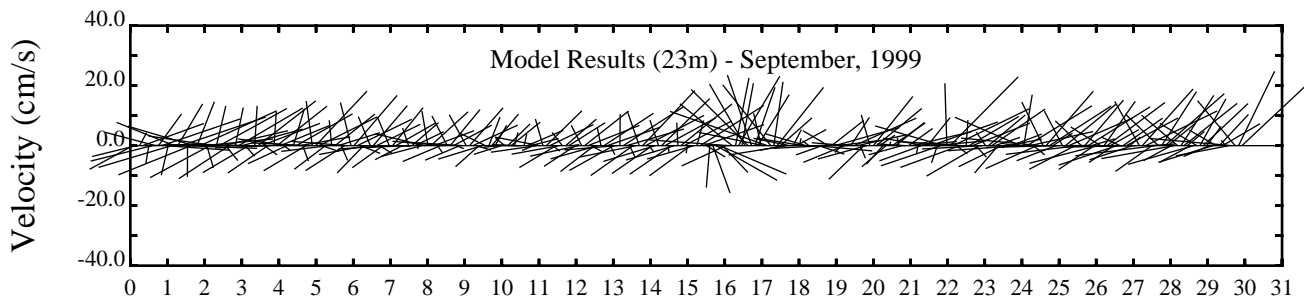
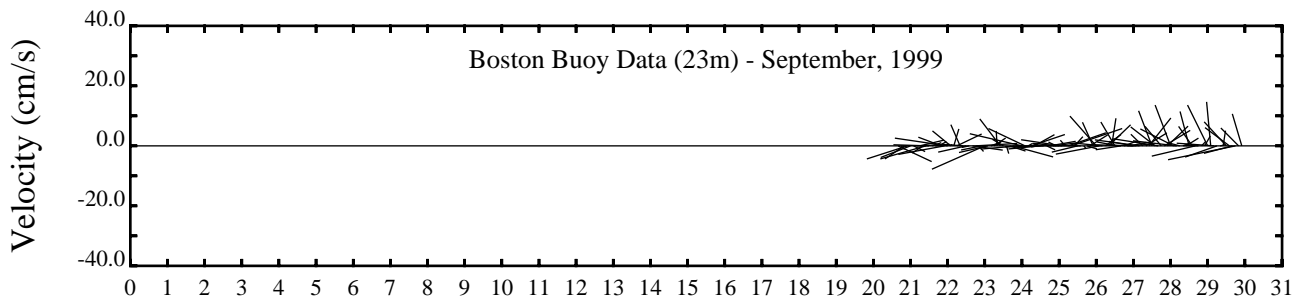
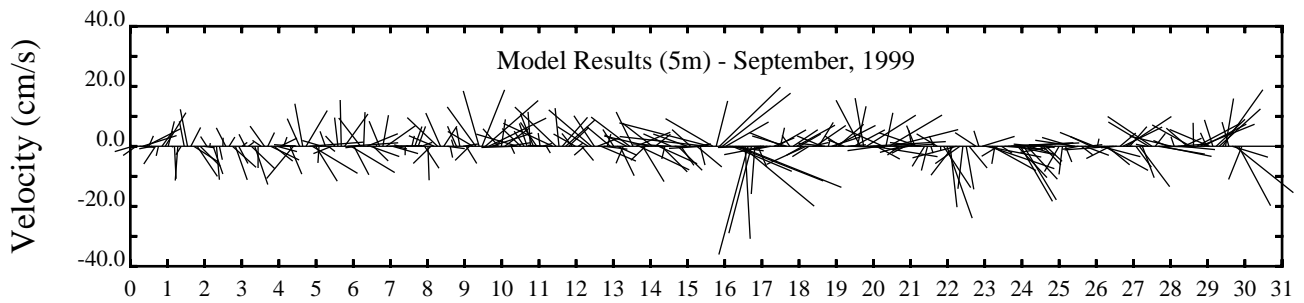
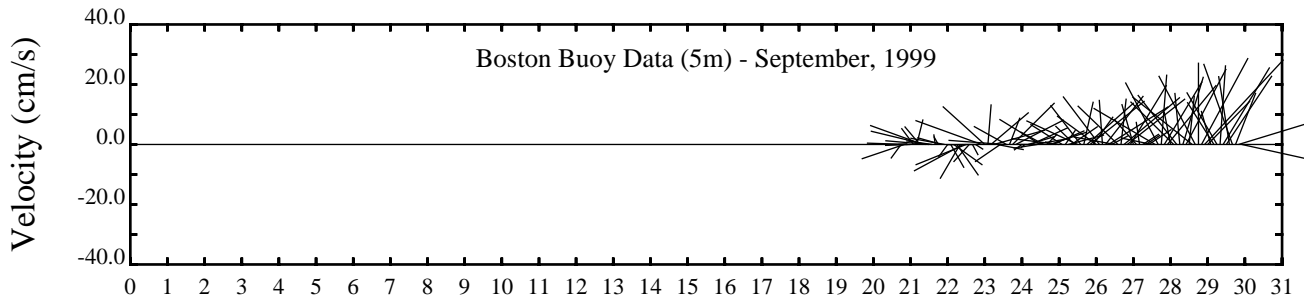
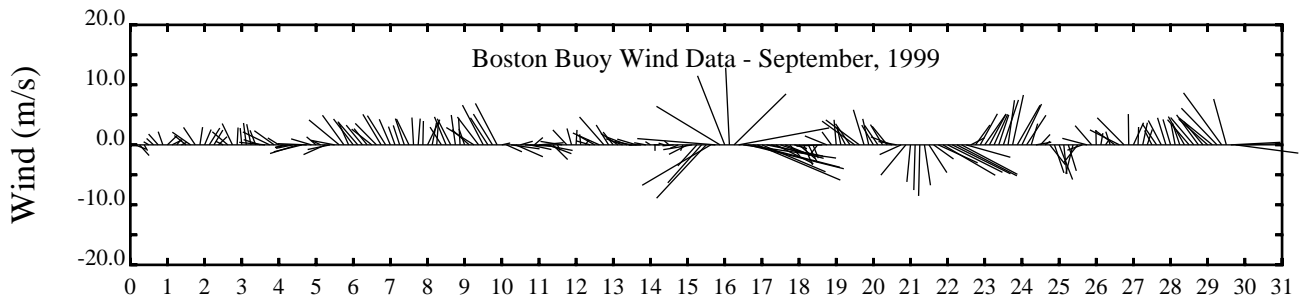




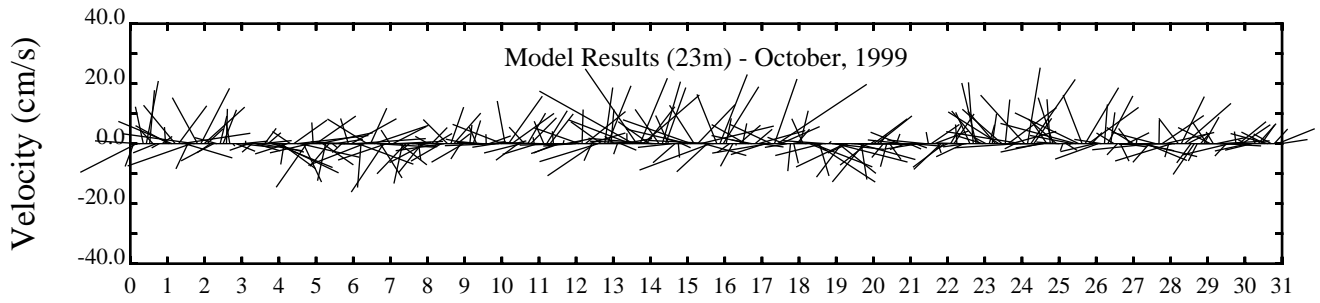
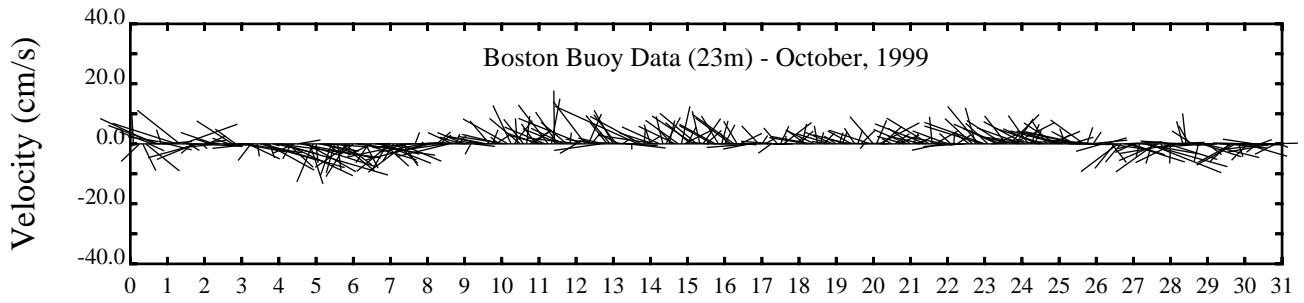
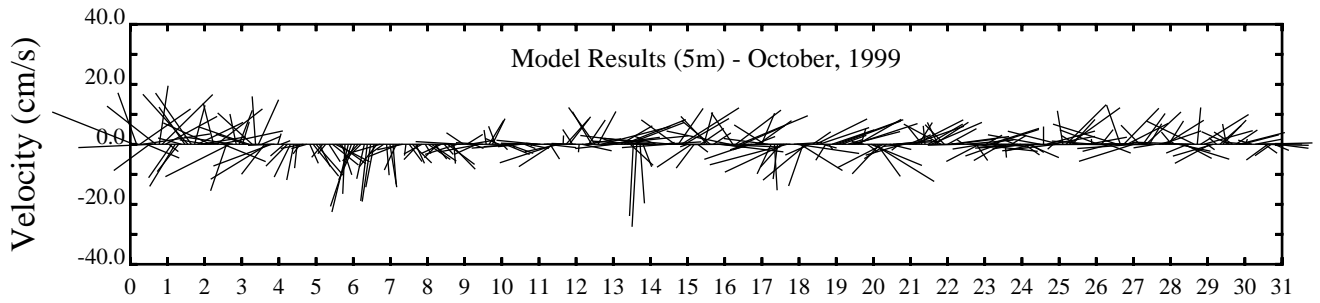
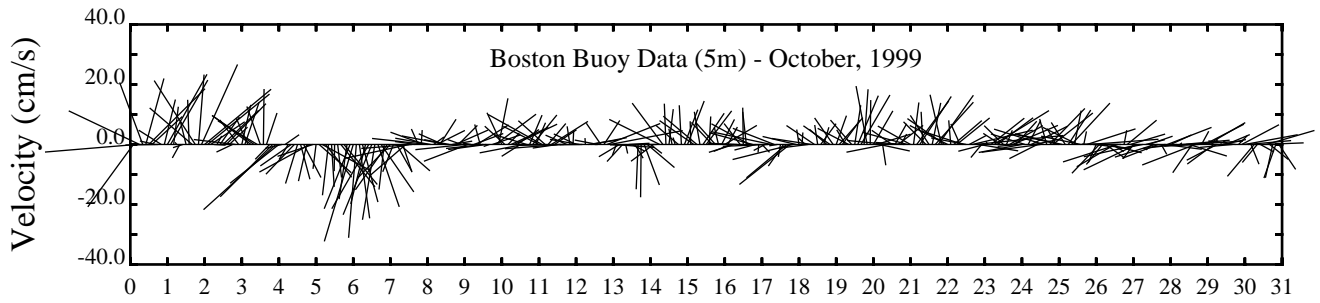
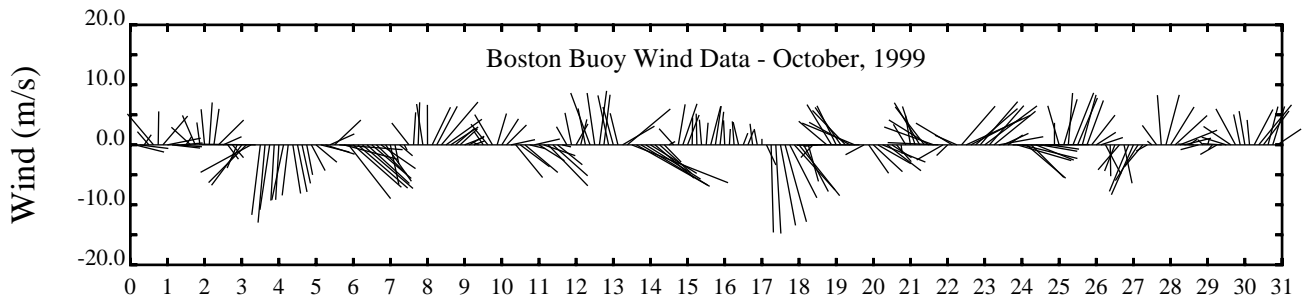
Day



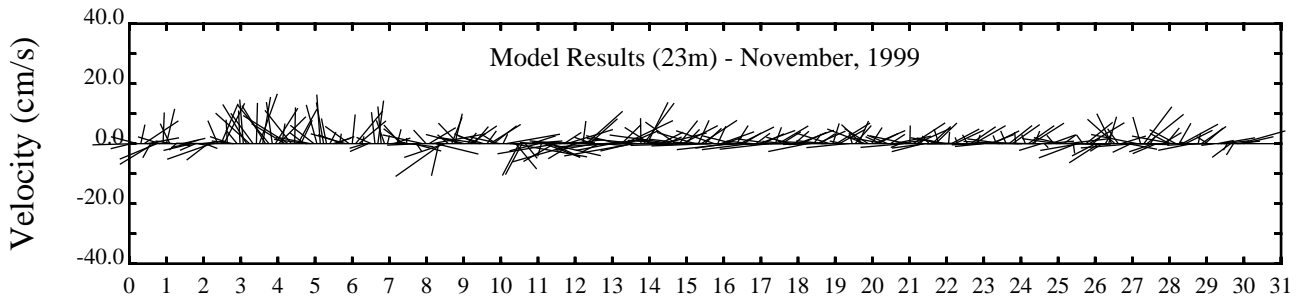
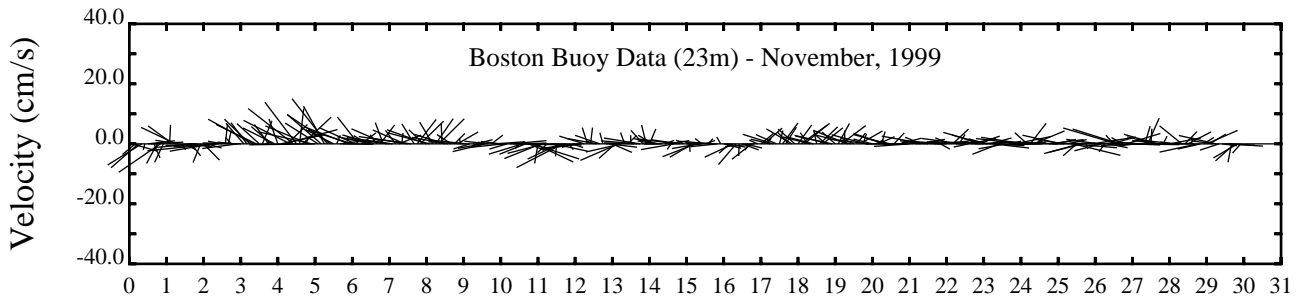
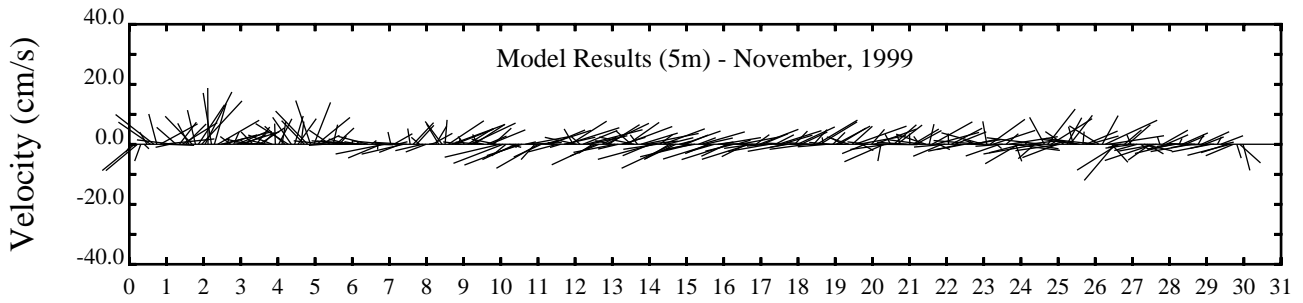
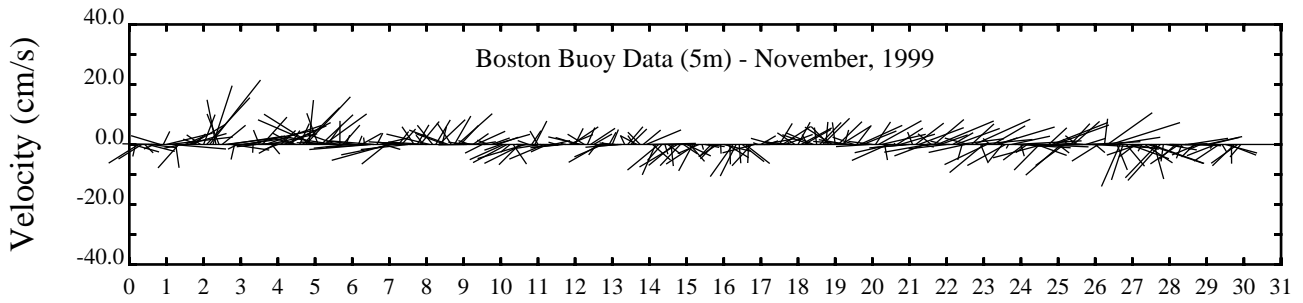
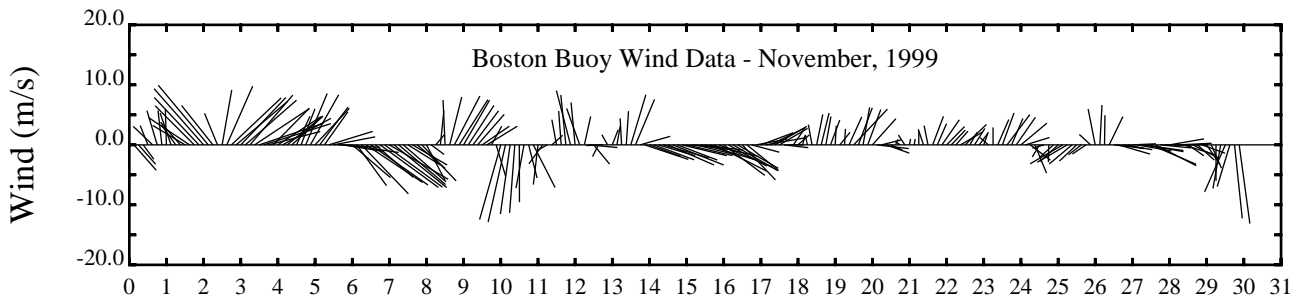


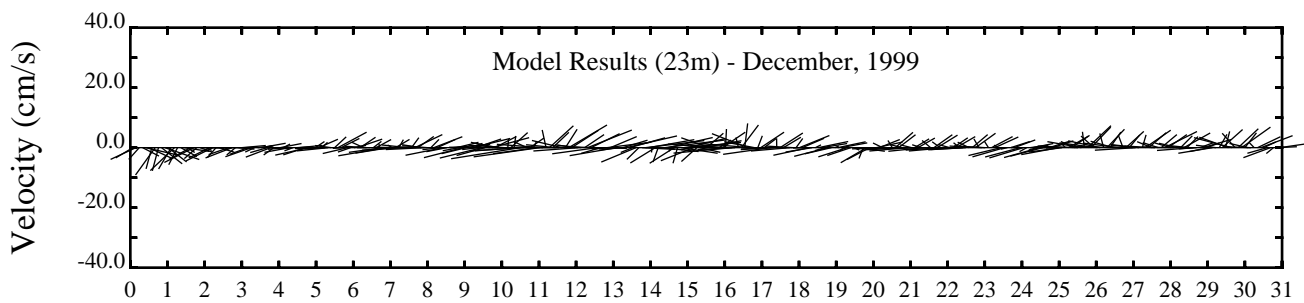
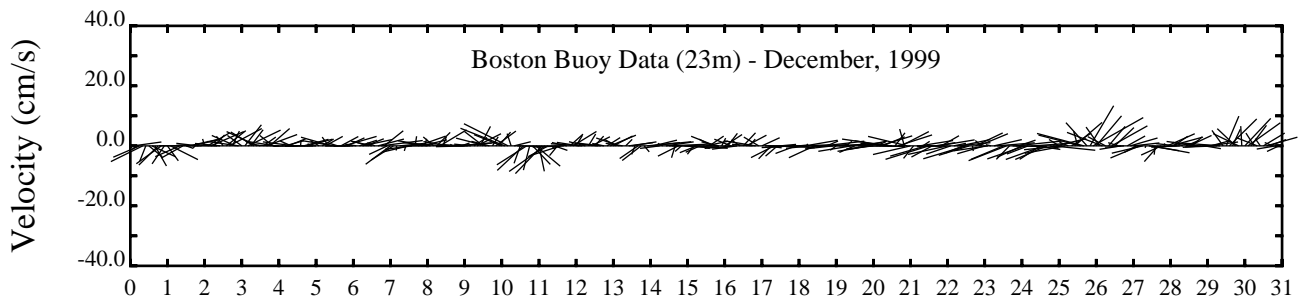
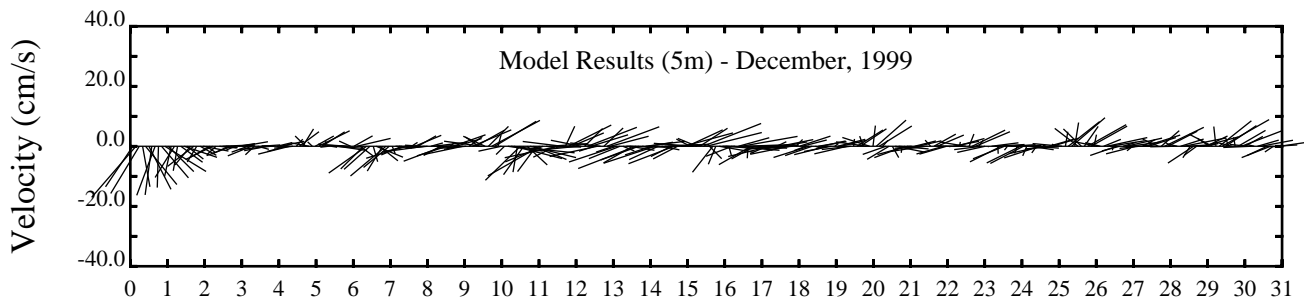
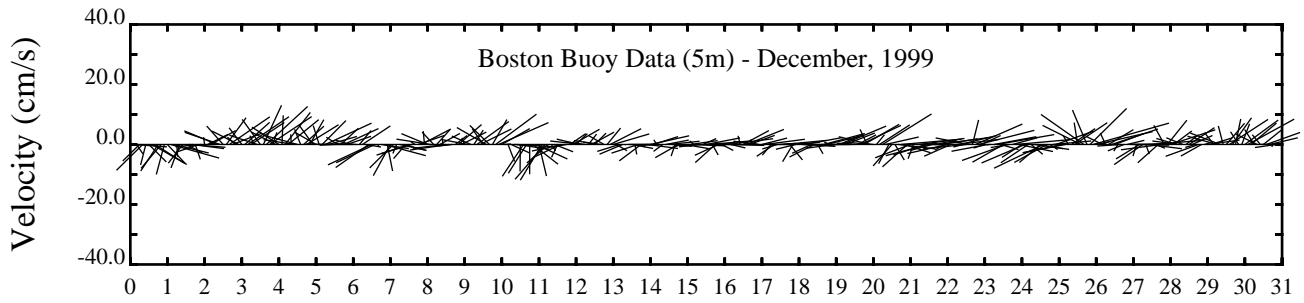
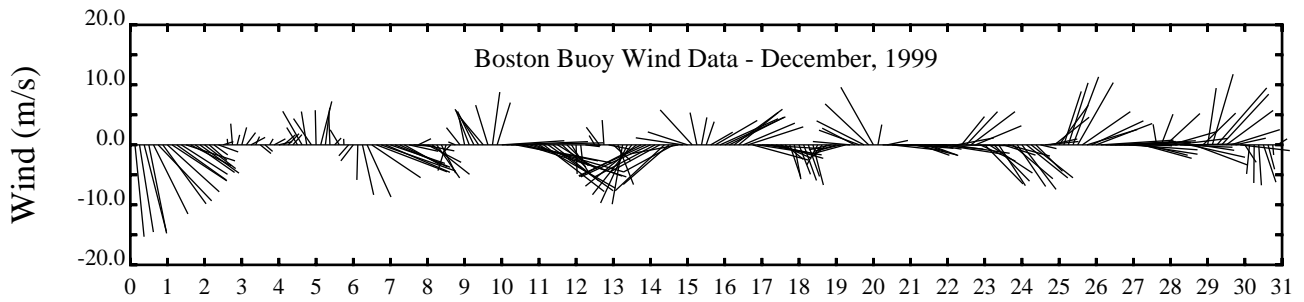


Day

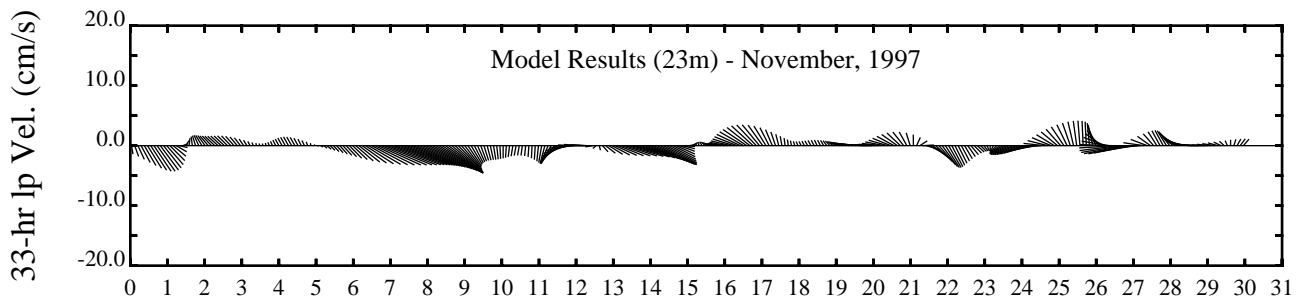
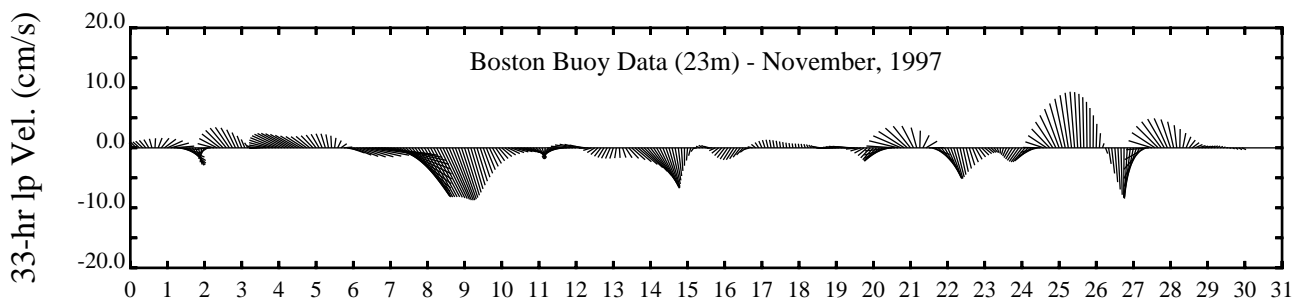
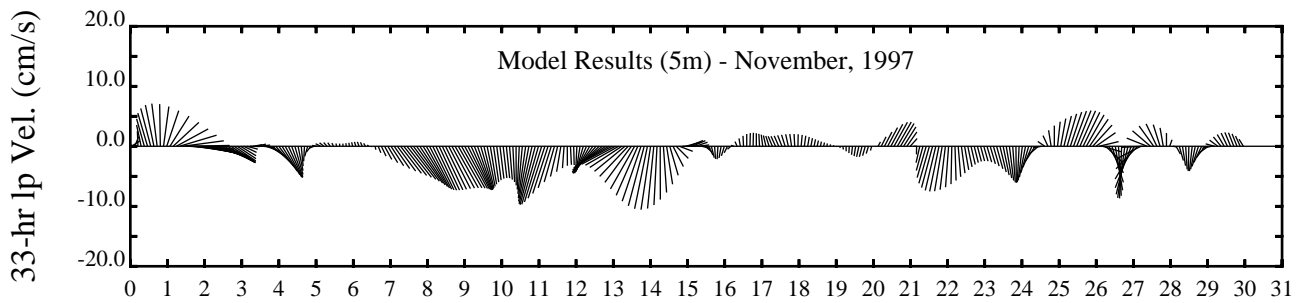
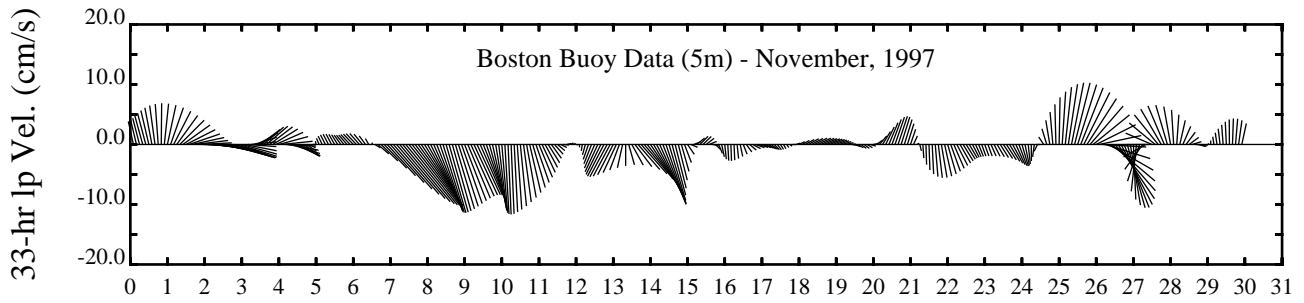
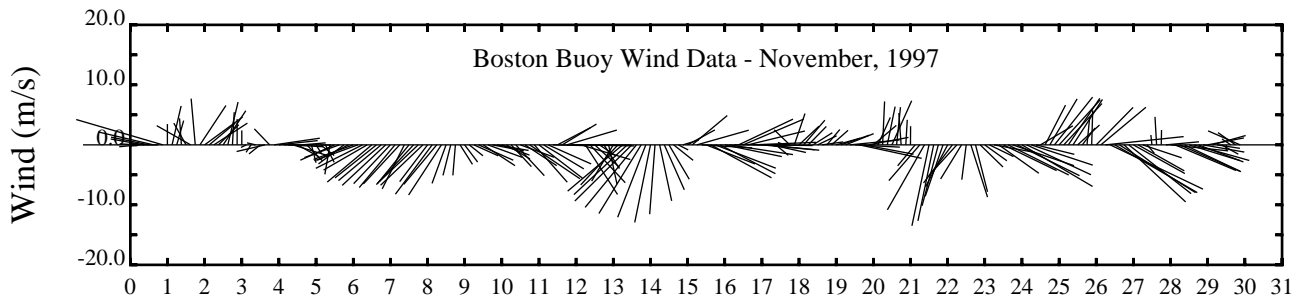


Day

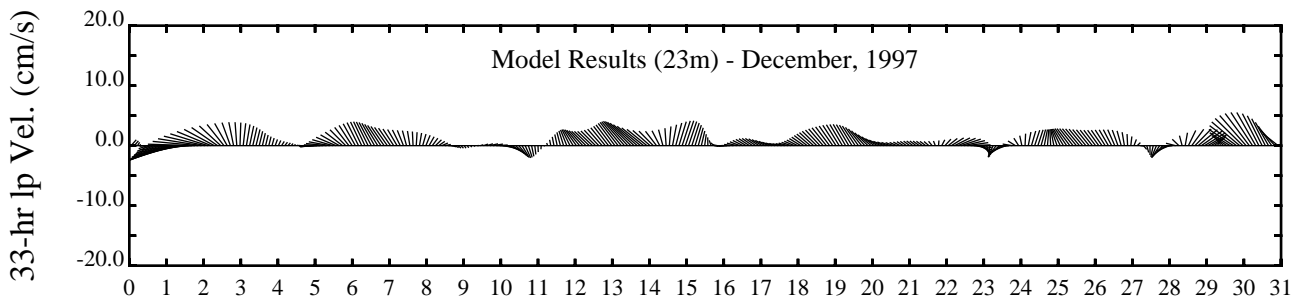
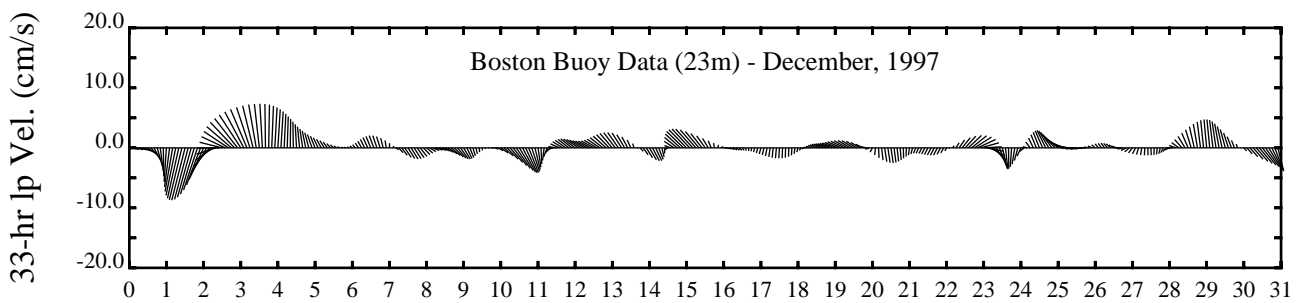
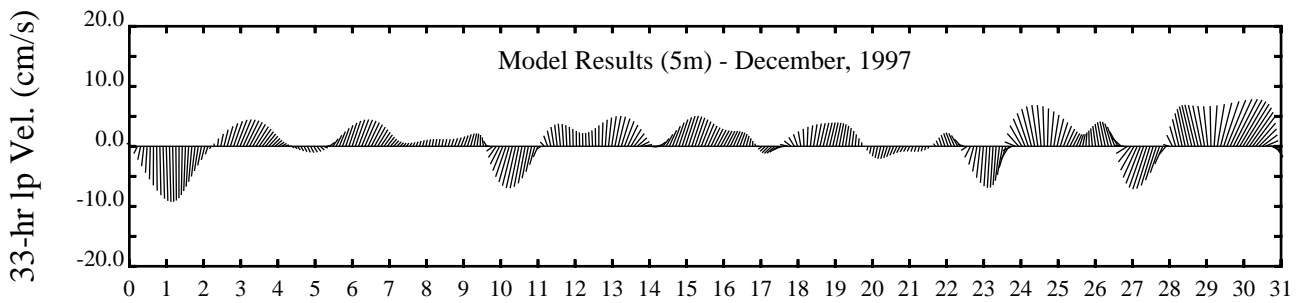
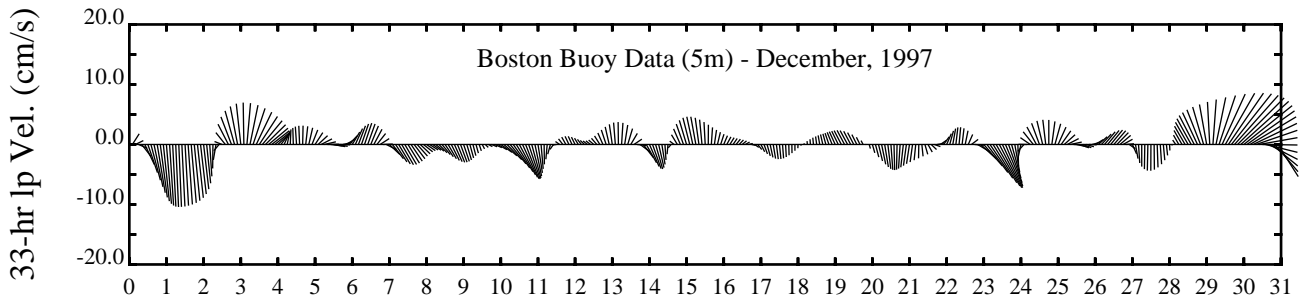
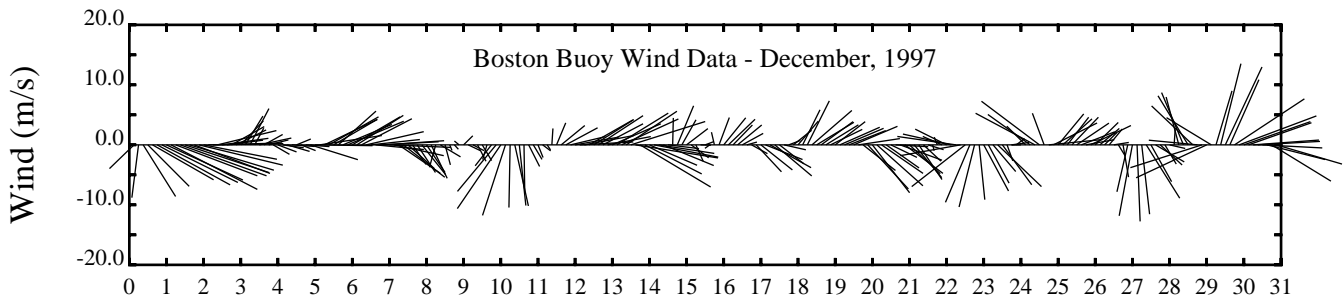




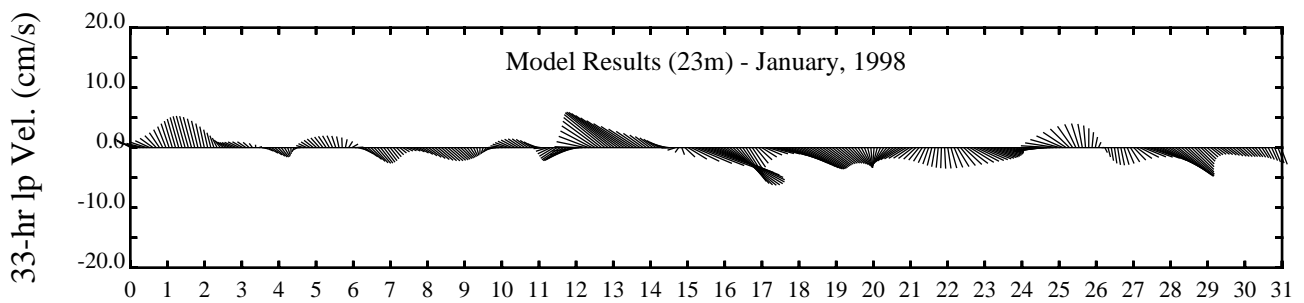
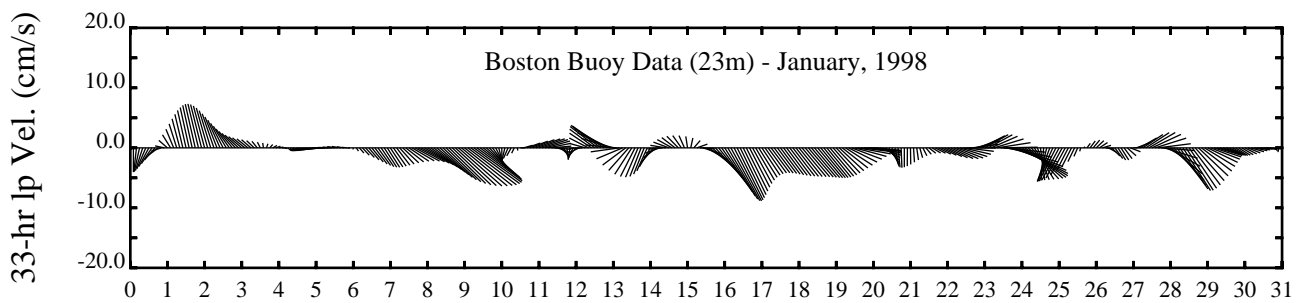
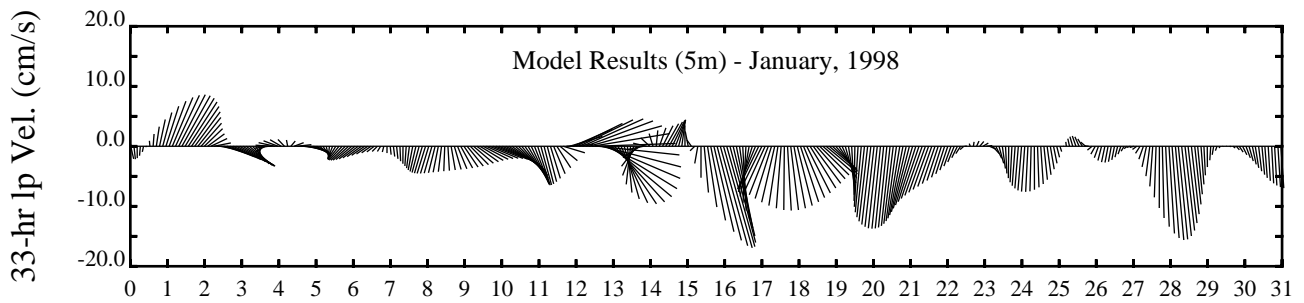
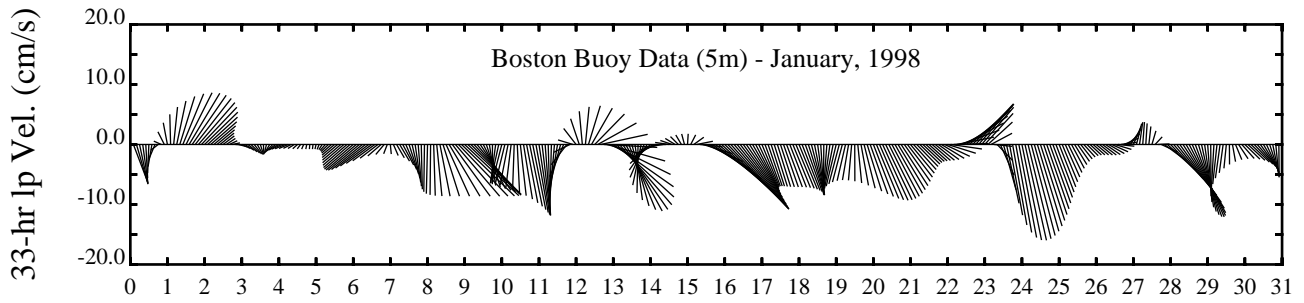
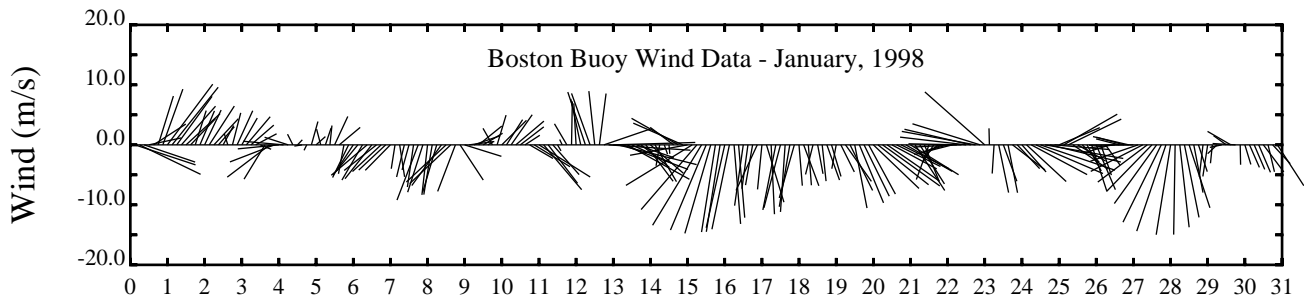
Day



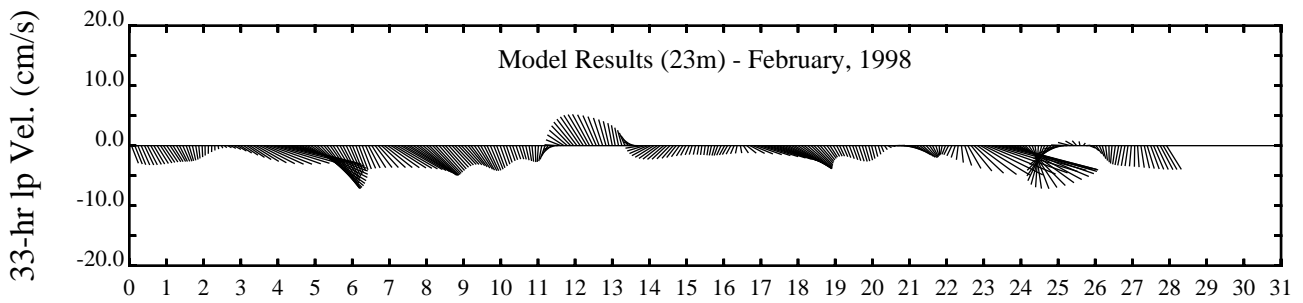
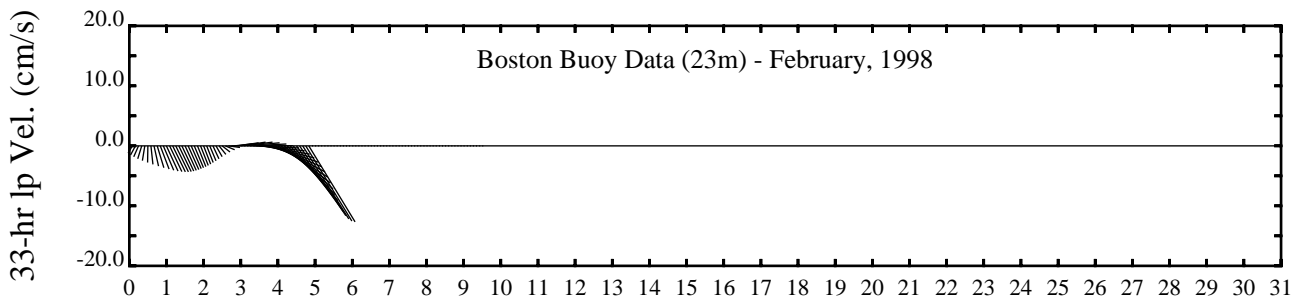
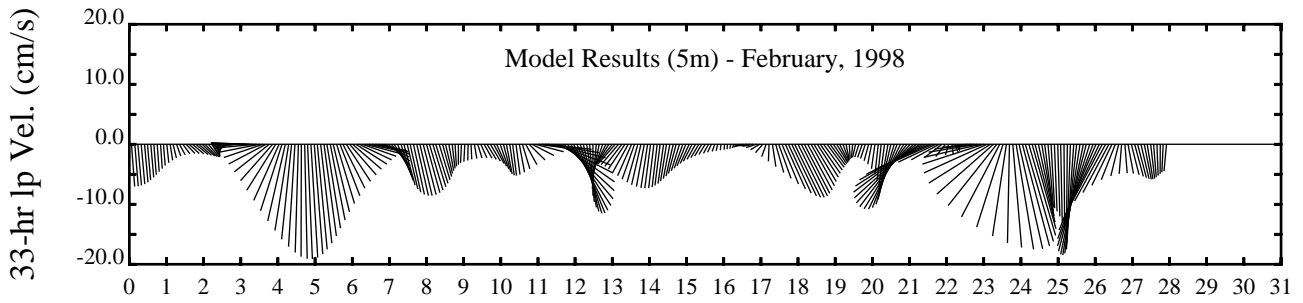
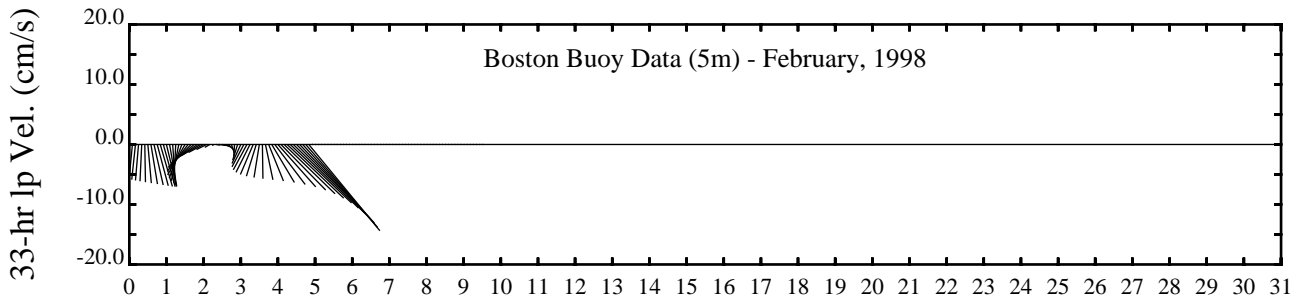
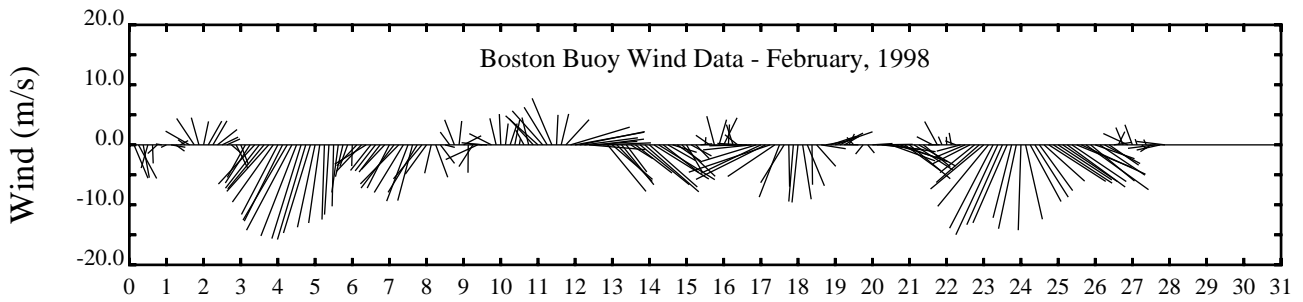
Day



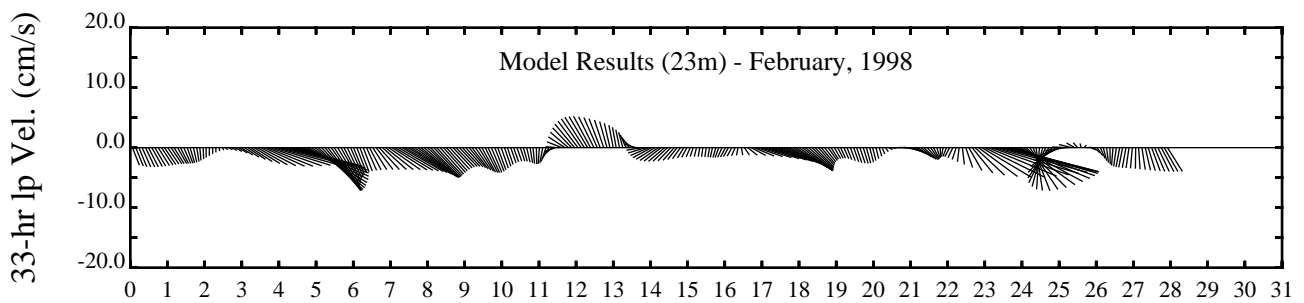
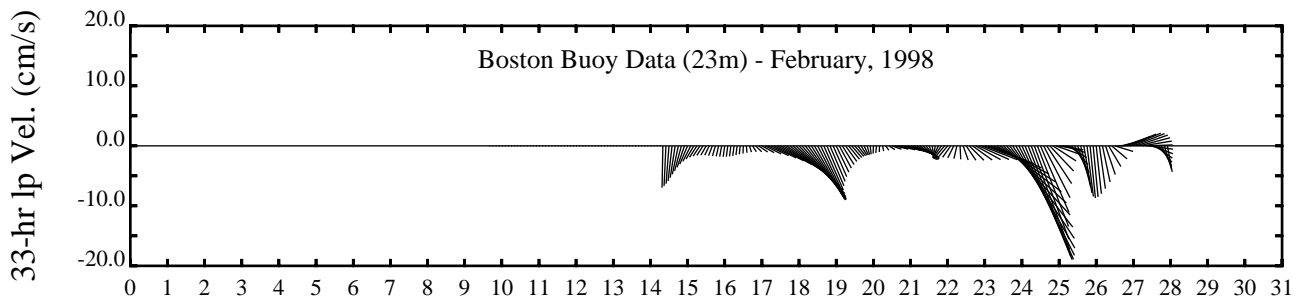
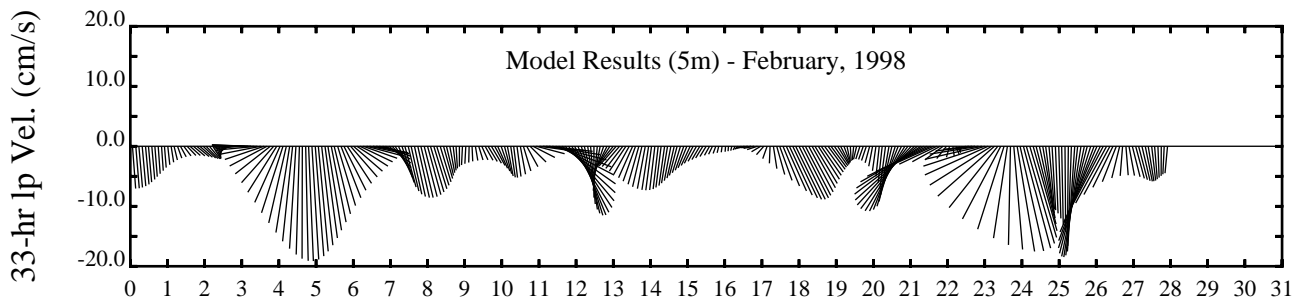
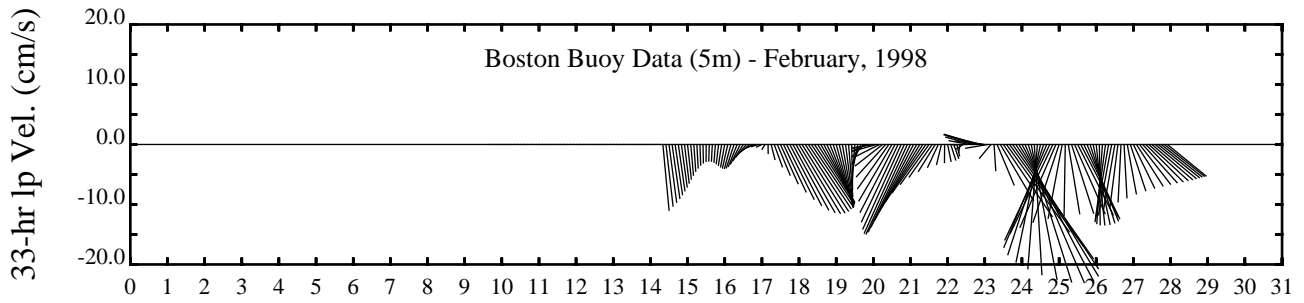
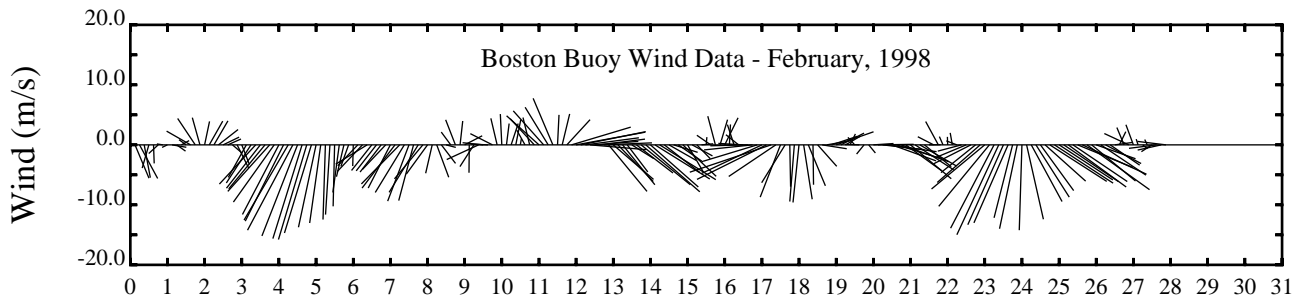
Day



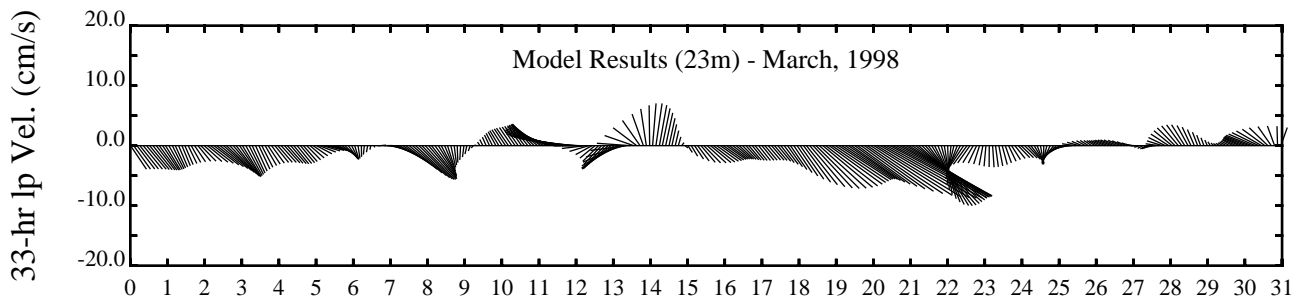
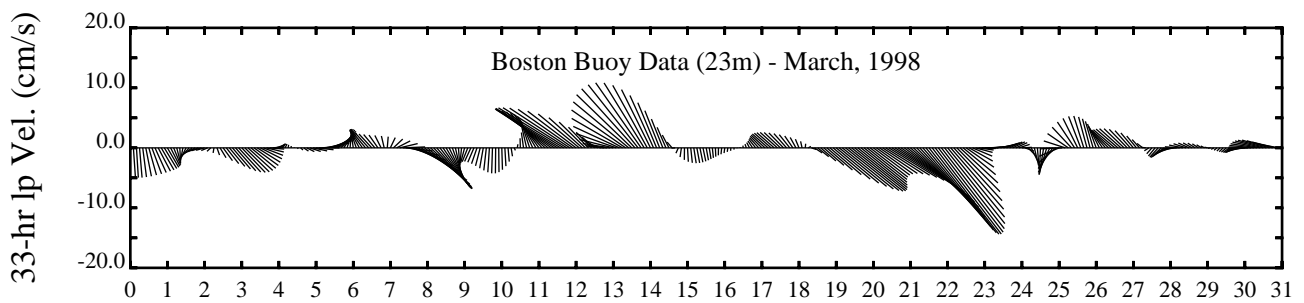
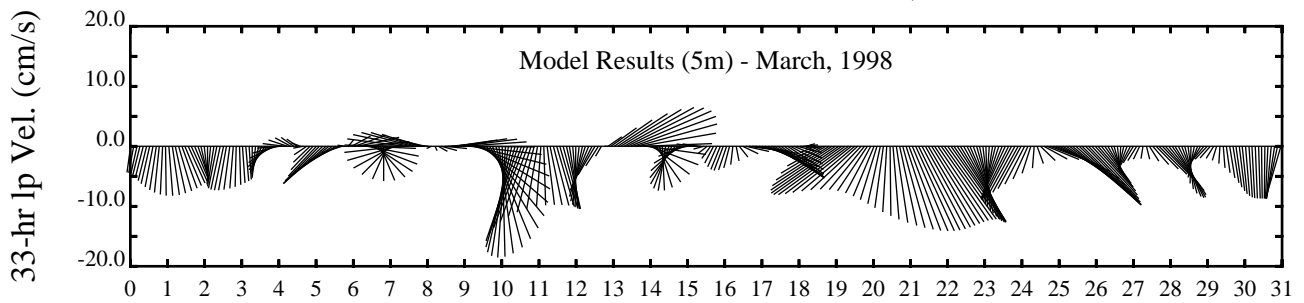
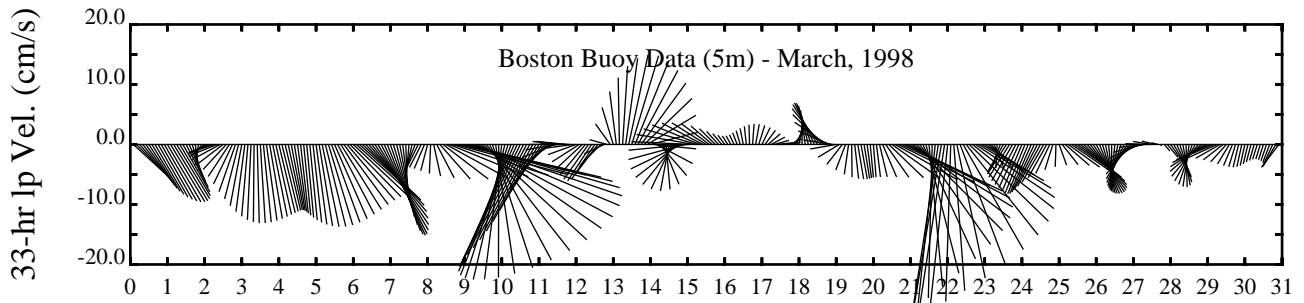
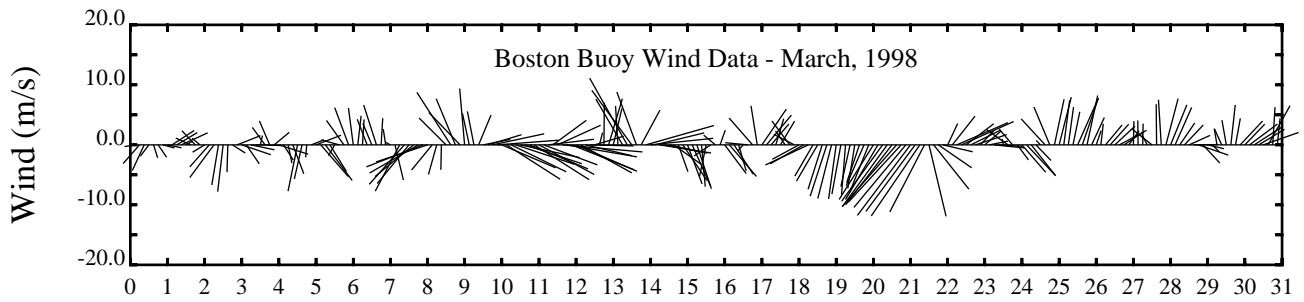
Day



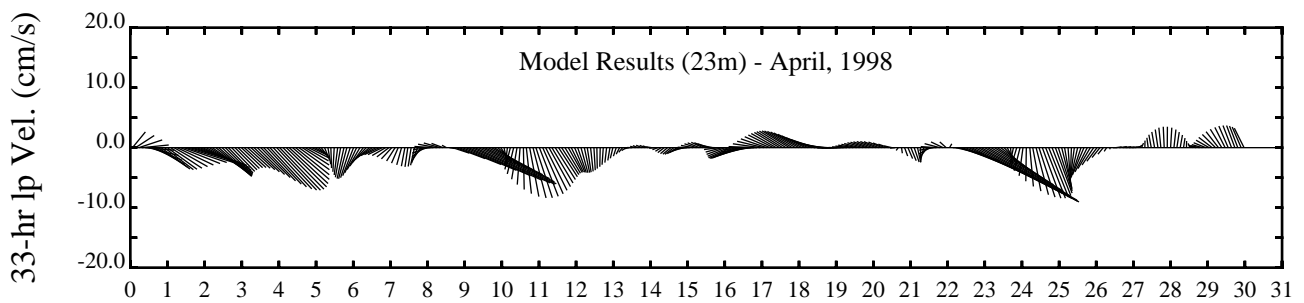
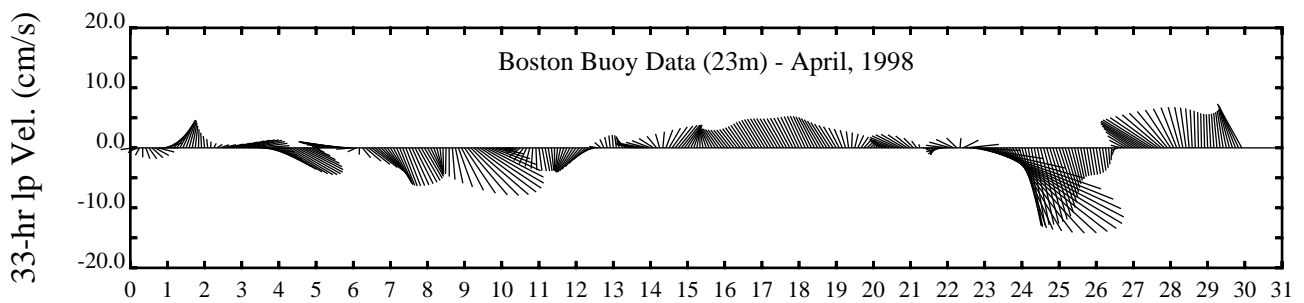
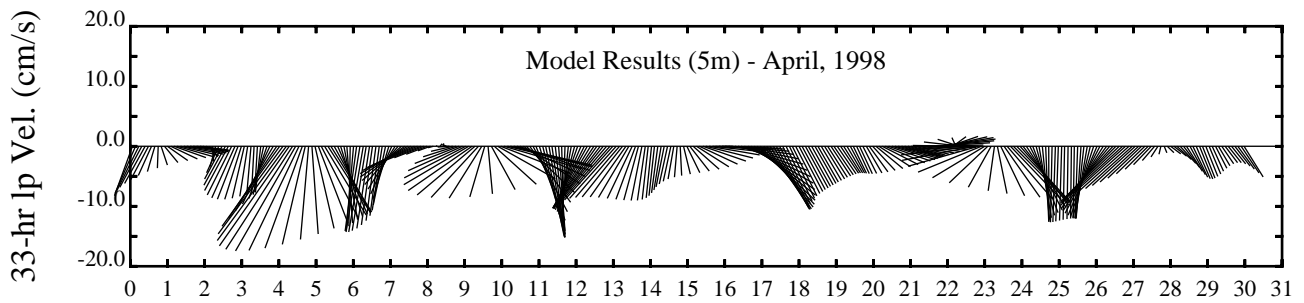
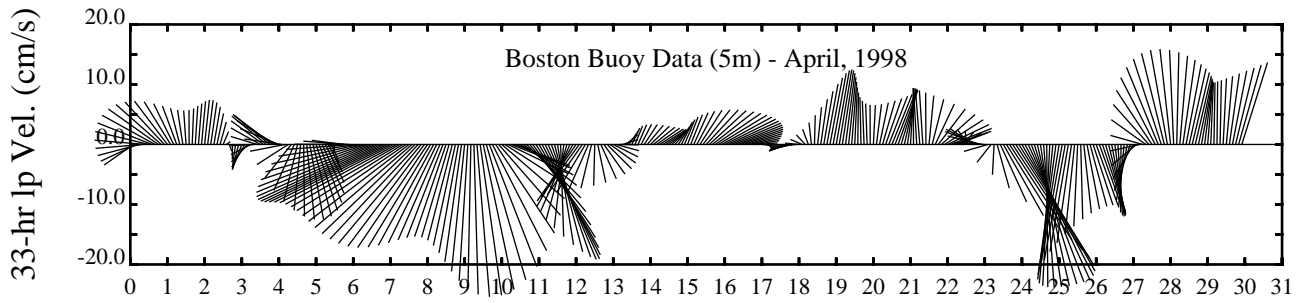
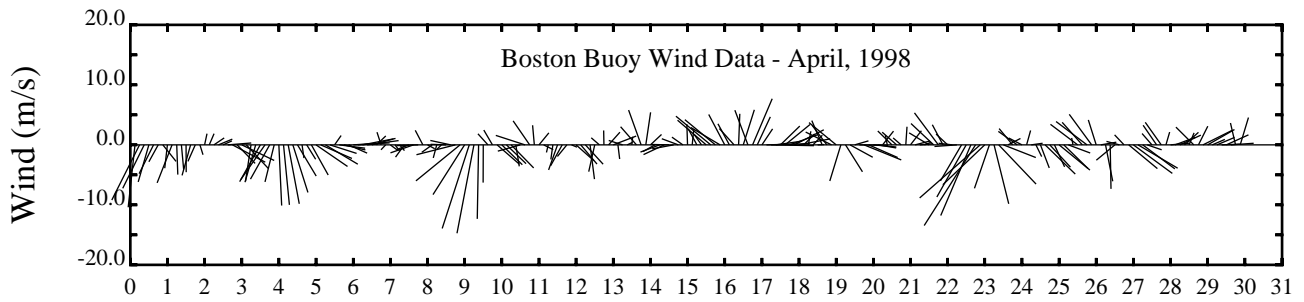
Day



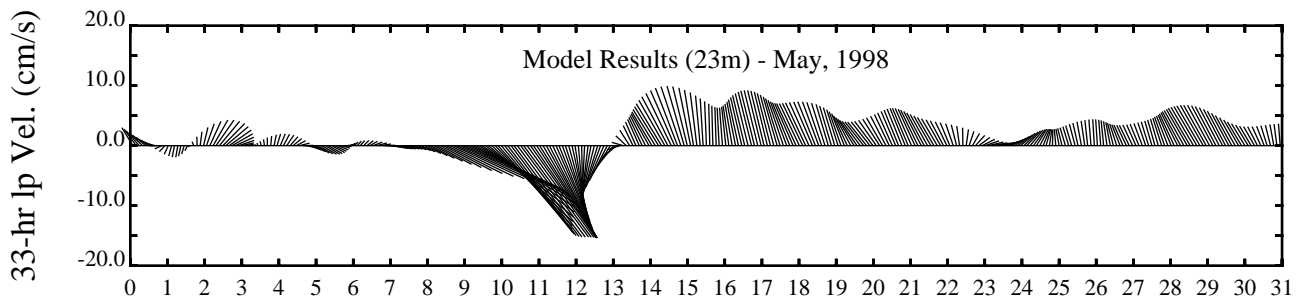
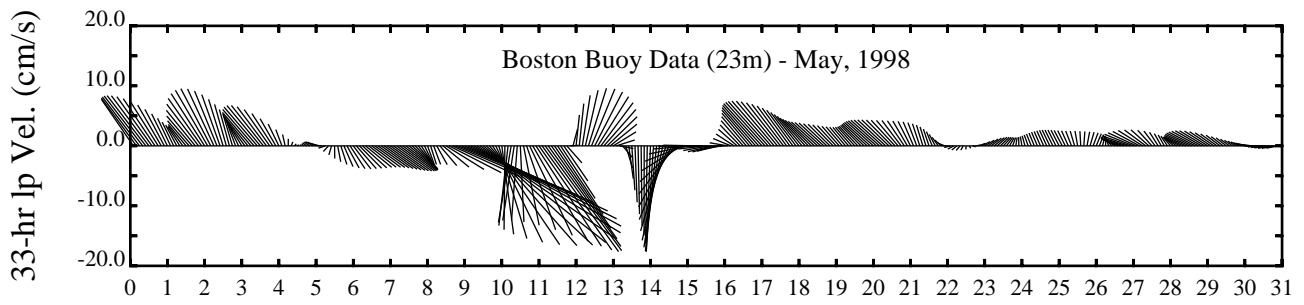
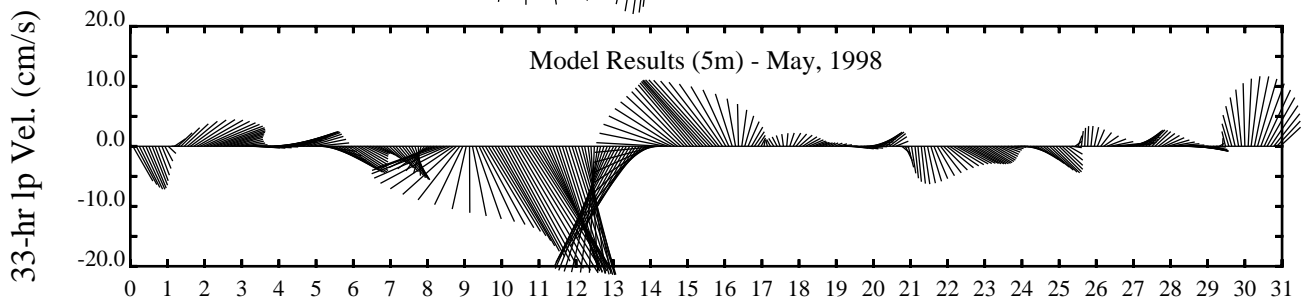
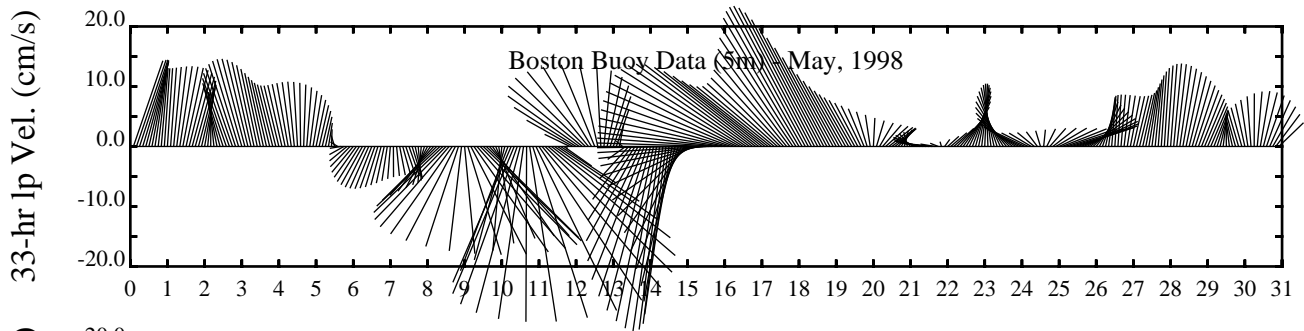
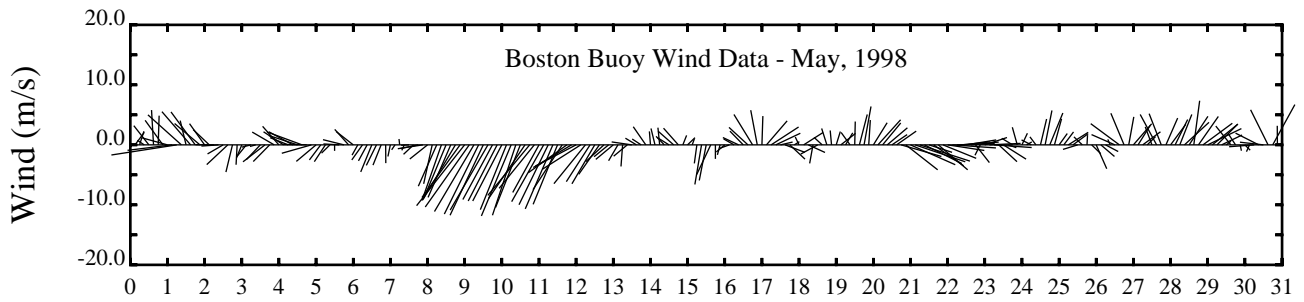
Day



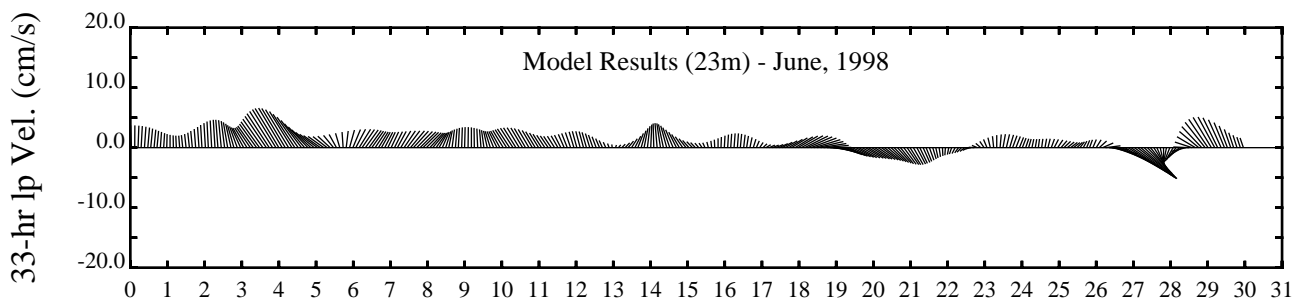
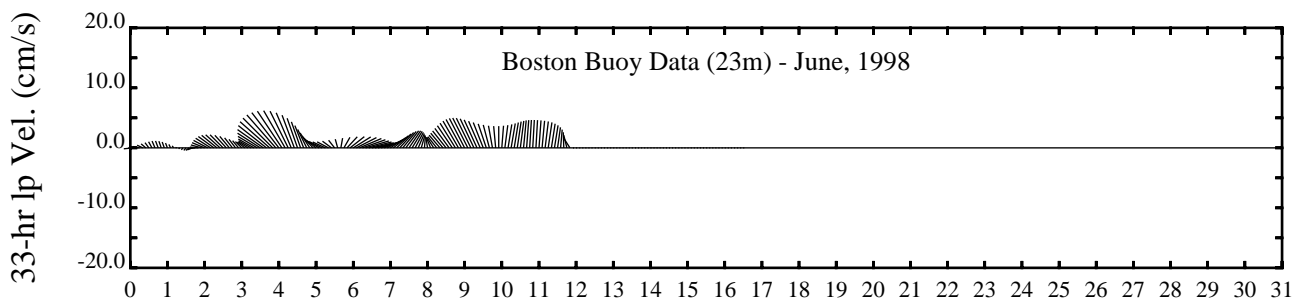
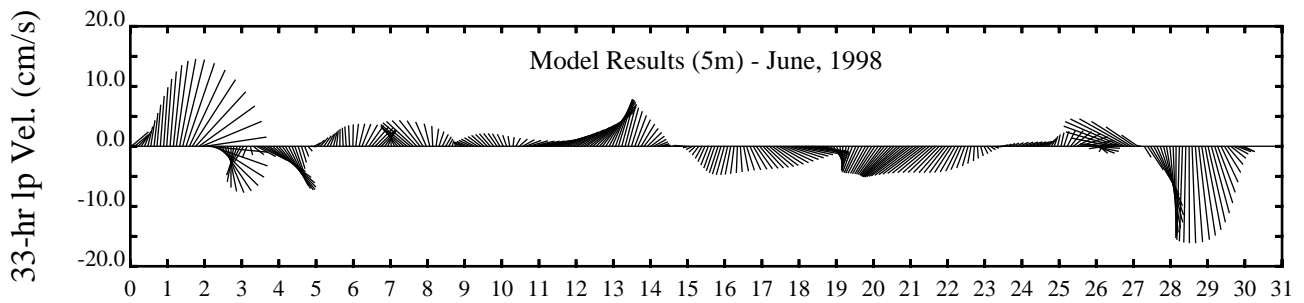
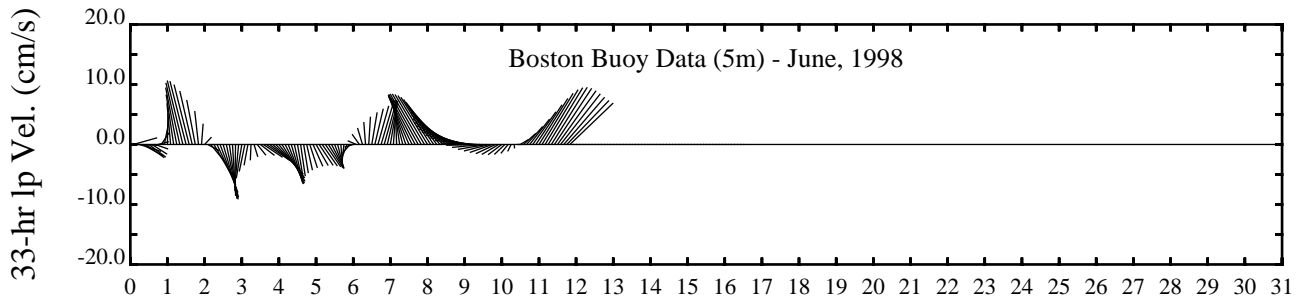
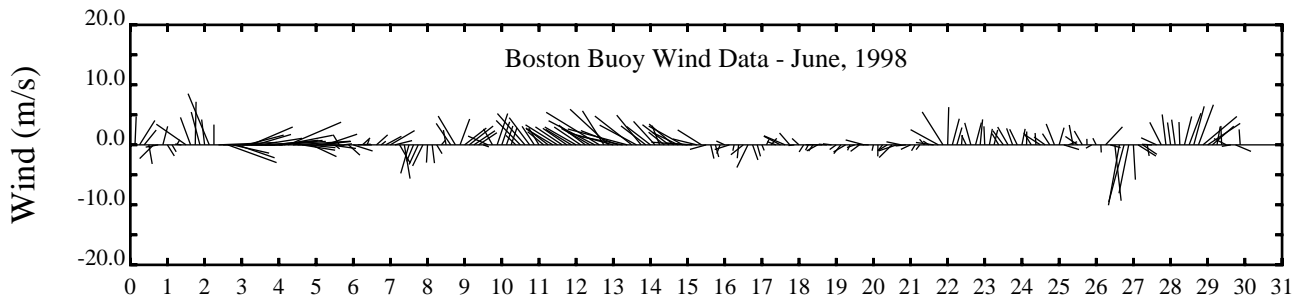
Day

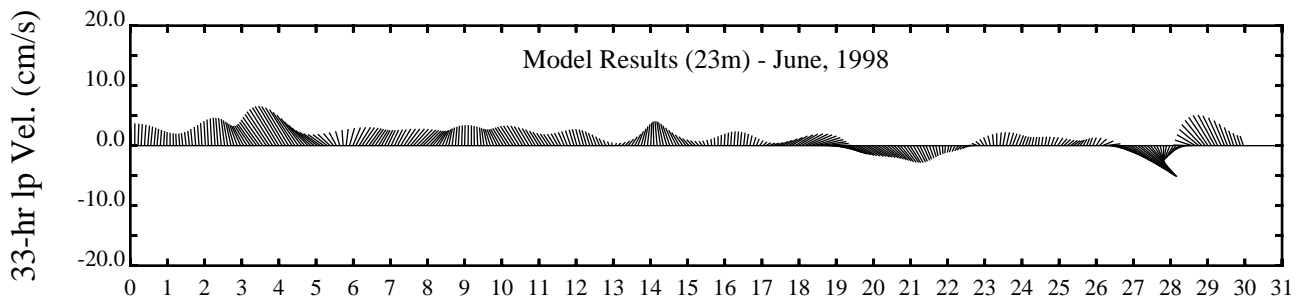
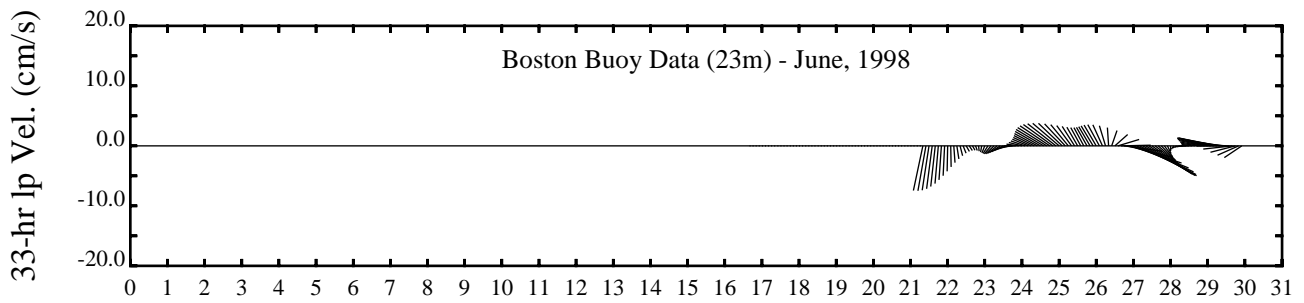
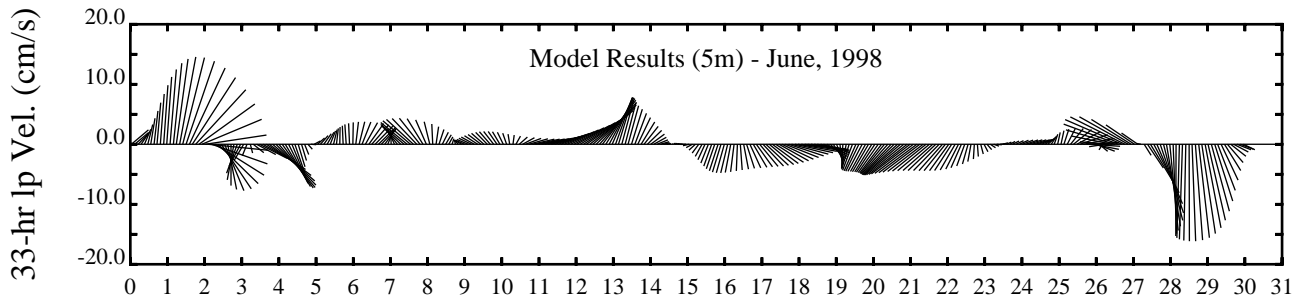
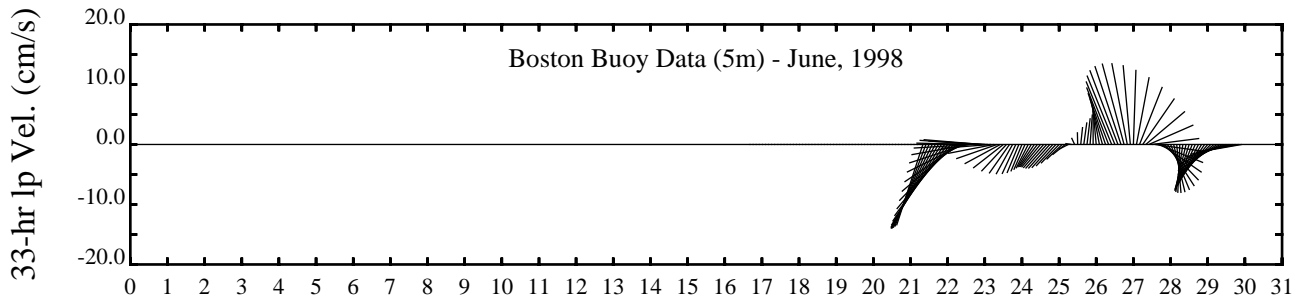
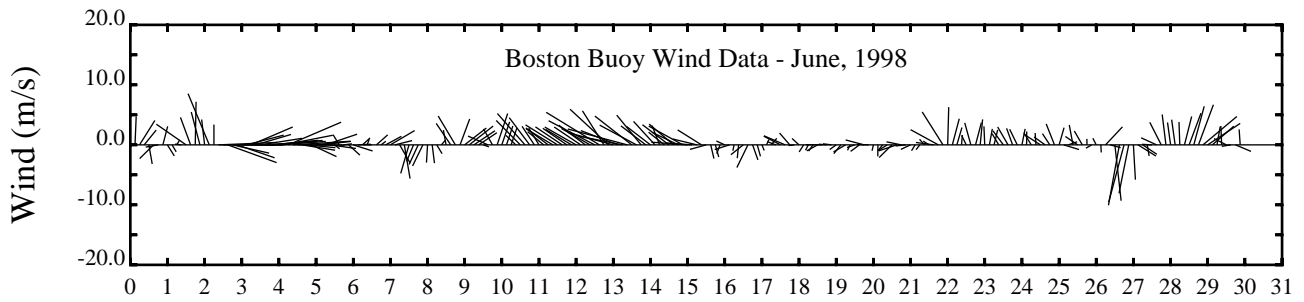


Day

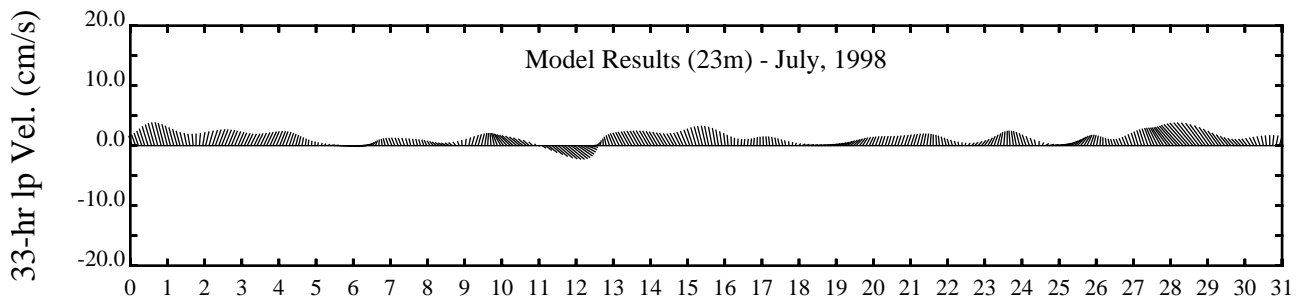
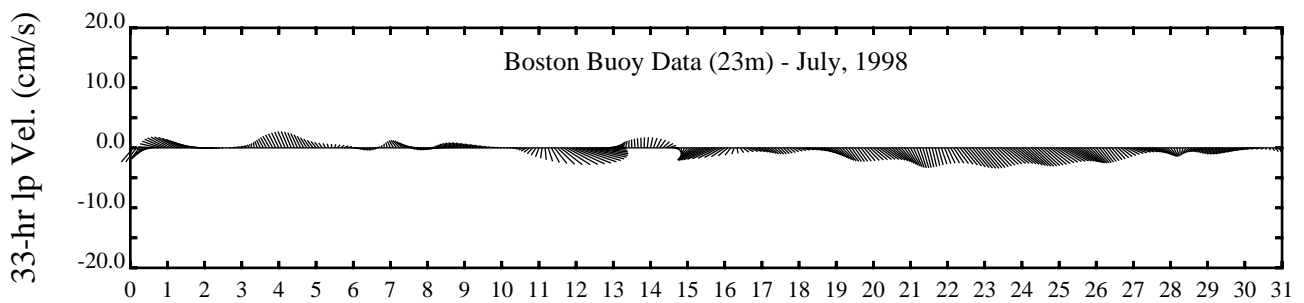
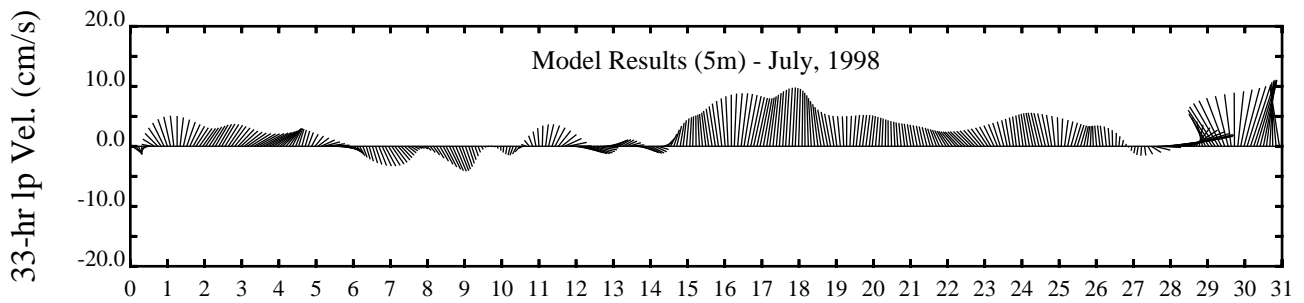
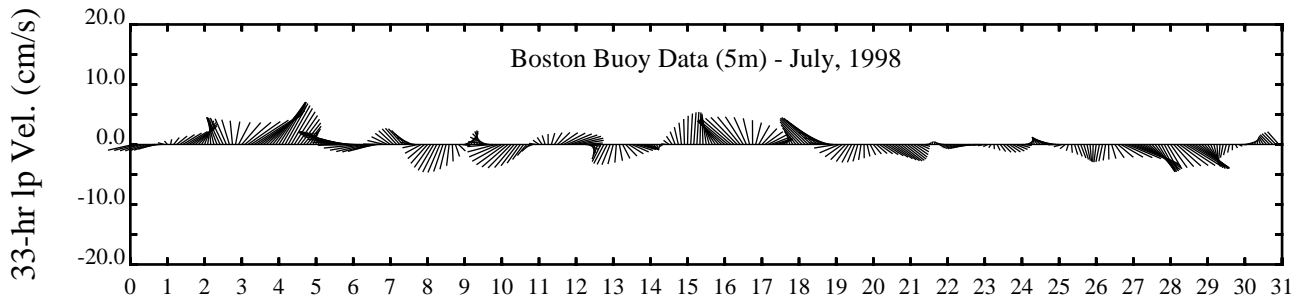
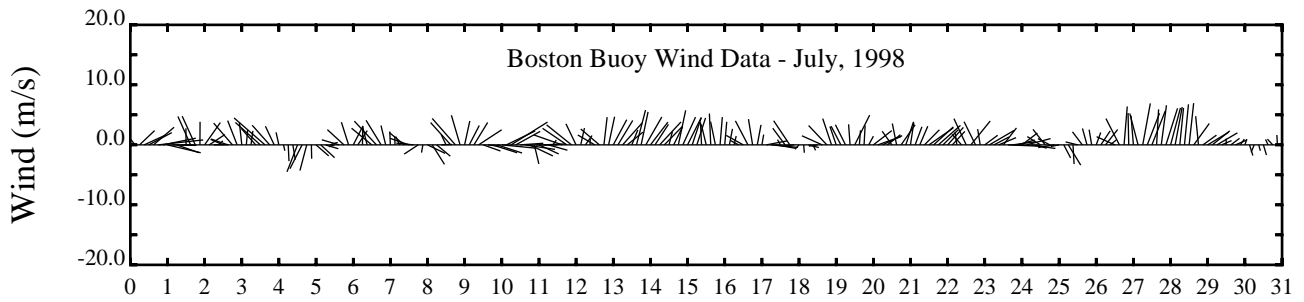


Day

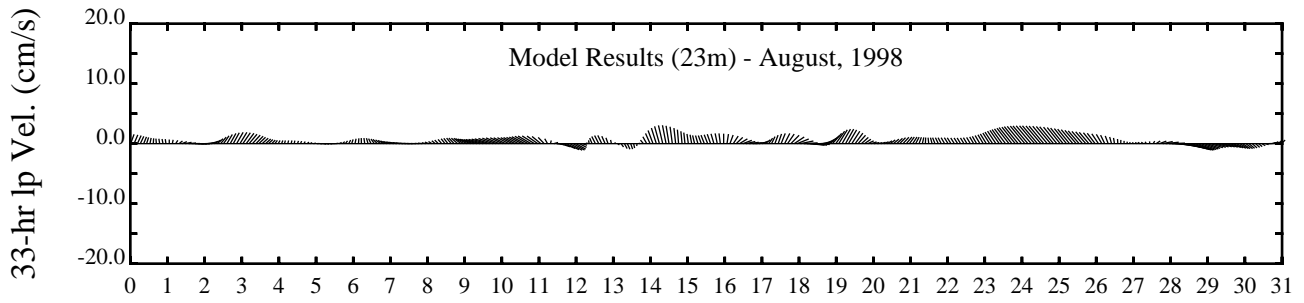
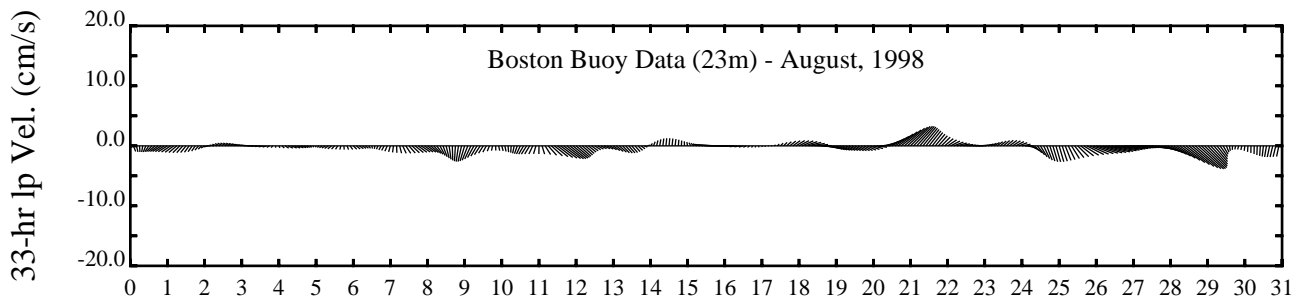
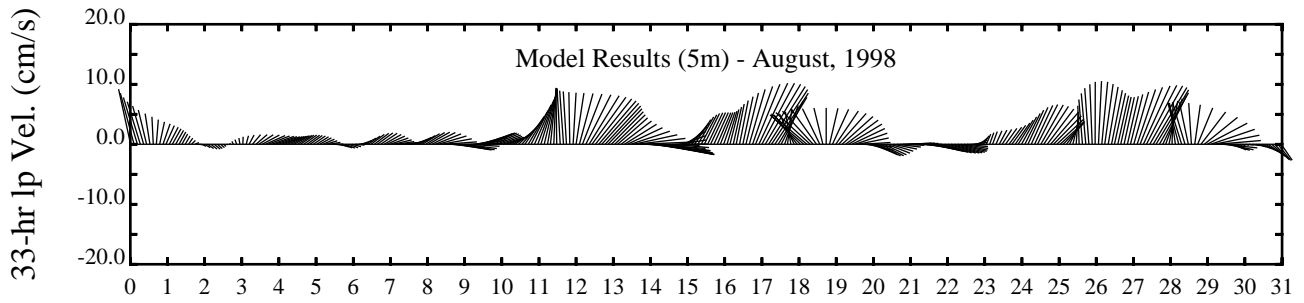
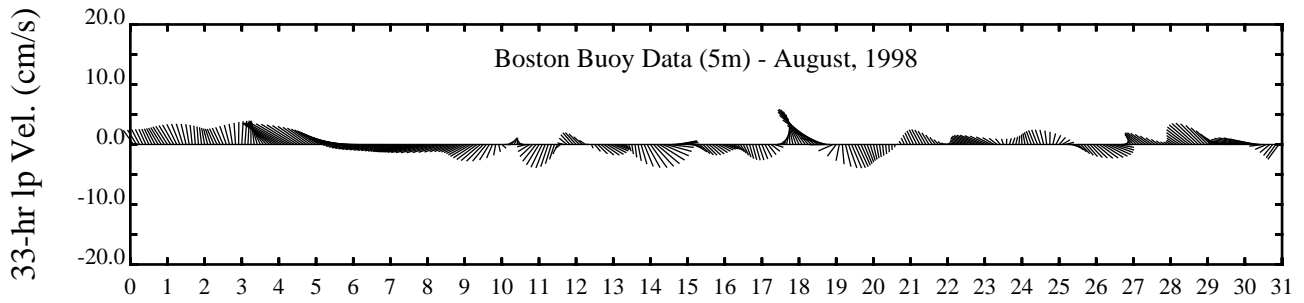
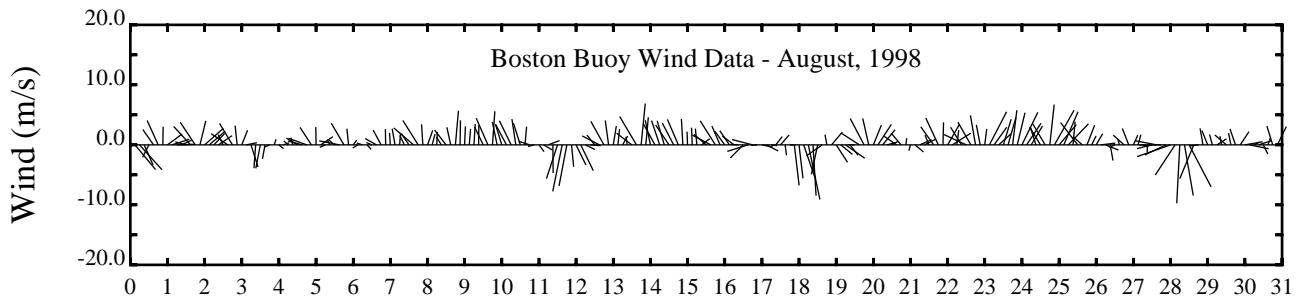




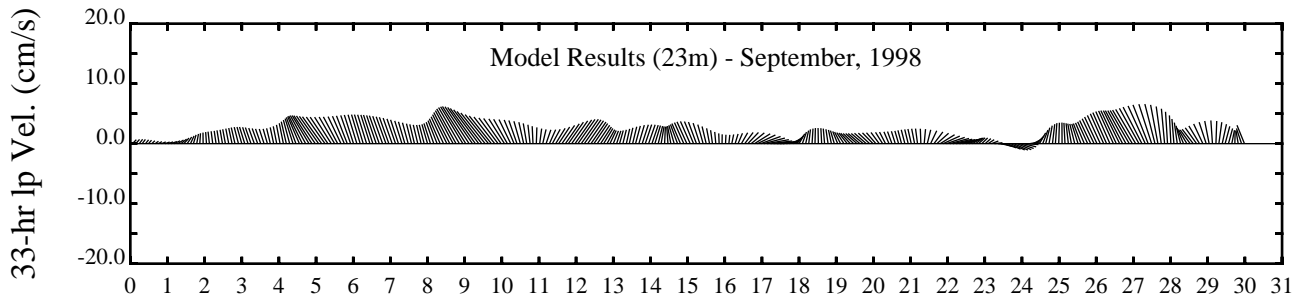
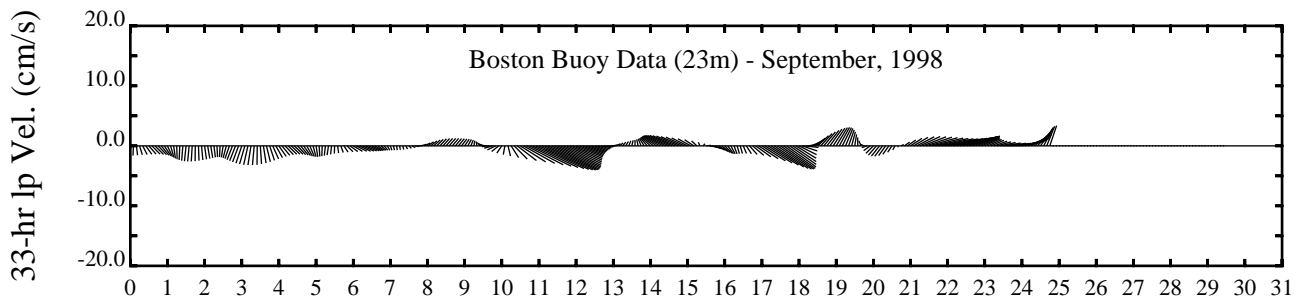
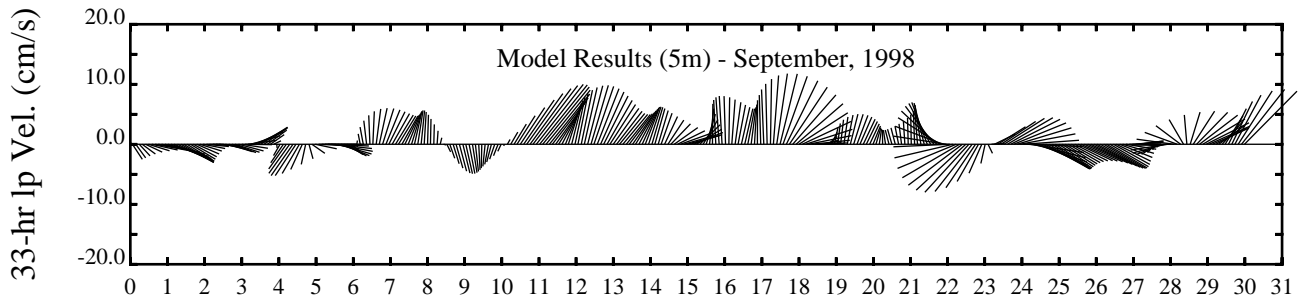
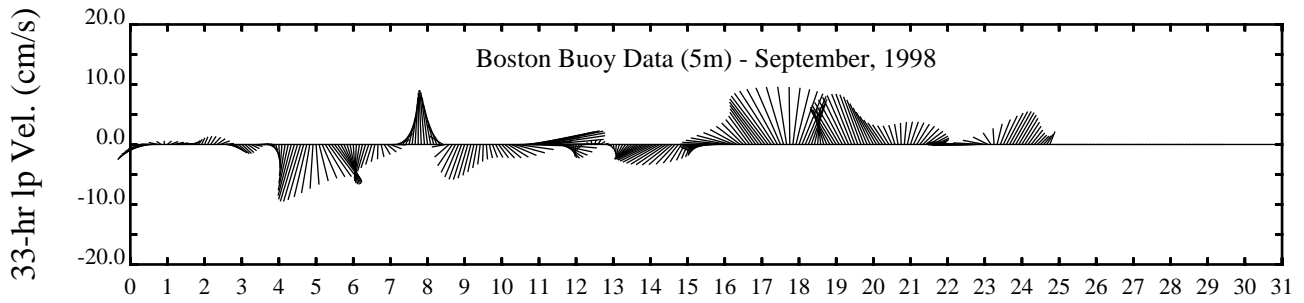
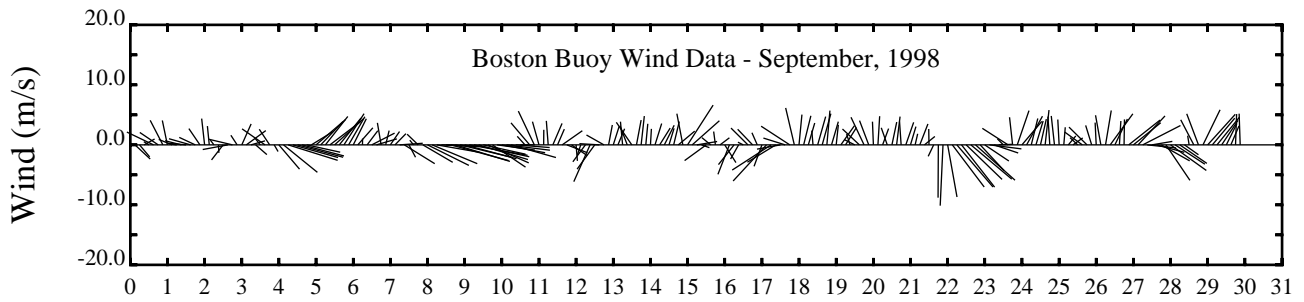
Day



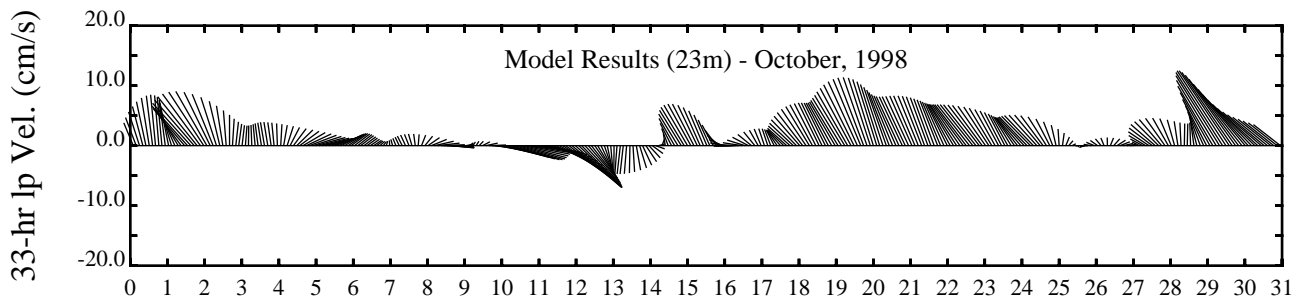
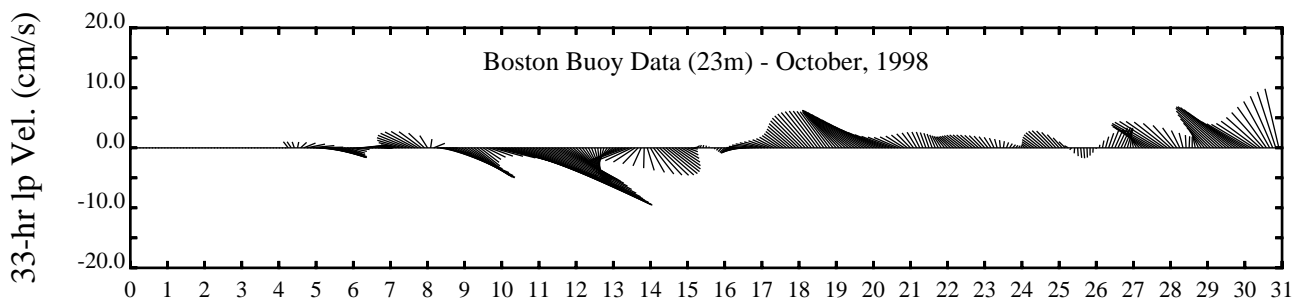
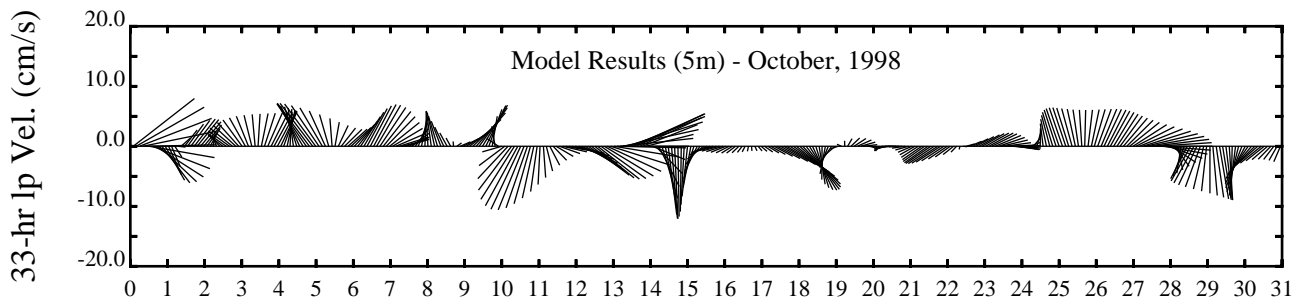
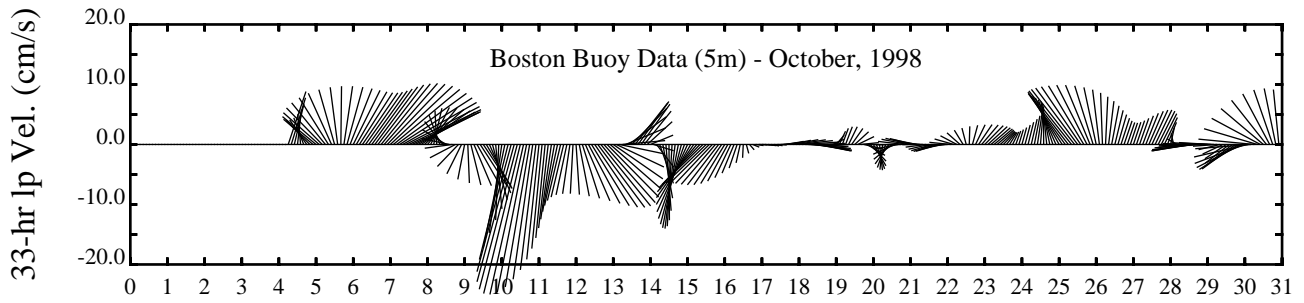
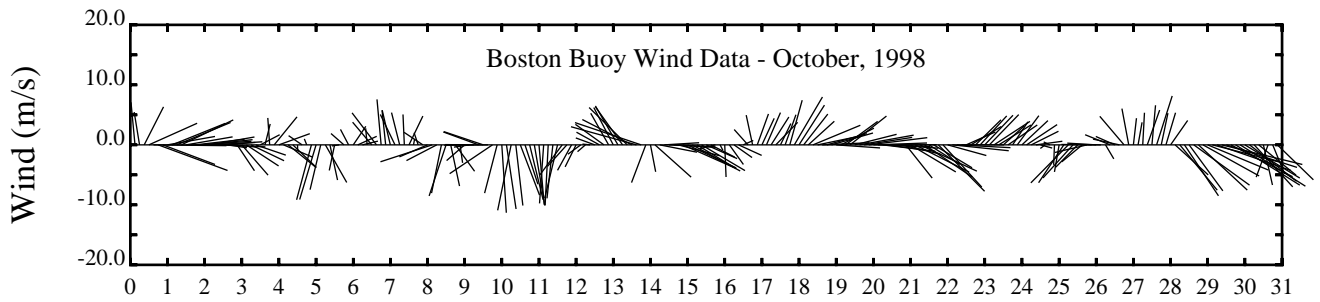
Day



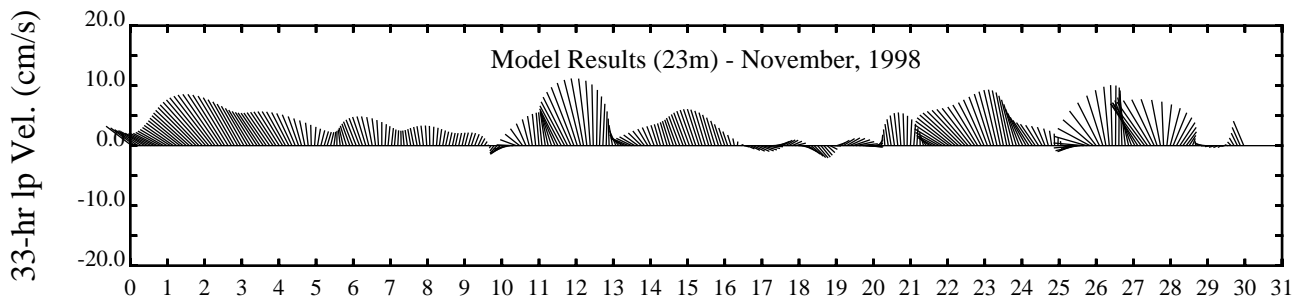
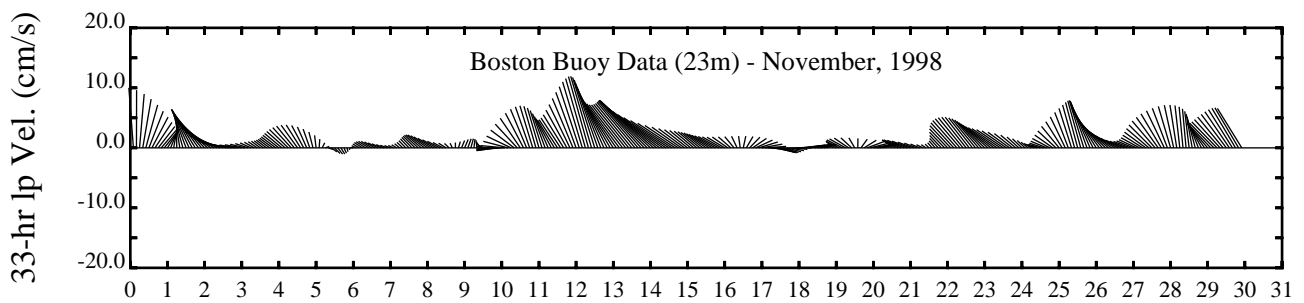
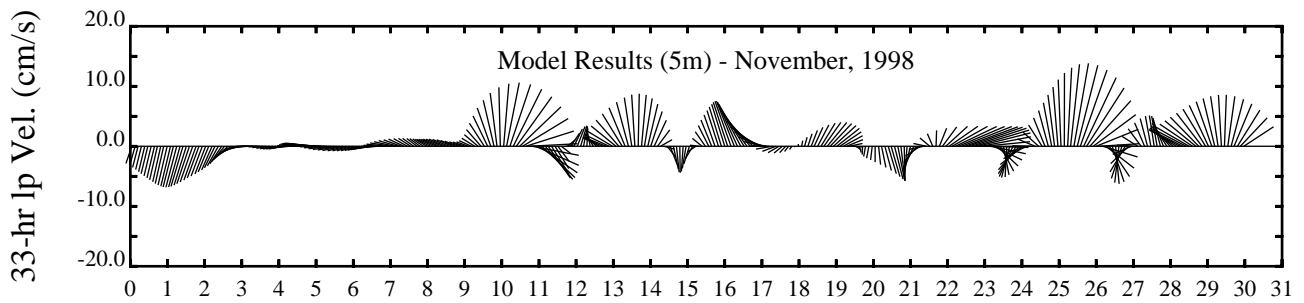
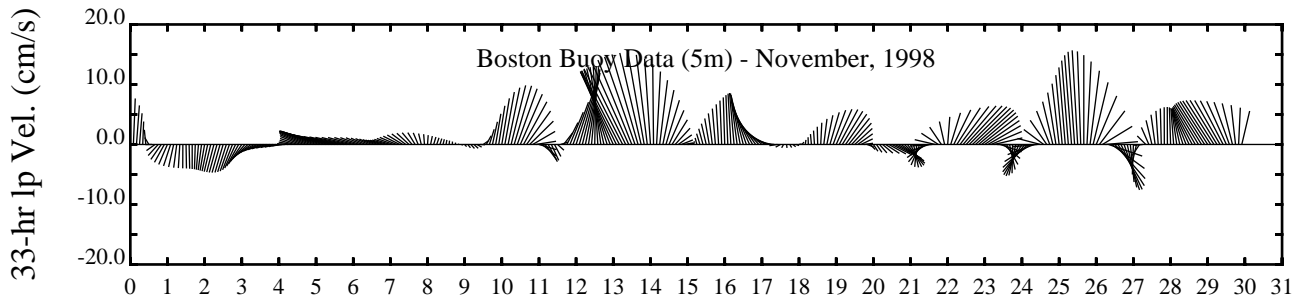
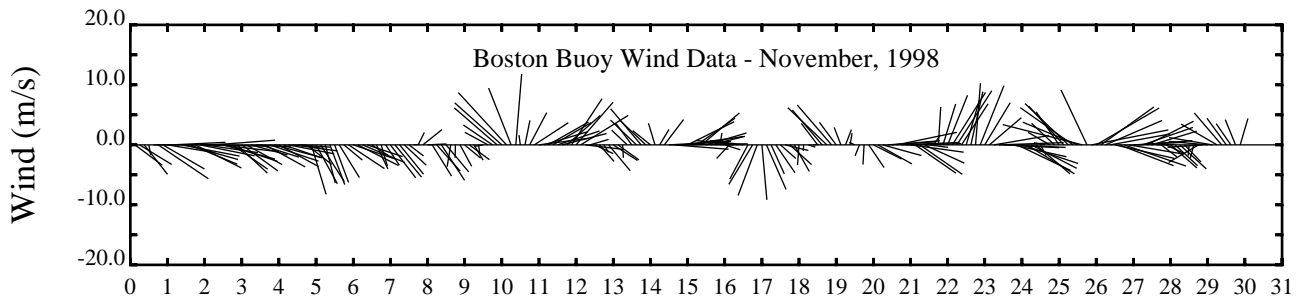
Day



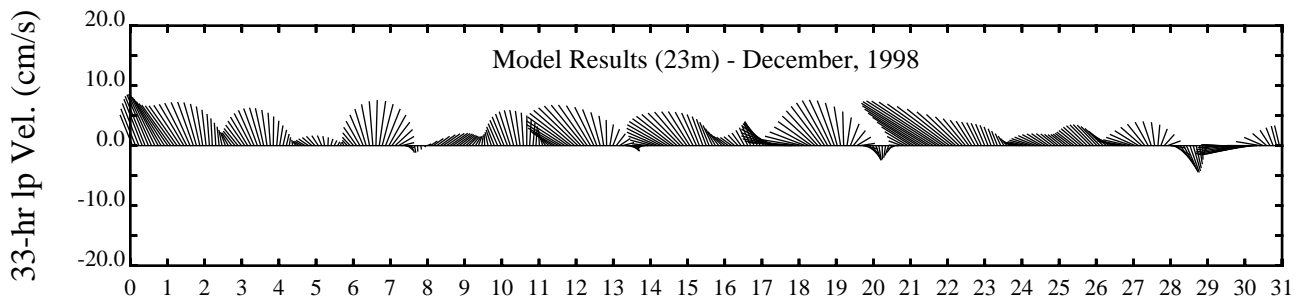
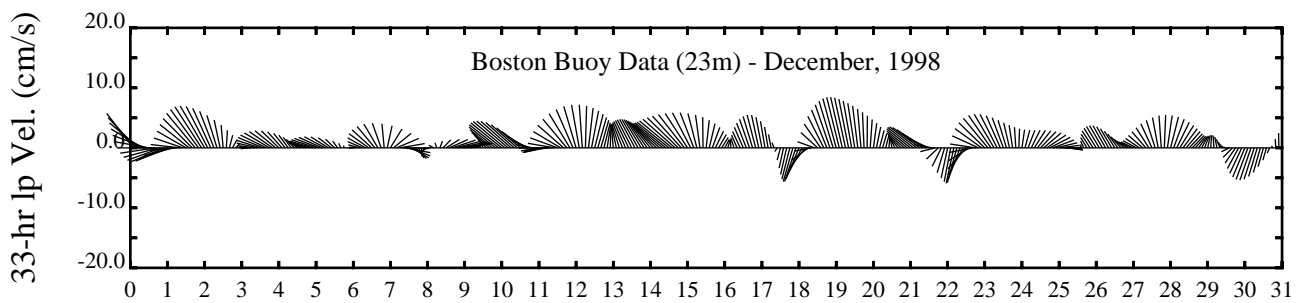
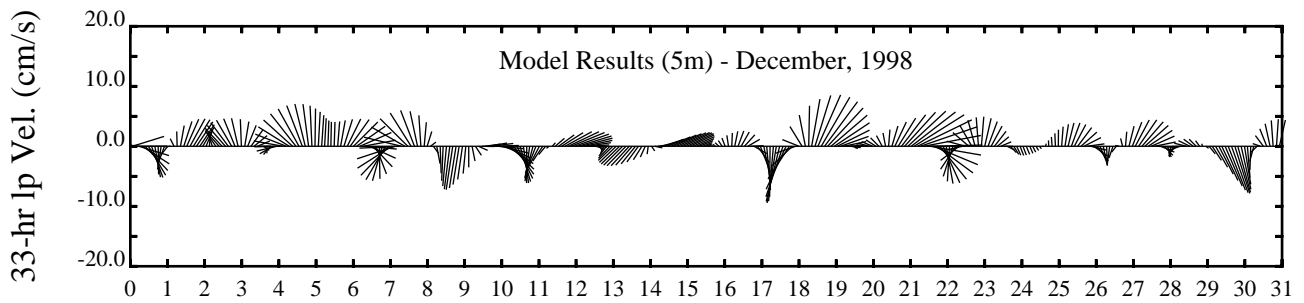
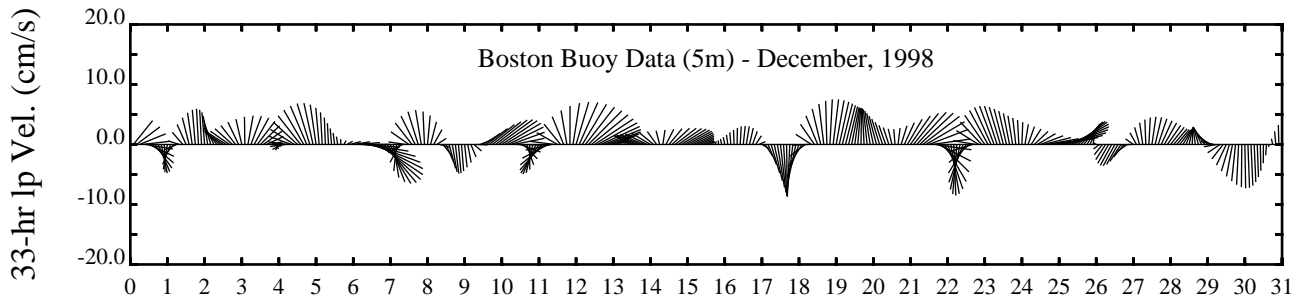
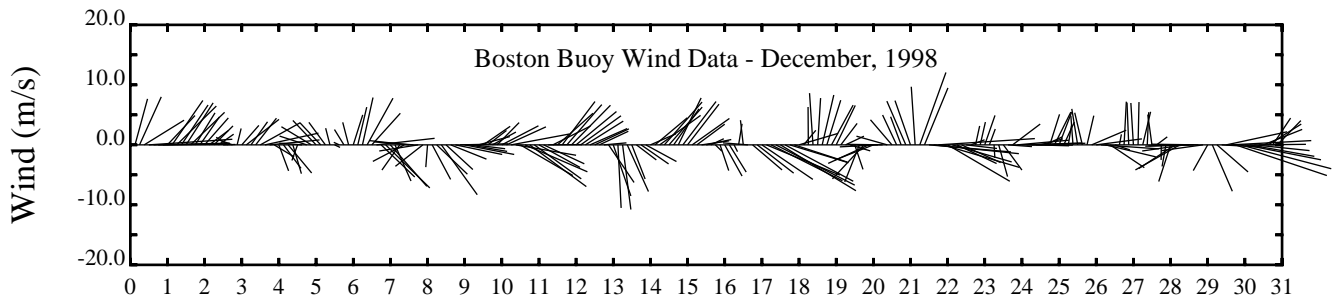
Day



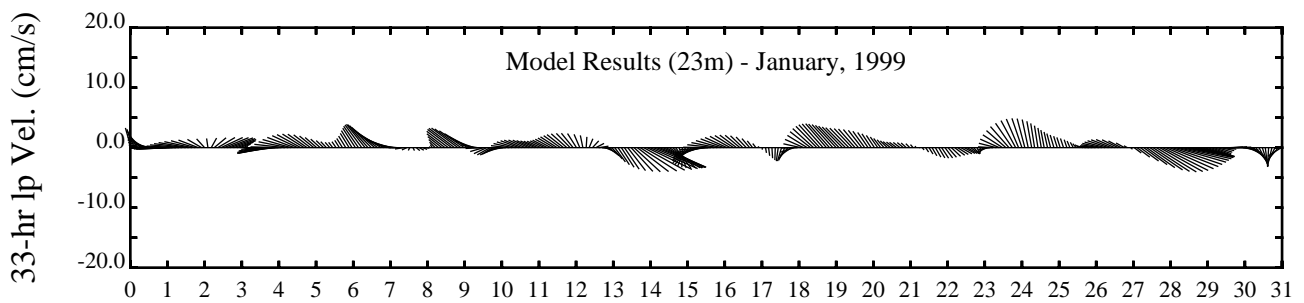
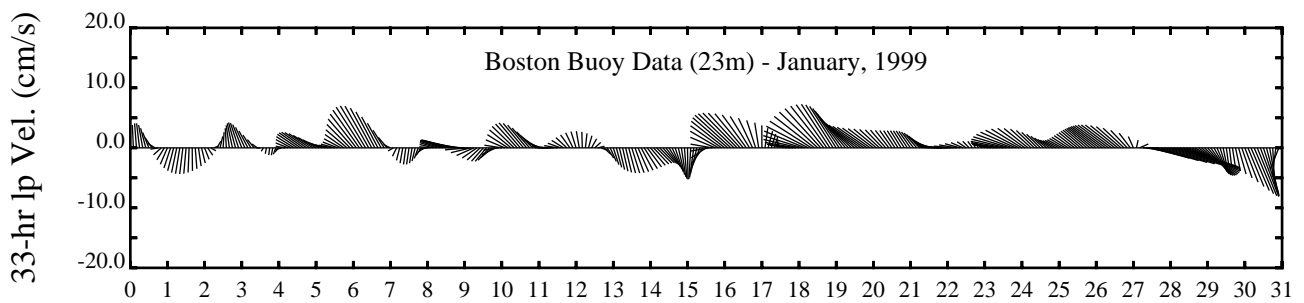
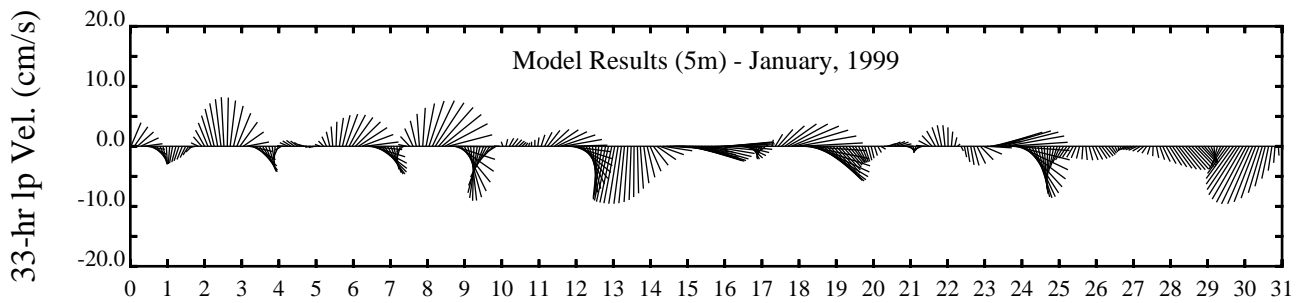
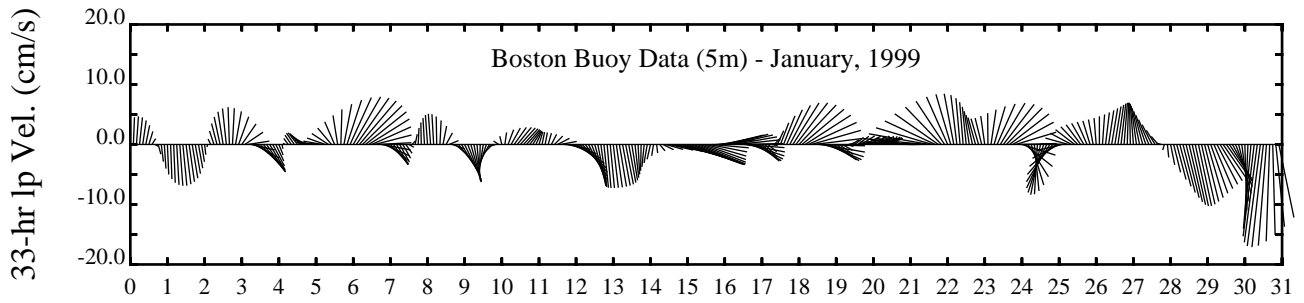
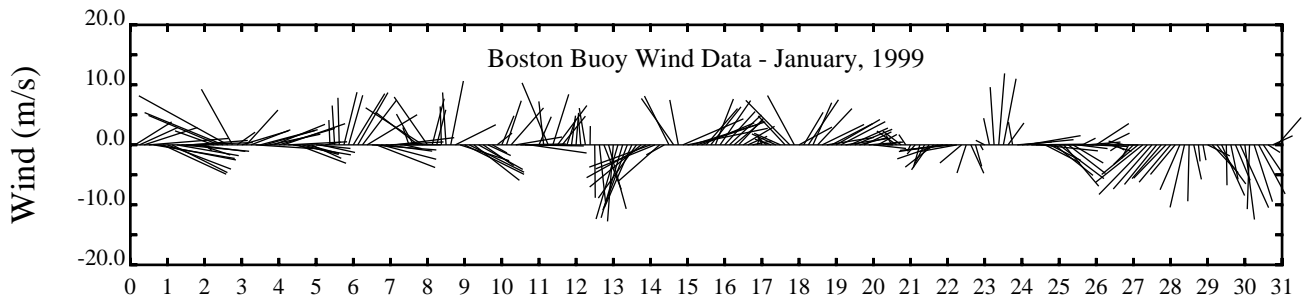
Day



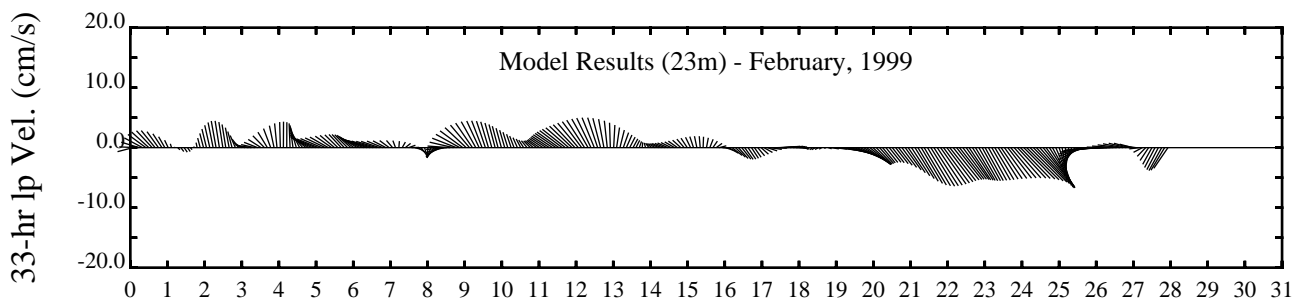
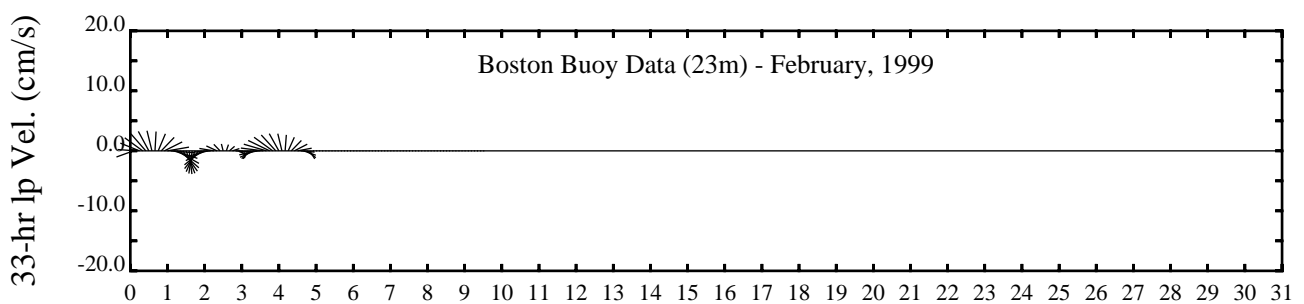
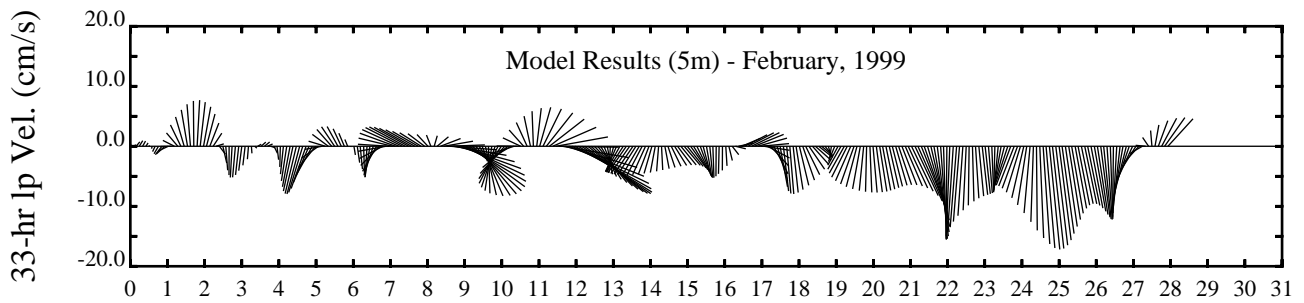
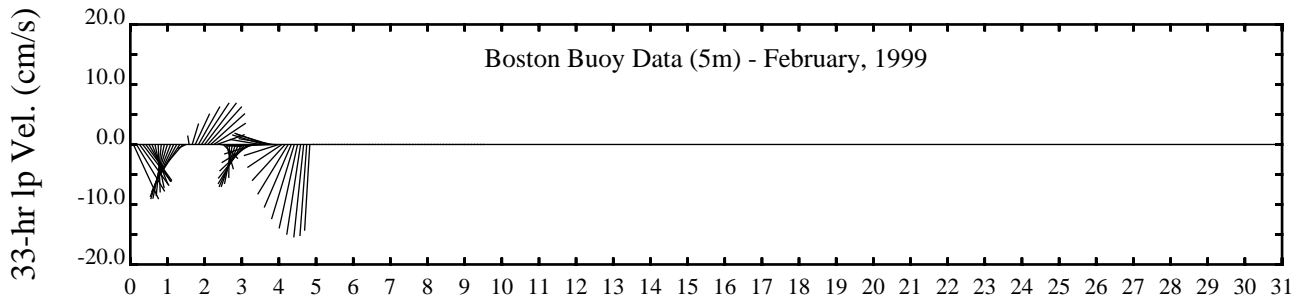
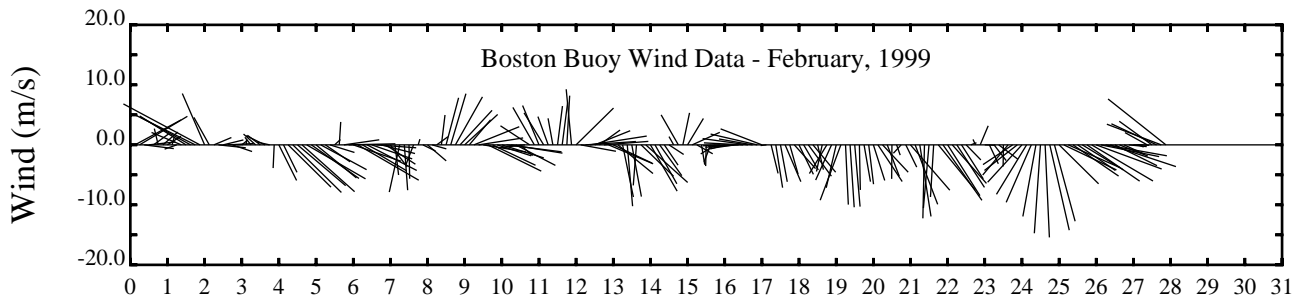
Day



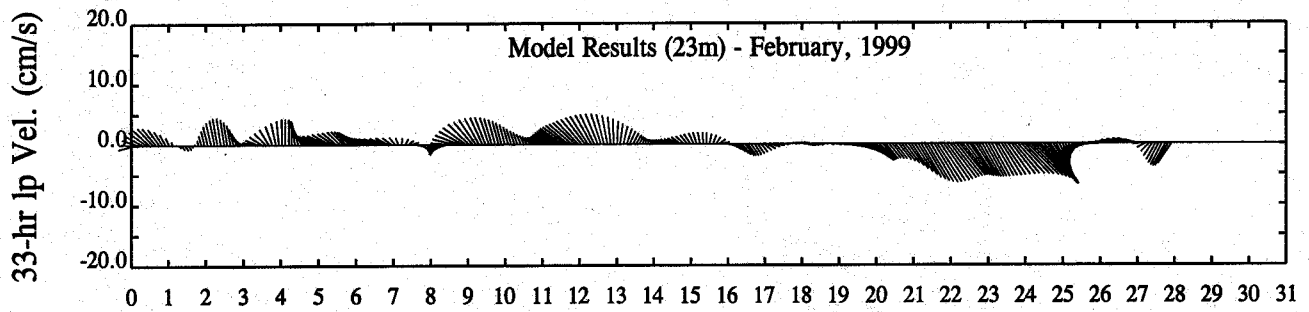
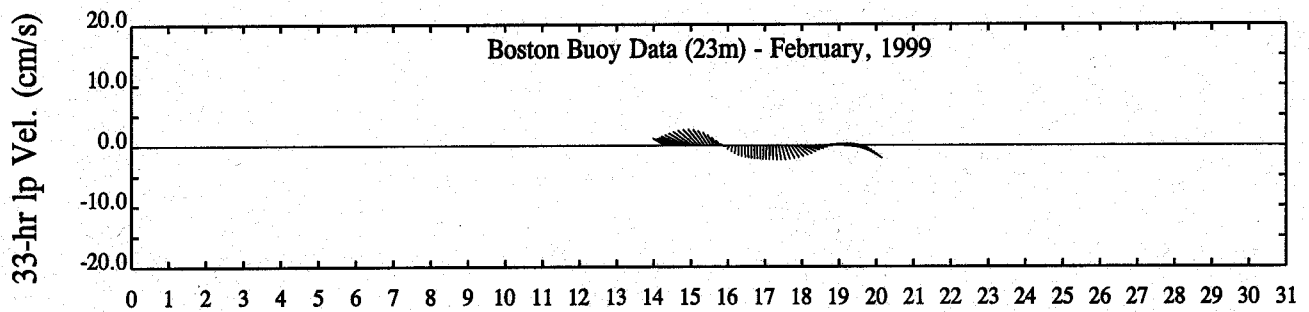
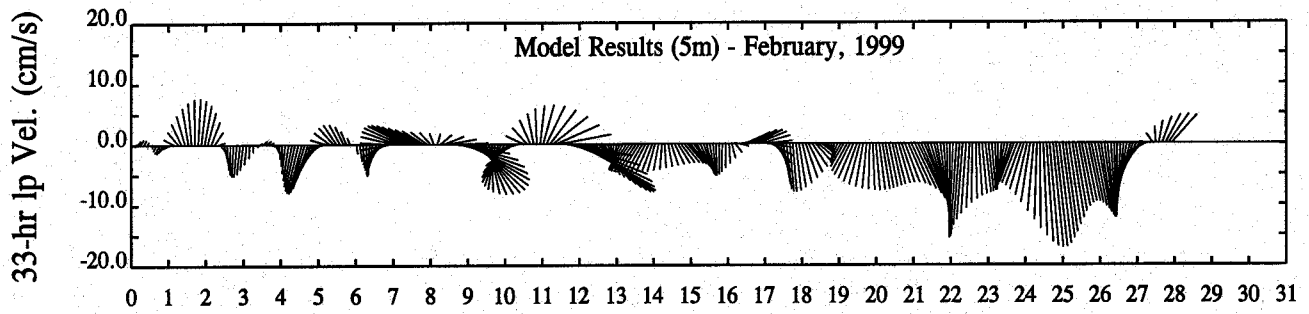
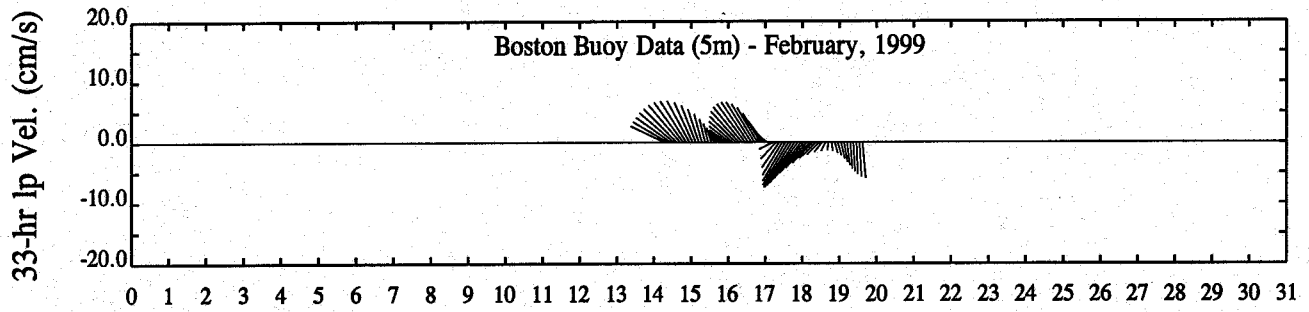
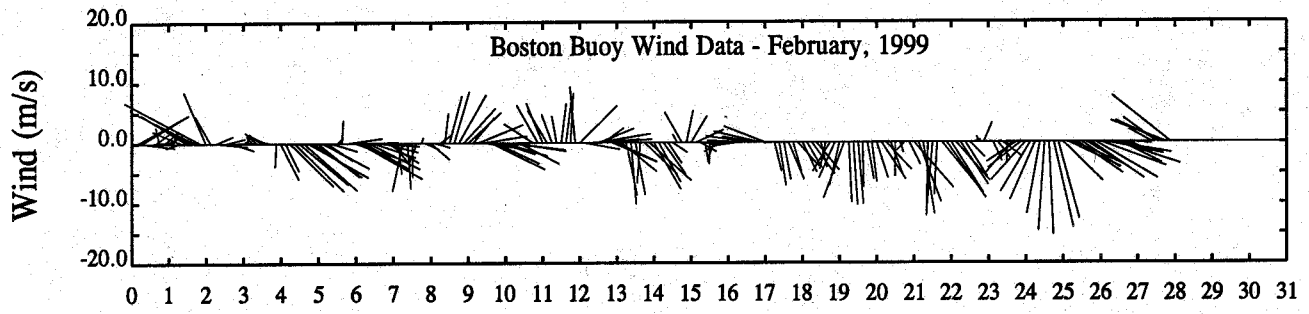
Day



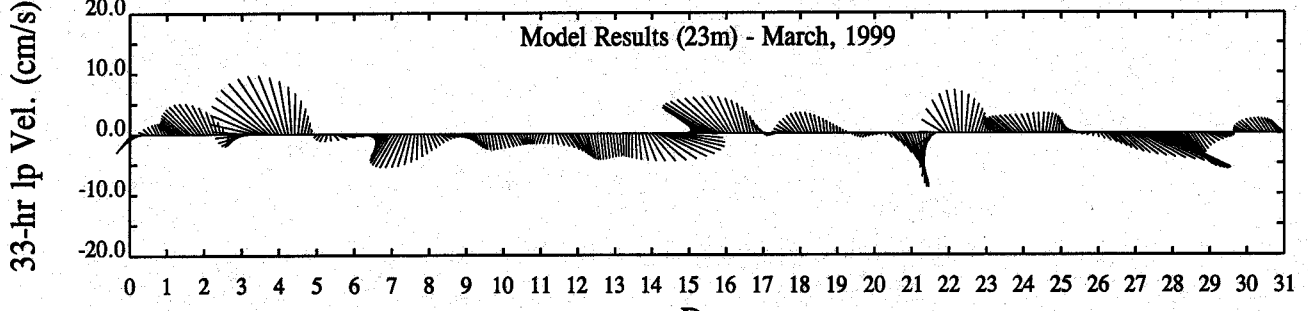
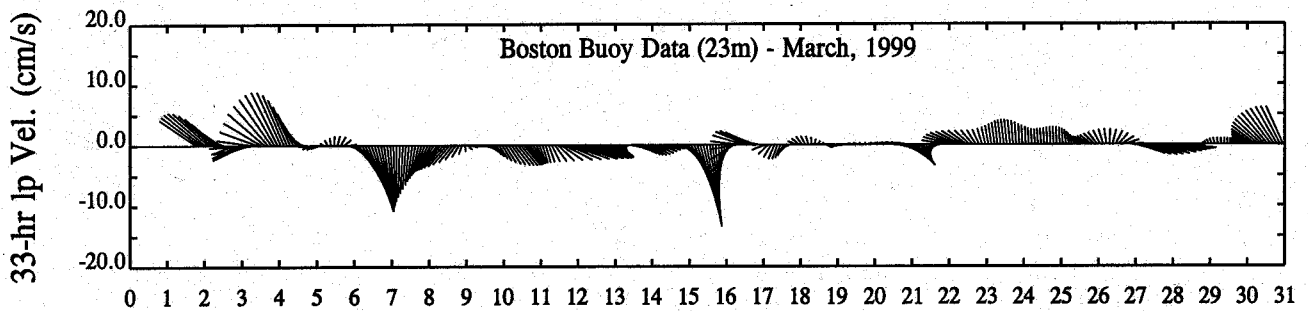
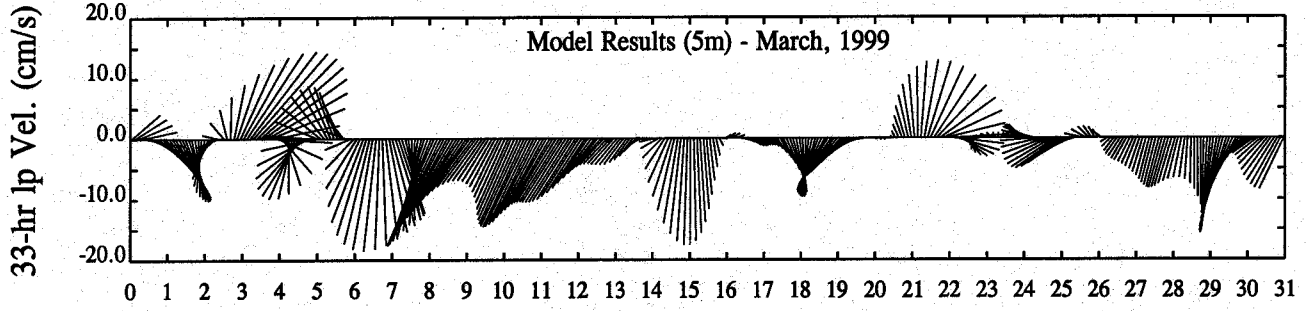
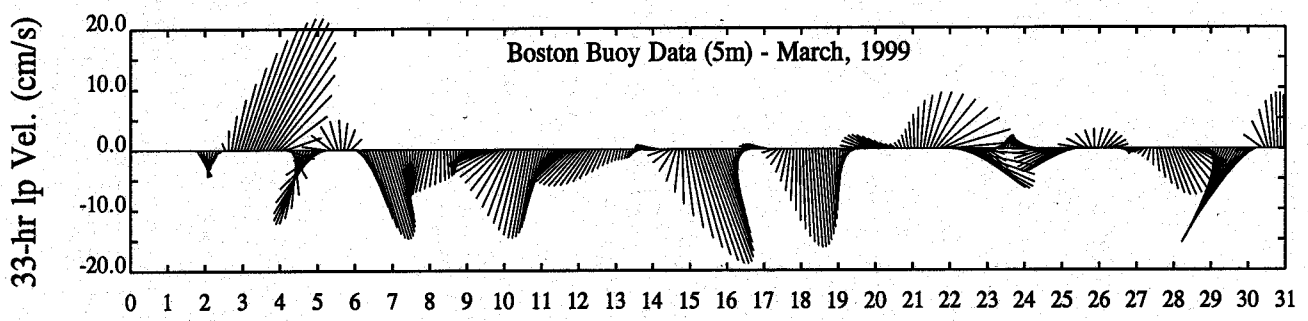
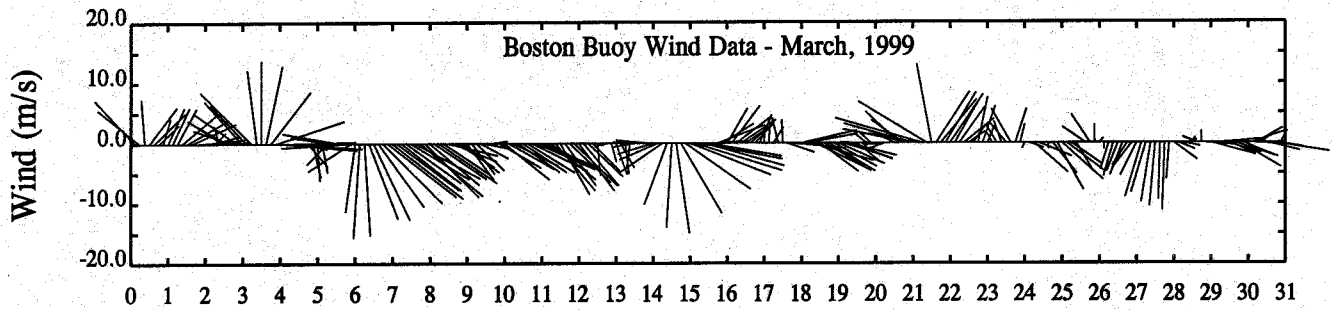
Day



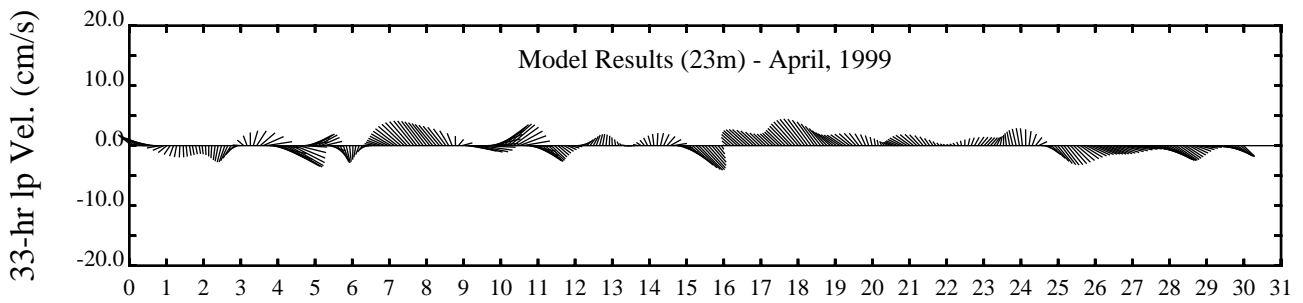
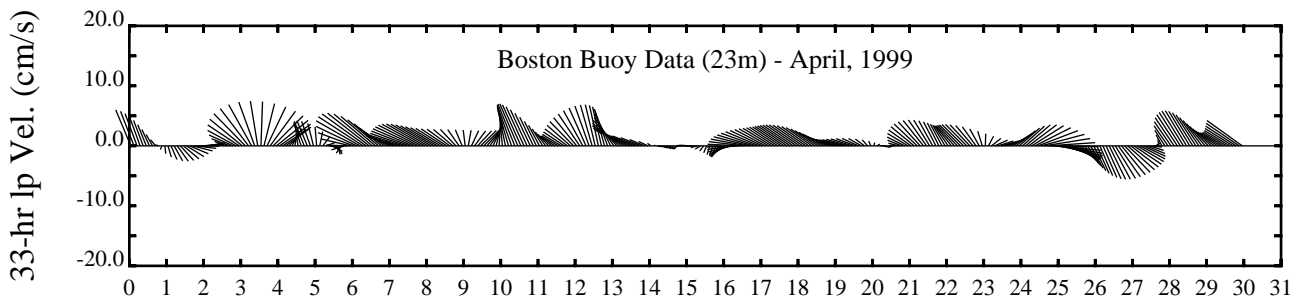
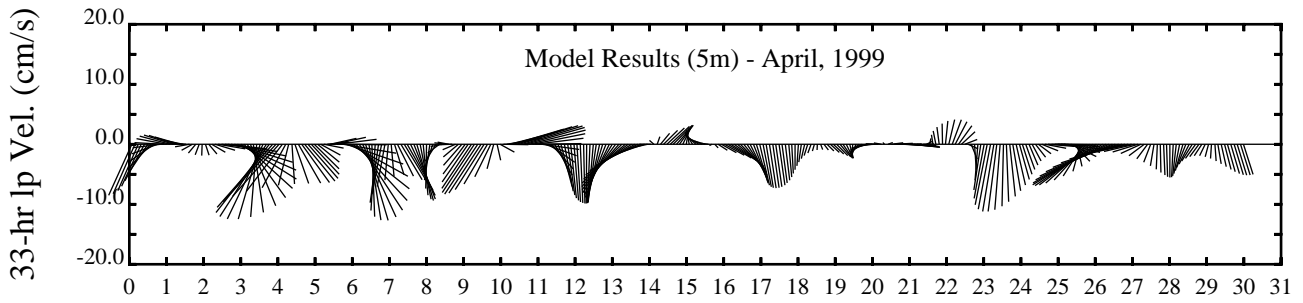
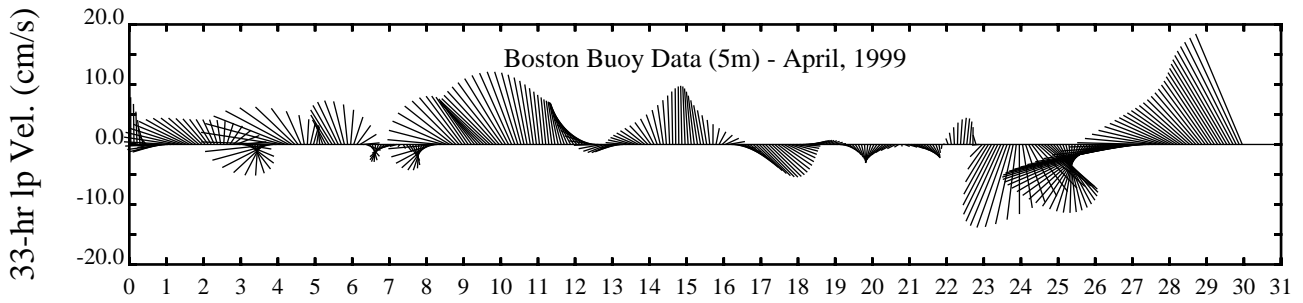
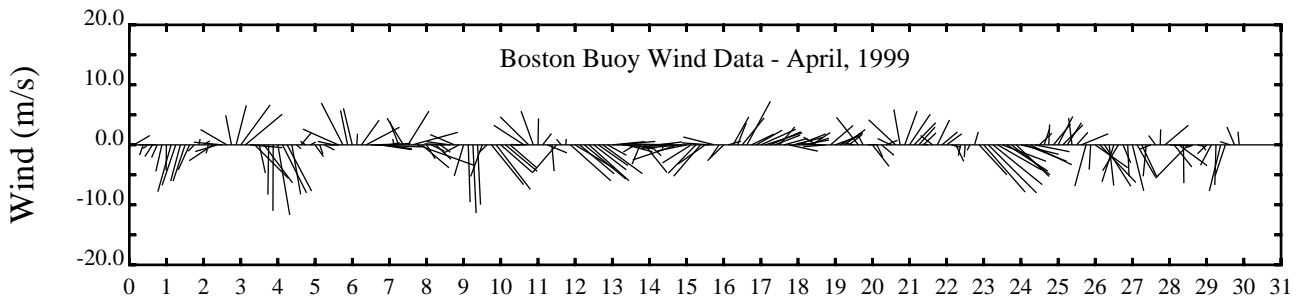
Day



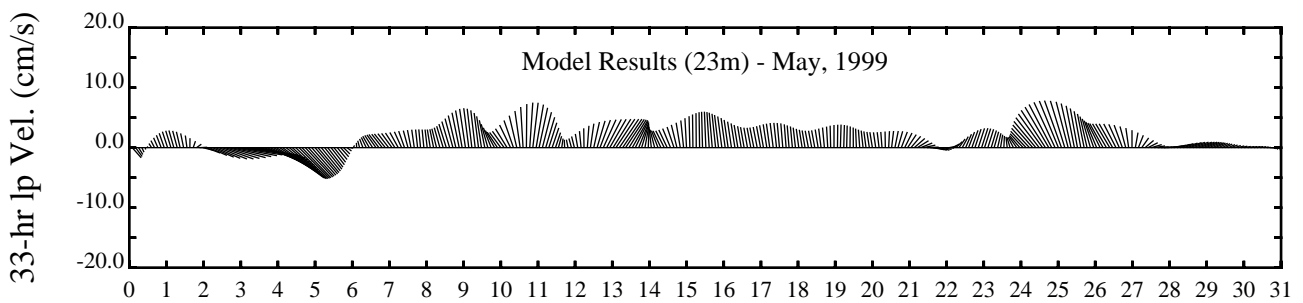
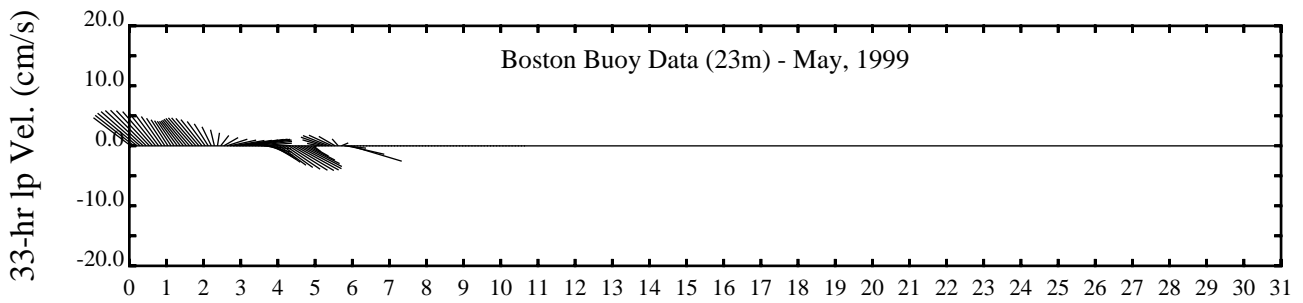
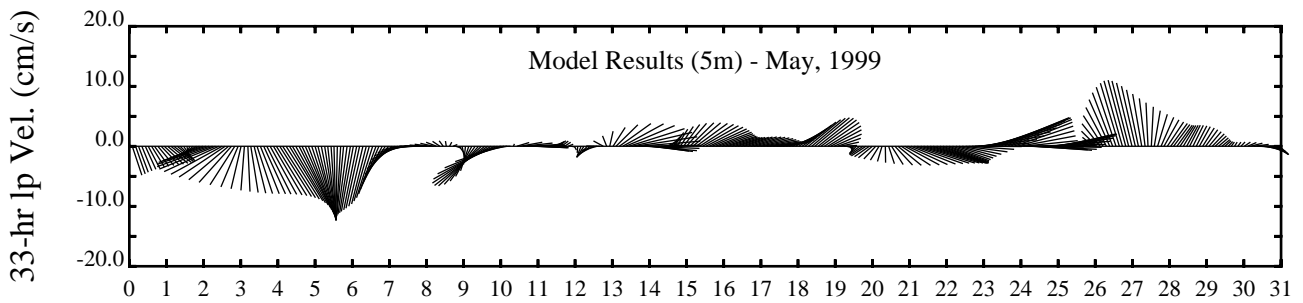
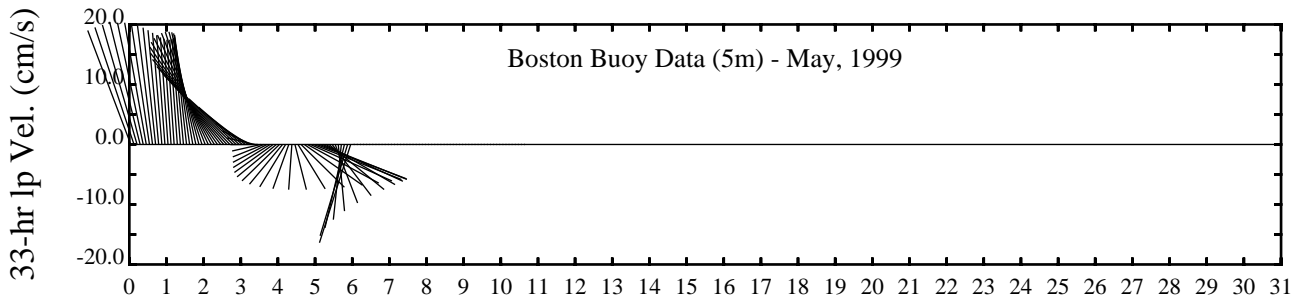
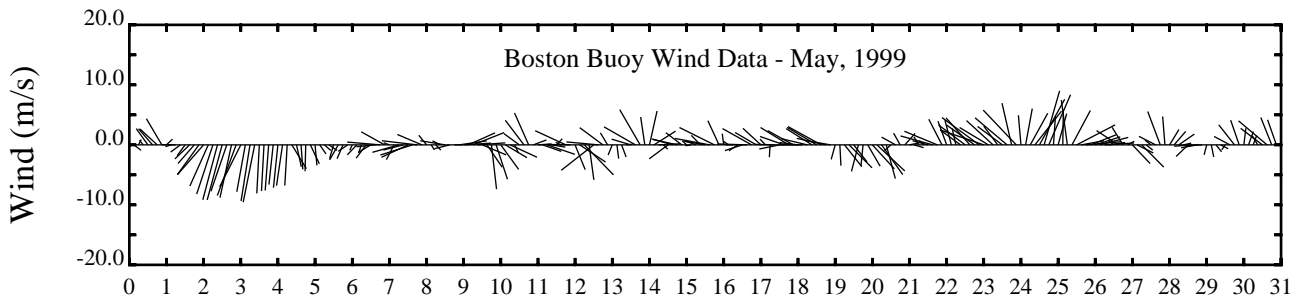
Day



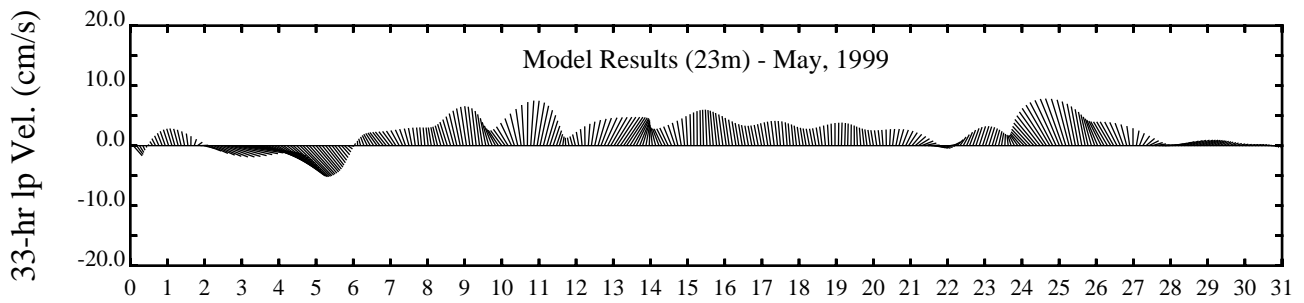
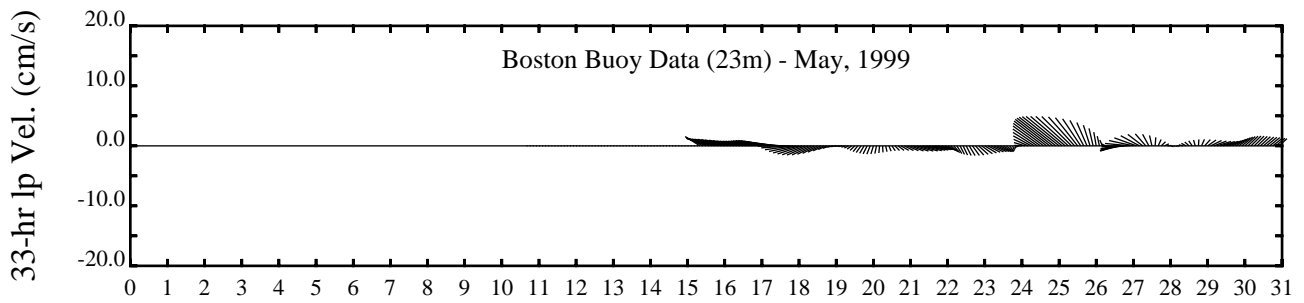
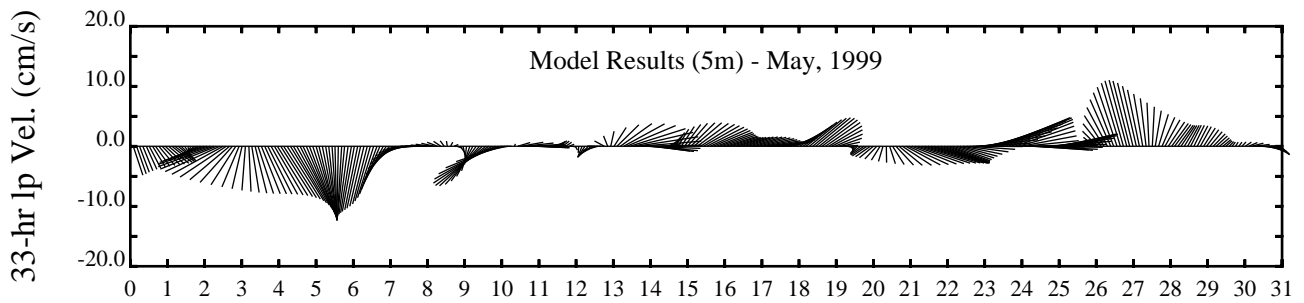
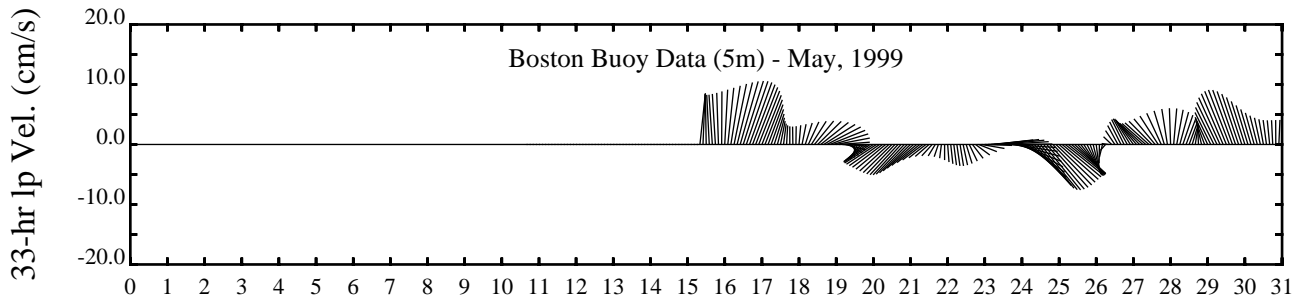
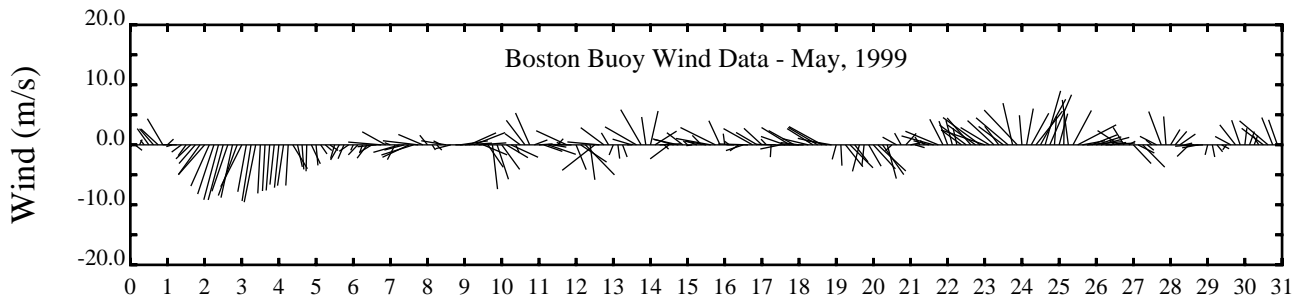
Day



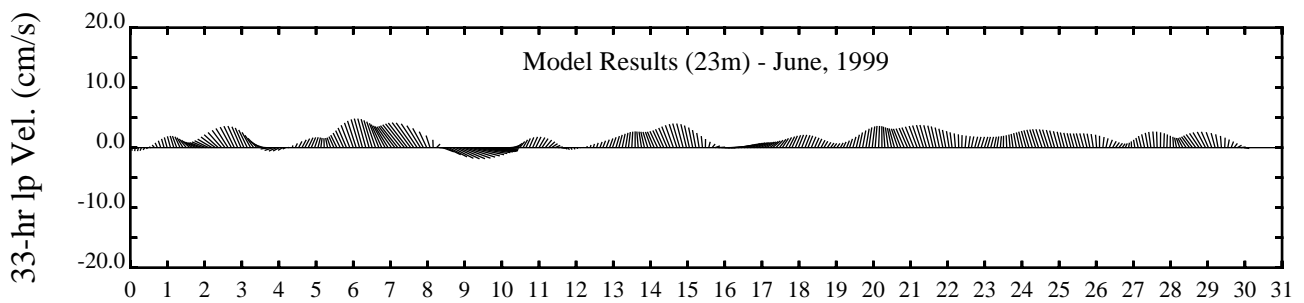
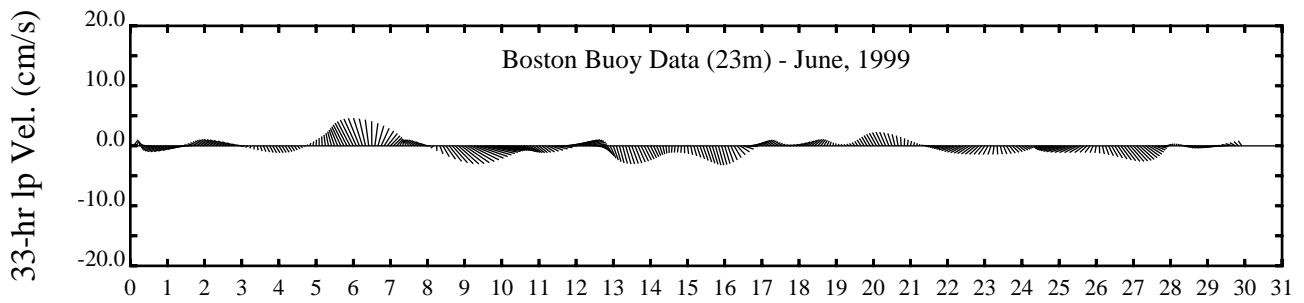
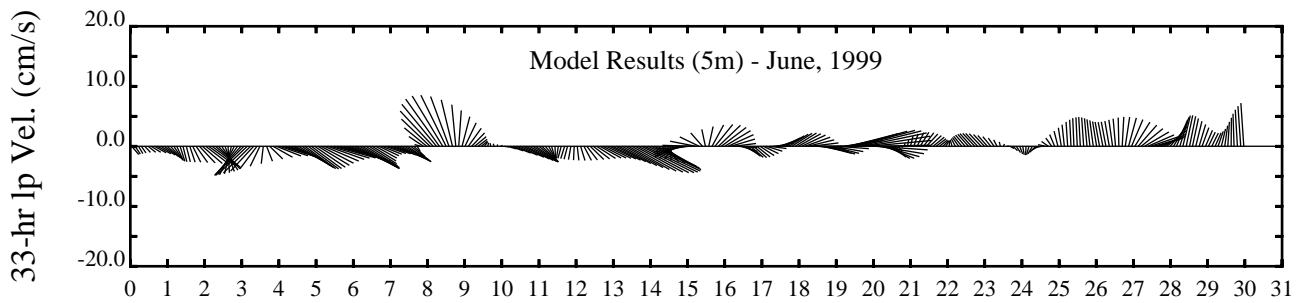
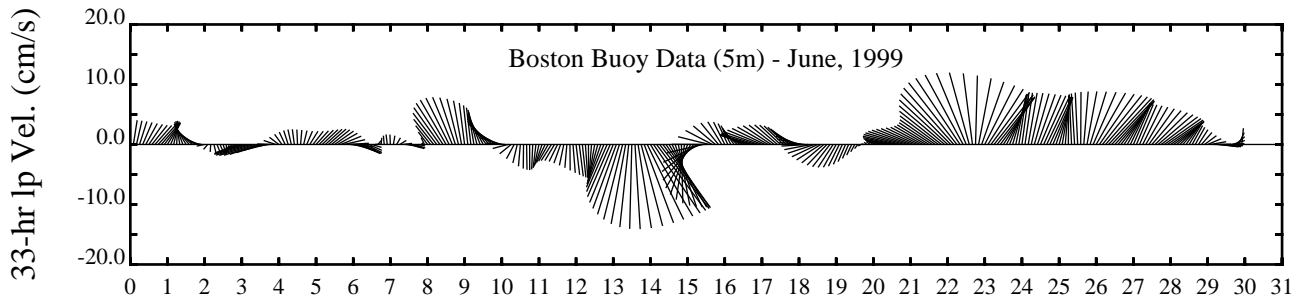
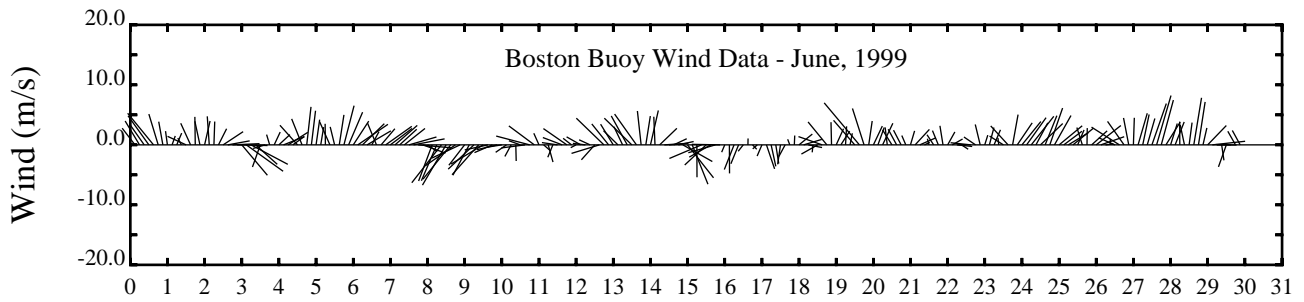
Day



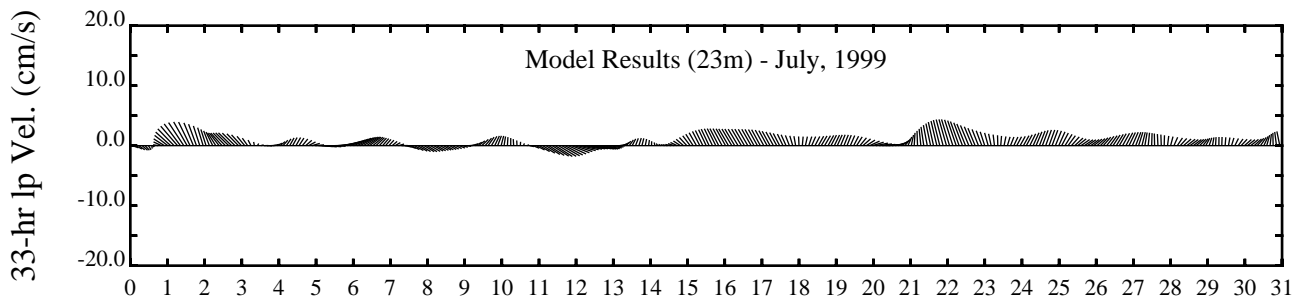
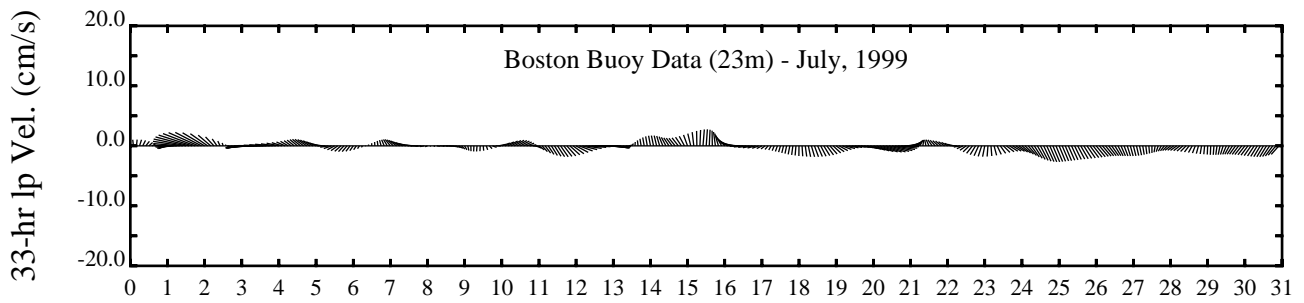
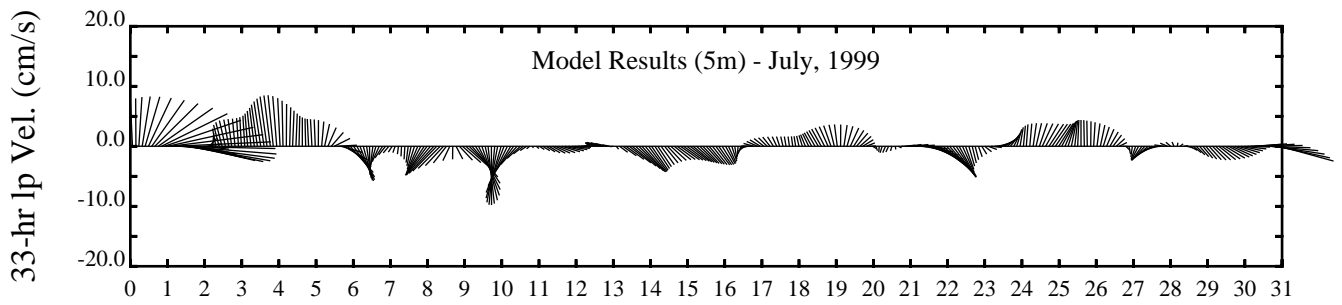
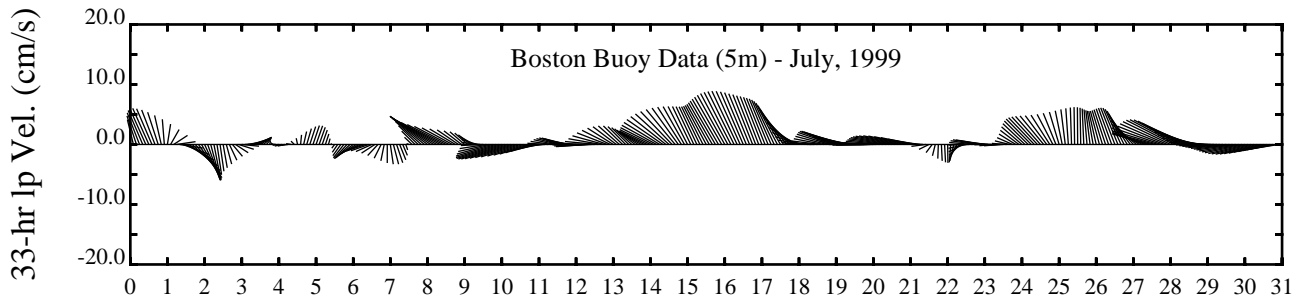
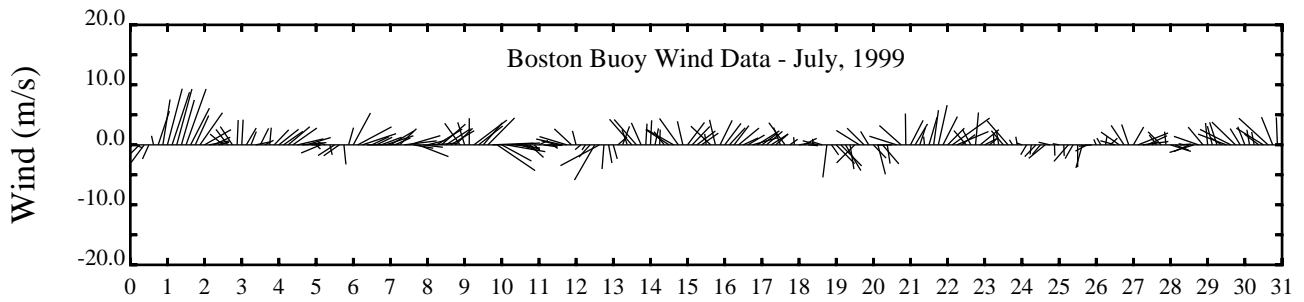
Day



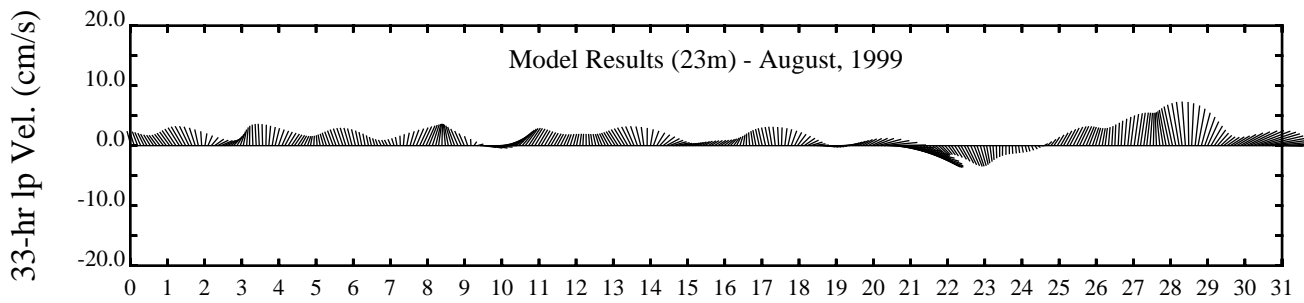
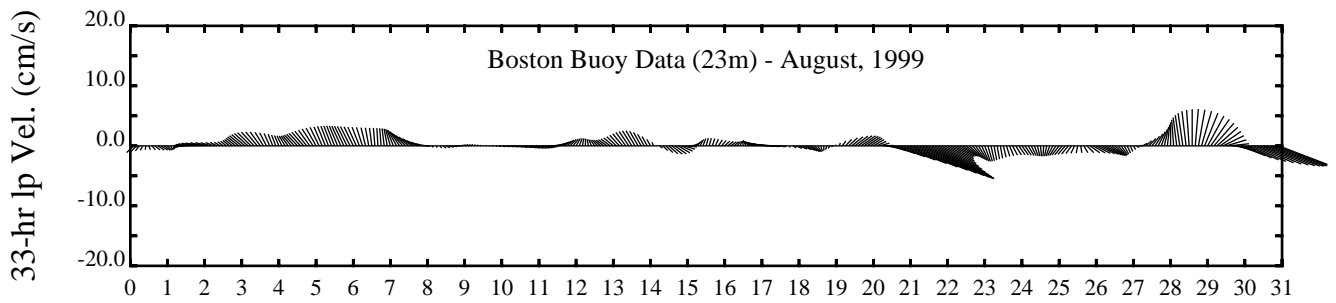
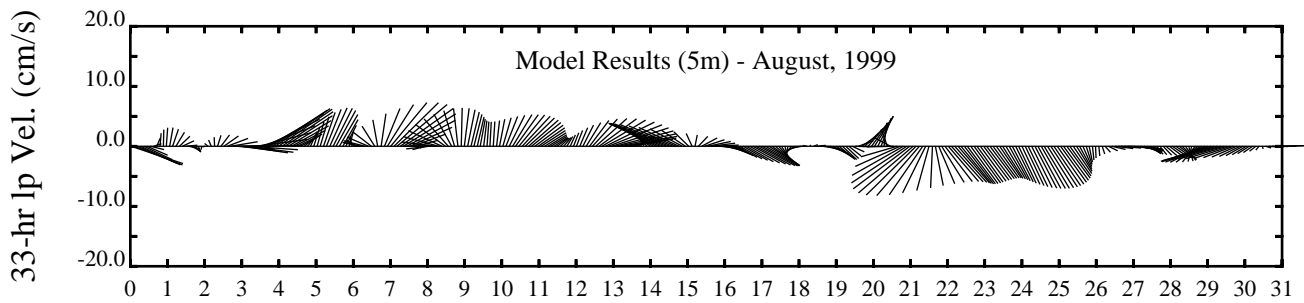
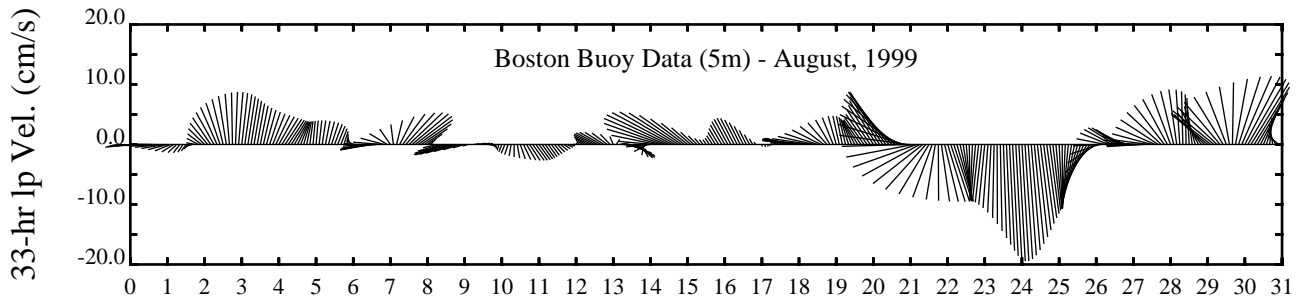
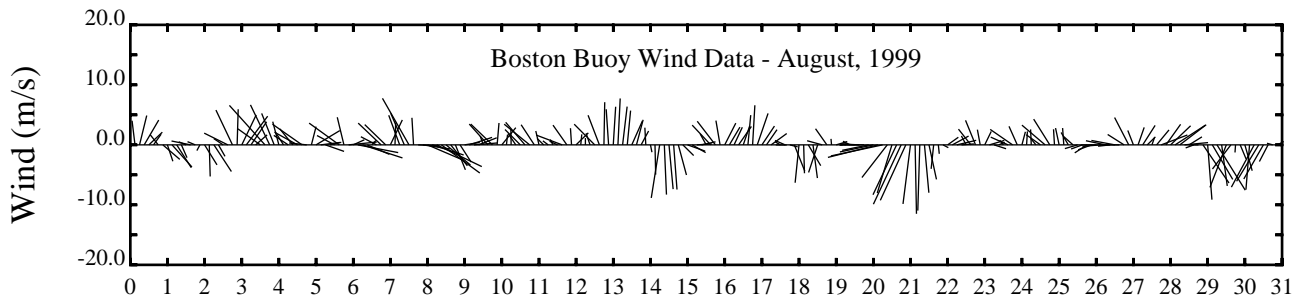
Day



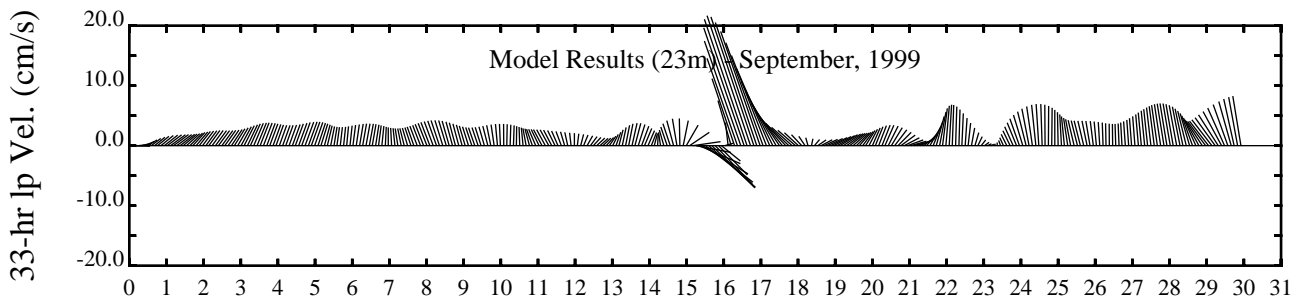
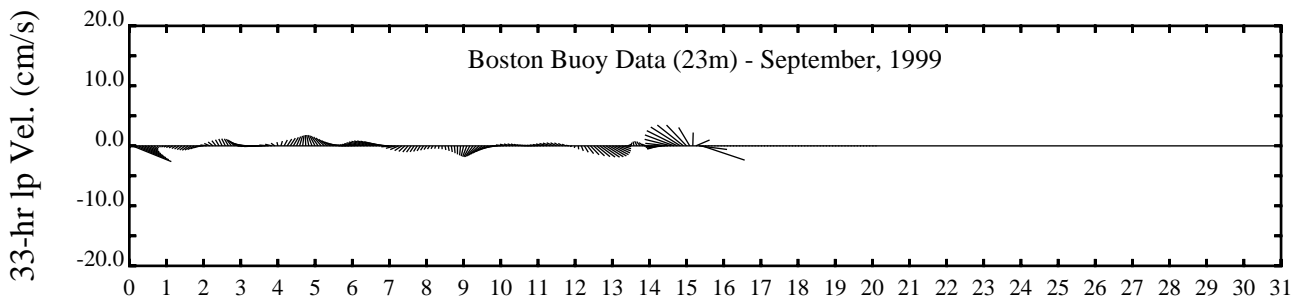
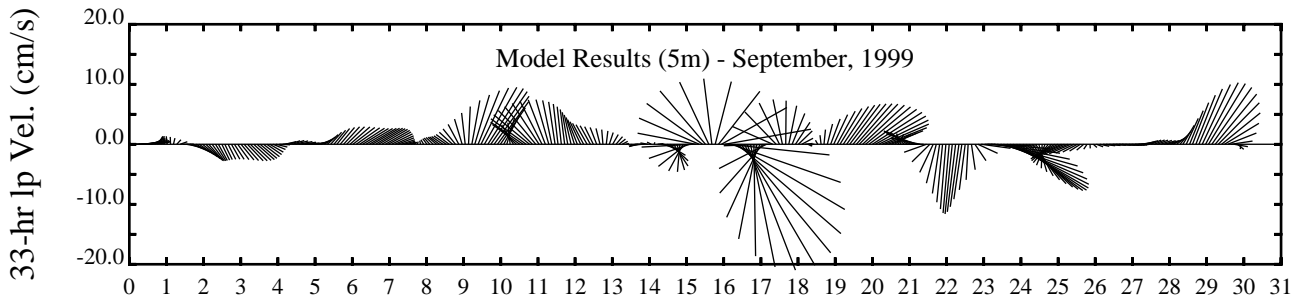
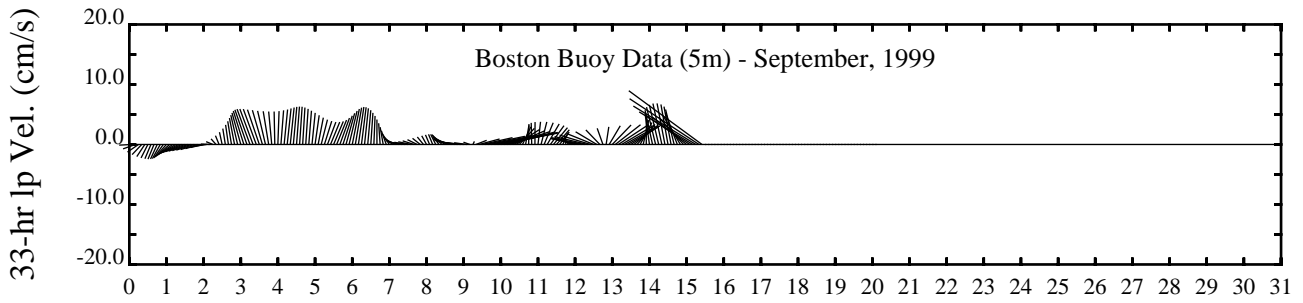
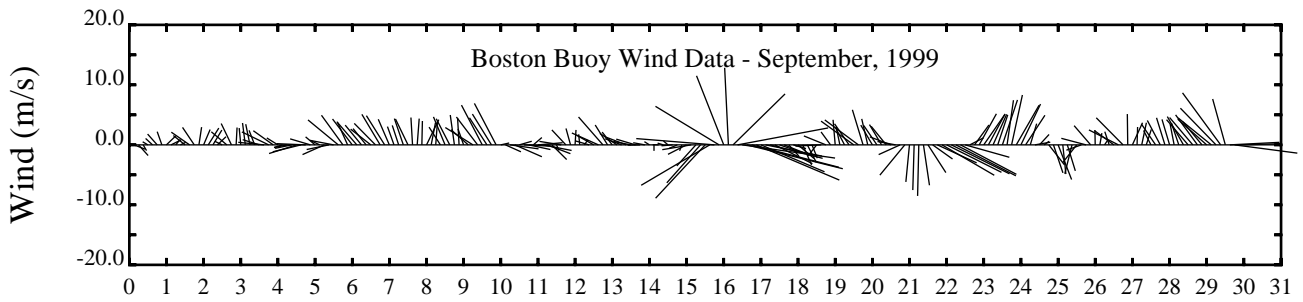
Day



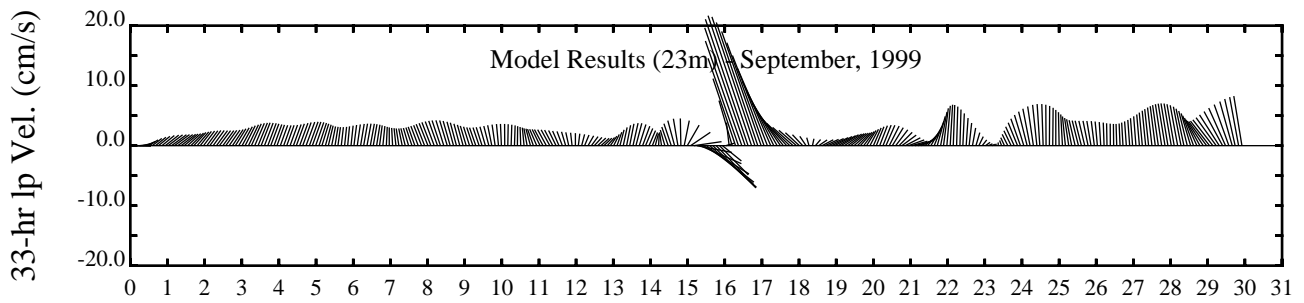
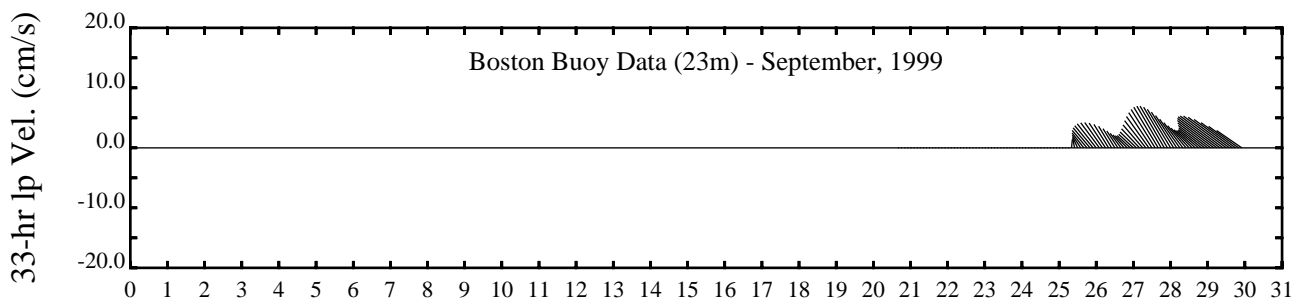
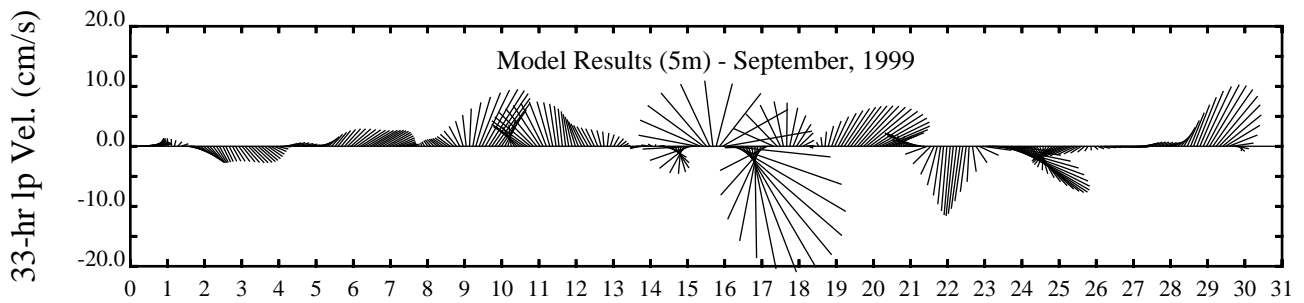
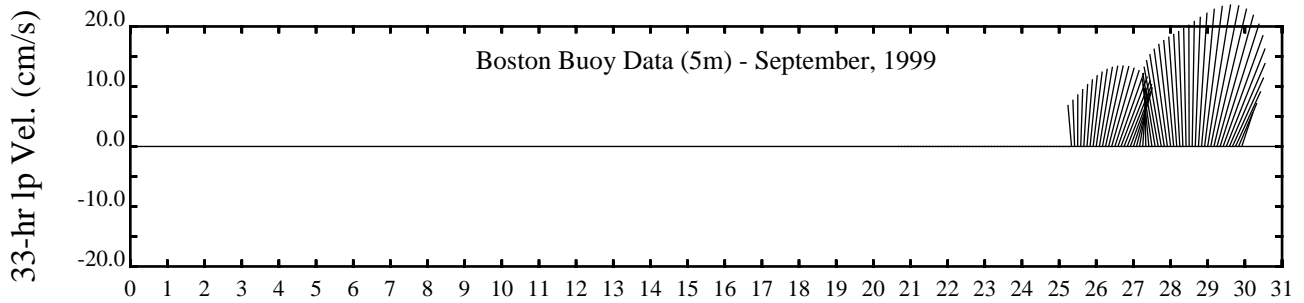
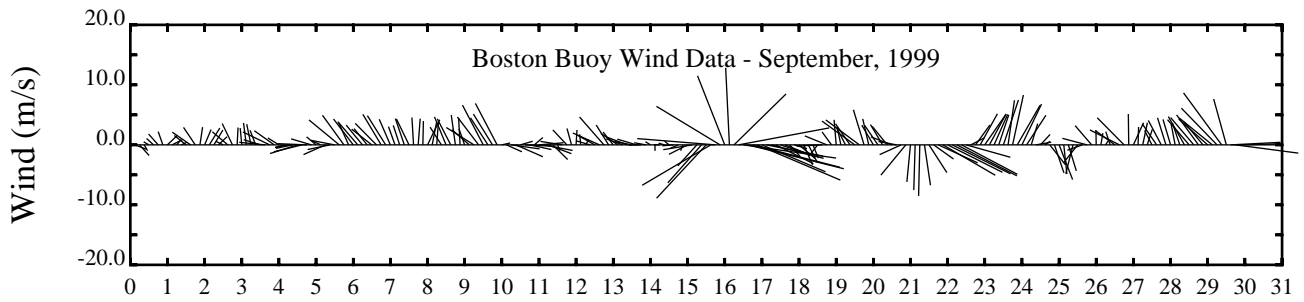
Day



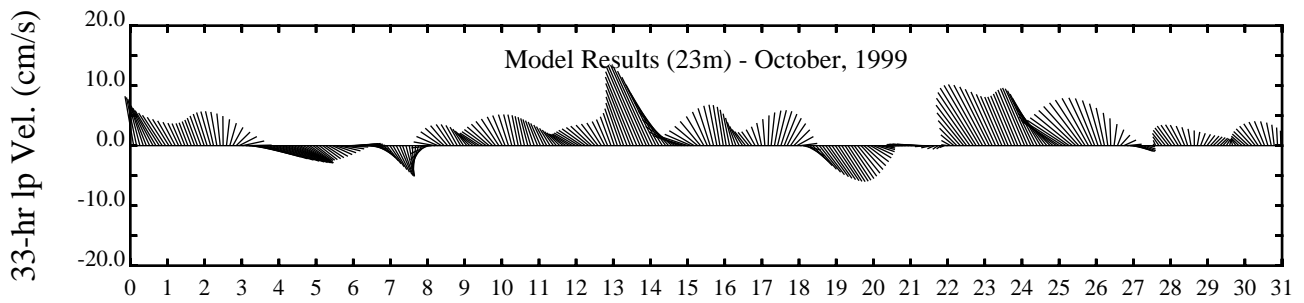
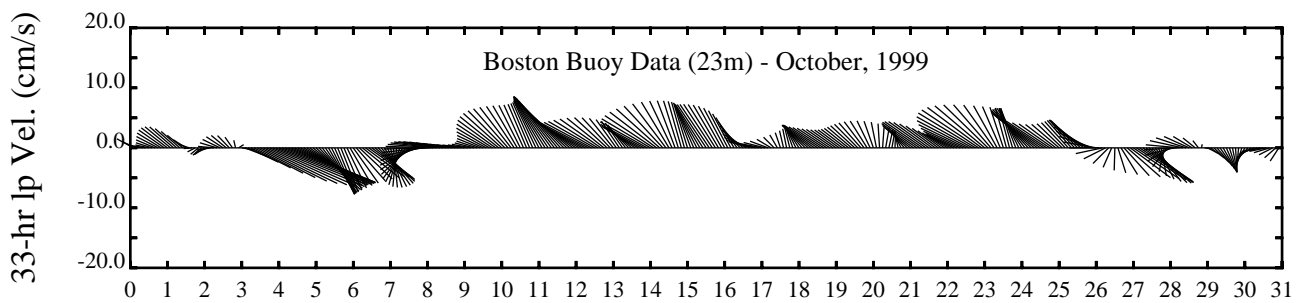
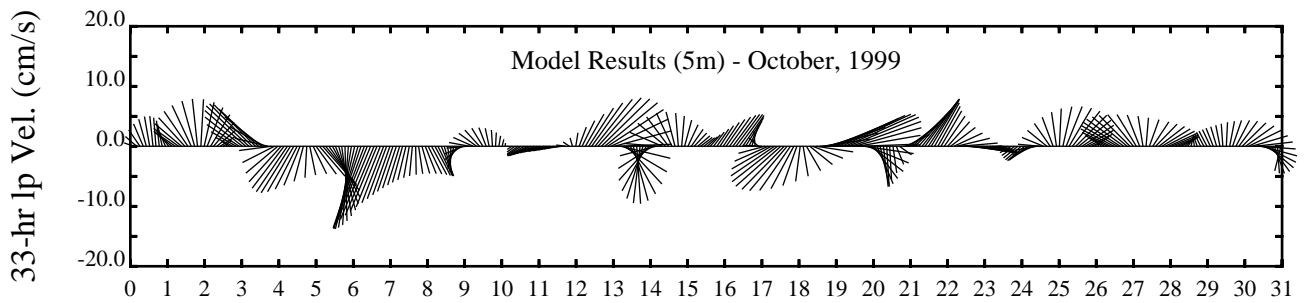
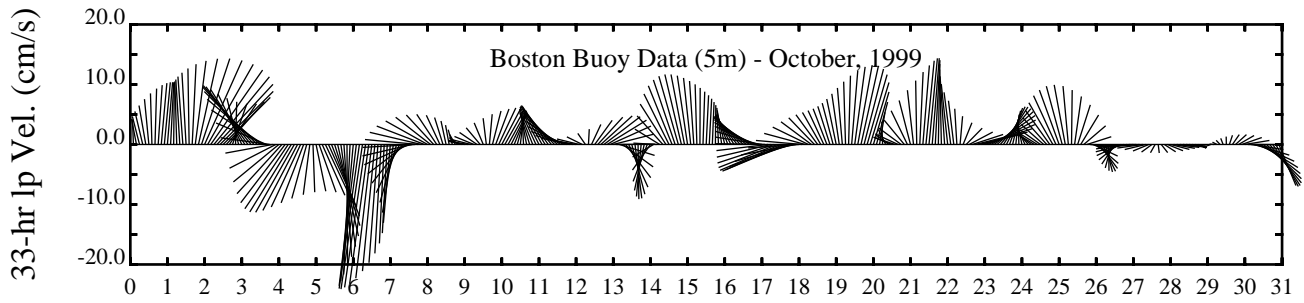
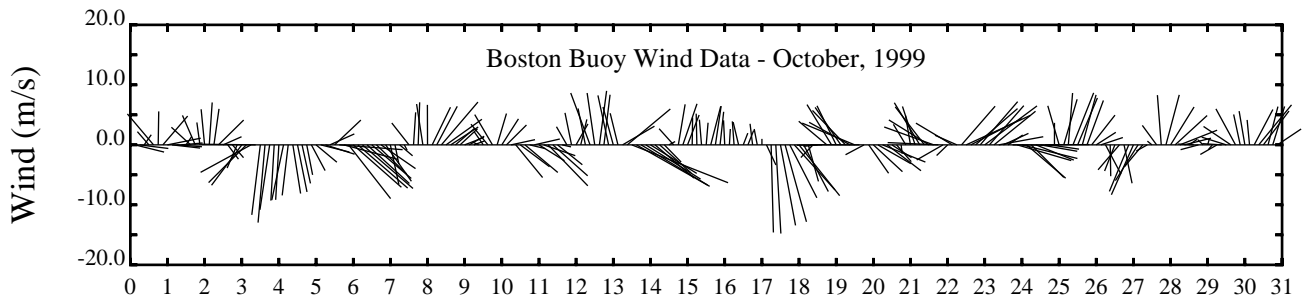
Day



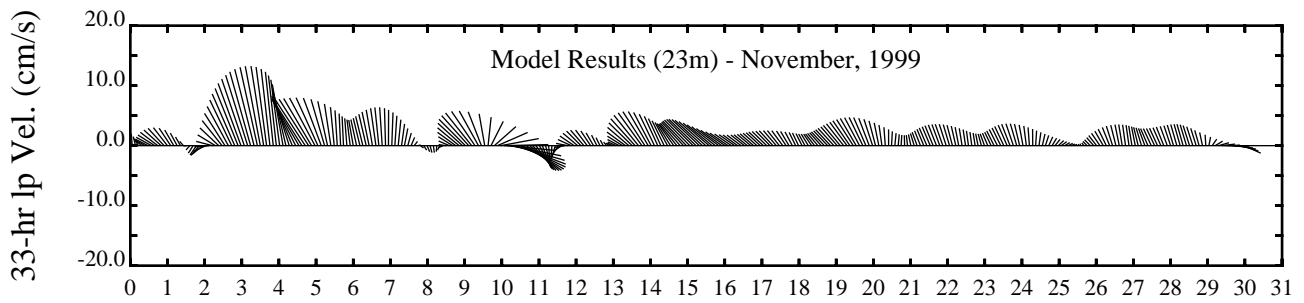
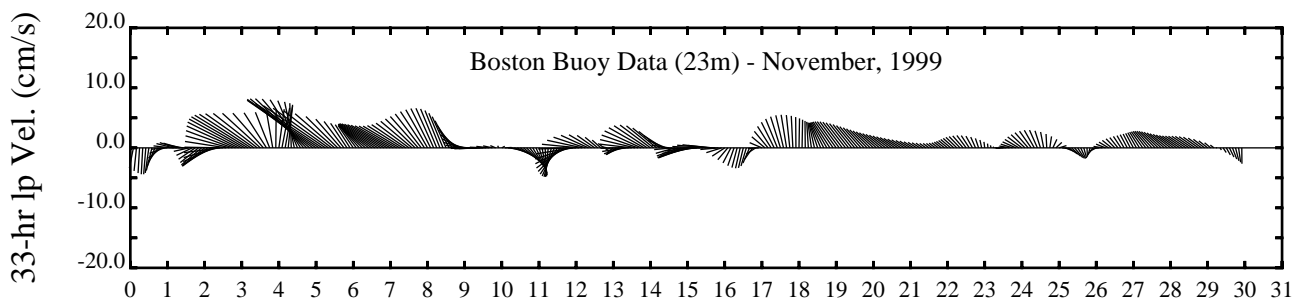
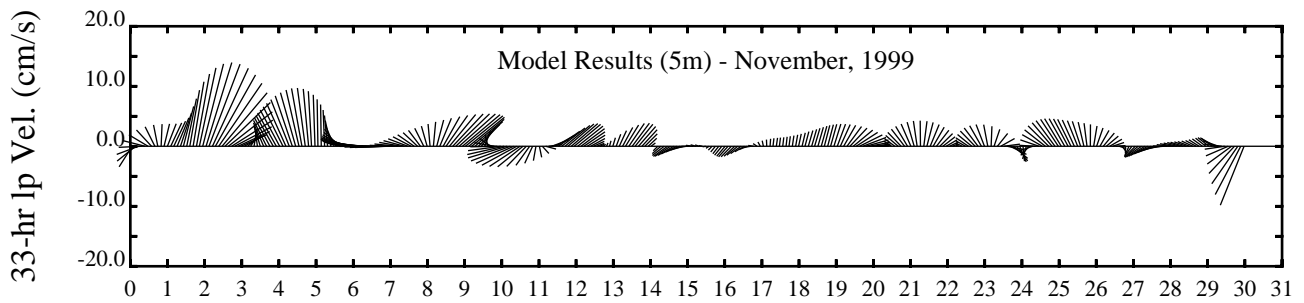
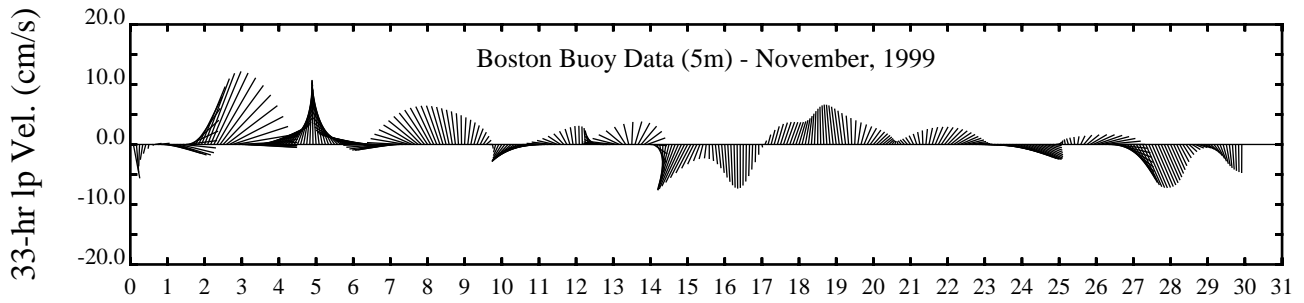
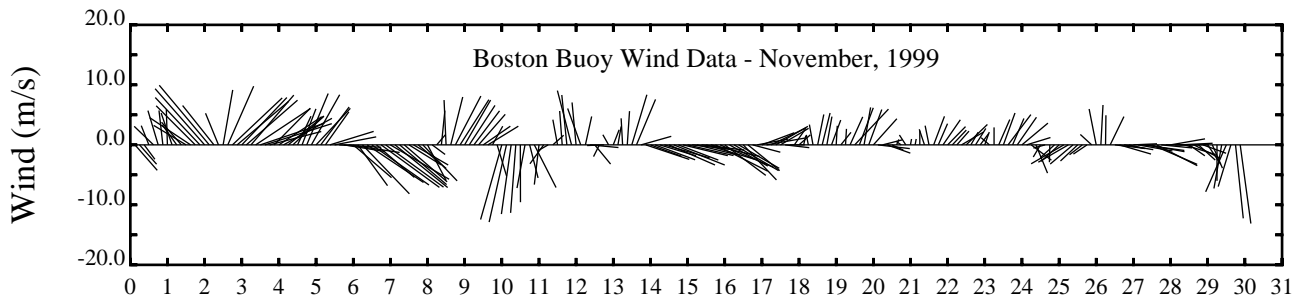
Day



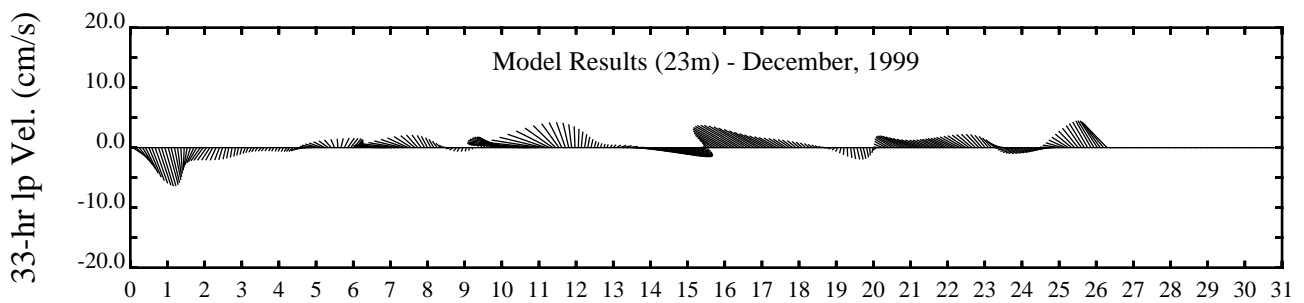
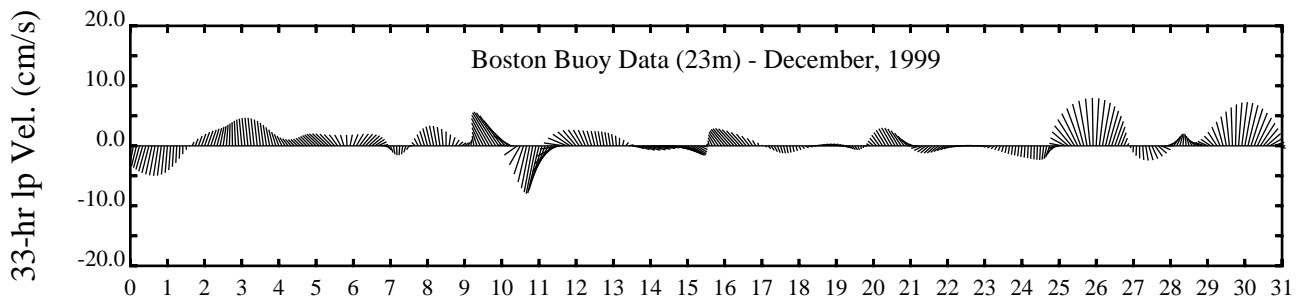
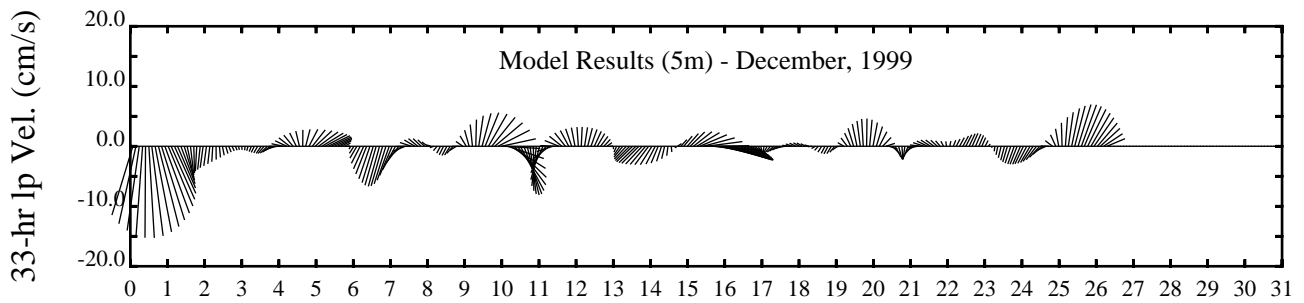
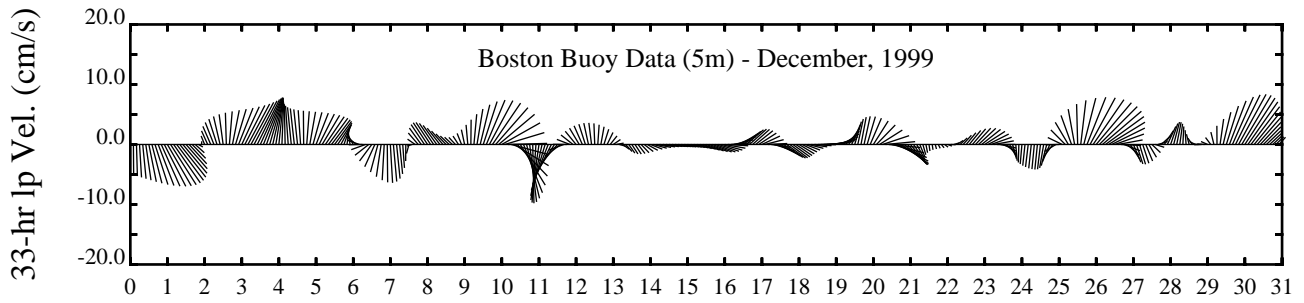
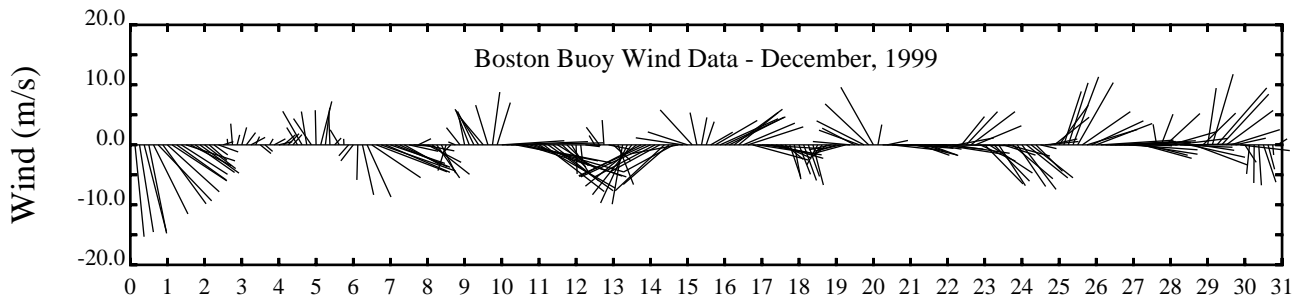
Day



Day

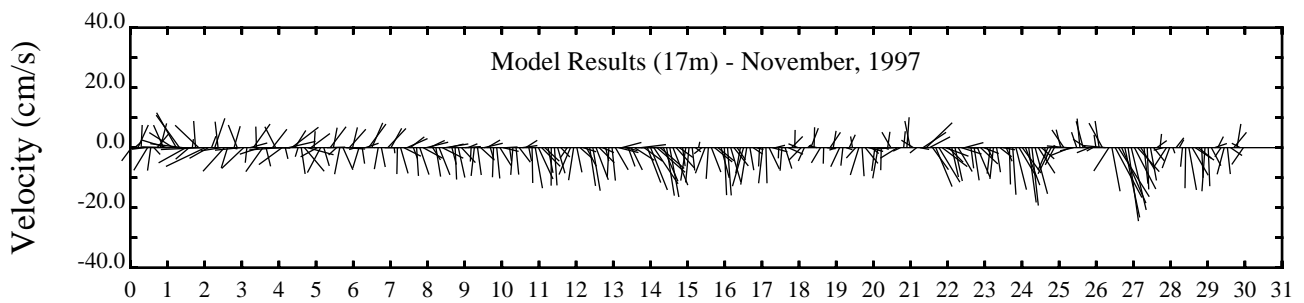
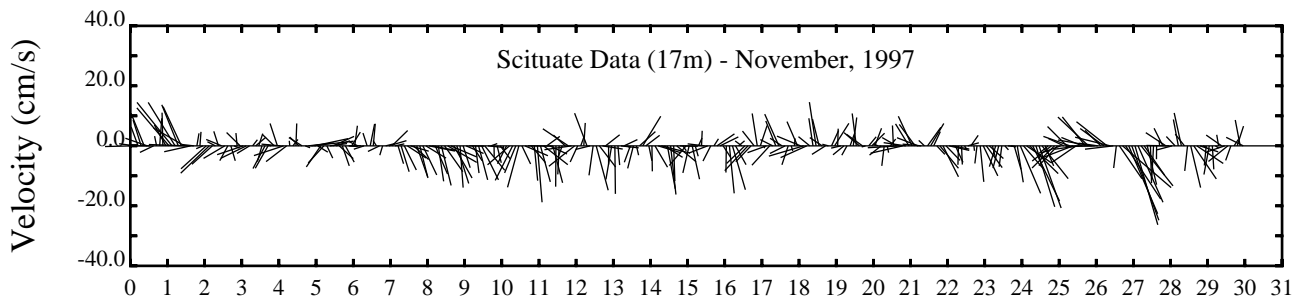
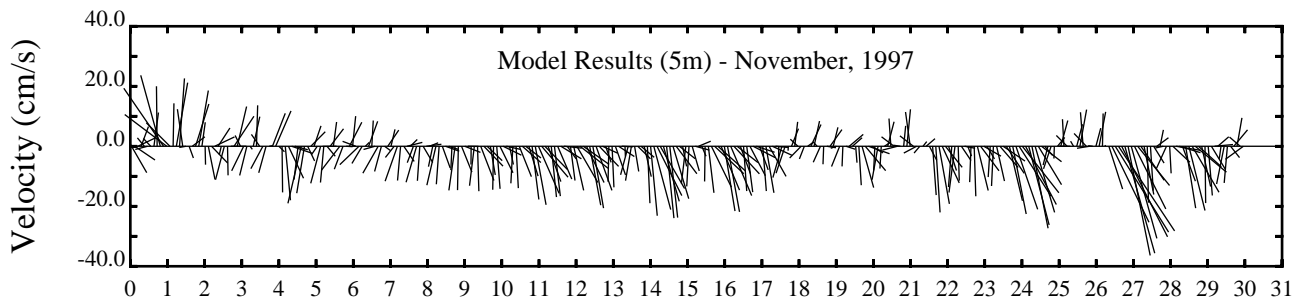
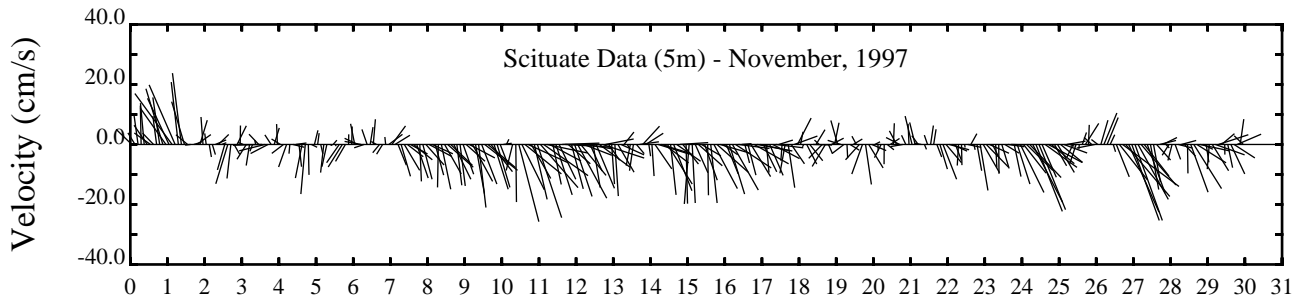
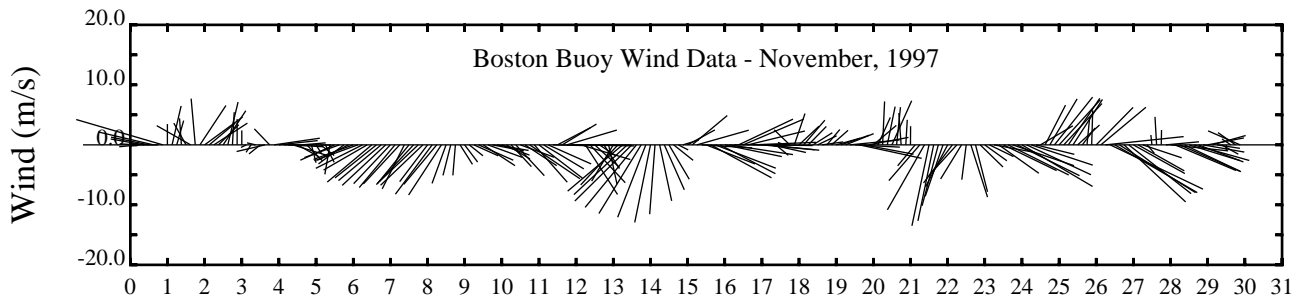


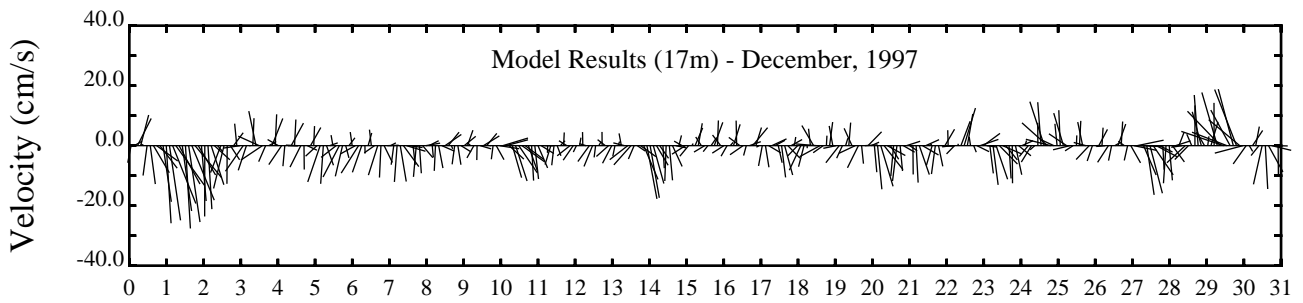
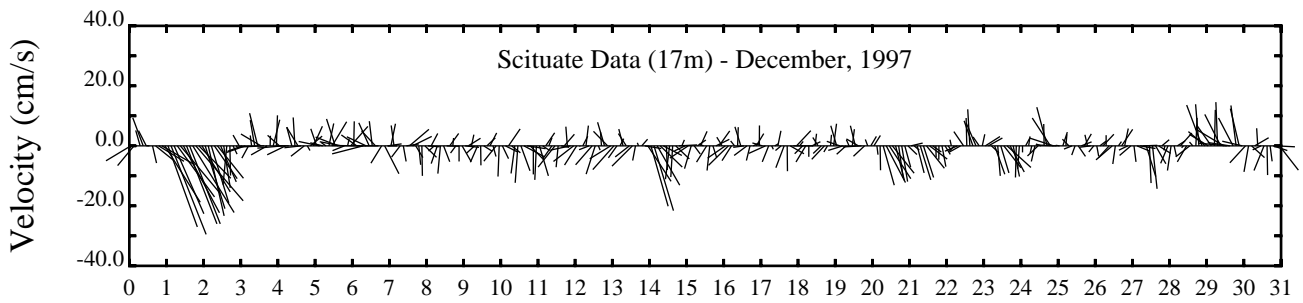
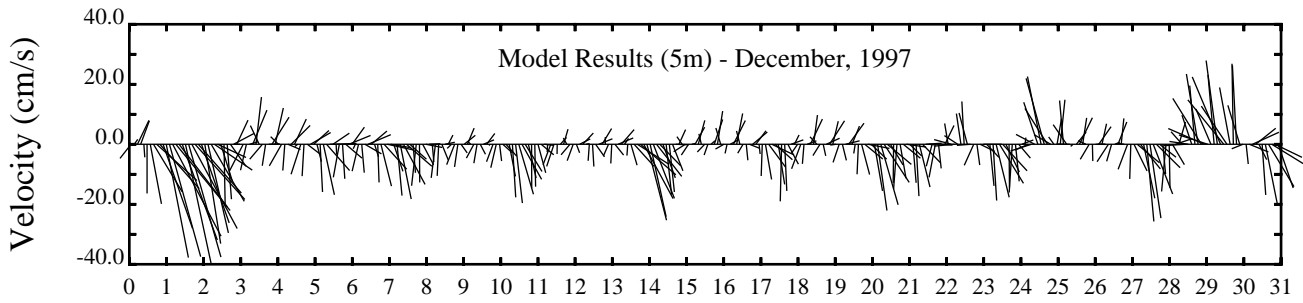
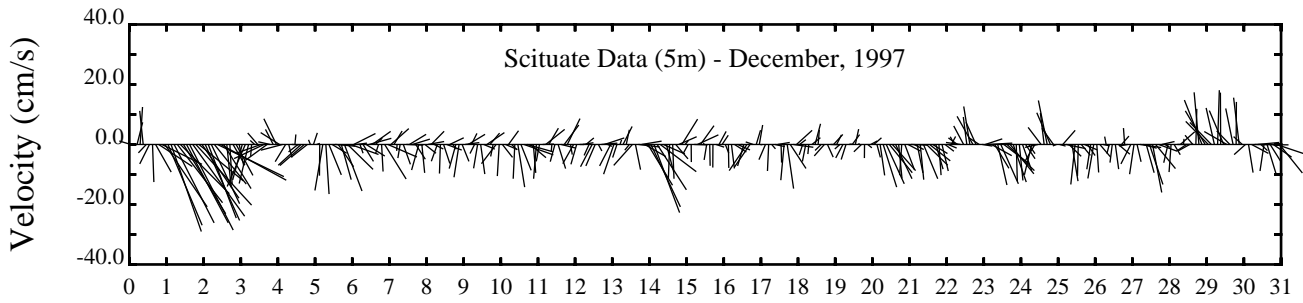
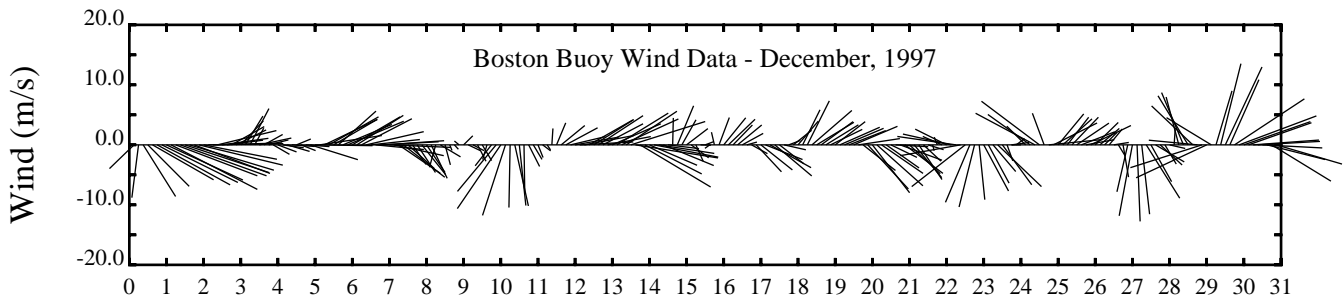
Day



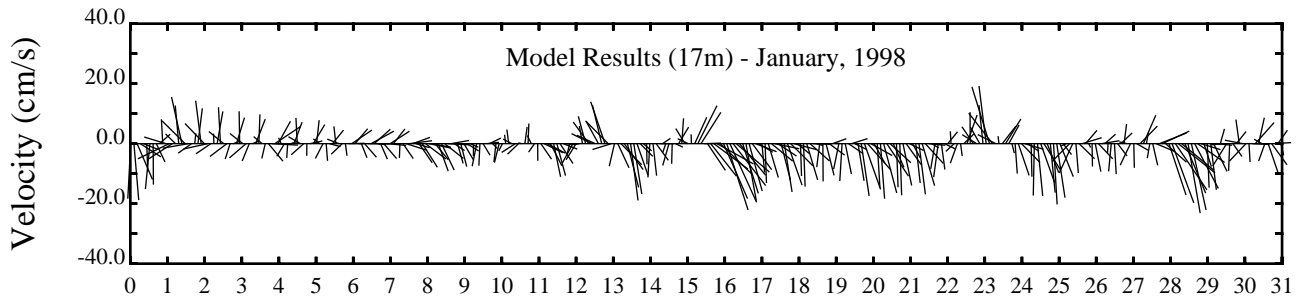
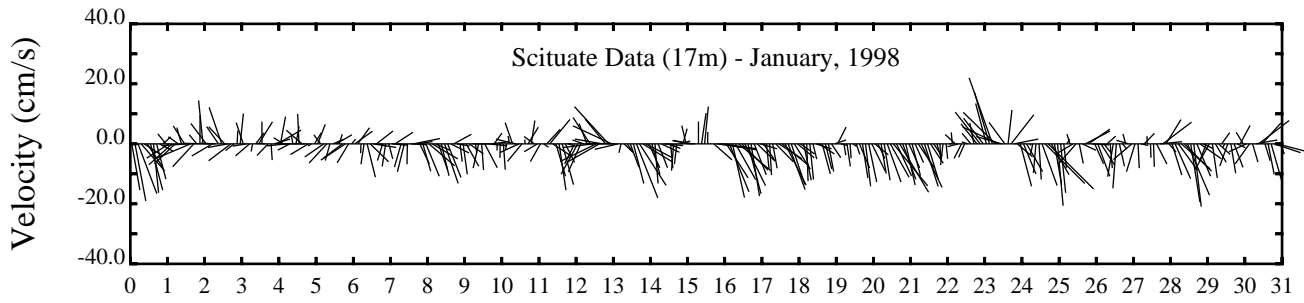
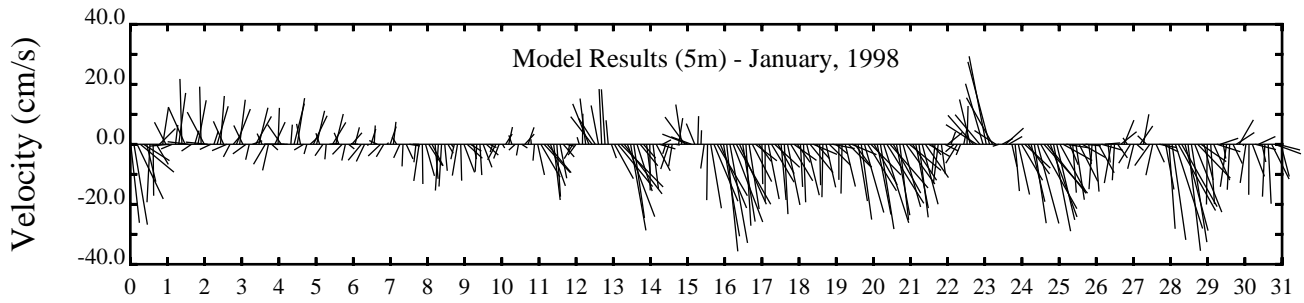
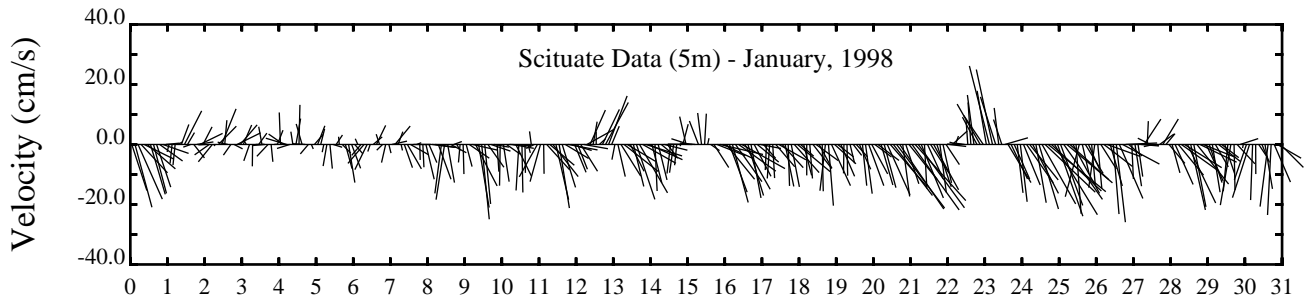
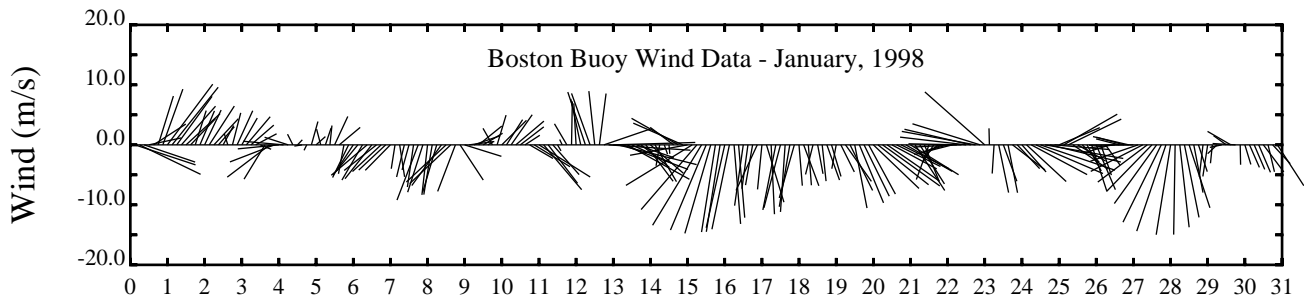
Day

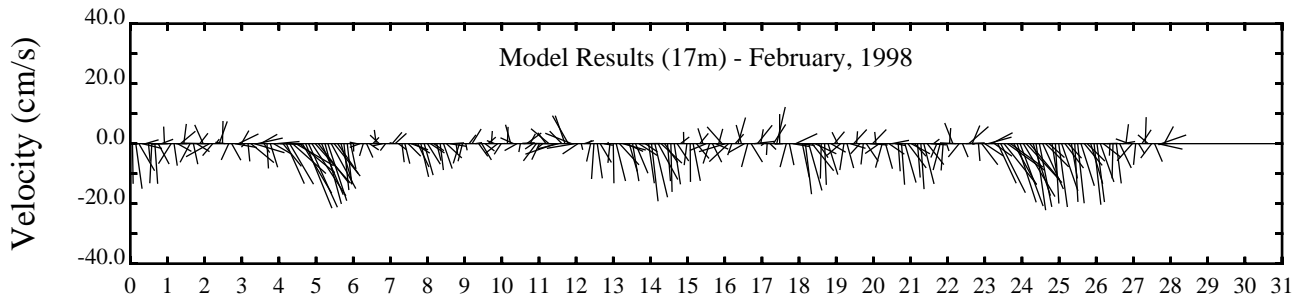
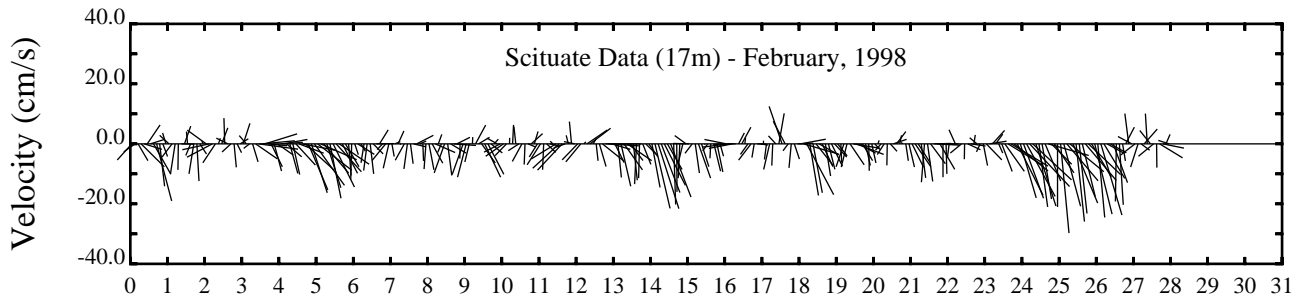
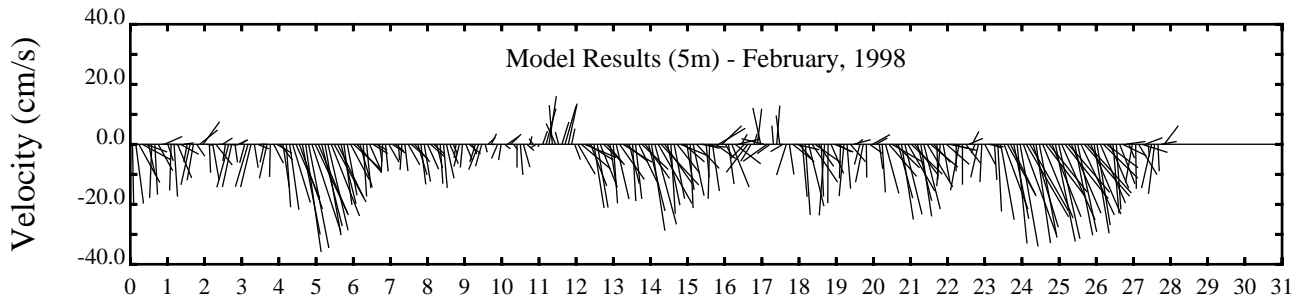
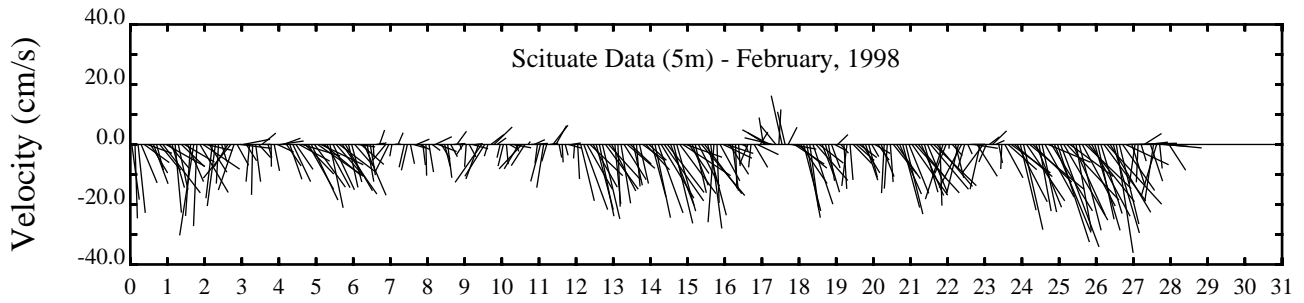
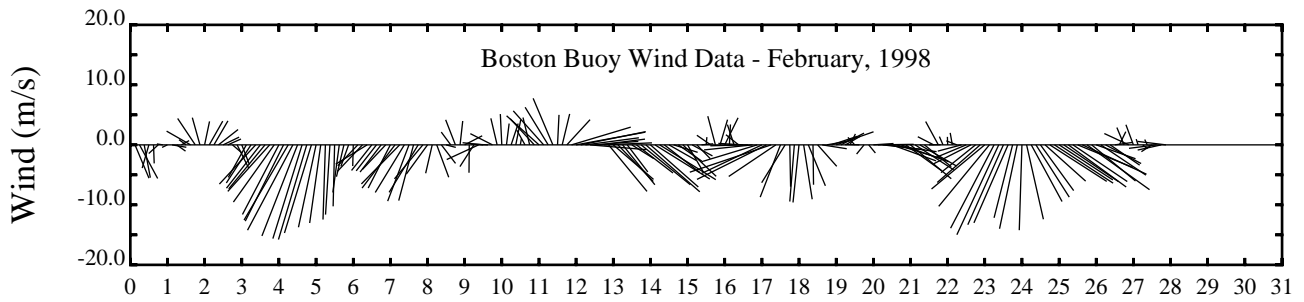
APPENDIX D
Monthly Current Meter Model versus
Data Comparisons at the Sciuate Buoy

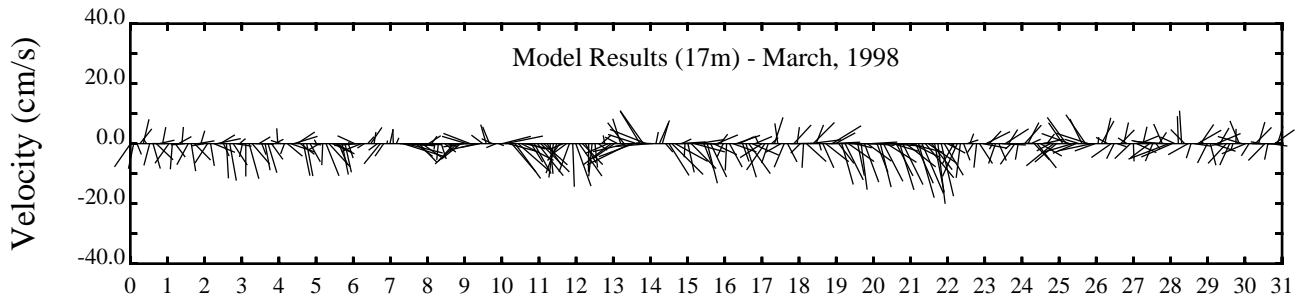
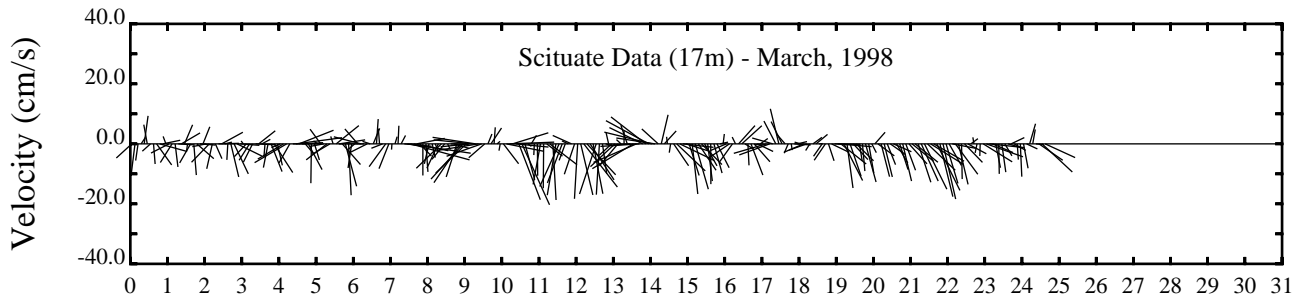
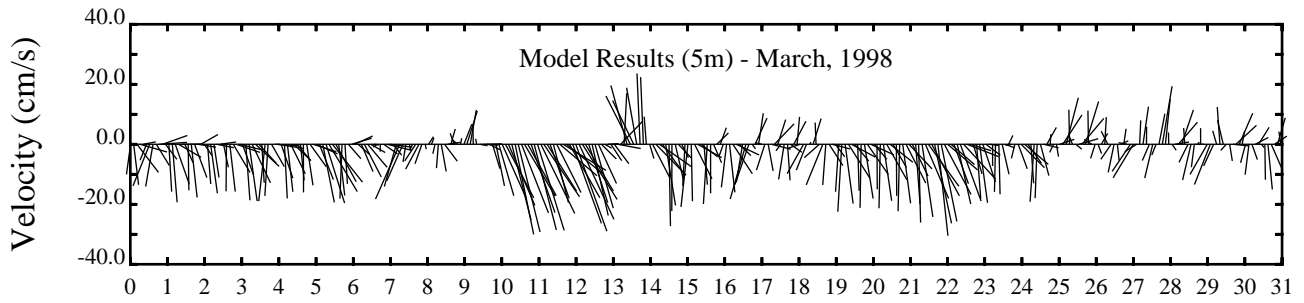
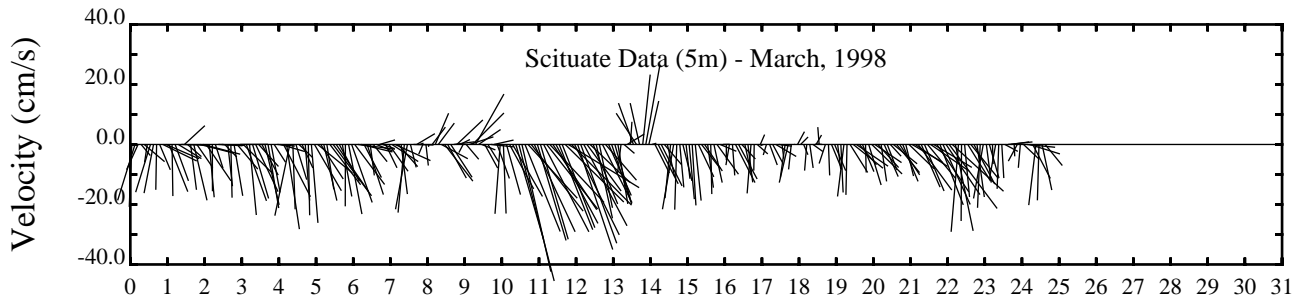
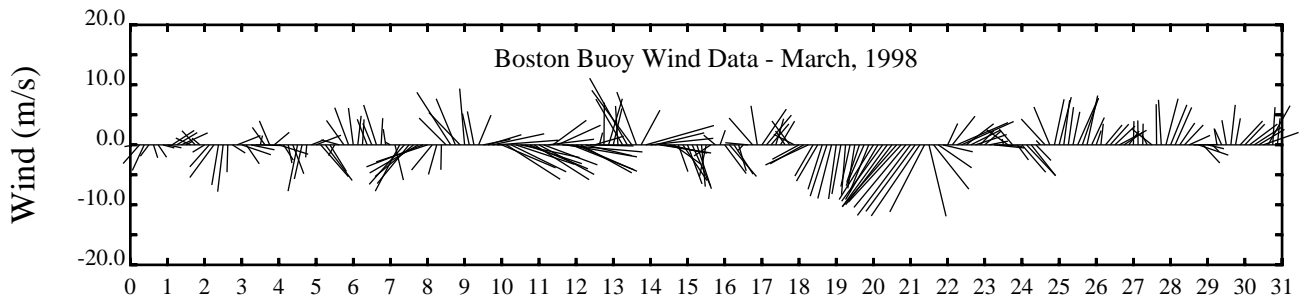




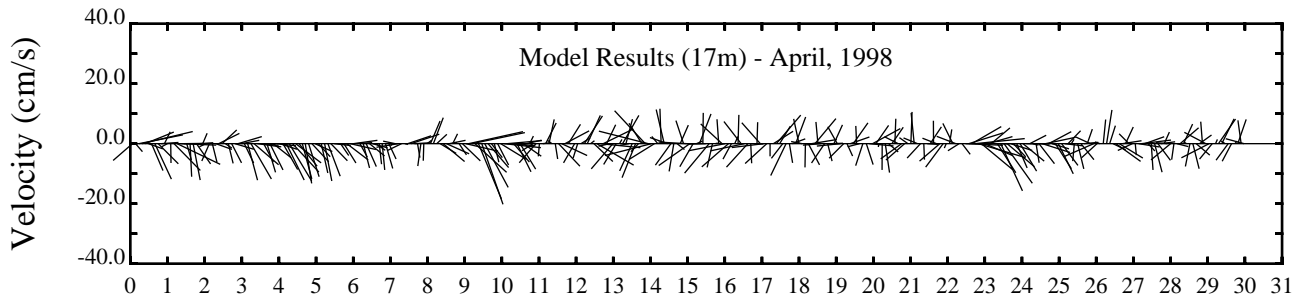
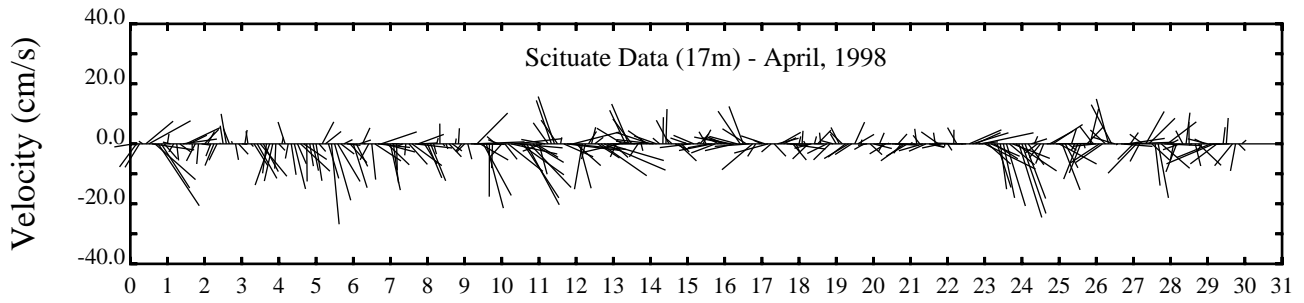
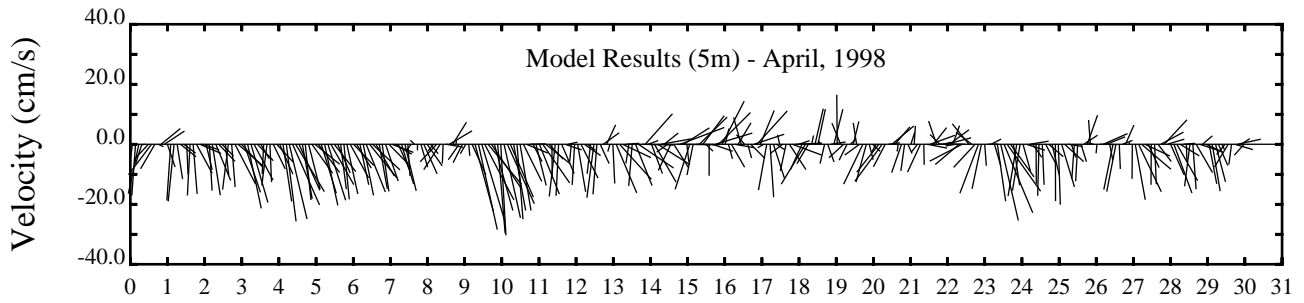
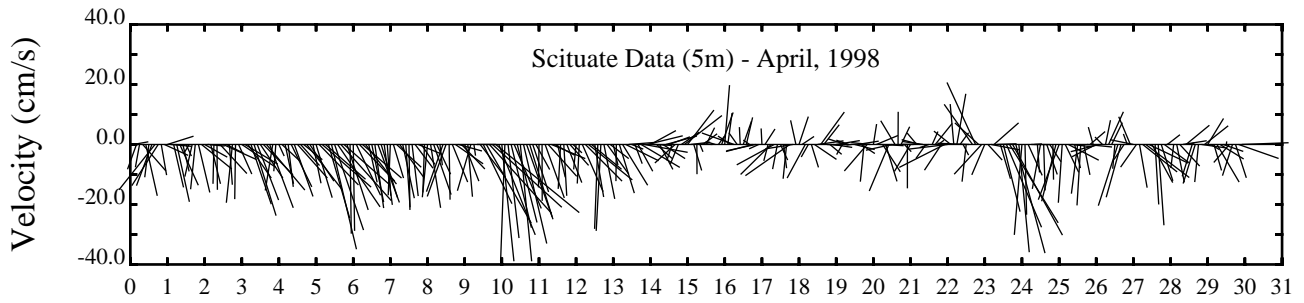
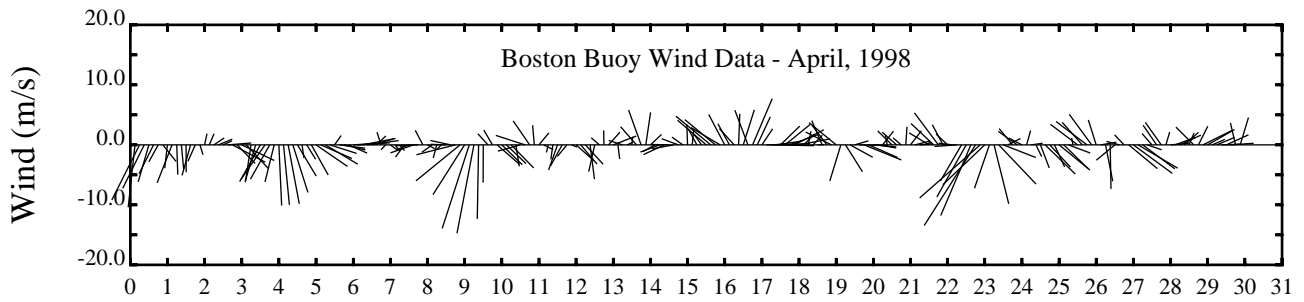
Day



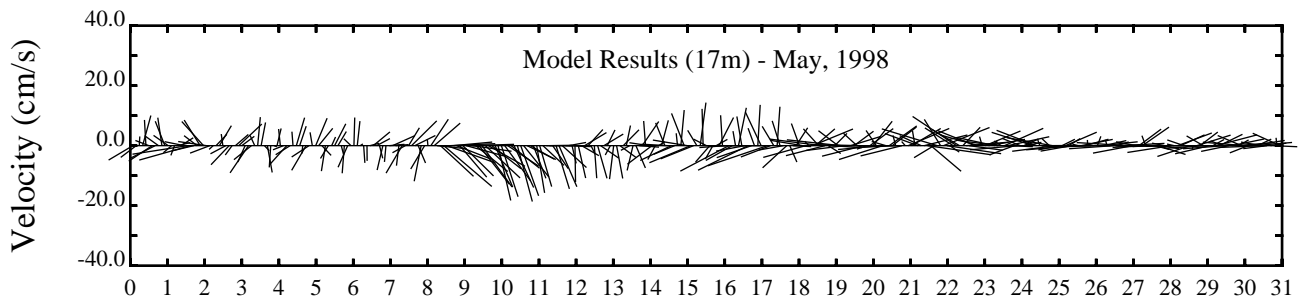
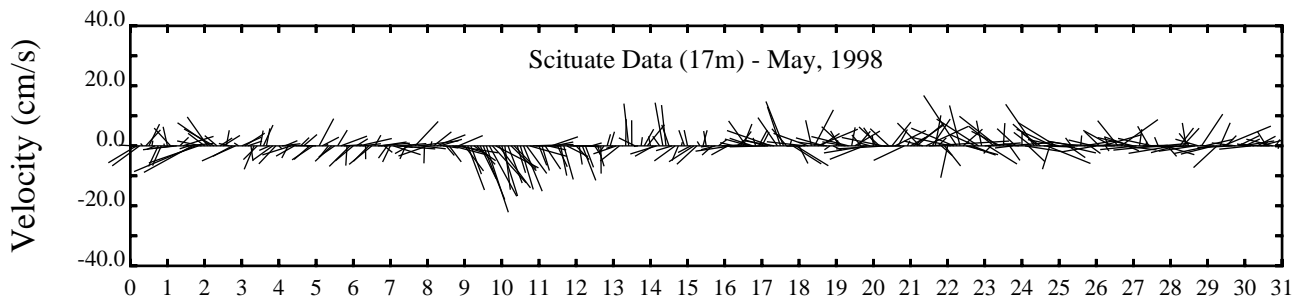
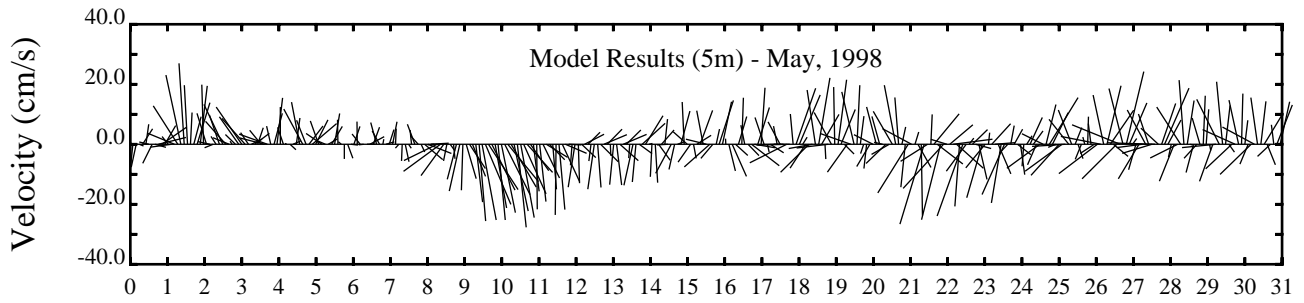
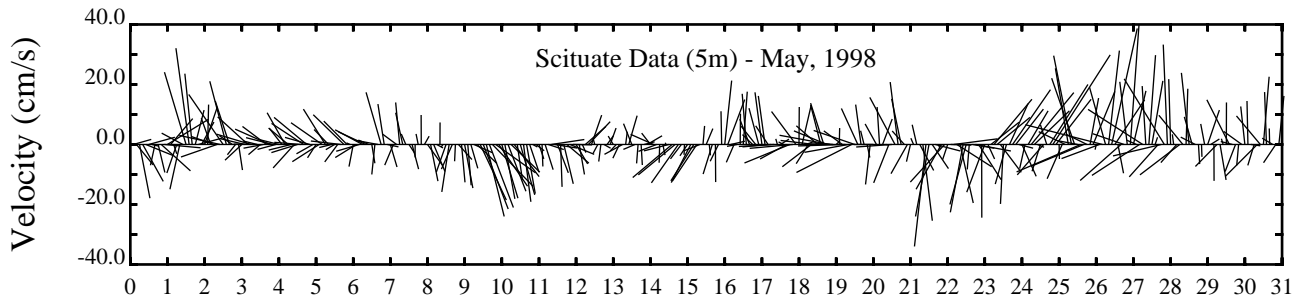
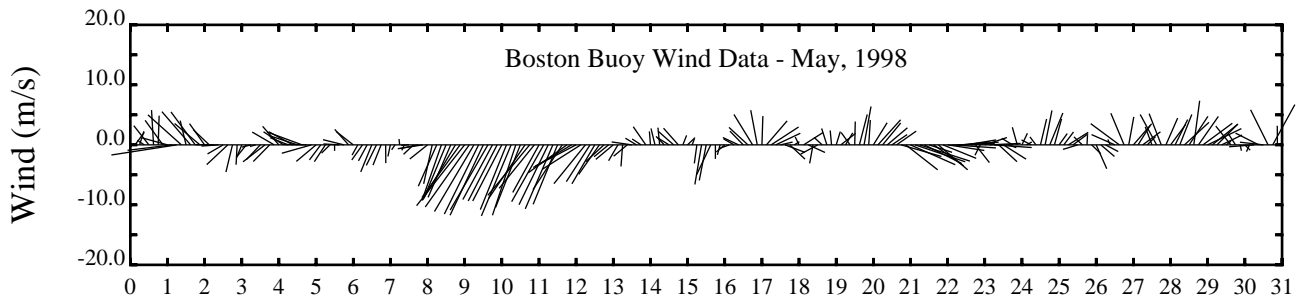




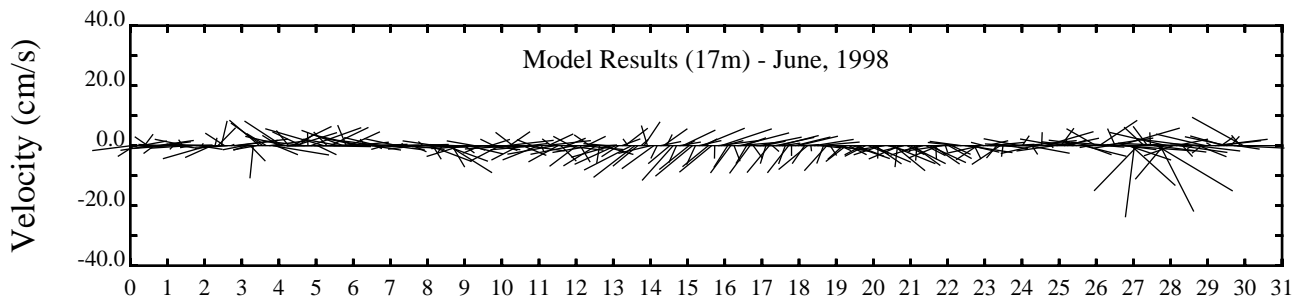
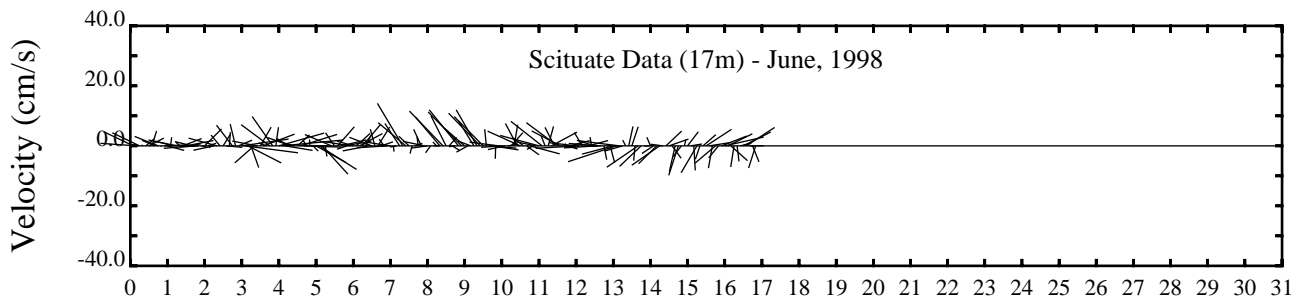
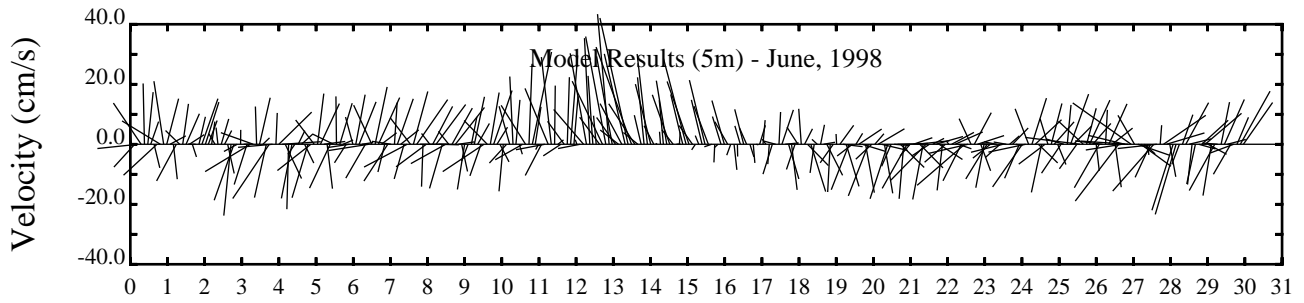
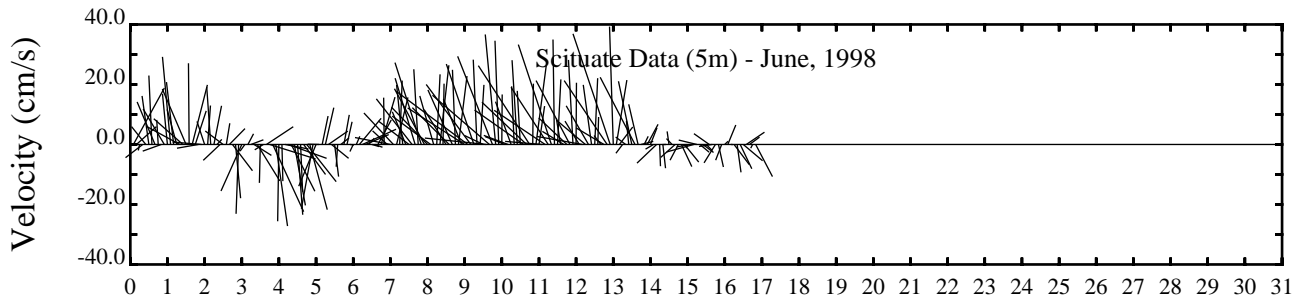
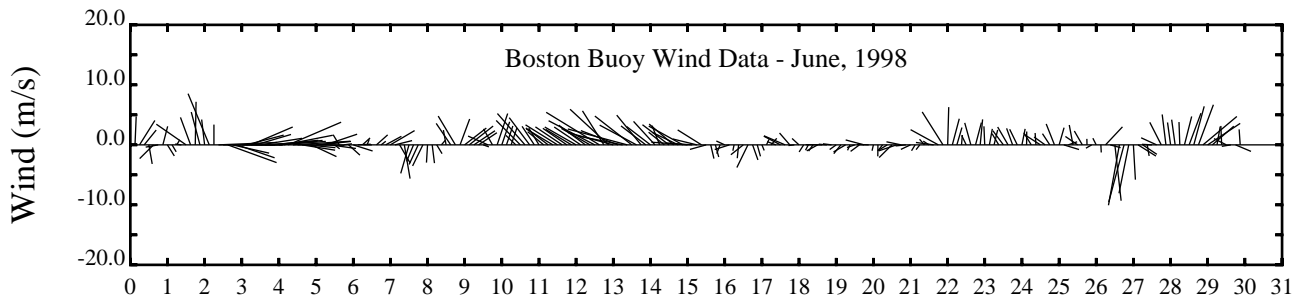
Day

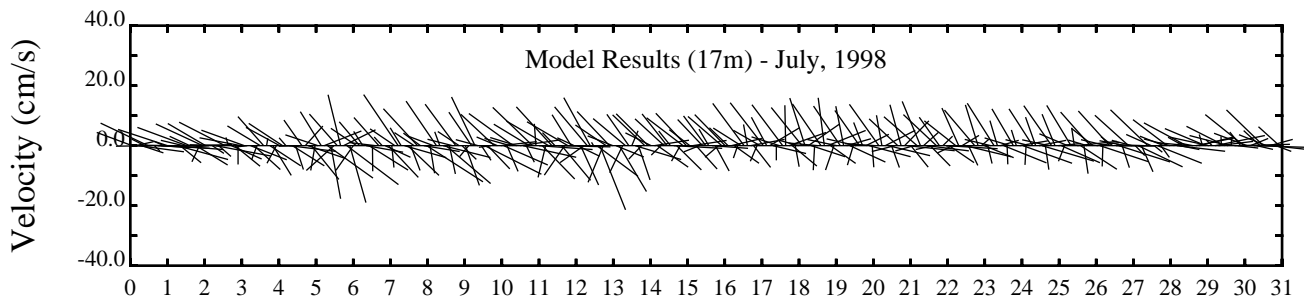
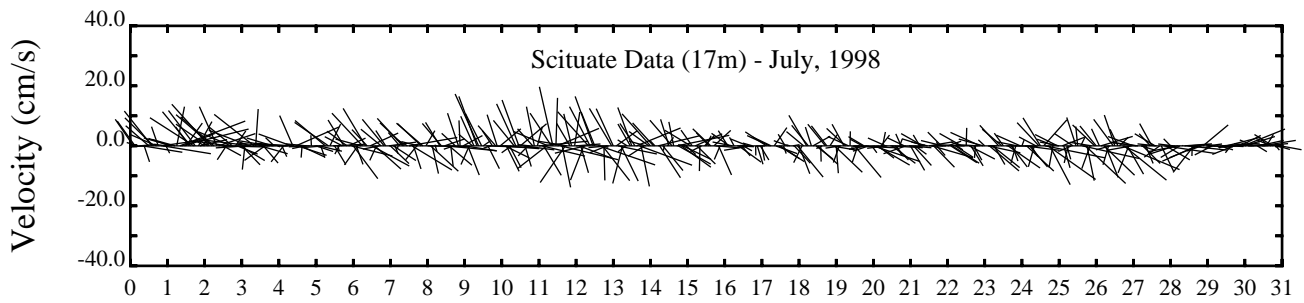
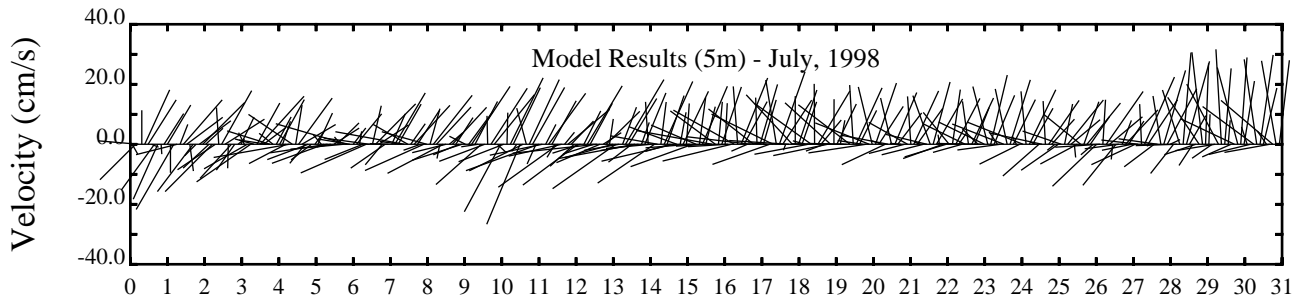
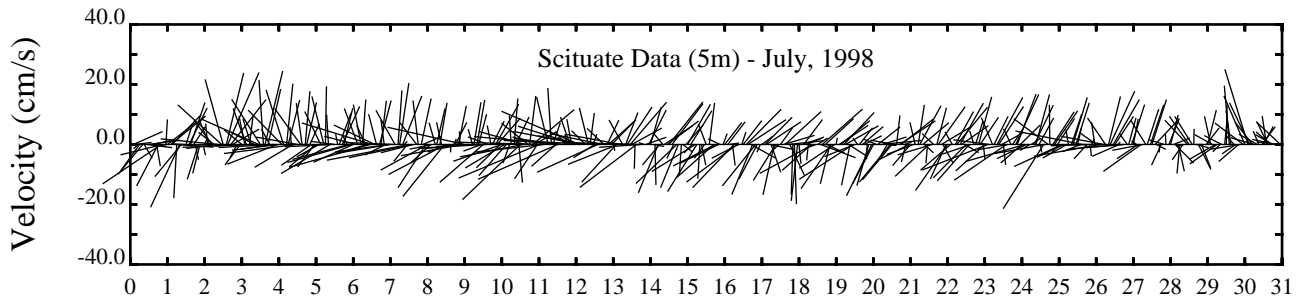
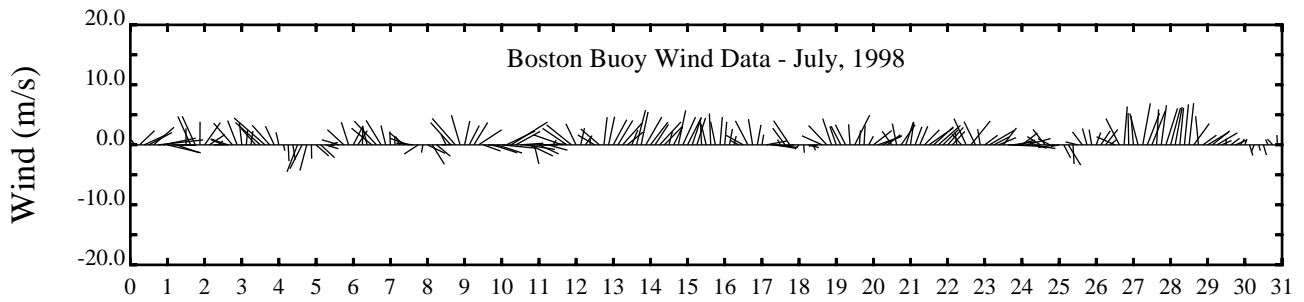


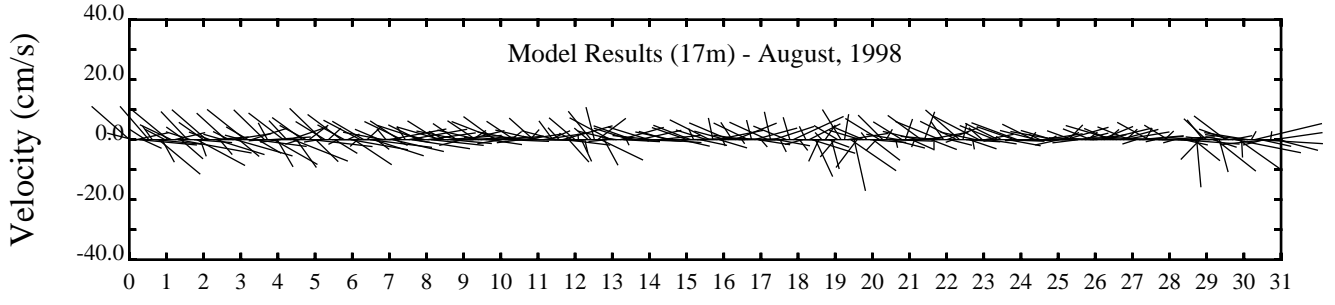
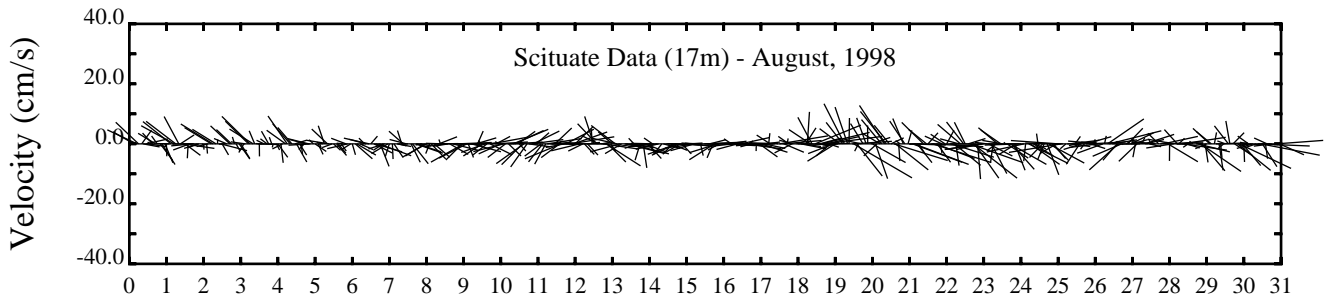
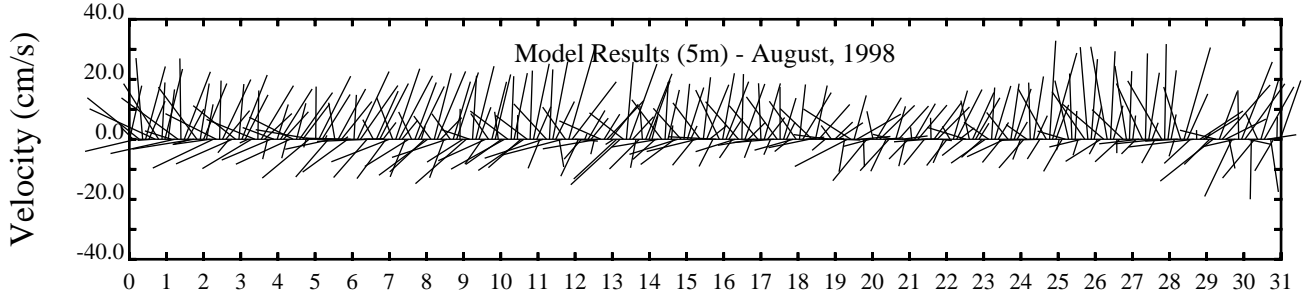
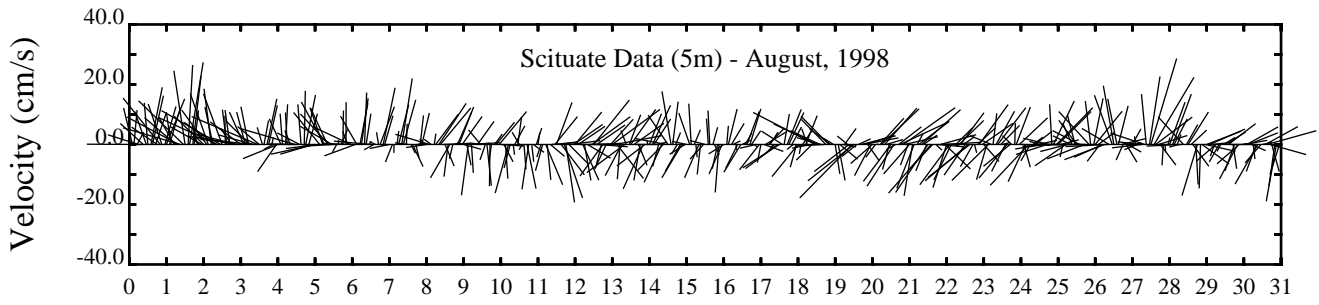
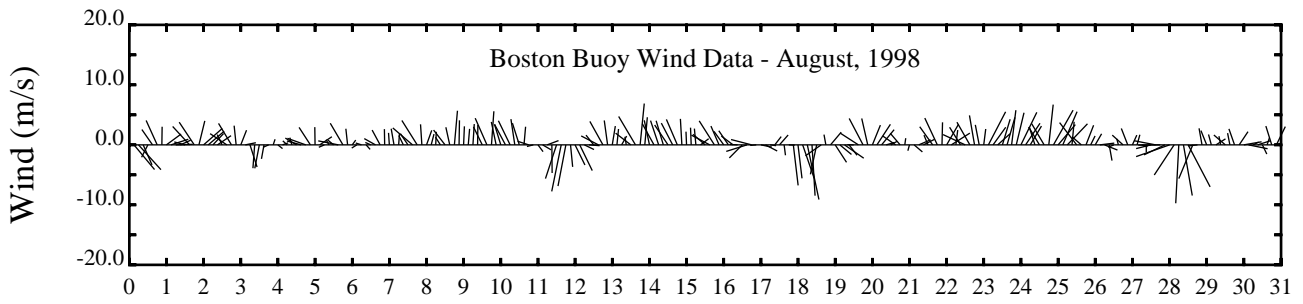
Day



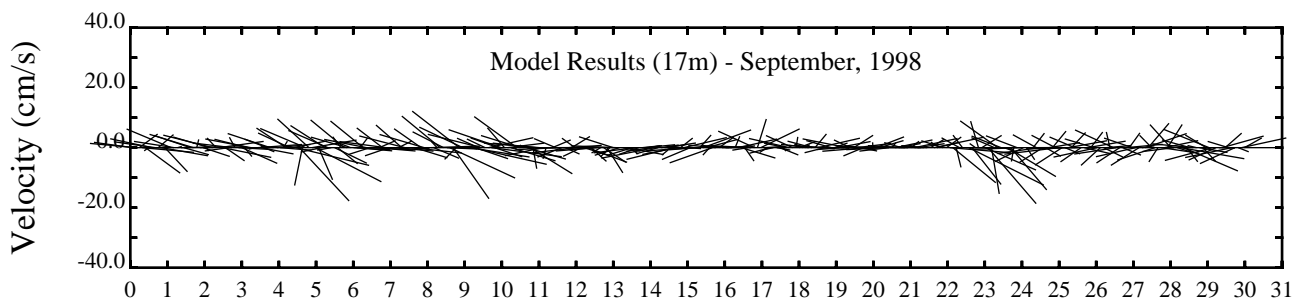
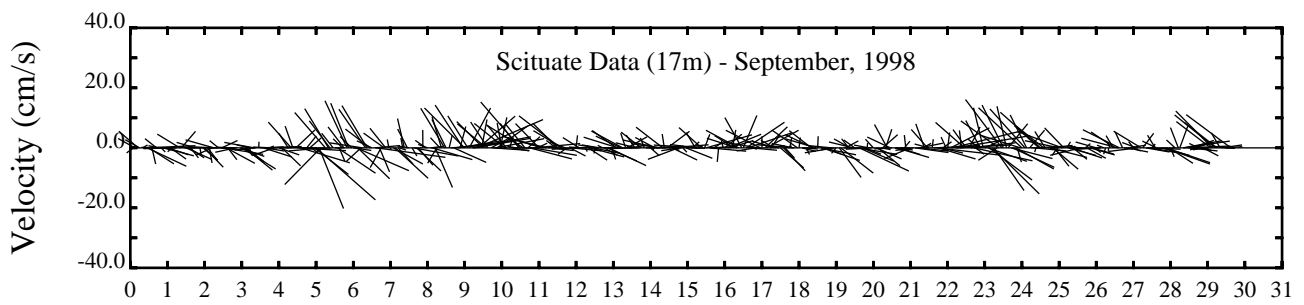
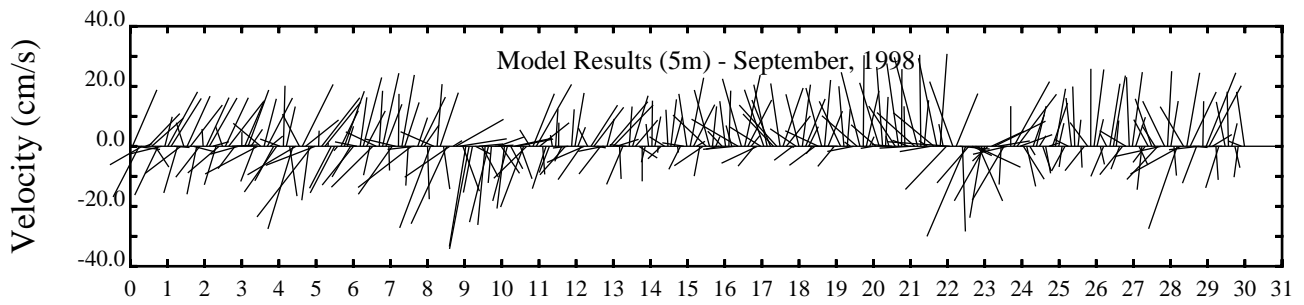
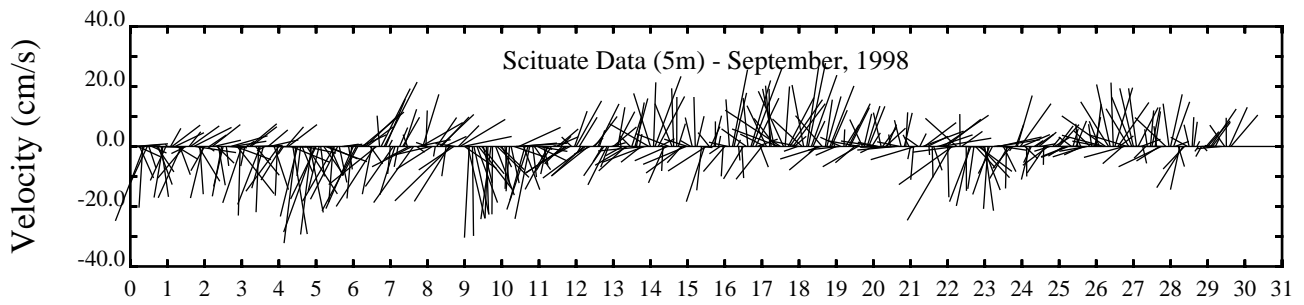
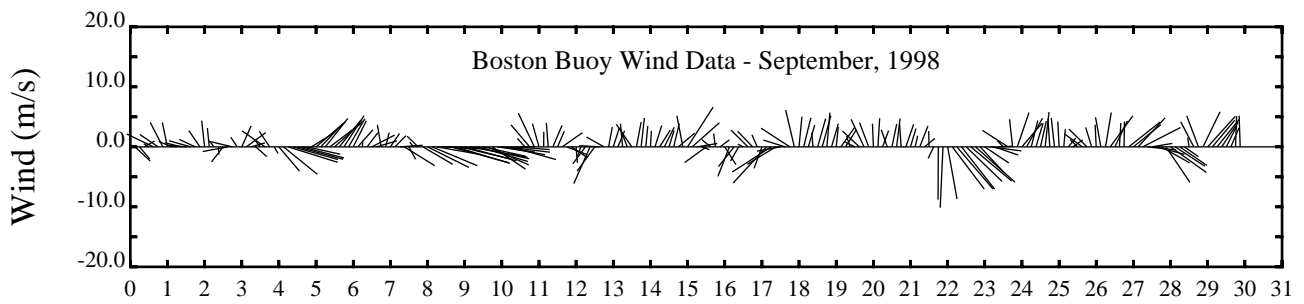
Day

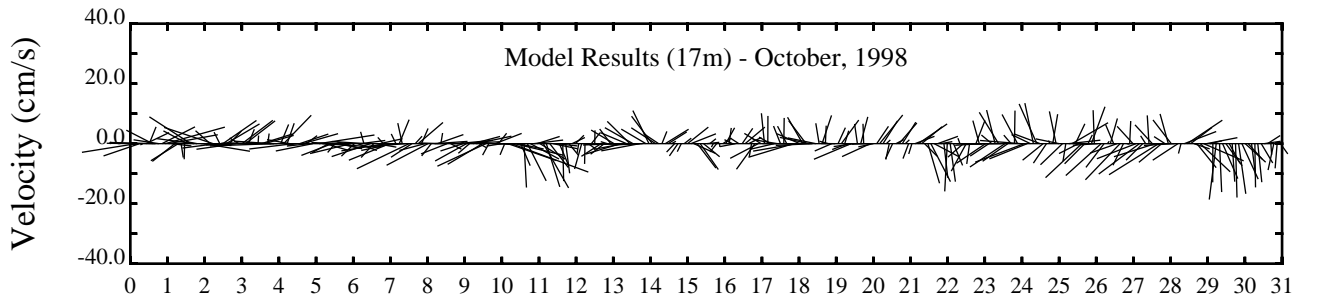
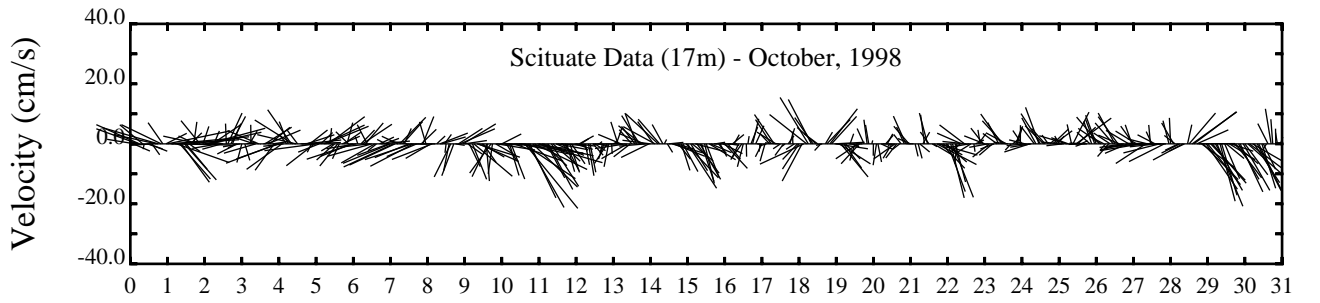
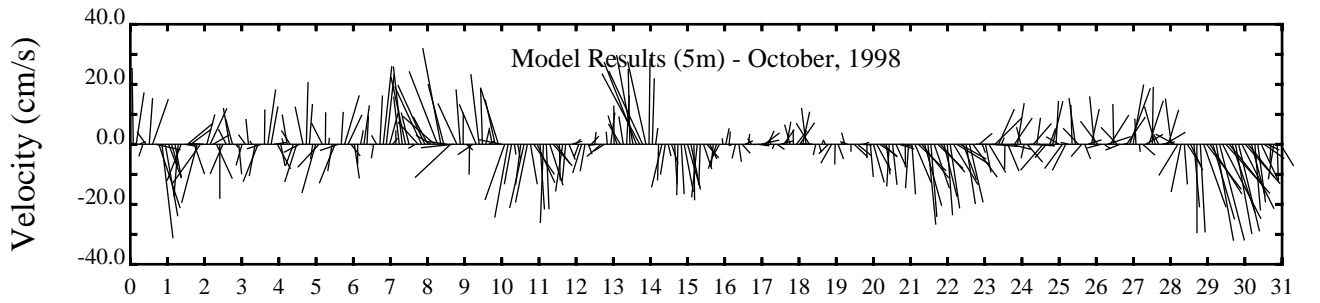
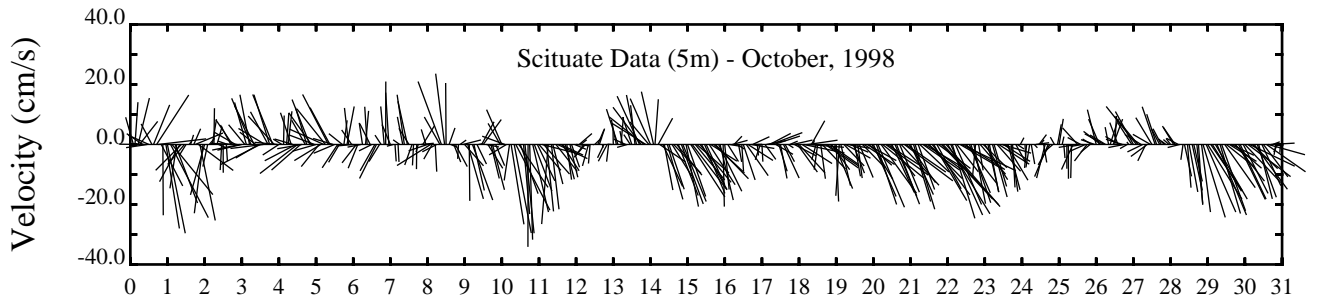
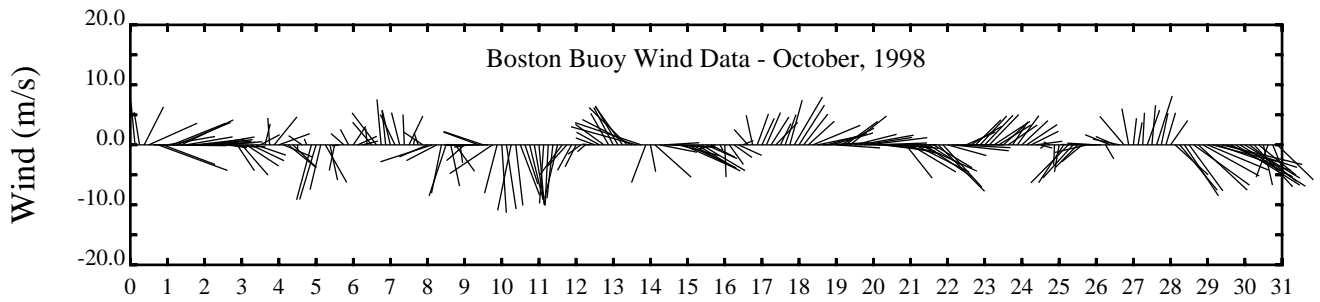


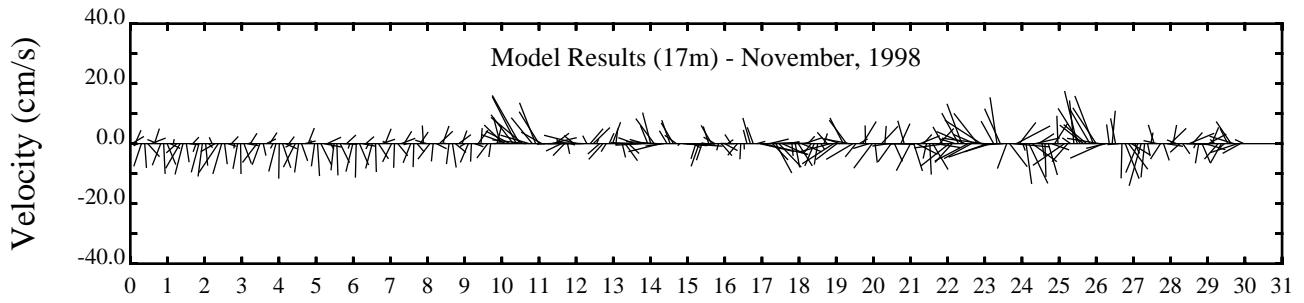
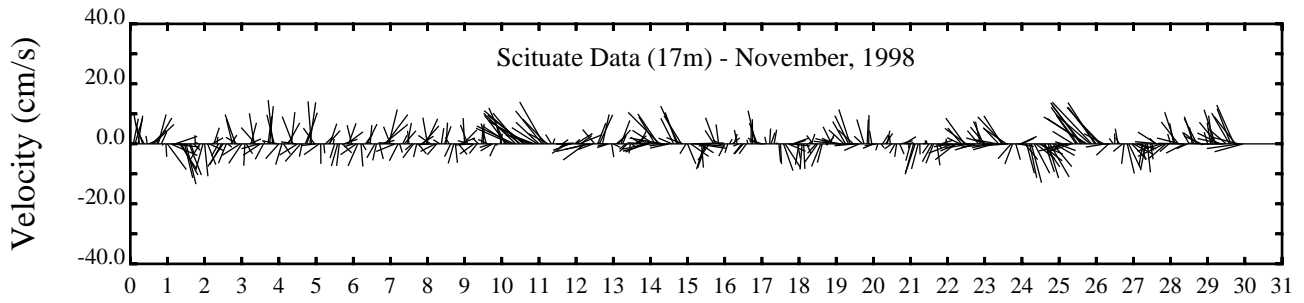
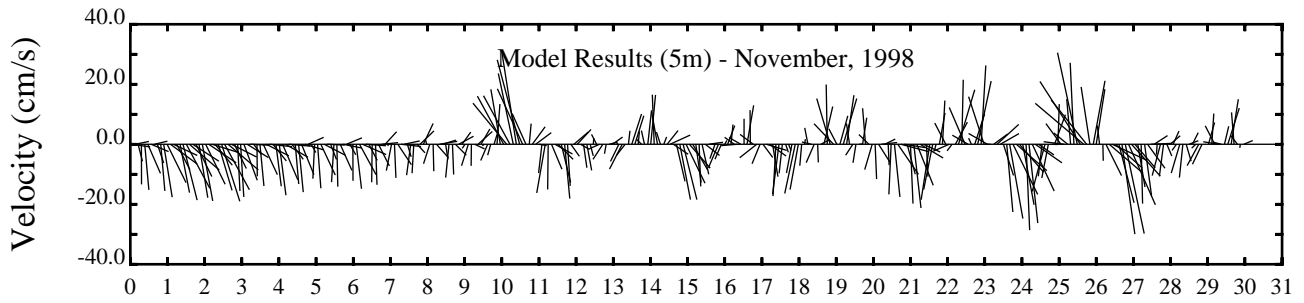
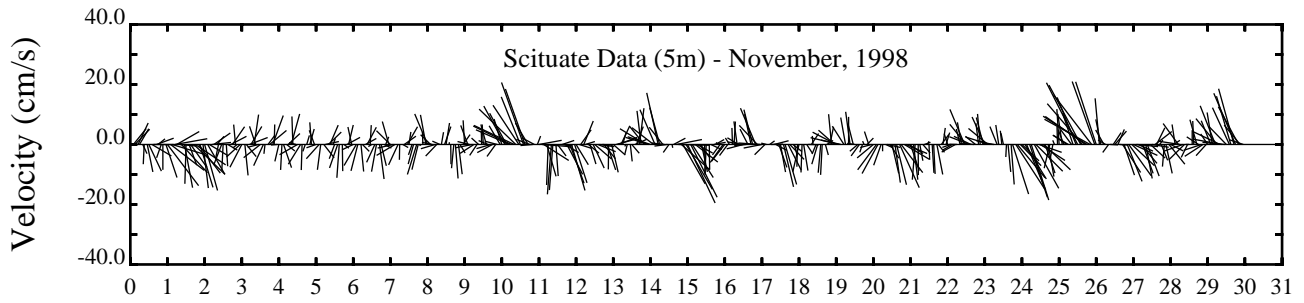
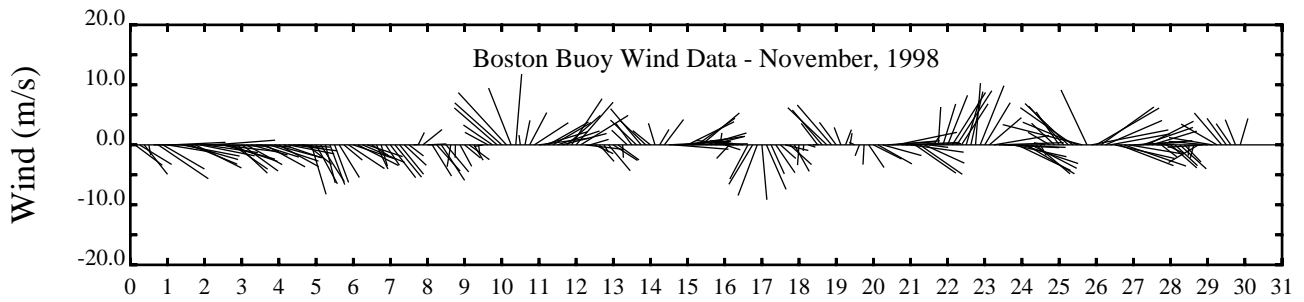


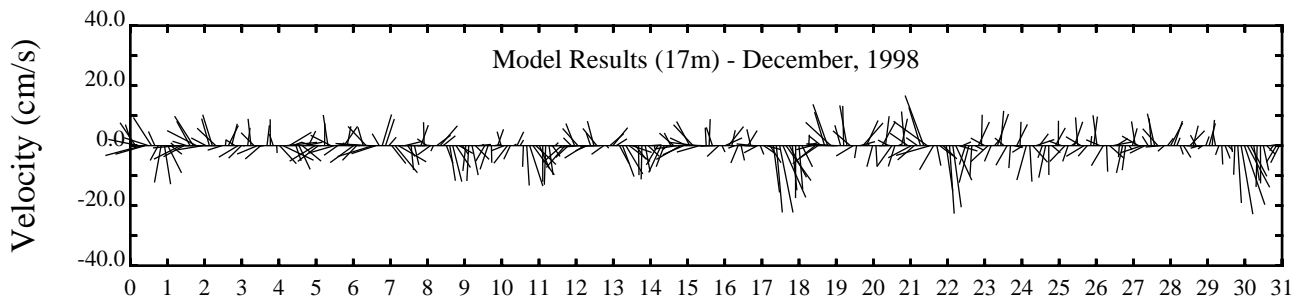
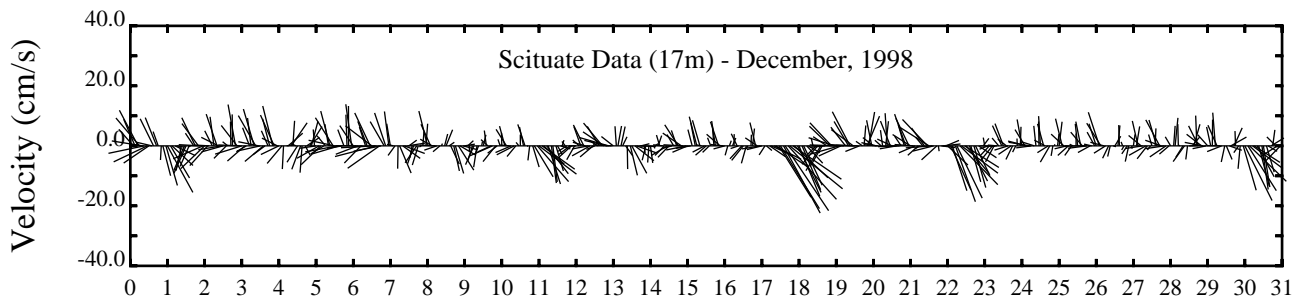
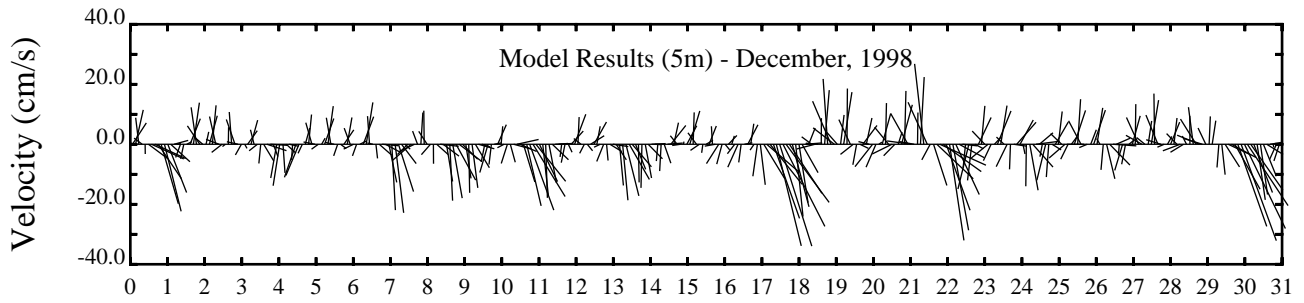
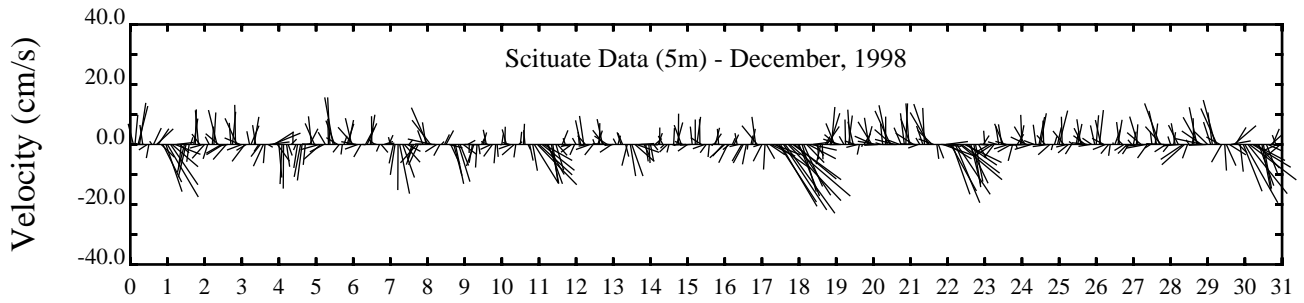
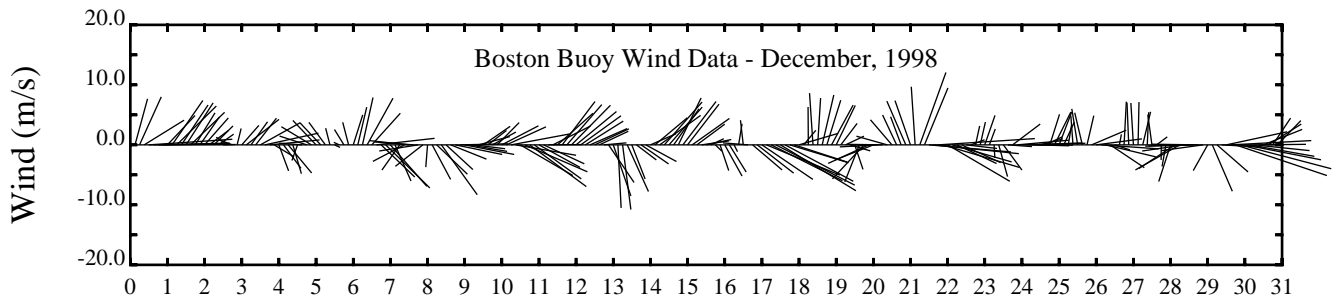


Day

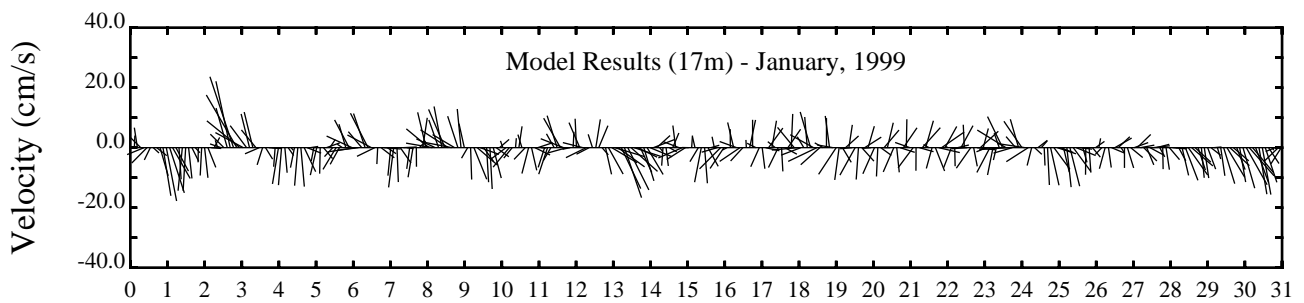
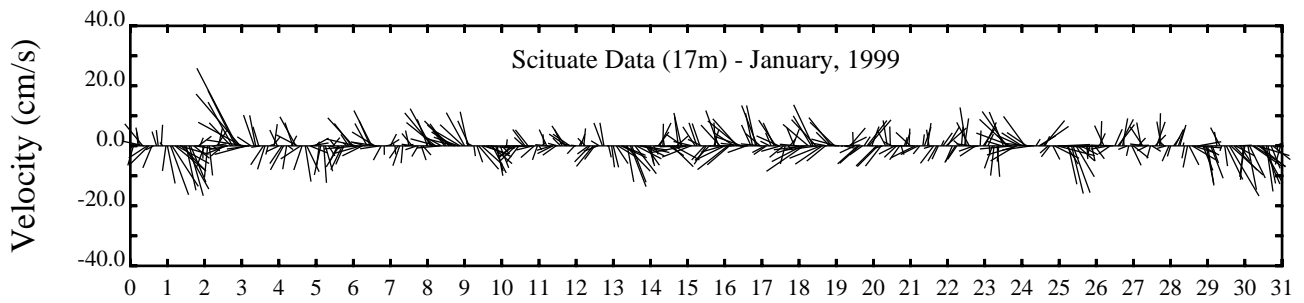
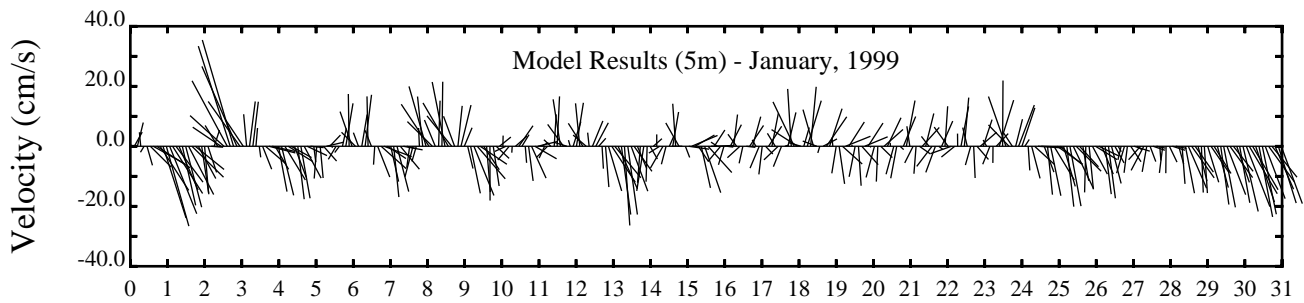
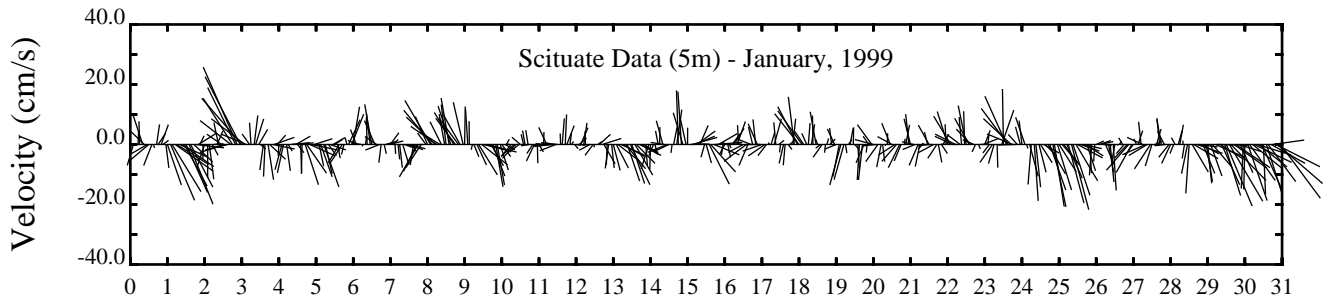
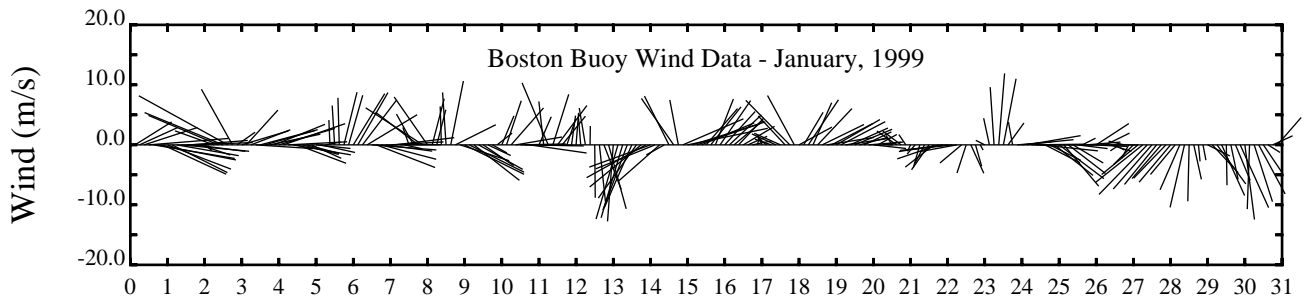




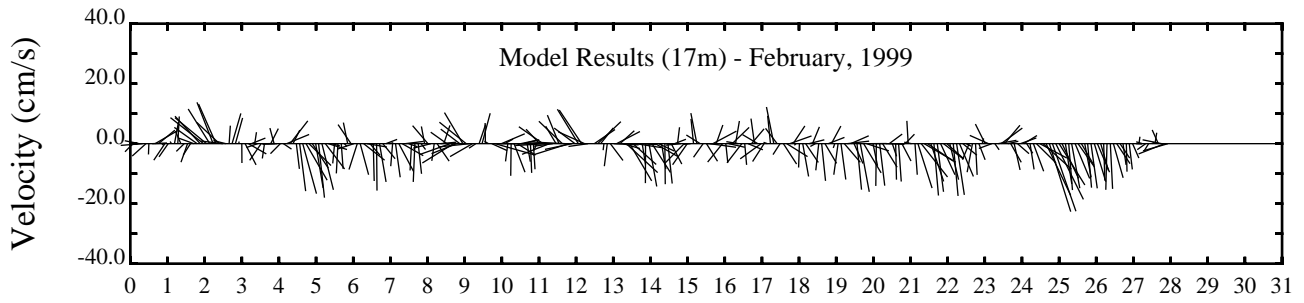
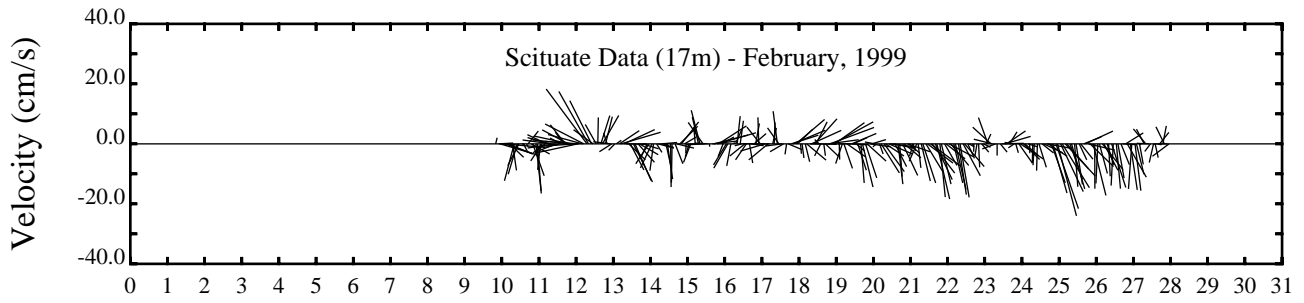
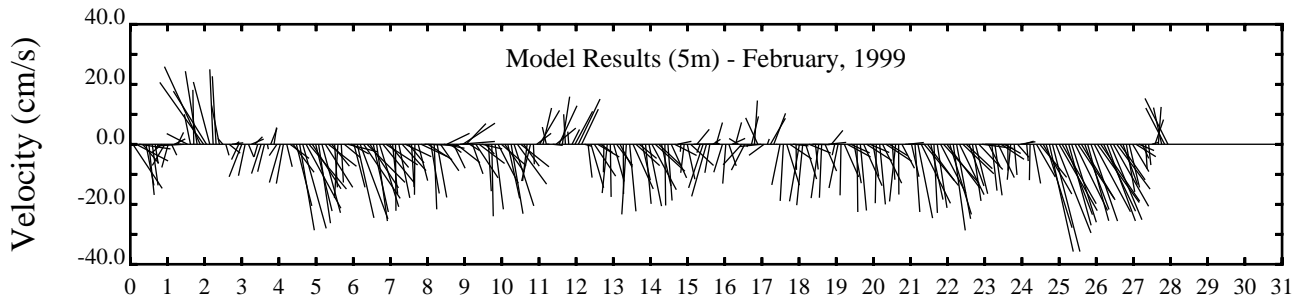
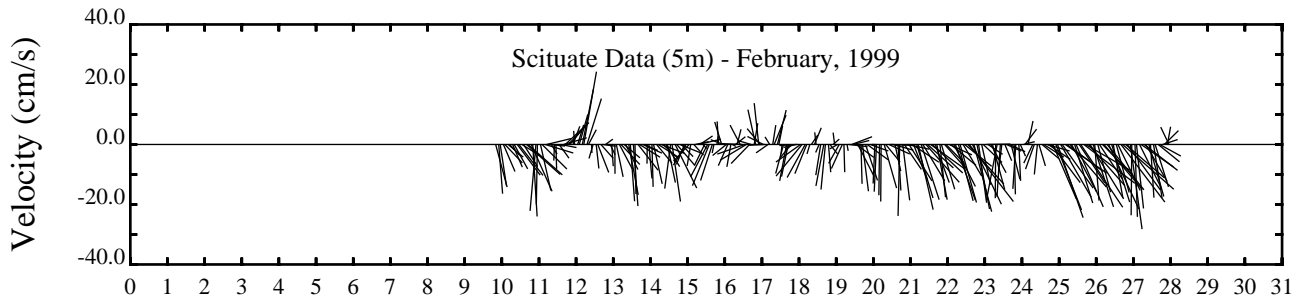
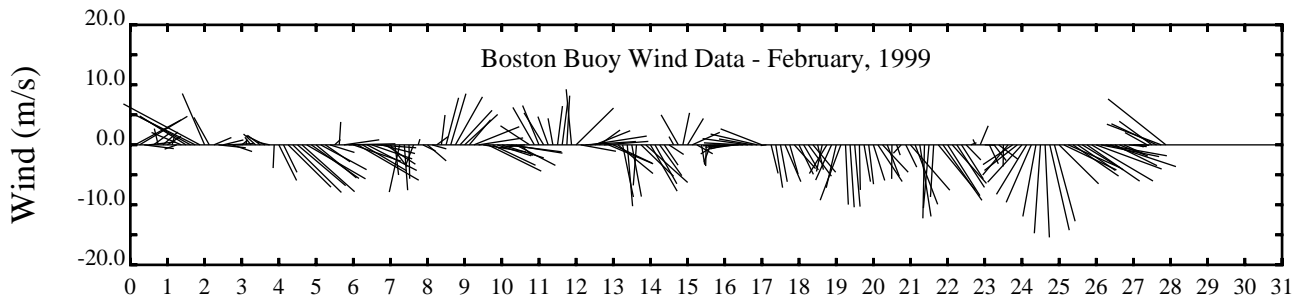


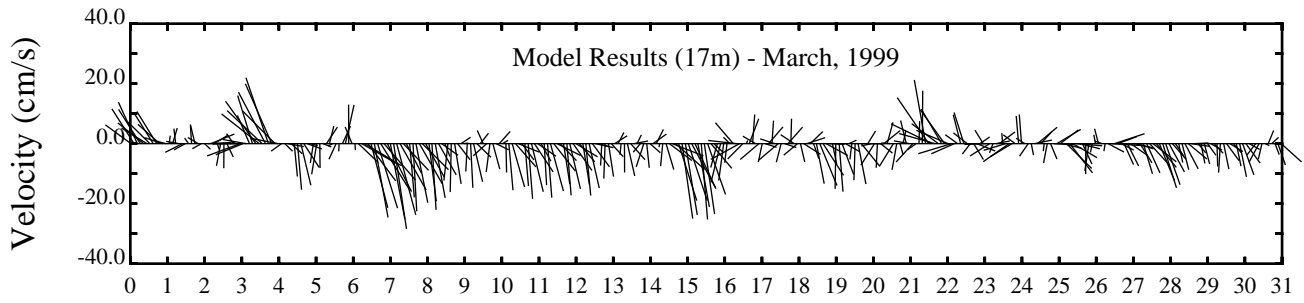
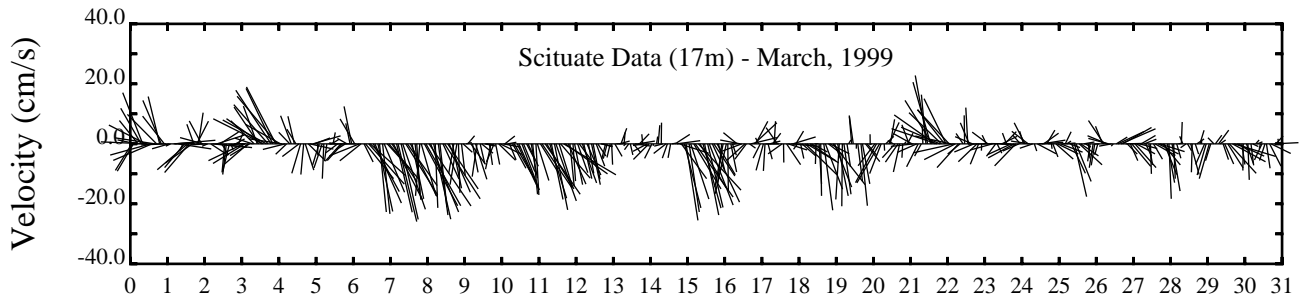
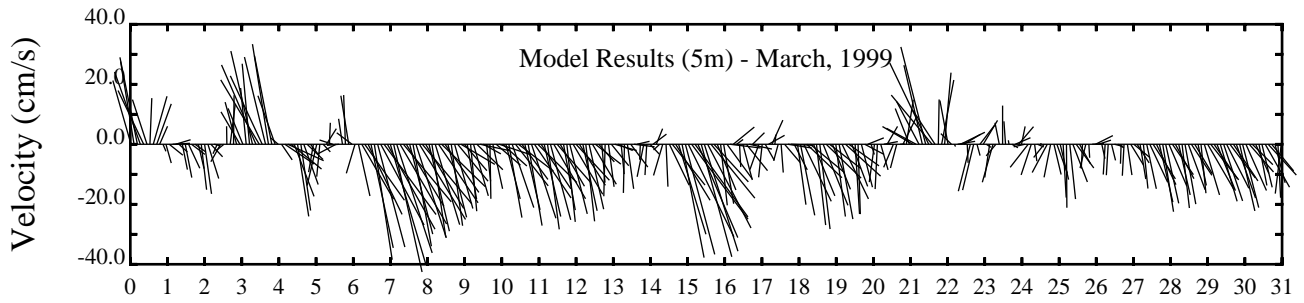
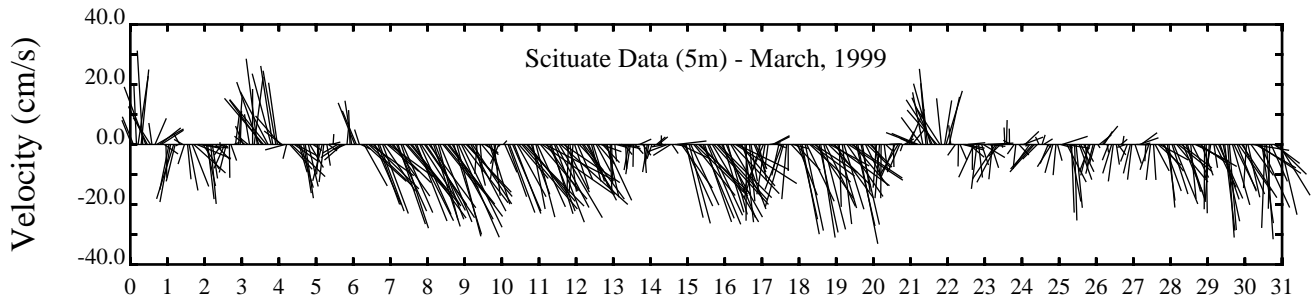
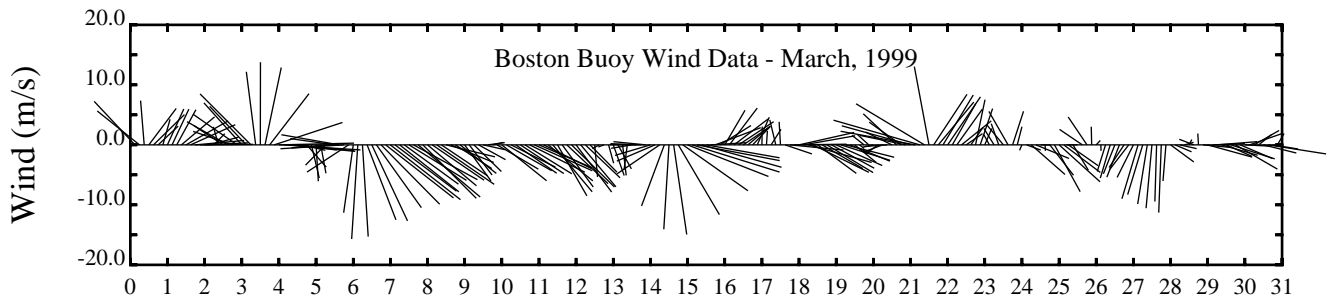


Day

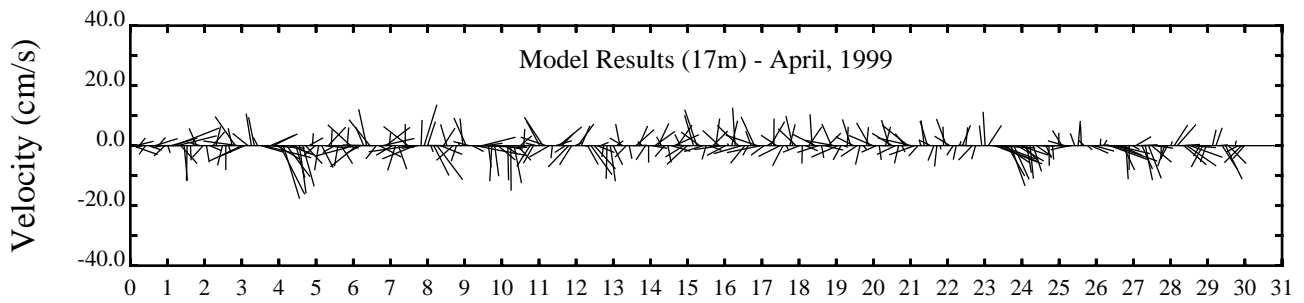
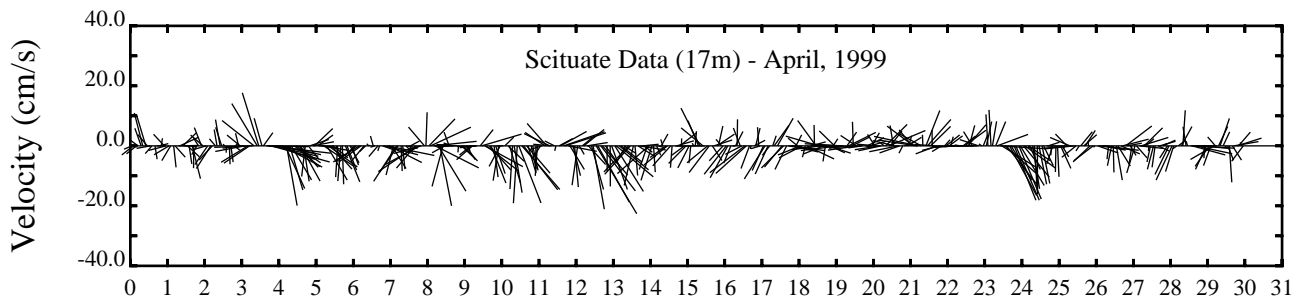
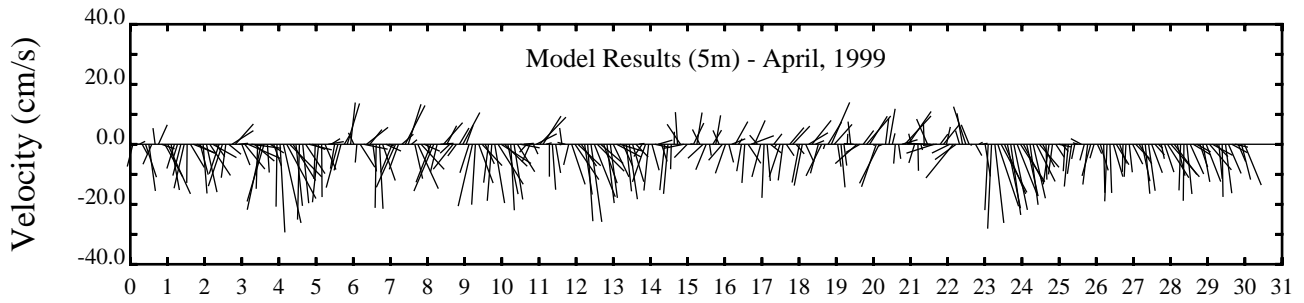
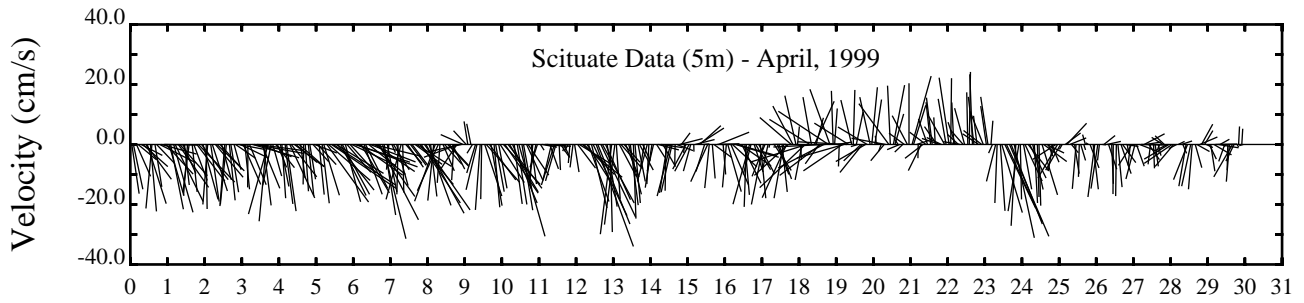
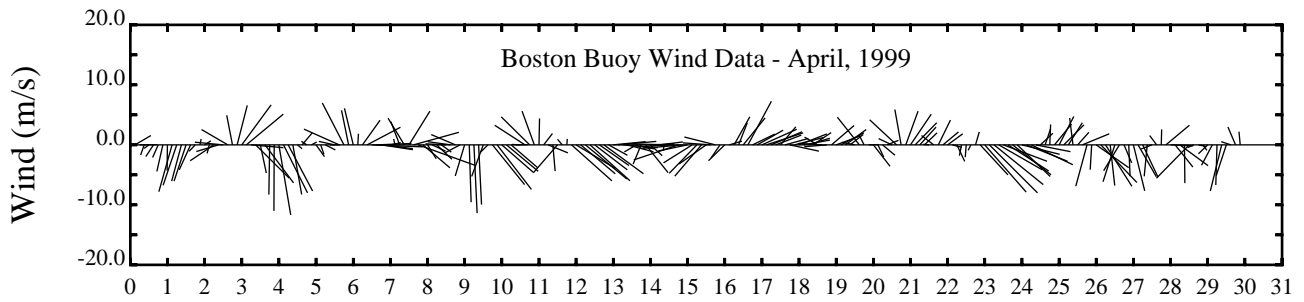


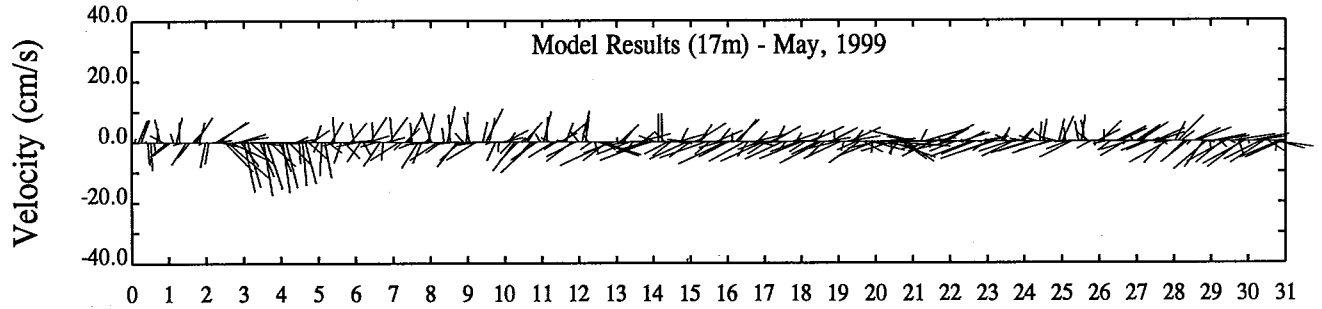
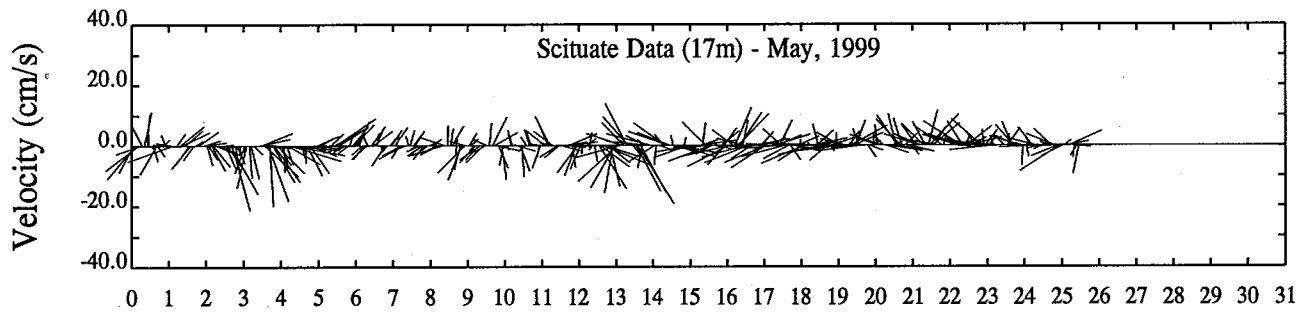
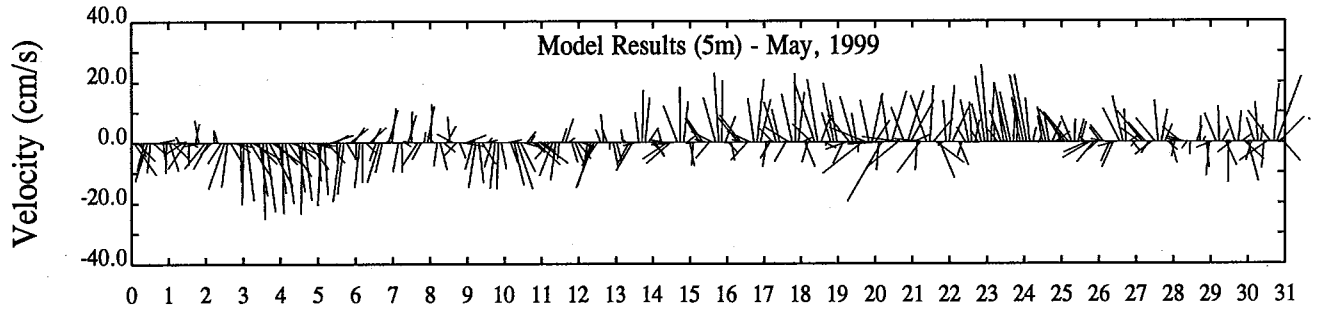
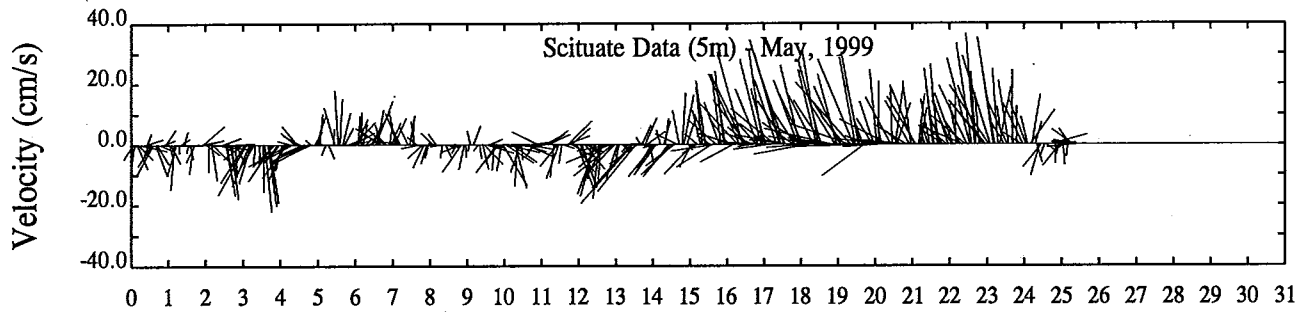
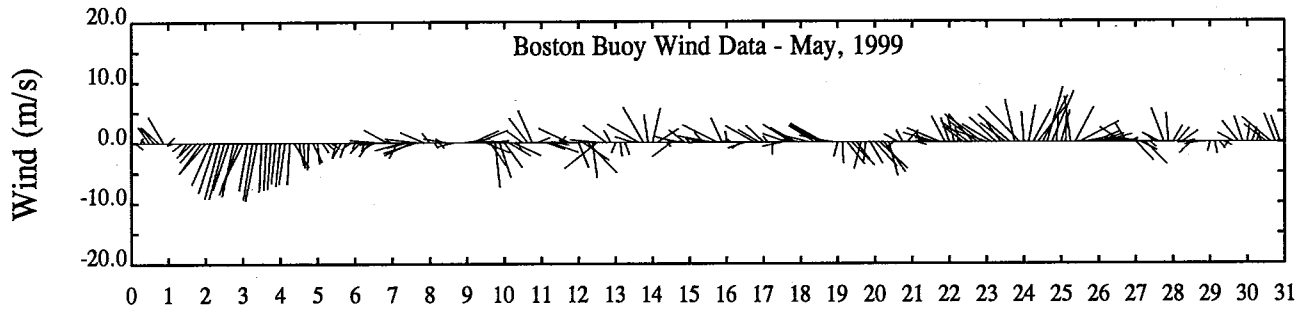
Day



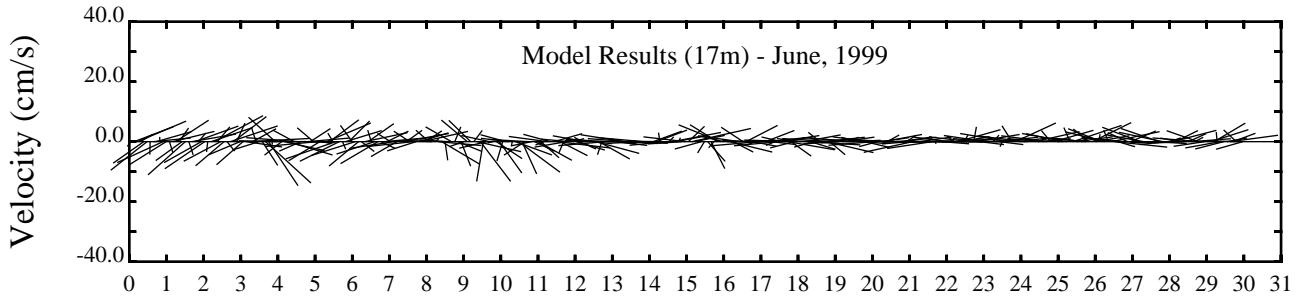
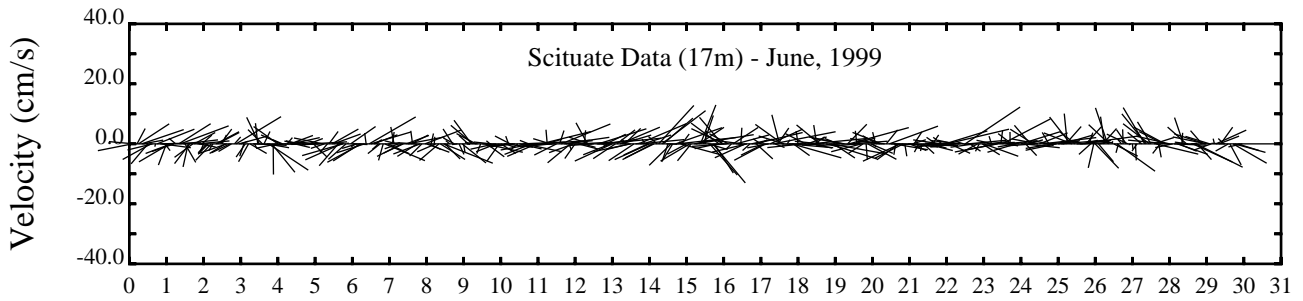
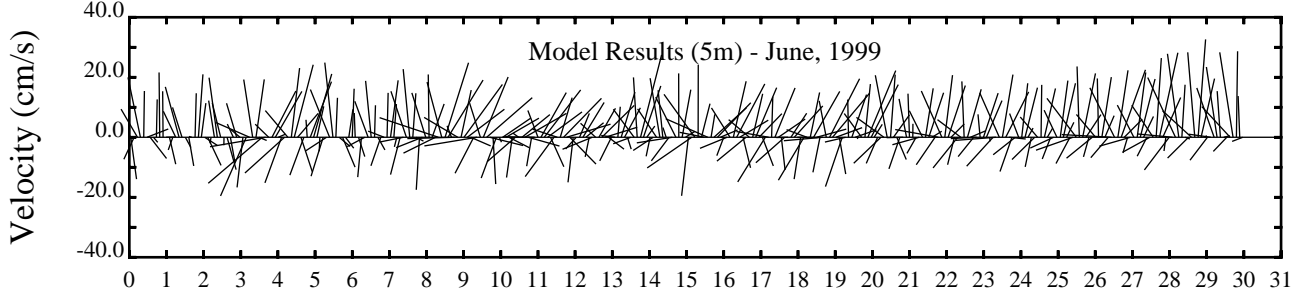
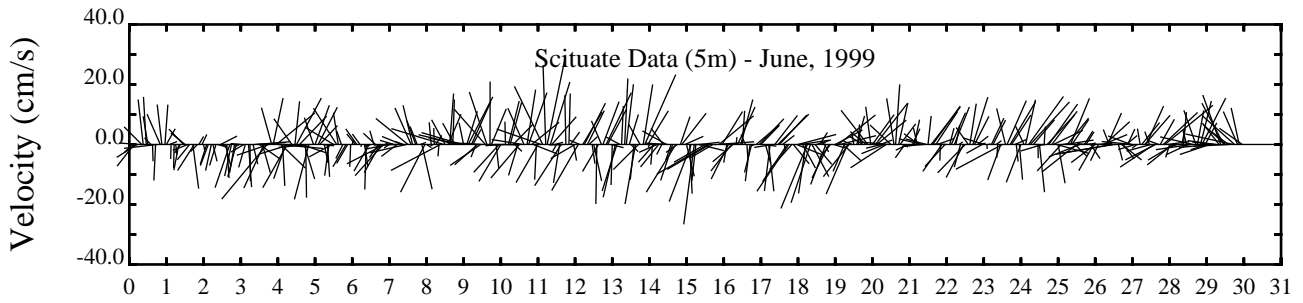
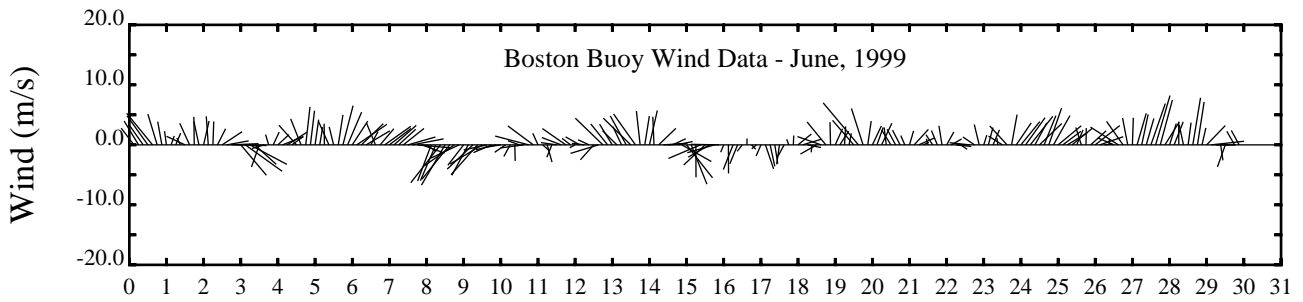


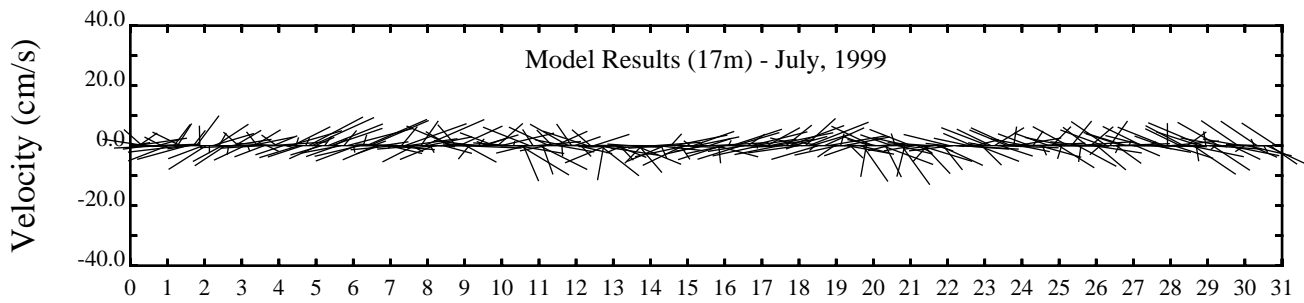
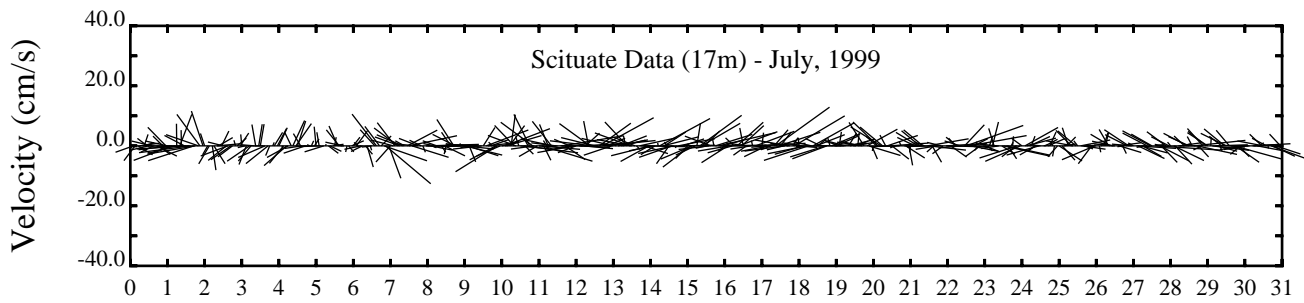
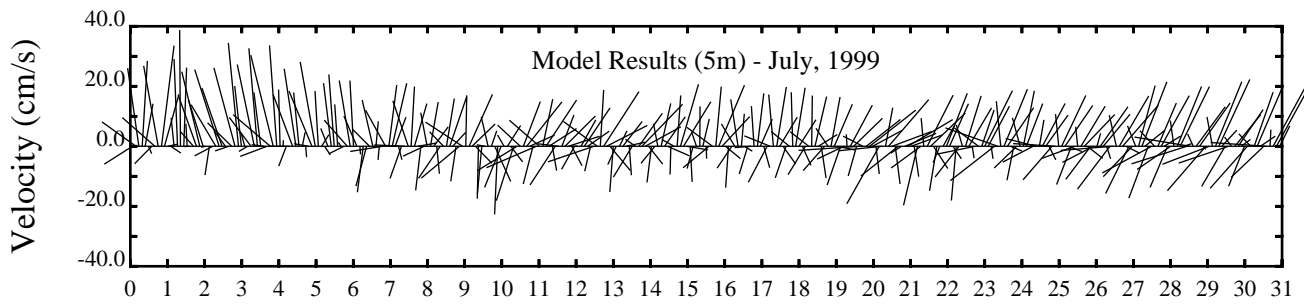
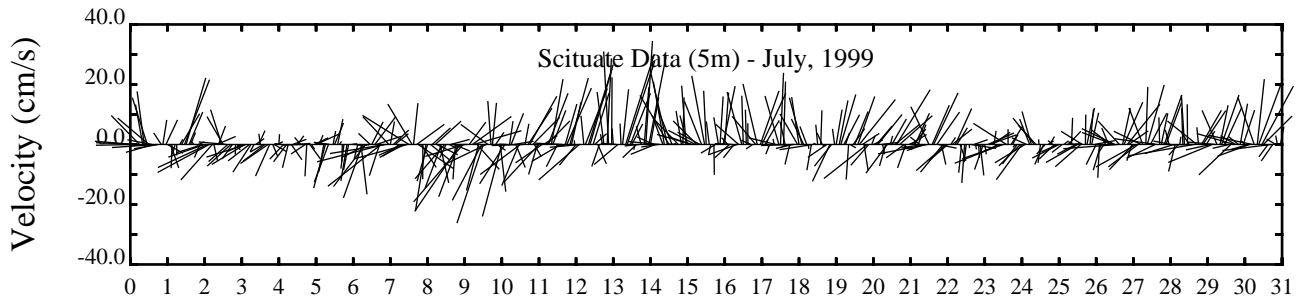
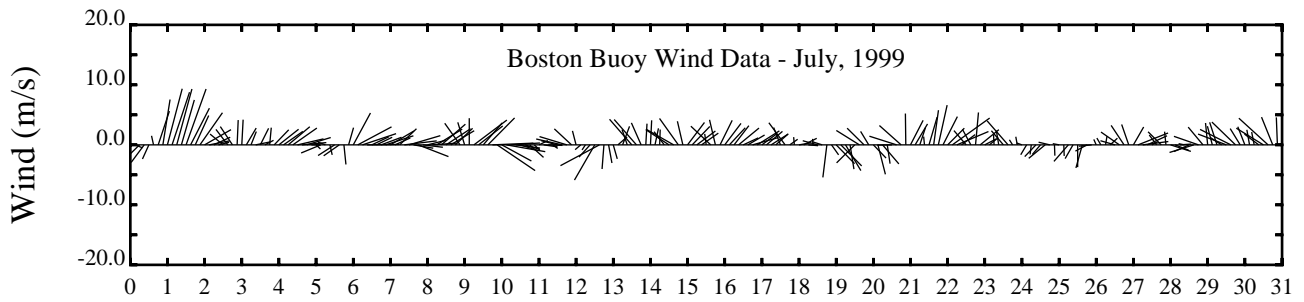
Day



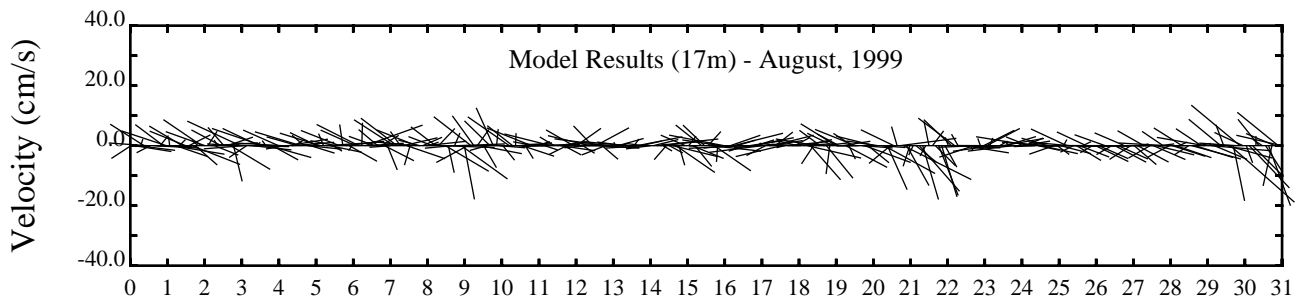
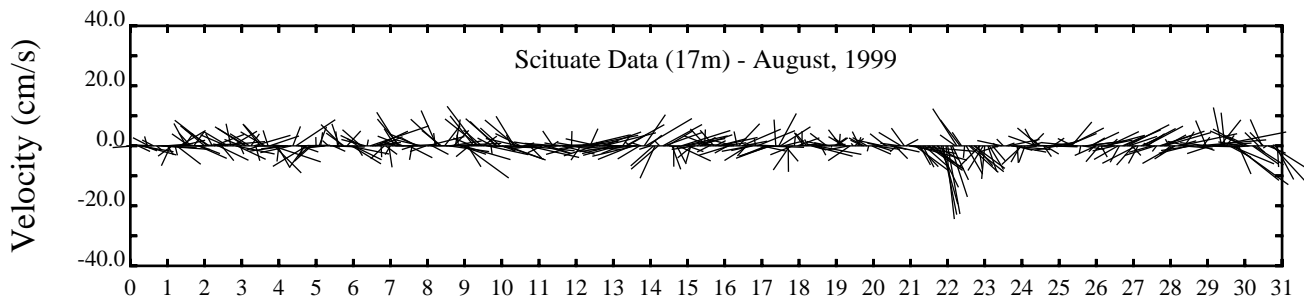
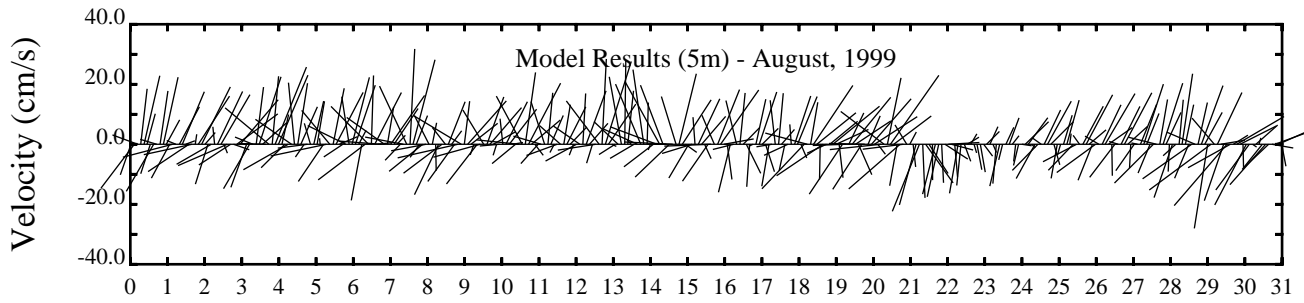
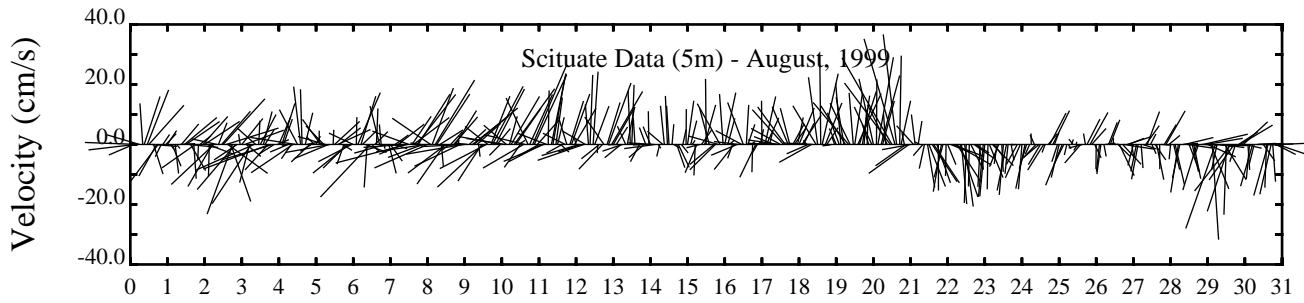
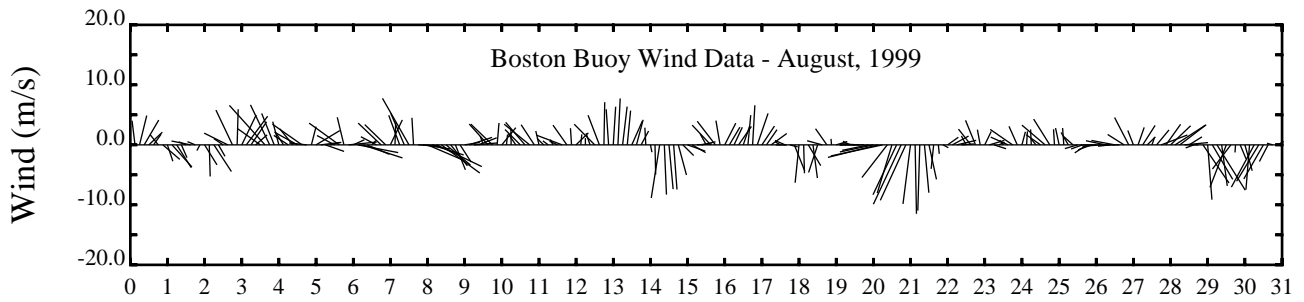


Day

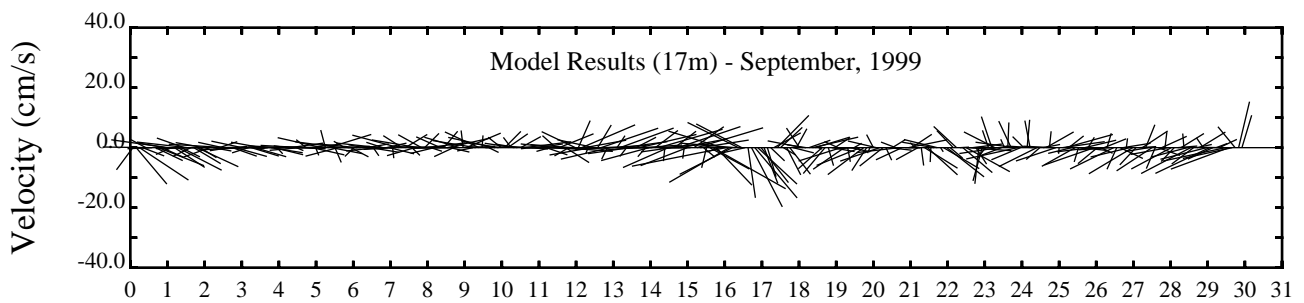
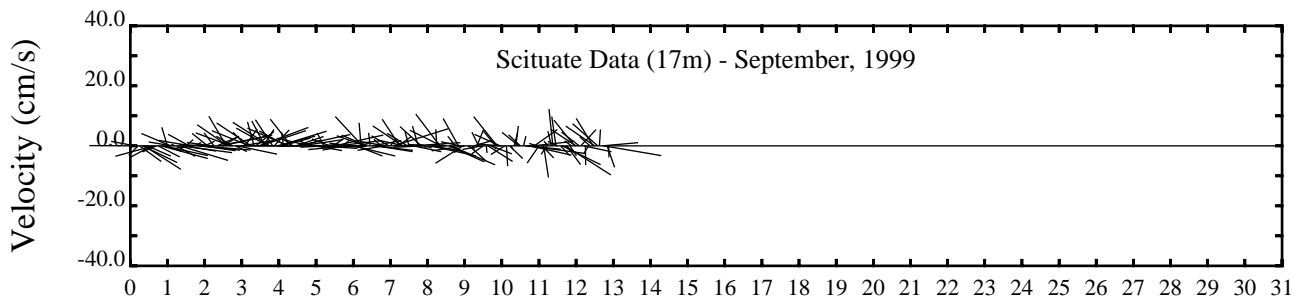
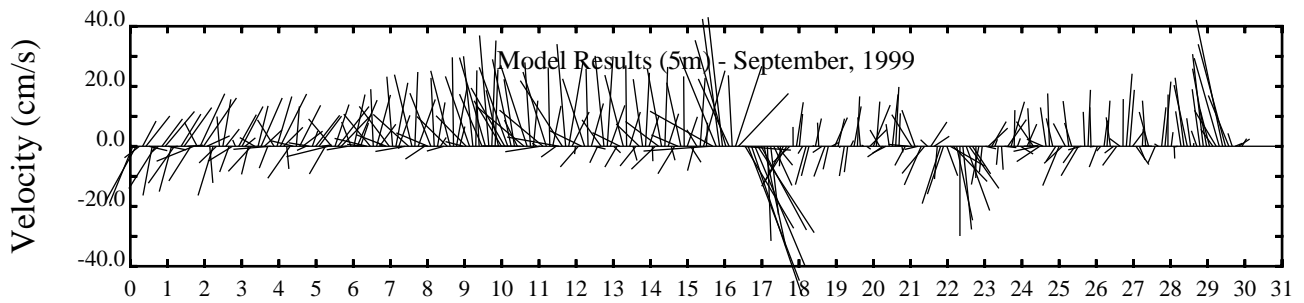
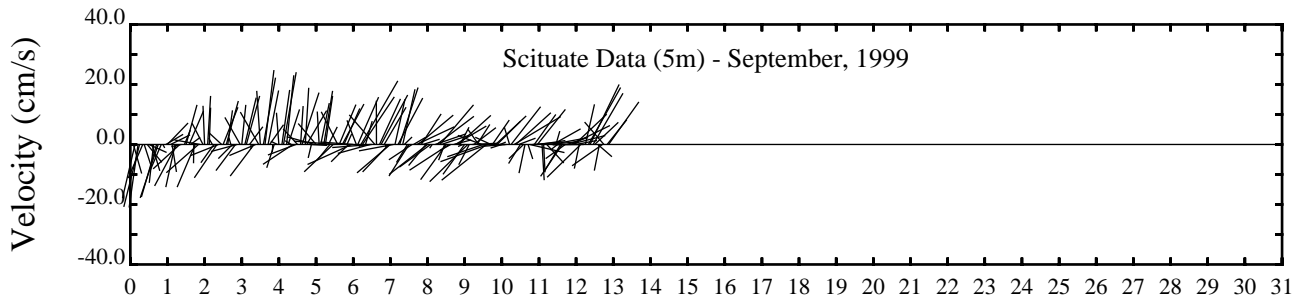
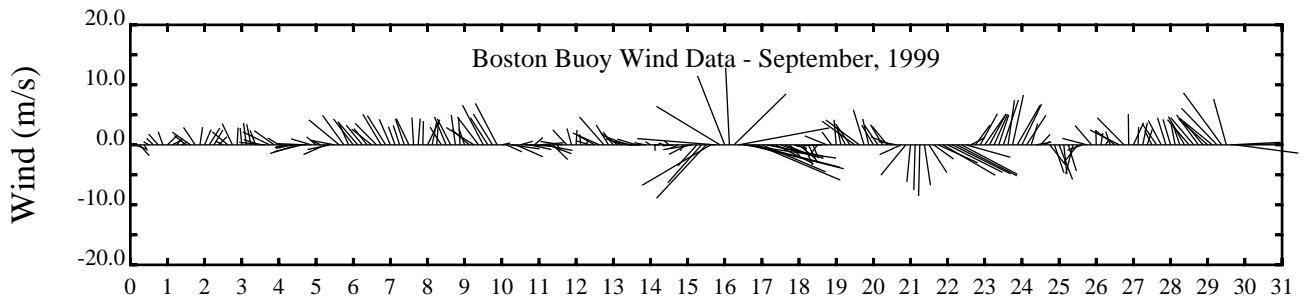


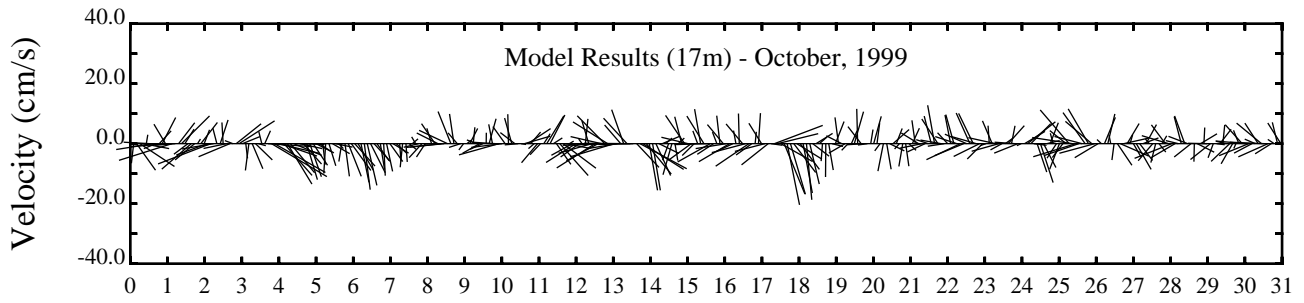
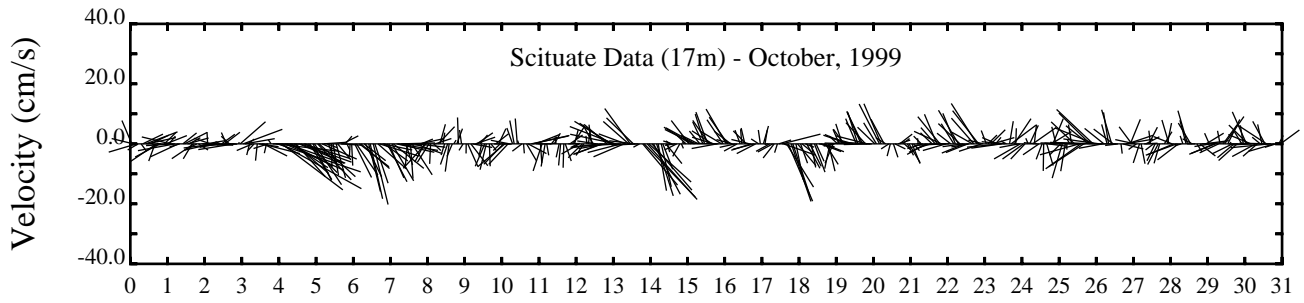
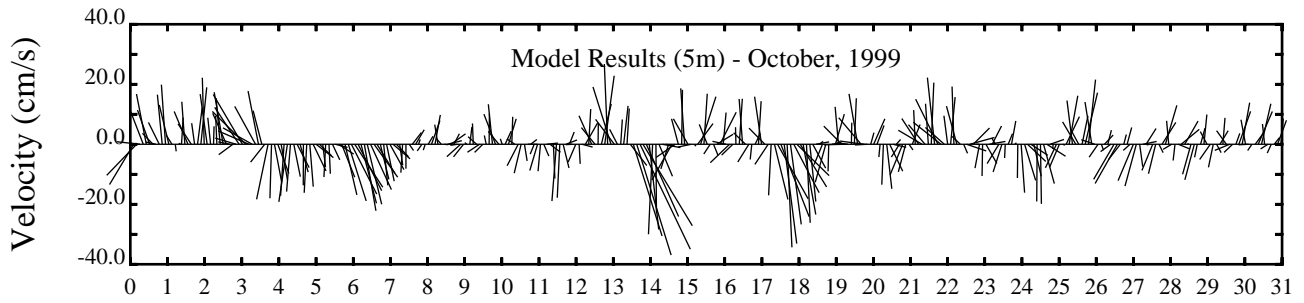
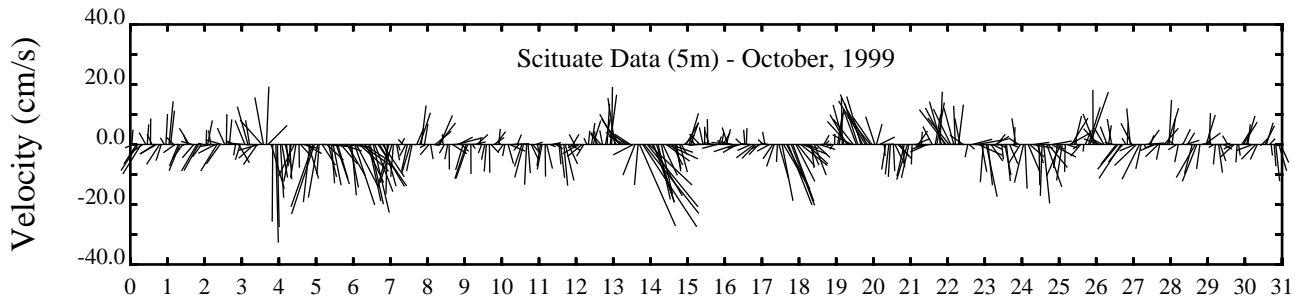
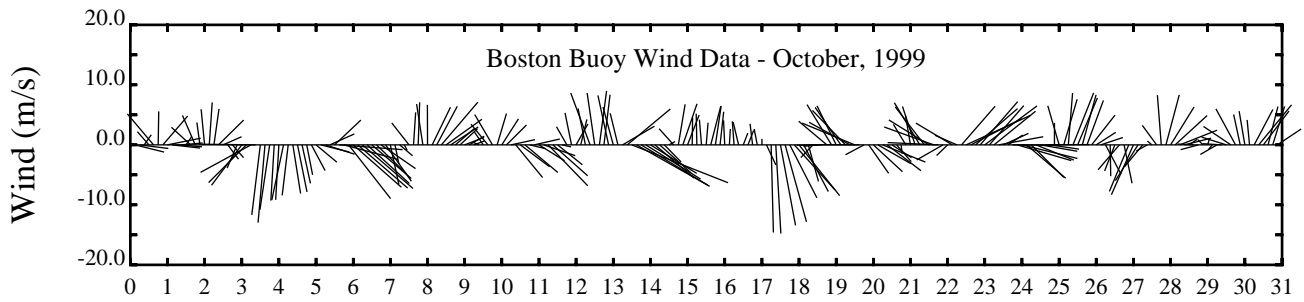


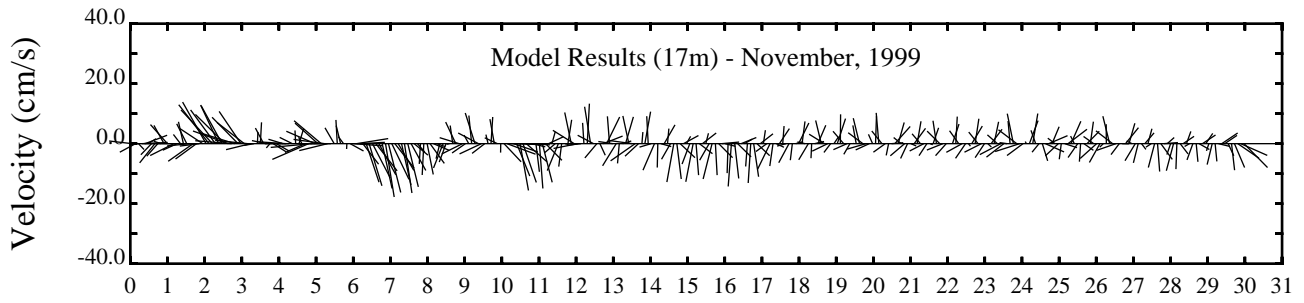
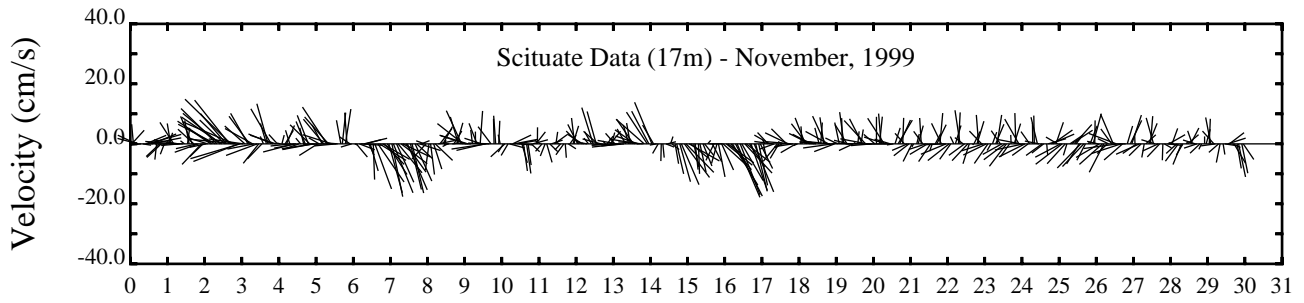
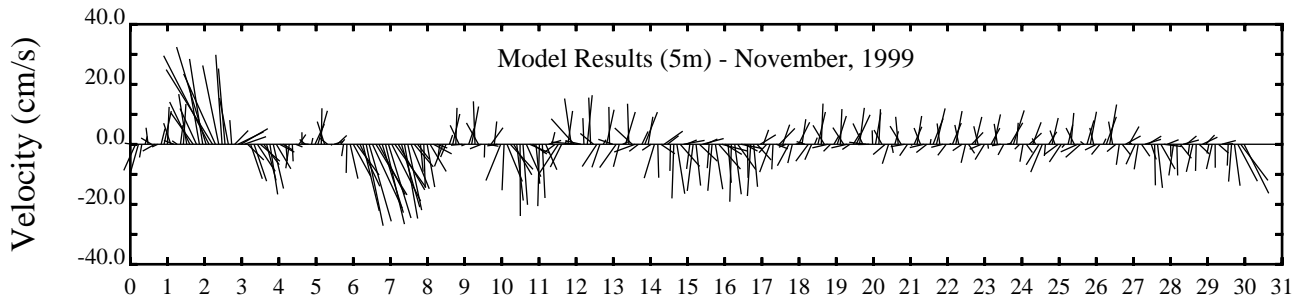
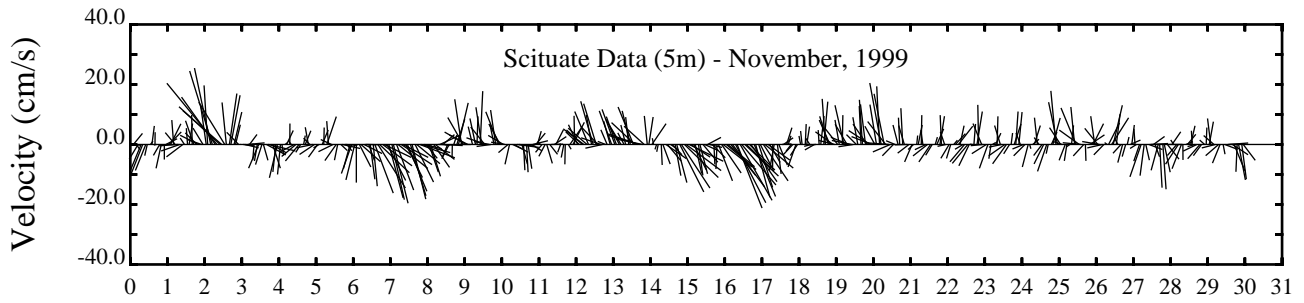
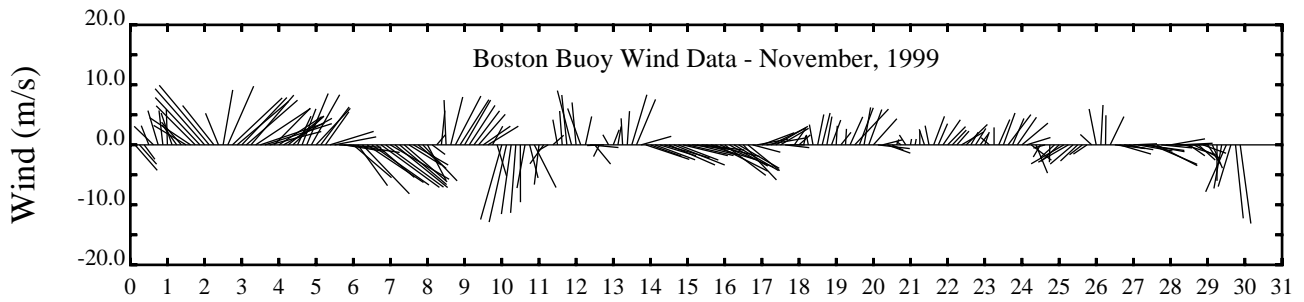
Day

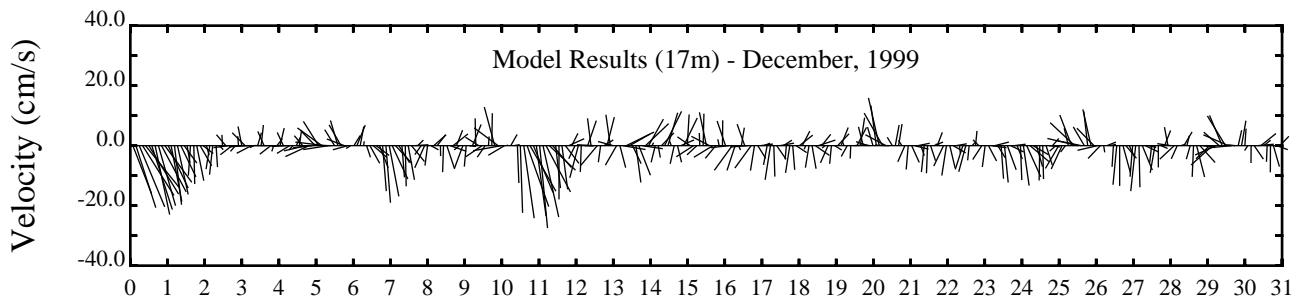
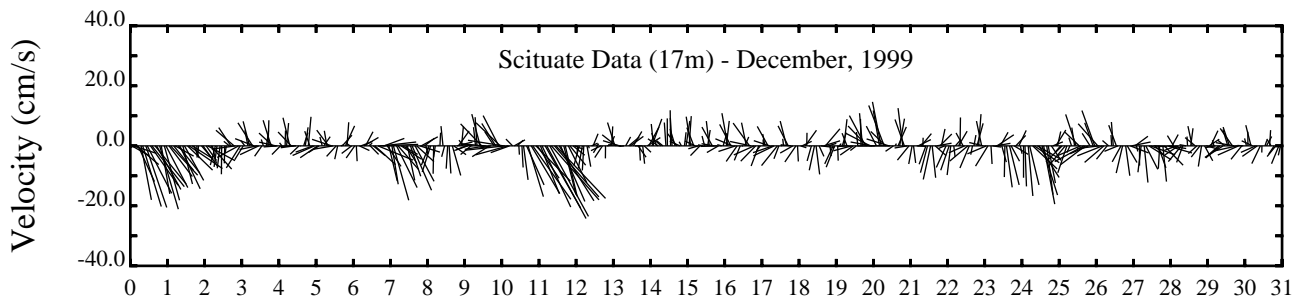
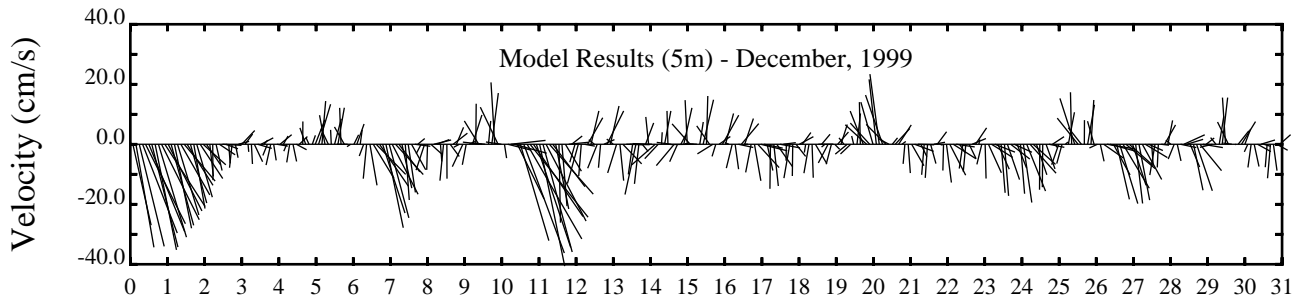
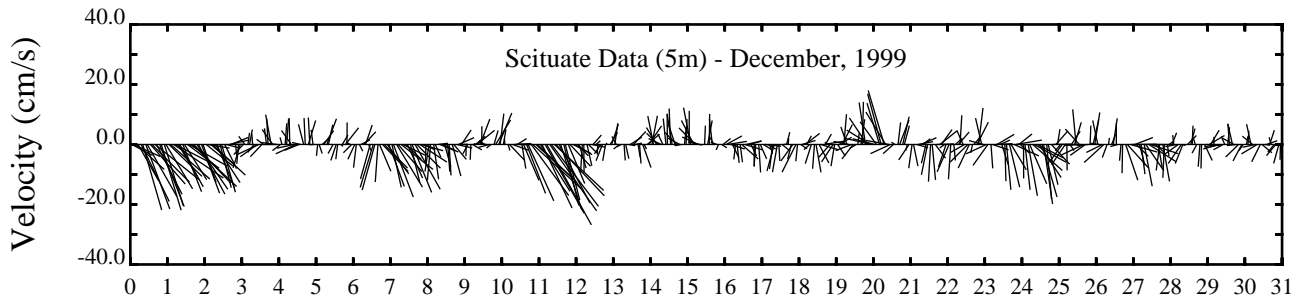
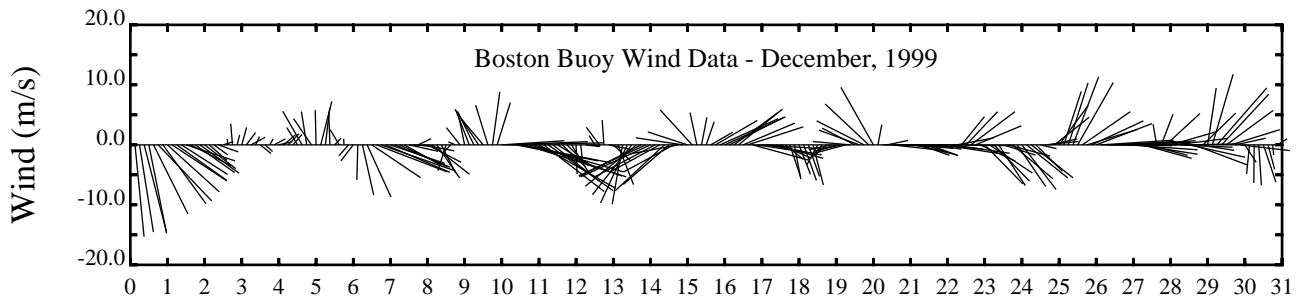


Day

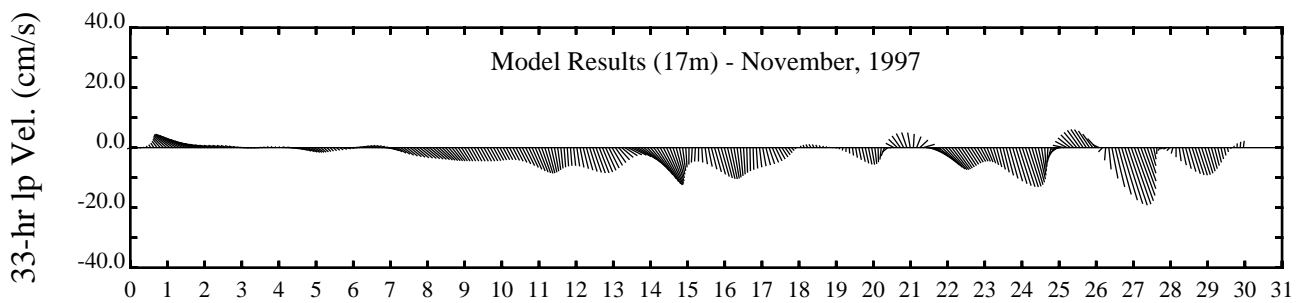
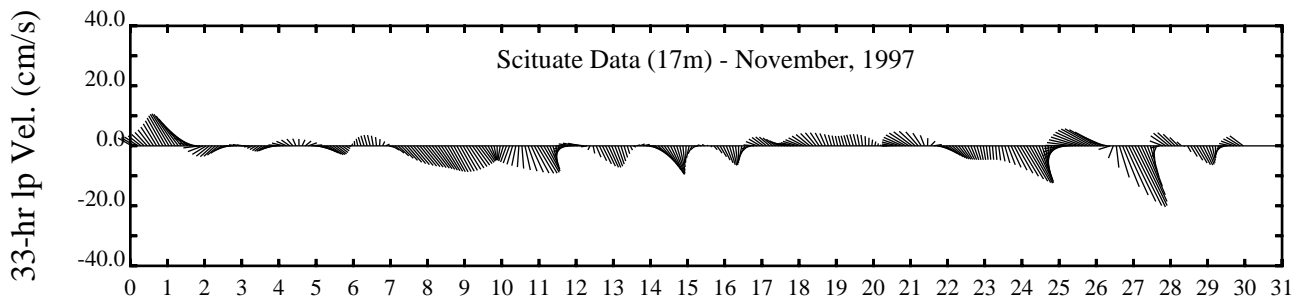
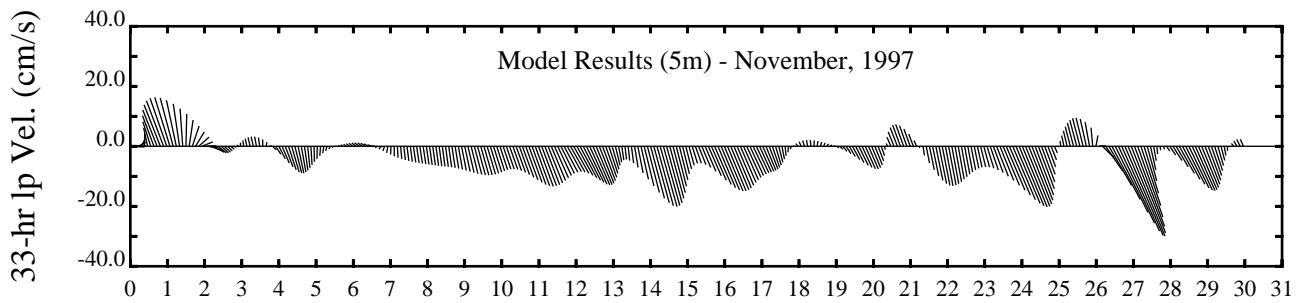
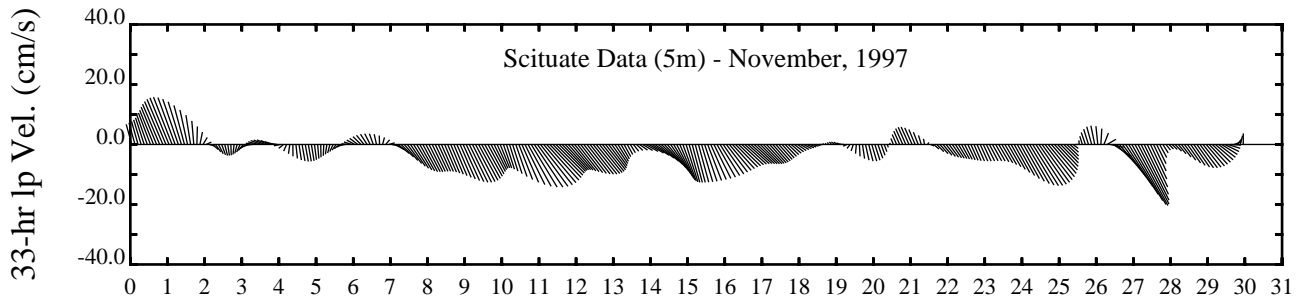
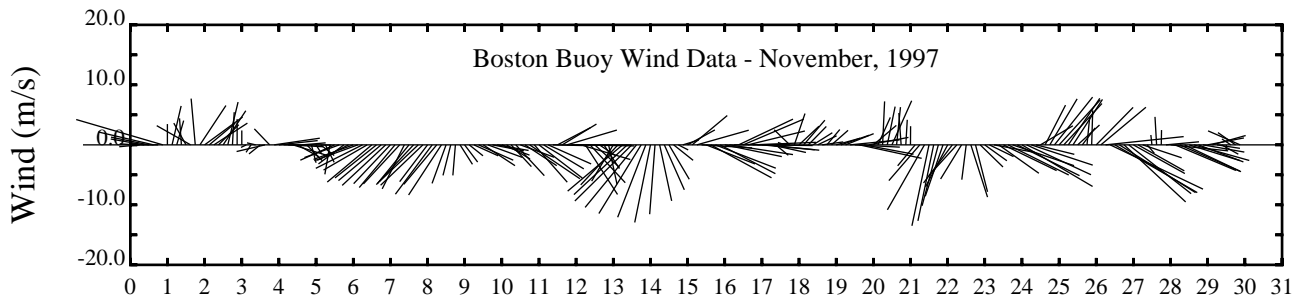


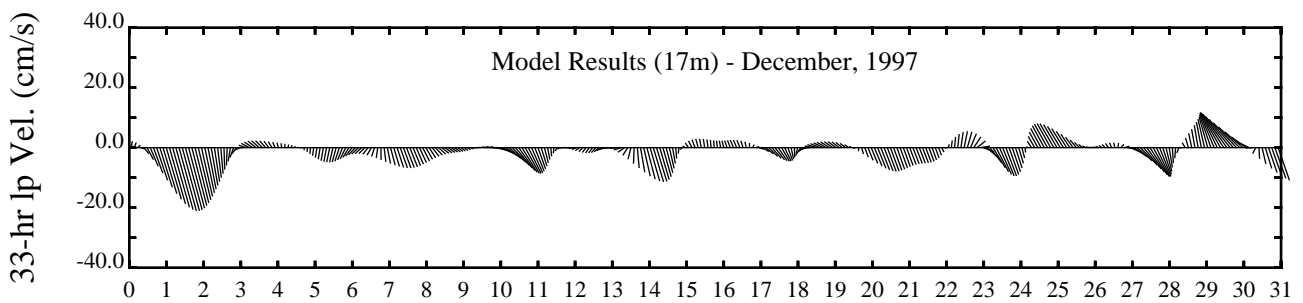
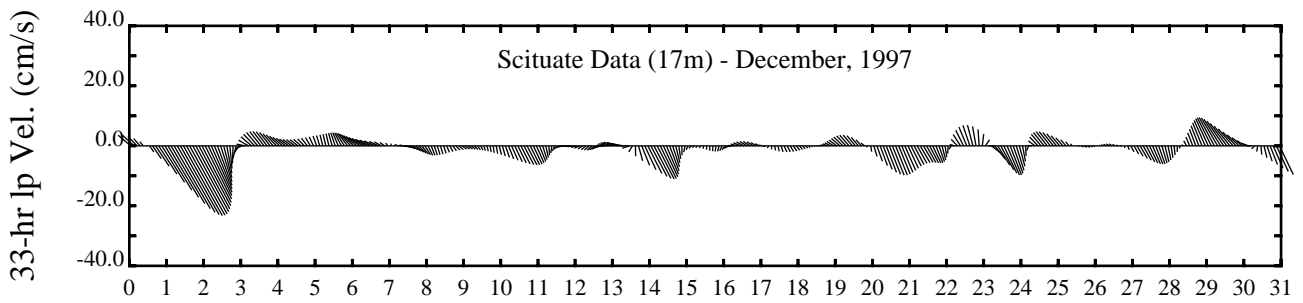
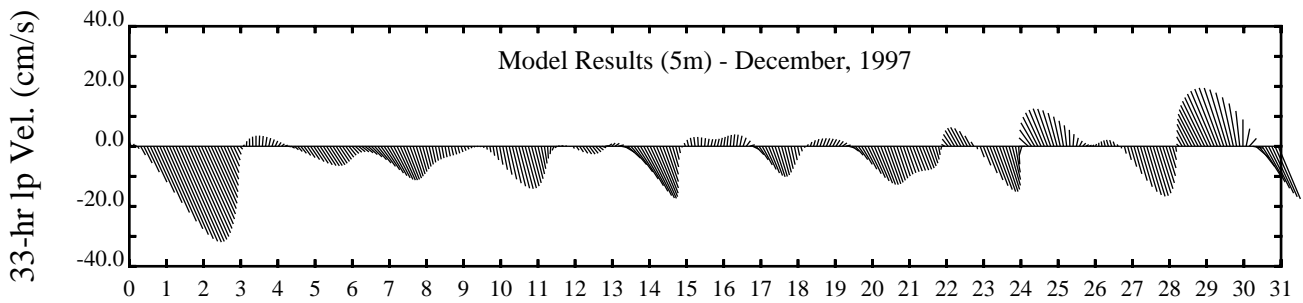
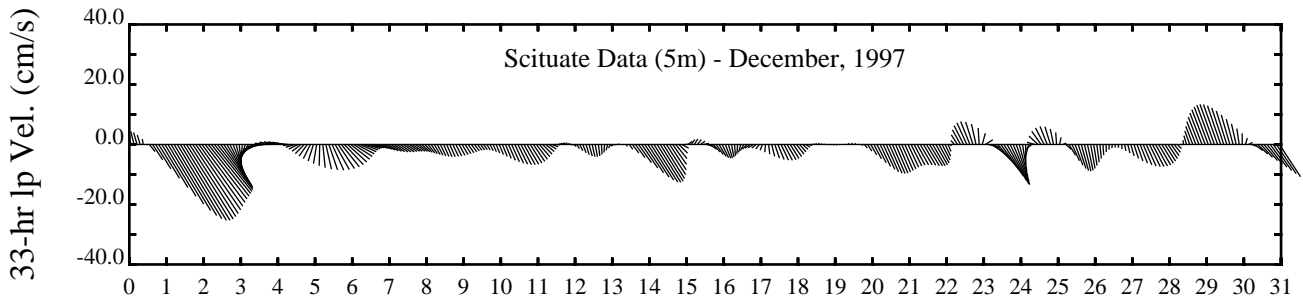
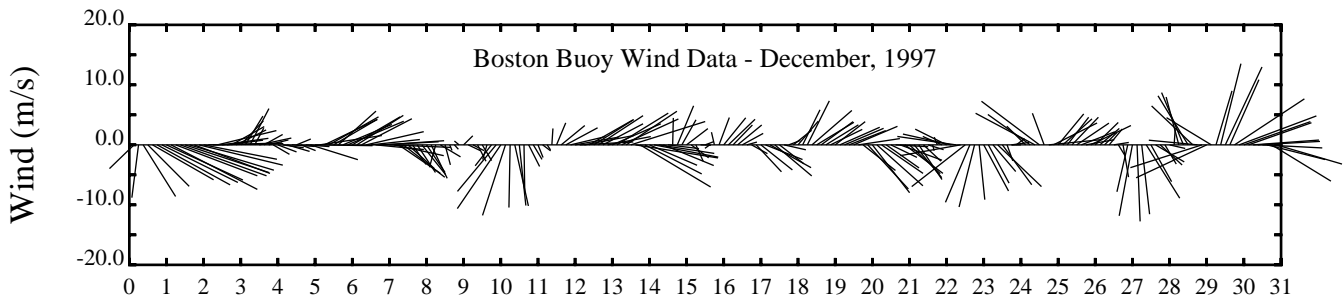




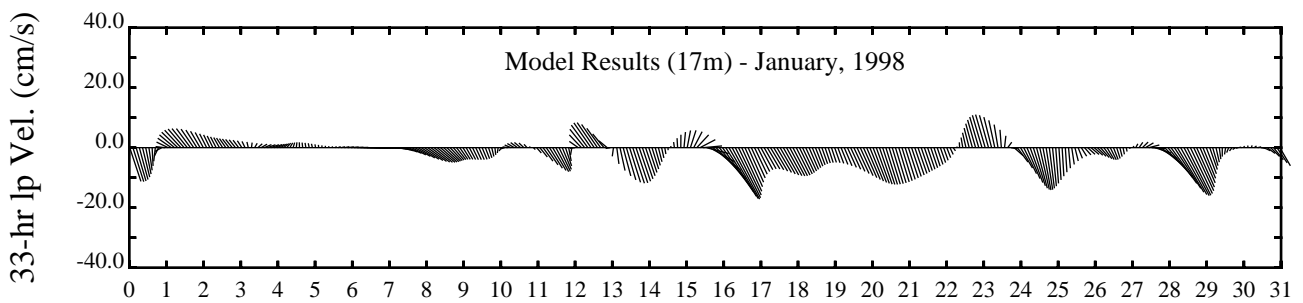
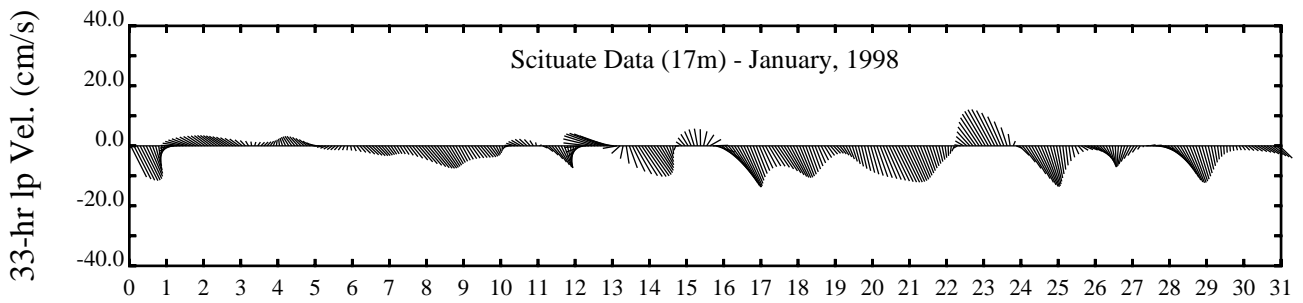
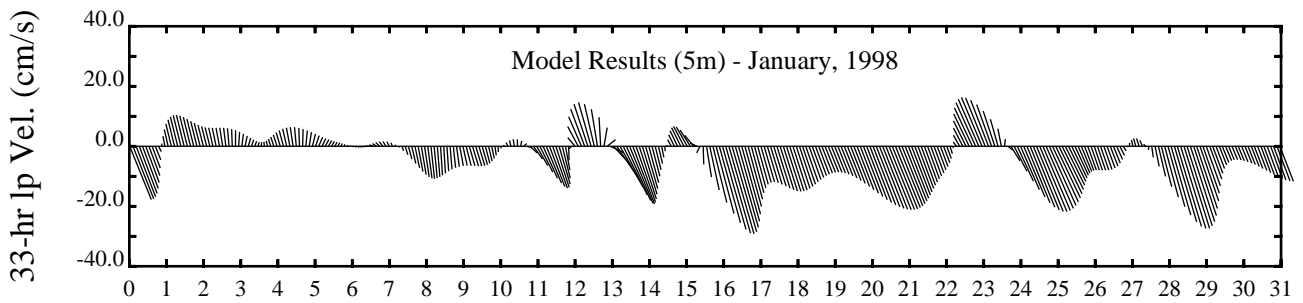
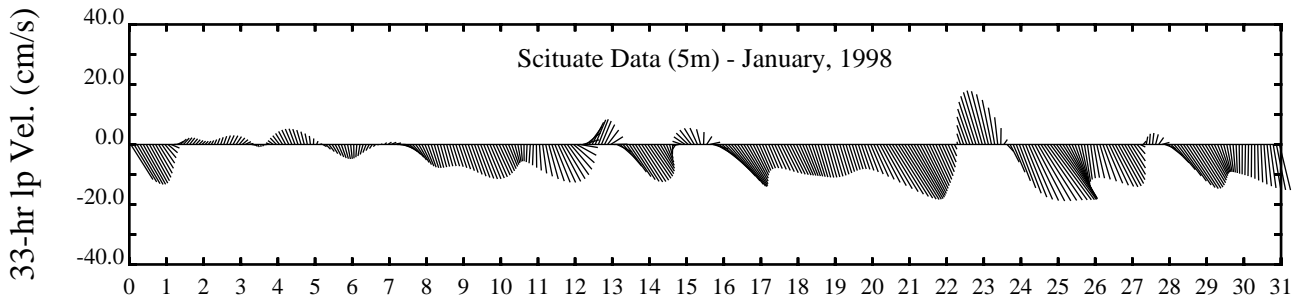
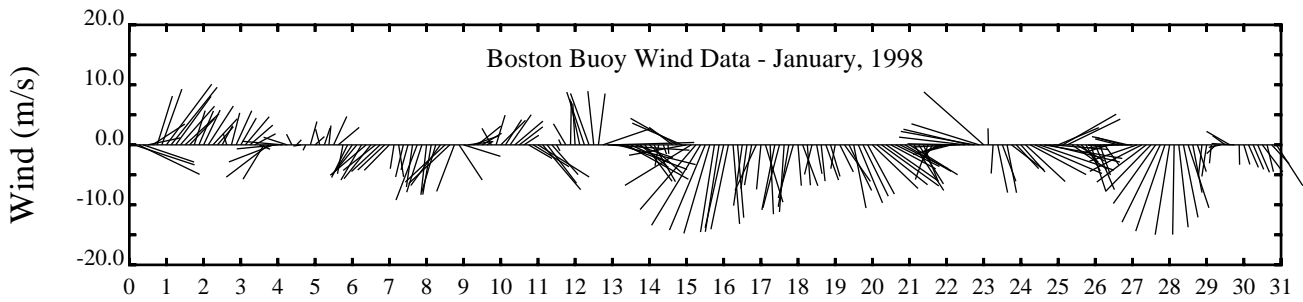


Day

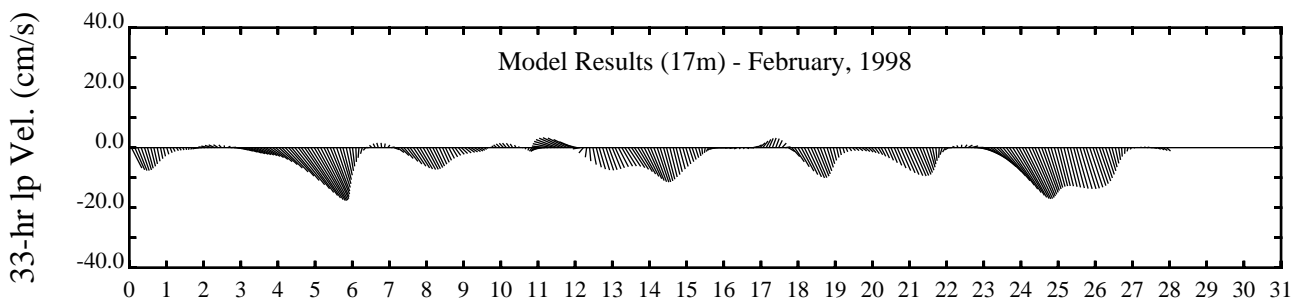
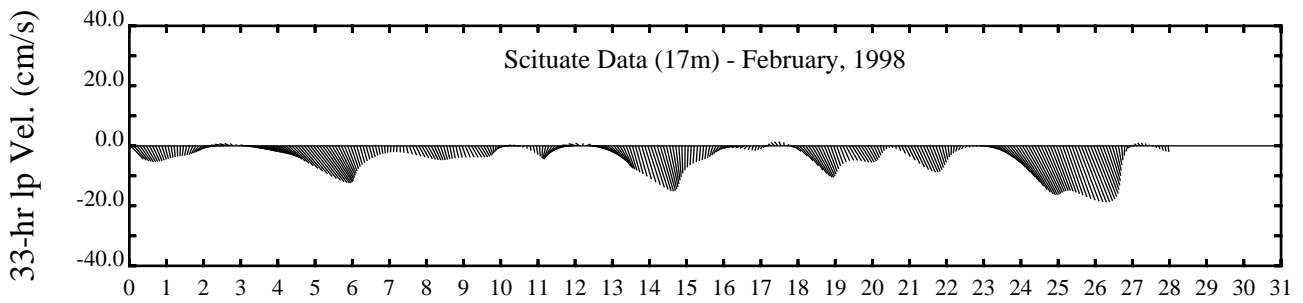
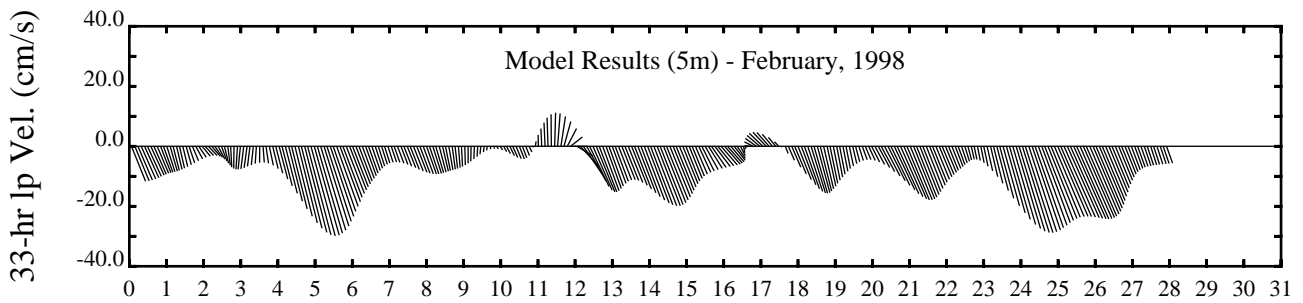
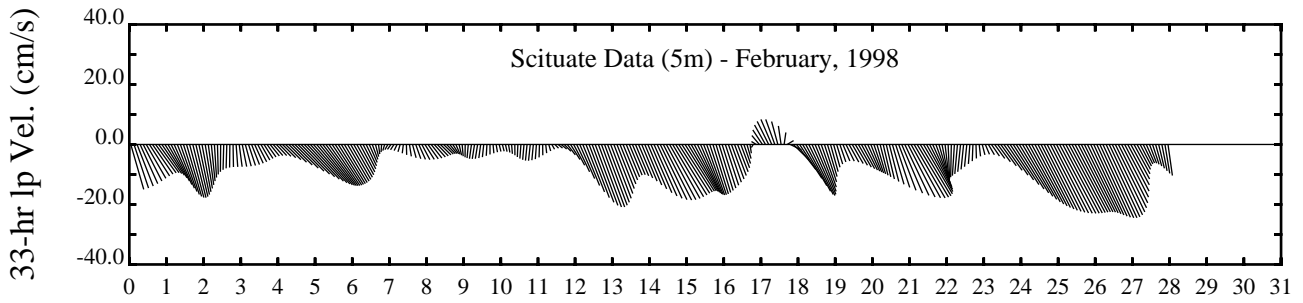
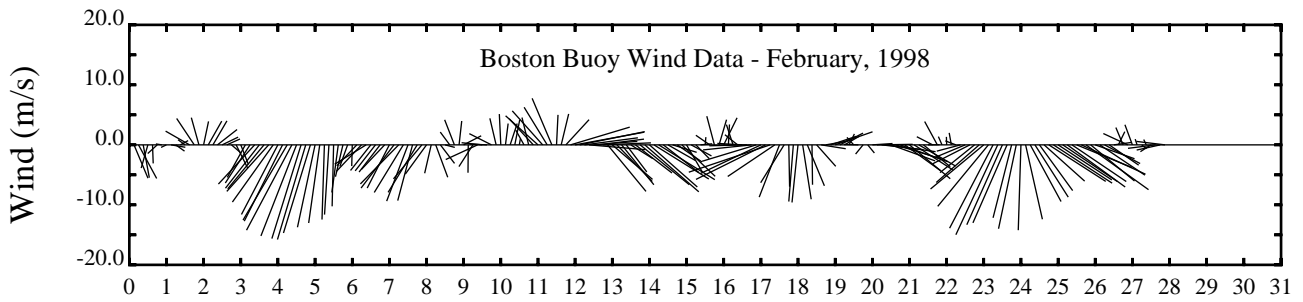




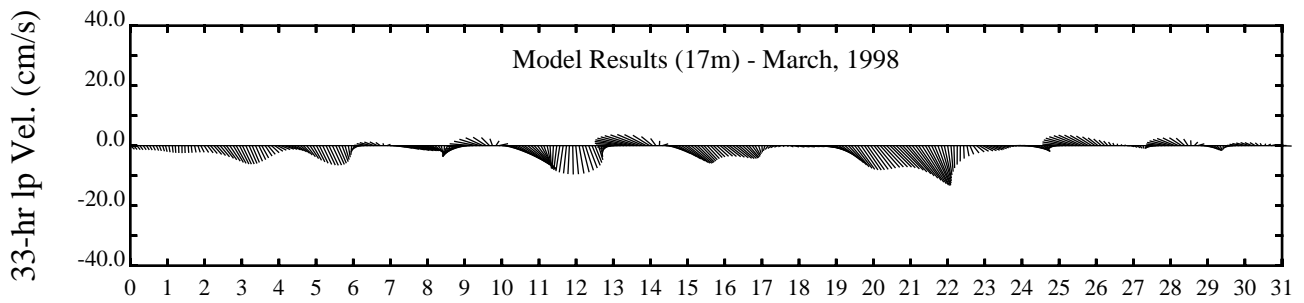
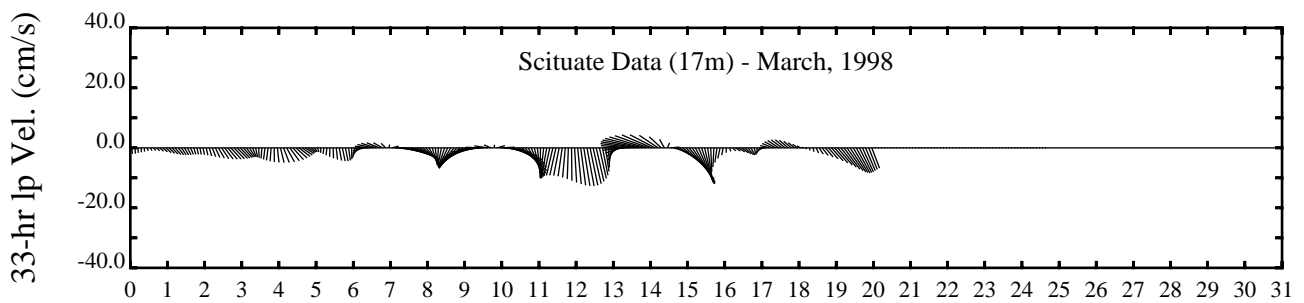
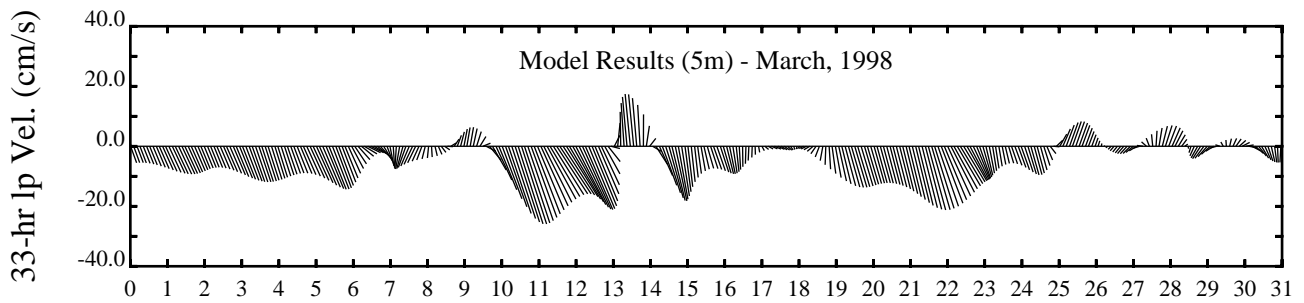
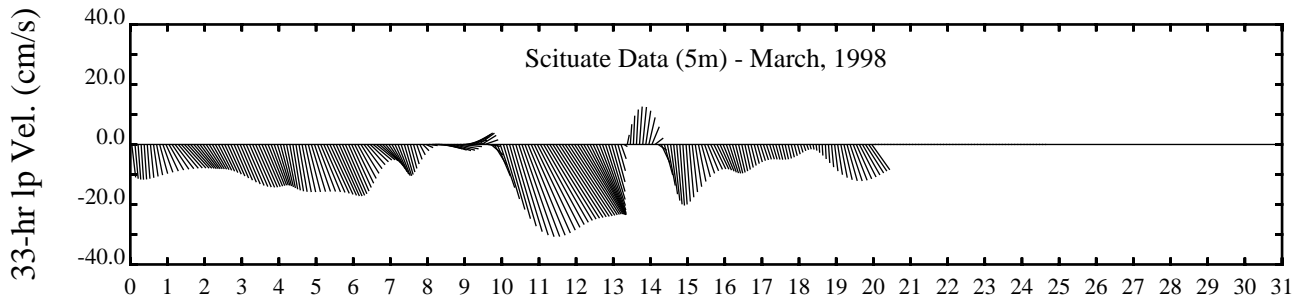
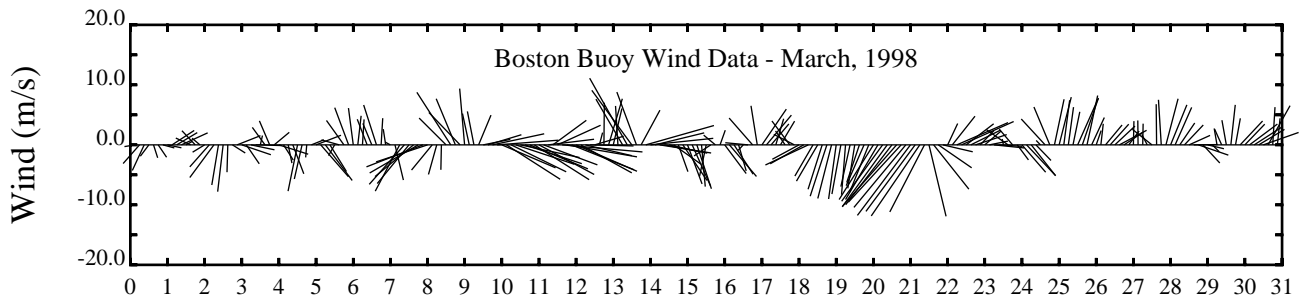
Day



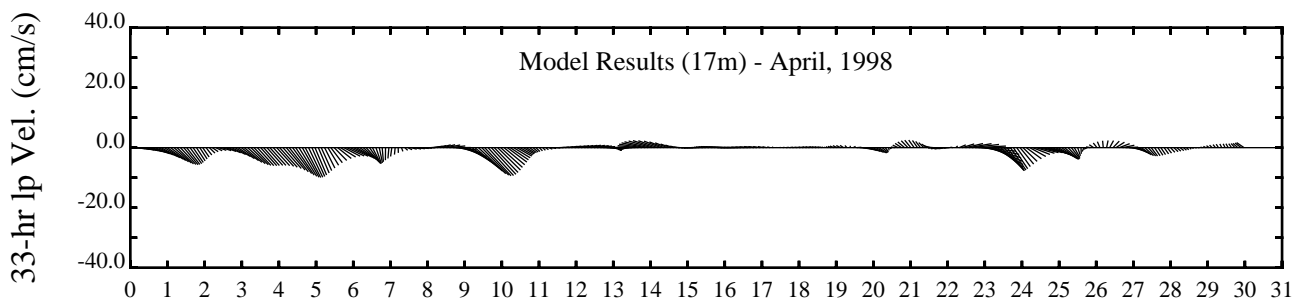
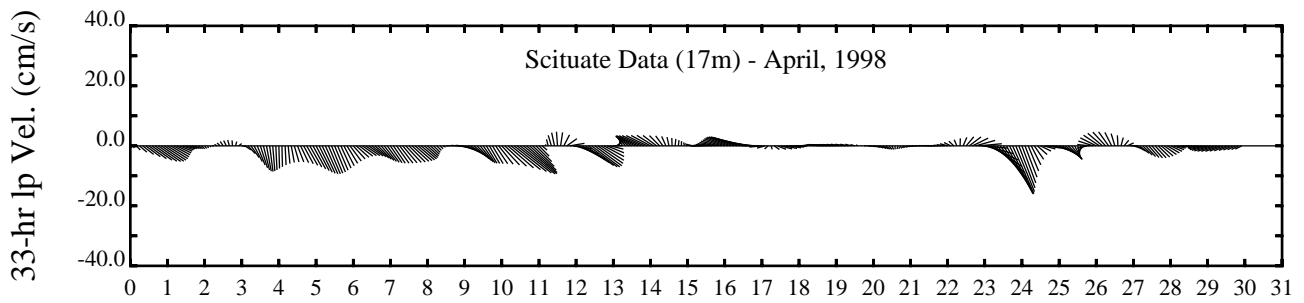
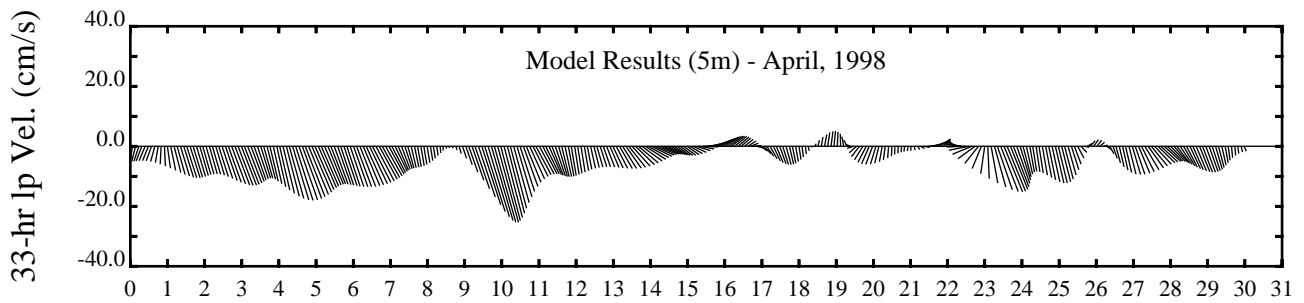
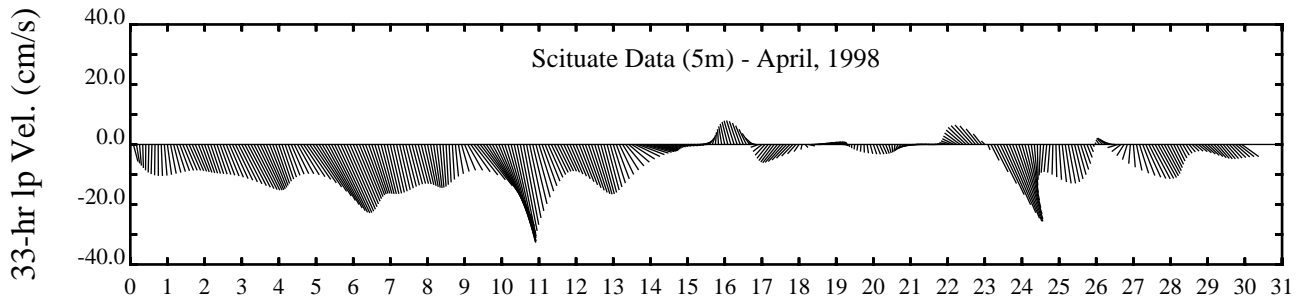
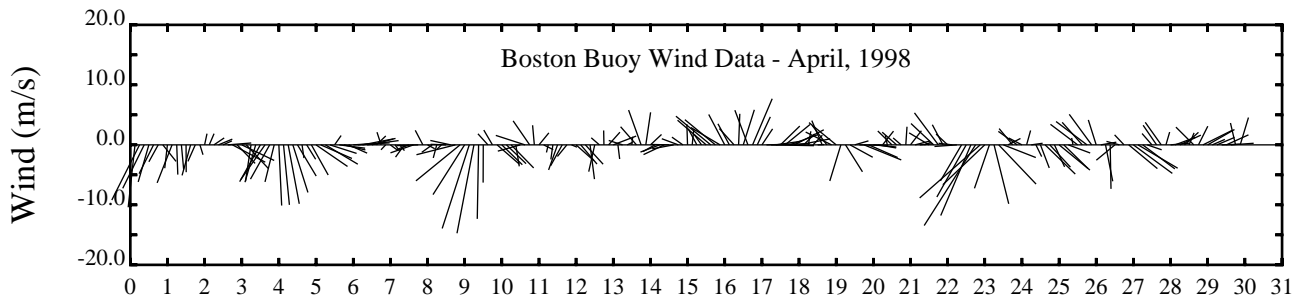
Day

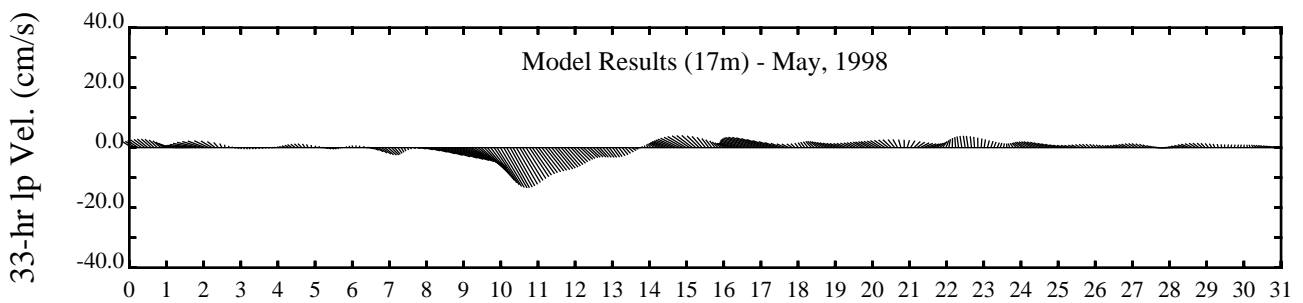
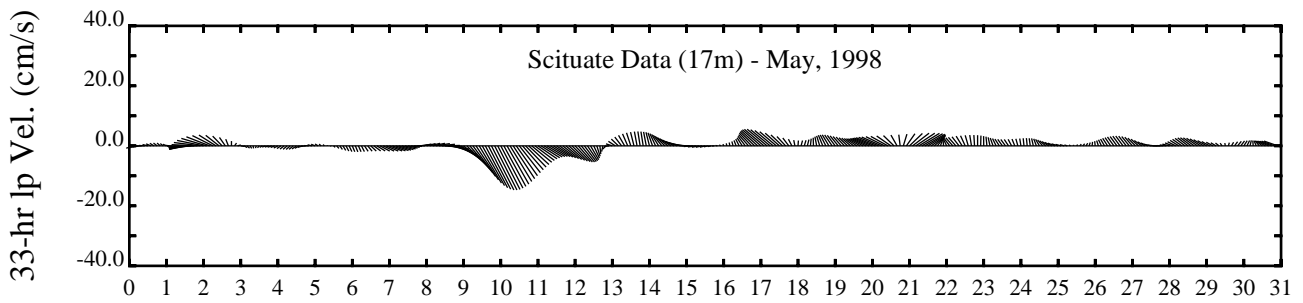
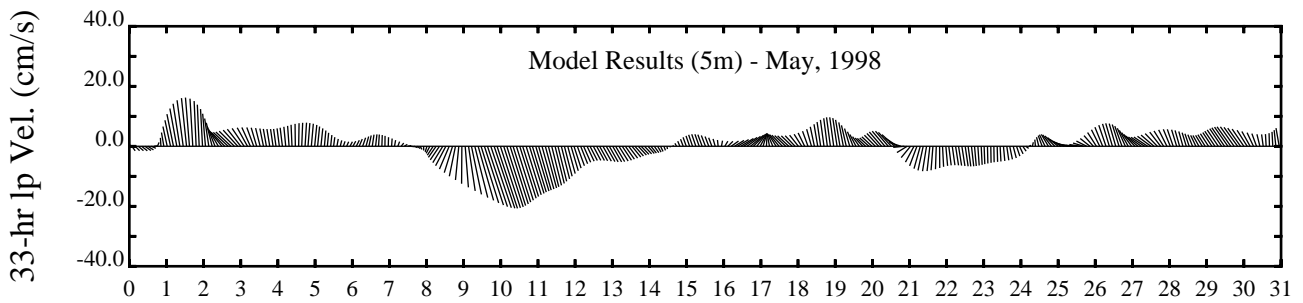
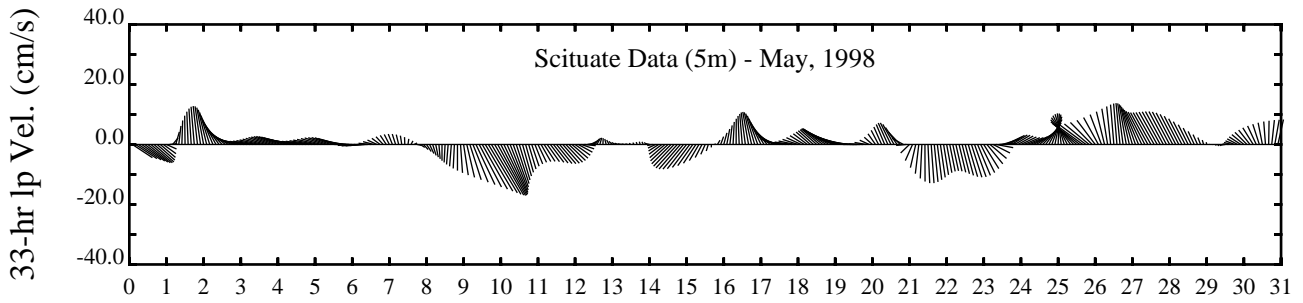
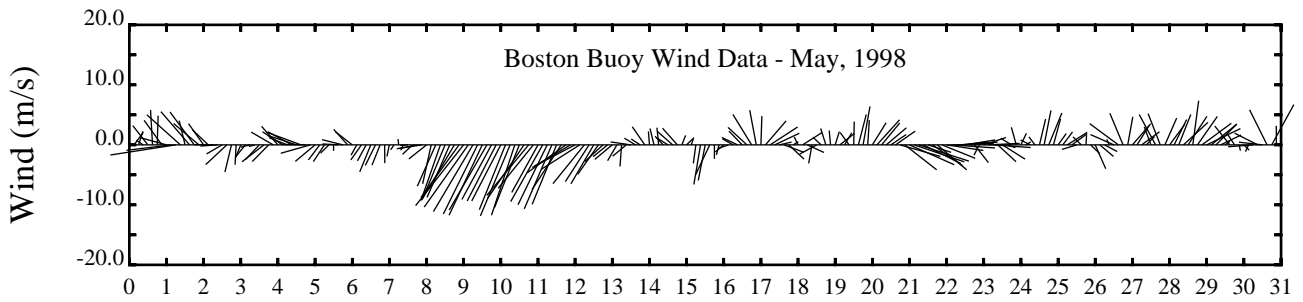


Day

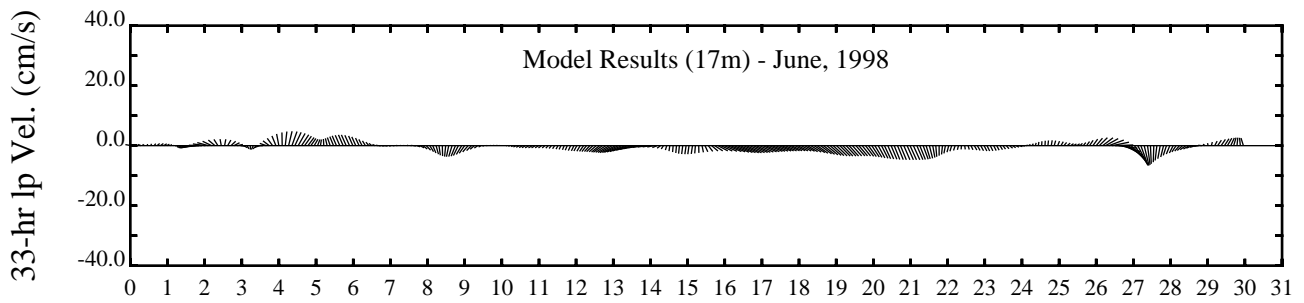
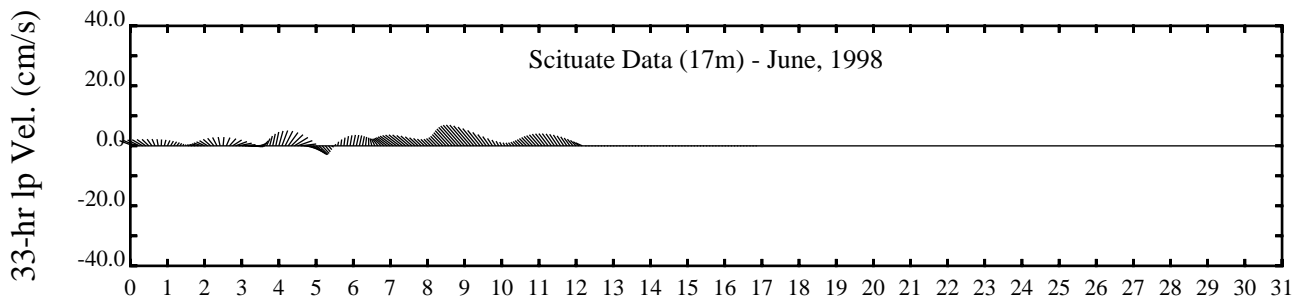
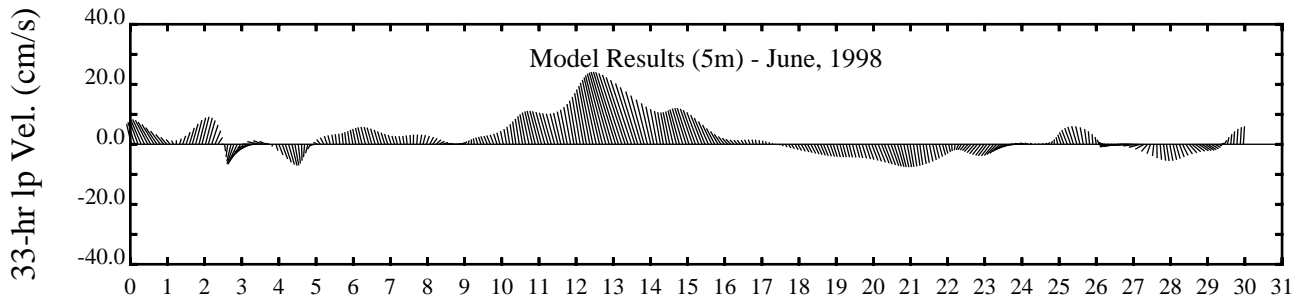
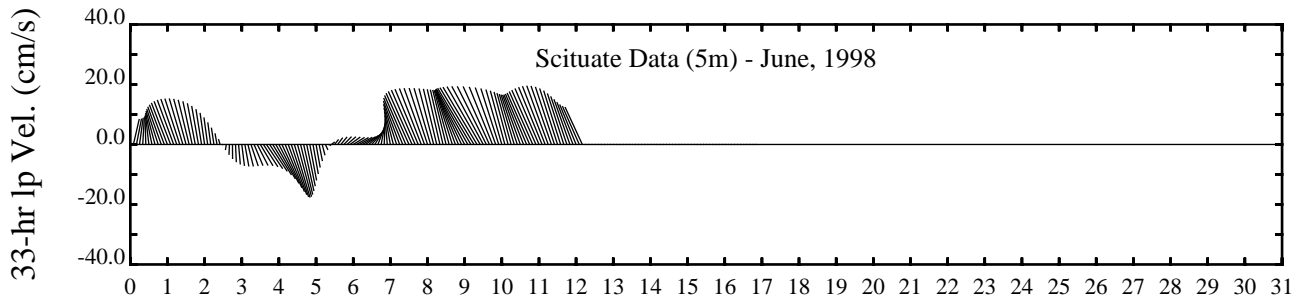
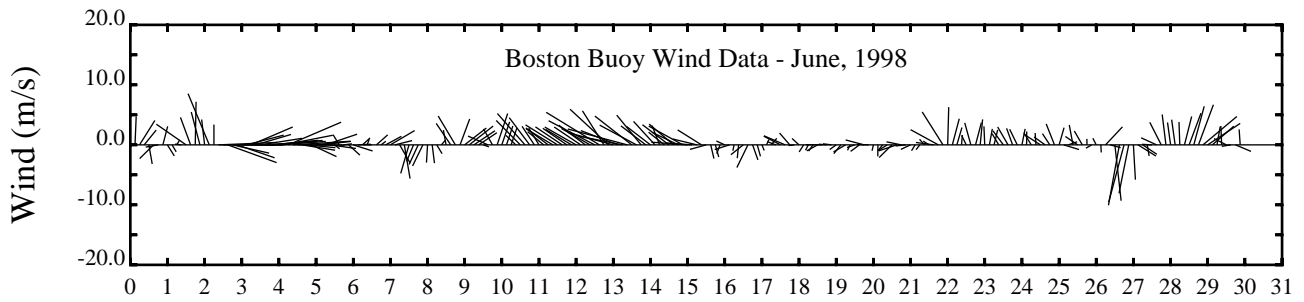


Day

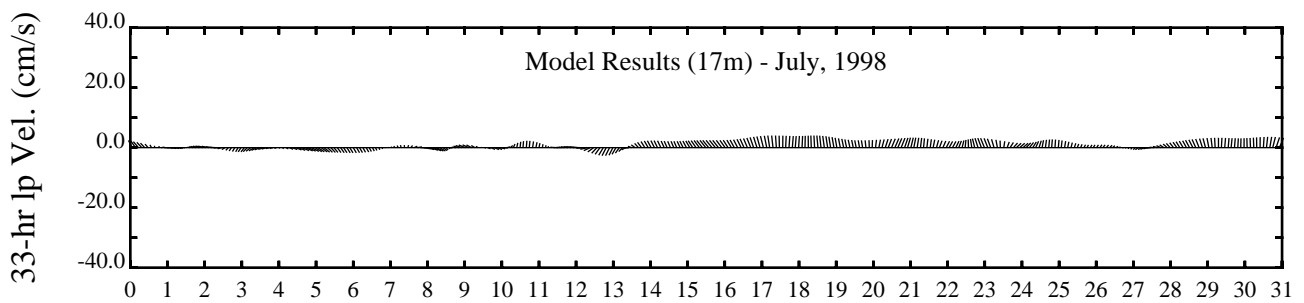
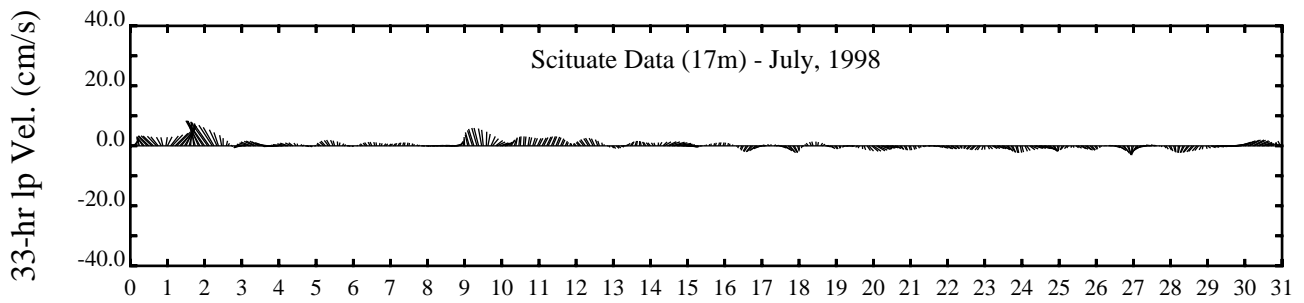
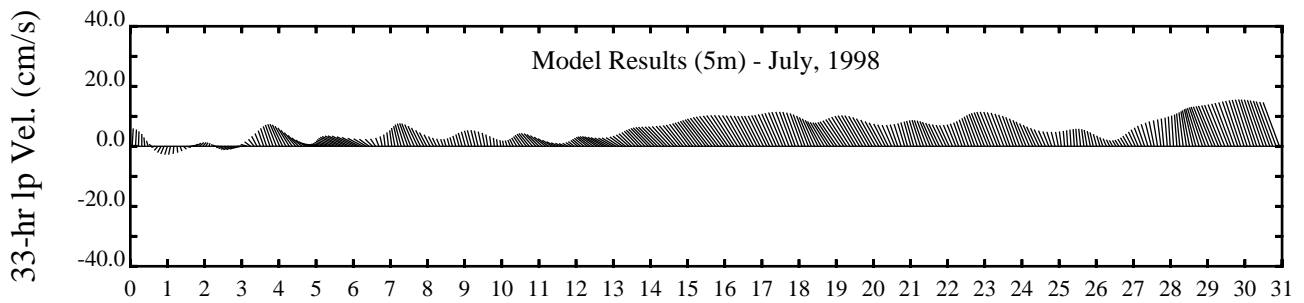
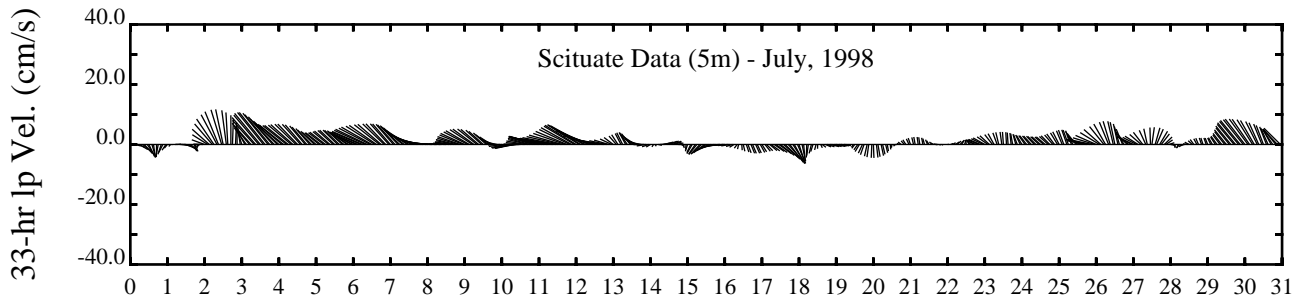
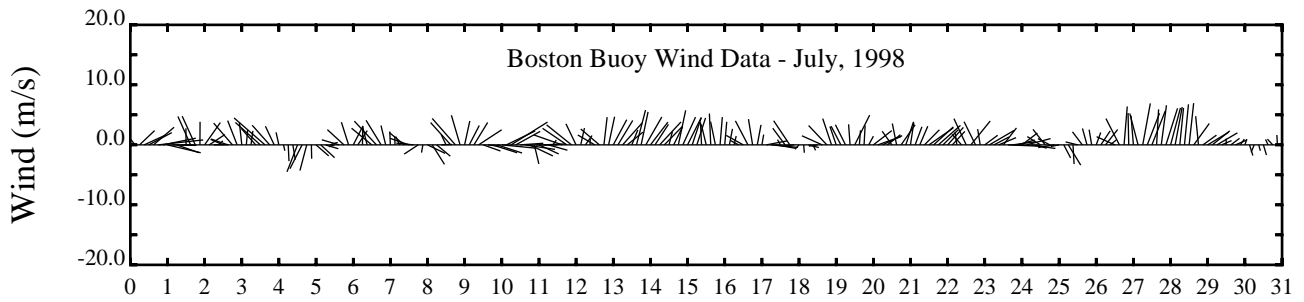




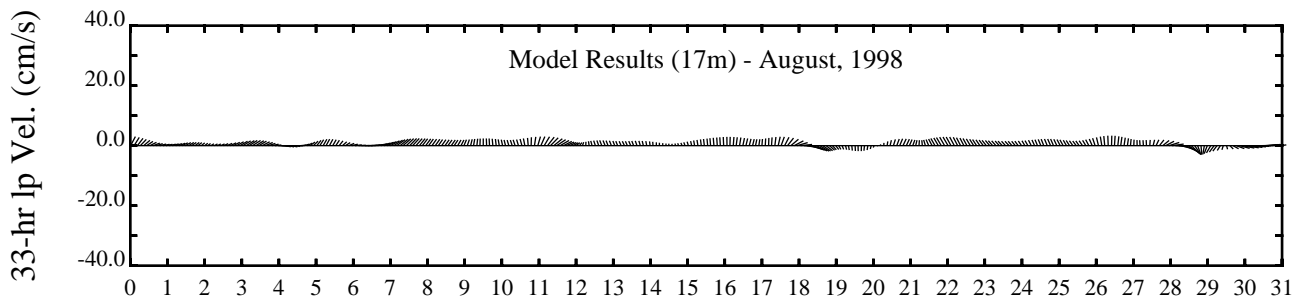
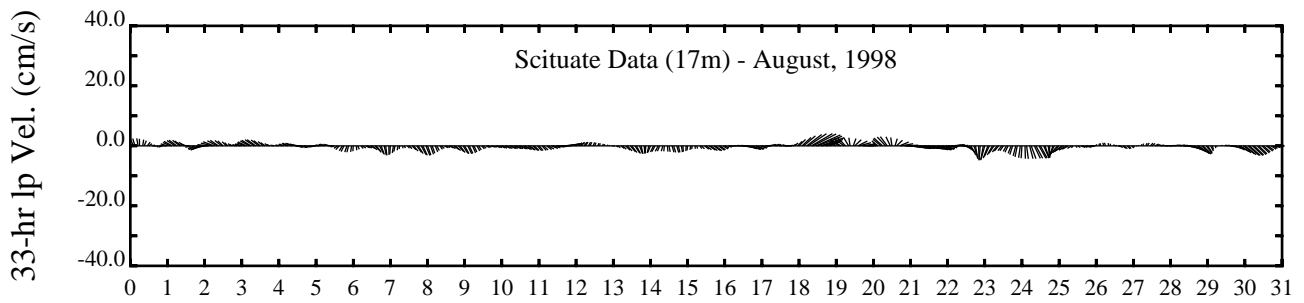
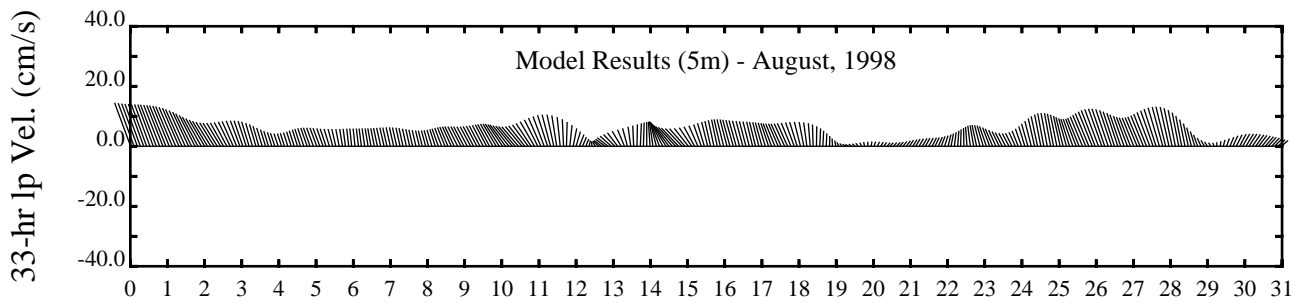
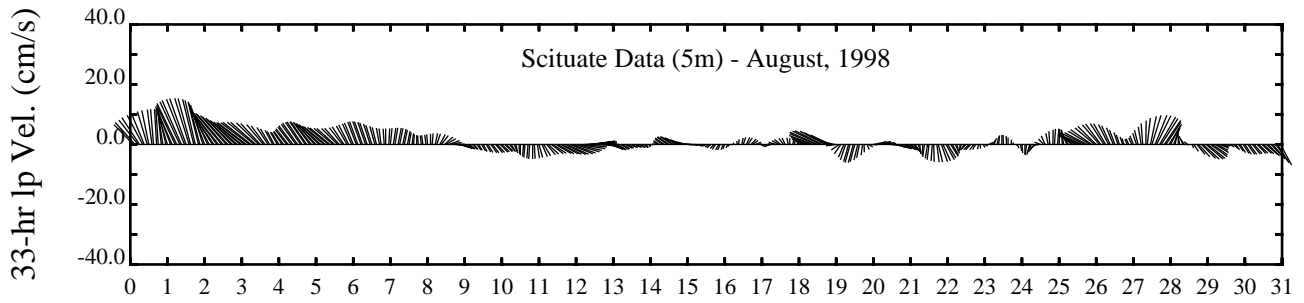
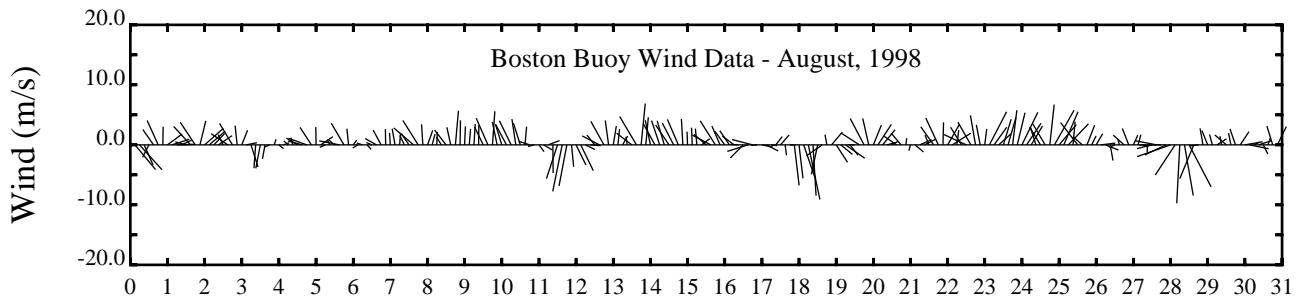
Day



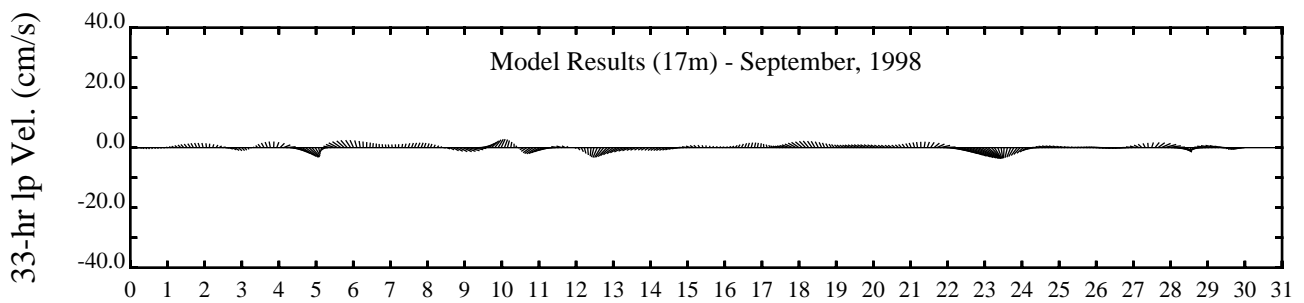
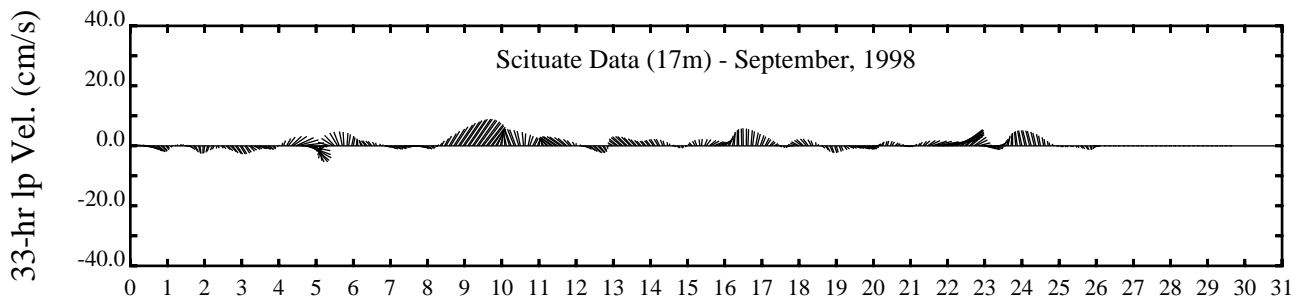
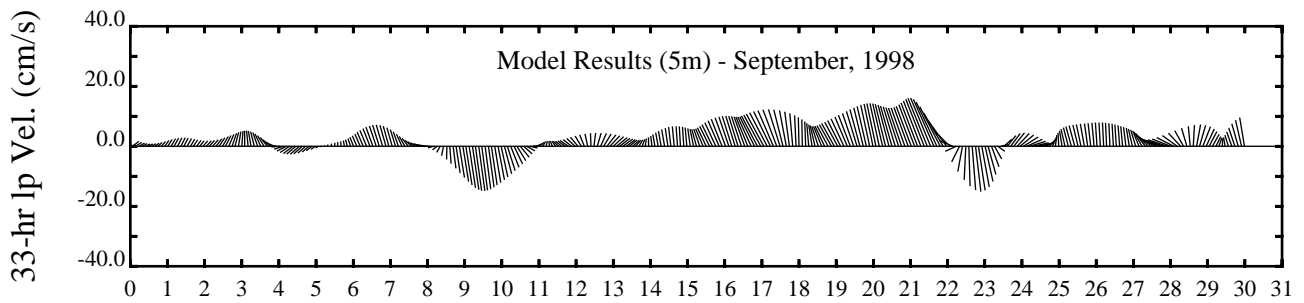
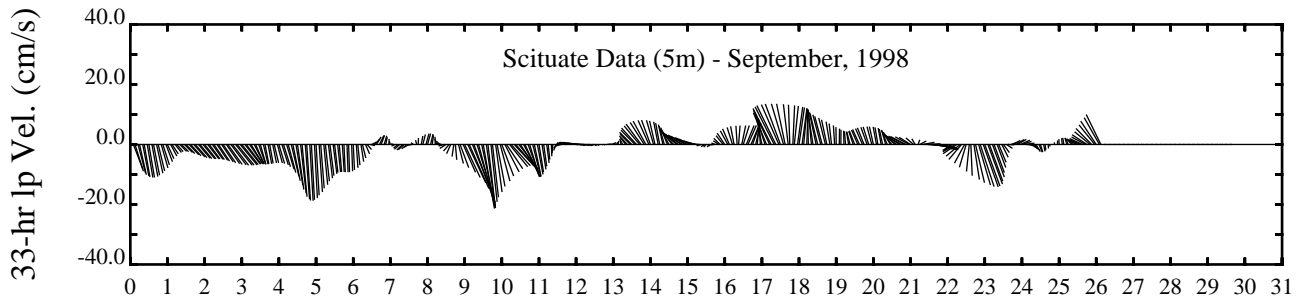
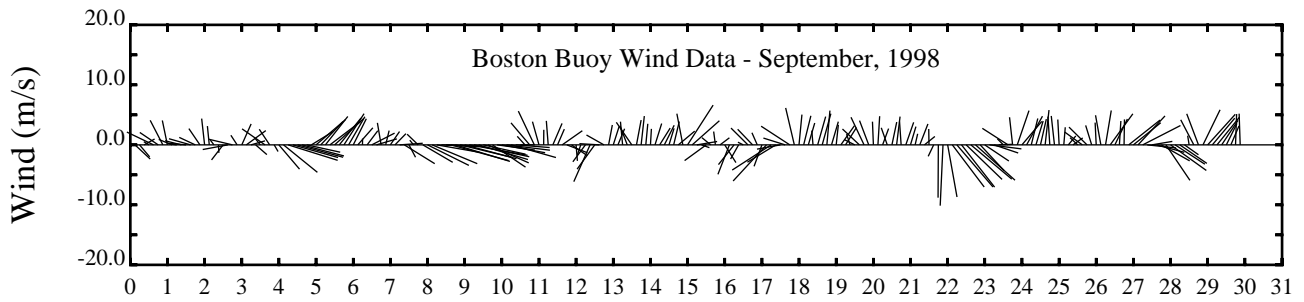
Day



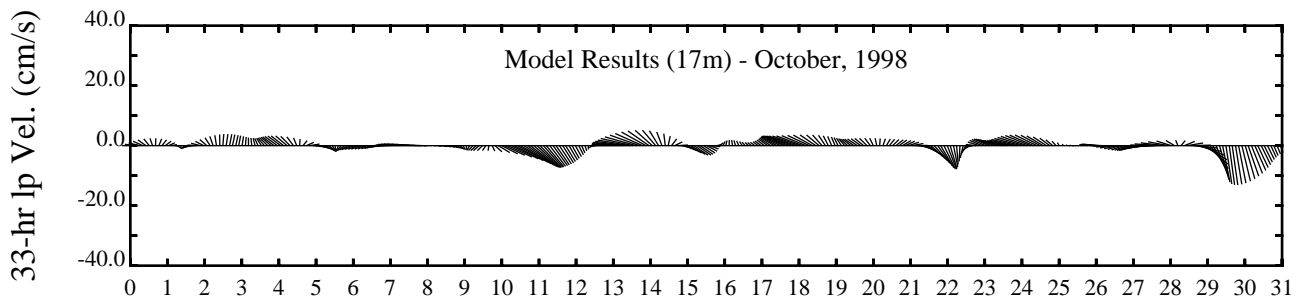
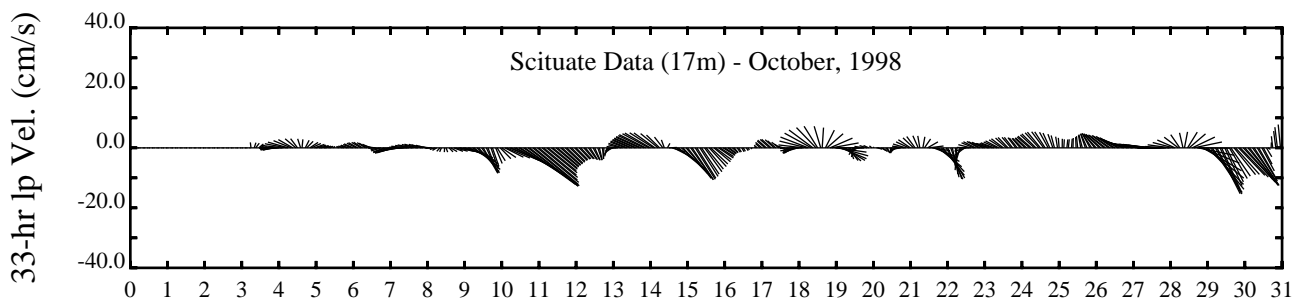
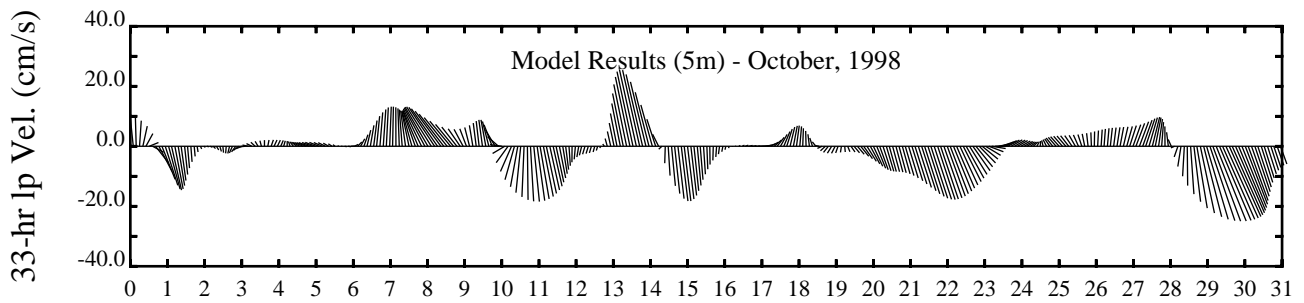
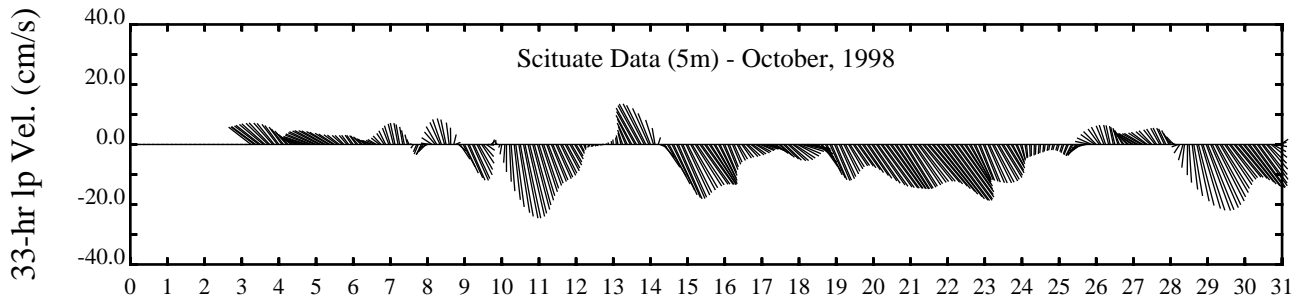
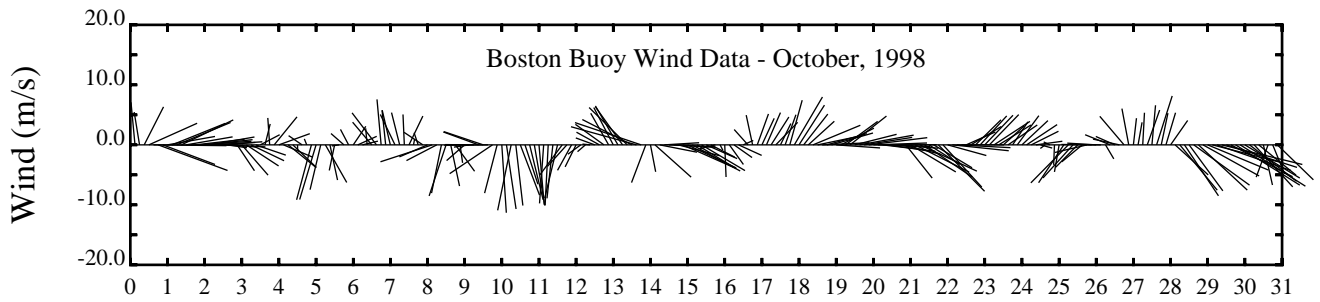
Day



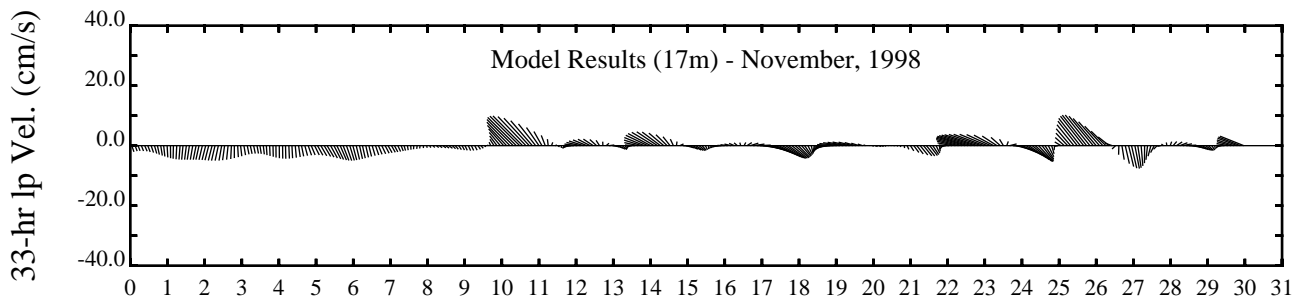
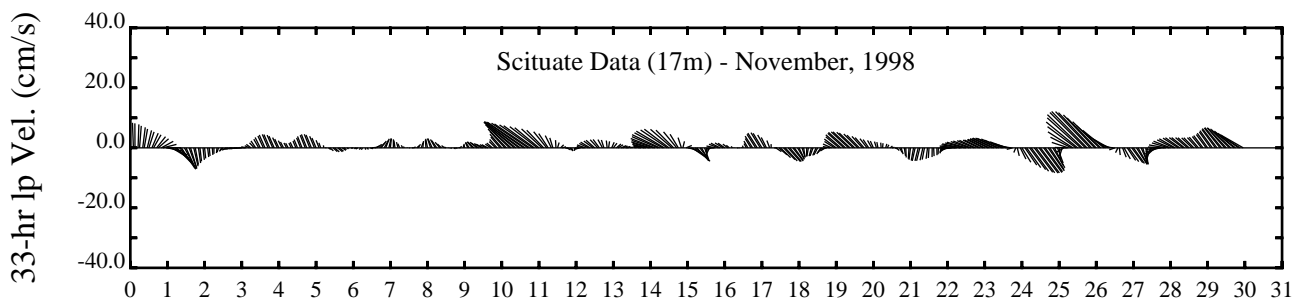
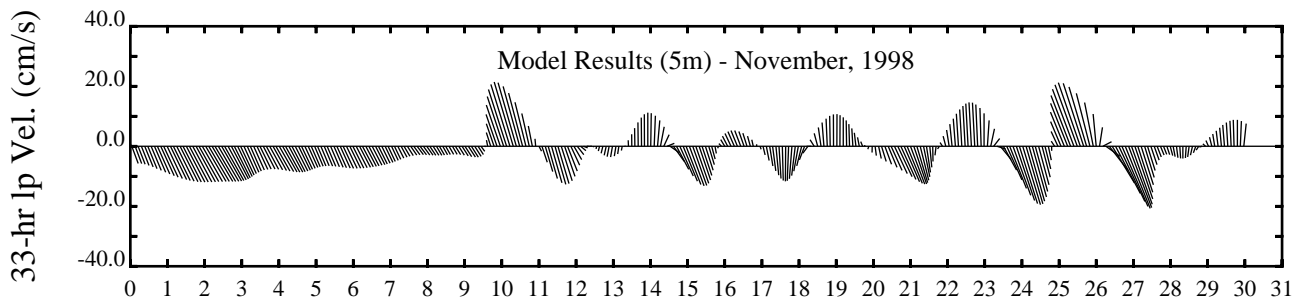
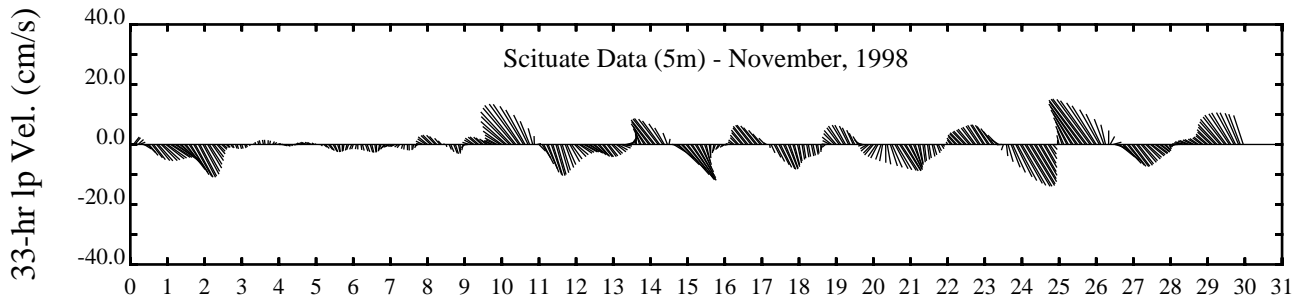
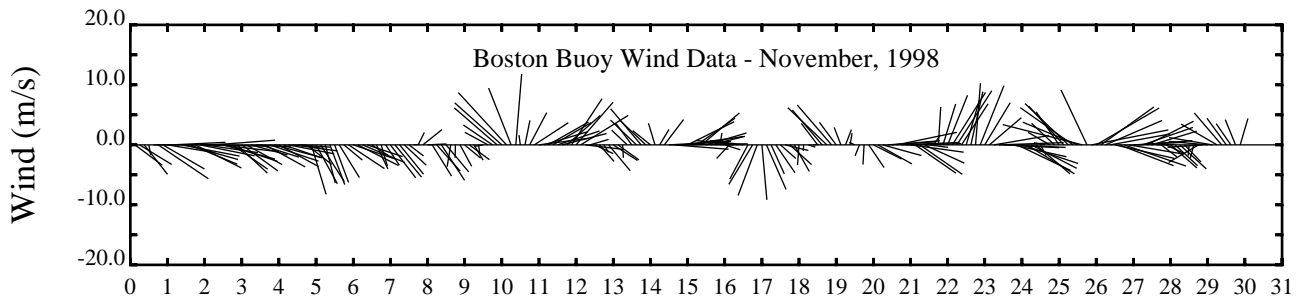
Day



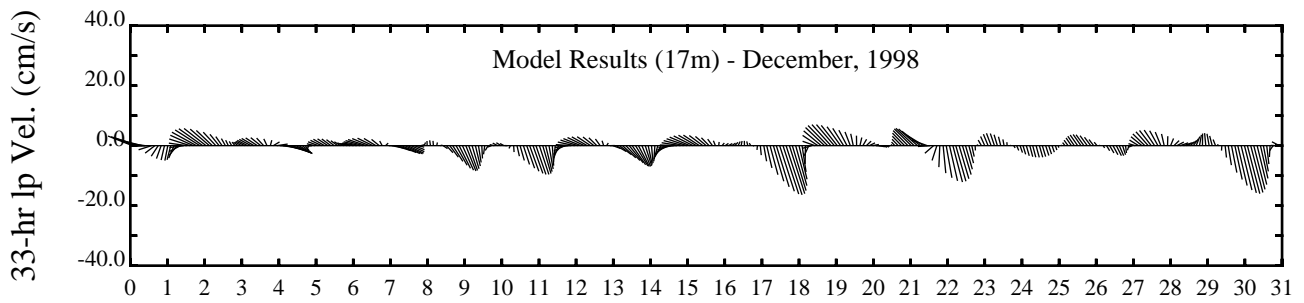
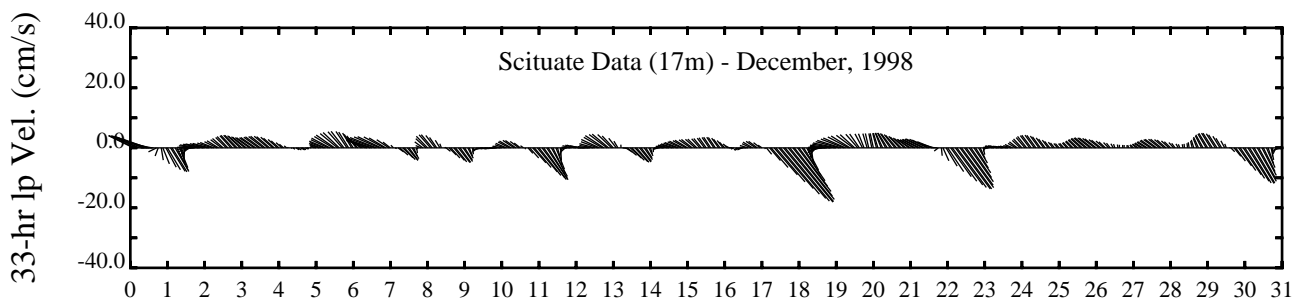
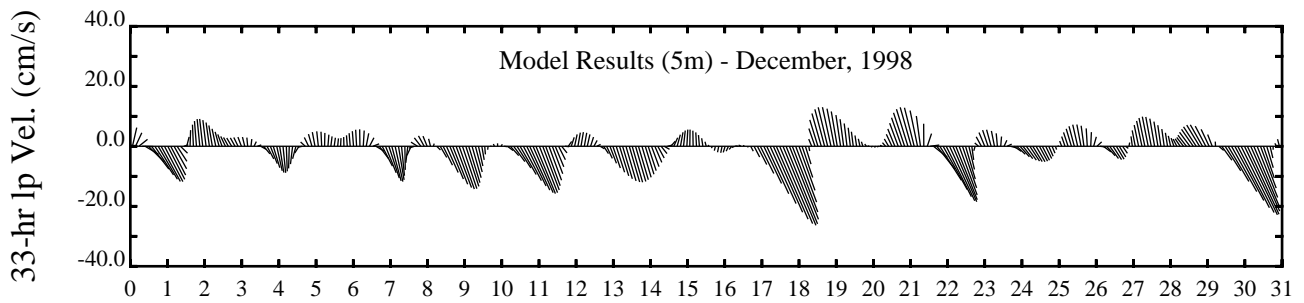
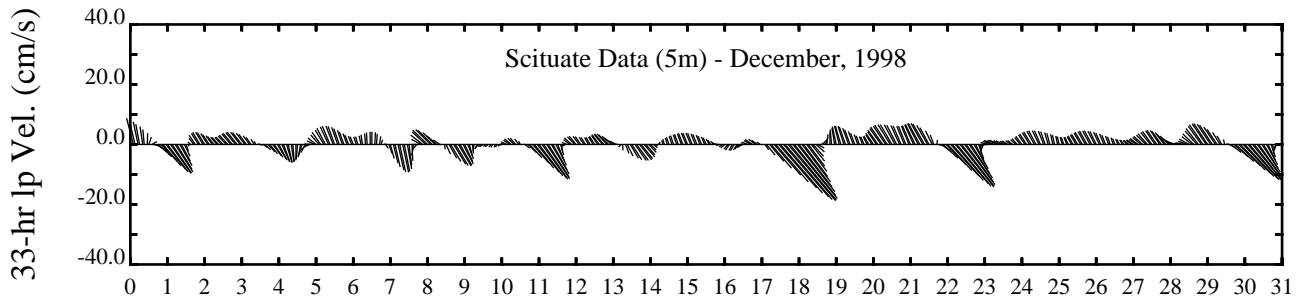
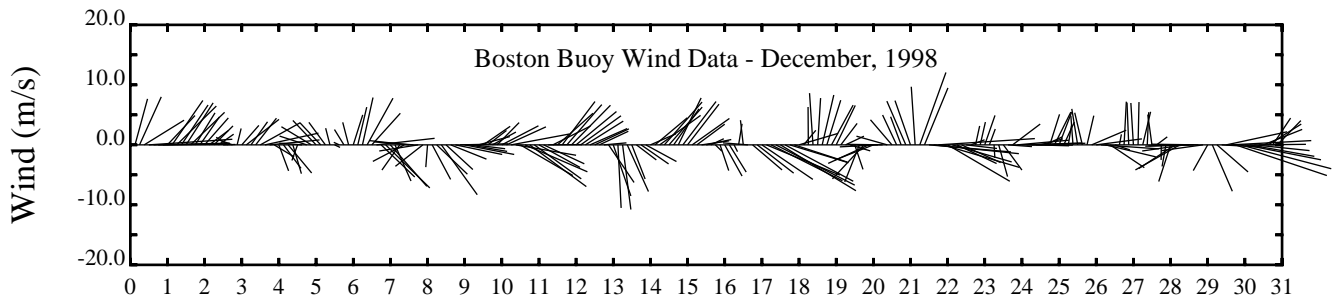
Day

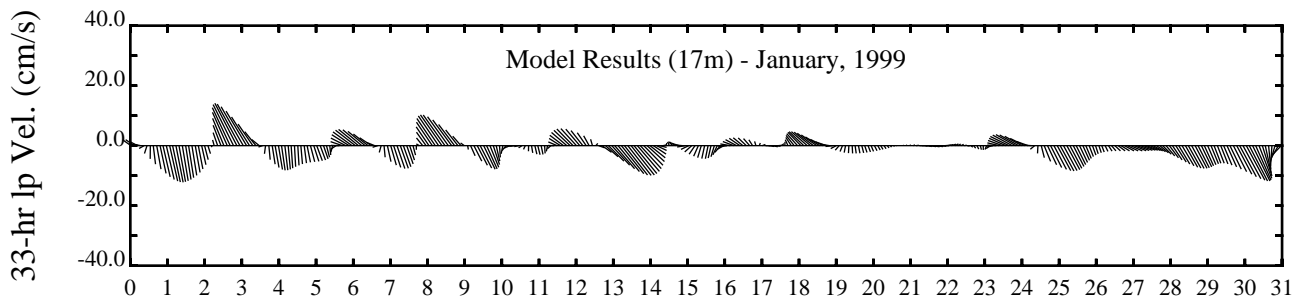
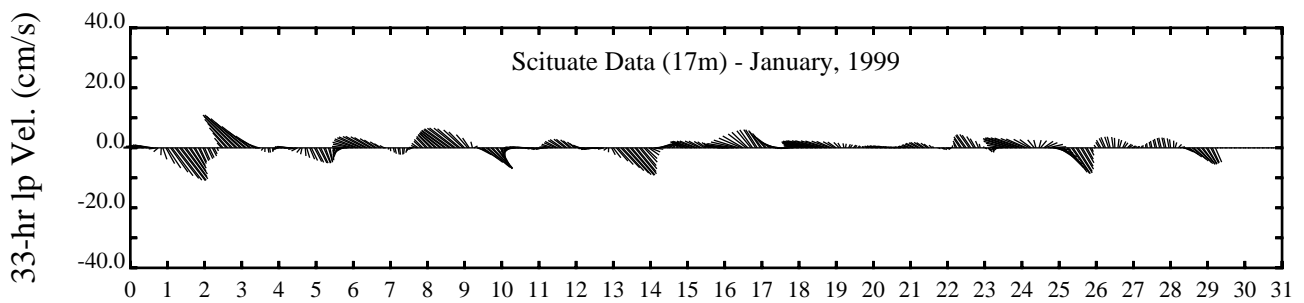
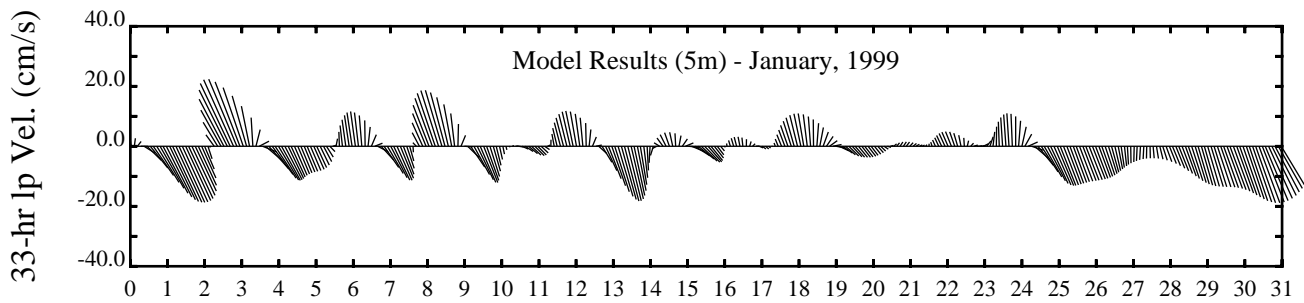
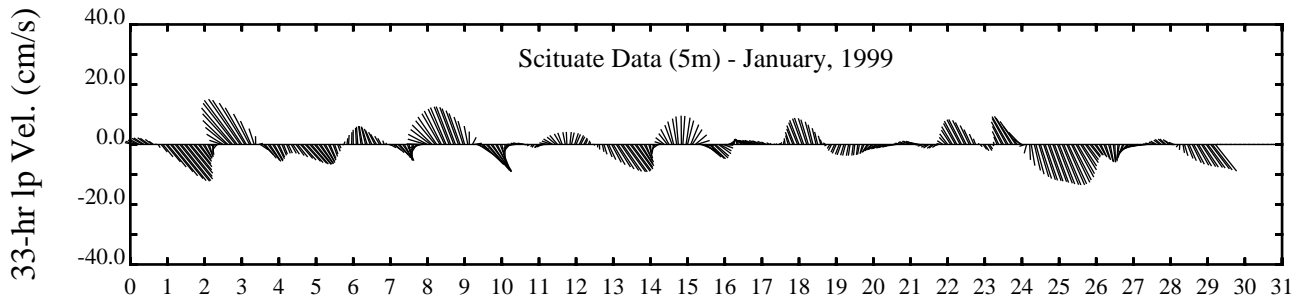
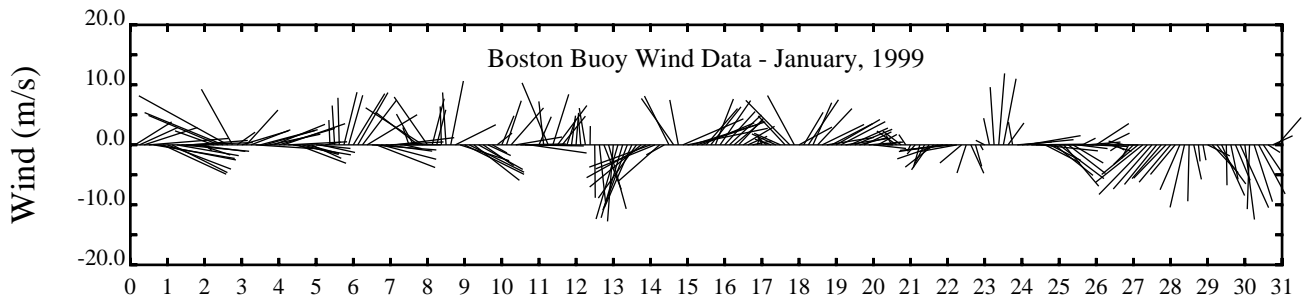


Day

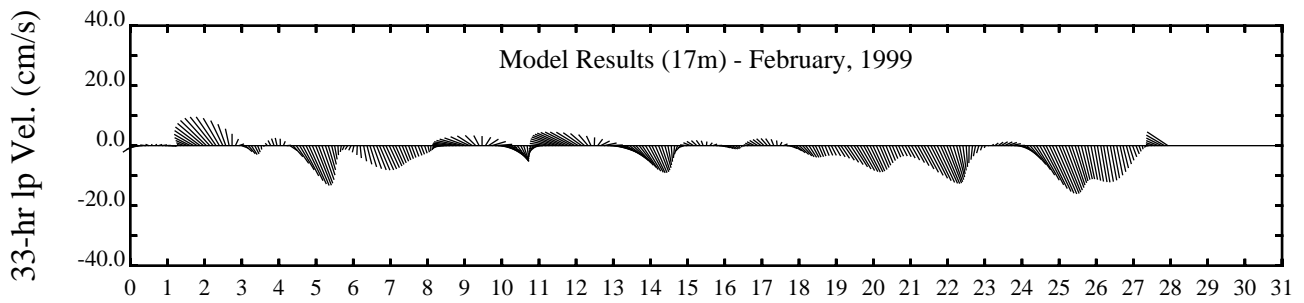
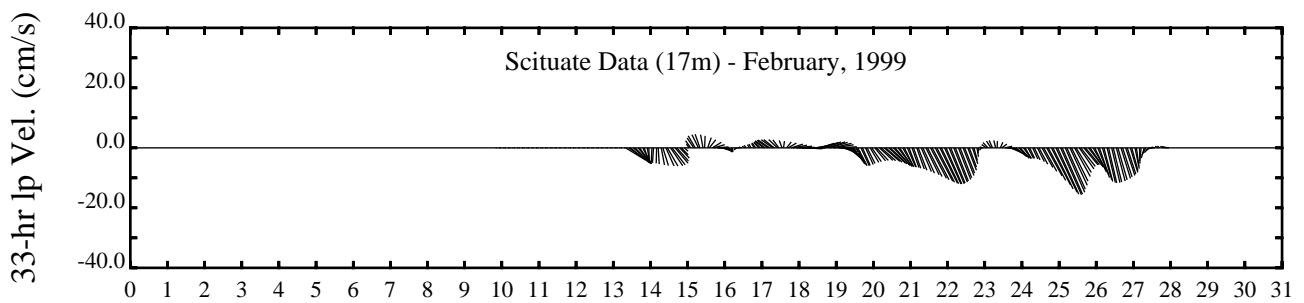
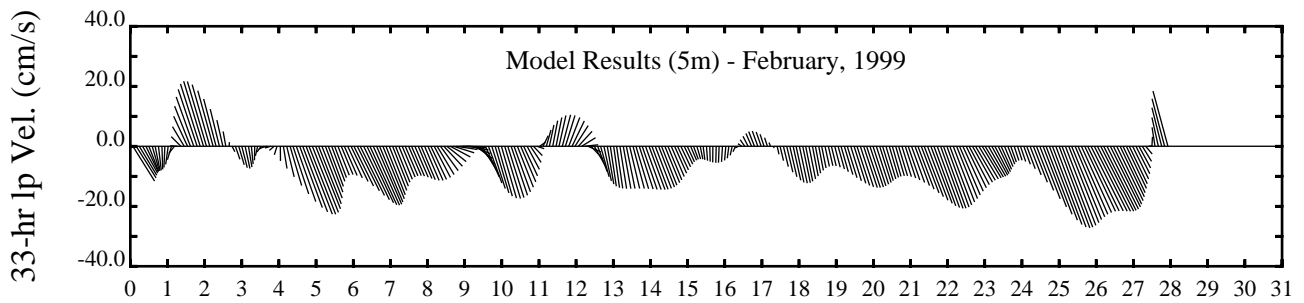
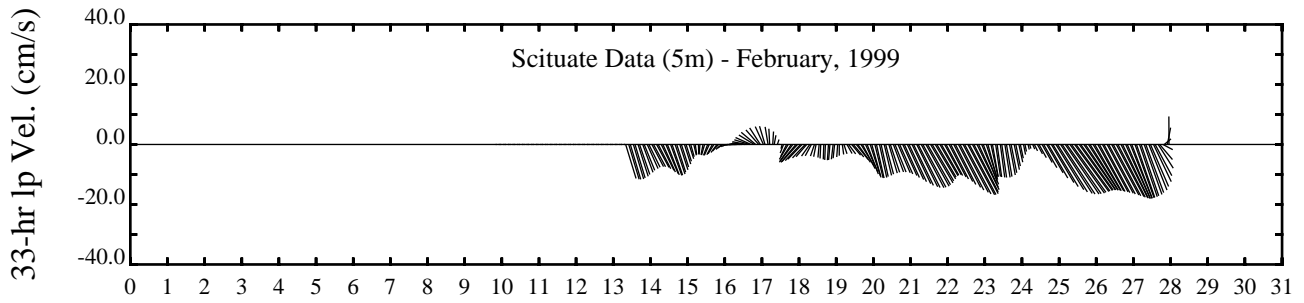
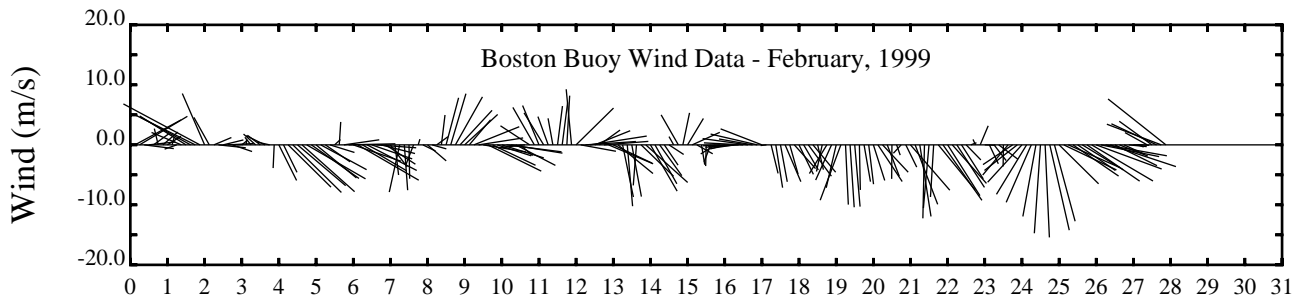


Day

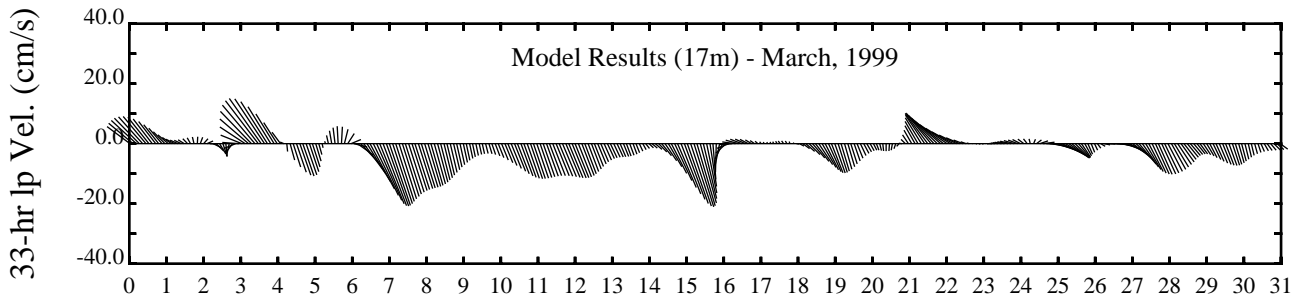
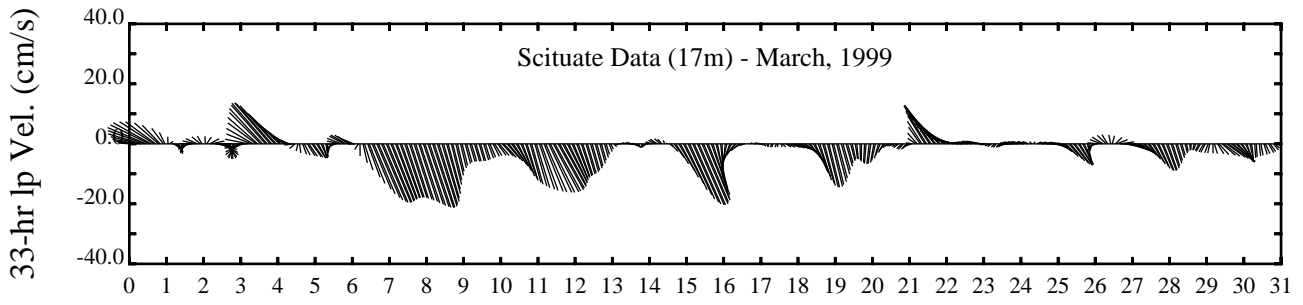
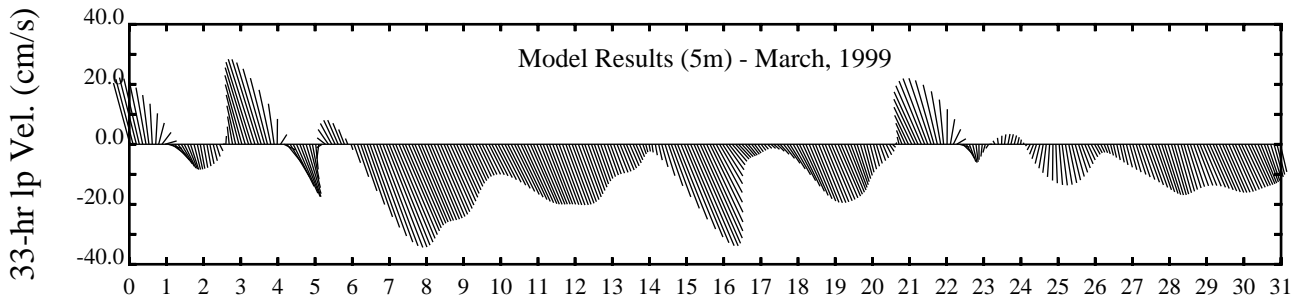
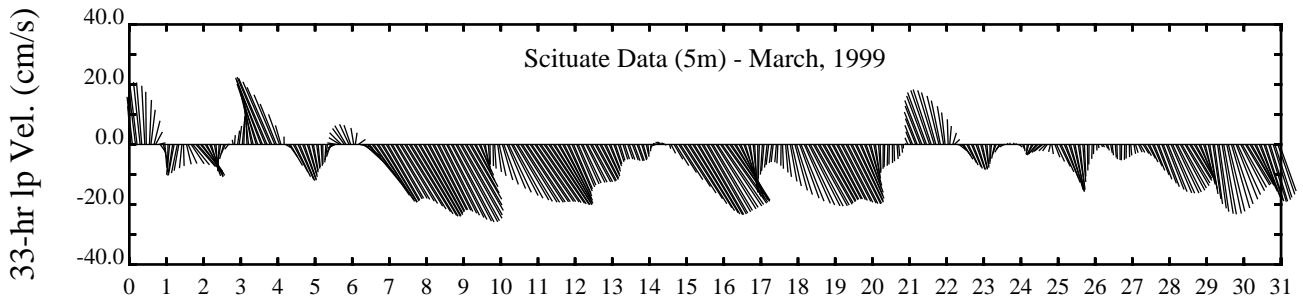
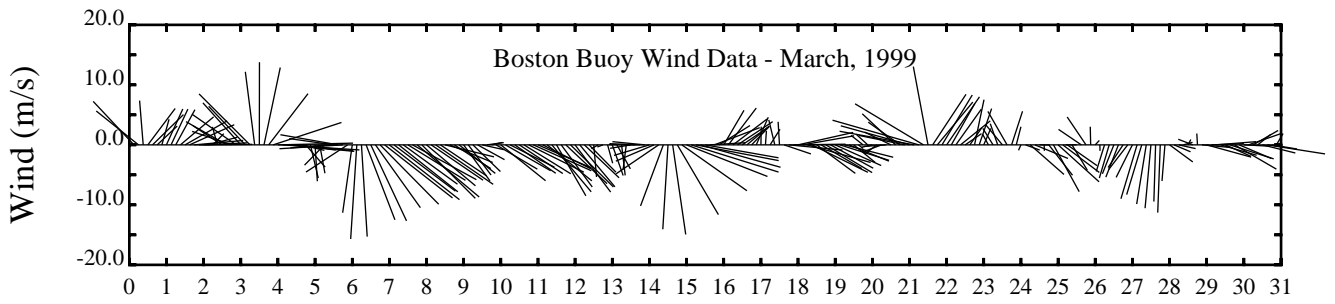




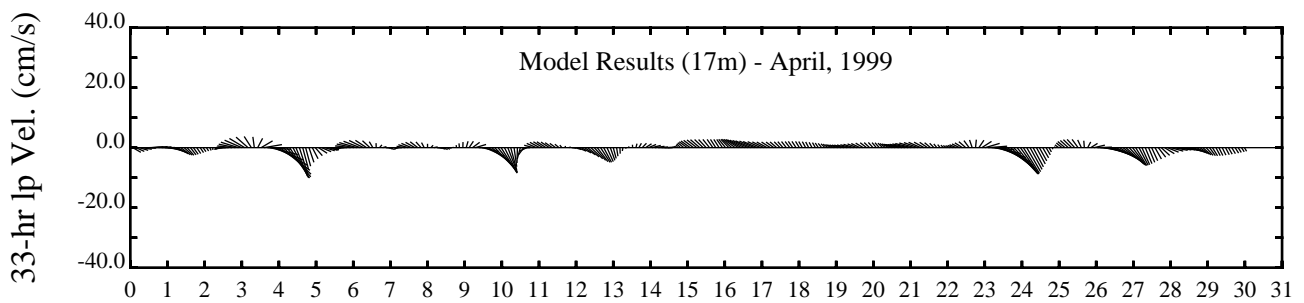
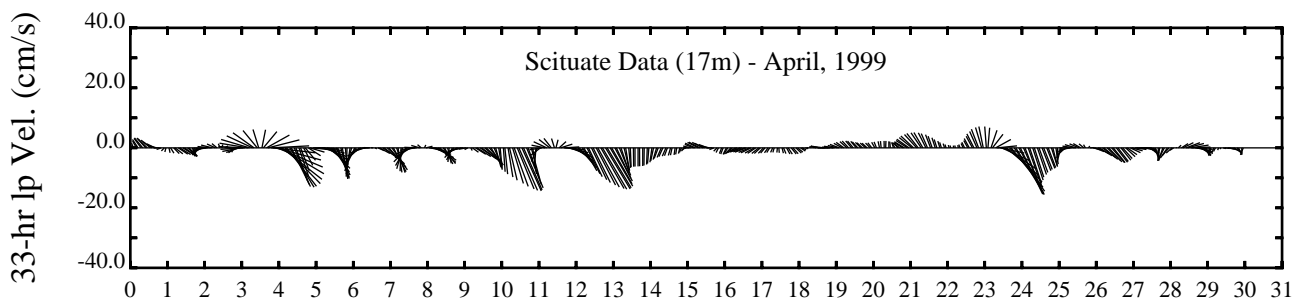
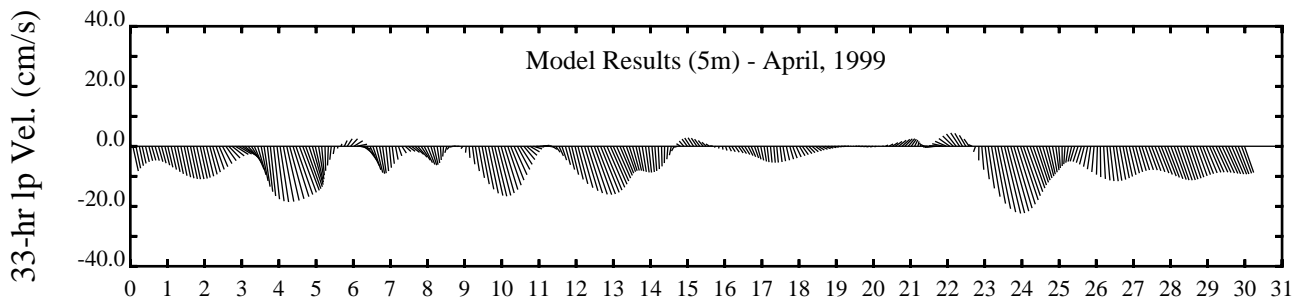
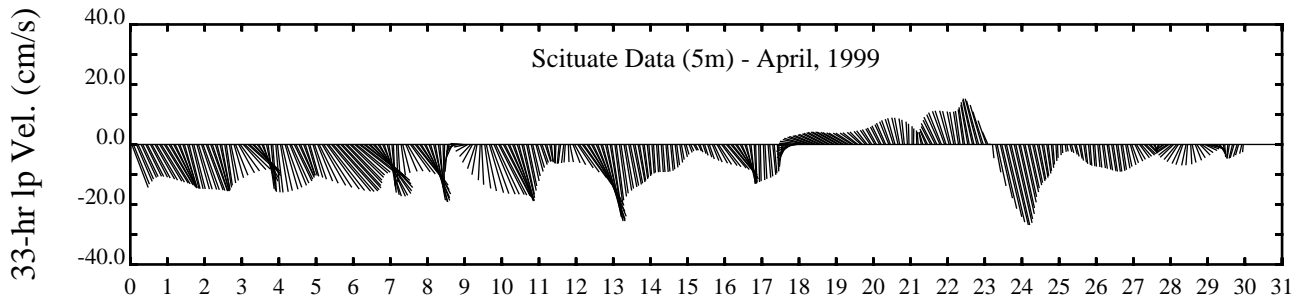
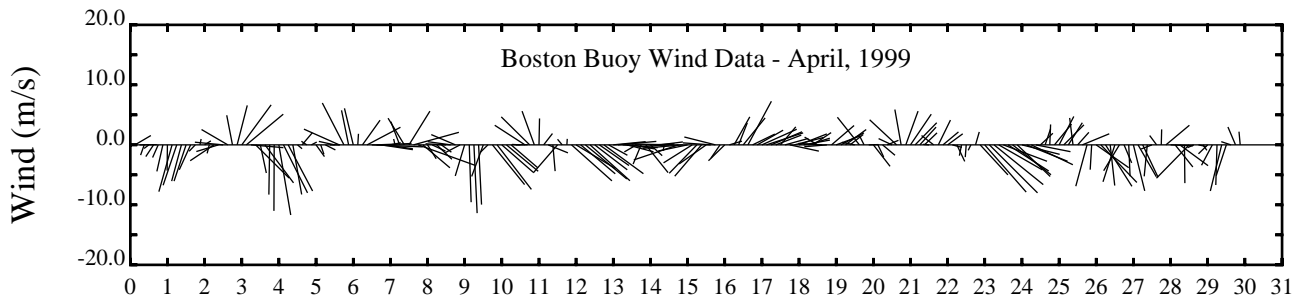
Day



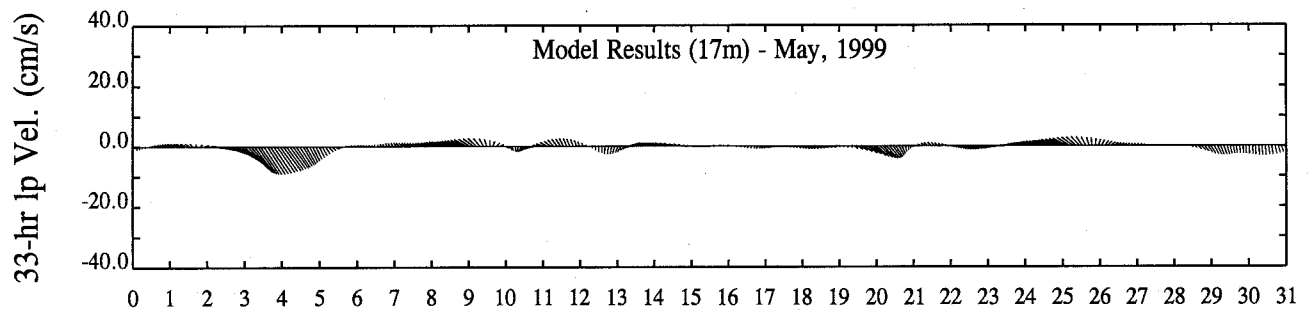
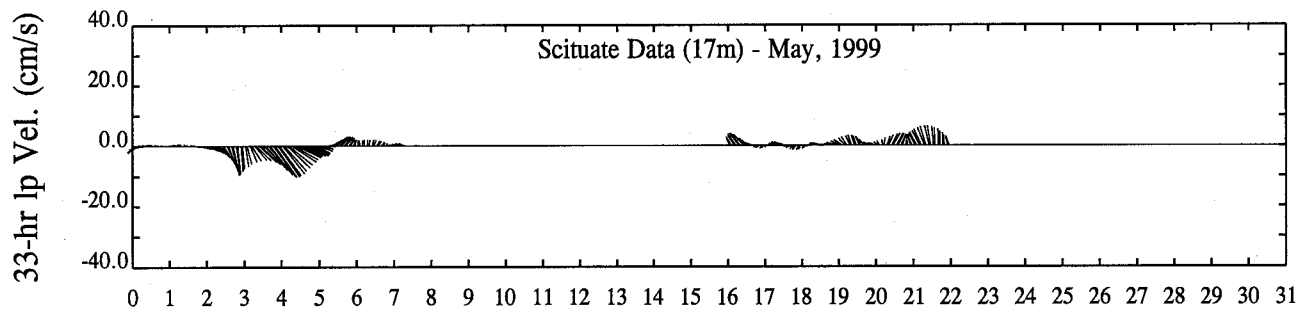
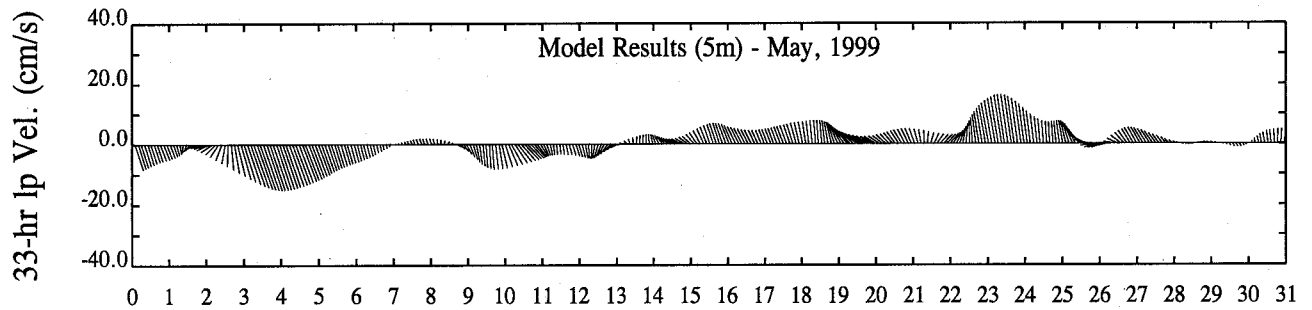
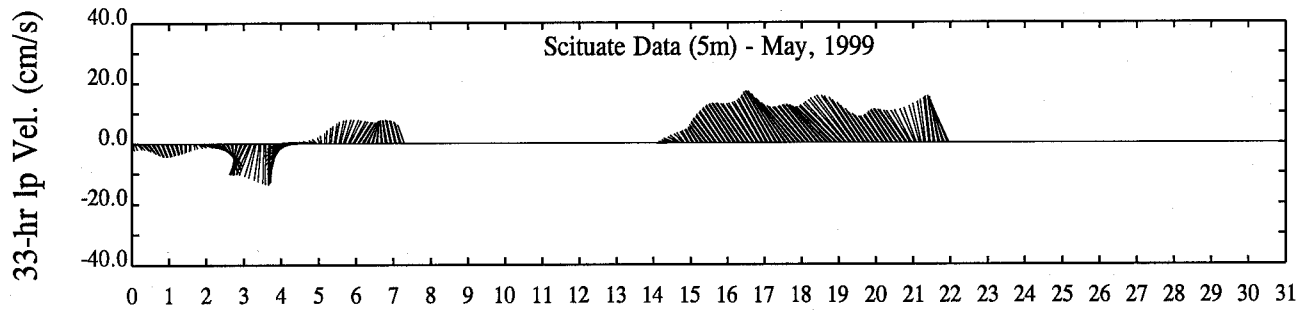
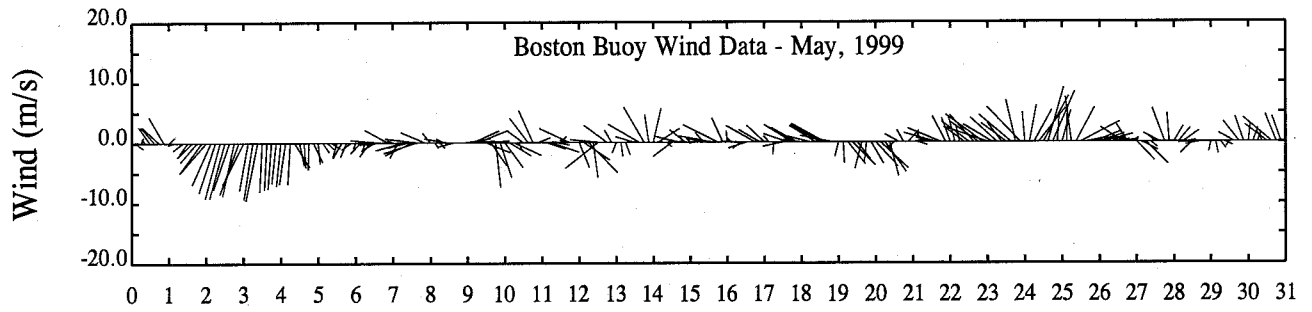
Day



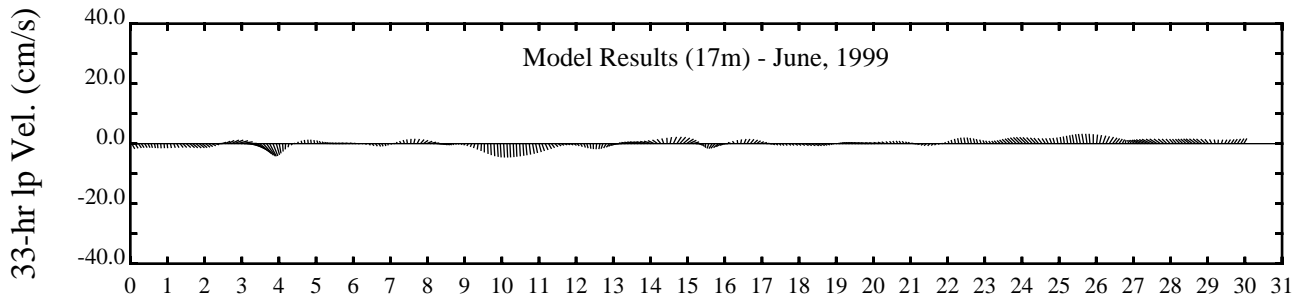
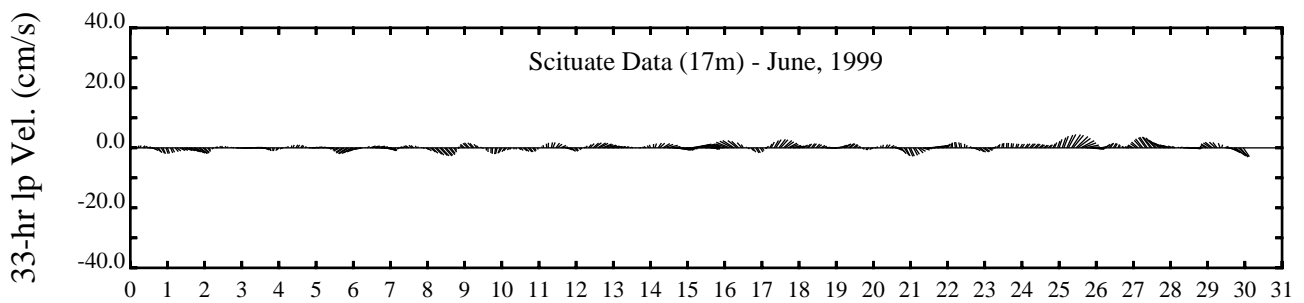
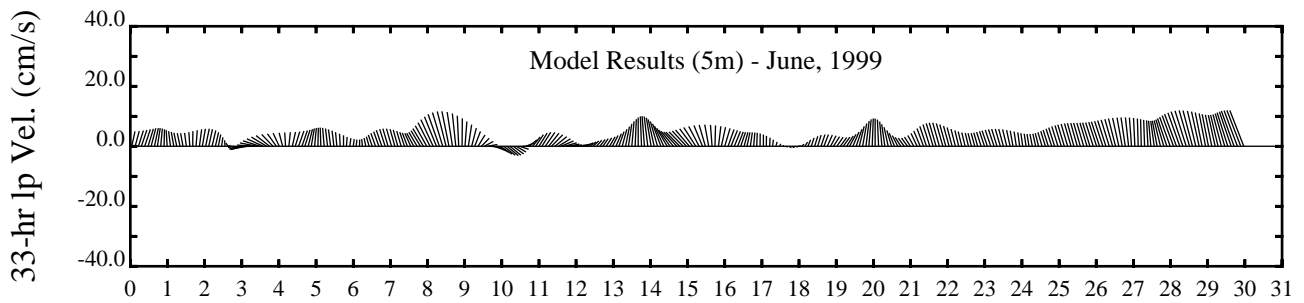
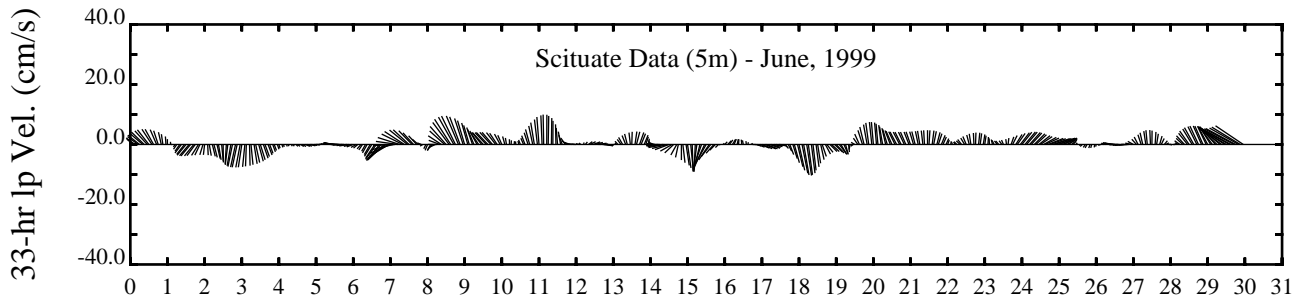
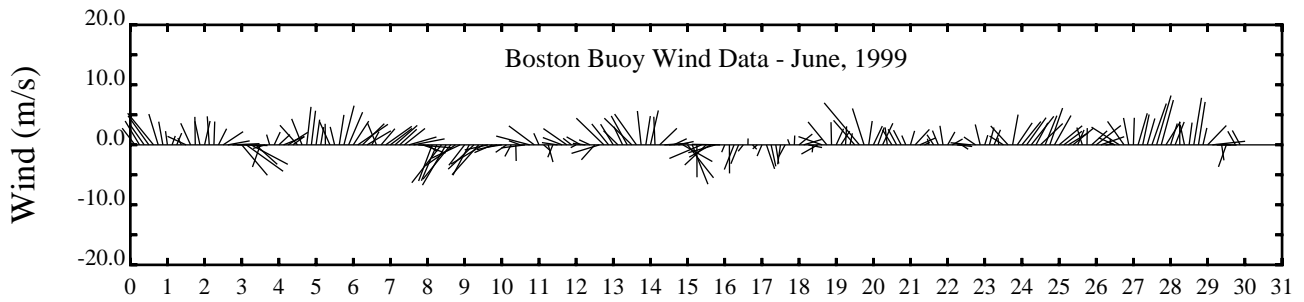
Day



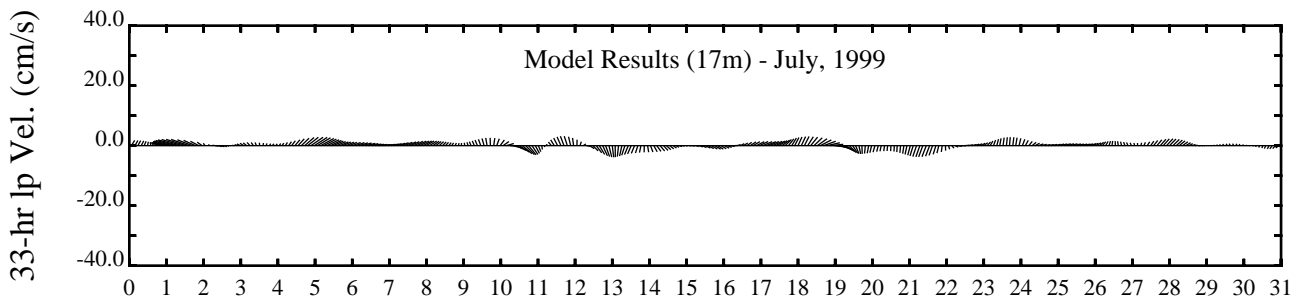
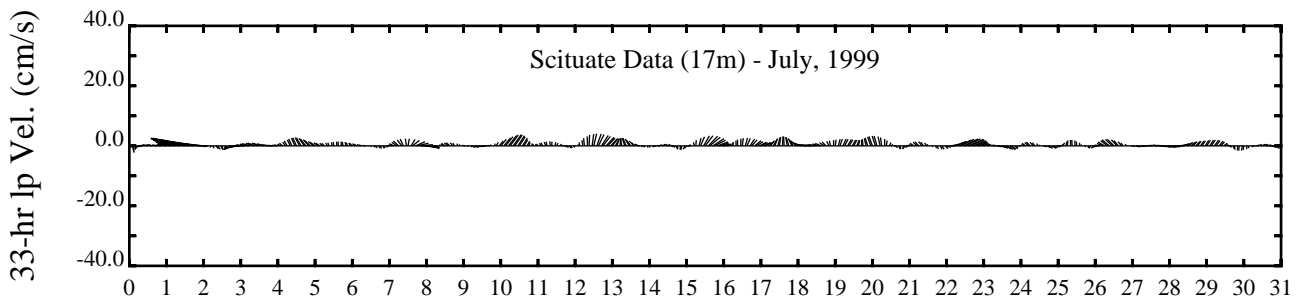
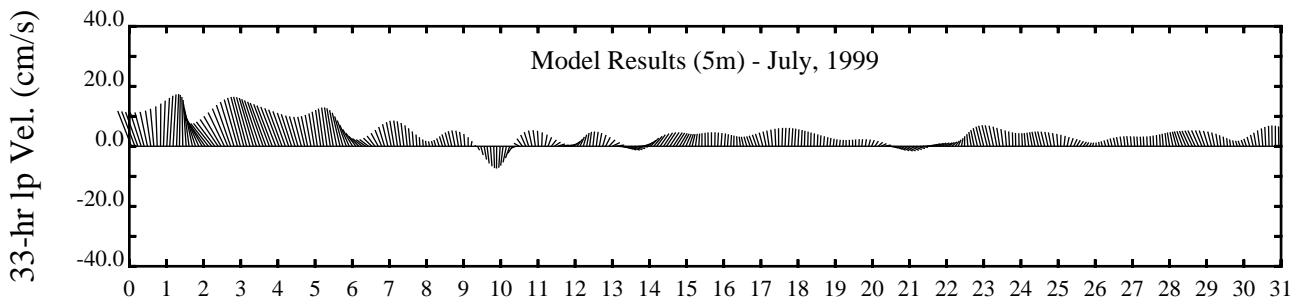
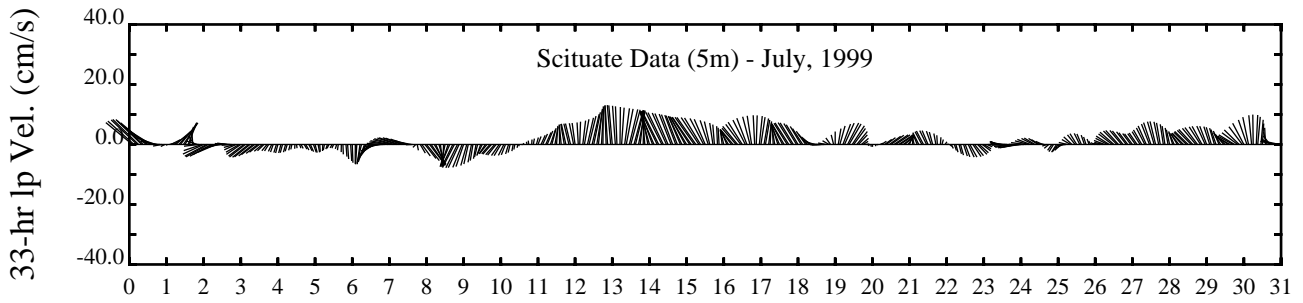
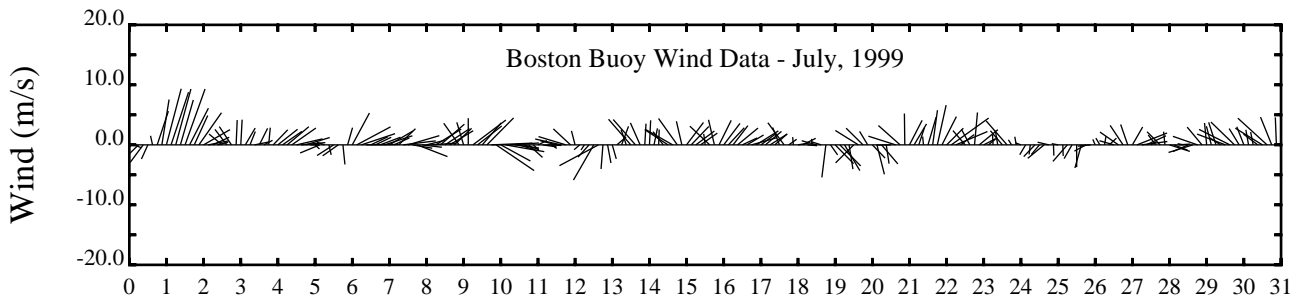
Day



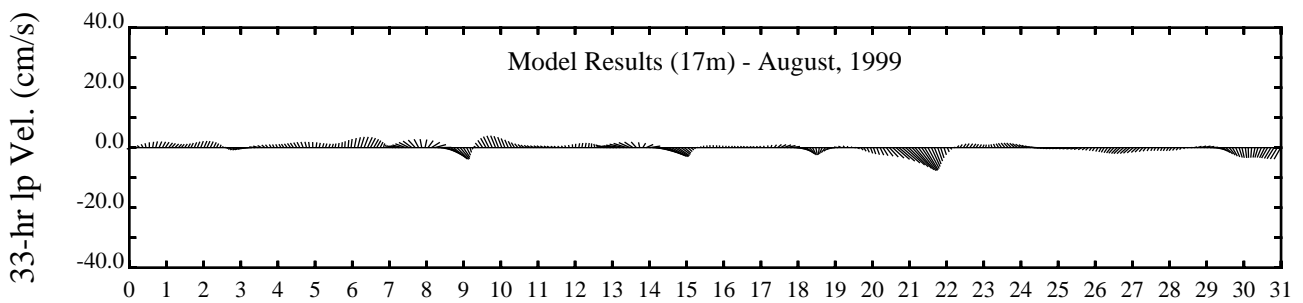
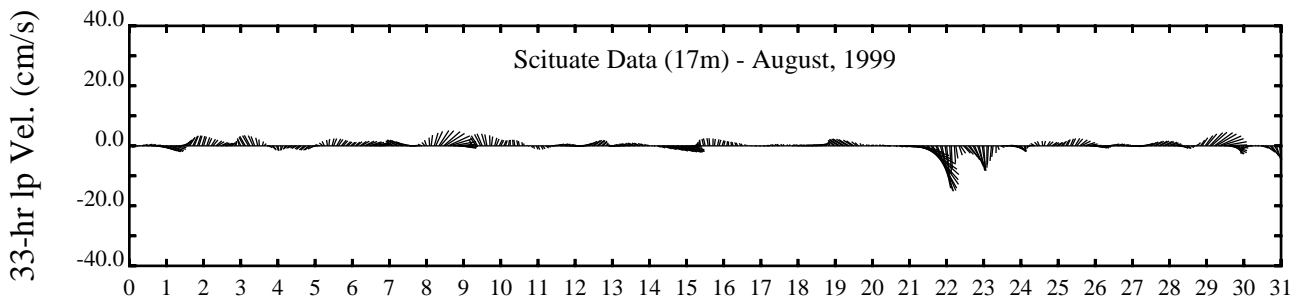
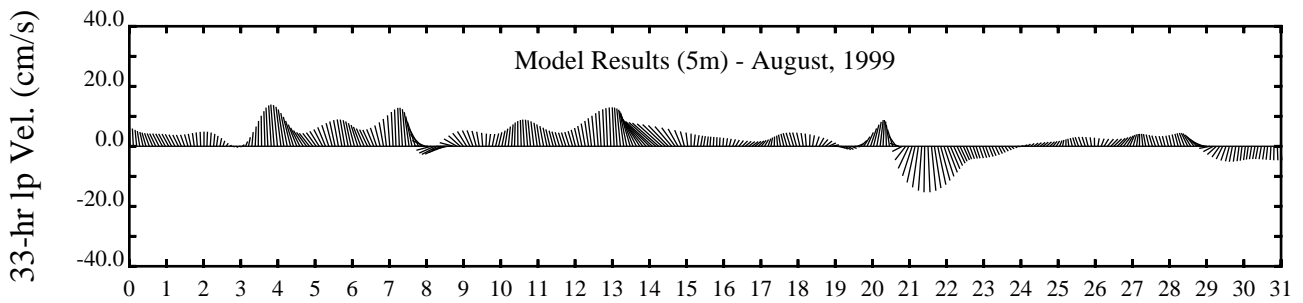
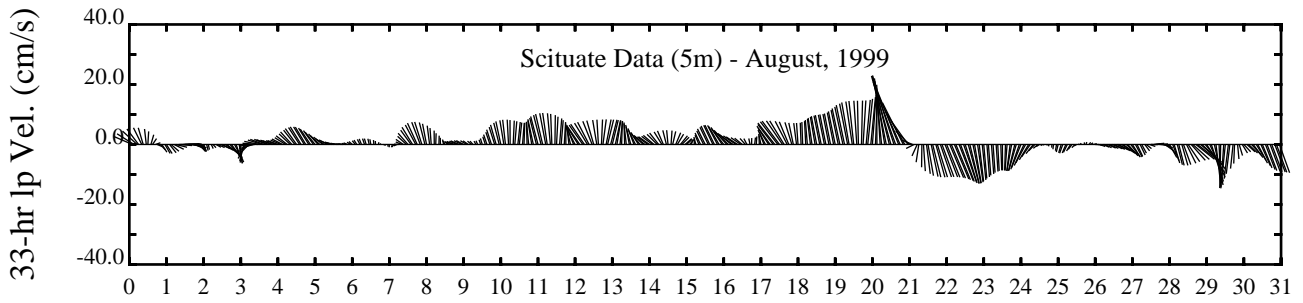
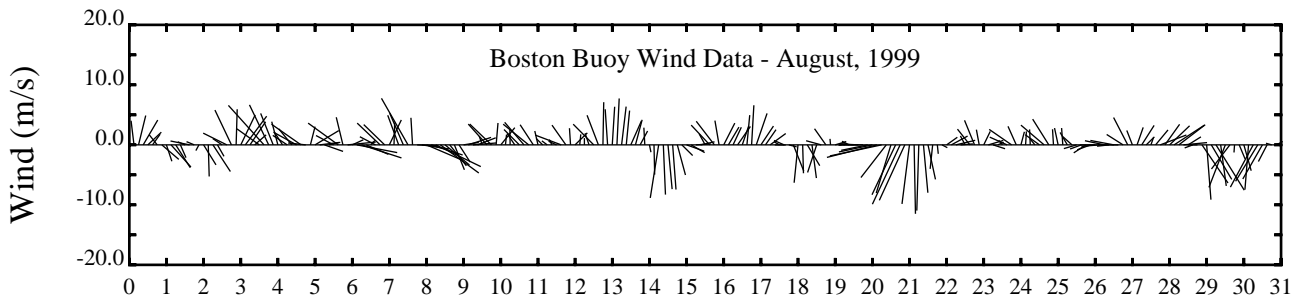
Day



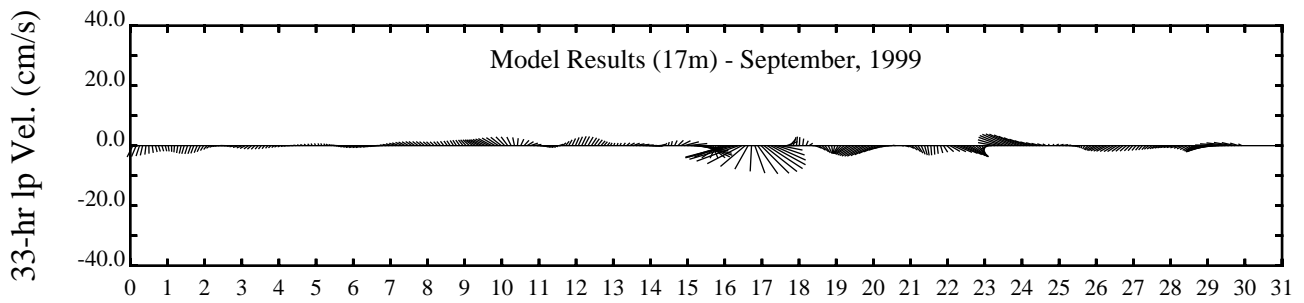
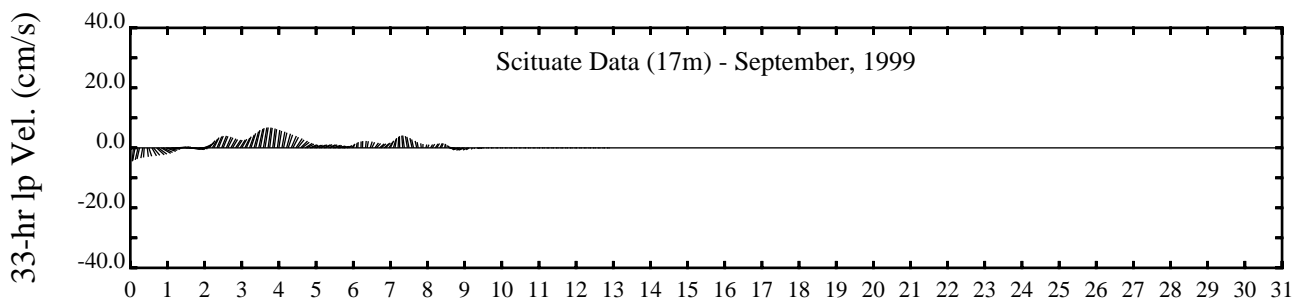
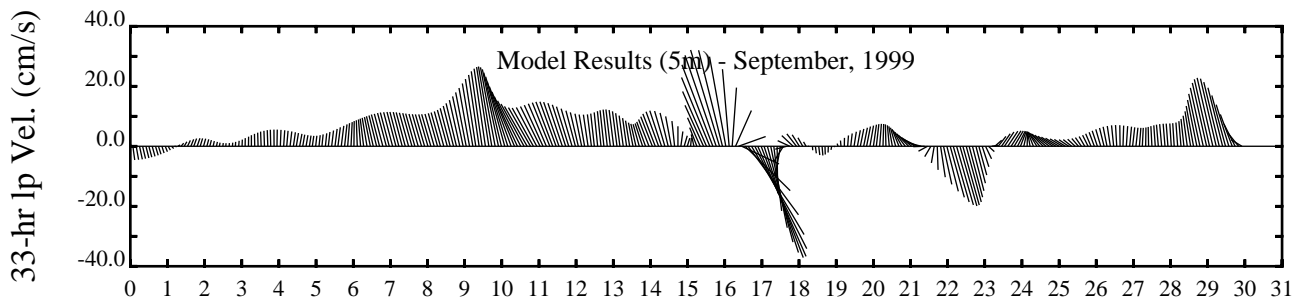
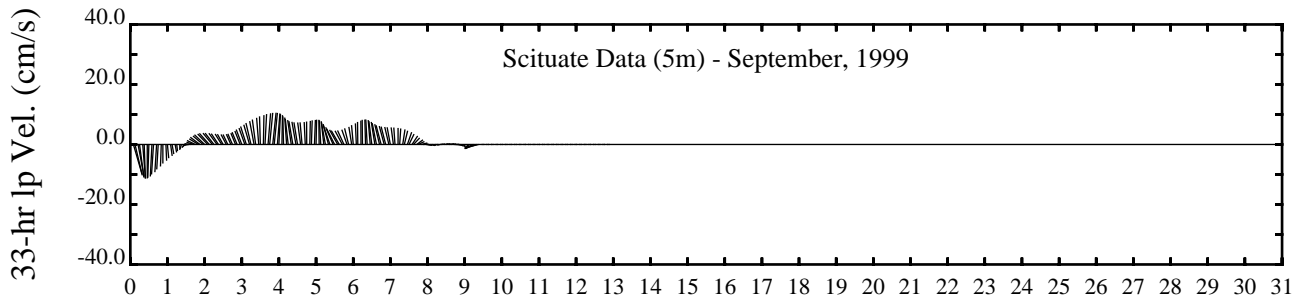
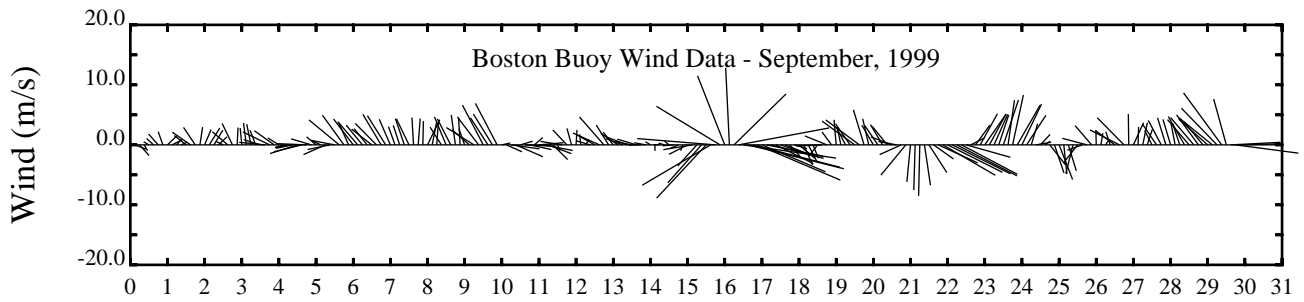
Day



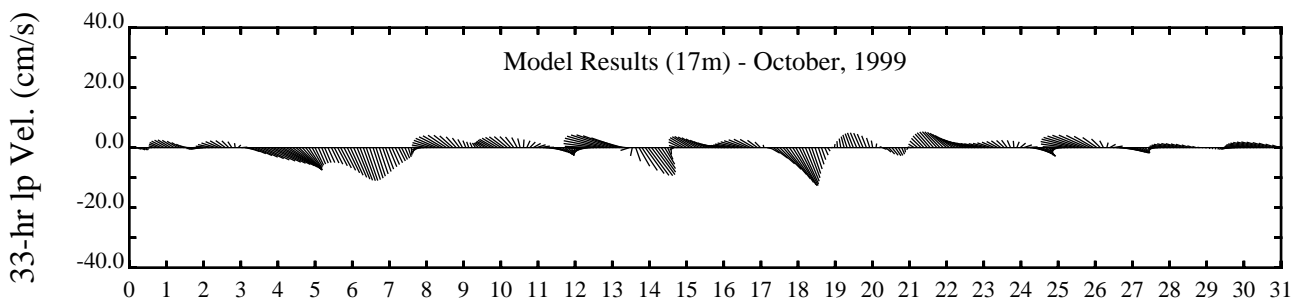
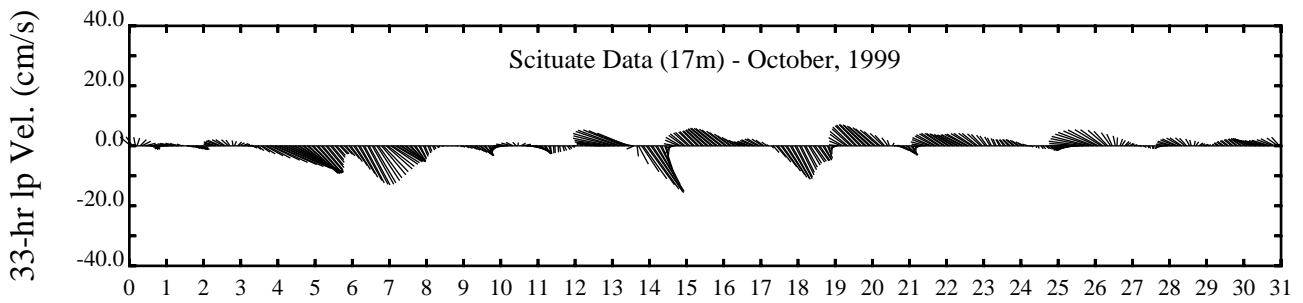
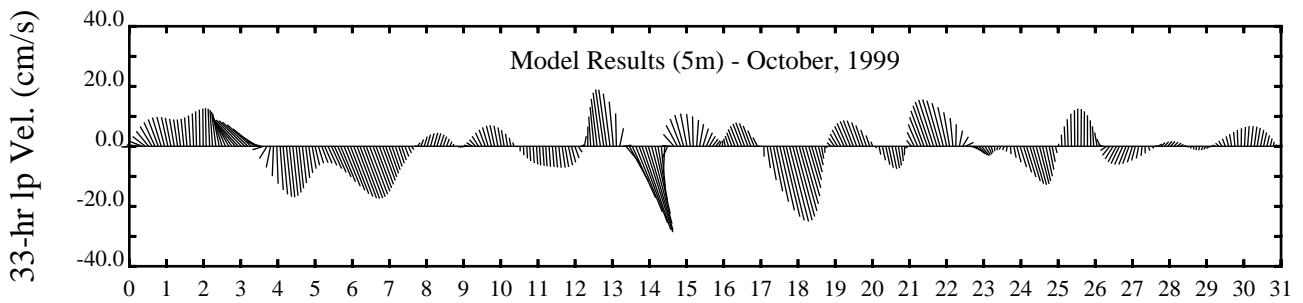
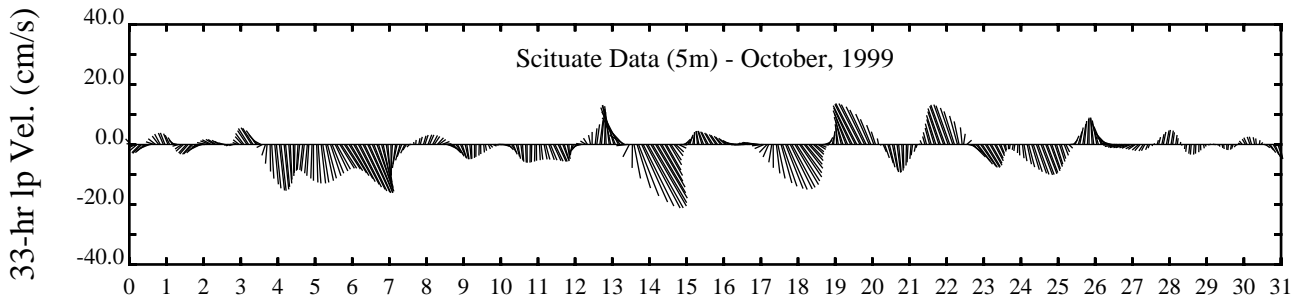
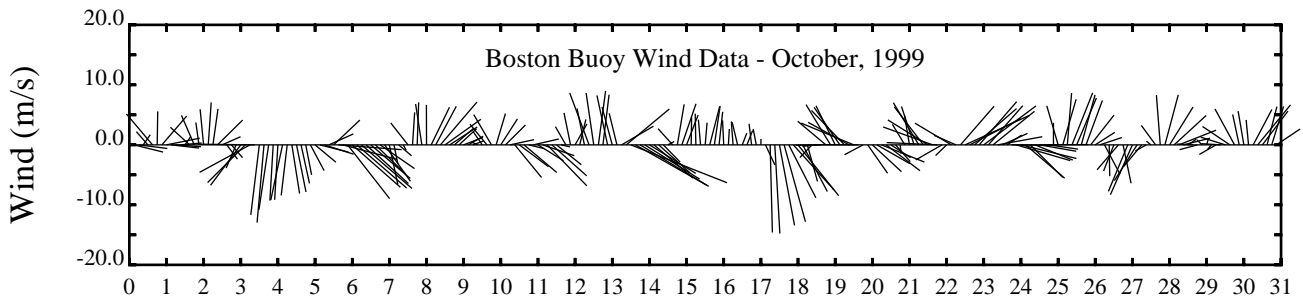
Day



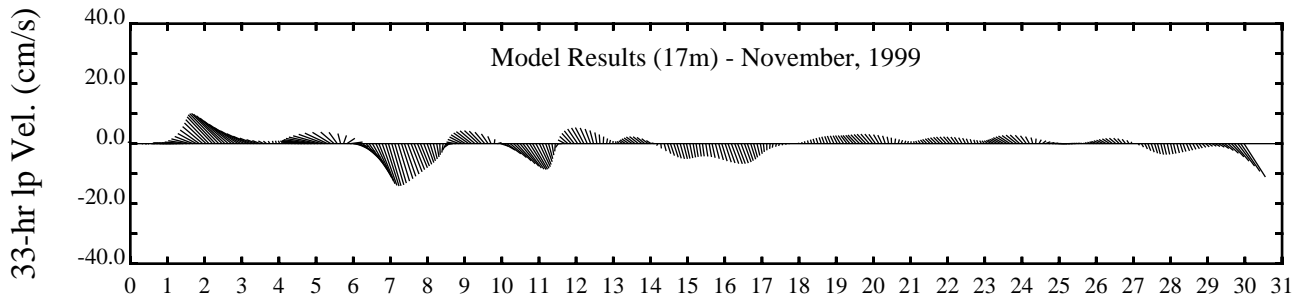
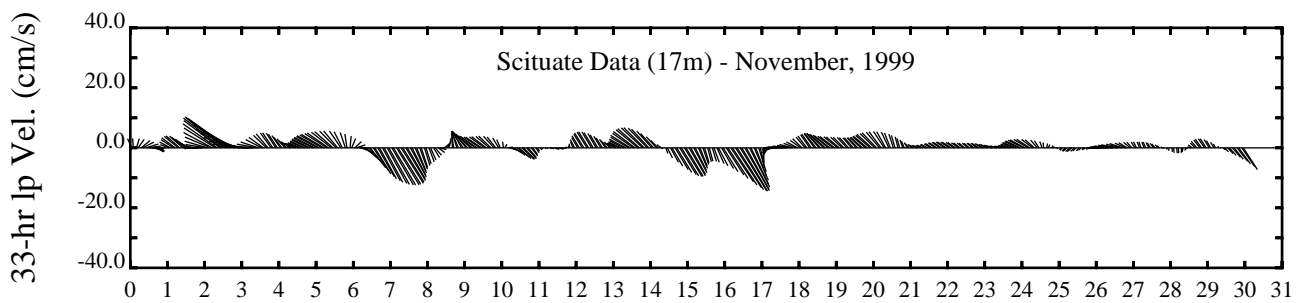
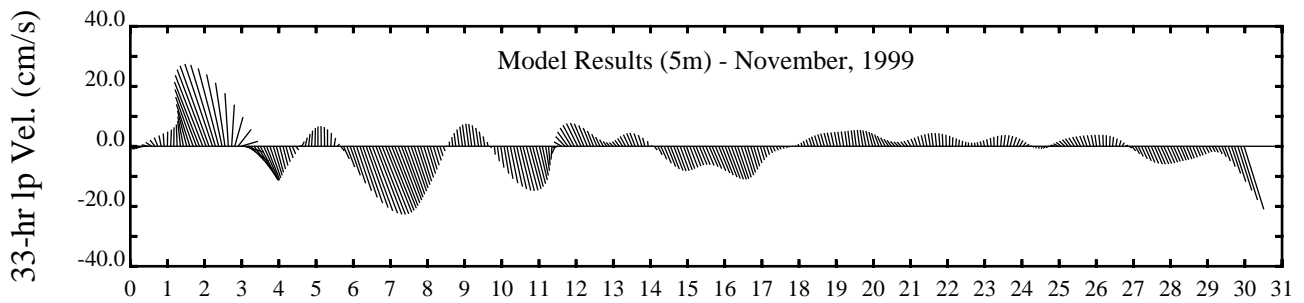
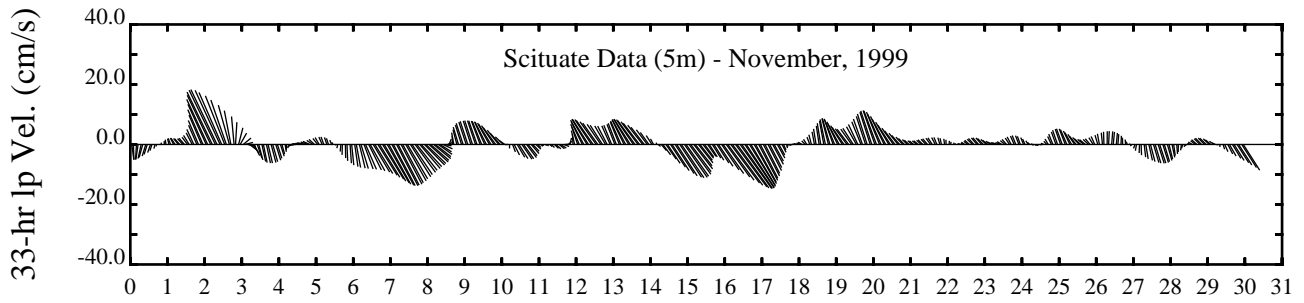
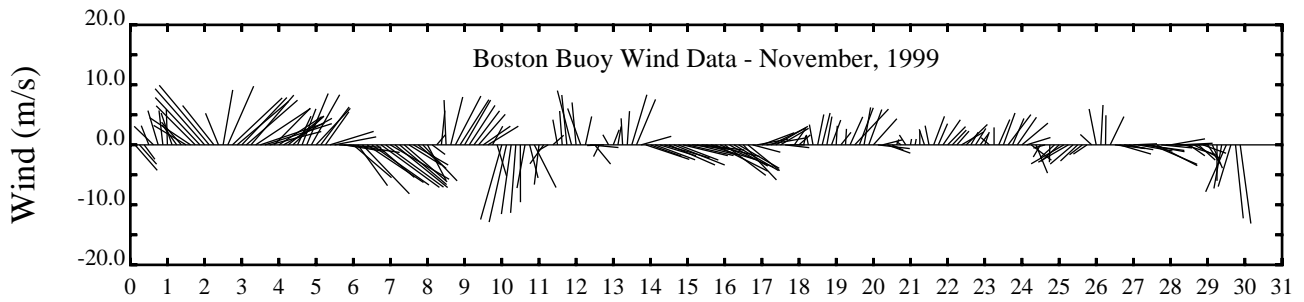
Day

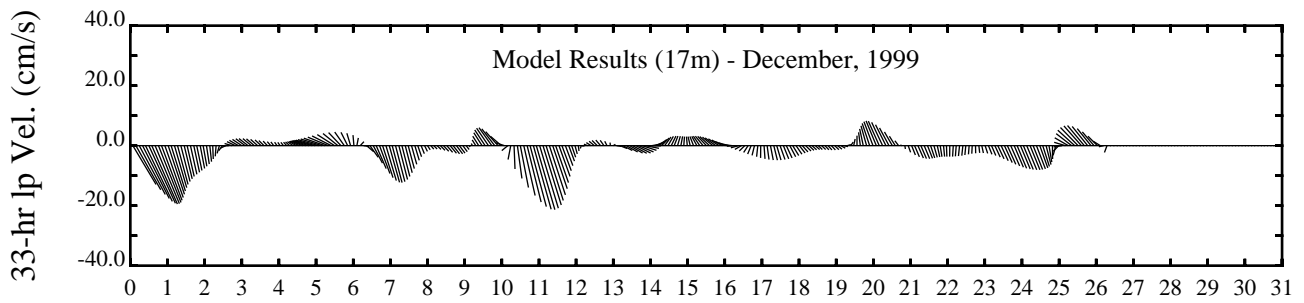
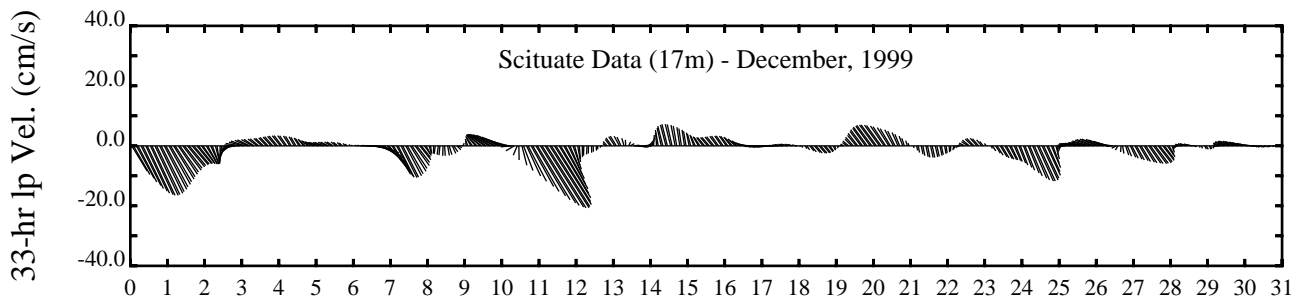
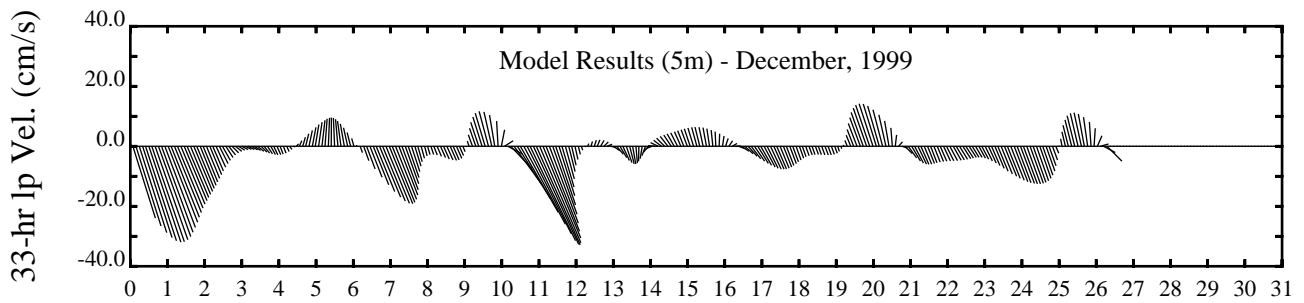
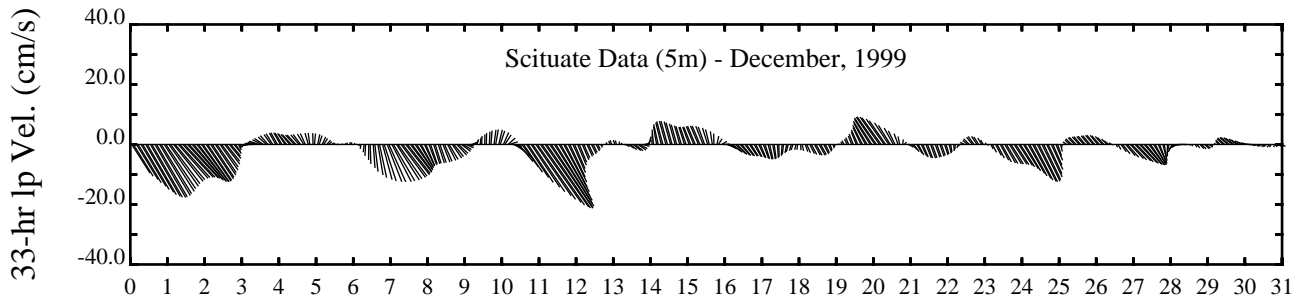
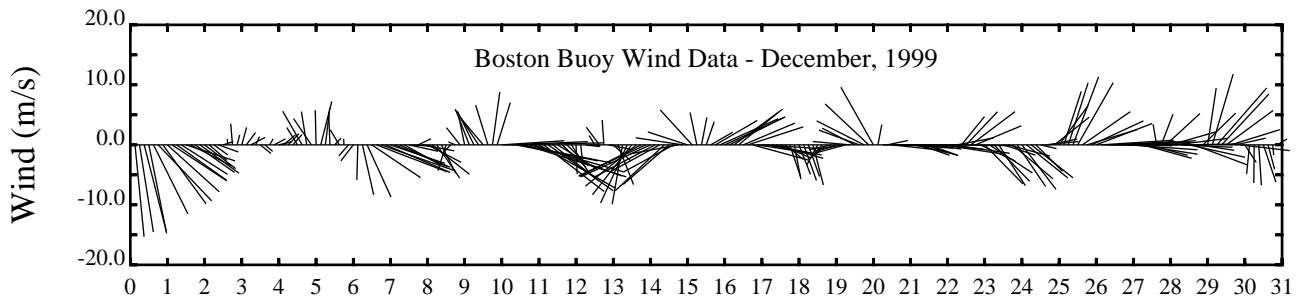


Day



Day





Day